PHYTOCHEMICAL AND ANTIPLASMODIAL STUDIES OF FIVE ETHNOBOTANICALLY-SELECTED SOUTH AFRICAN MEDICINAL PLANTS

Submitted in fulfilment of the academic requirements for the degree of

Doctor of Philosophy

UNIVERSITY OF
KWAZULU-NATAL

School of Chemistry and Physics

College of Agriculture, Engineering and Science (Pietermaritzburg)

By

Nasir Tajuddeen

Supervisor: Prof F R van Heerden

December 2019

PHYTOCHEMICAL AND ANTIPLASMODIAL STUDIES OF FIVE ETHNOBOTANICALLY-SELECTED SOUTH AFRICAN MEDICINAL PLANTS

By

Nasir Tajuddeen

2019

A thesis submitted to the School of Chemistry and Physics, College of Agriculture, Engineering and Science, University of KwaZulu-Natal, for the degree of Doctor of Philosophy.

This Thesis has been prepared according to **Format 4** as outlined in the guidelines from the College of Agriculture, Engineering and Science, which states:

This is a thesis in which chapters are written as a set of discrete research papers, with an overall introduction and final discussion, where one (or all) of the chapters have either been submitted for publication or have already been published. Typically, these chapters will have been published in internationally recognized, peer-reviewed journals.

Abstract

Vachellia xanthophloea, *Euclea natalensis*, *Ozoroa obovata*, *Gardenia thunbergia,* and *Pappea capensis* are traditionally used to treat malaria/fever in Africa. Previous studies showed that the extracts of *V. xanthophloea*, *G. thunbergia*, *P. capensis,* and *E. natalensis* have antiplasmodial activity. Therefore, in search of antiplasmodial compounds from South African plants, the five plants were investigated. Antiplasmodial screening of the ethyl acetate fraction of *V. xanthophloea* leaves against the 3D7 parasites showed moderate activity (IC_{50} = 10.6 µg/mL) and negligible cytotoxicity. Phytochemical investigation of the fraction afforded 16 compounds, ten flavonoids, a phenolic ester, a furofuran lignan, a carotenoid, and a fatty alcohol. The hexane fraction afforded a mixture of phytol and lupeol. Methyl gallate displayed the best antiplasmodial activity (IC_{50} = 1.2 µg/mL), better than the extract, and the cytotoxicity was not significant. The leaf extract of *O. obovata* inhibited *P. falciparum* viability by >90% at 50 µg/mL and was cytotoxic. Chromatographic purification of the extract afforded two biflavonoids, four flavonoid glycosides, a steroid glycoside, and a megastigmane derivative. The biflavonoids and flavonoid glycosides displayed nonselective antiplasmodial activities at 50 µg/mL. *E. natalensis* leaf extract displayed moderate antiplasmodial activity (IC_{50} = 25.6 µg/mL) and was not cytotoxic. Purification of the extract gave 11 compounds, six flavonoid glycosides, four triterpenoids, and a coumarin. The glycosides suppressed *P. falciparum* viability by more than 70% at 50 µg/mL but were also cytotoxic. An antiplasmodial assay of *P. capensis* leaf extract showed >80% inhibition of parasite viability at 50 µg/mL with cytotoxicity. Five flavonoid glycosides were subsequently isolated from the extract. The glycosides showed antiplasmodial activity at 50 µg/mL and were cytotoxic. *G. thunbergia* methanol leaf extract displayed good antiplasmodial activity (80% inhibition at 50 µg/mL) with little cytotoxicity. A saponin, two flavonoid glycosides, two metabolites of abscisic acid, a triterpenoid and a mixture of two sterols were isolated from the extract. The saponin and flavonoid glycosides inhibited the viability of *P. falciparum* at 50 µg/mL (>80%) but were also cytotoxic. This project has identified some extracts, e.g. *V. xanthophloea* and compounds, e.g. methyl gallate with promising antiplasmodial activity worthy of further development.

Declaration

I hereby declare that the experimental work described in thesis entitled "**Phytochemical and Antiplasmodial Studies of Five Ethnobotanically-Selected South African Medicinal Plants**" was carried out in the School of Chemistry and Physics, University of KwaZulu-Natal, Pietermaritzburg, to be submitted for the degree of Doctor of Philosophy in Chemistry under the supervision of **Prof. F. R. van Heerden**.

These studies represent original work by the author and have not otherwise been submitted in any form for any degree or diploma to any tertiary institution. Where use has been made of the work of others, it is duly acknowledged in the text.

Signed…  … Date…March 13, 2020

Nasir Tajuddeen

I hereby certify that this statement is correct.

Signed…  … Date… March 13, 2020

Prof. F. R. van Heerden

Supervisor

Declaration 2 - Plagiarism

I**, Nasir Tajuddeen,** declare that:

1. The research reported in this thesis, except where otherwise indicated, is my original research.
2. This thesis has not been submitted for any degree or examination at any other university.
3. This thesis does not contain other persons' data, pictures, graphs or other information, unless specifically acknowledged as being sourced from other persons'.
4. This thesis does not contain other persons' writing, unless specifically acknowledged as being sourced from other researchers. Where other written sources have been quoted, then:
    a. Their words have been re-written, but the general information attributed to them has been referenced.
    b. Where their exact words have been used, then their writing has been placed in italics and inside quotation marks and referenced.
5. This thesis does not contain text, graphics or tables copied and pasted from the internet, unless specifically acknowledged, and the source being detailed in the thesis and in the references sections.

Signed…  …

Declaration 3 - Publications

Publications from this thesis

Nasir Tajuddeen and Fanie R. Van Heerden. Antiplasmodial Natural Products – an update. *Malaria Journal*, in press.

Nasir Tajuddeen, Tarryn Swart, Heinrich C. Hoppe, and Fanie R. van Heerden. Antiplasmodial activity of *Vachellia xanthophloea* (Benth.) P.J.H. Hurter (African fever tree) and its active constituents. *Journal of Ethnopharmacology*, submitted for publication.

Nasir Tajuddeen, Tarryn Swart, Heinrich C. Hoppe, and Fanie R. van Heerden. Phytochemical and antiplasmodial studies of *Ozoroa obovata* (Oliv.) R. & A. Fern. *Chemistry and Biodiversity*, submitted for publication.

Nasir Tajuddeen, Tarryn Swart, Heinrich C. Hoppe, and Fanie R. van Heerden. Phytochemical and antiplasmodial investigation of *Euclea natalensis* A. DC. leaves: *South African Journal of Botany,* submitted for publication.

Nasir Tajuddeen, Tarryn Swart, Heinrich C. Hoppe, and Fanie R. van Heerden. Phytochemical and antiplasmodial studies of *Pappea capensis* (Eckl. & Zeyh.) leaves. *Natural Product Research*, submitted for publication.

Conference presentation

1. **Nasir Tajuddeen,** Dustin Laming, Heinrich Hoppe and Fanie R. van Heerden. Antiplasmodial activity of methoxylated flavonoids from *Vachellia xanthophloea* (Benth.) P.J.H. Hurter (African fever tree). Lecture presented at UKZN College of Agriculture Engineering and Science Post graduate Research Day, Westville campus, 25th October 2018.
2. **Nasir Tajuddeen,** Dustin Laming, Heinrich Hoppe and Fanie R. van Heerden. Antiplasmodial activity of methoxylated flavonoids from *Vachellia xanthophloea* (Benth.) P.J.H. Hurter (African fever tree). Poster presented at the 43rd South African Chemical Institute (SACI) National Convention, CSIR – ICC, Pretoria, 2nd – 7th December 2018.
3. **Nasir Tajuddeen,** Dustin Laming, Heinrich Hoppe and Fanie R. van Heerden. Antiplasmodial activity of *Vachellia xanthophloea* (Benth.) P.J.H. Hurter (African fever tree) and its active compounds. SACI/Chromsa Postgraduate Research Colloquium for KwaZulu-Natal, Durban University of Technology, Durban, 6th March 2019. Poster presentation.
4. **Nasir Tajuddeen,** Dustin Laming, Heinrich Hoppe and Fanie R. van Heerden, Antiplasmodial activity of *Vachellia xanthophloea* (Benth.) P.J.H. Hurter (African fever tree) and its active compounds. Poster presented at the SACI Frank Warren conference 2019 – Alpine Health, Drakensberg, 7th – 11th July 2019. Poster presentation.

Details of contributions to publications that form part and/or include research presented in this thesis (including publications in preparation, submitted, *in press* or published and giving details of the contributions of each author to the experimental work and writing of each publication)

List of manuscripts/ publications:

Chapter 1

Nasir Tajuddeen and Fanie R. van Heerden

Antiplasmodial Natural Products – an update

Contributions:

- NT and FVH designed and wrote the work

Chapter 2

Nasir Tajuddeen, Tarryn Swart, Heinrich C. Hoppe, and Fanie R. van Heerden

Antiplasmodial activity of *Vachellia xanthophloea* (Benth.) P.J.H. Hurter (African fever tree) and its active constituents

Contributions:

- NT and FVH designed the project
- NT collected the plant material and did the isolation and characterization of the chemical compounds
- TS and HCH did the biological screening
- FVH supervised the work
- NT wrote the manuscript in the current form

Chapter 3

Nasir Tajuddeen, Tarryn Swart, Heinrich C. Hoppe, and Fanie R. van Heerden

Phytochemical and antiplasmodial studies of *Ozoroa obovata* (Oliv.) R. & A. Fern

Contributions:

- NT and FVH designed the project
- NT collected the plant material and did the isolation and characterization of the chemical compounds
- TS and HCH did the biological screening
- FVH supervised the work
- NT wrote the manuscript in the current form

Chapter 4

Nasir Tajuddeen, Tarryn Swart, Heinrich C. Hoppe, and Fanie R. van Heerden

Phytochemical and antiplasmodial investigation of *Euclea natalensis* A. DC. leaves

Contributions:

- NT and FVH designed the project
- NT collected the plant material and did the isolation and characterization of the chemical compounds
- TS and HCH did the biological screening
- FVH supervised the work
- NT wrote the manuscript in the current form

Chapter 5

Nasir Tajuddeen, Tarryn Swart, Heinrich C. Hoppe, and Fanie R. van Heerden

Phytochemical and antiplasmodial studies of *Pappea capensis* (Eckl. & Zeyh.) leaves

Contributions:

- NT and FVH designed the project
- NT collected the plant material and did the isolation and characterization of the chemical compounds
- TS and HCH did the biological screening
- FVH supervised the work
- NT wrote the manuscript in the current for

Chapter 6

Nasir Tajuddeen, Tarryn Swart, Heinrich C. Hoppe, and Fanie R. van Heerden

Phytochemical and antiplasmodial investigation of *Gardenia thunbergia* L.f. leaves

Contributions:

- NT and FVH designed the project
- NT collected the plant material and did the isolation and characterization of the chemical compounds
- TS and HCH did the biological screening
- FVH supervised the work
- NT wrote the manuscript in the current for

Acknowledgments

During the course of this program, a number of individuals and organisations have contributed to my success. I would like to use this opportunity to show my appreciation for their contributions.

I would like to thank my supervisor Prof. Fanie R. van Heerden for the opportunity to be a member of her research group to conduct my research and for all the knowledge and guidance. I have learned a lot and none of this will have been possible without this opportunity.

I would also like to express my gratitude to the University of KwaZulu-Natal for the award of the UKZN doctoral scholarship. This provided me with much needed financial stability and peace of mind to focus on my research work.

My sincere appreciation also goes to the technical staff; Craig Grimmer of the NMR lab, Caryl Janse van Rensburg of the MS lab, Saidishnee Naidoo and Fayzil Shaik, you guys have been wonderful and your support is appreciated.

I am also grateful to Drs MB Isah and MA Ibrahim for introducing me to UKZN and Prof. Fanie.

Then to all members of the Natural Product Research group, it has been a great experience working with you guys. Your company and contributions have been invaluable in the lab.

Finally to my mother, siblings, fiancée (Fatima) and friends (especially Ummi), thank you for all your support, prayers and patience.

To the memory of my late Father.

Table of Content

Contents

List of Tables

List of Figures

Abbreviations

^{1}H NMR	Proton nuclear magnetic resonance
^{13}C NMR	Carbon-13 nuclear magnetic resonance
brs	Broad singlet
brd	Broad doublet
COSY	Correlation spectroscopy
CD_3OD	Deuterated methanol
$CDCl_3$	Deuterated chloroform
DEPT	Distortionless enhancement by polarization transfer
DMSO	Dimethyl sulfoxide
d	Doublet
dd	Doublet of doublets
dt	Doublet of triplets
ESI	Electrospray ionization
EIMS	Electron-impact mass spectrometry
g	Gram
GC-MS	Gas chromatography-mass spectrometry
Glc	Glucosyl
Hz	Hertz
H_2SO_4	Sulfuric acid
HRMS	High-resolution mass spectrometry
HSQC	Heteronuclear single quantum coherence
HMBC	Heteronulcear multiple bond correlation
HRESIMS	High-resolution electrospray impact mass spectrometry
HPLC	High-performance liquid chromatography
IC_{50}	Half-maximal inhibitory concentration
J	Coupling constant
LC	Liquid chromatography
m	Multiplet
mL	Millilitre
mg/mL	Milligram per millilitre

mL/min	Millilitre per minute
mm	Millimetre
m/z	Mass-to-charge
mg	Milligram
Min	Minutes
MS	Mass spectrometry
$MgSO_4$	Magnesium sulfate
MTT	3-(4,5-Dimethylthiazol-2-yl)-2,5-diphenyltetrazolium bromide
MHz	Megahertz
nm	Nanometer
NIST	National Institute of Standards and Technology
NOESY	Nuclear Overhauser effect spectroscopy
pLDH	Parasite lactate dehydrogenase
PBS	Phosphate-buffered saline
Rf	Retention factor
Rham	Rhamnosyl
Rt	Retention time
s	Singlet
t	triplet
TOF	Time of flight
TLC	Thin-layer chromatogramphy
UV	Ultraviolet
VLC	Vacuum-liquid chromatography
WHO	World Health Organization
δ	Chemical shift
°C	Degrees Celcius
µm	Micrometre
µL	Microlitre
µg/mL	Microgram per millilitre

CHAPTER 1: Introduction

1.1 Malaria and the malaria parasite

Malaria is a vector-borne infectious disease of humans and other animals. The etiologic agents are parasites belonging to the *Plasmodium* genus and they are spread by mosquitos. *Plasmodium falciparum*, *P. malariae*, *P. vivax*, and *P. ovale* are the four species implicated for malaria in humans. *Plasmodium vivax* and *P. falciparum* are responsible for 95% of all malaria infections.[1] It was recently recognized that the monkey malaria parasite, *P. knowlesi* can also cause severe malaria in humans.[2-4] *Plasmodium falciparum* is the prevalent species in Africa and it causes a form of the disease that is most likely to result in fatality, if not quickly treated.[5] The life cycle of *Plasmodium* involves multiple stages and each of these stages presents an opportunity for combating the parasite. The stages are:

Liver stage: The injection of parasites, called sporozoites, into the bloodstream of an uninfected human during a blood meal by a compromised mosquito initiates an infection. The infective sporozoites evade the host defense system by rapidly invading liver cells where they multiply into tissue schizonts containing large amounts of merozoites. The schizonts eventually burst, releasing the merozoites into the host's blood circulatory system and kick start the erythrocytic stage. In *P. ovale* and *P. vivax*, some sporozoites transform into dormant hypnozoites and can start another infection called 'relapse', a long time after the original affliction. Prophylactic drugs kill liver-stage parasites and are useful in preventing a relapse. Targeting the liver stage parasites arrests the development of malaria before clinical manifestations.[6,7]

Erythrocytic stage: In the bloodstream, erythrocyte cells are invaded by the released merozoites where they replicate asexually through ring, trophozoite and schizont forms, and rapidly increase the number of merozoites. These daughter cells attack more red blood cells, consume the host haemoglobin and release toxic wastes, all of which result in the clinical manifestations of the disease. The asexual reproduction in the red blood cells continues for several cycles and eventually, some merozoites transform into sexual forms called gametocytes to kick start the next phase of the life cycle in a mosquito. The majority of

antimalarials act on parasites at the erythrocytic stage and are important in controlling the clinical symptoms of the disease and death.[6,7]

Mosquito stage: Some gametocytes are transferred to an unifected mosquito when it feeds on the blood of an infected host. The gametocytes migrate to the midgut of the mosquito and undergo sexual reproduction to form infective sporozoites. The sporozoites end up in the salivary gland of the mosquito and continue the transmission. Drugs that are active against sexual stage parasites are important for malaria eradication since they prevent transmission.[6,7]

1.2 The burden of malaria

Despite the tremendous progress made in malaria treatment, the disease continues to cause serious morbidity and death. Malaria is widespread in the tropics and subtropics, but the burden is heaviest in Africa, which accounted for 93% of the estimated 435000 global malaria deaths in 2017. The problem is complicated by the high prevalence among pregnant women and the fact that 61% of the mortality is in children under the age of five.[8] Also, climatic conditions and the variation of seasonal temperature in sub-Saharan Africa favour malaria transmission.[9]

Analyses show that malaria exerts an enormous burden on the economic wellbeing of vulnerable societies. Poor communities suffer the devastation of malaria disproportionately, and this causes more poverty and stunted economic growth**.** This is because malaria constitutes a major obstacle to human capital development in malarious regions, and causes loss of working hours of individuals, families and whole communities. Malaria may also have an adverse demographic effect. This is because families give birth to more children in situations where the chance of offspring survival is not guaranteed due to the increased risk of infant and child mortality. The overall result is an increase in population and decrease in the general quality of life.[10]

1.3 Antimalarial drugs from nature

The importance of natural products as extracts or purified compounds in the search for drug candidates and inspiration for the design of novel drugs is well established. The influence of natural products is particularly pronounced in the area of anti-infective agents.[11] Plant natural

products have historically produced the most effective antimalarial drugs. The quinoline antimalarials such as chloroquine (**1.1**), sontoquin (**1.2**), pamaquine (**1.3**) and primaquine (**1.4**) were inspired by quinine (**1.5**).[1] Quinine is obtained from the bark of South American *Chinchona* trees and was the first effective antimalarial drug.[12] The discovery of chloroquine in the 1940s represented a turning point in the fight against malaria. Chloroquine was cheap, effective, easy to administer, widely available, and well-tolerated, even in infants and pregnant women.[13] However, chloroquine became ineffective in most malaria-endemic regions following the widespread development of resistance by *P. falciparum*.

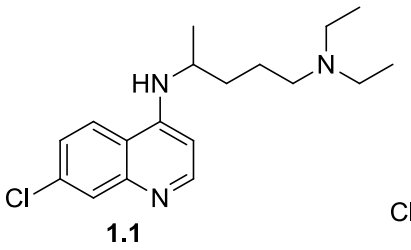

1.1

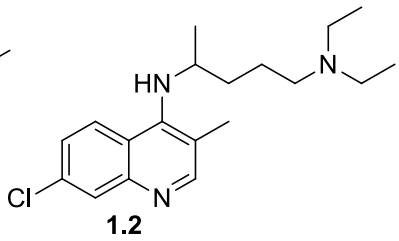

1.2

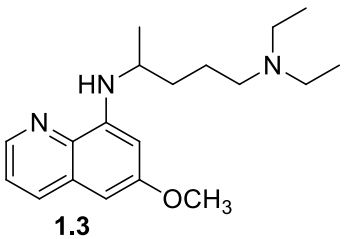

1.3

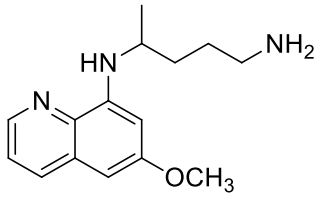

1.4

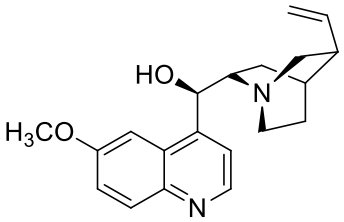

1.5

Lapachol (**1.6**), a hydroxynaphthoquinone with antimalarial activity, found in several plants of the Bignoniaceae, served as the inspiration for the design of atovaquone (**1.7**).[14] Atovaquone combined with proguanil (**1.8**) is sold under the brand name Malarone™ and is used for treatment and prophylaxis of malaria.[15]

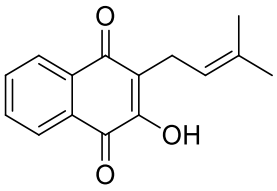

1.6

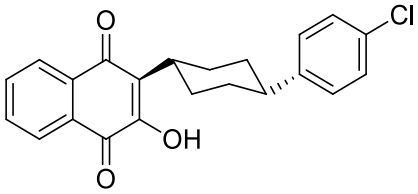

1.7

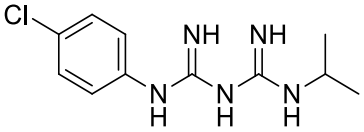

1.8

In the 1970s, artemisinin (**1.9**), the backbone of the current first-line antimalarial treatments, was isolated from the hexane extract of Chinese anti-fever plant, *Artemisia annua* or Qinghao.

The plant was traditionally used to treat malaria and fever.[12] Artemisinin, which is a sesquiterpene lactone endoperoxide, represented a new class of antimalarial agent, different from the conventional aminoquinolines. The low solubility of artemisinin meant that it had a poor oral activity and bioavailability. Attempts to overcome these shortcomings resulted in the preparation of some semi-synthetic derivatives. These derivatives include the oil-soluble artemether (**1.10**), artether (**1.11**), and sodium artesunate (**1.12**) and artelinate (**1.13**) which are soluble in water. Generally, the derivatives present a superior activity compared to artemisinin itself and the active metabolite is dihydroartemisinin (**1.14**).[1] Semi-synthetic artemisinin derivatives are made from dihydroartemisinin, which is in turn made by reducing the lactone functionality of artemisinin with sodium borohydride.[16]

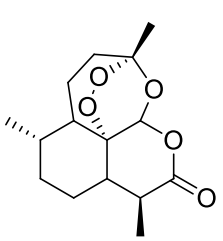

1.9

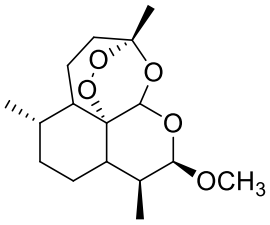

1.10

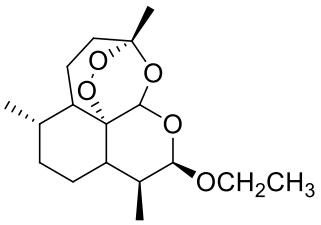

1.11

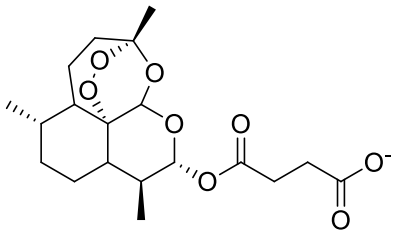

1.12

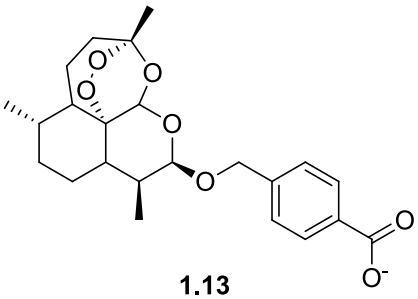

1.13

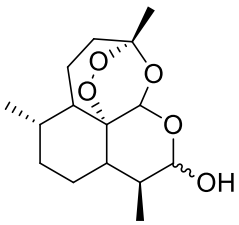

1.14

The World Health Organisation (WHO) recommends the use of artemisinin-based combination therapies, consisting of a rapid-acting artemisinin derivative and a longer-acting partner drug, such as an arylamino alcohol or a 4-aminoquinoline, for the treatment of uncomplicated malaria.[17] However, emerging cases of delayed drug response and resistance to artemisinin indicate that the search for new antiplasmodial agents is an urgent priority.

1.4 Antimalarial natural products research in South Africa

Approximately 10% of the world's flora is located in the Southern African region and comprises about 24500 plant taxa. The region, which defines the Flora of Southern Africa, has

a rich biodiversity of plants. Similarly, Southern Africa is home to a wide array of cultural groups with an active traditional health care system that takes advantage of the rich biodiversity to treat various diseases, such as malaria. The traditional uses of these medicinal plants have been documented in various databases and publications.[18] Some estimates indicate that the exploration of ethnobotanical knowledge resulted in the discovery of 74% of plant metabolites with pharmacological activity.[19] Incidentally, the most important antimalarial drugs were discovered from plants that were traditionally used to treat fever or malaria, indicating the immense value of traditional knowledge to antimalarial natural products research. As part of its effort towards controlling malaria, the South African government, through the Department of Science and Technology, funded investigation into the antimalarial activity of South African medicinal plants, with the ultimate aim of discovering new and affordable treatments for malaria.[20] Hence some major screening programs into the antiplasmodial activity of plants that are used for the treatment of malaria and/or fever in traditional medicine were carried out in South Africa.[20-24] These screening programs confirmed the antimalarial activity traditionally associated with some of these plants and identified some promising taxa for further investigation.

1.5 Aim of research

The aim of this project was the isolation, structure elucidation and antiplasmodial activity of compounds from five South African medicinal plants that are used in traditional medicine to treat malaria or fever.

The aim was achieved through the following objectives

i. Selection of plants based on ethnobotanical evidence of use in traditional medicine for the treatment of malaria or fever
ii. Phytochemical and antiplasmodial studies of *Vachellia xanthophloea* (Benth.) P.J.H.Hurter
iii. Phytochemical and antiplasmodial studies of *Ozoroa obovata* (Oliv.) R.Fern. & A.Fern. *var. obovata*
iv. Phytochemical and antiplasmodial studies of *Euclea natalensis* A. DC. subsp. *natalensis*
v. Phytochemical and antiplasmodial studies of *Pappea capensis* Eckl. & Zeyh.

vi. Phytochemical and antiplasmodial studies of *Gardenia thunbergia* L.f.

1.6 Structure of the thesis

The research work presented in this thesis is discussed as discrete chapters in the form of manuscripts. The opening chapter provides a general introduction where the theme and justification, as well as the aim and objectives of the project, are outlined. Chapter two comprehensively discussed the antiplasmodial natural products that were reported in the literature between 2010 and 2018 in the form of a review article. Chapters 3-7 contain the results obtained from the phytochemical and antiplasmodial studies of five South African plants that are used ethnobotanically in treating malaria and/or fever. Chapter eight provides a general conclusion summarising the research findings and some recommendations. The parts of the experimental section that is common to chapters 3-7 were detailed in chapter 3 and subsequently referred to in other chapters.

References

1. Schlitzer, M., Malaria chemotherapeutics part 1: History of antimalarial drug development, currently used therapeutics, and drugs in clinical development. *Chemmedchem* **2007,** 2, (7), 944-986.
2. Kantele, A.; Jokiranta, T. S., Review of cases with the emerging fifth human malaria parasite, *Plasmodium knowlesi*. *Clinical Infectious Diseases* **2011,** 52, (11), 1356-1362.
3. White, N. J., *Plasmodium knowlesi*: The fifth human malaria parasite. *Clinical Infectious Diseases* **2008,** 46, (2), 172-173.
4. Cox-Singh, J.; Davis, T. M. E.; Lee, K. S.; Shamsul, S. S. G.; Matusop, A.; Ratnam, S.; Rahman, H. A.; Conway, D. J.; Singh, B., *Plasmodium knowlesi* malaria in humans is widely distributed and potentially life threatening. *Clinical Infectious Diseases* **2008,** 46, (2), 165-171.
5. Gething, P. W.; Patil, A. P.; Smith, D. L.; Guerra, C. A.; Elyazar, I. R. F.; Johnston, G. L.; Tatem, A. J.; Hay, S. I., A new world malaria map: *Plasmodium falciparum* endemicity in 2010. *Malaria Journal* **2011,** 10.
6. Biamonte, M. A.; Wanner, J.; Le Roch, K. G., Recent advances in malaria drug discovery. *Bioorganic & Medicinal Chemistry Letters* **2013,** 23, (10), 2829-2843.

7. Oliveira, R.; Miranda, D.; Magalhaes, J.; Capela, R.; Perry, M. J.; O'Neill, P. M.; Moreira, R.; Lopes, F., From hybrid compounds to targeted drug delivery in antimalarial therapy. *Bioorganic & Medicinal Chemistry* **2015,** 23, (16), 5120-5130.
8. WHO, World Malaria Report 2017. WHO global malaria programme. In WHO Geneva: 2018.
9. Snow, R. W.; Sartorius, B.; Kyalo, D.; Maina, J.; Amratia, P.; Mundia, C. W.; Bejon, P.; Noor, A. M., The prevalence of *Plasmodium falciparum* in sub-Saharan Africa since 1900. *Nature* **2017,** 550, (7677), 515-518.
10. Sachs, J.; Malaney, P., The economic and social burden of malaria. *Nature* **2002,** 415, (6872), 680-685.
11. Newman, D. J.; Cragg, G. M., Natural products as sources of new drugs over the 30 years from 1981 to 2010. *Journal of Natural Products* **2012,** 75, (3), 311-335.
12. Klayman, D. L., Qinghaosu (artemisinin) - An antimalarial drug from China. *Science* **1985,** 228, (4703), 1049-1055.
13. Wellems, T. E., *Plasmodium* chloroquine resistance and the search for a replacement antimalarial drug. *Science* **2002,** 298, (5591), 124-126.
14. Schwikkard, S.; van Heerden, F. R., Antimalarial activity of plant metabolites. *Natural Product Reports* **2002,** 19, (6), 675-692.
15. Looareesuwan, S.; Chulay, J. D.; Canfield, C. J.; Hutchinson, D., Malarone (atovaquone and proguanil hydrochloride): a review of its clinical development for treatment of malaria. Malarone clinical trials study group. *The American Journal of Tropical Medicine and Hygiene* **1999,** 60, (4), 533-541.
16. Chaturvedi, D.; Goswami, A.; Saikia, P. P.; Barua, N. C.; Rao, P. G., Artemisinin and its derivatives: a novel class of anti-malarial and anti-cancer agents. *Chemical Society Reviews* **2010,** 39, (2), 435-454.
17. World Health Organisation. Overview of malaria treatment. https://www.who.int/malaria/areas/treatment/overview/en/ (29 August 2019),
18. Arnold, T. H.; Prentice, C.; Hawker, L.; Snyman, E.; Tomalin, M.; Crouch, N.; Pottas-Bircher, C., *Medicinal and magical plants of southern Africa: an annotated checklist*. National Botanical Institute: 2002.

19. Farnsworth, N. R.; Soejarto, D., Global importance of medicinal plants. In *The Conservation of Medicinal Plants*, Olayiwola Akerele, V. H., Hugh Synge, Ed. Cambridge University Press, UK.: 1991; Vol. 26, pp 25-51.
20. Clarkson, C.; Maharaj, V. J.; Crouch, N. R.; Grace, W. M.; Pillay, P.; Matsabisa, M. G.; Bhagwandin, N.; Smith, P. J.; Folb, P. I., In vitro antiplasmodial activity of medicinal plants native to or naturalised in South Africa. *Journal of Ethnopharmacology* **2004,** 92, (2-3), 177-191.
21. Bapela, M. J.; Meyer, J. J. M.; Kaiser, M., In vitro antiplasmodial screening of ethnopharmacologically selected South African plant species used for the treatment of malaria. *Journal of Ethnopharmacology* **2014,** 156, 370-373.
22. Mokoka, T. A.; Xolani, P. K.; Zimmermann, S.; Hata, Y.; Adams, M.; Kaiser, M.; Moodley, N.; Maharaj, V.; Koorbanally, N. A.; Hamburger, M.; Brun, R.; Fouche, G., Antiprotozoal screening of 60 South African plants, and the identification of the antitrypanosomal germacranolides schkuhrin I and II. *Planta Medica* **2013,** 79, (14), 1380-1384.
23. Nandkumar, N.; Ojewole, J. A. O., Studies on the antiplasmodial properties of some South African medicinal plants used as antimalarial remedies in Zulu folk medicine. *Methods and Findings in Experimental and Clinical Pharmacology* **2002,** 24, (7), 397-401.
24. Prozesky, E. A.; Meyer, J. J. M.; Louw, A. I., In vitro antiplasmodial activity and cytotoxicity of ethnobotanically selected South African plants. *Journal of Ethnopharmacology* **2001,** 76, (3), 239-245.

CHAPTER 2: Antiplasmodial natural products – An update

Nasir Tajuddeen and Fanie R. van Heerden

School of Chemistry and Physics, University of KwaZulu-Natal, Private Bag X01, Scottsville 3209, Pietermaritzburg, South Africa

Accepted review article, awaiting publication in ***Malaria Journal***

Abstract

Background

Malaria remains a significant public health challenge in regions of the world where it is endemic. An unprecedented decline in malaria incidences was recorded during the last decade due to the availability of effective control interventions, such as the deployment of artemisinin-based combination therapy and insecticide-treated nets. However, according to the World Health Organization, malaria is staging a comeback, in part due to the development of drug resistance. Therefore, there is an urgent need to discover new anti-malarial drugs. This article reviews the literature on natural products with antiplasmodial activity that was reported between 2010 and 2017.

Methods

Relevant literature was sourced by searching the major scientific databases, including Web of Science, ScienceDirect, Scopus, SciFinder, Pubmed and Google Scholar, using appropriate keyword combinations.

Results and Discussion

A total of 1524 compounds from 397 relevant references, assayed against at least one strain of *Plasmodium*, were reported in the period under review. Out of these, 39% were described as new natural products, and 29% of the compounds had $IC_{50} \leq 3.0$ µM against at least one strain of *Plasmodium*. Several of these compounds have the potential to be developed into viable anti-malarial drugs. Also, some of these compounds could play a role in malaria eradication by targeting gametocytes. However, the research into natural products with potential for blocking the transmission of malaria is still in its infancy stage and needs to be vigorously pursued.

Keywords: Malaria, *Plasmodium*, Antiplasmodial, Natural products, Plant metabolites, Marine natural products

Background

Malaria remains a serious parasitic disease in the world, with 219 million infections and 435,000 deaths cited for 2017 in the latest World Malaria Report [1]. An assessment of older and more recent malaria maps shows that the disease has been geographically restricted during the 20th century, and has remained endemic in the poor regions of the world where the climate is suitable for transmission [2-5]. In Africa, where the disease burden is the highest, there has been a general decline in the trend of *Plasmodium falciparum* malaria, from a prevalence of 40% in 1910 - 1929 to about 24% in 2010 – 2015 [6]. However, in the high transmission belt covering large parts of West and Central Africa, there is little change. This shrinkage of the malaria map has been interrupted by periods of rapid increase and decline in transmission [6]. The significant decline in malaria prevalence between 1945 and 1949, and again between 2005 and 2009 correlates with deliberate intervention programs. Each of these declines was preceded by a rise in malaria prevalence. The introduction of chloroquine (**1**) (Fig. 1) and dichlorodiphenyltrichloroethane (DDT) in 1945 and widespread use of insecticide-treated bed nets and artemisinin-based combination therapy (ACT) between 2005 and 2009 are partly credited for these declines. The rapid spread of resistance to chloroquine and emerging resistance to ACT in Africa, coupled with an increase in cases of vector-borne diseases in places like the USA, poses a threat to the gains that have been achieved in malaria control [6-9]. A World Health Organization (WHO) malaria report already shows a rise in malaria incidences in 2016 compared to 2015 [1]. Also, the sustained decline in mortality due to malaria since 2010 has stalled in some regions between 2015 and 2016, and has increased in other regions [1]. Therefore, the continued search for new anti-malarial agents remains an urgent priority.

Malaria chemotherapy has a strong historical link to natural products. The most successful anti-malarial agents have their origins in plant metabolites. The first successful anti-malarial drug was quinine (**2**), isolated from the bark of the South American *Cinchona* tree. This compound served as a lead structure in the development of the successful synthetic anti-malarial chloroquine (**1**), which, in recent years, has fallen out of favour as a result of the development of drug resistance by the parasite. Likewise, artemisinin (**3**) was isolated from the leaves of a Chinese medicinal plant, *Artemisia annua*. *Cinchona* bark and *Artemisia annua* were historically used to treat fever. Sophisticated target identification strategies following the sequencing of the *P. falciparum* genome in addition to the application of combinatorial chemistry hit identification strategies, did not lead to the expected increase in the number of new successful anti-malarial agents, and it is plausible that the next anti-malarial agents will be identified from a natural source again [10].

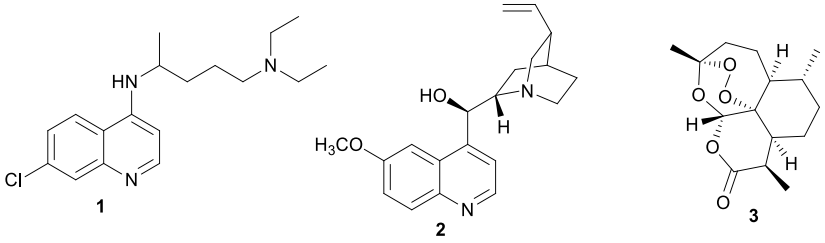

Fig. 1 Structures of anti-malarial drugs

Due to structural characteristics such as multiple stereocenters, flexible conformations, presence of heteroatoms, natural products are more likely than synthetic compounds to have multiple targets and/or new targets. Researchers investigating natural products as potential anti-malarial drugs need

to incorporate the screening of the compounds for the interaction with newly identified druggable targets, such as PfATP4 and DHODH, in order to identify hits/leads. Therefore, the continued exploration of natural products as antiplasmodial agents is of great scientific interest. Equally important is the need to review the literature in the field of malaria chemotherapy to provide a perspective for future research.

Plant-derived antiplasmodial compounds organized according to plant families covering the literature from 1990 to 2000 have been reviewed [11]. Similarly, reviews categorizing antiplasmodial compounds isolated from plants according to phytochemical classes have been conducted by Bero and co-workers (2005-2011) [12, 13], Nogueira and Lopes (2009-2010) [14], and Wright (2000-2010) [15]. Finally, reviews covering antiplasmodial marine natural products up to 2009 have been published by Laurent and Pietra, and Fattorusso and Taglialatela-Scafati [16, 17]. However, several new antiplasmodial chemotypes have been reported in the literature since 2010, in addition to the recent increase in antiplasmodial chemical scaffolds emerging from non-vegetal sources. Against this background, this article reviews the literature on natural products with antiplasmodial activity from 2010 to the end of 2017 and is organized according to structural types of compounds.

A thorough search of the relevant scientific databases, including Web of Science, ScienceDirect, Scopus, SciFinder, Pubmed and Google Scholar, was conducted. The keyword combinations of antiplasmodial, anti-malarial, *Plasmodium*, and malaria compounds together with plant, phytochemical, marine sponge, nudibranch, alga, cyanobacteria, mushroom, fungi, and *Streptomyces* were used in the search. Within the period under review, a total of 1524 compounds from 397 relevant references, assayed against at least one strain of *Plasmodium*, were reported. Of these compounds, 593 (39%) were described as new natural products. The number of compounds isolated from vegetal material was 1165 (76%), while 359 were from non-plant sources. Among the compounds isolated from non-plant sources, 192 (53%) were described as new, while 401 (34%) of the compounds isolated from plants were new. These numbers show that medicinal plants are still the most comprehensively explored source for antiplasmodial compounds, which may be related to ease of access. However, this review also shows the potential of non-plant material to furnish new chemotypes. Regarding the potency of these compounds, 857 (56%) had $IC_{50} \leq 10$ µM, 625 (41%) had $IC_{50} \leq 5.0$ µM, and 447 (29%) had $IC_{50} \leq 3.0$ µM against at least one strain of *Plasmodium*. The cut-off value for potency remains an issue of ongoing debate, but the industry standard for considering a pure compound to be active is generally accepted as $IC_{50} \leq 10$ µM [18].

The *in vitro* antiplasmodial activities described in this review were obtained with various *P. falciparum* strains with different drug sensitivities. The chloroquine-sensitive strains were 3D7, NF54, D6, HB3, F32, D10, TM4/8.2 and MRC-pf-20. Other strains used were the chloroquine-resistant strains Dd2, FcB1, *Pf*INDO, FcM29, MRC-pf-303, and the multidrug-resistant K1, TM90-C2A, TM93-C1088, W2, TM90-C2B, TM91-C235, NHP1337, FCR3, K1CB1 and W2mef strains. Different assays were used to determine the *in vitro* antiplasmodial activities of the compounds. The most commonly cited methods were the radioactive hypoxanthine-incorporation assay, the colourimetric enzyme-linked immunosorbent assays (ELISA) that measure *P. falciparum* lactate dehydrogenase protein (pLDH) and histidine-rich protein 2 (HRP2), a DNA-based fluorometric method using the PicoGreen (SYBR) assay, and microscopy. These methods have different sensitivities and the advantages and disadvantages have been investigated and reviewed [19-21]. Regardless of the *in vitro* assay method, in this review,

only compounds with IC_{50} ≤ 3.0 µM were considered to be of interest for further studies. Among the compounds that are discussed, 317 (70.9%) were isolated from 50 different plant families, while 130 were from non-plant sources comprising of different species of marine sponges, alga, fungi, ascidians, nudibranch, cyanobacteria and actinobacteria (Fig. 2).

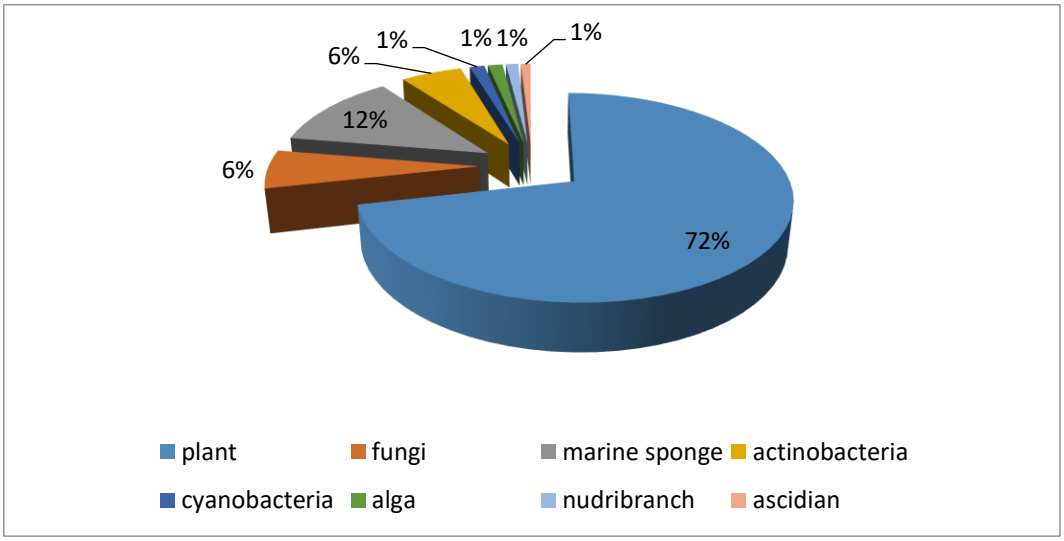

Fig. 2 Breakdown of sources for antiplasmodial compounds discussed in this review

The antiplasmodial natural products are organized in seven classes, i.e. endoperoxides, alkaloids, terpenes, polyphenols, quinones and polyketides, macrocycles, and cyclic phosphotriesters, with subclasses where applicable. The review concludes with a summary of the cellular targets in *Plasmodium* identified for natural products and natural products with transmission-blocking potential.

Endoperoxides

The profound success of artemisinin (**3**) and derivatives as drugs for the treatment of malaria prompted the selection of endoperoxides as the first class of compounds to be discussed in this review. Endoperoxide polyketides (Fig. 3) belonging to the 1,2-dioxane and 1,2-dioxolane structural class with proven antiplasmodial activity have been isolated from marine sponges. The structural variability includes different lengths of the 'western' side chain, different branching patterns, and a fully saturated or monounsaturated cyclohexane ring, all of which affect the bioactivity [22]. Plakortin (**4**), isolated from the marine sponge *Plakortis simplex*, is the archetype compound of this class. It demonstrated potent submicromolar antiplasmodial activity against chloroquine-sensitive and -resistant parasites [23, 24]. A plausible mechanism of action, inspired by results obtained with artemisinin and other trioxanes, was proposed for these structurally simpler molecules. It involves an initial reaction of the peroxidic bond with Fe(II) heme to form an *O*-centred radical, which is transformed into a *C*-centred radical following intramolecular rearrangement. The rearranged *C*-centred radical on the 'western' alkyl side-chain represents the toxic species that kills parasites. The minimum structural requirements for antiplasmodial activity of this class of compounds have been identified. The oxygen atoms of the endoperoxide bond must be accessible to Fe(II), and the molecule must adopt the appropriate conformation for the intramolecular rearrangement through a concerted intramolecular electron transfer [25]. The lower antiplasmodial activity of the peroxyketal derivative manadoperoxide C (**5**) and its analogues isolated from Indonesian-sourced *Plakortis* cfr. *simplex* was rationalized on the basis of these structural requirements. The 6-methoxy substituent of the

manadoperoxides constitutes a hindrance for Fe(II) to the peroxide bond, leading to lower activity [23]. The isolation of endoperoxide analogues **6-8** with a 1,2-diox-4-ene ring from *Plakortis simplex* allowed an extension of the structure-activity relationship (SAR). For structurally similar compounds, the unsaturated derivatives were more active due to stereochemical influence, although they were still less active than **4**. The lower activity compared to **4** could also be explained by the relative inaccessibility of the peroxide oxygen due to steric hindrance [22]. These results indicate that structural changes affecting the conformational behaviour of this class of compounds profoundly influence the antiplasmodial activity and this knowledge will be beneficial for the design of optimized analogues [23]. The related 1,2-dioxolane epiplakinidioic acid (**9**) was isolated from Puerto Rican-sourced *P. halichondrioides* and inhibited *P. falciparum* W2 strain. However, it was also cytotoxic against a panel of cancerous cell lines [26].

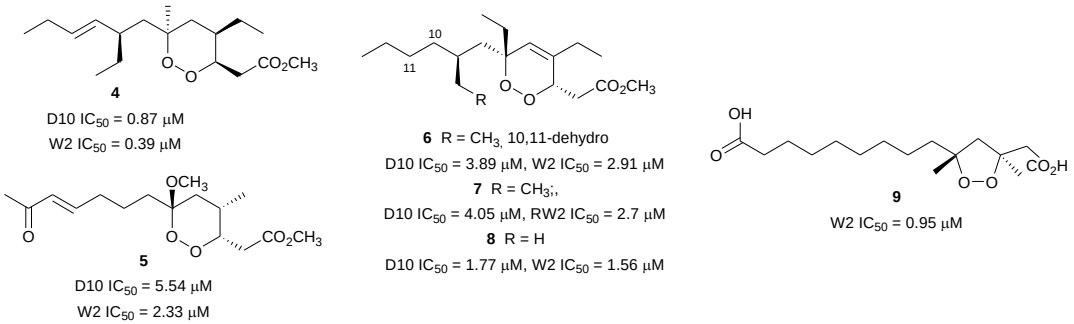

Fig. 3 Structures of polyketide-derived endoperoxides

The norditerpenoid cycloperoxides, diacarperoxides A (**10**), J (**11**), diacarnuperoxide N (**12**), and 2,3,6-epihurghaperoxide (**13**) (Fig. 4) were isolated from the South China Sea sponge *Diacarnus megaspinorhabdosa* and inhibited both the W2 and D6 *P. falciparum* strains. In contrast to the polyketide-derived counterparts, the SAR of the norditerpene endoperoxides has not been studied in detail. It was suggested that variations in the configuration at C-2, C-3, and C-6, or the cyclohexane ring and the side chains do not significantly affect activity [27, 28]. However, more detailed SAR studies need to be conducted to gain a better understanding of the activity.

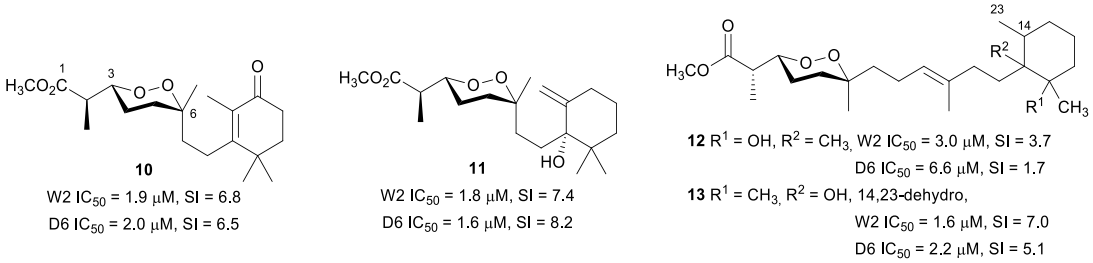

Fig. 4 Structures of norditerpene endoperoxides

Alkaloids

Among the 447 isolated natural products with IC_{50} ≤ 3.0 μM reported in this review, 31.9% are alkaloids.

Naphthylisoquinolines

The naphthylisoquinolines are a unique class of polyketide-derived biaryls of natural origin. These compounds are found exclusively in the Ancistrocladaceae from Central Africa and Southeast Asia,

and Dioncophyllaceae endemic to the coast of West Africa. The compounds are composed of naphthalene and isoquinoline moieties and are biosynthetically derived from the acetate-polymalonate pathway [29, 30]. The naphthalene and isoquinoline regions are coupled through a rotationally restricted C-C or C-N axes. This rotational hindrance gives rise to axial chirality, while the isoquinoline unit can have up to three stereocentres. Twelve of the monomeric naphthylisoquinolines (**14**-**25**) (Fig. 5) are discussed in this review. Dimeric naphthylisoquinolines have been described from species of the *Ancistrocladus* genus, and these dimers join four aryl units through three biaryl axes and thereby potentially doubling the number of stereocentres [31]. Seventeen of the dimeric naphthylisoquinolines (**26**-**42**) (Fig. 6) are mentioned in this report. The Ancistrocladaceae mostly produce C-6 oxygenated alkaloids with an *S*-configuration at C-3, and these are called the Ancistrocladaceae-type, while the alkaloids of Dioncophyllaceae exclusively have an *R*-configuration at C-3 and lack oxygenation at C-6, and are called the Dioncophyllaceae-type [30]. Several of these compounds displayed nanomolar selective inhibition of the *Plasmodium* parasite viability.

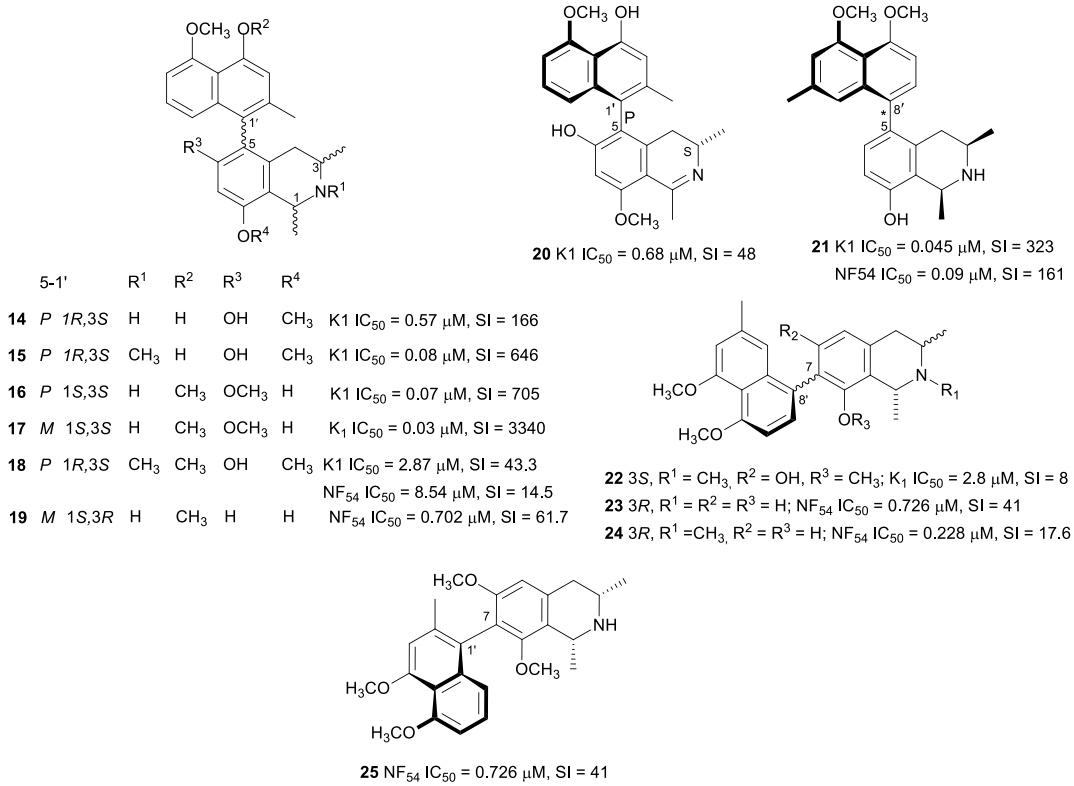

	5-1'		R^1	R^2	R^3	R^4	
14	*P*	*1R,3S*	H	H	OH	CH_3	K1 IC_{50} = 0.57 μM, SI = 166
15	*P*	*1R,3S*	CH_3	H	OH	CH_3	K1 IC_{50} = 0.08 μM, SI = 646
16	*P*	*1S,3S*	H	CH_3	OCH_3	H	K1 IC_{50} = 0.07 μM, SI = 705
17	*M*	*1S,3S*	H	CH_3	OCH_3	H	K_1 IC_{50} = 0.03 μM, SI = 3340
18	*P*	*1R,3S*	CH_3	CH_3	OH	CH_3	K1 IC_{50} = 2.87 μM, SI = 43.3 NF_{54} IC_{50} = 8.54 μM, SI = 14.5
19	*M*	*1S,3R*	H	CH_3	H	H	NF_{54} IC_{50} = 0.702 μM, SI = 61.7

Fig. 5 Structures of monomeric naphthylisoquinolines

Ancistectorines A_1 (**14**), *N*-methyl A_1 (**15**), A_2 (**16**), 5-*epi*-A_2 (**17**), A_3 (**20**), and C_1 (**22**) were isolated from the twigs of Chinese *Ancistrocladus tectorius* [32]. The six alkaloids potently inhibited the K1 strain of *P. falciparum* without cytotoxicity against rat skeletal myoblast (L6) cells. The 5,1'-coupled compounds **15**, **16**, and **17** were 3-7 times more active than chloroquine with **17** having an SI > 3000 [32]. The known *N*-methylated 5,1'-coupled ancistrocline (**18**) from the same plant also showed encouraging antiplasmodial activity against the K1 and NF54 strains. In addition to low cytotoxicity against L6 cells, compound **18** was 2-3 times more active against chloroquine-resistant K1 than the chloroquine-sensitive NF54 strain [33]. However, the additional methoxy group on the naphthalene unit of **18** led to >30 fold decrease in activity compared to **15**. The new dioncophyllines C_2 (**19**) and F (**21**), and the known ancistrocladisine A (**25**) and 5'-*O*-methyldioncophylline D (**23**) were isolated from the root bark of Congolese *Ancistrocladus ileboensis* [30]. The total synthesis of **21**, which was the first reported

natural 5,8'-coupled dioncophyllaceous alkaloid, was achieved by palladium-catalyzed Suzuki-Miyaura cross-coupling of the two aryl moieties. Furthermore, the leaves of *Ancistrocladus ileboensis* yielded the 7,8'-coupled dioncophylline D_2 (**24**), which was also previously unreported. Compounds **19**, **21**, **23**, **24**, and **25** were found to be active against the NF54 strain, with **21** displaying double the activity against the K1 over the NF54 strain. Furthermore, the new compounds were non-toxic to L6 cells with SI values ranging from 61 – 586 [30]. It is worthy to note that axial chirality influences the antiplasmodial activity of the naphthylisoquinolines when they exist as atropo-diastereomers. The *M*-configured analogues such as **17** generally showed superior selective antiplasmodial activity compared to the *P*-configured counterparts such as **16**.

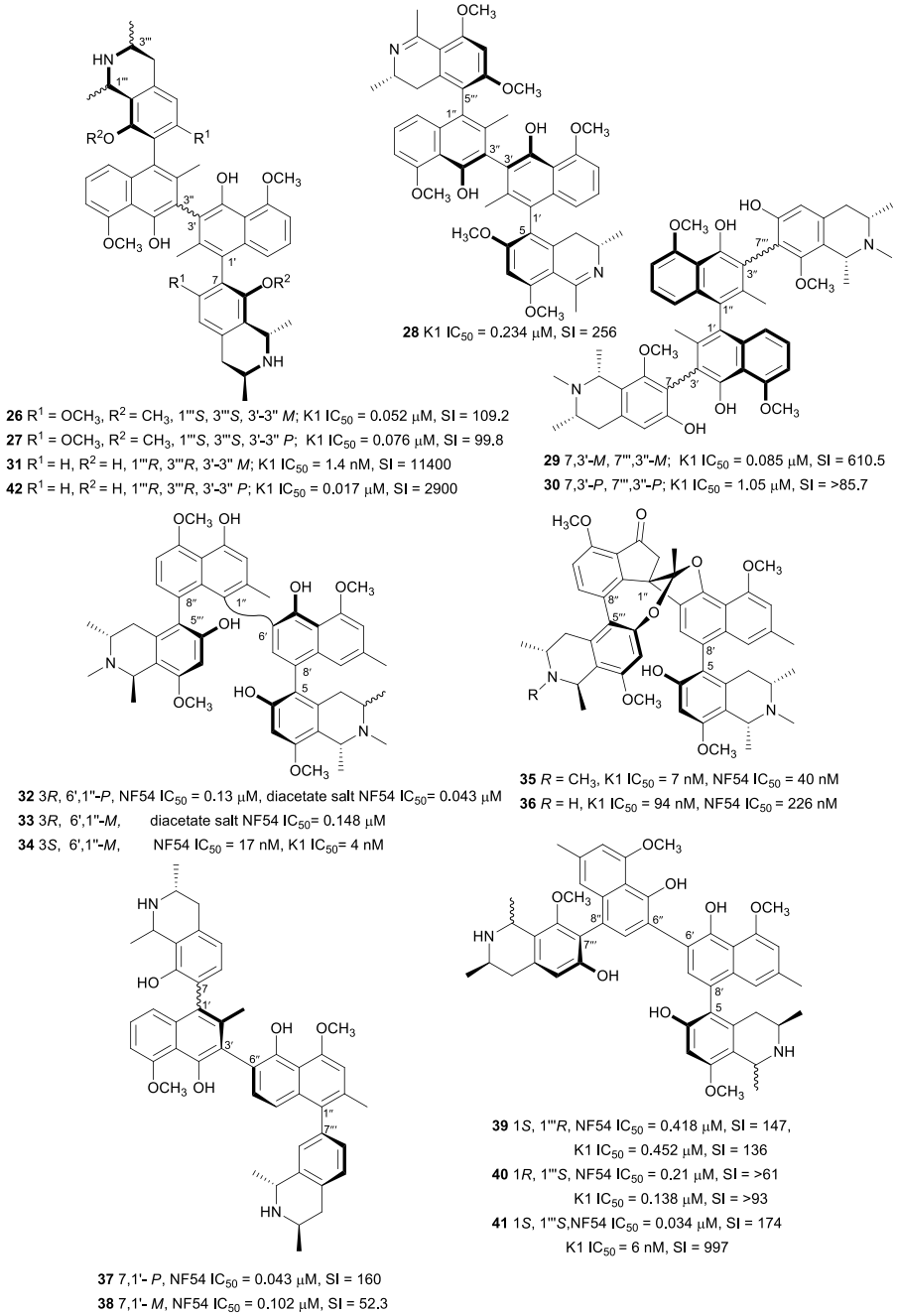

Fig. 6 Structures of dimeric naphthylisoquinolines

Dimerization of the naphthylisoquinoline core resulted in the rotationally-hindered 1,1'- or 3,3'-linked shuangancistrotectorines A-E (**26-30**) from the twigs of the Chinese *Ancistrocladus tectorius*. This was

the first report of a natural product featuring three consecutive stereo axes, which in addition to the tetrahydroquinoline stereocentres, confers up to seven stereogenic units [34]. Biological assessment of these compounds revealed sub-micromolar antiplasmodial activity against the K1 strain coupled to low toxicity against L6 cells (SI = 99.8-610.6), with compounds **26**, **27** and **30**, in particular, displaying antiplasmodial activity superior to that of chloroquine [34]. Similarly, jozimine A_2 (**31**), the first reported dioncophyllaceae-type sterically-hindered 3,3'-coupled dimeric naphthylisoquinoline isolated from a Congolese *Ancistrocladus* sp., displayed sub-nanomolar inhibitory activity, superior to that of chloroquine against the NF54 strain coupled to low cytotoxicity against L6 cells (SI >11400) [35]. Mbandakamines A (**32**) and B (**33**), the first dimeric naphthylisoquinolines featuring the unsymmetrical 6',1''-coupling of the naphthalene units were isolated from the leaf of another uncharacterized Congolese *Ancistrocladus* sp. The diacetate salts of these highly sterically-hindered compounds were more active against the NF54 strain than the free bases, possibly due to increased solubility [36]. Another unidentified Congolese *Ancistrocladus* sp. yielded the unsymmetrically 6',1''-coupled mbandakamine B_2 (**34**), together with two other unique dimers named spirombandakamines A_1 (**35**) and A_2 (**36**). Compounds **35** and **36**, which incorporate both a five-membered ketone ring alongside seven- and five-membered oxygenated heterocyclic rings into the dimeric structure, exhibited nanomolar antiplasmodial activity against both the K1 and NF54 parasite strains. The open-chain **34** was proposed as the biosynthetic precursor to the spiro-fused **35**, but the higher antiplasmodial activity of **34** as compared to **35** and **36** implies that cyclization is not beneficial to activity [37]. Jozilebomines A (**37**) and B (**38**), two unsymmetrical 3,6''-coupled dimers isolated from the root extract of the Congolese *Ancistrocladus ileboensis*, exhibited selective antiplasmodial activity against NF54 *P. falciparum* strain, with weak toxicity towards L6 cells (SI = 160 and 52.3, respectively). However, this activity was lower than the related symmetrically coupled jozimine A_2 (**31**) [38]. Three structurally unique heterodimeric naphthylisoquinolines, ealapasamines A-C (**39-41**), were isolated from the leaf of *Ancistrocladus ealensis*. The ealapasamines are the first reported unsymmetrical dimers in which the constituent monomeric naphthylisoquinoline units are linked at different positions, i.e. one 5,8'-coupled monomer links to another 7,8'-coupled unit at the 6' position of the respective naphthanyl subunits. This subsequently results in three different biaryl linkages, with the inter-naphthanyl biaryl axis being configurationally unstable. Compounds **39-41** were active against *P. falciparum* (K1 and NF54) with low nanomolar IC_{50} values and low toxicity to L6 cells [39].

The bioactivity of the dimeric naphthylisoquinolines, as with the monomers, is influenced by axial chirality as, for example, seen in the superior activity of jozimine A_2 over the atropo-diastereomer, 3'-*epi*-jozimine A2 (**42**) [29, 35]. So far, jozimine A_2 demonstrated the best antiplasmodial activity (IC_{50} = 1.4 nM) against the chloroquine-sensitive NF54 strain, while mbandakamine B_2 is the most active dimer against the chloroquine-resistant K1 strain (IC_{50} = 4.0 nM). With potent *in vitro* activities and high selectivity for the parasites over mammalian cell lines, the dimeric naphthylisoquinolines can be considered as viable anti-malarial hits. It will be worthwhile to study the mechanism of action as well as *in vitro* and *in vivo* potency against a comprehensive panel of drug-sensitive and -resistant parasites. Equally important for an anti-malarial drug is the need for oral bioavailability and hence pharmacokinetic studies are highly desirable. The synthesis of some dimeric naphthylisoquinolines has been reported, and since only small amounts of these potent compounds are present in plant material, the syntheses of these compounds will be essential for further developments [40].

Benzylisoquinolines and other isoquinolines

Three new tricyclic isoquinoline alkaloids (Fig. 7) were isolated from the leaf extract of *Cassia siamea* (Fabaceae), a plant traditionally used to treat periodic fever and malaria in Indonesia. Among the isolated compounds, cassiarin J (**43**) and the first halogenated cassiarin congener, cassiarin K (**44**), inhibited the *in vitro* growth of 3D7 *P. falciparum* [41]. However, both compounds **43** and **44** were less active than chemically simpler and the potent cassiarin A (**45**), suggesting that the role of the pyran ring of the cassiarins in antiplasmodial activity should be further explored in structure-activity relationship (SAR) investigations [42].

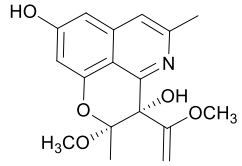

43 3D7 IC_{50} = 0.3 μM

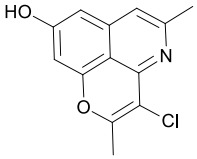

44 3D7 IC_{50} = 1.4 μM

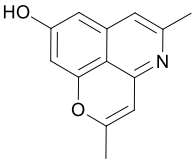

45 IC_{50} = 0.023 μM, SI = 7000

Fig. 7 Structures of cassiarins

The L-tyrosine-derived benzylisoquinoline alkaloids form a structurally diverse group of plant-derived compounds, many of which are associated with potent biological activities, and antiplasmodial activity is no exception. During the review period, the activity of one morphinanedienone alkaloid (**46**) (Fig. 8), six aporphines (**47-52**), six berberine-type compounds (**53-58**) and seven bisbenzyltetrahydroisoquinoline alkaloids (**59-65**) (Fig. 9) were reported. The morphinanedienone alkaloid, (-)-milonine (**46**) from the bark of *Dehaasia longipedicellata* (Lauraceae), exhibited sub-micromolar selective antiplasmodial activity against K1 parasites [43]. Carraz *et al.* reported that a derivative of a related morphinan, tazopsine, is active against the liver stages of the parasite and that this class of compounds may have potential as anti-malarial leads [44].

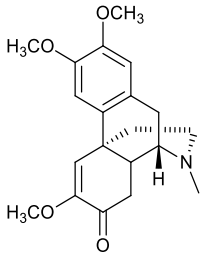

46

K1 IC_{50} = 0.097 μM, SI = >2062

Fig. 8 Structure of (-)-milonine

Following the screening of crude extracts of Malaysian medicinal plants, the extract of *Dehaasia longipedicellata* was identified as a promising antiplasmodial starting point. Chemical investigation of the bark extract afforded boldine (**47**) and (-)-*O*,*O*-dimethylgrisabine (**59**) as the most active constituents, both of which were active against the K1 strain of *P. falciparum,* with **59**, in particular, outperforming chloroquine in this assay. The compounds were not cytotoxic to a pancreatic cancer cell line (hTERT-HPNE) at 200 μM, indicating selective toxicity to the parasite [43]. Based on the antiplasmodial screening of 794 plant extracts from Papua New Guinea and Australia, four species were selected for further investigation, one of which was *Stephania zippeliana* (Menispemaceae) [45]. *Stephania zippeliana* yielded xylopine (**48**), which selectively inhibited the 3D7, FCR3, HB3, and K1, in addition to the D6 and W2 *P. falciparum* strains [46, 47]. Bioassay-guided fractionation of *Stephania*

venosa tubers yielded the aporphine alkaloids, stephanine (**49**), crebanine (**50**) and *O*-methylbulbocapnine (**51**) as antiplasmodial principles. Unfortunately, the most active alkaloid against 3D7 and W2 parasites, stephanine (**49**), was also the most cytotoxic to cancerous and non-cancerous cell lines [48]. Chemical interrogation of the root of *Thalictrum flavum* (Ranunculaceae) yielded the aporphine alkaloid, preocoteine (**52**), the protoberberines, pseudoberberin (**54**) and berberin (**55**), and the bisbenzylisoquinoline thaligosidine (**60**). The compounds exhibited antiplasmodial activity against the FcB1 strain. However, the activity of the quaternary protoberberines was not selective towards the parasite [49]. The tetrahydroprotoberberine alkaloid cheilanthifoline (**53**), isolated from *Corydalis calliantha* (Papaveraceae), an annual herb used in Bhutanese traditional medicine to treat malaria, also displayed activity against the TM4 strain of *P. falciparum* [50]. The aerial part of *Meconopsis simplicifolia* (Papaveraceae) is an ingredient in more than eight Bhutanese traditional medicine formulations and has displayed potent antiplasmodial activity against TM4/8.2 and K1CB1 strains of *P. falciparum* (IC_{50} = 0.4 and 6.39 µg/mL, respectively) [51]. Extraction and purification of the aerial components of *Meconopsis simplicifolia* yielded the protoberberine-type benzylisoquioline, simplicifolianine (**56**), which showed potent antiplasmodial activity against the TM4/8.2 and K1CB1 strains in the absence of significant cytotoxicity to Vero and human oral carcinoma (KB) cells [52].

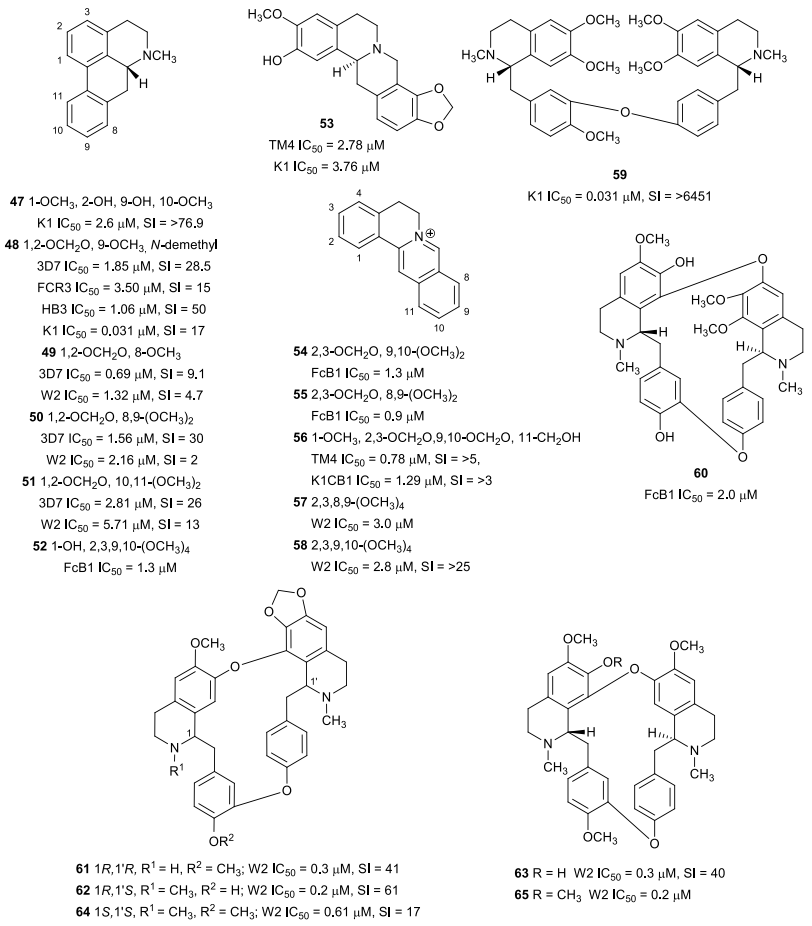

Fig. 9 Structures of benzylisoquinoline alkaloids

Three bisbenzylisoquinoline alkaloids, 2-norcepharanthine (**61**), cepharanoline (**62**), and fangchinoline (**63**), which were isolated from *Stephania rotunda* tuber as minor constituents, all showed potent antiplasmodial activity against the W2 strain with SI ≥ 40 [53]. Encouragingly, these compounds were twice as active as the major alkaloid of *Stephania rotunda*, cepharanthine (**64**), which was previously

reported to inhibit parasites *in vitro* and *in vivo* [54]. Further investigation found that the *Stephania rotunda* alkaloid **64** and the protoberberine-type benzylisoquinolines palmatine (**57**) and pseudopalmatine (**58**) also inhibited the *in vitro* viability of *P. falciparum* W2. However, while **64** was found to be cytotoxic against K562S cells, this was not the case for **58** at the highest tested concentration (IC_{50} > 25 µM). These findings supported the use of *Stephania rotunda* in malaria treatment by traditional healers in Cambodia [55]. Desgrouas *et al.* concluded that cepharanthine (**64**) affected the ring stage of the parasite [56, 57]. Furthermore, in *in vitro* studies, **64** had a synergistic antiplasmodial effect with the anti-malarial drugs chloroquine, atovaquone, and piperaquine, but had an antagonistic effect with dihydroartemisinin and mefloquine [56, 57]. In *in vivo* experiments, combinations of **64** and chloroquine, and **64** and amodiaquine were assayed in mice. Both combinations delayed parasitic growth and extended the life expectancies of the mice compared to the drugs alone [57]. Fangchinoline (**63**) and the methyl ether tetrandrin (**65**), both produced by *Stephania tetrandra*, are not only cytotoxic against cancer cell lines, but also reverse resistance of multidrug-resistant human cancer cells by inhibiting P-glycoprotein activity, thereby increasing drug concentration in the cells [58]. The resistance-reversal effect was also observed with *Plasmodium*; Ye and Van Dyke reported that **65** in combination with chloroquine resulted in a 44 fold potentiation of parasite killings [59]. These authors also reported on the structure-activity relationship of bisbenzylisoquinoline [59]. For activity, the configuration of C-1' of the 'right-hand' ring should be *S*. The configuration of C-1 of the 'left-hand' ring has little influence on the antiplasmodial activity. Furthermore, the position of the bridges connecting the two monomeric benzylisoquinolines also plays a role and compounds with ether bridges between C-8 to C-7', and between 11 and 12' (head-head and tail-tail dimer) have the highest antiplasmodial activity.

Phenanthrene derivatives: phenanthridine, phenanthroindolizidine and phenanthrene alkaloids

The dichloromethane bark extract of *Cryptocarya nigra* (Lauraceae) afforded the phenanthrene alkaloid 2-hydroxyatherosperminine (**66**) (Fig. 10), which was found to be active against the *P. falciparum* K1 strain. The significantly improved activity of **66** over the C-2 deoxy analogue atherosperminine indicates a possible important region of the pharmacophore [60].

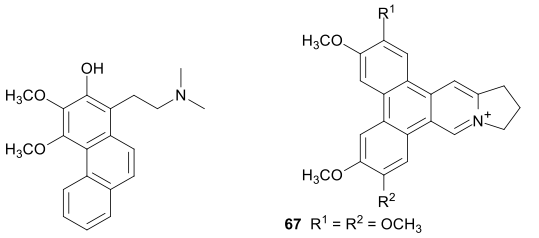

66
K1 IC_{50} = 0.75 µM

67 $R^1 = R^2 = OCH_3$
3D7 IC_{50} = 0.42 µM, SI = 20
68 $R^1 = OCH_3$, $R^2 = H$
3D7 IC_{50} = 0.028 µM, SI = >1964
69 $R^1 = H$, $R^2 = OCH_3$
3D7 IC_{50} = 0.058 µM, SI = >966

Fig. 10 Structures of phenanthrene alkaloids

The methanol extract of *Ficus septica* (Moraceae) twigs exhibited *in vitro* antiplasmodial activity against the 3D7 strain (IC_{50} = 2.0 µg/mL). Bioassay-guided fractionation of the chloroform fraction of the active methanol extract led to the isolation of the known compounds, dehydrotylophorine (**67**), dehydroantofine (**68**) and tylophoridicine (**69**) (Fig. 10). The three phenanthroindolizidine alkaloids inhibited the 3D7 strain with sub-micromolar IC_{50} and had low cytotoxicity. The selective

antiplasmodial activity of these alkaloids indicates that other alkaloids of this class should be further explored [61].

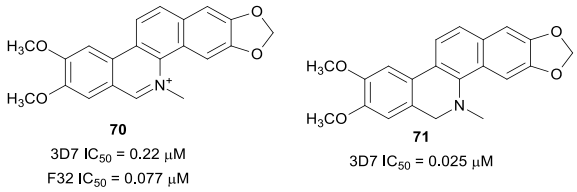

Fig. 11 Structures of nitidine (**70**) and dihydronitidine (**71**)

The benzophenanthridine alkaloid nitidine (**70**) (Fig. 11) was isolated as the main antiplasmodial compound from *Zanthoxylum chalybeum* (Rutaceae) and *Zanthoxylum rhoifolium* [62, 63]. Compound **70** displayed rapid activity against chloroquine-sensitive and -resistant parasites with little evidence of cross-resistance, consistent with previous reports [64]. Treatment of *Plasmodium berghei*-infected mice with **70** gave an ED_{50} value of 18.9 mg/kg/day without mice mortality. Nitidine (**70**) did not interfere with parasite DNA replication and was found to localize in the parasite cytoplasm. The mechanism of action of **70** might be similar to that of chloroquine since it formed a complex with heme and inhibited the formation of β-haematin *in vitro* [62]. In contrast to the rapid activity of **70**, dihydronitidine (**71**), isolated from *Zanthoxylum heitzii* bark, displayed a slow-acting drug effect against 3D7 parasites. This slow-acting effect, coupled with the fact that **71** will not carry a charge at the digestive vacuole pH, which is purportedly necessary for drug accumulation, suggests that the compounds might act via a different mechanism of action [65]. The poor water solubility of **71** might also limit its viability as an anti-malarial lead.

Terpenylindoles

The monoterpenoid indole alkaloid uleine (**72**) (Fig. 12) was isolated as the major antiplasmodial alkaloid from the trunk bark of the Brasilian tree *Aspidosperma parvifolium* (Apocynaceae) and was more active against the W2 than the 3D7 strain, with low cytotoxicity against the Hep G2A16 and Vero cell lines [66]. Compound **72** was found to localize in the parasite digestive vacuole as a result of the presence of a basic aliphatic amino group, which undergoes protonation in the acidic digestive vacuole and accumulates in suitable concentrations to inhibit heme polymerization [67]. Uleine has also been isolated from *Aspidosperma olivaceum* [68]. Traditionally, the Nkundo people in the DR Congo use various parts of *Greenwayodendron suaveolens* (Annonaceae) to treat malaria. Some species of monkeys chew the bitter leaves, presumably for zoopharmacognostic purposes [69]. Two sesquiterpenyl indole alkaloids, *N*-acetylpolyveoline (**73**) and polyalthenol (**74**) (Fig. 12), isolated from the root bark of *Greenwayodendron suaveolens*, are active against the K1 strain. While polyathenol was found to be cytotoxic against MRC-5 cells, **73** was more selective (SI = 10.6) [69].

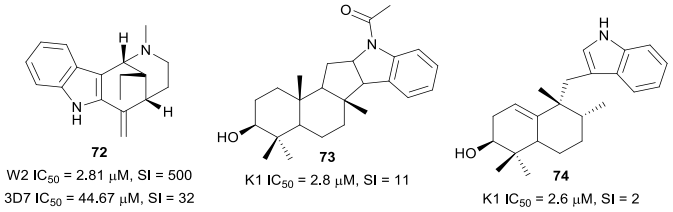

Fig. 12 Structures of terpenyl alkaloids

Bisindoles and related indoles

Flinderole A (**75**) and isoborreverine (**78**) were isolated from the bark of the Australian tree *Flindersia acuminata* (Rutaceae) and flinderoles B (**76**) and C (**77**), and dimethylisoborreverine (**79**) from *Flindersia amboinensis* from Papua New Guinea [56]. These indole alkaloids (Fig. 13) exhibited selective antiplasmodial activity against a wide panel of drug-sensitive and -resistant parasites. In a further investigation to ascertain which stage of the development cycle of the parasite is affected by the most active compound **79**, it was observed that **79** was more active against *P. falciparum* trophozoites, with treated parasites showing changes in digestive vacuole morphology and a reduced formation of haemozoin [46, 70]. A different *Flindersia* species, *Flindersia pimenteliana*, was the source of the new pimentelamine C (**80**), the known borreverine (**81**) and 4-methylborreverine (**82**), which were reported to be active against *P. falciparum* 3D7 and Dd2 with low toxicity to HEK-293 cells [71]. Compound **80**, which was isolated as the trifluoroacetate salt from the plant leaves, is one of three new indole alkaloids incorporating an ascorbic acid moiety. Interestingly, the other two analogues without a polar *N*-oxide moiety on the ethylamine unit attached to the indole skeleton were inactive [71]. This suggests a SAR role for the ethylamine unit that could be further explored.

Two bisindole alkaloids with a vobasinyl-iboga skeleton tabernaelegantine B (**83**) and D (**84**) (Fig. 14), isolated from *Muntafara sessilifolia* (Apocynaceae) stem bark, inhibited the FcB1 plasmodial strain but these compounds were also cytotoxic against L6 and MRC-5 cells [72]. However, the C-3' oxidized analogues **85** and **86**, in particular, showed better selectivity towards the parasite suggesting the position of the linkage between the monomeric units might influence the bioactivities of these compounds [72]. This observation is supported by the nanomolar antiplasmodial activity of another vobasinyl-iboga alkaloid, voacamine, which also has a C-3/ C-11' linkage [73]. A reinvestigation of *Geissospermum laeve* (Apocynaceae) using a dereplication strategy led to the isolation of new bisindole alkaloids, 3',4',5',6'-tetradehydrogeissospermine (**87**) and geissolosimine (**88**), from the bark of the tree [74].Compound **88** has also been isolated from the bark of *Geissospermum vellosii* [75]. The compounds exhibited non-selective antiplasmodial activity against FcB1 parasites [74]. Moreover, **88** was also active against the D10 strain with low toxicity to Chinese hamster ovarian cells [75].

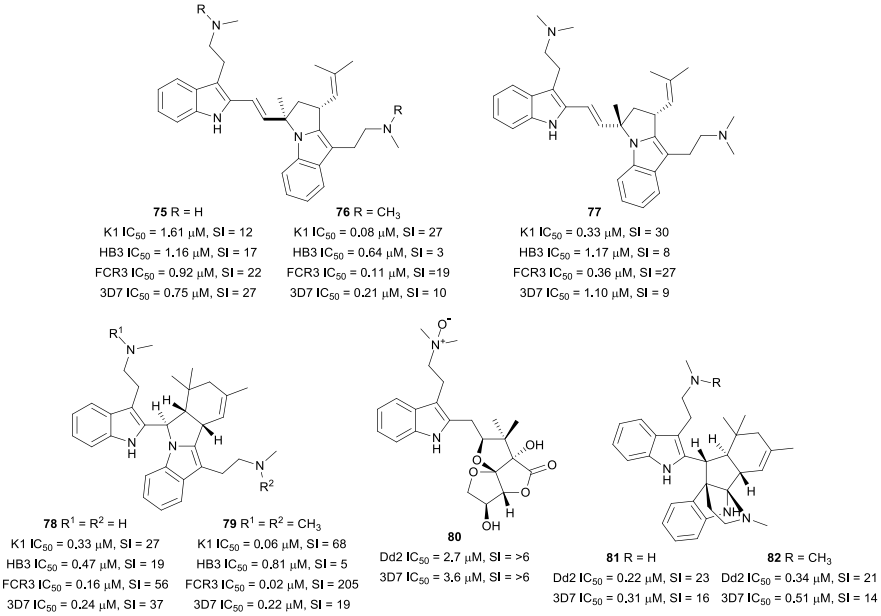

Fig. 13 Structures of bisindole alkaloids **75**-**82**

Divarine (**89**), longicaudatine (**90**), longicaudatine F (**91**) and longicaudatine Y (**92**) from the stem bark of *Strychnos malacoclados* (Loganiaceae) inhibited the growth of the 3D7 and W2 parasite strains. A cytotoxicity assay on WI-38 human fibroblasts with the most active **90** showed that the antiplasmodial activity is not specific. However, the structurally similar longicaudatine F (**91**), possessing an open ring in place of the six-membered oxygen heterocycle in **90**, was 40 times more selective against the parasite, despite the slightly lower antiplasmodial activity [76]. A phytochemical investigation of *Strychnos icaja* root provided a new bisindole, strychnobaillonine (**93**), and the known strychnohexamine (**94**) (Fig. 14). The alkaloids were active against the 3D7 strain of *P. falciparum*, and the trisindole **94** was also cytotoxic against WI-38 cells (SI <10), whereas **93** was not cytotoxic at the highest tested concentration (10 µg/mL) [77]. Interestingly, while monomers of *Strychnos* alkaloids do not have antiplasmodial activity, polymerization increases the basic nature of the monomers and confers antiplasmodial potency. This suggests that some degree of basicity is essential for antiparasitic activity of the *Strychnos* alkaloids and that compounds might localize in the parasite acidic digestive vacuole [78].

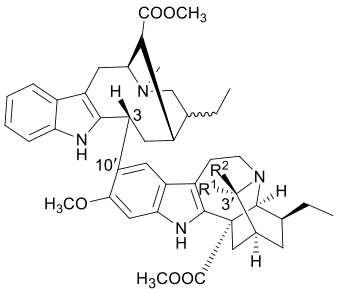

83 $R^1 = R^2$ = H, β-ethyl
FcB1 IC_{50} = 2.7 µM, SI = 1.0
84 $R^1 = R^2$ = H, α-ethyl
FcB1 IC_{50} = 1.2 µM, SI = 0.4
85 $R^1 = R^2$ = O, β-ethyl
FcB1 IC_{50} = 10.4 µM, SI = 4.0

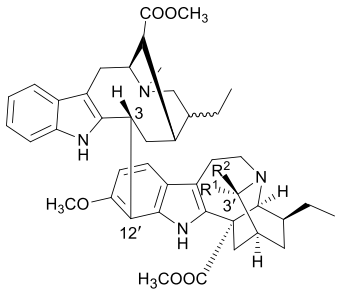

86 $R^1 = R^2$ = O, β-ethyl
FcB1 IC_{50} = 4.4 µM, SI = >31

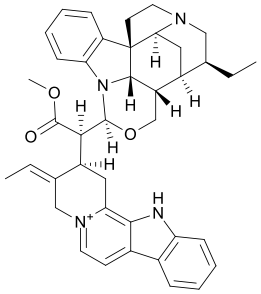

87
FcB1 IC_{50} = 2.9 µM, SI = 1.0

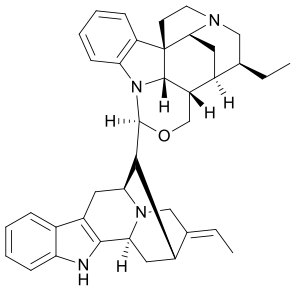

88
FcB1 IC_{50} = 1.9 µM
D10 IC_{50} = 0.96 µM, SI = 18

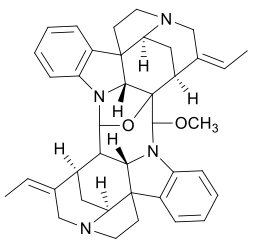

89
3D7 IC_{50} = 1.38 µM
W2 IC_{50} = 0.50 µM

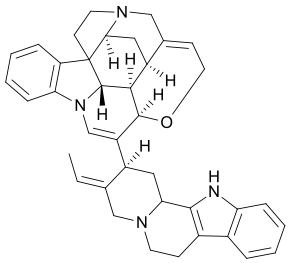

90
3D7 IC_{50} = 0.68 µM, SI = 4
W2 IC_{50} = 0.57 µM,SI = 5

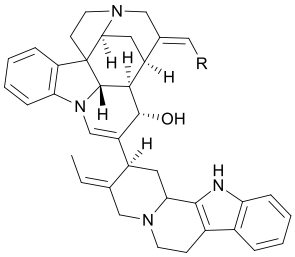

91 R = OH
3D7 IC_{50} = 1.19 µM, SI = 41
W2 IC_{50} = 1.05 µM,SI = 46

92 R = H
3D7 IC_{50} = 1.51 µM
W2 IC_{50} = 0.73 µM

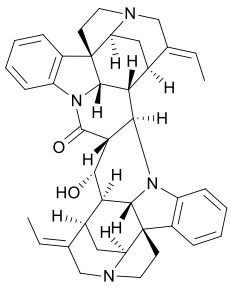

93
3D7 IC_{50} = 1.1 µM, SI = >14

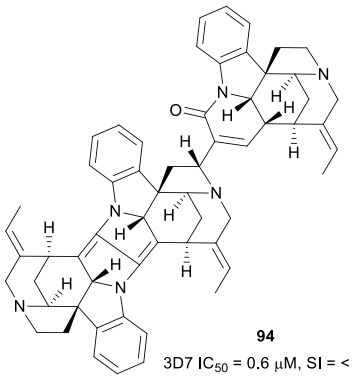

94
3D7 IC_{50} = 0.6 µM, SI = <10

Fig. 14 Structures of bisindole alkaloids **83**-**94**

It was previously reported that ellipticine (**95**) (Fig. 15), isolated from *Aspidosperma vargasii* (Apocynaceae) bark, has *in vitro* and *in vivo* anti-malarial activity [79]. In search of more active analogues, semi-synthetic derivatives of **95** were prepared. 9-Nitroellipticine (**96**), in which ring A was modified, was more active than **95**, while the 7-nitro derivative was the least active [80]. The indole-quinazoline alkaloid tryptoquivaline (**97**), obtained from the culture broth of *Neosartorya spinosa* KKU-1NK1 (sexual state of *Aspergillus* fungus species), was active against K1 parasites. The compound was slightly cytotoxic to Vero cells (SI = 25) but was inactive against a panel of cancer cell lines [81].

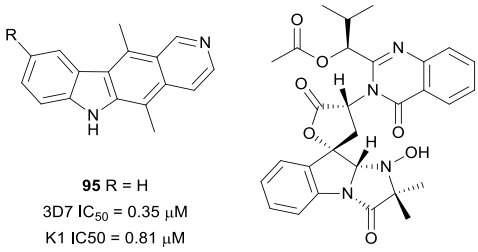

Fig. 15 Structures of indole derivatives **95**-**97**

β-Carbolines

The β-carboline-indole alkaloid hyrtiosulawesine (**98**) (Fig. 16), isolated from the root of *Aristolochia cordigera* (Aristolochiaceae), inhibited the *in vitro* viability of *P. falciparum* (3D7) without any toxicity to Hep G2 cells. Similar inhibition of the FcB1 strain was observed with synthetic **98** [82]. However, the glucoside derivative of **98** was only half as active as **98** [83]. Marinacarboline A (**99**) isolated from *Marinactinospora thermotolerans* SCSIO 00652*,* an actinomycetes species from South China Sea marine sediments, was 18 times more active against the multi-drug resistant Dd2 strain than against the chloroquine-sensitive 3D7. The compound was not significantly cytotoxic to a panel of tumour cell lines (IC_{50} > 50 μM) [84]. The New Zealand ascidian *Pseudodistoma opacum* was the source of a new antiplasmodial alkylguanidine-substituted β-carboline alkaloid, opacalin A (**100**). The poor cytotoxicity of **100** against L6 cells indicates a selective antiparasitic activity against the K1 strain [85]. β-Carboline-1-propionic acid (**101**) was isolated from the root of *Eurycoma longifolia* (Simaroubaceae), a popular southeast Asian medicinal plant. It exhibited antiplasmodial activity against the 3D7 strain, but the cytotoxicity was not reported [86].

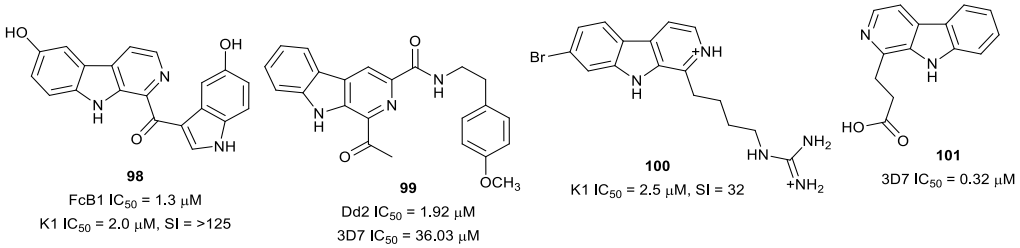

Fig. 16 Structures of β-carbolines

Piperidine, pyridone and pyrimidine alkaloids

The leaf decoction of *Carica papaya* (Caricaceae), which is traditionally used to treat malaria in Indonesian Papua and Maluku islands, displayed *in vitro* antiplasmodial activity (51% inhibition at 4.8 μg/mL) [87]. Purification of an alkaloid-enriched fraction of the plant leaves yielded the dimeric piperidine alkaloids **102**-**104** (Fig. 17) as the antiplasmodial principles, while the monomeric carpamic

acid and methyl carpamate were inactive. Carpine (**102**), with the best activity, was the major alkaloid but it was inactive *in vivo* (11.9% suppression of *P. berghei* parasite at 5 mg/kg). The *in vivo* activity of a hydroalcoholic extract of papaya leaves suggests that other metabolites in the extracts might potentiate the antiplasmodial activity of the active compounds [87]. The observed lack of *in vivo* efficacy of **102** highlights the complex relationship between metabolites in natural extracts and emphasizes the need to validate *in vitro* potencies in animal models. Nevertheless, potent and selective activity of compounds can be exploited by medicinal chemistry methods in designing improved analogues. Cassine (**105**) and spectaline (**106**) from *Senna spectabilis* leaf were active against 3D7 *P. falciparum in vitro*. However, the 3-*O*-acetyl semi-synthetic derivatives were less active than the natural piperidine parents [88]. Ingamine A (**107**), together with two new ingamine-type piperidine alkaloids, (22*S*)-hydroxyingamine A (**108**) and dihydroingenamine D (**109**), were isolated from the marine sponge *Petrosid Ng5 Sp5*. Compounds **107-109** showed sub-micromolar antiplasmodial activity against D6 and W2 parasites without cytotoxicity against cancerous and noncancerous cells at 10 µg/mL [89]. An antiplasmodial high-throughput screen of the ethanolic extract of marine sponges from the Solomon Islands identified the active *Heliclona* sp. with an *in vitro* activity of <1 µg/mL. Bioassay-guided fractionation of the extract from this sponge led to the isolation of haliclonacyclamine A (**110**). The bis-piperidine **110** was more active against chloroquine-resistant FcB1 than chloroquine-sensitive 3D7 parasites, with low cytotoxicity against MCF7 cancer cells. It suppressed parasitaemia in *Plasmodium vinckei petteri*-infected mice by 45% after four days of treatment with 10 mg/kg/day [90]. Most of the antiplasmodial piperidine alkaloids mentioned here are cyclic dimers. The potent, selective activity of these compounds makes them attractive as lead templates in anti-malarial drug design.

The new pyridone alkaloid **111** (Fig. 17), with a 1,4-dihydroxy-5-phenyl-2-pyridinone skeleton, was isolated from the Ascomycetes fungus, *Septoria pistaciarum.* Compound **111** was active against *P. falciparum* D6 and W2 strains, but it was also cytotoxic against Vero cells. Three other analogues without a free *N*-hydroxy group on the pyridone heterocycle were inactive, suggesting a SAR role for substituents on the ring nitrogen [91].

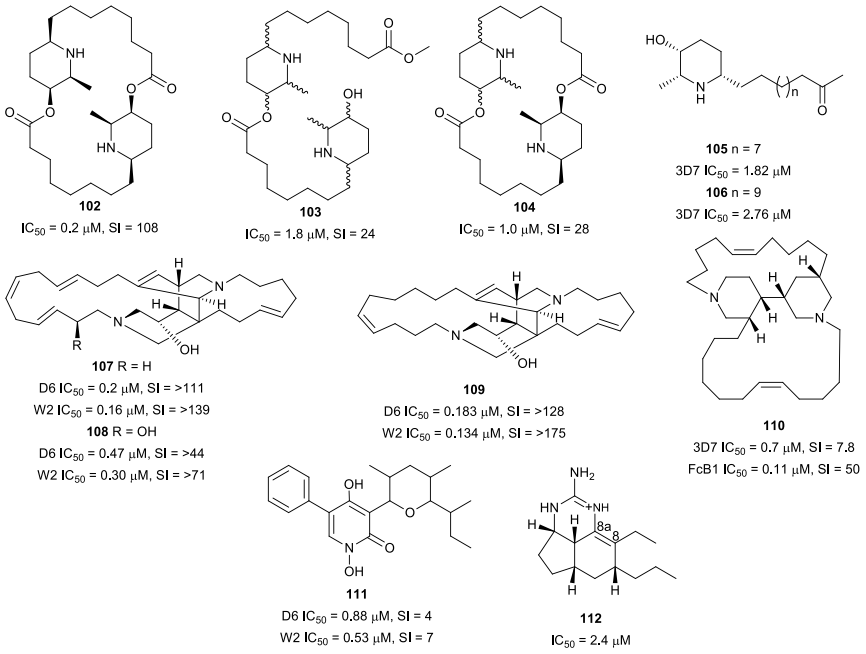

Fig. 17 Structures of piperidines **102-110**, pyridone **111**, and pyrimidine alkaloid **112**

The extract of *Biemna laboutei*, a marine sponge collected at Salary Bay in Madagascar, showed antiplasmodial activity with IC_{50} of 3.2 µg/mL. Chemical investigation of the active extract yielded new tricyclic pyrimidine alkaloids named netamines. Among the isolated alkaloids, netamine K (**112**), with a $\Delta^{8,8a}$-double bond in the tricyclic skeleton, exhibited activity against *P. falciparum* without toxicity to KB cells at the highest tested concentration of 1 µM [92].

Pyrroles

A series of 14 structurally related bromopyrrole alkaloids (Fig. 18) derived from sponges of the *Agelas* and *Axinella* genera were assayed for antiplasmodial activity against the K1 strain. Dibromopalau'amine (**113**) had the highest activity against the parasite, although it was also cytotoxic against L6 cells. The slightly less potent spongiadicin B (**114**) and dispacamide B (**115**) were more selective against the parasite (SI = 32.7 and > 67.2, respectively). Preliminary SAR observations in this series indicated that the aminoimidazole ring and the level of oxidation are important for antiplasmodial activity. Analogues lacking the imidazole ring were inactive while those in which the ring is not oxidized were less active. Some bromopyrrole alkaloids inhibited *Plasmodium* type II fatty acid synthase (FAS II) enzyme (Table 1), suggesting that this might be part of the mechanism of action [93].

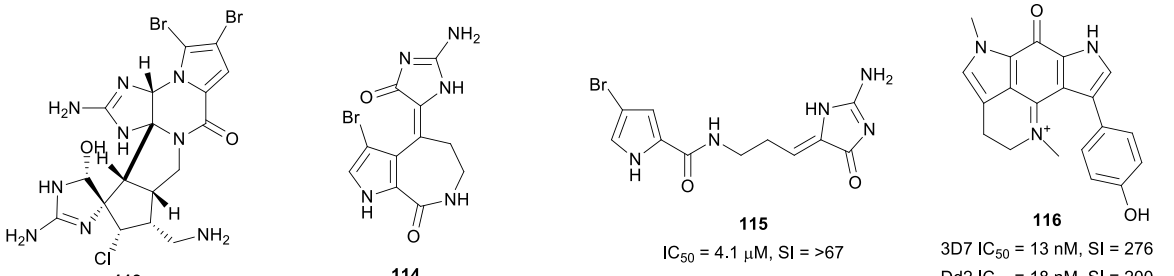

113
IC_{50} = 2.65 µM, SI = 3

114
IC_{50} = 3.36 µM, SI = 33

115
IC_{50} = 4.1 µM, SI = >67

116
3D7 IC_{50} = 13 nM, SI = 276
Dd2 IC_{50} = 18 nM, SI = 200

121
3D7 IC_{50} = 1.88 µM, SI = >63
Dd2 IC_{50} = 0.36 µM, SI = >333

122
D6 IC_{50} = 53 nM, SI = 130
W2 IC_{50} = 53 nM, SI = 130

123 R = O
D6 IC_{50} = 2.8 µM, SI = 1.0
W2 IC_{50} = 2.0 µM, SI = 1.4
124 R = H, OH
D6 IC_{50} = 170 nM, SI = 58
W2 IC_{50} = 130 nM, SI = 75

117 $\Delta^{7,8}$ R^1 = R^2 = CH_3 3D7 IC_{50} = 36 nM, SI = 51,
Dd2 IC_{50} = 39 nM, SI = 51
118 R^1 = H, R^2 = CH_3 3D7 IC_{50} = 25 nM, SI = 48,
Dd2 IC_{50} = 22 nM, SI = 54
119 R^1 = CH_3, R^2 = H 3D7 IC_{50} = 0.39 µM, SI = 3,
Dd2 IC_{50} = 0.30 µM, SI = 4
120 $\Delta^{7,8}$ R^1 = H, R^2 = CH_3 3D7 IC_{50} = 40 nM, SI = 35,
Dd2 IC_{50} = 21 nM, SI = 66

Fig. 18 Structures of pyrrole alkaloids

The new bispyrroloiminoquinone tsitsikammamine C (**116**), with nanomolar antiplasmodial activity against 3D7 and Dd2 *P. falciparum* strains, together with the equally active makaluvamines G (**117**), J-L (**118-120**), were isolated from the marine sponge *Zyzzya* sp. [94]. Compounds **116** and **118** were equally active against both parasite schizonts and trophozoites. Subcutaneous treatment of *P. berghei* infected mice with **117** at 8 mg/kg/day for four days suppressed parasitaemia by 48% with no apparent toxicity to mice. Damirone A (**121**), with a benzoquinone group in place of the iminoquinone moiety

of the makaluvamines, was less active, suggesting that the iminoquinone group is crucial for activity. Methylation of the iminium nitrogen led to an increase in activity [94]. Bioassay- and LC-MS-guided fractionation of an active extract from the Alaskan-sourced *Latrunculia* sp. sponge yielded discorhabdins A (**122**), and C (**123**), and dihydrodiscorhabdin C (**124**) [95]. The most potent pyrroloiminoquinones, **122** and **124**, with nanomolar antiplasmodial activity against D6 and W2 strains, were also the most selective (SI = 130 and 75, respectively). In an *in vivo* experiment, *P. berghei*-infected mice were treated with **122** and **124** at 10 mg/kg/day and although 50% suppression of parasitaemia was observed with **122** after 2 days of treatment, both compounds resulted in symptoms of severe toxicity [95].

Other alkaloids

Concoctions prepared from *Buxus* plant species are used for the treatment of malaria in various traditional medicine systems [96, 97]. An alkaloid-enriched fraction from the leaves of *Buxus sempervirens* (Buxaceae), which exhibited selective antiplasmodial activity (IC_{50} = 0.36 µg/mL, SI = 20.3), was subjected to bioassay-guided fractionation and yielded the cycloartane alkaloid, *O*-tigloylcyclovirobuxeine B (**125**) (Fig. 19), as the major antiplasmodial compound. The antiplasmodial activity of **125** against the NF54 strain was slightly less than that of the crude alkaloid fraction, but the compound was not significantly cytotoxic against L6 cells. Compound **125** was also detected in significant quantities in a leaf decoction of *Buxus sempervirens* that was prepared in accordance with ethnobotanical protocols [98]. Purification of the chloroform fraction of an extract from the combined twigs, leaves, and fruits of *Buxus cochinchinensis* yielded a number of bioactive triterpenoids, including the cycloartane alkaloid, *N*-benzoyldihydrocyclomicrophylline F (**126**). This compound inhibited both Dd2 *P. falciparum* and HT-29 human colon cancer cells, suggesting non-selective activity [99]. Two pregnane-type steroidal alkaloids, mokluangin A (**127**) and irehline (**128**), isolated from the root of *Holarrhena pubescens* (Apocynaceae), were active against K1 *P. falciparum* with low cytotoxicity against NCI-H187 lung cancer cells (IC_{50} = 30.6 and 27.7 µM, respectively) [100]. Two new cassane diterpene alkaloids, caesalminines A (**129**) and B (**130**) (Fig. 19), possessing a tetracyclic furanoditerpenoid skeleton were isolated from the seeds of *Caesalpinia minax* (Fabaceae). The compounds, which were proposed to be biosynthetically derived from the aminolysis of the geranylgeranyl pyrophosphate precursor, inhibited K1 *P. falciparum* [101].

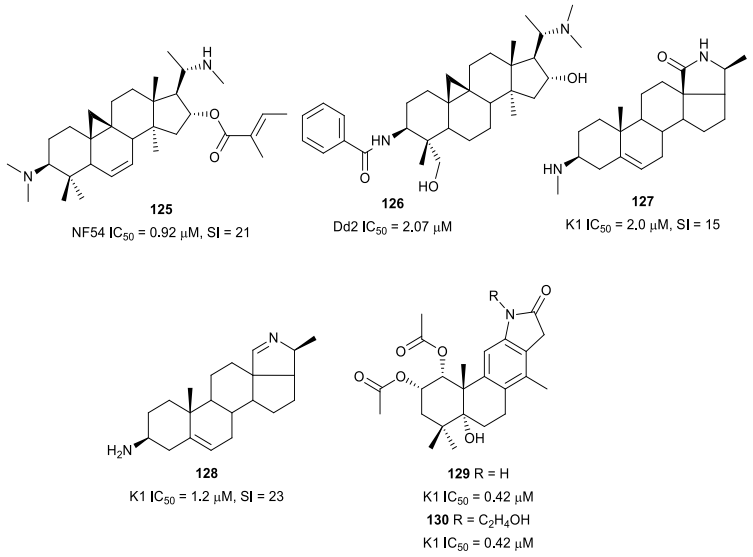

Fig. 19 Structures of steroidal alkaloids

A new Amaryllidaceae alkaloid, (+)-5,6-dehydrolycorine (**131**) (Fig. 20), isolated from the bulbs of *Lycoris radiata* (Amaryllidaceae), inhibited the *in vitro* viability of *P. falciparum* (D6 and W2), albeit with associated cytotoxicity against eight human tumour cell lines, indicating non-specific antiparasitic activity [102]. Similarly, the macrocyclic lactams cripowellin A-D (**132-135**) (Fig. 20), which were isolated from the alkaloid-enriched extract of *Crinum erubescens* (Amaryllidaceae), inhibited the Dd2 strain with nanomolar IC_{50} values but were also cytotoxic against cancerous A2780 cells. Importantly, the presence of the 1,3,5-trioxepane-ring in **132** and **134** correlated with improved activity [103]. Another bioassay-guided purification, this time of *Crinim firmifolium* leaf extract, led to the isolation of the new 2-alkylquinolinones **136** and the known **137**, which were both active against the 3D7 and Dd2 strains with mild cytotoxicity against A2780 mammalian ovarian cancer cells [104]. Incorporation of a branched alkyl into **137** to form **138** improved antiplasmodial activity, suggesting that branching of the alkyl side chain is beneficial to potency [104].

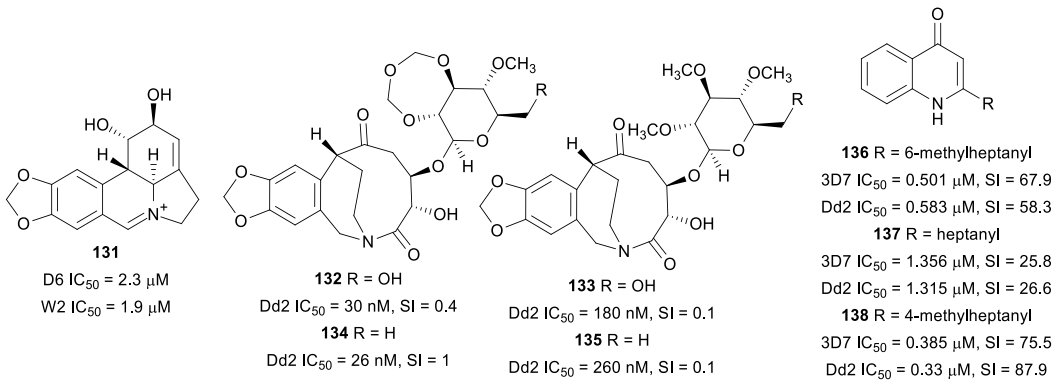

Fig. 20 Structures of (+)-5,6-dehydrolycorine **131**, lactams **132-135** and quinolinone alkaloids **136-138**

The bromotyrosine alkaloid psammaplysin H (**139**) was isolated from a marine *Pseudoceratina* sponge together with the known psammaplysin F (**140**), previously isolated from a *Hyattella* sponge, and both exhibited antiplasmodial activity against the 3D7 strain (Fig. 21) [105].

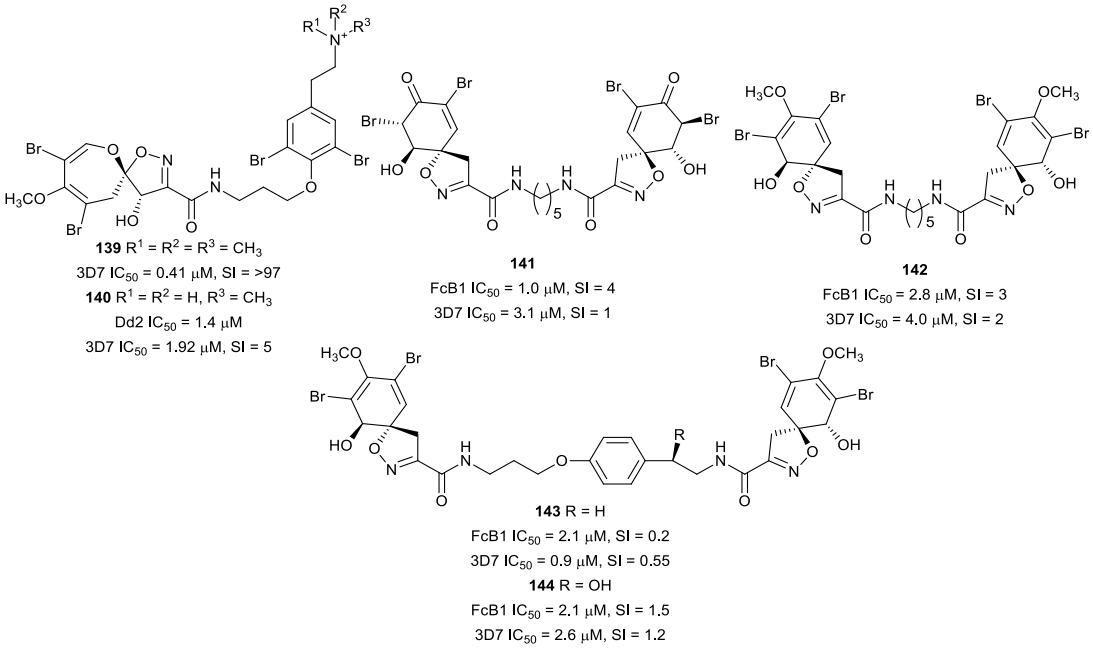

Fig. 21 Structures of bromotyrosine alkaloids

Psammaplysin H (**139**), which has a trimethylated quaternary terminal nitrogen, was not toxic to HEK293 and HepG2 mammalian cells, while **140** suffered from reduced activity coupled with significant cytotoxicity [106]. Preliminary SAR studies indicated that substitution on the terminal nitrogen influences the selective antiplasmodial activity. Four other antiplasmodial bromotyrosine derivatives, aplysinone D (**141**), homoaerothionin (**142**), 11,19-dideoxyfistularin 3 (**143**), and 11-hydroxyfistularin (**144**), were isolated from *Suberea ianthelliformis*, a marine sponge from the Solomon Islands. Unfortunately, these compounds were also cytotoxic against Vero cells [107].

Interrogation of the marine sponge *Monanchora unguiculata*, collected at the Mitsio islands of Madagascar, yielded four new guanidine alkaloids ptilomycalins E-H (**145-148**), along with the known crambescidin 800 (**149**) and fromiamycalin (**150**) (Fig. 22). The compounds exhibited sub-micromolar antiplasmodial activity against the 3D7 strain but were also cytotoxic against KB cells [108]. Similarly, four new antiplasmodial tricyclic thiazine alkaloids thiaplakortones A-D (**151-154**) (Fig. 22), isolated from the Australian marine sponge *Plakortis lita*, showed nanomolar inhibition against the 3D7 and Dd2 parasites, with low toxicity to human HEK293 cells (SI = >62 - >500) [109]. The decalin-tetramic acid metabolite phomasetin (**155**) was obtained following the culturing of the *Pyrenochaetopsis* sp. RK10-F058 fungus. Biological assessment revealed that **155** was active against *P. falciparum* 3D7 with moderate cytotoxicity against cancerous HeLa, HL-60 and src^{ts}-NRK cells. The same culture broth yielded two more decalin metabolites, possessing a cyclopentanone-fused decalin skeleton and a serine-derived *N*-methylated amino acid instead of the tetramic acid moiety. However, they were >21 times less active than **155**, indicating that the cyclized tetramic acid group might be crucial for potent activity [110]. Aplidiopsamine A (**156**) (Fig. 22), with a rare pyrrolo-quinoline conjugated to an adenine nucleobase, was isolated from the Australian ascidian *Aplidiopsis confluata.* The new metabolite was active against the 3D7 and Dd2 strains without significant toxicity against HEK-293 cells [111].

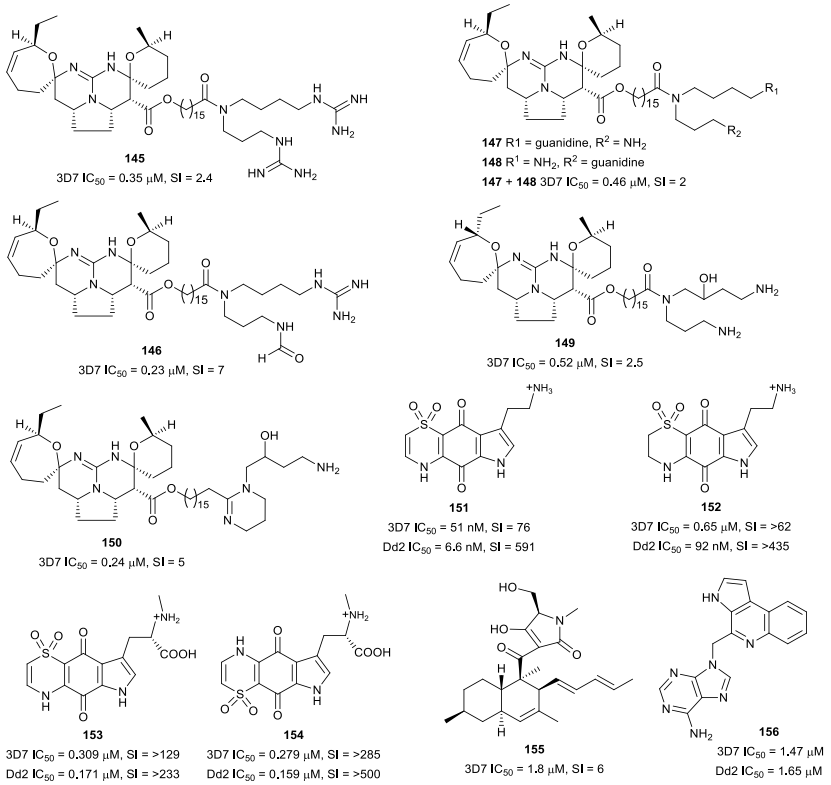

Fig. 22 Structures of guanidines **145-150**, thiazines **151- 154**, phomasetin **155** and aplidiopsamine A **156**

An extract from the leaves of *Prosopis glandulosa* (Fabaceae), collected in Nevada, yielded a new tertiary indolizidine alkaloid $\Delta^{1,6}$-juliprosopine (**157**) (Fig. 23). Interestingly, the leaf extract of the same plant collected in Texas produced the known quaternary alkaloid juliprosine (**158**) but not **157**. The two compounds inhibited the D6 and W2 strains without any toxicity to Vero cells at the highest tested concentration of 23.8 µg/mL [112]. Allonorsecurinine (**159**), previously reported as a synthetic compound, was isolated with *ent*-norsecurinine (**160**) from the antiplasmodial plant *Phyllanthus fraternus* (Phyllanthaceae) (methanol extract IC_{50} = 0.44 µg/mL against 3D7) [113]. The two securinega alkaloids were more active against chloroquine-resistant W2 than against chloroquine-sensitive 3D7 parasites. No cytotoxicity was observed against human umbilical vein endothelial cells at the highest concentration of 100 µM [114]. The root bark extract of the Ugandan anti-malarial medicinal plant *Citropsis articulata* (Rutaceae) displayed 77% inhibition of FcB1 *P. falciparum* at 10 µg/mL with low cytotoxicity against Vero cells. A pyranoacridone alkaloid, 5-hydroxynoracronycine (**161**), was isolated as the most active constituent against the same parasite strain. However, the compound was also moderately cytotoxic against Vero cells (SI = 10) [115].

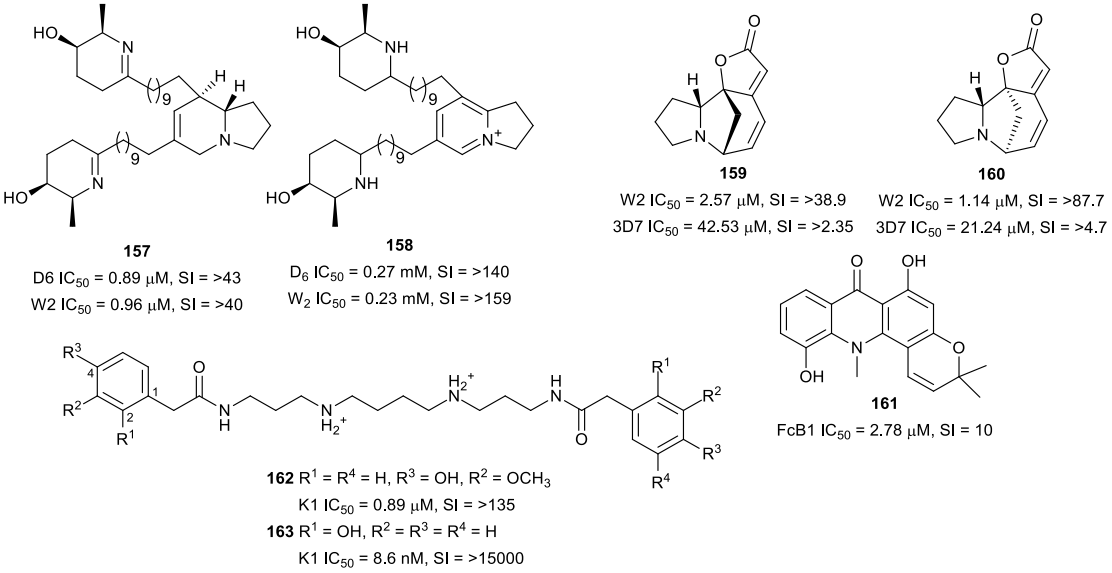

Fig. 23 Structures of other alkaloids **157-163**

The polyamine diamide orthidine F (**162**) (Fig. 23) from the New Zealand-sourced ascidian *Aplidium orthium* was active against K1 *P. falciparum* without cytotoxicity against L6 cells. A synthetic 2-hydroxyphenylacetamide derivative **163** was >100 times more active while retaining selectivity. Preliminary SAR indicated that the two arylamide terminals and the spermine fragment are essential for antiplasmodial activity. Similarly, the hydroxy group at C-2 of the aromatic rings is important for improved antiplasmodial activity [116].

Terpenes

Among the 447 isolated natural products with $IC_{50} \leq 3.0$ µM reported in this review, 30.8% are terpenoids.

Monoterpenes

The iridoid specicoside (**164**) (Fig. 24), isolated from an antiplasmodial ethyl acetate extract of *Kigelia africana* (Bignoniaceae), was active against the *P. falciparum* W2, CAM10 and SHF4 strains without cytotoxicity against LLC/MK-2 cells. Specicoside (**164**) acted in synergy with artemether in inhibiting the W2mef strain but had an antagonistic effect with *p*-hydroxycinnamic acid, which is also present in *Kigelia africana* [117, 118].

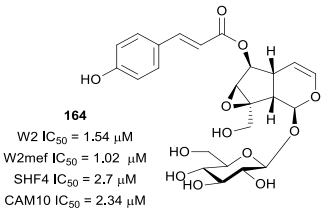

Fig. 24 Structure of specioside

Sesquiterpenes

A phytochemical investigation of the active chloroform extract of *Drimys brasiliensis* (Winteraceae) stem bark (*P. falciparum* FcR3, IC_{50} 3.0 µg/mL) led to the isolation of drimane sesquiterpenes but the most active compound was 1β-(*p*-coumaroyloxy)polygodial (**165**) (Fig. 25) [119]. Preliminary antiplasmodial screening of *Salacia longipes* var. *camerunensis* (Celastraceae) seed extract showed that it was active against the W2 strain with an IC_{50} of 2.28 µg/mL. Extensive purification of the active extract afforded the β-agarofuran sesquiterpenoids salaterpenes A-D (**166-169**) (Fig. 25), which were also active against W2 parasites [120]. The root extract of *Ferula pseudalliacea* (Apiaceae) yielded an antiplasmodial metabolite sanandajin (**170**), the first isolated disesquiterpene-coumarin. This compound, a cadinenyl ester of the sesquiterpene coumarin glabanic acid, inhibited the K1 parasite and had moderate cytotoxicity against L6 cells [121].

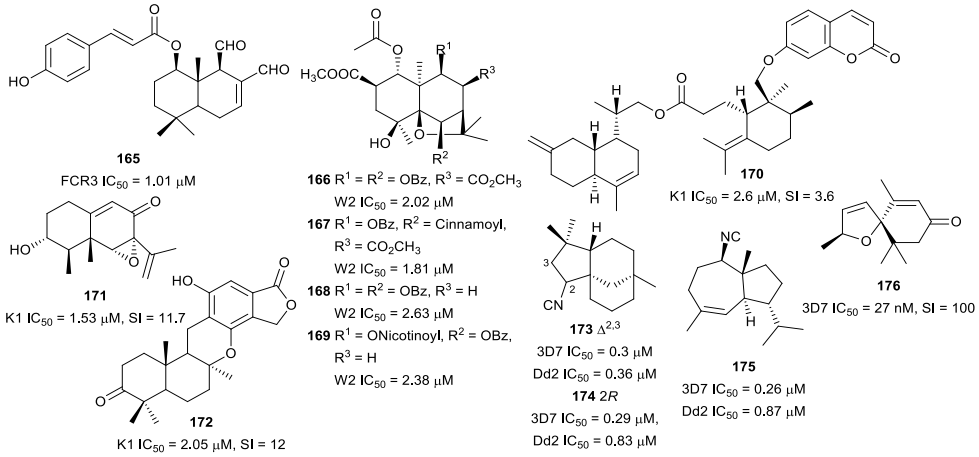

Fig. 25 Structures of sesquiterpenes **165-176**

The eremophilane sesquiterpenoid sporogen-AO1 (**171**), produced by the soil fungus *Penicillium copticola* PSURSPG138, inhibited K1 parasites but was also cytotoxic against human oral epidermoid carcinoma (KB) and Vero cells [122]. The endophytic fungus *Phomopsis archeri*, isolated from *Vanilla albidia* cortex stem, yielded an extract with antiplasmodial activity (IC_{50} = 5.0 µg/mL) from which an aromatic sesquiterpene phomoarcherin B (**172**) (Fig. 25), with antiplasmodial activity but also moderate cytotoxicity against cholangiocarcinoma and KB cells, was isolated [123]. The Australian

nudibranch *Phyllidia ocellata* has produced three new isonitrile sesquiterpenes, 2-isocyanoclovene (**173**), 2-isocyanoclovane (**174**) and 4,5-*epi*-10-isocyanoisodauc-6-ene (**175**), with selective antiplasmodial activity against the 3D7 and Dd2 strains. The isothiocyanate and formamide analogues were significantly less active, further reinforcing the argument that the isonitrile functionality is crucial for the potent activity of isonitrile terpenes [124]. Young *et al*. adapted a β-haematin inhibition assay to allow for the assaying of small amounts of marine natural products and was able to prove that six terpenoid isonitriles inhibit heme crystallization at different levels [125]. The sesquiterpene-derived spiro heterocycle 3,4-dehydrotheaspirone (**176**) (Fig. 25) has been isolated from *Laumoniera bruceadelpha* (Simaroubaceae) bark extract and was found to inhibit 3D7 parasites selectively [126].

Sesquiterpene lactones

Many species in the genus *Chloranthus* (Chloranthaceae), known in traditional Chinese medicine as "Sikuaiwa", have been documented as a treatment for malaria. A library of 44 lindenane-type sesquiterpenoid monomers and dimers isolated from different *Chloranthus* species and *Sarcandra glabra* (Chloranthaceae) were assayed for antiplasmodial activity. Potent activity was observed for twenty-six of the compounds (**177-202**) (Fig. 26).

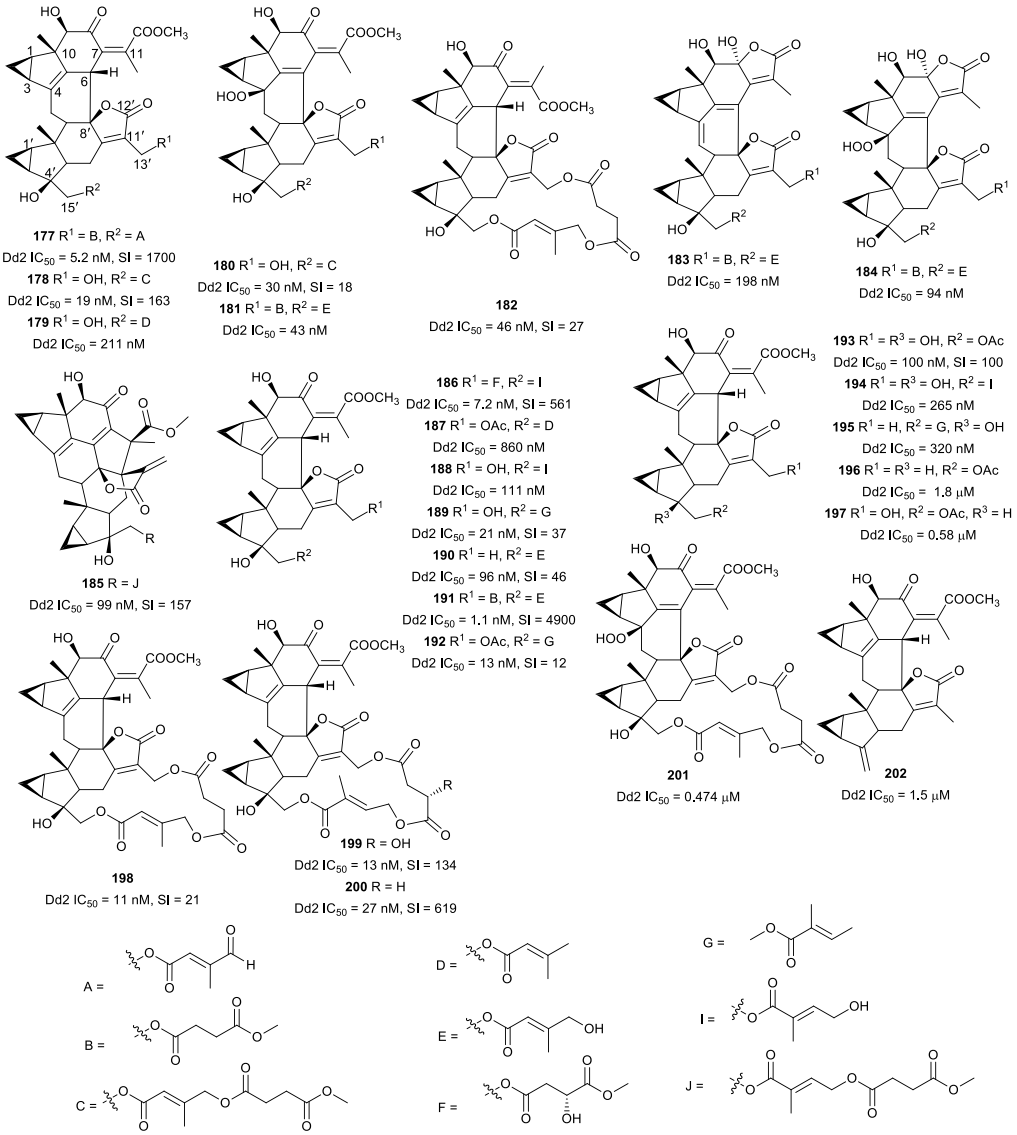

Fig. 26 Structures of dimeric sesquiterpene lactones **177-202**

Compounds with IC_{50} ≤ 100 nM were also assessed for cytotoxicity on embryonic lung tissue (WI-38) cells, and some compounds, e.g. fortunilide A (**177**), sarglabolide J (**186**), and chlorajaponilide C (**191**) had potencies comparable to that of artemisinin and were not cytotoxic. Preliminary SAR observations indicated that all the active compounds were dimers, had a Δ^4 double bond and a hydroxy group at C-4', and contain a (*Z*)-5-hydroxy-4-oxopent-2-enoate ester. The presence and nature of the ester groups at C-13' and C-15' affected the antiplasmodial activity, suggesting that these ester groups could be manipulated to optimize potency [127]. The potent and selective antiplasmodial activity warrants further exploration of this group of compounds.

Thirteen plants used in Burkina Faso to treat malaria were investigated, and due to the promising *in vitro* and *in vivo* anti-malarial activity, *Dicoma tomentosa* (Asteraceae) was selected for further studies [128]. Bioassay-guided purification of the whole plant extract yielded the known germacranolide sesquiterpene lactone, urospermal A 15-*O*-acetate (**203**) (Fig. 27) as the major antiplasmodial compounds. The compound exhibited antiplasmodial activity against the 3D7 and W2 strains without evidence of haemolysis, indicating a direct action on the parasite. However, **203** was cytotoxic against WI38 human fibroblasts SI = 3.3, suggesting non-selective activity [129]. The root of an antiplasmodial *Dicoma* species from South Africa, *Dicoma anomala* subsp. *gerrardii* was the source of a eudesmanolide-type sesquiterpene lactone, dehydrobrachylaenolide (**204**), which inhibited D10 *P. falciparum* but was less active against the K1 strain and moderately cytotoxic against CHO cells (SI = 9). Semi-synthetic derivatives of **204**, in which the α-methylene ketone and lactone were reduced, were less active. This indicates that the exocyclic methylene group is essential for activity [130].

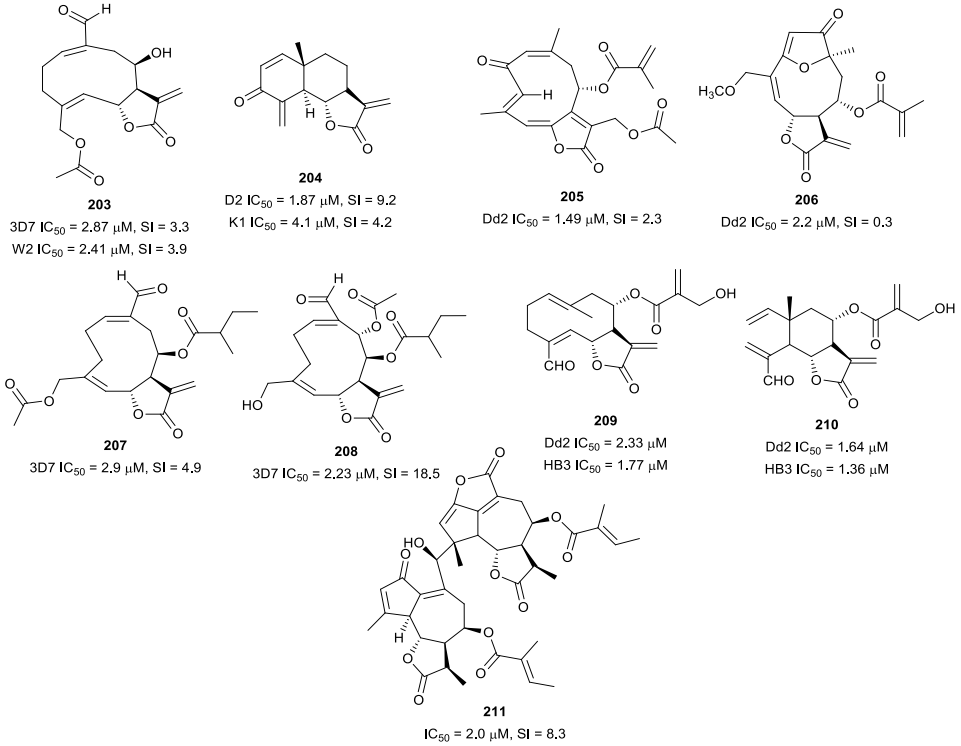

Fig. 27 Structures of sesquiterpene lactones **203-211**

The dichloromethane extract of *Trichospira verticillata* (Asteraceae) exhibited antiplasmodial activity against Dd2 *P. falciparum* with an IC_{50} of approximately 5 µg/mL. Fractionation of the extract afforded the new germacranolide trichospirolide A (**205**) (Fig. 27) as the most active constituent. However, it was also toxic to A2780 ovarian cancer and HEK293 cells [131]. Another antiplasmodial

germacranolide, 15-*O*-methylgoyazensolide (**206**), was isolated from the leaf and twig extract of *Piptocoma antillana* (Asteraceae). It was equally active against the Dd2 strain and A2780 human ovarian cancer cells, indicating a non-selective antiplasmodial activity [132]. Antiplasmodial screening of 12 plants used in traditional medicine against malaria in Benin resulted in an extract of the aerial parts of *Acanthospermum hispidum* (Asteraceae) with potent activity against 3D7 and W2 parasites (IC_{50} = 7.5 and 4.8 µg/mL, respectively) [133]. Two acanthospermolide-type sesquiterpene lactones (**207** and **208**) were subsequently isolated as the major antiplasmodial compounds without haemolytic activity [134]. Compound **208** was less cytotoxic against WI38 human fibroblasts than **207**, indicating that **208** was more selective in the toxicity to 3D7 parasites [134]. Two other sesquiterpene lactones, vernopicrin (**209**) and vernomelitensin (**210**), from *Vernonia guineensis* (Asteraceae) leaves were also active against Dd2 and Hb3 parasite strains without haemolysis [135]. The dichloromethane extract of *Eupatorium perfoliatum* (Asteraceae) aerial parts inhibited *P. falciparum* with low cytotoxicity (IC_{50} = 2.7 µg/mL and SI = 27). The new dimeric guaianolide, diguaiaperfolin (**211**), was isolated as the main antiplasmodial compound from the active extract, but the compound was moderately cytotoxic against L6 cells (SI = 8) [136].

All the different classes of sesquiterpene lactones reported so far exhibited non-selective antiplasmodial activity. The bioactivities of sesquiterpene lactones have been ascribed to the presence of an α-methylene-γ-lactone moiety in the structures. The conjugate Michael acceptor property of this highly reactive functionality allows it to react with the thiol group of crucial cell proteins hence the unselective activity. SAR studies around this enigmatic functionality to make sesquiterpene lactones more selective are essential if these compounds are to enjoy further development as anti-malarial scaffolds.

Diterpenes

Three new cassane diterpenes (Fig. 28) from an active chloroform extract of *Caesalpinia sappan* (Fabaceae) seeds (IC_{50} = 0.38 µg/mL against K1), caesalsappanins G-I (**212-214**), inhibited K1 *P. falciparum* [137]. Cytotoxicity studies against a panel of cancer cell lines showed moderate selectivity for the parasite (SI = 10.5-17.6). The three active compounds have a hydroxy group at C-12, whereas compounds lacking the C-12 hydroxy were less active [137]. The dichloromethane extract of *Caesalpinia bonducella* root showed *in vivo* dose-dependent antiplasmodial activity [138]. A phytochemical investigation of the root afforded norcaesalpin D (**215**) as the antiplasmodial component. This cassane diterpenoid was active against 3D7, Dd2, and artemisinin-resistant (IPC 5202 Battambang, IPC 4912 Mondolkiri-Cambodia) strains. No cytotoxicity was observed against mammalian LLC-MK2 cells at the highest concentration (200 µg/mL) tested [139].

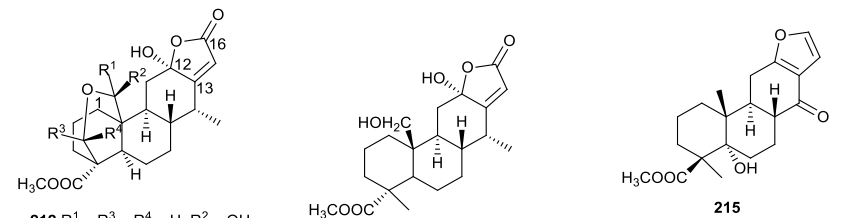

Fig. 28 Structures of cassane diterpenes **212-215**

The leaf extract of *Aphanamixis grandifolia* (Meliaceae) produced the diterpenoid lactones amphadilactones A-F and H-I (**216-223**) (Fig. 29) [140, 141]. The structures of amphadilactones E and F feature a novel carbon skeleton with a 1,1,2,2-tetrasubstituted cyclobutane moiety. Compounds **216-223** inhibited the Dd2 strain with sub-micromolar IC_{50} values. The interesting structures and antiplasmodial activity of **216-219** have motivated the total synthesis of the compounds [142].

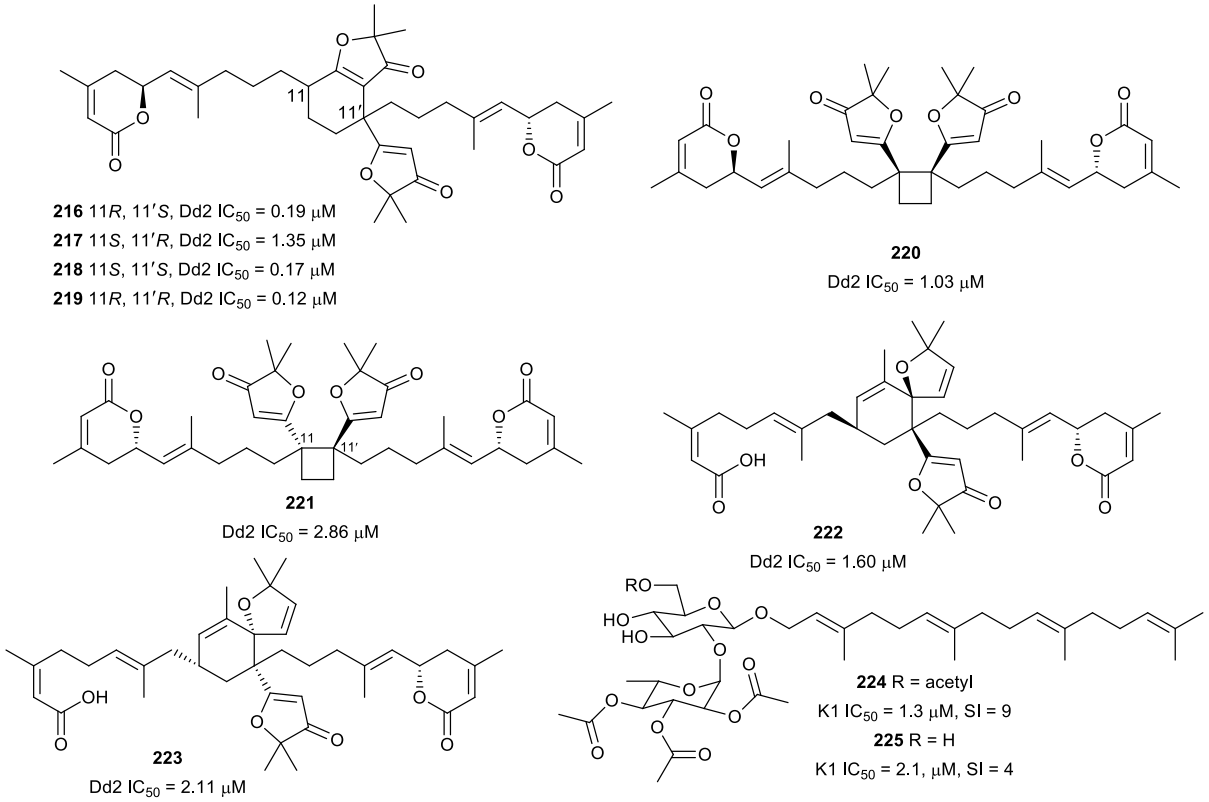

Fig. 29 Structures of diterpenes **216-225**

Furthermore, compounds **216-219** showed potent inhibition of diacylglycerol *O*-acyltransferase-1 (DGAT-1) isozyme. *P. falciparum* encodes only one DGAT enzyme, *Pf*DGAT, and it is necessary for parasite proliferation during the intraerythrocytic stage [143]. With the unprecedented carbon frameworks, it is worthwhile to investigate whether the new amphadilactones exert antiplasmodial activity by inhibiting *Pf*DGAT [140, 141]. The hexane and dichloromethane bark extracts of *Cupania cinerea* (Sapindaceae), an Ecuadorian ethnobotanical plant, were active against *P. falciparum* K1 strain (IC_{50} = 2.9 and 3.1 μg/mL, respectively) [144]. Subsequent bioassay-guided purification of the extracts yielded the new linear diterpenoid glycosides cupacinoside (**224**) and 6'-de-*O*-acetylcupacinoside (**225**), both displaying antiplasmodial activity against K1 parasites but also cytotoxicity against L6 cells [145].

The serrulatane diterpenoid **226**, which was isolated from the aerial parts of *Eremophila microtheca* (Scrophulariaceae), was not active at 10 μM against *P. falciparum*. However, a semi-synthetic amide derivative **227** exhibited antiplasmodial activity against the 3D7 and Dd2 strains without being cytotoxic to HEK293 cells at 80 μM [146]. Two new pre-segetane and jatrophane diterpenoids euphorbesulins A (**228**) and G (**229**) (Fig. 30), from the twigs of *Euphorbia esula* (Euphorbiaceae), have also shown activity against the *P. falciparum* Dd2 strain [147].

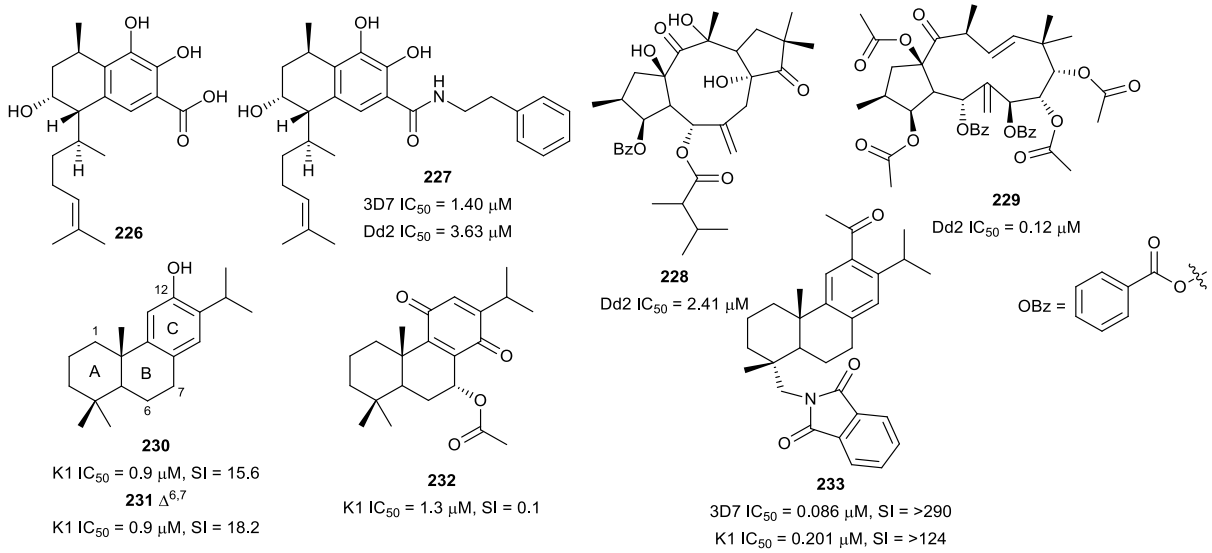

Fig. 30 Structures of diterpenes **226-233**

Antiplasmodial screening of 150 Iranian ethnomedicinal plants identified *Salvia sahendica* (Lamiaceae) hexane root extract with potent activity against the K1 strain (70% inhibition at 0.85 µg/mL) [148]. A subsequent phytochemical investigation led to the isolation of abietane diterpenoids as the bioactive constituents and ferruginol (**230**), Δ^9-ferruginol (**231**) and 7α-acetoxyroyleanone (**232**) inhibited K1 parasites. However, **232** was also toxic to L6 cells, indicating a non-selective antiplasmodial activity. Chemical modifications, which included deacetylation and dehydrogenation of ring B, and hydroxylation of the benzoquinone ring of **232**, led to a reduction in activity without improving selectivity [148]. However, the semi-synthetic phthalimide derivative **233** of ferruginol had an improved selective antiplasmodial activity. Preliminary SAR studies of a library of semi-synthetic derivatives of ferruginol indicated that a hydroxy group at C-12 is beneficial for activity while an acetate group at C-12 reduced the activity against the K1 strain, but improved the activity against the 3D7 strain. Chlorination of the phthalimide group was detrimental to activity [149].

A marine sponge from Thailand, *Stylissa cf. massa*, has produced some bifunctionalized amphilectane diterpenoids. The most active metabolite, 8-isocyano-15-formamidoamphilect-11(20)-ene (**234**) (Fig. 31), exhibited antiplasmodial activity against the K1 strain and was not cytotoxic against MCF-7 breast cancer cells. Analogues bearing an isocyanate and isothiocyanate functionalities were up to ten times less active, indicating that the isonitrile group improved activity. Also, an analogue with only the formamide functional group but lacking an isonitrile group, was not active against *P. falciparum*, suggesting that the formamide group does not contribute to antiplasmodial activity [150]. Two more isonitrile amphilectanes, monamphilectines B (**235**) and C (**236**), were isolated from the Carribean marine sponge *Svenzea flava* collected off the coast of Puerto Rico [151]. The new metabolites were described as the first marine natural products with an α-substituted monocyclic β-lactam ring. The compounds were active against the 3D7 parasites with nanomolar IC_{50} values. Interestingly, 8,15-diisocyano-11(20)-amphilectene (**237**), which differs from the new compound by the absence of the substituted β-lactam moiety, was also active, which suggests that the β-lactam moiety does not contribute to antiplasmodial potency and further confirms the crucial role of the isocyanide (isonitirile) functionality [151]. Potent antiplasmodial activity against W2 parasites was also reported for monamphilectine A (**238**), with an unsubstituted β-lactam ring [152].

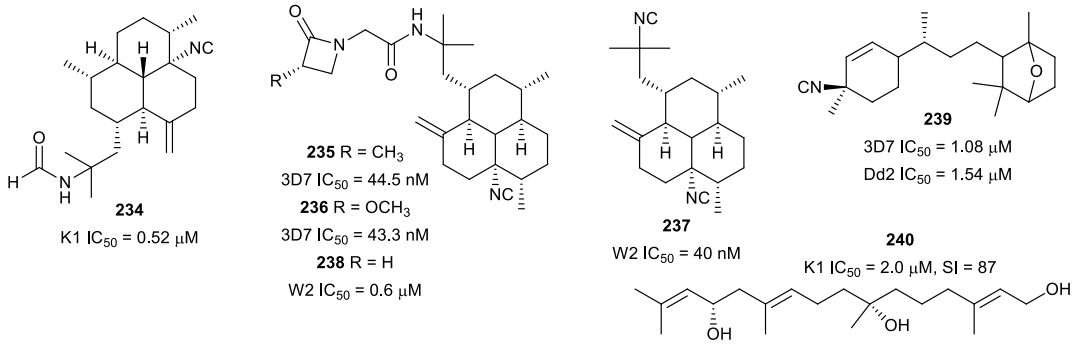

Fig. 31 Structures of isocyano diterpenes **234-239** and bifurcatriol

Pustulosaisonitrile-1 (**239**), which was isolated from the Australian nudibranch *Phyllidiella pustulosa*, exhibited antiplasmodial activity against 3D7 and Dd2 *P. falciparum* strains [153]. Diastereoisomers of **239**, obtained by enantio- and stereoselective total synthesis, were as active as the natural compound, but also showed cross-resistance [153]. The antiplasmodial activity of isonitrile terpenoids has been demonstrated to be due to inhibition of haemozoin formation [125, 154]. Therefore, further development of this class of compound will depend on the ability to avoid cross-resistance. A new linear diterpenoid, bifurcatriol (**240**), featuring two stereogenic centres, was isolated from the Irish brown alga *Bifurcaria bifurcata* and was active against K1 *P. falciparum* with negligible cytotoxicity against L6 cells [155].

The stem extract of *Drypetes gerrardii* var *gerrardii* (Putranjivaceae) exhibited potent antiplasmodial activity against *P. falciparum* (IC_{50} = 0.5 μg/mL). Two new metabolites, the diterpene-derived phenanthrenone drypetenone D (**241**) and phenanthrenone heterodimer drypetenone E (**242**) (Fig. 32), were subsequently isolated from this extract. These compounds were active against the NF54 strain with low cytotoxicity against L6 cells (SI = 71 and 31, respectively). However, the more active and selective monomer **241** did not show *in vivo* activity in *P. berghei*-infected mice [156]. The phenanthrenone derivatives fimbricalyx A (**243**) and B (**244**), isolated from *Strophioblachia fimbricalyx* (Euphorbiaceae) root, also inhibited *P. falciparum* K1. Interestingly, the new fimbricalyx B exhibited nanomolar antiplasmodial activity, better than mefloquine, without being cytotoxic against Vero and human cancerous cells at 10 μM [157].

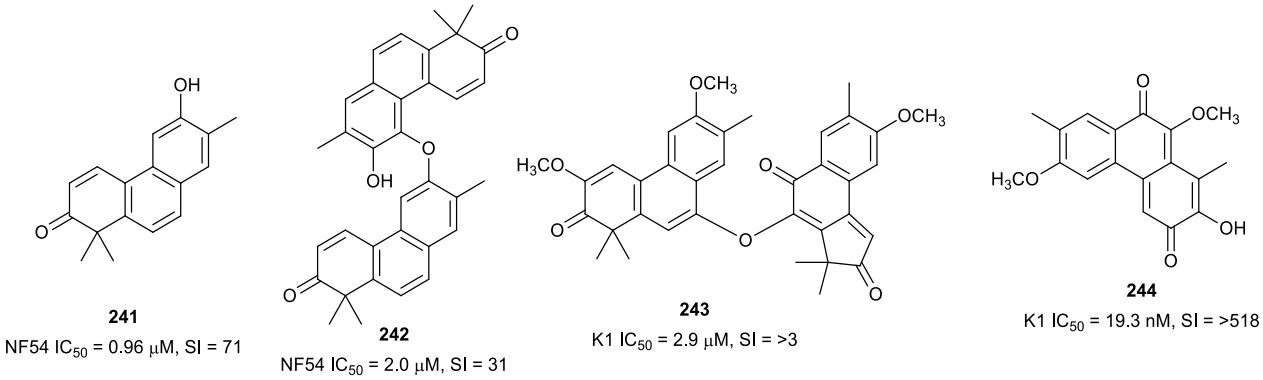

Fig. 32 Structures of other diterpenoids

Triterpenes

The chloroform extract of a combination of *Buxus cochinchinensis* (Buxaceaea) leaves, twigs and fruits yielded five betulin coumaroyl esters (**245-249**) (Fig. 33) [99]. The lupane esters **245, 248** and **249** were also isolated from the methanolic supercritical fluid extract of *B. sempervirens* together with five other new coumaroyl and feruloyl esters of betulin (**250-254**) [158]. The coumaroyl and feruloyl esters have either a *Z*- or *E*-configuration and are attached to betulin at either C-3 or C-23. The esters were active against *P. falciparum* Dd2, HB3 and NHP1337 strains without cytotoxicity against HeLa cells. Ester **250**, with an *E*-feruloyl group attached at C-23, was the most active with sub-micromolar IC_{50} values, whereas analogues with *E* or *Z* coumaroyl or *Z*-feruloyl at C-23 were slightly less active. Also, C-3 modified analogues were less active than the C-23 modified counterparts. These observations identify the importance of the *E*-feruloyl moiety and suggest that modification at C-23 is more advantageous for activity. Importantly, the esterified betulin derivatives were more active than betulin and 23-hydroxybetulin, and the diacetate ester was inactive [99, 158]. Betulone (**255**), isolated from the bark of *Cupania cinerea* (Sapindaceae), inhibited *P. falciparum* K1 and had moderate cytotoxicity against L6 cells [145].

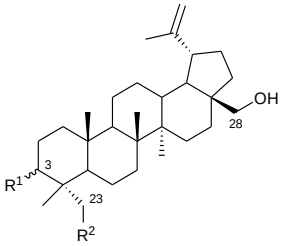

245 R^1 = β-(*E*)-*p*-coum, R^2 = OH
Dd2 IC_{50} = 0.65 μM, SI = >31
HB3 IC_{50} = 1.9 μM, SI = >11
NHP1337 IC_{50} = 1.4 μM, SI = >14
246 R^1 = α-(*E*)-*p*-coum, R^2 = OH
Dd2 IC_{50} = 1.28 μM, SI = >16
247 R^1 = α-(*Z*)-*p*-coum, R^2 = OH
Dd2 IC_{50} = 1.02 μM, SI = >20
248 R^1 = β-OH, R^2 = (*E*)-*p*-coum
Dd2 IC_{50} = 0.26 μM, SI = >77
HB3 IC_{50} = 0.9 μM, SI = 31
NHP1337 IC_{50} = 0.85 μM, SI = 33
249 R^1 = β-OH, R^2 = (*Z*)-*p*-cou
Dd2 IC_{50} = 0.63 μM, SI = >32
HB3 IC_{50} = 0.8 μM, SI = 8.8
NHP1337 IC_{50} = 1.53 μM, SI = 4.6
coum = coumaroyl

250 R^1 = OH R^2 = (*E*)-feruloyl
HB3 IC_{50} = 0.5 μM, SI = >20
NHP1337 IC_{50} = 0.27 μM, SI = 65
251 R^1 = OH R^2 = (*Z*)-feruloyl
250 + **251** (3:1)
HB3 IC_{50} = 1.0 μM, SI = 20
NHP1337 IC_{50} = 0.31 μM, SI = 65
252 R^1 = β-(*Z*)-*p*-coum, R^2 = OH
245 + **252** (1:4)
HB3 IC_{50} = 2.3 μM, SI = 9.6
NHP1337 IC_{50} = 1.6 μM, SI = 14
253 R^1 = (*E*)-feruloyl, R^2 = OH
254 R^1 = (*Z*)-feruloyl, R^2 = OH
253 + **254** (2:1)
HB3 IC_{50} = 3.0 μM, SI = >6.7
NHP1337 IC_{50} = 2.3 μM, SI = >8.7

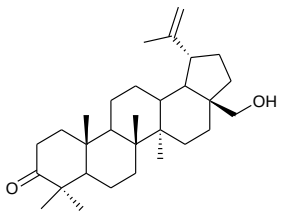

255
K1 IC_{50} = 3.0 μM, SI = 7.4

Fig. 33 Structures of betulin derivatives

Happi and co-workers investigated the chemical constituents of *Entandrophragma congoense* (Meliaceae) bark, a plant used in Cameroonian traditional medicine against malaria. They isolated the apotirucallane triterpenoids prototiamins A-G (**256-262**) and the known **263** as the major constituents and gladoral A (**264**) was obtained as a minor metabolite (Fig. 34) [159]. The compounds displayed antiplasmodial activity against NF54 *P. falciparum* strain with varying levels of toxicity to L6 cells (SI = 4 - 107). Triterpenoid **256**, with a sub-micromolar IC_{50} value, was the most selective against the parasite [160, 161]. Comparing the activities of the compounds allowed some preliminary SAR assumptions. Compounds **256** and **257** differ only in the orientation of the hydroxy group at C-24 and presence or absence of acetylation at C-7 of ring B. Analogue **256**, with an α-oriented OH group and acetylation of the OH at C-7, was twice as active and four times more selective than **257**. Compound **258**, which has a similar structure to **256** but with an epoxide ring between C-24 and C-25 instead of the free α-OH in **256**, was >8 times less selective. These observations suggest a SAR role for these positions that could be exploited further to optimize potency and selectivity. Another tirucallane triterpenoid, isoflindissone lactone (**265**), was isolated from the dichloromethane extract of *Boswellia serrata* (Burseraceae) oleo-gum resin by bioassay-guided purification of an extract that inhibited *P. falciparum* with IC_{50} = 2.6 μg/mL. Compound **265** was active against the NF54 parasite strain with low toxicity against L6 cells (IC_{50} = 40 μM) [162]. The ethyl acetate stem bark extract of *Kigelia africana*

(Bignoniaceae) inhibited *P. falciparum* W2 strain and two field isolates, CAM10 and SHF4 (IC_{50} = 11.15, 4.74 and 3.91 µg/mL, respectively). Phytochemical investigations of this active extract yielded the known triterpenoid **266** alongside other metabolites. Compound **266** was active against the W2 and CAM10 strains, with moderate cytotoxic against monkey kidney (LLC-MK2) cells (IC_{50} = 9.4 µg/mL) [117]. A synergistic effect was observed with a combination of **266** and artemether on the W2mef parasite strain, but the compound had an antagonistic effect with quinine [118].

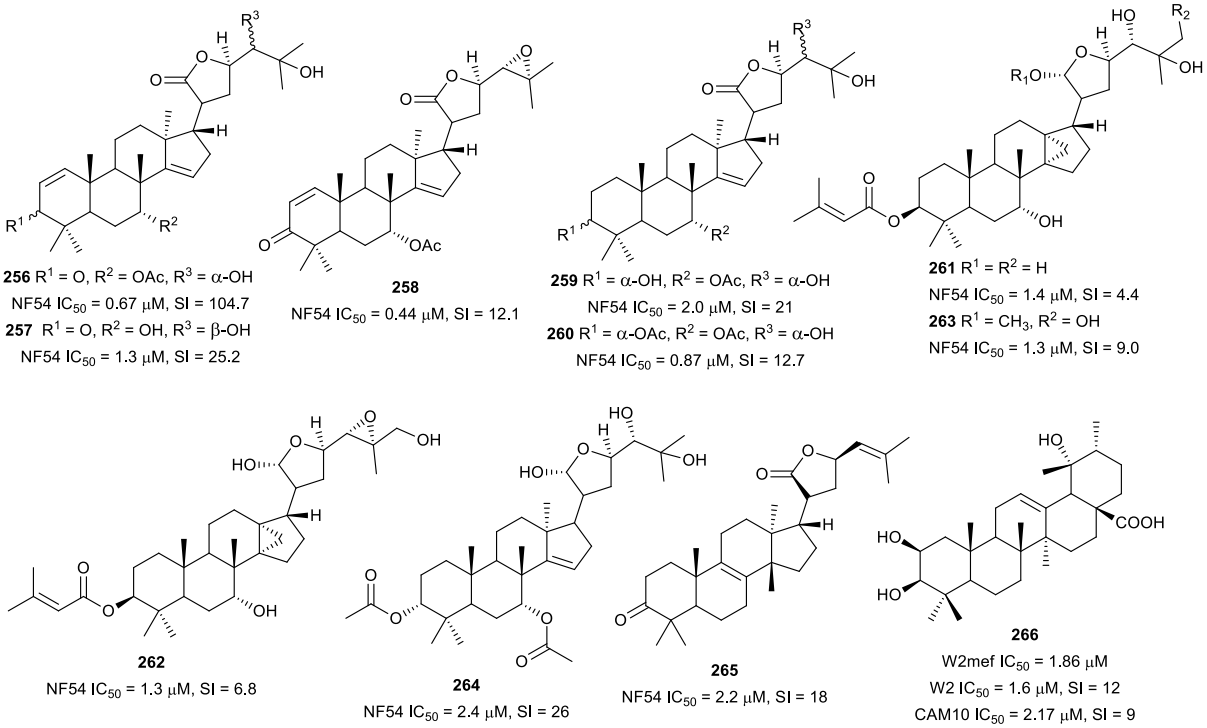

Fig. 34 Structures of triterpenes **256-266**

Bioassay-guided fractionation of the methanol extract from the aerial parts of *Momordica balsamina* (Cucurbitaceae) afforded the new curcurbitacins, balsaminol F (**267**), the glycoside balsaminoside B (**268**) and the known kuguaglycoside A (**269**) (Fig. 35). Glycosides **268** and **269** displayed antiplasmodial activity against the 3D7 and Dd2 strains, while the aglycone **267** was much less active. This suggests that the sugar unit is beneficial to the antiplasmodial activity. However, the compounds were not selective when the cytotoxicity against MCF-7 breast cancer cells is compared to the antiplasmodial activity. Interestingly, the triacetyl semi-synthetic derivative **270** of balsaminol F was 22 and 50 times (for 3D7 and Dd2, respectively) more active than the parent compound without cytotoxicity against MCF-7 cells. However, the activity was lost with the corresponding tribenzoyl ester derivative of balsaminol F [163]. Similar improvement in potency and selectivity was observed when karavilagenin C (**271**), which was isolated from *Momordica balsamina*, and was esterified at C-3 and/or C-23 to give different alkanoyl and benzoyl/cinnamoyl derivatives. For the alkanoyl analogues, the diacetyl and dipropanoyl derivatives were more active than the mono analogues, while the monobutanoyl compound was more active than the dibutanoyl counterpart. Moreover, all the mono-aroyl/cinnamoyl derivatives were superior compared to the diaroyl/cinnamoyl counterparts [164]. These observations allow the conclusion that for bulky groups, mono-esterification is optimal for activity, while di-esterification is favoured for the smaller groups. It will be worthwhile to study the preferred point of esterification for the monoesters.

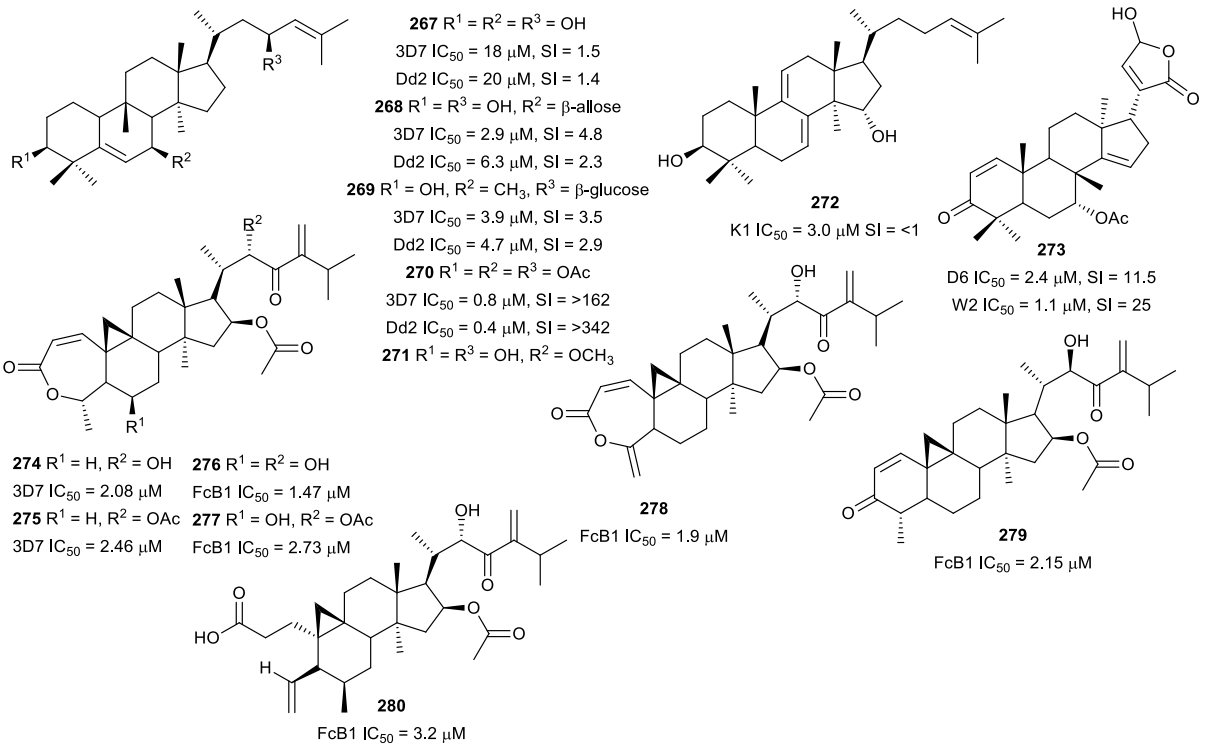

Fig. 35 Structures of triterpenes **267-280**

The root bark of *Greenwayodendron suaveolens* (Annonaceae) afforded polycarpol (**272**) as one of the active metabolites against K1 *P. falciparum*, but it was also cytotoxic against MRC-5 cells (SI = <1) [69]. Antiplasmodial assay of 14 Kenyan medicinal plants identified the methanol root bark extract of *Turraea robusta* (Meliaceae) as the most active against NF54 and K1 parasites (IC_{50} = 2.4 and 3.5 μg/mL, respectively) [165]. Azadironolide (**273**) was subsequently isolated as the most active antiplasmodial compound from the plant stem bark with moderate cytotoxicity against Vero cells [166]. An ethnomedicinal survey of plant use in the Northern sector of Kibale National Park in western Uganda indicated that *Neoboutonia macrocalyx* (Euphorbiaceae) is used to treat malaria [167]. Chemical investigation of the plant leaf afforded the new cycloartane triterpenoids neomacrolactone (**274**), 22α-acetoxyneomacrolactone (**275**), 6-hydroxyneomacolactone (**276**), 22α-acetoxy-6-hydroxyneomacrolactone (**277**) and 4-methylene-neomacrolactone (**278**), and the previously reported 22-de-*O*-acetyl-26-deoxyneoboutomellerone (**279**) (Fig. 35). These compounds exhibited antiplasmodial activity against FcB1 *P. falciparum*, but were generally cytotoxic against KB and MRC-5 cells. Interestingly, neomacroin (**280**) with an open ring A, thus lacking an α,β-unsaturated carbonyl conjugated to the cyclopropane ring, showed low cytotoxicity but was slightly less potent (IC_{50} = 3.2 μM) [168]. Two more novel triterpenoids, salvadione C (**281**) and perovskone B (**282**) (Fig. 36), with rare carbon skeletons were isolated from an antiplasmodial hexane extract of *Salvia hydrangea* (Lamiaceae). The antiplasmodial activity against K1 parasites was selective when compared to cytotoxicity against L6 cells. The rare carbon scaffolds can be rationalized by a Diels-Alder-type addition of an acyclic monoterpene to a diterpenoid. The monoterpene in the case of **281** is myrcene and *trans*-β-ocimene for **282**, and the additional oxepane ring in **281** confers structural rigidity. These structural types were only previously reported in salvadiol from *Salvia bucharica* and perovskone from *Perovskia abrotanoides* (Lamiaceae) [169]. Three new triterpenoid saponins, maesargentoside I, III, IV (**283-285**) from the leaf extract of *Maesa argentea* (Myrsinaceae) have displayed non-selective antiplasmodial activity against K1 *P. falciparum* [170]. The medicinal mushroom *Ganoderma*

boninense produced a new nortriterpenoid with a 3,4-seco-27-norlanostane rearranged skeleton. The metabolite ganoboninketal C (**286**) inhibited *P. falciparum* 3D7 strain with low cytotoxicity against A549 cells [171]. The antiplasmodial activity of squalene (**287**), isolated from *Uapaca paludosa* (Euphorbiaceae) trunk bark extract, was reported for the first time. However, it was also cytotoxic against KB and Vero cells [172].

The ethyl acetate extract of the soil fungus *Neosartorya tatenoi* KKU-2NK23 exhibited antiplasmodial activity (IC_{50} = 3.09 µg/mL). A chemical investigation of the fungal material yielded the known meroterpenoid aszonapyrone A (**288**) (Fig. 36). The compound was active against the K1 strain with low cytotoxicity against KB cells (IC_{50} = 48.18 µg/mL). However, the compound was cytotoxic against cancerous NCI-H187 cells, suggesting some level of selectivity in the toxicity to cells. An analogue of **288**, which had a free hydroxy group at C-3 instead of the acetoxy in **288**, was inactive, suggesting a SAR role at this position and indicating that acetylation of the free hydroxy is beneficial to activity [173].

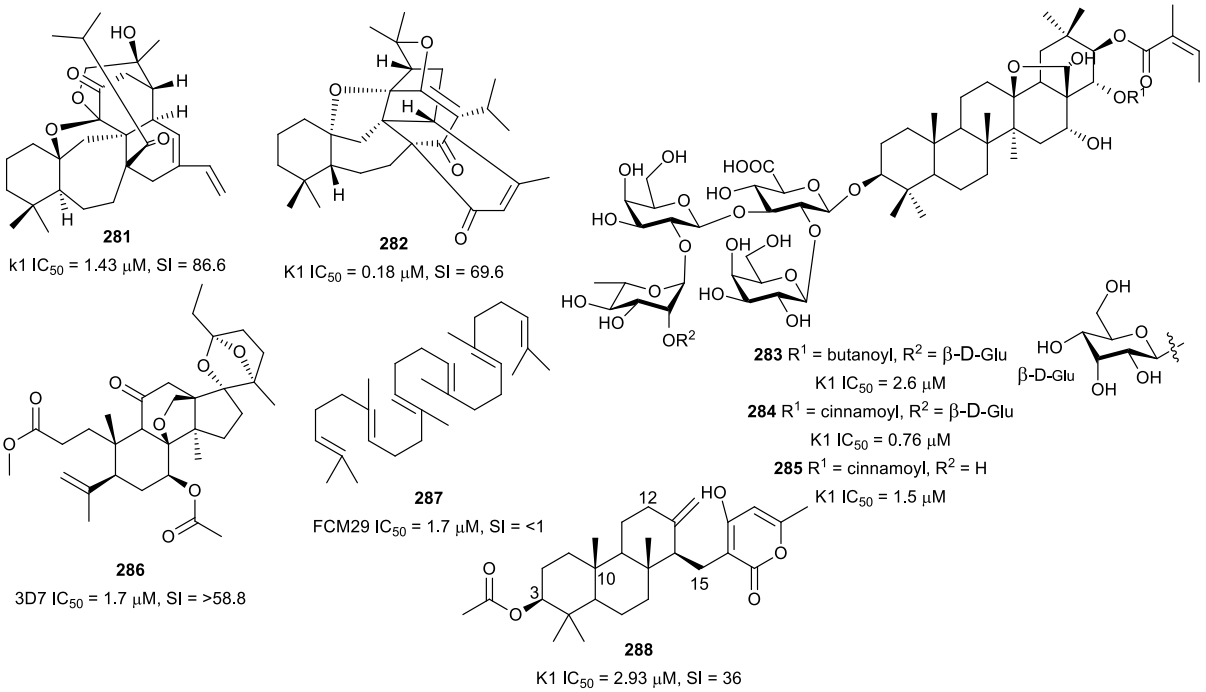

Fig. 36 Structures of other triterpenes

Steroids

An analysis of 65,000 small molecules using the *in silico* similarity ensemble approach (SEA), predicted antiplasmodial activity for selected physalins. Physalins B, D, F and G were then isolated from *Physalis angulata* (Solanaceae) and evaluated for *in vitro* and *in vivo* anti-malarial activity. Physalins B (**289**) and F (**290**) (Fig. 37) had *in vitro* activity against W2 parasite but were also cytotoxic (SI = 12 and 6, respectively). Interestingly, all the mice treated with **290** died from an exacerbated infection due to the increase in parasitaemia that was attributed to an immunosuppressive effect of the compound. However, physalin D (**291**), without the immunosuppressive effect, decreased parasitaemia in *P. berghei* infected mice by 65% at 100 mg/kg [174]. The *n*-butanol fraction of *Caesalpinia volkensii* (Fabaceae) methanol stem bark extract inhibited *P. falciparum* D6 and W2 strains (IC_{50} = 4.5 and 1.3 µg/mL, respectively) better than the less polar fractions. Bioassay-guided purification led to the

isolation of the new steroid glycoside 3-*O*-[β-D-glucopyranosy-(1→2)-*O*-β-D-xylopyranosyl]stigmasterol (**292**) with antiplasmodial activity against the D6 and W2 strains. Crucially, the aglycone, which was isolated from the chloroform fraction, was inactive, suggesting that the two sugars potentiate antiplasmodial activity [175]. The marine red alga *Halymenia floresii* has produced a new steroid, halymeniaol (**293**), which inhibited 3D7 *P. falciparum* and was not cytotoxic [176]. Chemical reinvestigation of the Caribbean sponge *Pandaros acanthifolium* has yielded two new steroid glycosides, pandaroside G (**294**) and pandaroside G methyl ester (**295**). The two compounds were active against the K1 strain as well as cytotoxic against L6 cells, indicating non-selective toxicity. The compounds did not inhibit recombinant *P. falciparum* fatty acid biosynthesis enzymes at the highest tested concentration (20 µg/mL) [177].

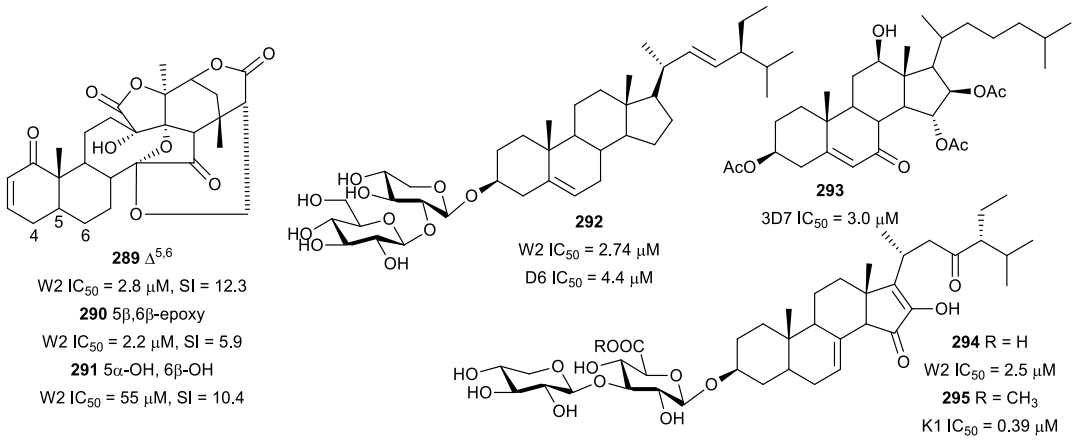

Fig. 37 Structures of steroids

Limonoids

African great apes such as Chimpanzees have been observed to ingest the non-nutritional bitter bark and sap of *Khaya anthotheca* (Meliaceae) in the wild and it has been proposed that this unusual feeding is for medicinal purposes [178, 179]. In an effort to identify bioactive constituents from this plant, the seed petroleum ether extract was tested against *P. falciparum* and showed good activity (IC_{50} = 0.96 µg/mL). Bioassay-guided purification of the extract yielded the known limonoids grandifolione (**296**) and 7-deacetylkhivorin (**297**) (Fig. 38) as the active antiplasmodial constituents. The compounds inhibited the K1 strain and **296** was less toxic towards L6 cells than **297**, SI = 64 and 11, respectively [180]. Two new antiplasmodial limonoids, kostchyienones A (**298**) and B (**299**), were isolated from the root extract of *Pseudocedrela kostchyi* (Meliaceae). Previous investigations indicated that the extract inhibited *P. falciparum* schizont development [181]. Antiplasmodial activity of the new compounds against 3D7 and *Pf*INDO strains was selective and the compounds were not toxic to HEK239T cells (IC_{50} >200 µg/mL). The antiplasmodial activity of limonoids has been attributed to the presence of the α,β-unsaturated carbonyl moiety in the structures, which may be involved in Michael-type addition reactions [182].

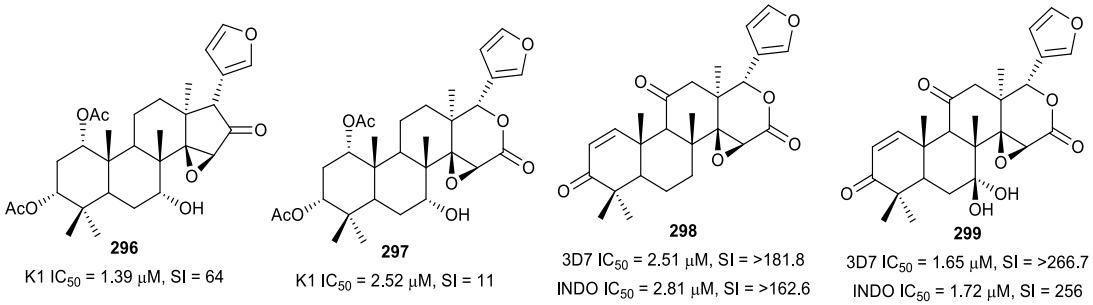

Fig. 38 Structures of limonoids

Quassinoids

The leaf of the tropical Amazonian medicinal plant *Quassia amara* (Simaroubaceae) is used traditionally by people in French Guinea for the preparation of popular anti-malarial remedies, alone or in combination with other plants [183]. The plant leaf extract was prepared according to traditional instructions and found to be active against *P. falciparum in vitro* and *in vivo*, without signs of general toxicity [184]. The known quassinoid simalikalactone D (**300**) (Fig. 39), identified as the main antiplasmodial component of *Quassia amara*, had an IC_{50} of 10 nM against the FcB1 parasite and showed *in vivo* efficacy (oral) [185]. The known cytotoxicity of quassinoids prompted investigations into the toxicity of **300**. The compound displayed antiproliferative activity against cancerous KB cells (IC_{50} = 6.3 nM) but was less cytotoxic against HeLa and noncancerous Vero cells (IC_{50} = 2 and 10 µM, respectively). Similarly, Raji B cells mitotic activity was inhibited at concentrations larger than 45 nM, but no apoptosis or necrosis was observed at a concentration of up to 200 µM of **300**. The compound did not inhibit heme crystallization or parasite-induced host erythrocyte membrane permeability.

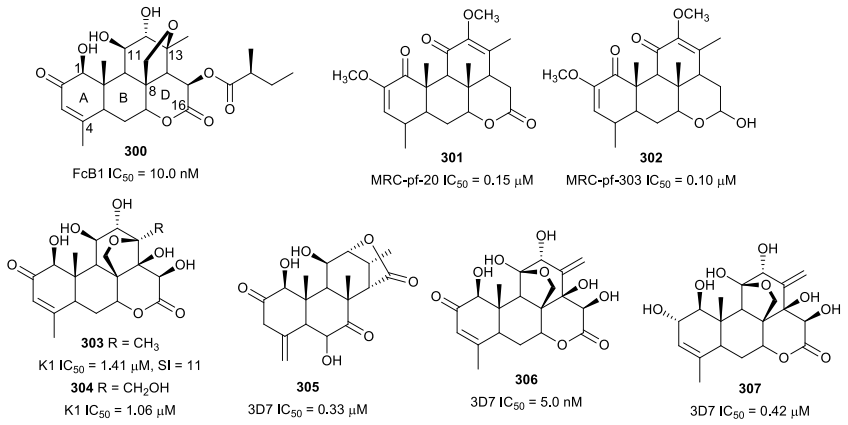

Fig. 39 Structures of quassinoids

Moreover, **300** showed a stage-specific activity by inhibiting DNA replication in mature trophozoites. An additive effect was observed in combination studies with **300** and the traditional anti-malarials chloroquine, artemisinin and analogues. Interestingly, a synergistic effect was observed with atovaquone, opening the possibility of combination therapy to combat drug resistance and mitigate toxicity [186]. Two more quassinoid metabolites of *Quassia amara*, quassin (**301**) and neo-quassin (**302**) isolated from the stem bark, inhibited the MRC-pf-20 and MRC-pf-303 strains. However, the two compounds and the control (artesunate) were less active than the crude stem bark extract (IC_{50} = 0.0025 µg/mL), and the extract was not toxic to mice. A combination treatment with artesunate and **301** or **302** showed synergism at a ratio of 1:2 and additive interaction at a 2:1 ratio; a similar result

was obtained when **301** and **302** were combined [187]. These findings suggest that other metabolites in the stem bark extract might potentiate the antiplasmodial activity of these two compounds. The frequent ethnomedicinal usage, superior activity, and general lack of toxicity of *Quassia amara* extract make it an attractive herbal anti-malarial remedy worthy of further development.

The acetone stem extract of *Brucea javanica* (Simaroubaceae) produced the antiplasmodial quassinoids bruceine D (**303**) and H (**304**) (Fig. 39). Bruceine D (**303**) was also isolated from the roots of the plant. Both compounds inhibited *P. falciparum* K1 strain, but **303** was also cytotoxic against cancerous human KB and NCI-H187 cells [188, 189]. *Eurycoma longifolia* (Simaroubaceae) root extract yielded the new 18-dehydro-6α-hydroxyeurycomalactone (**305**), alongside known eurycomanone (**306**) and eurycomanol (**307**), with nanomolar antiplasmodial activity [86].

The bioactivity of quassinoids has been correlated with the presence of an α,β-unsaturated ketone in ring A. Quassinoids possessing an oxymethylene bridge joining C-8 and C-13 have also shown pronounced activity [188]. These two structural features are considered essential for potent antiplasmodial activity but might also be responsible for the cytotoxicity of the compounds. Furthermore, hydroxy groups at C-11 and C-12 have been implicated in the cytotoxicity of quassinoids [189]. Thus, medicinal chemistry approaches could be employed to optimize the antiplasmodial activity and reduce cytotoxicity of this class of compounds, especially since there might be a different mechanism of action from the traditional anti-malarials.

Polyphenols

Among the 447 isolated natural products with IC_{50} ≤ 3.0 μM reported in this review, 17.4% are polyphenols.

Biflavonoids

Traditional healers in Congo-Kinshasa claim that the chewing of *Garcinia kola* (Clusiaceae) nuts in small quantities daily can ward off malaria. This ethnomedicinal use was validated by the activity of seed extracts against *P. falciparum in vitro* and *P. berghei in vivo* [190, 191]. Moreover, 5 μg/mL of a 70% ethanolic extract of the seed inhibited *P. falciparum* by 87%. Subsequent bioassay-guided fractionation led to the isolation of three biflavanones GB1a (**308**), GB1 (**309**) and GB2 (**310**) (Fig. 40), as the antiplasmodial principles. All three compounds exhibited sub-micromolar antiplasmodial activity against the FCR3 strain with low cytotoxicity against cancerous KB3-1 cells (SI = 77 to 900). *In vivo* treatment of *P. berghei*-infected mice with 100 mg/kg of the principal and most active constituent, **309**, led to 52% suppression of parasites. The compound was orally active, which is crucial for an anti-malarial lead, and no visible signs of toxicity were observed in the treated mice [192]. Another biflavonoid, volkensiflavone (**311**), with antiplasmodial activity against the F32 and FcM29 *P. falciparum* strains, was isolated from *Allanblackia floribunda* (Clusiaceae). Two structural analogues of **311** with an additional hydroxy at C-3' on the lower flavone unit were >10 times less active, suggesting a SAR that could be further exploited [193].

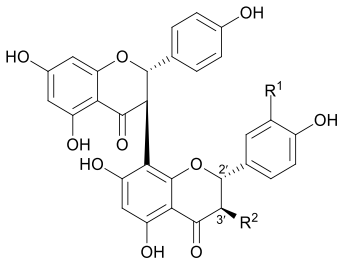

308 $R^1 = R^2 = H$
FCR3 IC_{50} = 0.65 μM, SI = 77
309 $R^1 = H$, $R^2 = OH$
FCR3 IC_{50} = 0.16 μM, SI = >900
310 $R^1 = R^2 = OH$
FCR IC_{50} = 0.21 μM, SI = >700
311 $\Delta^{2'3'}R^1 = R^2 = H$
F32 IC_{50} = 1.83 μM
FCM 29 IC_{50} = 1.72 μM

Fig. 40 Structures of biflavonoids

Prenylated flavonoids

The ethyl acetate extract of *Artocarpus styracifolius* (Moraceae) stem bark (10 μg/mL) inhibited FcB1 *P. falciparum* by 87%. A phytochemical investigation of this extract yielded prenylated flavonoids, the new styracifolin B (**312**), together with known artonin B (**313**), artonin F (**314**), heterophyllin (**315**) and artoheterophyllin B (**316**) (Fig. 41) [194]. The compounds displayed antiplasmodial activity against FcB1 parasites with varying degrees of cytotoxicity against KB and MRC-5 cells (IC_{50} = 4.7-97 μM). An assessment of the structural features of the flavonoids shows that the two most cytotoxic compounds **312** and **315** had a prenyl chain at C-3. The C-3 prenyl side chain was transformed into a furan ring that was fused to flavonoid ring B in the most selective analogue (**314**) [194]. A crude extract from *Macaranga triloba* (Euphorbiaceae) inflorescence showed antiplasmodial activity against the 3D7 strain with an IC_{50} of 2.01 μg/mL [195]. The prenylated flavonoids nymphaeol C (**317**) and 6-farnesyl-3',4',5,7-tetrahydroxyflavanone (**318**) were isolated from this extract and inhibited the 3D7 parasites. The compounds also displayed varying levels of cytotoxicity to cancerous HL-60, MCF-7 and HeLa cells (IC_{50} = 1.3-23 μg/mL), suggesting some degree of selectivity in the toxicity to cellular components [195]. The antiplasmodial activity of *Tephrosia purpurea* (Fabaceae), a widely distributed medicinal plant, was validated *in vitro* against the D6 and W2 strains [196, 197]. A phytochemical investigation of *Tephrosia purpurea* subsp. *leptostachya* afforded a new antiplasmodial prenylflavone, (*E*)-5-hydroxytephrostachin (**319**) (Fig. 41). It was not cytotoxic to cancerous HepG2 cells at 100 μM while being moderately cytotoxic against non-cancerous human cells, indicating selectivity against D6 parasites [198].

The aerial parts of the related *Tephrosia subtriflora* were also active against *P. falciparum* 3D7, D6 and KSM 009 field isolate (IC_{50} = 4.5-11.4 μg/mL [199]. The prenylated flavonoid MS-II (**320**) was subsequently isolated from the active extract and inhibited the 3D7, KSM 009 and artemisinin-sensitive F32-TEM strains. The compound was not cytotoxic against Hep2 and Vero cells at 247.5 μM, suggesting a selective antiplasmodial activity [199]. Furthermore, the root extract of *Tephrosia aequilata*, which inhibited 3D7 *P. falciparum* by 100% at 10 μg/mL, produced the new aequichalcone C (**321**). It inhibited the 3D7 strain without being cytotoxic against HEK-293 cells up to 40 μM, indicating selectivity [200]. Another prenylated flavonoid, carpachromene (**322**), was isolated from *Flindersia pimenteliana* (Rutaceae) as one of the antiplasmodial principles, and it was not cytotoxic against HEK-293 cells at 40 μM [71].

Although many prenylated flavonoids are active against the malaria parasite, many of these compounds are also cytotoxic, and selectivity is a problem. Fröhlich *et al.* reported that prenylated chalcones isolated from hops (*Humulus lupulus*, Cannabaceae) interfere with haem degradation in *P. falciparum*, suggesting a possible mechanism of action [201].

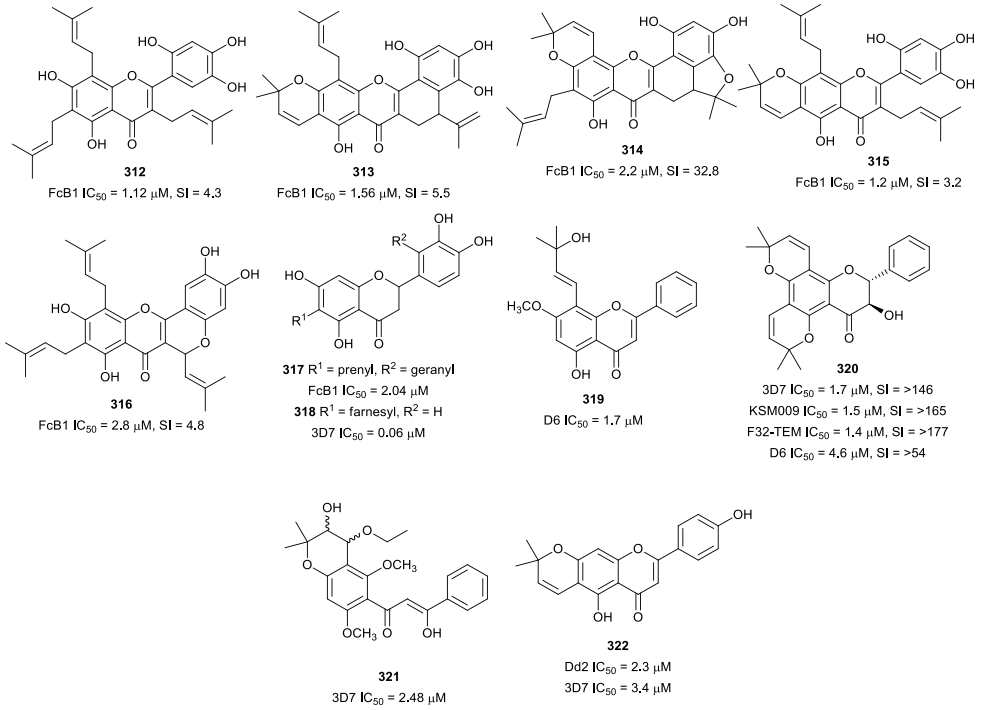

Fig. 41 Structures of prenylated flavonoids

Other flavonoids

Methanol supercritical fluid extraction yielded four kaempferol 3-*O*-rhamnosides (**323-326**) from *Platanus occidentalis* (Platanaceae) and three kaempferol 3-*O*-glucosides (**327-330**) from *Quercus laceyi* (Fagaceae) (Fig. 42) [158]. The glycoside esters exhibited activity against HB3 parasites but were 2-11 times less active against a multidrug-resistant NHP1337 clone. The glucosides **327-330** were also cytotoxic against HeLa cells, while rhamnosides **323-326** were more selective against HB3 parasites (SI = 6-34) [158]. An ethnobotanical survey of medicinal plants used by the people in the Comoros Islands indicated that a decoction of *Flacourtia indica* (Salicaceae) stem and leaves is used against malaria. But, extracts prepared from the aerial parts of this plant displayed only weak activity against K1 parasites (IC_{50} = 49 μg/mL) for dichloromethane and >50 μg/mL for polar extracts [202]. However, in support of the ethnomedical use of the plant, a 95% ethanol extract of *Flacourtia indica* inhibited the 3D7 strain (IC_{50} = 0.5 μg/mL) but was inactive against K1 at the highest tested concentration (10 μg/mL). Chemical investigation of the active extract afforded six phenolic compounds (Fig. 42) of which the flavonolignans, mururin A (**331**) and catechin-[5,6-e]-4β-(3,4-dihydroxyphenyl)dihydro-2(3*H*)-pyranone (**332**) exhibited selective antiplasmodial activity. Compound **331** inhibited 3D7 and K1 *P. falciparum*, while **332** was active only against the 3D7 strain. Both compounds also inhibited β-haematin formation similar to chloroquine and H_2O_2-mediated heme degradation (Table 1), suggesting a possible mechanism of action [203].

The known flavonoid, 3',4',7-trihydroxyflavone (**333**), isolated from *Albizia zygia* (Fabaceae) extract, inhibited K1 *P. falciparum* but was also cytotoxic against L6 cells [204]. (-)-Epigallocatechin-3-gallate (EGCG) (**334**), the major polyphenol in green tea (*Camellia sinensis*, Theaceae), displayed antiplasmodial activity against 3D7 *P. falciparum*. EGCG also inhibited chaperone and ATPase functions by targeting *Pf*Hsp70-1 and *Pf*Hsp70-z (Table 1) [205]. A previous study had shown that EGCG

did not interfere with the parasite folate pathway. Moreover, the antiplasmodial activity of green tea and **334** was demonstrated previously, and EGCG was shown to have an additive effect in combination with artemisinin [206]. However, a higher IC_{50} value (37.2 µM) for EGCG against 3D7 parasites was reported in that study, even though comparable assay methods were used to evaluate the activity. The availability, low cost, and lack of toxicity of green tea coupled with the potentiating effect on the antiplasmodial activity of artemisinin could be exploited to design new artemisinin combination therapies [206].

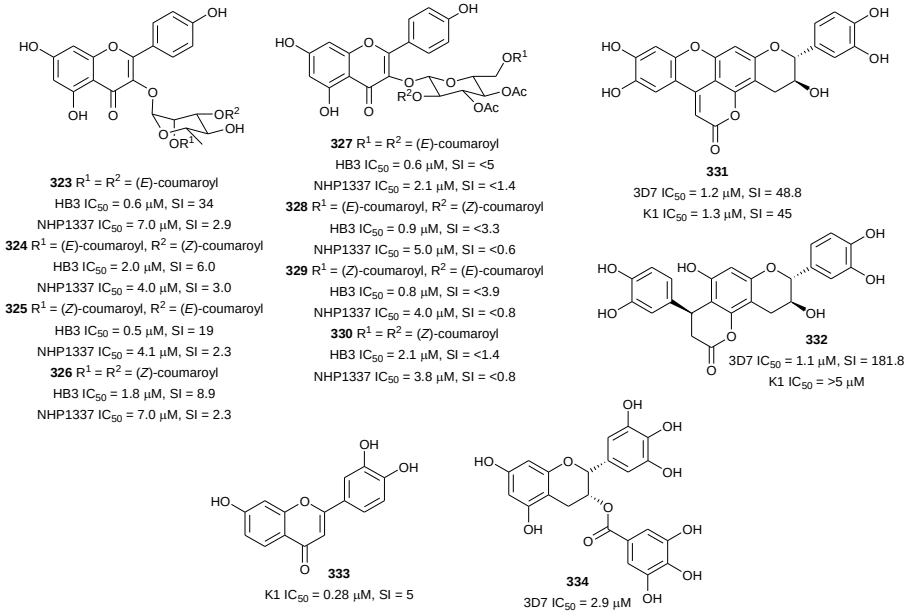

Fig. 42 Structures of other flavonoids

Coumarins and lactones

Bioassay-guided fractionation of the rhizome extract of the Korean medicinal plant, *Angelica purpuraefolia* (Apiaceae) led to the isolation of the pyranocoumarins 3'-decanoyl-*cis*-khellactone (**335**) and 4'-decanoyl-*cis*-khellactone (**336**) as the main antiplasmodial compounds (Fig. 43). Both compounds inhibited D10 parasite strains without cytotoxicity against cancerous SK-OV-3 cells, suggesting selectivity towards the parasite [207]. The known metabolite 2-isopropenyl-6-acetyl-8-methoxy-1,3-benzodioxin-4-one (**337**), with an additional oxygen atom in the lactone ring, was also isolated as the main antiplasmodial constituent from a *Carpesium divaricatum* (Asteraceae) extract [208]. The dichloromethane extract of *Malleastrum* sp. (Meliaceae) showed antiplasmodial activity against the Dd2 strain with IC_{50} = 1.3 µg/mL. A new butanolide lactone, malleastrumolide A (**338**), was subsequently isolated from the active extract and was found to inhibit Dd2 parasites, but it was also cytotoxic against A2780 cancer cells [209].

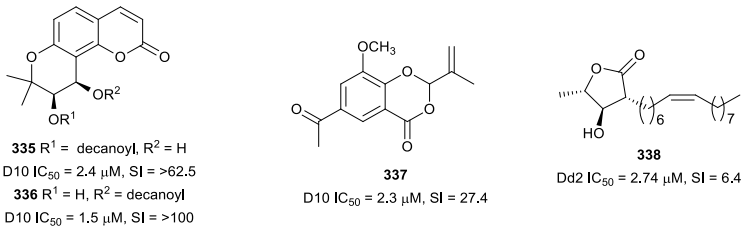

Fig. 43 Structures of coumarins and lactones

Phenolic acids, phenylethanoids, phenylpropanoids and other shikimic acid-derived metabolites

The leaf extract of *Dacryodes edulis* (Burseraceae), a West African traditional medicinal plant, exhibited antiplasmodial activity against 3D7 and Dd2 parasites (IC_{50} = 6.45 and 8.62 µg/mL, respectively) [210]. Antiplasmodial screening of the stem bark extract showed that it was also active with an IC_{50} of 4.34 and 6.43 µg/mL against 3D7 and Dd2 strains, respectively. Chemical investigations of the stem bark extract afforded methyl gallate (**339**) (Fig. 44) as the most active compound against the same parasite strains without cytotoxicity against LLC-MK2 cells. Preliminary investigations showed that **339** acts on late-stage parasite trophozoites and schizonts. Compound **339** also acts in synergism with quinine but had an additive effect with artemether [211]. A new gallic acid ester, 2,3,4-trihydroxy-2-methylbutyl gallate (**340**), with activity against D6 and W2 *P. falciparum*, was isolated from the aerial parts of *Limonium leptophyllum* (Plumbaginaceae). The compound was almost twice as active against the chloroquine-resistant W2 strain as against the chloroquine-sensitive D6 strain [212].

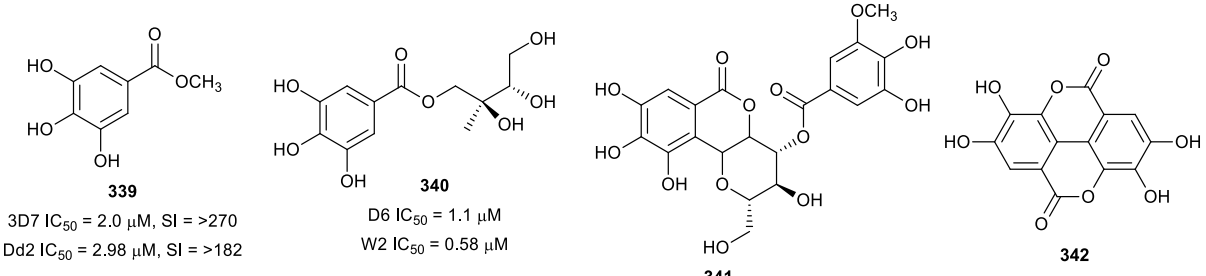

Fig. 44 Structures of coumarins and lactones

Likewise, a galloylated norbegenin derivative, 4-*O*-(3'-methylgalloyl)norbergenin (**341**), was obtained as the most active antiplasmodial constituent of *Diospyros sanza-minika* (Ebenaceae) stem bark extract. Norbegenin, which was also isolated from the same extract, was 32 times less active (40.15 µM), indicating that the additional galloyl group is beneficial to the antiplasmodial activity [213]. Antiplasmodial activity was demonstrated for *Anogeissus leiocarpus* (Combretaceae) methanol bark extract (IC_{50} = 18.8 µg/mL) and ellagic acid (**342**) was isolated as the most active antiplasmodial metabolite of the extract against 3D7 *P. falciparum* [214]. The *in vitro* and *in vivo* anti-malarial activity of ellagic acid was previously demonstrated with little cytotoxicity. It also has a synergistic effect in combination with chloroquine and artesunate [215].

The leaf extract of South American folkloric medicinal plant *Jacaranda glabra* (Bignoniaceae) exhibited antiplasmodial activity against the K1 strain. Bioassay-guided purification was subsequently used to isolate the phenylethanoid glucosides jacaglabrosides A-D (**343-346**) (Fig. 45). All four jacaranone-based glucosides (**343-346**) inhibited *P. falciparum* K1 strain. Compound **344-346** were not cytotoxic, but **343** showed cytotoxicity against L6 cells [216]. The ethyl acetate fraction of *Magnolia grandiflora* (Magnoliaceae) fruit and twig extracts inhibited Dd2 *P. falciparum* (IC_{50} = 10 µg/mL). The known, 4'-*O*-methyl honokiol (**347**) was the most active among the isolated bioactive neolignans against the Dd2 strain. The position and number of substituents on the neolignan aromatic rings affected the bioactivity. Honokiol, which is structurally similar to **347** but is not methoxylated, was six times less active (IC_{50} = 16.5 µM). However, magnolol, which is isomeric to honokiol, was only slightly less active (IC_{50} = 3.4 µM) than **347**, while an additional methoxy group on magnolol (3-methoxymagnolol)

resulted in a 30 fold decrease in activity [217]. More SAR studies are needed to fully understand the effect of substituents on the antiplasmodial activity of simple neolignans. A new dihydrobenzofuranoid neolignan, ococymosin (**348**), was obtained from the antiplasmodial hexane stem extract (IC_{50} = 1.25 µg/mL) of *Ocotea cymosa* (Lauraceae) as the most active metabolite against the Dd2 strain [218]. The antiplasmodial screening of a library of marine- and plant-derived extracts showed that *Grevillea* (Poorinda Queen, Proteaceae) leaf and twigs extract displayed antiplasmodial activity. Subsequent bioassay-guided purification of the active extract yielded the hemiquinone-containing phenylpropanoid glycosides robustasides D (**349**) and G (**350**) (Fig. 45) as the main antiplasmodial constituents. Both compounds were more active against chloroquine-resistant *P. falciparum* than to chloroquine-sensitive strains. Compound **350** was more active against the Dd2 and K1 strains whereas **349** was more active against the multidrug-resistant TM93-C1088 and TM90-C2B strains. Treatment of *P. berghei* infected mice with 32 mg/kg dose of **350** twice a day for four days suppressed parasitaemia by 95% without evidence of toxicity [219]. The phenylpropanoid glycoside vanicoside F (**351**), isolated as a major constituent of *Polygonum hydropiper* (Polygonaceae) aerial parts, also inhibited *P. falciparum* D6 and W2 strains without cytotoxicity against Vero cells [220].

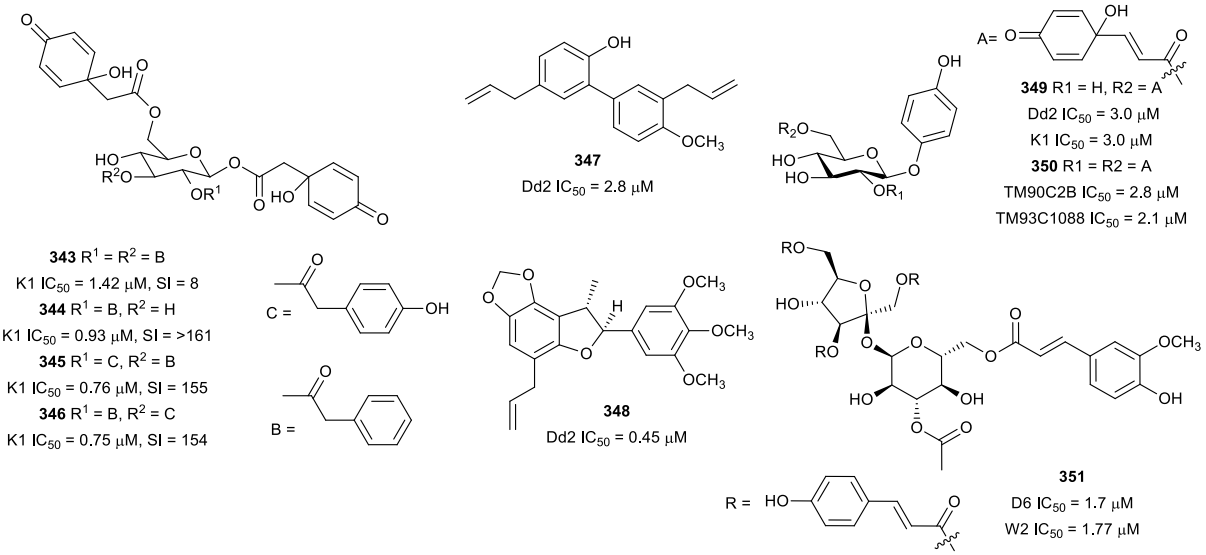

Fig. 45 Structures of phenylethanoids and phenylpropanoids

The culture broth of the *Penicillium* sp. FKI-4410 (*Penicillium viticola* sp. nov) fungus afforded some tropolones, among which puberulic acid (**352**) and a new derivative viticolin B (**353**) (Fig. 46) showed activity. Compound **352** showed potent nM activity against K1 and FCR3 parasites and was not cytotoxic against MCR-5 cells, whereas **353** was less active and selective. Treatment of *P. berghei*-infected mice with 2 mg/kg of **352** for three days suppressed parasitaemia by 69%, comparable to chloroquine and artesunate. A preliminary SAR of the tropone compounds suggests that a hydroxy group at C-7 and a methoxy group at C-2 are important for activity while a carboxylic acid function at C-4 improves selectivity [221].

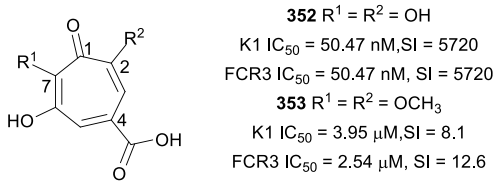

Fig. 46 Structures of tropones

A phytochemical reinvestigation of *Cleistochlamys kirkii* (Annonaceae) leaf extract led to the isolation of new polyoxygenated cyclohexenones cleistodienediol (**354**), cleistodienol B (**355**) and the known cleistodienol A (**356**) (Fig. 47). The configuration of the exocyclic double bond in **356** was revised based on the similarity of the nuclear magnetic resonance spectroscopic and optical rotation data with those of **354**. The absolute configuration of **354** was established by X-ray diffraction analysis, which showed that it adopts a half-chair conformation. All three compounds inhibited 3D7 and Dd2 *P. falciparum* strains but were also cytotoxic against noncancerous HEK-293 and cancerous MDA-MB-231 cells. The additional acetylation of compound **356** led to a decrease in activity and selectivity, suggesting a SAR role that could be further explored [222].

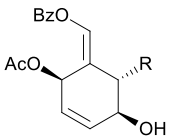

354 R = OH
3D7 IC_{50} = 0.20 μM, SI = 14
Dd2 IC_{50} = 0.48 μM, SI = 5.6
356 R = OAc
3D7 IC_{50} = 0.62 μM, SI = 4
Dd2 IC_{50} = 3.4 μM, SI = 1

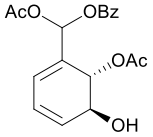

355
3D7 IC_{50} = 1.2 μM, SI = 3
Dd2 IC_{50} = 2.2 μM, SI = 1.6

Fig. 47 Structures of oxygenated cylcohexenones

The strobilurins are used commercially in agriculture as fungicides. An investigation of the extracts from the fungus *Favolaschia tonkinensis* led to the isolation of the β-methoxyacrylate derivatives, 9-methoxystrobilurins A, B, and G (**357**-**359**), and oudemansin B (**360**) (Fig. 48). The compounds were active against K1 *P. falciparum* strain and weakly cytotoxic against Vero cells [223].

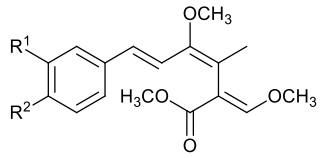

357 R^1 = R^2 = H
K1 IC_{50} = 1.35 μM, SI = 55
358 R^1 = OCH_3, R^2 = Cl
K1 IC_{50} = 0.85 μM, SI = 26

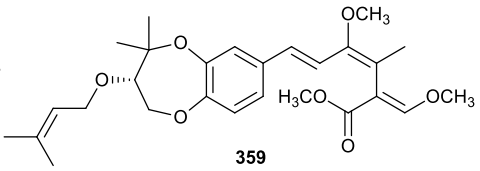

359
K1 IC_{50} = 0.06 μM, SI = 799

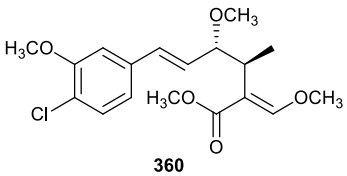

360
K1 IC_{50} = 1.12 μM, SI = 36

Fig. 48 Structures of strobilurins

Xanthones

The extract from fruit pericarp of *Pentadesma butyracea* (Clusiaceae) exhibited antiplasmodial activity against W2 parasites with IC_{50} = 1.8 μg/mL. Bioassay-guided purification of the extract yielded the new prenylxanthone pentadexanthone (**361**), together with the known cratoxylone (**362**), garcinone E (**363**) and α-mangostin (**364**) (Fig. 49). All four xanthones were active against *P. falciparum* W2 strain [224]. The antiplasmodial activity of **363** from the same plant against FcB1 was previously reported, but it was also cytotoxic against MCF-7 cells [225]. Xanthone **364** was isolated from *Garcinia mangostana* (mangosteen, Clusiaceae) husk and it inhibited FCR3 *P. falciparum* but, surprisingly, it was much less active against the 3D7 strain. Intraperitoneal treatment of *P. berghei* infected mice with **364** at 100 mg/kg suppressed parasitaemia by 80%. Oral treatment produced only 27% suppression. The compound was not cytotoxic to U-937 cells (LC_{50} = 130.6 μM), but produced haemolysis of red blood cells at 69.7 μM [226]. Another prenylated xanthone, macluraxanthone (**365**), was isolated from an antiplasmodial extract of *Allanblackia floribunda* (Clusiaceae) and had activity against the F32 and FcM29 parasites [193]. *Hypericum lanceolatum* (Hypericaceae) is a multipurpose medicinal plant that

is used by the people in the southwest province of Cameroon to treat fever [227]. In an effort to rationalize this ethnomedicinal use scientifically, the stem bark ethyl acetate fraction was assayed and antiplasmodial activity was observed against the W2mef parasite, IC_{50} = 5.02 µg/mL. A bioassay-guided purification of the extract afforded 5-hydroxy-3-methoxyxanthone (**366**) as the most active compound. It inhibited *P. falciparum* SHF4 field isolate but was slightly less active against the W2mef strain. The compound was not cytotoxic against LLC-MK2 cells at the highest concentration tested (100 µg/mL). Interestingly, the 3-hydroxy-5-methoxy isomer of **366** was inactive, suggesting that substitution pattern of the xanthone skeleton play a crucial role in the bioactivity [228]. *Garcinia* species produce a unique group of metabolites called caged *Garcinia* xanthones (CGXs) in which the C-ring of the xanthone skeleton has a prenyl substituent that has been transformed to form a tricyclic ring. It was observed that these compounds with interesting bioactivities tend to localize in cell mitochondria and cause damage to it [229]. Gambogic acid (**367**) (Fig. 49), the representative CGX, was isolated from *Garcinia* (Gamboge) resin and exhibited antiplasmodial activity against Dd2 parasites with a sub-micromolar IC_{50} value. Chemically modified analogues **368** and **369** that incorporated a triphenylphosphonium group into the CGX skeleton displayed low nanomolar activity against parasite trophozoites and schizonts, whereas replacement of the CGX scaffold with a planar xanthone structure led to a reduction in activity. These observations indicate the beneficial effect of conjugating a triphenylphosphonium moiety to the CGXs and the vital role of the CGX scaffold in the activity of these compounds. The CGXs caused mitochondrial fragmentation and morphological changes within the parasite but did not affect the mitochondrial electron transport chain. This suggests a different mechanism of action from other anti-malarial drugs, such as atovaquone, that target parasite mitochondria. The cytotoxicity of the compounds against HEK293 cells was in the µM range making them selectively toxic to the parasite at the active concentration (SI >100) [230]. A tetrahydroxanthone dimer, dicerandrol D (**370**), from the endophytic fungus *Diaporthe* sp. (CY-5188) also inhibited *P. falciparum* with a sub-micromolar IC_{50} value and moderate cytotoxicity. The bioactivity is influenced by the configuration and the C-12 epimer, dicerandrol B, was inactive [231].

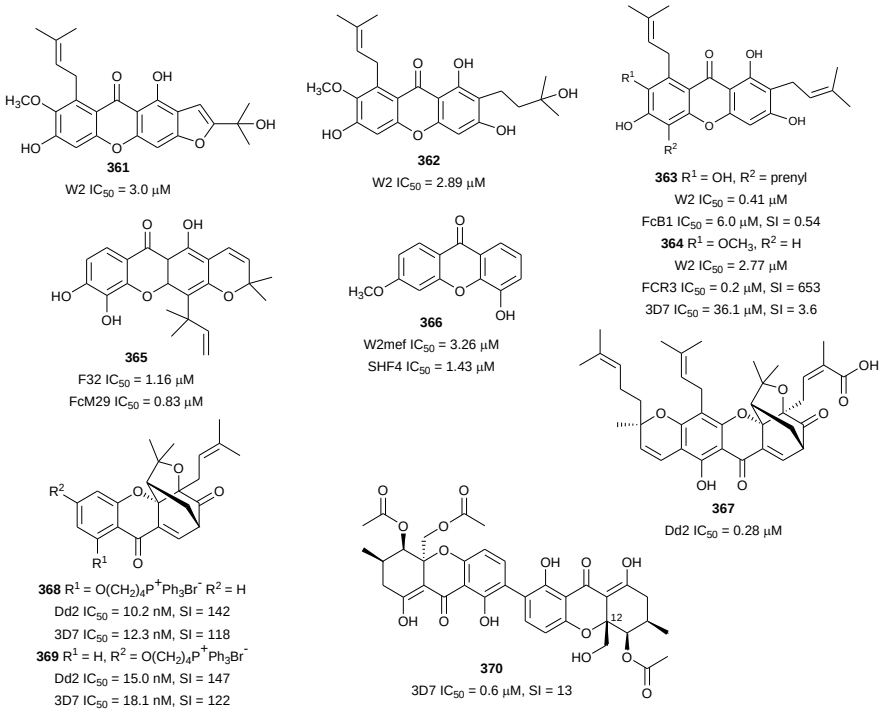

Fig. 49 Structures of xanthones

Phloroglucinol derivatives

Two new dimeric phloroglucinols mallotojaponins B (**371**) and C (**372**) (Fig. 50) were obtained from *Mallotus oppositifolius* (Euphorbiaceae) leaf and inflorescence ethanol extract. Both compounds were active against the Dd2 parasite and cytotoxic against cancerous A2780 cells. Also, the compounds displayed cytocidal activity against the HB3 (LD_{50} 14.6 and 0.81 µM for **371** and **372**, respectively) and Dd2 strains (LD_{50} = 6.7 and 0.8 µM for **371** and **372**, respectively). Mallotophenone, isolated from the same plant, lacked the prenyl chain of the mallotojaponins and was inactive. Also, **372** with two prenyl chains was more active than the monoprenylated **371**, suggesting that prenylation is essential for the antiplasmodial activity of these compounds [232]. The synthesis of mallotojaponin C (**372**) was demonstrated in a three-step procedure [233]. Seven new polycyclic polyprenylated acylphloroglucinols (PPAPs), symphonones A (**373**), C-E (**374-376**), G (**377**), H (**378**), and 14-deoxy-7-epi-isogarcinol (**379**) have been isolated from *Symphonia globulifera* (Clusiaceae) root bark extract. It was previously observed that the extract inhibited *P. falciparum* by 97% at a concentration of 10 µg/mL. These benzophenone derivatives were active against FcB1 *P. falciparum* but were also cytotoxic against MRC-5 cells [234].

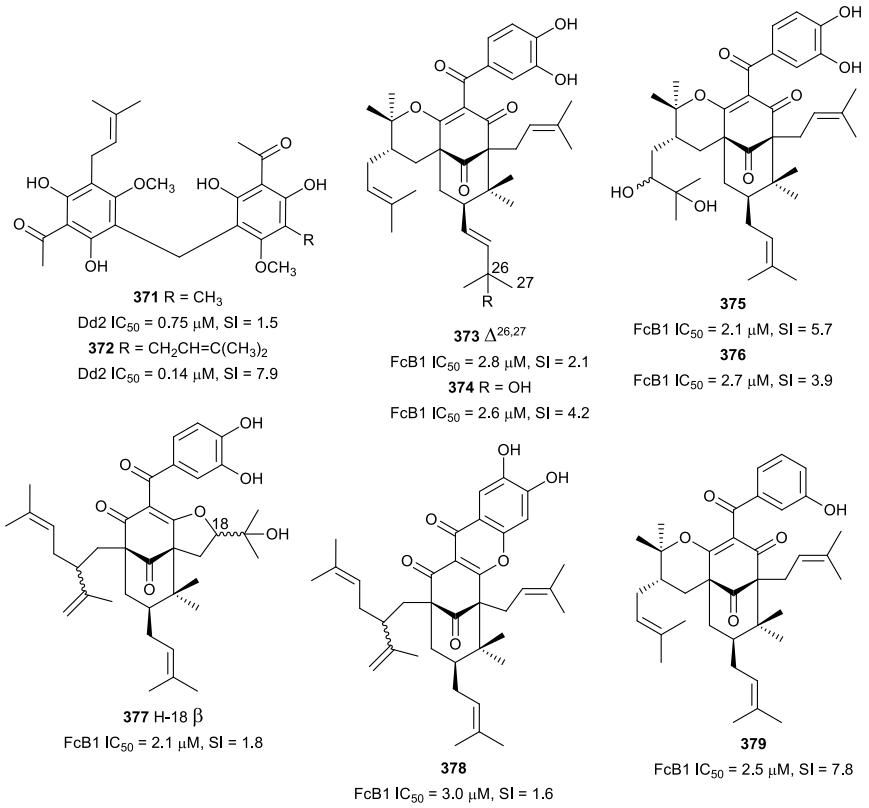

Fig. 50 Structures of phloroglucinol derivatives

β-Triketones

This interesting antiplasmodial scaffold is present in compounds isolated from plants of the Myrtaceae. These compounds have been isolated as adducts of phloroglucinol and terpenes as well as simple acylated syncarpic acid derivatives. A new phloroglucinol β-triketone rhodomyrtosone F (**380**) (Fig. 51) from *Syncarpia glomulifera* (Myrtaceae) stem bark extract, displayed sub-micromolar inhibition of Dd2 *P. falciparum* and only inhibited HEK293 cells by 58% at 50 µM, suggesting selective toxicity to parasites [235]. Likewise, rhodomyrtone (**381**), from the flower extract of *Angophora*

woodsiana (Myrtaceae), was active against 3D7 and Dd2 parasites but moderately cytotoxic [236]. Tomentosone A (**382**), with a novel hexacyclic ring system that features a bisfurano moiety, was isolated from the dichloromethane extract of *Rhodomyrtus tomentosa* leaves (Myrtaceae). The compound inhibited 3D7 and Dd2 parasites without being cytotoxic against HEK293 cells at 40 µM [237].

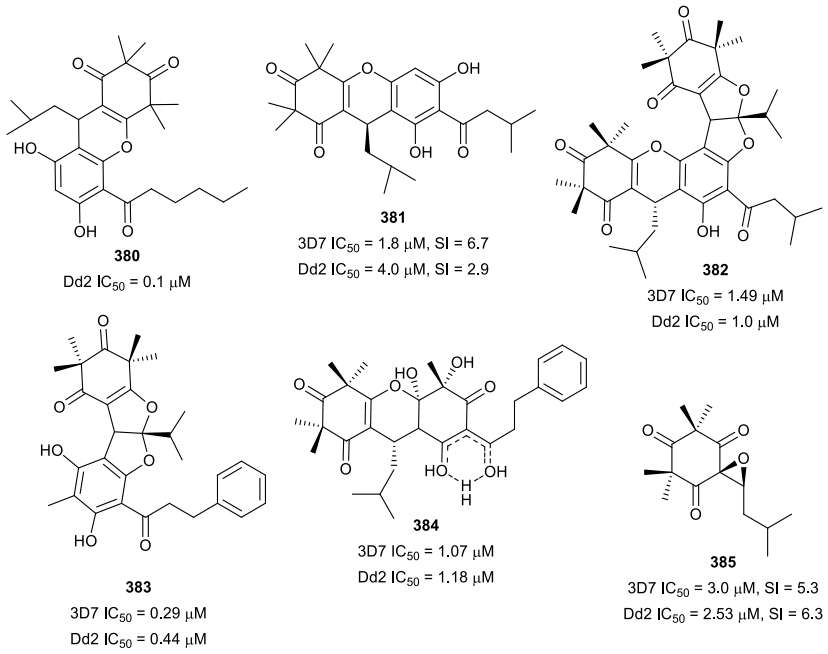

Fig. 51 Structures of β-triketones

Watsonianones B (**383**) and C (**384**), from the flowers of *Corymbia watsoniana* (Myrtaceae), have also shown antiplasmodial activity [238]. Watsonianone C is the first 4,4a,9,9a-tetrahydro-2*H*-xanthene-1,3,5,7(6*H*,8*H*)-tetraone to be reported while watsonianone B possesses the rare bisfurano moiety present in **382** and is only the fourth fused bisfurano-β-triketone to be reported. Compounds **383** and **384** exerted antiplasmodial activity on the parasite ring stage with **383** acting predominantly on early ring stage trophozoites. Tomentosone A (**382**), with an additional syncarpic acid moiety and an isobutyl instead of the ethylphenyl group, was less active than **383**. The beneficial role of the ethylphenyl over the isobutyl chain was further demonstrated by the activity of rhodomyrtosone A, which was 50 times less than that of **383** [238]. Woodsianone B (**385**), a simple acylated syncarpic acid derivative with an epoxide-containing isopentyl side chain, was also obtained from *Angophora woodsiana* and inhibited the 3D7 and Dd2 parasites [236]. Unfortunately, the terpene-β-triketone adducts demonstrated only weak antiplasmodial activity, and this was attributed to poor water solubility of the compounds. Indeed, the more water-soluble analogues have shown better activity. It is plausible that improving the water solubility might lead to more active compounds. The β-triketone pharmacophore can be considered as a novel antiplasmodial scaffold [236].

Other polyphenols

Atranorin (**386**) was isolated from the antiplasmodial *Kigelia africana* (Bignoniaceae) bark extract and inhibited the CAM10, SHF4 and W2 parasite strains. The polyphenolic depside **386** also inhibited W2mef parasites and showed synergism in combination with artemether [117, 118].

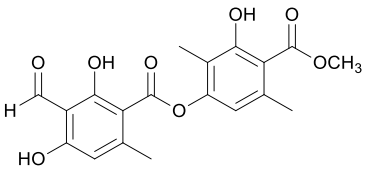

386
W2mef IC_{50} = 1.78 μM
W2 IC_{50} = 2.9 μM, SI = 16.8
SHF4 IC_{50} = 2.78 μM, SI = 26.7
CAM10 IC_{50} = 2.81 μM, SI = 26.5

Fig. 52 Structure of atranorin

Quinones and polyketides

Anthraquinones

An antiplasmodial screening of 6900 extracts identified *Kniphofia ensifolia* (Asphodelaceae) dichloromethane extract as active against Dd2 parasites (IC_{50} = 6 μg/mL) [239]. Bioassay-guided fractionation afforded the bisanthraquinones chryslandicin (**387**) and 10-(chrysophanol-7-yl)-10-hydroxy-chrysophanol anthrone (**388**), and the phenylanthraquinone, knipholone (**389**) as active principles (Fig. 53). The compounds displayed activity against Dd2 *P. falciparum* but were also moderately cytotoxic to cancerous A2780 cells [239]. Inhibition of the 3D7 strain was previously reported for all the three compounds, but **387** and **388** were not cytotoxic against KB cells [240]. Aloe-emodin, which was also isolated from *Kniphofia ensifolia*, was less active against the Dd2 parasites (IC_{50} = 58 μM) and did not exhibit antiproliferative activity against A2780 cells. However, a semi-synthetic derivative of aloe-emodin, the 3,4-di-*O*-methylcaffeoyl ester **390**, potently inhibited *P. falciparum* without being cytotoxic [239]. The crude extract of *Kniphofia foliosa* root also inhibited *P. falciparum* W2 and D6 strains with IC_{50} = 11.29 and 8.92 μg/mL, respectively. A reinvestigation of the extract yielded a new bisanthraquinone, 10-(chrysophanol-7-yl)-10-methoxy-chrysophanol anthrone (**391**), and the compound was more active against the chloroquine-resistant W2 strain than against the D6 strain [241].

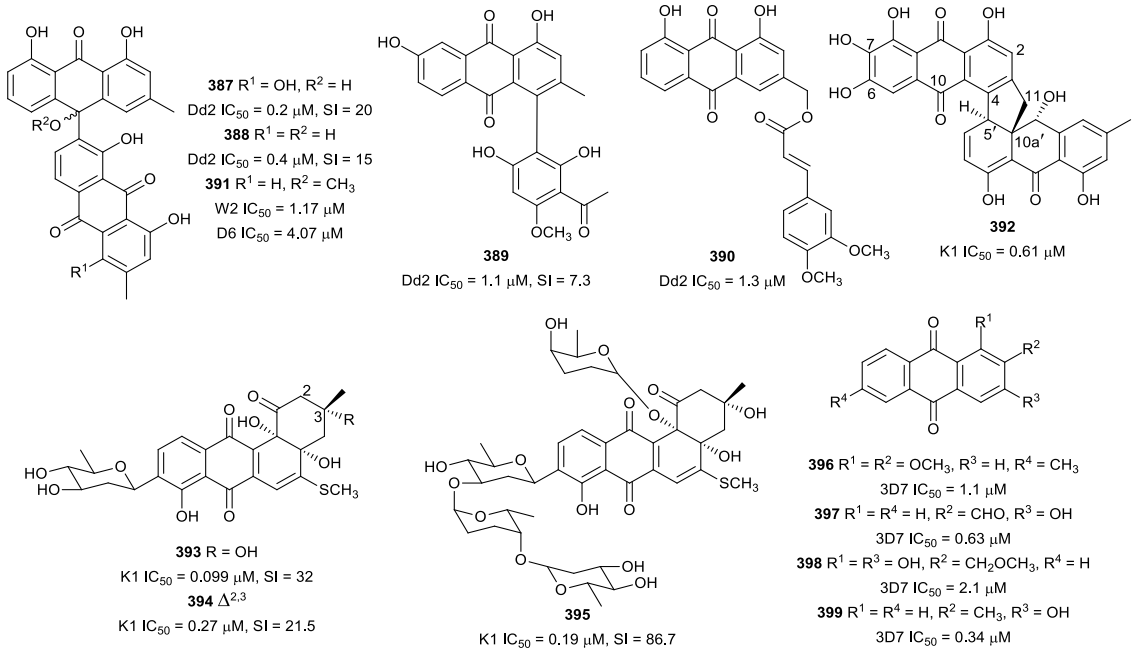

387 R^1 = OH, R^2 = H
Dd2 IC_{50} = 0.2 μM, SI = 20
388 R^1 = R^2 = H
Dd2 IC_{50} = 0.4 μM, SI = 15
391 R^1 = H, R^2 = CH_3
W2 IC_{50} = 1.17 μM
D6 IC_{50} = 4.07 μM

389
Dd2 IC_{50} = 1.1 μM, SI = 7.3

390
Dd2 IC_{50} = 1.3 μM

392
K1 IC_{50} = 0.61 μM

393 R = OH
K1 IC_{50} = 0.099 μM, SI = 32
394 $\Delta^{2,3}$
K1 IC_{50} = 0.27 μM, SI = 21.5

395
K1 IC_{50} = 0.19 μM, SI = 86.7

396 R^1 = R^2 = OCH_3, R^3 = H, R^4 = CH_3
3D7 IC_{50} = 1.1 μM
397 R^1 = R^4 = H, R^2 = CHO, R^3 = OH
3D7 IC_{50} = 0.63 μM
398 R^1 = R^3 = OH, R^2 = CH_2OCH_3, R^4 = H
3D7 IC_{50} = 2.1 μM
399 R^1 = R^4 = H, R^2 = CH_3, R^3 = OH
3D7 IC_{50} = 0.34 μM

Fig. 53 Structures of anthraquinones

The leafhopper pathogenic fungus *Torrubiella sp.* BCC 28517 also produced a dimeric anthraquinone, torrubiellin B (**392**), with activity against K1 *P. falciparum*. The new compound, which had rare C-4 – C-5' and C-11 – C-10a' linkages, was cytotoxic against cancerous human KB, NCI-H187 and MCF-7 cells. The structural analogue torrubiellin A, with two less hydroxy groups (C-6 and C-7), was ten times less active against parasites [242]. Antiplasmodial screening of crude extracts of marine actinomycetes from Thailand identified *Streptomyces sp.* BCC45596 to have potent activity with IC_{50} = 1.45-3.56 µg/mL. Bioassay-guided purification of the extracts led to the isolation of two new *C*-glycosylated benz[α]anthraquinones, urdamycinone E (**393**) and G (**394**), and the known urdamycin E (**395**). Sub-micromolar antiplasmodial activity was obtained for these compounds against the K1 strain. However, the compounds also showed antiproliferative activity against cancerous KB, MCF-7, NCI-H187 cells, but were less cytotoxic against non-cancerous Vero cells [243]. The antiplasmodial activity of four more anthraquinones (**396-399**) from an active root extract of *Rennellia elliptica* (Rubiaceae) was demonstrated [244].

Naphthoquinones

The leaf extract of *Pentas longiflora* (Rubiaceae), which is used in Kenyan folk medicine to treat malaria, was active against *P. falciparum* [245]. Antiplasmodial investigation of the root extract showed a better activity against the W2 and D6 parasites than the leaf extract (IC_{50} = 0.93 and 0.99 µg/mL, respectively). Phytochemical investigation yielded the pyranonaphthoquinones, pentalongin (**400**) and psychorubrin (**401**) (Fig. 54) with antiplasmodial activity against W2 and D6 strains. However, both compounds were also cytotoxic [246]. The ethyl acetate extract of *Markhamia tomentosa* (Bignoniaceae) stem bark showed activity against the W2 and K1 strains (IC_{50} = 1.46 and 2.81 µg/mL, respectively). Two furanonaphthoquinones (**402** and **403**) were isolated from the extract and inhibited the W2 and K1 parasites. However, **402** and **403** were also cytotoxic against L6 cells [247]. Plumbagin (**404**) is the major phytochemical in the extracts of several *Plumbago* species (Plumbaginaceae), including *Plumbago indica* and *Plumbago zeylanica*, with anti-malarial activity [248, 249]. Plumbagin (**404**) inhibited 3D7 and K1 *P. falciparum* strains and suppressed parasitaemia in *P. berghei*-infected mice by 41% after treatment (25 mg/kg body weight). Acute and subacute toxicity was observed in mice after oral administration of **404** above 100 and 25 mg/kg body weight, respectively. The relatively poor *in vivo* anti-malarial activity of **404** might be due to low bioavailability in living cells [250].

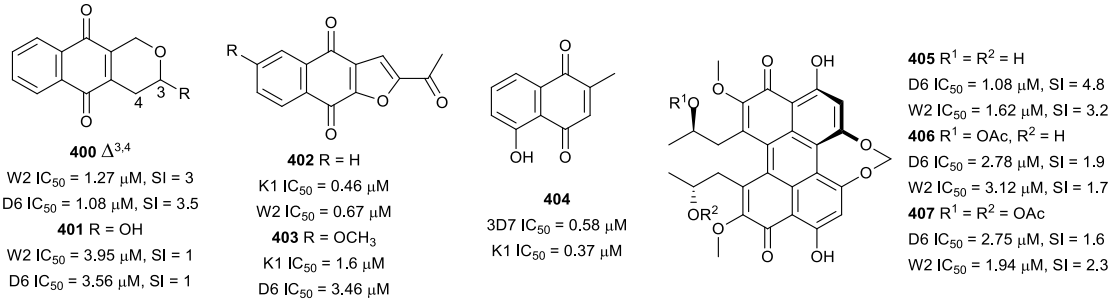

Fig. 54 Structures of other quinones

Perylenequinones

The perylenequinones cercosporin (**405**), 14-*O*-acetylcercosporin (**406**), and di-*O*-acetylcercosporin (**407**) (Fig. 54) were isolated from the culture medium of the plant pathogenic fungus, *Septoria*

pistaciarum. Compound **405** was also obtained from an extract of the endophytic fungus *Mycosphaerella* sp. F2140. The phytotoxins **405-407** inhibited *P. falciparum* D6 and W2 strain but were also cytotoxic against MCF-7 and Vero cells. Interestingly, a new cercosporin analogue with a hydroxy and a methoxy group instead of the methylenedioxy bridge in **405-407** was inactive. This suggests a SAR role at these two positions that could be exploited for optimized antiparasitic activity [251, 252].

Other polyketides

The Solomon Island-sourced marine sponge, *Xestospongia testudinaria* produced a halenaquinone-type polyketide 3-ketoadociaquinone A (**408**) (Fig. 55), which selectively inhibited the FcB1 and 3D7 strains. Halenaquinone, which differs from **408** only in the absence of the dioxothiazine ring, was inactive, indicating that a dioxothiazine ring is necessary for the antiplasmodial activity of the compound [253]. The crude extract of terrestrial *Streptomyces* sp. BCC71188 from Thailand inhibited *P. falciparum* (IC_{50} = 0.19 µg/mL). Two benzoquinone polyketides, geldanamycin (**409**) and 17-demethoxyreblastatin (**410**) were isolated from the extract and showed antiplasmodial activity against the K1 strain. The quinone moiety in **409** appears to contribute to the cytotoxicity since the structural analogue **410** with a phenol group instead of the quinone was more selective against the parasite [254]. Two new antiplasmodial azaphilones, longirostrerone A (**411**) and C (**412**), were isolated from the ethyl acetate extract of the Thailand soil fungus, *Chaetomium longirostre*. Both compounds inhibited K1 *P. falciparum* but were also cytotoxic against cancerous KB cells. Compound **411** was also cytotoxic against NCIH-187 and MCF-7 cancer cells, whereas **412** was inactive, indicating selective cytotoxicity [255]. Longirostrerone D, which differs from **411** in the configuration of the isochromeno-lactone ring junction and had a double bond in the butyrolactone ring, was inactive. Likewise, longirostrerone B, which lacks the lactone moiety, was less active. These observations suggest that the nature of the six-membered ring attached to isochromene, the lactone ring, and the configuration of the compounds play a role in the activity and further modifications might produce analogues that are more selective.

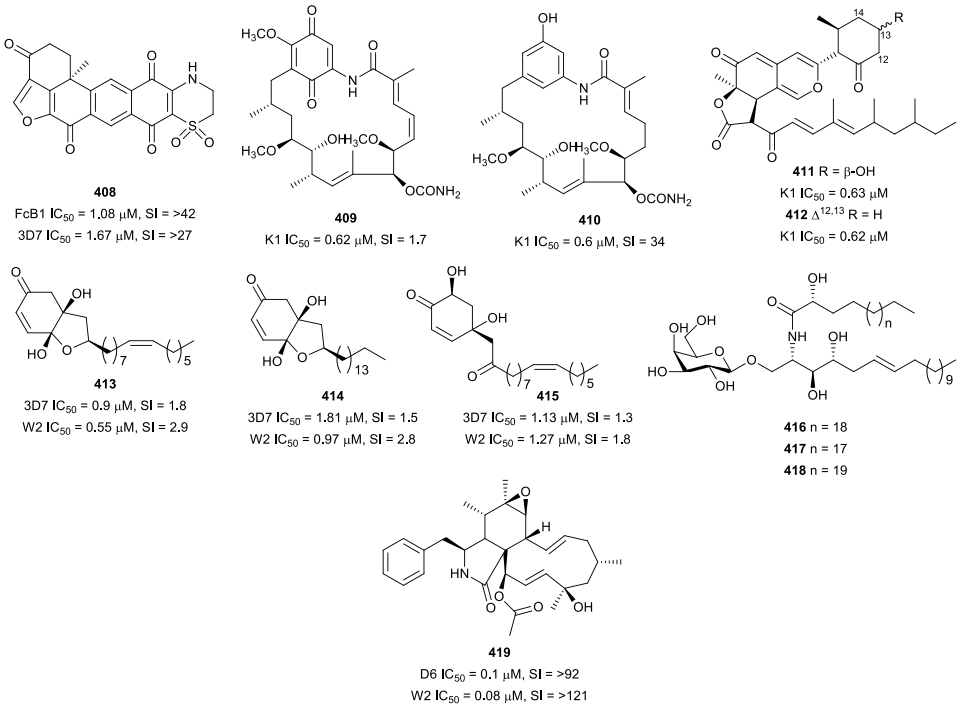

Fig. 55 Structures of other polyketides

Three other new cyclohexenones, poupartones A-C (**413-415**) were isolated from the ethyl acetate leaf extract of *Poupartia borbonica* (Anacardiaceae) by bioassay-guided fractionation [256]. The extract was previously shown to inhibit the 3D7 strain of *P. falciparum* with IC_{50} = 3.28 µg/mL. The compounds were active against W2 and 3D7 parasites but were also cytotoxic against HeLa and WI38 cells. No haemolytic activity was observed with the compounds, indicating that the antiplasmodial activity was due to direct action on the parasites. Treatment of *P. berghei*-infected mice with **413** (15 mg/kg/day for four days) led to 69.5% parasite suppression, but it was also toxic to the mice. A toxicity assay of **413** using the zebrafish embryo model indicated that the compound might be cardiotoxic [256].

The Senegalese marine sponge, *Axinyssa djiferi* produced an antiplasmodial mixture containing three glycosphingolipids axidjiferosides A-C (**416-418**) (Fig. 55). The mixture represented 2.16% of the dried sponge lipid content, while axidjiferoside A (**416**) constituted 60% of the mixture. The compounds were identified as homologs of β-galactopyranosylceramide, containing a 2-amino-1,3,4-trihydroxy-octadecene sphingoid base. Moreover, the fatty acid methyl ester of the major compound (**416**) was identified as 2-hydroxytetracosanoic acid. The mixture exhibited antiplasmodial activity against the FcB1 strain (IC_{50} = 0.53 µM) and was not cytotoxic against a panel of cancerous cells. The activity also appeared to be parasite selective because *Leishmania donovani* and *Trypanosoma brucei* were not susceptible to the mixture [257]. The endophytic fungus *Diaporthe miriciae* produced epoxycytochalasin H (**419**) with potent antiplasmodial activity against D6 and W2 parasite strains. The compound was not cytotoxic against Vero cells, indicating that the toxicity to the parasite is selective [258].

Macrocycles

Macrolides

The bromophycolides are diterpene-benzoate macrolides that were isolated from the Fijian marine red alga *Callophycus serratus* and had antiplasmodial activity [259]. A reinvestigation of *Callophycus serratus* afforded bromophycolides R (**420**), S (**421**), and U (**422**) (Fig. 56) with antiplasmodial activity and moderate cytotoxicity against cancerous cells [260]. Bromophycolides with 15- and 16-membered rings have shown potent antiplasmodial activity. No significant influence of the lactone ring size on activity was observed between 15- and 16-membered lactone rings. The macrolide ring appears to improve bioactivity considering that non-macrocyclic diterpene-benzoic acids and diterpene-phenols were less active. Furthermore, isolation of the less active 14-membered ring callophycolide A (IC_{50} = 5.4 µM), which lacked the bromine atoms and a cyclohexane ring, showed that these features are not essential but improve the potency [259, 261]. Some bromophycolides target haem crystallization, suggesting that the mechanism of action involves the inhibition of haemozoin formation (Table 1) [262]. Bastimolide A (**423**), a 40-membered ring polyhydroxy macrolide with 10 stereocentres and a rare *tert*-butyl terminus, was isolated from marine cyanobacterium, *Okeania hirsuta* (PAB-19MAY11-4)[242]. The planar structure and absolute configuration of the macrocyclic lactone, which consist of a 1,3-diol, one 1,3,5-triol, and six 1,5-diols, were established by X-ray crystallography. It was hypothesized that the rare *tert*-butyl group near the lactone ester in the bastimolide structure protects the lactone ring against hydrolysis. The compound inhibited multidrug-resistant strains TM90-C2A, TM90-C2A, TM91-C235 and W2 with nanomolar IC_{50} values. Surprisingly, the chloroquine-

sensitive HB3 strain was less susceptible to **423** (IC_{50} in μM). Additionally, the semi-synthetic (2*E*)-isomer was more active against the HB3 strain than the (2*Z*) natural product. Further investigation of *O. hirsuta* yielded bastimolide B, in which lactonization produced a 24-membered ring and a highly oxidized side chain that terminated in a *tert*-butyl group. Bastimolide B was not as active as **423**, suggesting that the lactone ring size affects the potency [263, 264]. The Thailand marine sponge *Pachastrissa nux* exhibited antiplasmodial activity against K1 *P. falciparum* (IC_{50} = 0.7 μg/mL).

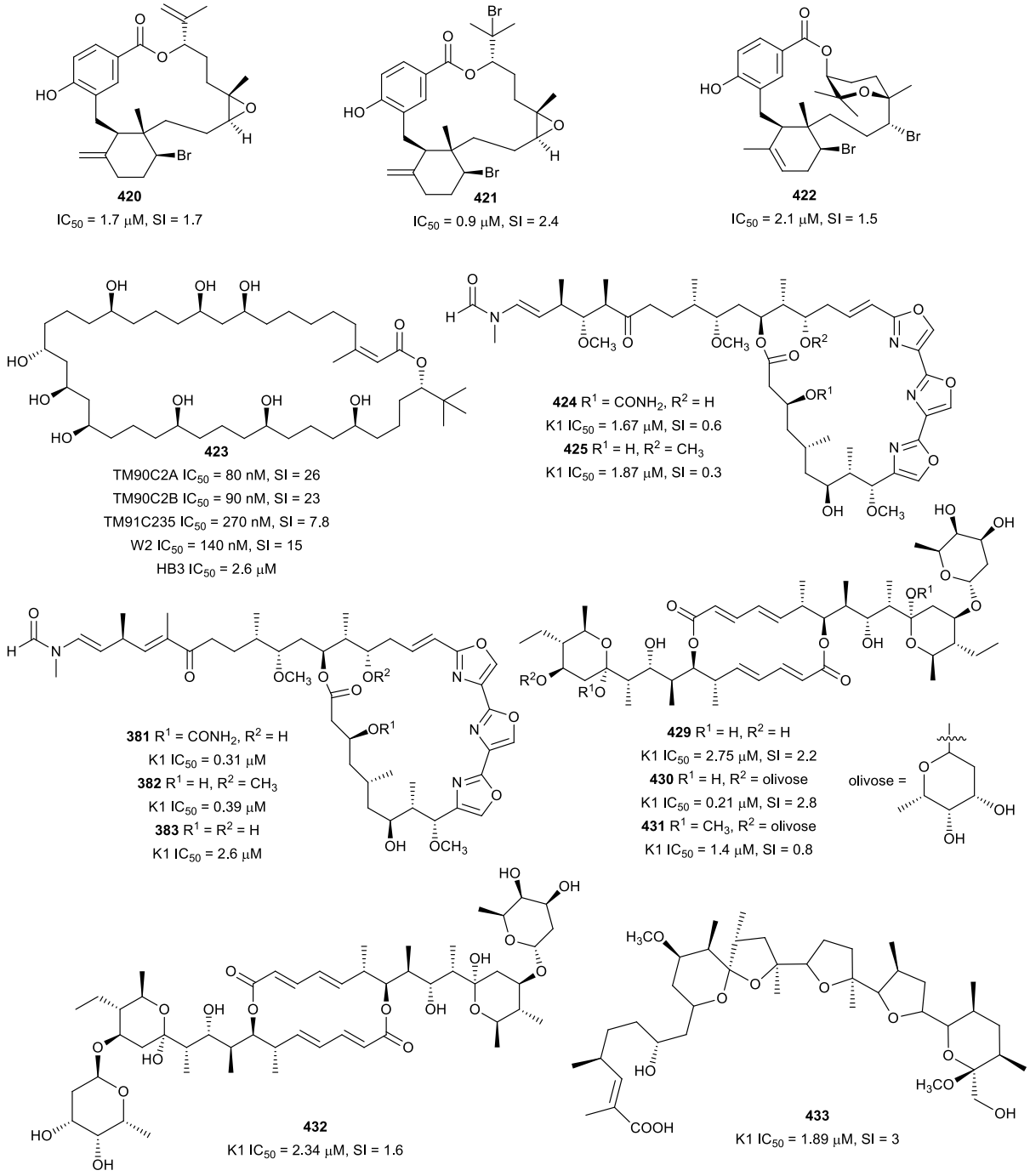

Fig. 56 Structures of macrolides

The 25-membered ring trisoxazole macrolides kabiramides B (**424**), D (**425**), and J-L (**426-428**) (Fig. 56) were subsequently isolated from the extract and were shown to inhibit K1 parasites. However, the compounds were also cytotoxic against cancerous MCF-7 cells and normal human fibroblasts [265,

266]. Likewise, the crude extract of terrestrial *Streptomyces* sp. BCC71188 afforded the macrolides, monoglycosylelaiolide (**429**), azalomycin B (**430**), and 11,11'-*O*-dimethylelaiophylin (**431**) as active metabolite against the K1 strain, but these compounds were also cytotoxic against cancerous and Vero cells [254]. *Streptomyces* sp. BCC72023, isolated from rice stems, produced the macrolide, efomycin G (**432**) and 29-*O*-methylabierixin (**433**), with activity against K1 *P. falciparum* [267].

Resorcylic acid lactones

The mycelial culture of the filamentous fungus, *Paecilomyces* sp. SC0924 produced the new 14-membered ring β-resorcylic acid lactones (RALs, Fig. 57) paecilomycins A (**434**), E (**435**), F (**436**), together with aigilomycin B (**437**) and aigialomycin F (**438**), all with potent antiplasmodial activity. Paecilomycin E (**435**) and aigialomycin F (**438**) showed sub-micromolar inhibition of 3D7 parasites, with all the compounds more potent against the 3D7 than the Dd2 strain, suggesting resistance by the Dd2 strain. The compounds were not cytotoxic against Vero cells at 50 µM [268]. Cochliomycins A-F are structural analogues of the paecilomycins and were initially isolated from the culture broth of *Cochliobolus lunatus* in trace quantities [269, 270]. Two cochliomycin analogues were subsequently isolated in larger amounts from an optimized fermentation broth, and the natural cochliomycins and some derivatives were obtained by semi-synthesis. In contrast to the paecilomycins, the cochliomycins generally showed poor antiplasmodial activity. However, semi-synthetic acetonide derivative **439** inhibited *P. falciparum* (SI = 184) selectively whereas the hydroxylated parent was inactive. Also, cochliomycin C, the chlorinated derivative of paecilomycin F (**436**), was inactive.

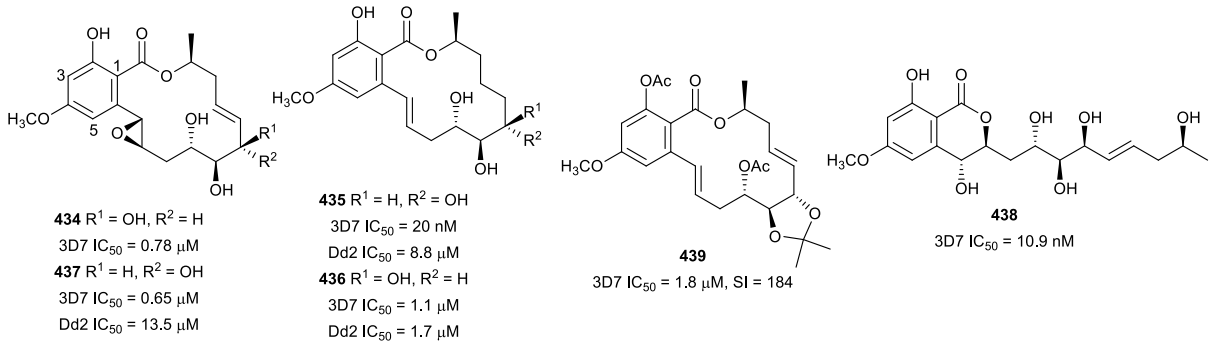

Fig. 57 Structures of resorcyclic acid lactones

SAR deductions from the RAL structures indicate that the presence of acetyl and acetonide groups on the lactone ring hydroxy groups improve activity, with the acetonide derivative having a superior activity. A chlorine atom on the aromatic C-5 decreases activity while the C-2 phenolic group is important for selective activity. The presence of an enone moiety in the lactone macrocycle contributes to cytotoxicity whereas the configuration of the 1,2,3-triol or 1,2-diol stereocentres had a negligible effect on the activity [271].

Cyclodepsipeptides and other peptides

The cyclodepsipeptides lagunamides A-C (**440-442**) (Fig. 58) were obtained from the marine cyanobacterium, *Lyngbya majuscula.* The planar lagunamide macrocyclic scaffold consists of peptide and polyketide substructures, and the main differences are in the polyketide part. Lagunamides A and B are 26-membered macrocycles whereas lagumanide C has an additional methylene carbon in the polyketide structure. The compounds exhibited potent antiplasmodial activity against NF54 *P.*

falciparum strain and were also cytotoxic against cancerous cells [272, 273]. The double bond in the side chain of **441** might be responsible for the lower activity. Mollemycin A (**443**), a glyco-hexadepsipeptide with a polyketide residue, was isolated from an Australian *Streptomyces* sp. CMBM0244 and had a potent nanomolar antiplasmodial activity. It was equally active against the 3D7 and Dd2 strains and only slightly cytotoxic against human fibroblast cells (SI > 20), suggesting selectivity against the parasites [274].

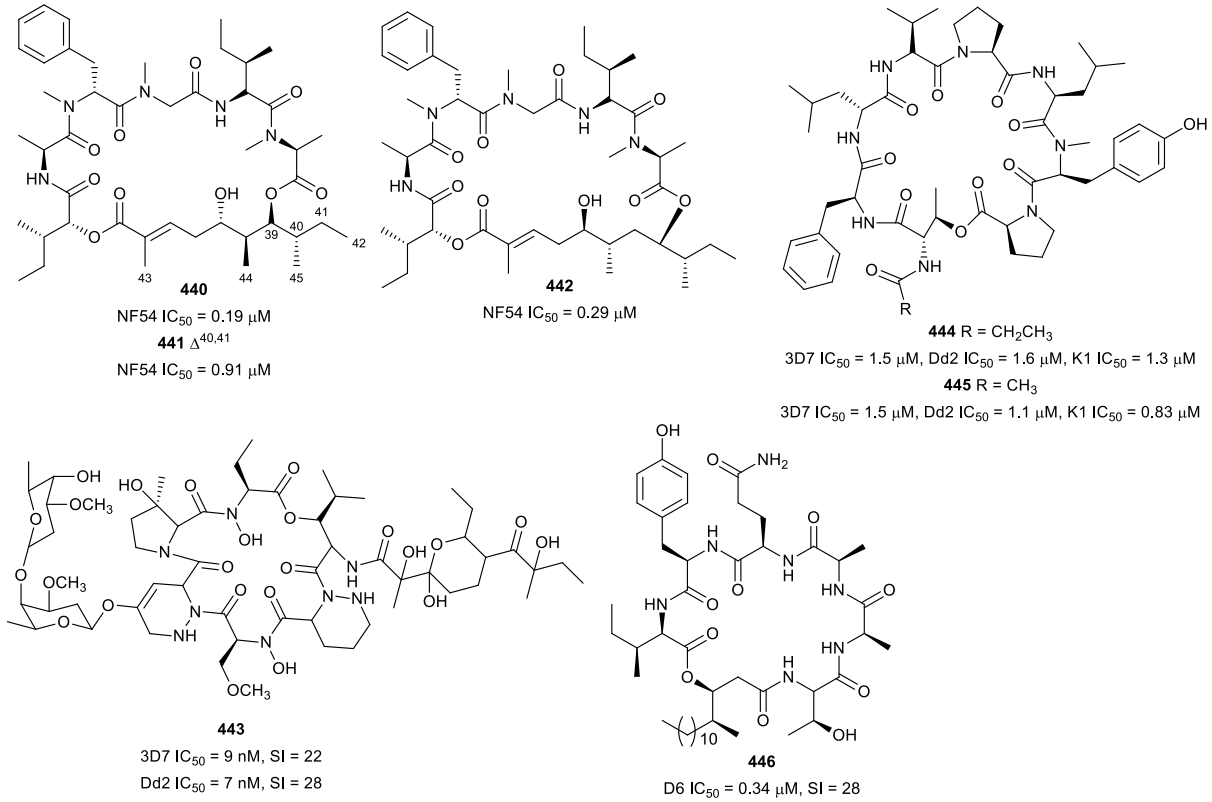

Fig. 58 Structures of cyclodepsipeptides

Two other antiplasmodial octacyclodepsipeptides, octaminomycins A (**444**) and B (**445**), were isolated from Indonesian soil *Streptomyces* sp. RK85-270. The octaminomycin amino acid sequence was established as cyclo-(Pro-*N*-MeTyr-Leu-Pro-Val-Leu-Phe-Thr). Furthermore, the only structural difference is the presence of propionyl and acetyl chains on the threonine nitrogen in **444** and **445**, respectively. Both compounds were active against 3D7, Dd2 and K1 strains, and were not cytotoxic at 30 μM [275]. A new cyclodepsipeptide incorporating a 3-hydroxy-4-methylpentadecanoic acid moiety, fusaripeptide A (**446**), was obtained from *Mentha longifolia* (Lamiaceae) root endophytic fungus, *Fusarium* sp. from Saudi Arabia. The amino acid sequence was established as cyclo-(Ala-Ala-Thr-Ile-Tyr-Glu). Compound **446** exhibited antiplasmodial activity against D6 *P. falciparum* and was moderately cytotoxic against cancerous L5178Y and PC12 cells [276].

Carmaphycin B (**447**) (Fig. 59), with an amino acid sequence of L-Val-L-Met sulfone-L-Leu, was isolated from the cyanobacterium, *Symploca* sp. The tripeptide with hexanoyl and an α,β-epoxyketone groups on the *N* and carboxyl ends, respectively, had potent nM *in vitro* and *in vivo* antiplasmodial activity, but it was also cytotoxic against HepG2 cells. The synthetically modified analogue **448** with a D-Val-L-Nle-L-Leu amino acid sequence showed improved antiplasmodial activity and selectivity (SI = 379). The peptides act in synergy with artemisinin and kill the parasite by targeting the β5 subunit of

Plasmodium proteasome (Table 1) [277]. A marine actinobacteria from Papua New Guinea, *Streptomyces bangulaensis*, produced the antiplasmodial tetrapeptide, actinoramide A (**449**). The compound displayed sub-micromolar antiplasmodial activity against *P. falciparum* Dd2, HB3, 7G8, GB4, and cp250 strains, and no cytotoxicity. The 25-epimer of **449**, 25-*epi*-actinoramide A was about 20-fold less active, suggesting an influence of the configuration on activity. Actinoramide F, which is structurally similar to **449** but has a 5-amino-5,6-dihydrouracil terminus instead of the cyclic 2-amino-4-ureidobutanoic acid of **449,** was inactive. This suggests that the terminal substructure of the actinoramides is crucial for antiplasmodial activity [278]. Furthermore, a new antiplasmodial cyclic tetrapeptide, apicidin F (**450**) was isolated from the rice fungus pathogen, *Fusarium fujikuroi*, and the amino acid composition was established to be L-tryptophan, D-pipecolic acid, L-phenylalanine, and L-2-aminooctanedioic acid [279].

Cyclopeptide alkaloids are 13, 14 or 15-membered ring polyamides with a styrylamine unit, a β-hydroxy amino acid and other common amino acid forming the macrocycle. The macrocyclic polyamide has an attached side chain which could be basic or neutral. Spinanine B (**451**) (Fig. 59), a cyclopeptide alkaloid from the stem bark of *Ziziphus spina-christi* (Rhamnaceae), inhibited the K1 strain of *P. falciparum* without cytotoxicity to MRC-5 cells at 64 µM [280]. Evaluation of the antiplasmodial activity of 19 cyclopeptide alkaloids facilitated some SAR conclusions. Preliminary SAR studies indicated that the 13-membered ring cyclopeptide alkaloids were generally more active than the 14 and 15 membered analogues. Also, a methoxy group on the styrylamine moiety was more favourable for antiplasmodial activity than a hydroxy group [281, 282].

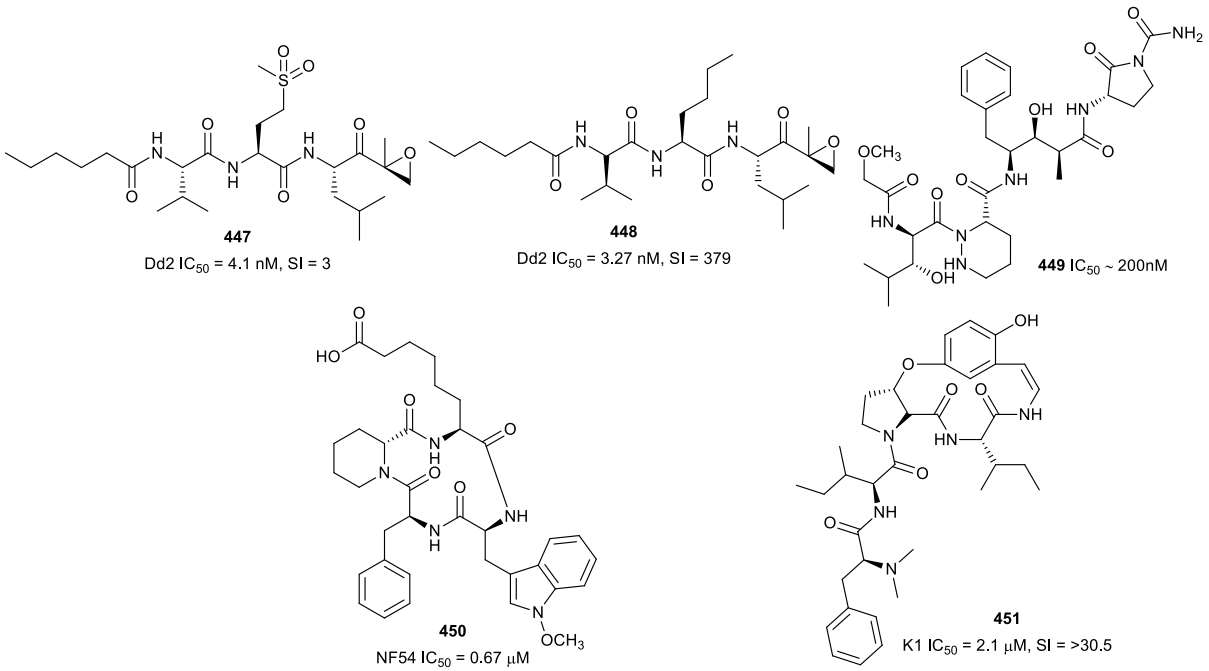

Fig. 59 Structures of other peptides

Cyclic phosphotriesters

A marine actinobacteria, *Salinospora* sp., produced a new class of antiplasmodial scaffolds based on a bicyclic phosphotriester core, substituted with alkyl chains. Among the new compounds, salinipostins A-D, F-G, and I (**452**-**458**) (Fig. 60) potently inhibited W2 *P. falciparum* without cytotoxicity. Preliminary

SAR findings indicated that an increase in alkyl chain length attached to the phosphoester oxygen (R^2) and vinyl carbon (R^1) led to increased activity while branching of the R^1 alkyl causes a slight reduction in activity. The most active **452** had sub-micromolar IC_{50} values and stage-specific activity on early stage parasite ring forms, but parasite trophozoites were less susceptible. The compound did not affect parasite schizonts, indicating that it acts by disrupting the processes required for the establishment or growth of intracellular parasites. Salinispostin A (**452**) did not inhibit haemozoin formation but appears to cause cellular disorganization and disintegration of internal structures. Moreover, experiments for resistance selection under three different conditions failed to identify mutant resistant strains, suggesting that the compound may be less susceptible to resistance development. These compounds represent a new class of antiplasmodial agents, and further biological studies on them are warranted [283].

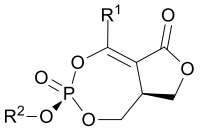

452 $R^1 = CH_3(CH_2)_3$, $R^2 = C_{15}H_{31}$
W2 IC_{50} = 0.05 μM

453 $R^1 = CH_3(CH_2)_3$, $R^2 = C_{14}H_{29}$
W2 IC_{50} = 0.139 μM

454 $R^1 = CH_3(CH_2)_3$, $R^2 = C_{13}H_{27}$
W2 IC_{50} = 0.415 μM

455 $R^1 = (CH_3)_2CHCH_2$, $R^2 = C_{14}H_{29}$
W2 IC_{50} = 0.082 μM

456 $R^1 = CH_3(CH_2)_2$, $R^2 = C_{15}H_{31}$
W2 IC_{50} = 0.266 μM

457 $R^1 = CH_3(CH_2)_2$, $R^2 = C_{14}H_{29}$
W2 IC_{50} = 1.52 μM

458 $R^1 = CH_3CH_2$, $R^2 = C_{15}H_{31}$
W2 IC_{50} = 0.126 μM

Fig. 60 Structures of cyclic phosphotriesters

Mechanism of action of antiplasmodial natural products: *Plasmodium* cellular targets identified for natural products

Understanding the mechanism of action of bioactive molecules facilitates the development of leads into improved therapeutic compounds and aids in the understanding of resistance evolution. Natural products have proven to be a prolific source of drug leads, but limited knowledge about the mechanism of action often impedes further development [284]. In order to understand the mechanism of action of anti-malarial natural products, it is necessary to identify the molecular targets in the parasite. The anti-malarial drugs in current use are based on pharmacophores acting on a small number of targets as their mechanism of action. The use of these compounds as monotherapy resulted in the emergence of multidrug-resistant parasites [285, 286]. Many of the candidates currently in the anti-malarial drug pipeline are based on chemical modification to overcome the handicaps of the traditional anti-malarials [287]. Eventual development of resistance to these new therapies when they become clinically useful is inevitable. Therefore, it is imperative to discover new therapeutics with novel targets and mechanisms of action. The increased understanding of the *Plasmodium* parasite biology following the sequencing of its genome has led to the identification of novel potential drug targets that are thought to be essential for parasite survival [288].

Crucial enzymes and macromolecules in the parasite fatty acid, haemoglobin, protein, Ca^{2+} metabolism, glyoxalase detoxification system, and protein folding pathways have been inhibited by natural products. Reports on natural products as inhibitors of potential and proven antiplasmodial targets together with the mechanism of action are summarized in Table 1. Natural products have also modulated their parasite killing effect by disrupting the haem detoxification systems as well as induction of oxidative stress and lipid peroxidation in the parasite (Table 1). Some natural products

have also been reported to mediate antiplasmodial activity by inducing morphological and ultrastructural changes that are detrimental to parasite viability [230, 289].

Natural products with transmission-blocking potentials

Malaria chemotherapy has focused mainly on controlling the disease. Thus, most anti-malarial drugs act on asexual blood stage parasites that are responsible for the clinical manifestations of the disease. However, there has been a shift in focus towards malaria elimination strategies. In this regard, compounds with activity against asymptomatic gametocytes and liver stage parasites, including hypnozoites (prophylaxis) are crucial to the eradication agenda. As yet, artesunate, artemether, methylene blue and primaquine are the known gametocidal agents, with primaquine being the only approved prophylactic and gametocytocidal drug [309]. Some natural products have shown transmission blocking potential by exhibiting activity against one or more of these parasite life cycle stages. These natural products are summarized in Table 2. Similarly, extracts from *Zanthoxylum heitzii*, *Vernonia amygdalina*, *Artemisia afra*, *Trichilia emetica*, *Turraea floribunda*, and *Leonotis leonurus* have shown gametocidal activity [65, 310, 311]. The standardized commercial preparation NeemAzal®, an azadirachtin-enriched neem extract, has also demonstrated potent transmission-blocking activity *ex vivo* and *in vivo* [312, 313]. The targeting of gametocytes is indeed of great importance in the fight against malaria. The limited information available in the literature on drugs with this activity may be a reflection of the difficulty of assaying gametocidal activity.

Table 1 Mechanism of action of antiplasmodial natural products.

Pathway	Mechanism of action	Target	Compound	Compound class	Reference
Fatty acid metabolism	Inhibition of type II fatty acid synthase (FAS II) enzymes	*Plasmodium falciparum* enoyl-ACP reductase (*Pf*FabI)	Oroidin	Bromopyrrole alkaloid	[290]
			Luteolin 7-*O*-β-D-glucopyranoside	Flavonoid glycoside	[291]
			Anthecularin	Sesquiterpene lactone	[292]
			4-Hydroxyanthecotulide	Sesquiterpene lactone	[293]
			4-Acetoxyanthecotulide	Sesquiterpene lactone	[293]
			Mucusisoflavone C	Flavonoid	[294]
			3-*O*-Methylquercetin	Flavonoid	[294]
			Isowighteone	Flavonoid	[294]
			Evernic acid	Phenolic acid	[295]
			Psoromic acid	Phenolic acid	[295]
			Methylenebissantin	Flavonoid	[296]
		Plasmodium falciparum β-ketoacyl-ACP reductase (*Pf*FabG)	Anthecularin	Sesquiterpene lactone	[292]
			4-Hydroxyanthecotulide	Sesquiterpene lactone	[293]
			4-Acetoxyanthecotulide	Sesquiterpene lactone	[293]
			Psoromic acid	Phenolic acid	[295]
		Plasmodium falciparum β-hydroxyacyl-ACP dehydratase (*Pf* FabZ)	Evernic acid	Phenolic acid	[295]
			Vulpic acid	Phenolic acid	[295]
			Psoromic acid	Phenolic acid	[295]
			Catechin gallate	Catechin	[297]
			Bromopyrrolohomoarginin	Bromopyrrole alkaloid	[93]

Detoxification of haem	Inhibition of β-haematin formation	Haem crystallization	Bromophycolide A	Macrocyclic meroditerpene	[262]
			Bergenin	Phenolic glycoside	[298]
			Fraxetin	Coumarin	[299]
			1,3,6-Trihydroxy-2-(3-methyl but-dienyl)-7-methoxy-8-(3- methyl but-2-enyl)xanthen-9-one	Xanthone	[300]
			2-(6-*O*-Benzoyl-β-D-gluco pyranosyloxy)-7-(1α, 2α, 6α-trihydroxy-3-oxocyclohex-4-enoyl)-5-hydroxybenzyl alcohol	Phenolic glycoside	[301]
			Dimethylisoborreverine	Indole alkaloid	[46]
			Nitidine	Benzophenanthridine alkaloid	[62]
	Inhibition of β-haematin formation, inhibition of H_2O_2 and glutathione mediated hemin degradation		Axisonitrile-3	Sesquiterpene isonitrile	[154]
			Diisocyanoadociane	Diterpene isonitrile	[154]
	Inhibition of β-haematin formation, inhibition of H_2O_2 mediated haemin degradation		Catechin-[5,6-e]-4β-(3,4-dihydroxyphenyl) dihydro-2(3H)- pyranone	Phenylpropanoid catechin	[203]
			Mururin A	Phenylpropanoid catechin	[203]
		Plasmodium falciparum glutathione transferase (*Pf*GST)	JB42C	Sesquiterpene lactone	[302]
			Tral-1	Coumarin catechin	[302]

Oxidative stress	Production of ROS and lipid peroxidation product	Trafficking, transmembrane and vesicular transport parasite proteins	Plakortin	Polyketide endoperoxide	[303]
Haemoglobin degradation	Inhibition of food vacuole falcipains	Falcipain 2	2,3,6-Trihydroxy benzoic acid	Phenolic acid	[304]
			2,3,6-Trihydroxy methyl benzoate	Phenolic ester	[304]
			Symplostatin 4	Depsipeptide	[284]
		Falcipain 2' and 3	Symplostatin 4	Depsipeptide	[284]
Glyoxalase detoxification system	Inhibition of *Plasmodium falciparum* glyoxalase I (PfGLOI)	(*Pf*GLOI)	Puberulic acid	Tropone	[305]
			Hinokitiol	Tropone	[305]
			Tropolone	Tropone	[305]
Protein folding	Inhibition of *Plasmodium falciparum* Hsp70-1 (PfHsp70-1) chaperone function	(*Pf*Hsp70-1)	Malonganenone A	Purine alkaloid	[306]
			Malonganenone B	Purine alkaloid	[306]
			Malonganenone C	Alkaloid	[306]
			Lapachol	Naphthoquinone	[306]
	Inhibition of chaperone and ATPase functions	PfHsp70-1, PfHsp70-z	Epigallocatechin 3-gallate	Catechin	[205]
Protein degradation	inhibition of Pf20S proteasome	β5 subunit	Carmaphycin B	Tripeptide	[277]
Ca^{2+} metabolism	Inhibition of SERCA-type Ca^{2+}-ATPase	PfATP6	Artemisinins	Sesquiterpene endoperoxide	[307]
Protein biosynthesis	Inhibition of cytoplasmic lysyl-tRNA synthetase	*Pf* lysyl-tRNA synthetase	Cladosporin	Isocoumarin	[308]

Table 2 Natural products with transmission-blocking potential

Compound	Parasite	Active on	Activity	IC_{50}	Reference
Dihydronitidine	*Plasmodium berghei*	Early mosquito stage	Inhibition of ookinete formation	1.7 µM	[65]
Heitziquinone	*P. berghei*	Early mosquito stage	Inhibition of ookinete formation	17 µM	[65]
Mallotojaponin C	*P. falciparum* NF54	stage V gametocytes	Gametocytocidal	3.6 µM	[232]
Carmaphycin B	*P. falciparum* NF54	stage V gametocytes	Gametocytocidal	160 nM	[277]
Carmaphycin B	*P. berghei*	liver stage		61.6 nM	
Parthenine	*P. falciparum* NF54	stage V gametocytes	Gametocytocidal. Inhibition of microgamete exflagellation. Prevent oocysts development in mosquito at 3.84 µM		[314]
		Early mosquito stage	Inhibition of ookinete formation	100% inhibition at 191 µM	[314]
Parthenolide	*P. falciparum* NF54	stage V gametocytes	Gametocytocidal. Inhibition of microgamete exflagellation. prevent oocysts development in mosquito at 4 µM		[314]
Deacetylnimbin	*P. berghei*	Early mosquito stage	Inhibition of ookinete formation	100% inhibition at 100 µM	[315]
Azadirachtin	*P. falciparum* NF54	stage V gametocytes	100% inhibition of microgamete exflagellation		[316]
	P. berghei	stage V gametocytes	Gametocytocidal. Inhibition of microgamete exflagellation	3.25 µM	[316]
Vernodalol	*P. berghei*	Early mosquito stage	Inhibition of early sporogenic stages development	18.7 µM	[310]
Vernolide	*P. berghei*	Early mosquito stage	9-33% inhibition of early sporogenic stages development at 50 µM		[310]
Usnic acid	*P. berghei*	liver stage		2.3 µM	[295]
Vulpic acid	*P. berghei*	liver stage		10.2 µM	[295]
Psoromic acid	*P. berghei*	liver stage		31.6 µM	[295]

Evernic acid	*P. berghei*	liver stage		77.3 µM	[295]
Balsaminol F	*P. berghei*	liver stage	Inhibition of intracellular development	>95% inhibition at 15 µM	[163]
BalsaminosideB	*P. berghei*	liver stage	Inhibition of intracellular development	>95% inhibition at 15 µM	[163]
Triacetylbalsaminol F	*P. berghei*	liver stage	Inhibition of intracellular development	>95% inhibition at 15 µM	[163]
6-Deoxy-8-*O*-methylrabelomycin	*P. berghei*	liver stage		18.5 µM	[317]
X-14881 E	*P. berghei*	liver stage		3.0 µM	[317]
Marilone A	*P. berghei*	liver stage	Inhibition of liver cell infection	12.1 µM	[318]

Conclusions

The present review covered the antiplasmodial natural products reported between 2010 and 2017. A breakdown of the statistics of compounds and the biological source reported per year is given in Fig. 61.

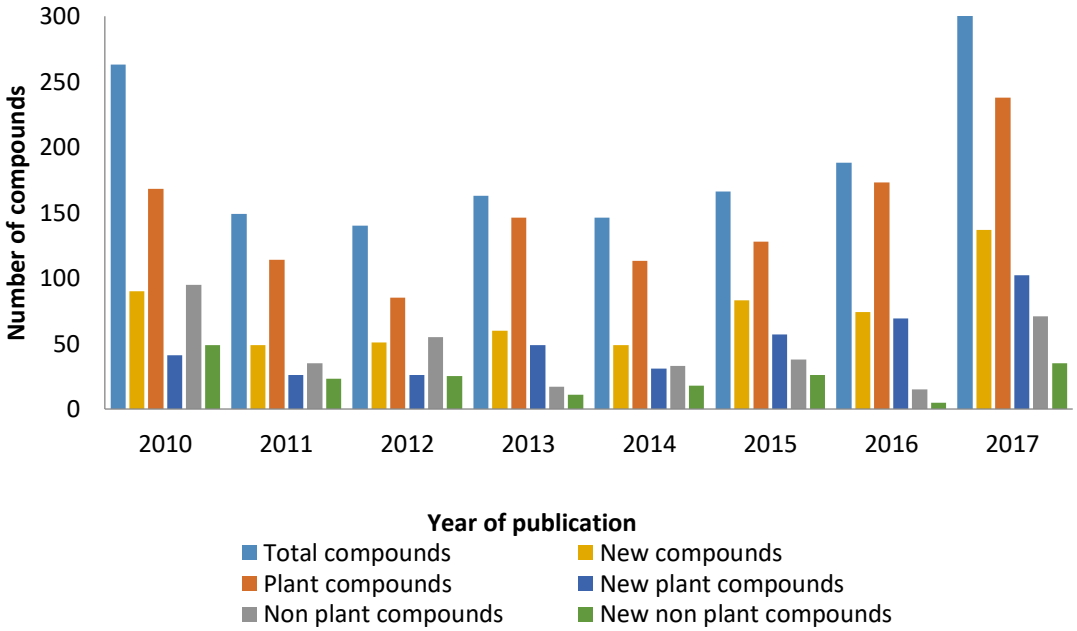

Fig. 61 Summary of biological source from which antiplasmodial natural products were isolated between 2010 and 2017

A total of 447 compounds derived from plant, microrganisms and marine organisms were found to have $IC_{50} \leq 3.0$ µM against at least one strain of asexual blood-stage *P. falciparum*. Some of these compounds show potent selective activity against parasites. However, others were equally cytotoxic against cancerous and/or noncancerous cells. Notwithstanding the cytotoxicity, we have considered these compounds to be promising anti-malarial hits of which the cytotoxicity could be mitigated by medicinal chemistry approaches as was demonstrated, for example, with ferruginol (**230**) and carmaphycin B (**447**) [149, 277]. Also, some of these compounds could serve as templates for designing novel antiplasmodial pharmacophores using the strategy of diversity-oriented synthesis. More than half of the compounds belong to three major chemical classes comprising alkaloids (31.9%), terpenoids (30.8%) and polyphenols (17.4%). This is consistent with the phytochemical distribution of antiplasmodial compounds from earlier reviews [12, 13]. This review also discussed compounds with potent selective antiplasmodial activities that belong to classes from which antiplasmodial activity has not been previously reported. Such novel antiplasmodial scaffolds, e.g. the tropolones and cyclic phosphotriesters, are important in the battle against malaria because these compounds might possess a novel mechanism of action and expand the therapeutic arsenal against the disease.

Many of the plants were investigated based on the ethnobotanical history of use against malaria, while the non-plant materials were mostly investigated because of their chemical profiles. This underscores the need to employ the dual approach of ethnobotanical reputation and chemical profiling in the search for anti-malarial natural products. Although fewer marine and microorganisms have been screened for antiplasmodial compounds compared to plants, the diverse nature of metabolites

produced by these alternative sources presents a compelling case for intensive exploration. Only a small number of *in vivo* studies to validate the *in vitro* efficacy of these compounds have been conducted. This is not surprising considering that natural products are usually isolated in small amounts, which is barely sufficient for *in vitro* testing. Nevertheless, the need for *in vivo* confirmation of observed *in vitro* potency could not be overemphasized. Therefore, efficient total synthesis of the most promising compounds identified in this review should be prioritized.

It is now accepted that the *Plasmodium* parasite transmission from infected host to uninfected mosquitoes should be blocked to curtail the spread of malaria. Compounds with activity against sexual and liver stage parasites are therefore crucial to the malaria eradication agenda. Sadly, only a few chemical compounds have proven ability to kill liver and sexual stage parasites. In spite of the fruitful relationship between malaria chemotherapy and natural products, only a few natural products have been evaluated for activity against the parasite gametocytes and liver forms. As this review has shown, the few investigated natural products have shown promise. Therefore, the exploration of natural products in this regard cannot be overemphasized. The compounds covered in this review will be a good starting point, since natural products, unlike the synthetic counterparts, might have multi-stage activity. Priority should be given to compounds of which the mode of action does not involve the inhibition of haemozoin formation since stage V gametes, which are the transmissible form of the parasite, do not digest haemoglobin. Standardized assay methods for evaluating late stage gametocidal and liver stage activities have been developed that will aid in the high-throughput screening of natural products [319, 320].

Abbreviations

ACT: artemisinin-based combination therapy; ATPase: adenosine triphosphatase; CGX: Caged *Garcinia* xanthones; DDT: dichlorodiphenyltrichloroethane; DGAT: diacylglycerol O-acyltransferase; DNA: Deoxyribonucleic acid; EGCG: Epigallocatechin-3-gallate; ELISA: enzyme-linked immunosorbent assays; Glu: glutamic acid; HRP2: histidine-rich protein 2; Ile: isoleucine; LC-MS: liquid chromatography - mass spectrometry; Leu: leucine; Met: methionine; MeTyr: methyl tyrosine; Nle: norleucine; µM: micromolar; nM: nanomolar; NMR: nuclear magnetic resonance spectroscopy; PfDGAT: *Plasmodium falciparum* diacylglycerol O-acyltransferase; PfHsp: *Plasmodium falciparum* heat shock protein; Phe: phenylalanine; pLDH: Plasmodium lactate dehydrogenase protein; PPAP: polyprenylated acylphloroglucinol; Pro: proline; ROS: reactive oxygen species; SAR: structure-activity relationship; SI: selectivity index; Thr: threonine; USA: United States of America; Val: valine; WHO: World Health Organization.

References

1. WHO. World Malaria Report 2017. Geneva, World Health Organization; 2018.
2. Kiszewski A, Mellinger A, Spielman A, Malaney P, Sachs SE, Sachs J. A global index representing the stability of malaria transmission. Am J Trop Med Hyg. 2004;70:486-98.
3. Snow RW, Guerra CA, Noor AM, Myint HY, Hay SI. The global distribution of clinical episodes of *Plasmodium falciparum* malaria. Nature. 2005;434:214.
4. Hay SI, Guerra CA, Tatem AJ, Noor AM, Snow RW. The global distribution and population at risk of malaria: past, present, and future. Lancet Infect Dis. 2004;4:327-36.
5. Russell PF. World-wide malaria distribution, prevalence, and control. Am J Trop Med Hyg. 1956;5:937-65.
6. Snow RW, Sartorius B, Kyalo D, Maina J, Amratia P, Mundia CW, et al. The prevalence of *Plasmodium falciparum* in sub-Saharan Africa since 1900. Nature. 2017;550:515.

7. Howard J. Tick- and mosquito-borne diseases more than triple, since 2004, in the US. https://edition.cnn.com/2018/05/01/health/ticks-mosquito-borne-diseases-cdc-study/index.html. Accessed 30 July 2018.
8. Lu F, Culleton R, Zhang M, Ramaprasad A, von Seidlein L, Zhou H, et al. Emergence of indigenous artemisinin-resistant *Plasmodium falciparum* in Africa. N Engl J Med. 2017;376:991-3.
9. Talisuna AO, Bloland P, d'Alessandro U. History, dynamics, and public health importance of malaria parasite resistance. Clin Microbiol Rev. 2004;17:235-54.
10. Wells TN, Van Huijsduijnen RH, Van Voorhis WC. Malaria medicines: a glass half full? Nat Rev Drug Discovery. 2015;14:424.
11. Schwikkard S, van Heerden FR. Antimalarial activity of plant metabolites. Nat Prod Rep. 2002;19:675-92.
12. Bero J, Frédérich M, Quetin-Leclercq J. Antimalarial compounds isolated from plants used in traditional medicine. J Pharm Pharmacol. 2009;61:1401-33.
13. Bero J, Quetin-Leclercq J. Natural products published in 2009 from plants traditionally used to treat malaria. Planta Med. 2011;77:631-40.
14. Nogueira CR, Lopes LM. Antiplasmodial natural products. Molecules. 2011;16:2146-90.
15. Wright CW. Recent developments in research on terrestrial plants used for the treatment of malaria. Nat Prod Rep. 2010;27:961-8.
16. Laurent D, Pietra F. Antiplasmodial marine natural products in the perspective of current chemotherapy and prevention of malaria. A review. Mar Biotechnol. 2006;8:433-47.
17. Fattorusso E, Taglialatela-Scafati O. Marine antimalarials. Mar Drugs. 2009;7:130-52.
18. Gertsch J. How scientific is the science in ethnopharmacology? Historical perspectives and epistemological problems. J Ethnopharmacol. 2009;122:177-83.
19. Krettli AU, Adebayo JO, Krettli LG. Testing of natural products and synthetic molecules aiming at new antimalarials. Curr Drug Targets. 2009;10:261-70.
20. Wein S, Maynadier M, Van Ba CT, Cerdan R, Peyrottes S, Fraisse L, et al. Reliability of antimalarial sensitivity tests depends on drug mechanisms of action. J Clin Microbiol. 2010;48:1651-60.
21. Mokgethi-Morule T, N'Da DD. Cell based assays for anti-*Plasmodium* activity evaluation. Eur J Pharm Sci. 2016;84:26-36.
22. Chianese G, Persico M, Yang F, Lin H-W, Guo Y-W, Basilico N, et al. Endoperoxide polyketides from a Chinese *Plakortis simplex:* Further evidence of the impact of stereochemistry on antimalarial activity of simple 1,2-dioxanes. Bioorg Med Chem. 2014;22:4572-80.
23. Fattorusso C, Persico M, Calcinai B, Cerrano C, Parapini S, Taramelli D, et al. Manadoperoxides A-D from the Indonesian sponge *Plakortis* cfr. *simplex*. Further insights on the structure-activity relationships of simple 1,2-dioxane antimalarials. J Nat Prod. 2010;73:1138-45.
24. Fattorusso E, Parapini S, Campagnuolo C, Basilico N, Taglialatela-Scafati O, Taramelli D. Activity against *Plasmodium falciparum* of cycloperoxide compounds obtained from the sponge *Plakortis simplex*. J Antimicrob Chemother. 2002;50:883-8.
25. Taglialatela-Scafati O, Fattorusso E, Romano A, Scala F, Barone V, Cimino P, et al. Insight into the mechanism of action of plakortins, simple 1,2-dioxane antimalarials. Org Biomol Chem. 2010;8:846-56.
26. Jiménez-Romero C, Ortiz I, Vicente J, Vera B, Rodríguez AD, Nam S, et al. Bioactive cycloperoxides isolated from the Puerto Rican sponge *Plakortis halichondrioides*. J Nat Prod. 2010;73:1694-700.
27. Yang F, Wang R-P, Xu B, Yu H-B, Ma G-Y, Wang G-F, et al. New antimalarial norterpene cyclic peroxides from Xisha Islands sponge *Diacarnus megaspinorhabdosa*. Bioorg Med Chem Lett. 2016;26:2084-7.
28. Yang F, Zou Y, Wang R-P, Hamann MT, Zhang H-J, Jiao W-H, et al. Relative and absolute stereochemistry of diacarperoxides: antimalarial norditerpene endoperoxides from marine sponge *Diacarnus megaspinorhabdosa*. Mar Drugs. 2014;12:4399-416.
29. Bringmann G, Tasler S. Oxidative aryl coupling reactions: a biomimetic approach to configurationally unstable or axially chiral biaryl natural products and related bioactive compounds. Tetrahedron. 2001;57:331-43.
30. Li J, Seupel R, Feineis D, Mudogo V, Kaiser M, Brun R, et al. Dioncophyllines C2, D2, and F and related naphthylisoquinoline alkaloids from the Congolese liana *Ancistrocladus ileboensis* with potent activities against *Plasmodium falciparum* and against multiple myeloma and leukemia cell lines. J Nat Prod. 2017;80:443-58.
31. Hallock YF, Manfredi KP, Dai J-R, Cardellina JH, Gulakowski RJ, McMahon JB, et al. Michellamines D–F, new HIV-inhibitory dimeric naphthylisoquinoline alkaloids, and korupensamine E, a new antimalarial monomer, from *Ancistrocladus korupensis*. J Nat Prod. 1997;60:677-83.
32. Bringmann G, Zhang G, Ölschläger T, Stich A, Wu J, Chatterjee M, et al. Highly selective antiplasmodial naphthylisoquinoline alkaloids from *Ancistrocladus tectorius*. Phytochemistry. 2013;91:220-8.
33. Bringmann G, Seupel R, Feineis D, Xu M, Zhang G, Kaiser M, et al. Antileukemic ancistrobenomine B and related 5,1'-coupled naphthylisoquinoline alkaloids from the Chinese liana *Ancistrocladus tectorius*. Fitoterapia. 2017;121:76-85.
34. Xu M, Bruhn T, Hertlein B, Brun R, Stich A, Wu J, et al. Shuangancistrotectorines A–E, dimeric naphthylisoquinoline alkaloids with three chiral biaryl axes from the Chinese plant *Ancistrocladus tectorius*. Chem Eur J. 2010;16:4206-16.

35. Bringmann G, Zhang G, Büttner T, Bauckmann G, Kupfer T, Braunschweig H, et al. Jozimine A2: The first dimeric Dioncophyllaceae-type naphthylisoquinoline alkaloid, with three chiral axes and high antiplasmodial activity. Chem Eur J. 2013;19:916-23.
36. Bringmann G, Lombe BK, Steinert C, Ioset KN, Brun R, Turini F, et al. Mbandakamines A and B, unsymmetrically coupled dimeric naphthylisoquinoline alkaloids, from a Congolese *Ancistrocladus* species. Org Lett. 2013;15:2590-3.
37. Lombe BK, Bruhn T, Feineis D, Mudogo V, Brun R, Bringmann G. Antiprotozoal spirombandakamines A1 and A2, fused naphthylisoquinoline dimers from a Congolese *Ancistrocladus* plant. Org Lett. 2017;19:6740-3.
38. Li J, Seupel R, Bruhn T, Feineis D, Kaiser M, Brun R, et al. Jozilebomines A and B, naphthylisoquinoline dimers from the Congolese liana *Ancistrocladus ileboensis*, with antiausterity activities against the PANC-1 human pancreatic cancer cell Line. J Nat Prod. 2017;80:2807-17.
39. Tshitenge DT, Feineis D, Mudogo V, Kaiser M, Brun R, Bringmann G. Antiplasmodial ealapasamines A-C, 'mixed naphthylisoquinoline dimers from the Central African liana *Ancistrocladus ealaensis*. Sci Rep. 2017;7:5767.
40. Bringmann G, Gulder T, Hertlein B, Hemberger Y, Meyer F. Total synthesis of the *N*,*C*-coupled naphthylisoquinoline alkaloids ancistrocladinium A and B and related analogues. J Am Chem Soc. 2010;132:1151-8.
41. Deguchi J, Hirahara T, Hirasawa Y, Ekasari W, Widyawaruyanti A, Shirota O, et al. New tricyclic alkaloids, cassiarins G, H, J, and K from leaves of *Cassia siamea*. Chem Pharm Bull. 2012;60:219-22.
42. Morita H, Oshimi S, Hirasawa Y, Koyama K, Honda T, Ekasari W, et al. Cassiarins A and B, novel antiplasmodial alkaloids from *Cassia siamea*. Org Lett. 2007;9:3691-3.
43. Zahari A, Cheah FK, Mohamad J, Sulaiman SN, Litaudon M, Leong KH, et al. Antiplasmodial and antioxidant isoquinoline alkaloids from *Dehaasia longipedicellata*. Planta Med. 2014;80:599-603.
44. Carraz M, Jossang A, Franetich JF, Siau A, Ciceron L, Hannoun L, et al. A plant-derived morphinan as a novel lead compound active against malaria liver stages. Plos Medicine. 2006;3:2392-402.
45. Fernandez LS, Jobling MF, Andrews KT, Avery VM. Antimalarial activity of natural product extracts from Papua New Guinean and Australian plants against *Plasmodium falciparum*. Phytother Res. 2008;22:1409-12.
46. Fernandez LS, Sykes ML, Andrews KT, Avery VM. Antiparasitic activity of alkaloids from plant species of Papua New Guinea and Australia. Int J Antimicrob Agents. 2010;36:275-9.
47. Likhitwitayawuid K, Angerhofer CK, Chai H, Pezzuto JM, Cordell GA, Ruangrungsi N. Cytotoxic and antimalarial alkaloids from the tubers of *Stephania pierrei*. J Nat Prod. 1993;56:1468-78.
48. Le PM, Srivastava V, Nguyen TT, Pradines B, Madamet M, Mosnier J, et al. Stephanine from *Stephania venosa* (Blume) Spreng showed effective antiplasmodial and anticancer activities, the latter by inducing apoptosis through the reverse of mitotic exit. Phytother Res. 2017;31:1357-68.
49. Ropivia J, Derbré S, Rouger C, Pagniez F, Le Pape P, Richomme P. Isoquinolines from the roots of *Thalictrum flavum* L. and their evaluation as antiparasitic compounds. Molecules. 2010;15:6476-84.
50. Wangchuk P, Bremner JB, Rattanajak R, Kamchonwongpaisan S. Antiplasmodial agents from the Bhutanese medicinal plant *Corydalis calliantha*. Phytother Res. 2010;24:481-5.
51. Wangchuk P, Keller PA, Pyne SG, Taweechotipatr M, Tonsomboon A, Rattanajak R, et al. Evaluation of an ethnopharmacologically selected Bhutanese medicinal plants for their major classes of phytochemicals and biological activities. J Ethnopharmacol. 2011;137:730-42.
52. Wangchuk P, Keller PA, Pyne SG, Lie W, Willis AC, Rattanajak R, et al. A new protoberberine alkaloid from *Meconopsis simplicifolia* (D. Don) Walpers with potent antimalarial activity against a multidrug resistant *Plasmodium falciparum* strain. J Ethnopharmacol. 2013;150:953-9.
53. Chea A, Bun S-S, Azas N, Gasquet M, Bory S, Ollivier E, et al. Antiplasmodial activity of three bisbenzylisoquinoline alkaloids from the tuber of *Stephania rotunda*. Nat Prod Res. 2010;24:1766-70.
54. Chea A, Hout S, Bun S-S, Tabatadze N, Gasquet M, Azas N, et al. Antimalarial activity of alkaloids isolated from *Stephania rotunda*. J Ethnopharmacol. 2007;112:132-7.
55. Baghdikian B, Mahiou-Leddet V, Bory S, Bun S-S, Dumetre A, Mabrouki F, et al. New antiplasmodial alkaloids from *Stephania rotunda*. J Ethnopharmacol. 2013;145:381-5.
56. Desgrouas C, Chapus C, Desplans J, Travaille C, Pascual A, Baghdikian B, et al. *In vitro* antiplasmodial activity of cepharanthine. Malar J. 2014;13:327.
57. Desgrouas C, Dormoi J, Chapus C, Ollivier E, Parzy D, Taudon N. *In vitro* and *in vivo* combination of cepharanthine with anti-malarial drugs. Malar J. 2014;13:90.
58. Sun YF, Wink M. Tetrandrine and fangchinoline, bisbenzylisoquinoline alkaloids from *Stephania tetrandra* can reverse multidrug resistance by inhibiting P-glycoprotein activity in multidrug resistant human cancer cells. Phytomedicine. 2014;21:1110-9.
59. Ye Z, van Dyke K. Antimalarial activity of various bisbenzylisoquinoline and aporphine-benzylisoquinoline alkaloids and their structure-activity relationships against chloroquine – sensitive and resistant *Plasmodium falciparum* malaria *in vitro*. Malar Contr Elim. 2015;5:1.
60. Nasrullah AA, Zahari A, Mohamad J, Awang K. Antiplasmodial alkaloids from the bark of *Cryptocarya nigra* (Lauraceae). Molecules. 2013;18:8009-17.
61. Kubo M, Yatsuzuka W, Matsushima S, Harada K, Inoue Y, Miyamoto H, et al. Antimalarial phenanthroindolizine alkaloids from *Ficus septica*. Chem Pharm Bull. 2016;64:957-60.

62. Bouquet J, Rivaud M, Chevalley S, Deharo E, Jullian V, Valentin A. Biological activities of nitidine, a potential anti-malarial lead compound. Malar J. 2012;11:67.
63. Muganga R, Angenot L, Tits M, Frédérich M. *In vitro* and *in vivo* antiplasmodial activity of three Rwandan medicinal plants and identification of their active compounds. Planta Med. 2014;80:482-9.
64. Gakunju D, Mberu E, Dossaji S, Gray A, Waigh R, Waterman P, et al. Potent antimalarial activity of the alkaloid nitidine, isolated from a Kenyan herbal remedy. Antimicrob Agents Chemother. 1995;39:2606-9.
65. Goodman CD, Austarheim I, Mollard V, Mikolo B, Malterud KE, McFadden GI, et al. Natural products from *Zanthoxylum heitzii* with potent activity against the malaria parasite. Malar J. 2016;15:481.
66. Dolabela MF, Póvoa MM, Brandão GC, Rocha FD, Soares LF, de Paula RC, et al. *Aspidosperma* species as sources of anti-malarials: Uleine is the major anti-malarial indole alkaloid from *Aspidosperma parvifolium* (Apocynaceae). Malar J. 2015;14:498.
67. de Oliveira AB, Dolabela MF, Póvoa MM, Santos CAM, de Pilla Varotti F. Antimalarial activity of ulein and proof of its action on the *Plasmodium falciparum* digestive vacuole. Malar J. 2010;9:O9.
68. Chierrito TP, Aguiar AC, de Andrade IM, Ceravolo IP, Gonçalves RA, de Oliveira AJ, et al. Anti-malarial activity of indole alkaloids isolated from *Aspidosperma olivaceum*. Malar J. 2014;13:142.
69. Muganza DM, Fruth B, Nzunzu JL, Tuenter E, Foubert K, Cos P, et al. *In vitro* antiprotozoal activity and cytotoxicity of extracts and isolated constituents from *Greenwayodendron suaveolens*. J Ethnopharmacol. 2016;193:510-6.
70. Fernandez LS, Buchanan MS, Carroll AR, Feng YJ, Quinn RJ, Avery VM. Flinderoles A−C: Antimalarial bis-indole alkaloids from *Flindersia* species. Org Lett. 2008;11:329-32.
71. Robertson LP, Duffy S, Wang Y, Wang D, Avery VM, Carroll AR. Pimentelamines A–C, indole alkaloids isolated from the leaves of the Australian tree *Flindersia pimenteliana*. J Nat Prod. 2017;80:3211–7.
72. Girardot M, Deregnaucourt C, Deville A, Dubost L, Joyeau R, Allorge L, et al. Indole alkaloids from *Muntafara sessilifolia* with antiplasmodial and cytotoxic activities. Phytochemistry. 2012;73:65-73.
73. Ramanitrahasimbola D, Rasoanaivo P, Ratsimamanga-Urverg S, Federici E, Palazzino G, Galeffi C, et al. Biological activities of the plant-derived bisindole voacamine with reference to malaria. Phytother Res. 2001;15:30-3.
74. Fox Ramos AE, Alcover C, Evanno L, Maciuk A, Litaudon M, Duplais C, et al. Revisiting previously investigated plants: A molecular networking-based study of *Geissospermum laeve*. J Nat Prod. 2017;80:1007-14.
75. Mbeunkui F, Grace MH, Lategan C, Smith PJ, Raskin I, Lila MA. In vitro antiplasmodial activity of indole alkaloids from the stem bark of *Geissospermum vellosii*. J Ethnopharmacol. 2012;139:471-7.
76. Tchinda AT, Ngono AR, Tamze V, Jonville MC, Cao M, Angenot L, et al. Antiplasmodial alkaloids from the stem bark of *Strychnos malacoclados*. Planta Med. 2012;78:377-82.
77. Tchinda AT, Jansen O, Nyemb J-N, Tits M, Dive G, Angenot L, et al. Strychnobaillonine, an unsymmetrical bisindole alkaloid with an unprecedented skeleton from *Strychnos icaja* roots. J Nat Prod. 2014;77:1078-82.
78. Frédérich M, Jacquier M-J, Thépenier P, De Mol P, Tits M, Philippe G, et al. Antiplasmodial activity of alkaloids from various *Strychnos* species. J Nat Prod. 2002;65:1381-6.
79. Rocha e Silva L, Montoia A, Amorim R, Melo M, Henrique M, Nunomura SM, et al. Comparative *in vitro* and *in vivo* antimalarial activity of the indole alkaloids ellipticine, olivacine, cryptolepine and a synthetic cryptolepine analog. Phytomedicine. 2012;20:71-6.
80. Montoia A, Rocha e Silva LF, Torres ZE, Costa DS, Henrique MC, Lima ES, et al. Antiplasmodial activity of synthetic ellipticine derivatives and an isolated analog. Bioorg Med Chem Lett. 2014;24:2631-4.
81. Rajachan O-A, Kanokmedhakul K, Sanmanoch W, Boonlue S, Hannongbua S, Saparpakorn P, et al. Chevalone C analogues and globoscinic acid derivatives from the fungus *Neosartorya spinosa* KKU-1NK1. Phytochemistry. 2016;132:68-75.
82. Liew LP, Fleming JM, Longeon A, Mouray E, Florent I, Bourguet-Kondracki M-L, et al. Synthesis of 1-indolyl substituted β-carboline natural products and discovery of antimalarial and cytotoxic activities. Tetrahedron. 2014;70:4910-20.
83. Pereira MD, da Silva T, Aguiar ACC, Oliva G, Guido RV, Yokoyama-Yasunaka JK, et al. Chemical composition, antiprotozoal and cytotoxic activities of indole alkaloids and benzofuran neolignan of *Aristolochia cordigera*. Planta Med. 2017;83:912-20.
84. Huang H, Yao Y, He Z, Yang T, Ma J, Tian X, et al. Antimalarial β-carboline and indolactam alkaloids from *Marinactinospora thermotolerans*, a deep sea isolate. J Nat Prod. 2011;74:2122-7.
85. Chan ST, Pearce AN, Page MJ, Kaiser M, Copp BR. Antimalarial β-carbolines from the New Zealand ascidian *Pseudodistoma opacum*. J Nat Prod. 2011;74:1972-9.
86. Yusuf H, Mustofa M, Susidarti RA, Asih PBS, Suryawati S. A new quassinoid of four isolated compounds from extract *Eurycoma longifolia* Jack roots and their in-vitro antimalarial activity. Int J Res Pharm Biomed Sci. 2013;4:728-34.
87. Julianti T, De Mieri M, Zimmermann S, Ebrahimi SN, Kaiser M, Neuburger M, et al. HPLC-based activity profiling for antiplasmodial compounds in the traditional Indonesian medicinal plant *Carica papaya* L. J Ethnopharmacol. 2014;155:426-34.
88. Pivatto M, Baccini LR, Sharma A, Nakabashi M, Danuello A, Viegas Júnior C, et al. Antimalarial activity of piperidine alkaloids from *Senna spectabilis* and semisynthetic derivatives. J Braz Chem Soc. 2014;25:1900-6.
89. Ilias M, Ibrahim MA, Khan SI, Jacob MR, Tekwani BL, Walker LA, et al. Pentacyclic ingamine alkaloids, a new antiplasmodial pharmacophore from the marine sponge *Petrosid* Ng5 Sp5. Planta Med. 2012;78:1690-7.

90. Mani L, Petek S, Valentin A, Chevalley S, Folcher E, Aalbersberg W, et al. The *in vivo* anti-plasmodial activity of haliclonacyclamine A, an alkaloid from the marine sponge, *Haliclona* sp. Nat Prod Res. 2011;25:1923-30.
91. Kumarihamy M, Fronczek FR, Ferreira D, Jacob M, Khan SI, Nanayakkara ND. Bioactive 1,4-dihydroxy-5-phenyl-2-pyridinone alkaloids from *Septoria pistaciarum*. J Nat Prod. 2010;73:1250-3.
92. Gros E, Al-Mourabit A, Martin MT, Sorres J, Vacelet J, Frederich M, et al. Netamines H–N, tricyclic alkaloids from the marine sponge *Biemna laboutei* and their antimalarial activity. J Nat Prod. 2014;77:818-23.
93. Scala F, Fattorusso E, Menna M, Taglialatela-Scafati O, Tierney M, Kaiser M, et al. Bromopyrrole alkaloids as lead compounds against protozoan parasites. Mar Drugs. 2010;8:2162-74.
94. Davis RA, Buchanan MS, Duffy S, Avery VM, Charman SA, Charman WN, et al. Antimalarial activity of pyrroloiminoquinones from the Australian marine sponge *Zyzzya* sp. J Med Chem. 2012;55:5851-8.
95. Na M, Ding Y, Wang B, Tekwani BL, Schinazi RF, Franzblau S, et al. Anti-infective discorhabdins from a deep-water Alaskan sponge of the genus *Latrunculia*. J Nat Prod. 2009;73:383-7.
96. Neves JM, Matos C, Moutinho C, Queiroz G, Gomes LR. Ethnopharmacological notes about ancient uses of medicinal plants in Trás-os-Montes (northern of Portugal). J Ethnopharmacol. 2009;124:270-83.
97. Leporatti ML, Pavesi A, Posocco E. Phytotherapy in the *Valnerina marche* (central Italy). J Ethnopharmacol. 1985;14:53-63.
98. Althaus JB, Jerz G, Winterhalter P, Kaiser M, Brun R, Schmidt TJ. Antiprotozoal activity of *Buxus sempervirens* and activity-guided isolation of *O*-tigloylcyclovirobuxeine-B as the main constituent active against *Plasmodium falciparum*. Molecules. 2014;19:6184-201.
99. Pan L, Acuña UM, Chai H, Park H-Y, Ninh TN, Van Thanh B, et al. New bioactive lupane triterpene coumaroyl esters isolated from *Buxus cochinchinensis*. Planta Med. 2015;81:1133.
100. Cheenpracha S, Boapun P, Limtharakul T, Laphookhieo S, Pyne SG. Antimalarial and cytotoxic activities of pregnene-type steroidal alkaloids from *Holarrhena pubescens* roots. Nat Prod Res. 2017:1-7.
101. Ma G, Sun Z, Sun Z, Yuan J, Wei H, Yang J, et al. Antimalarial diterpene alkaloids from the seeds of *Caesalpinia minax*. Fitoterapia. 2014;95:234-9.
102. Hao B, Shen S-F, Zhao Q-J. Cytotoxic and antimalarial Amaryllidaceae alkaloids from the bulbs of *Lycoris radiata*. Molecules. 2013;18:2458-68.
103. Presley CC, Krai P, Dalal S, Su Q, Cassera M, Goetz M, et al. New potently bioactive alkaloids from *Crinum erubescens*. Bioorg Med Chem. 2016;24:5418-22.
104. Presley CC, Du Y, Dalal S, Merino EF, Butler JH, Rakotonandrasana S, et al. Isolation, structure elucidation, and synthesis of antiplasmodial quinolones from *Crinum firmifolium*. Bioorg Med Chem. 2017;25:4203-11.
105. Yang X, Davis RA, Buchanan MS, Duffy S, Avery VM, Camp D, et al. Antimalarial bromotyrosine derivatives from the Australian marine sponge *Hyattella* sp. J Nat Prod. 2010;73:985-7.
106. Xu M, Andrews KT, Birrell GW, Tran TL, Camp D, Davis RA, et al. Psammaplysin H, a new antimalarial bromotyrosine alkaloid from a marine sponge of the genus *Pseudoceratina*. Bioorg Med Chem Lett. 2011;21:846-8.
107. Mani L, Jullian V, Mourkazel B, Valentin A, Dubois J, Cresteil T, et al. New antiplasmodial bromotyrosine derivatives from *Suberea ianthelliformis* Lendenfeld, 1888. Chem Biodiversity. 2012;9:1436-51.
108. Campos P-E, Wolfender J-L, Queiroz EF, Marcourt L, Al-Mourabit A, Frederich M, et al. Unguiculin A and ptilomycalins E–H, antimalarial guanidine alkaloids from the marine sponge *Monanchora unguiculata*. J Nat Prod. 2017;80:1404-10.
109. Davis RA, Duffy S, Fletcher S, Avery VM, Quinn RJ. Thiaplakortones A–D: Antimalarial thiazine alkaloids from the Australian marine sponge *Plakortis lita*. J Org Chem. 2013;78:9608-13.
110. Nogawa T, Kato N, Shimizu T, Okano A, Futamura Y, Takahashi S, et al. Wakodecalines A and B, new decaline metabolites isolated from a fungus *Pyrenochaetopsis* sp. RK10-F058. J Antibiot. 2018;71:123.
111. Carroll AR, Duffy S, Avery VM. Aplidiopsamine A, an antiplasmodial alkaloid from the temperate Australian ascidian, *Aplidiopsis confluata*. J Org Chem. 2010;75:8291-4.
112. Rahman AA, Samoylenko V, Jacob MR, Sahu R, Jain SK, Khan SI, et al. Antiparasitic and antimicrobial indolizidines from the leaves of *Prosopis glandulosa* var. *glandulosa*. Planta Med. 2011;77:1639.
113. Komlaga G, Cojean S, Dickson RA, Beniddir MA, Suyyagh-Albouz S, Mensah ML, et al. Antiplasmodial activity of selected medicinal plants used to treat malaria in Ghana. Parasitol Res. 2016;115:3185-95.
114. Komlaga G, Genta-Jouve G, Cojean S, Dickson RA, Mensah ML, Loiseau PM, et al. Antiplasmodial *Securinega* alkaloids from *Phyllanthus fraternus*: Discovery of natural (+)-allonorsecurinine. Tetrahedron Lett. 2017;58:3754-6.
115. Lacroix D, Prado S, Kamoga D, Kasenene J, Bodo B. Structure and in vitro antiparasitic activity of constituents of *Citropsis articulata* root bark. J Nat Prod. 2011;74:2286-9.
116. Liew LP, Kaiser M, Copp BR. Discovery and preliminary structure–activity relationship analysis of 1,14-sperminediphenylacetamides as potent and selective antimalarial lead compounds. Bioorg Med Chem Lett. 2013;23:452-4.
117. Zofou D, Kengne ABO, Tene M, Ngemenya MN, Tane P, Titanji VP. *In vitro* antiplasmodial activity and cytotoxicity of crude extracts and compounds from the stem bark of *Kigelia africana* (Lam.) Benth (Bignoniaceae). Parasitol Res. 2011;108:1383-90.

118. Zofou D, Tene M, Tane P, Titanji VP. Antimalarial drug interactions of compounds isolated from *Kigelia africana* (Bignoniaceae) and their synergism with artemether, against the multidrug-resistant W2mef *Plasmodium falciparum* strain. Parasitol Res. 2012;110:539-44.
119. Claudino VD, Da Silva KC, Cechinel Filho V, Yunes RA, Monache FD, Giménez A, et al. Drimanes from *Drimys brasiliensis* with leishmanicidal and antimalarial activity. Mem Inst Oswaldo Cruz. 2013;108:140-4.
120. Mba'ning BM, Lenta BN, Noungoué DT, Antheaume C, Fongang YF, Ngouela SA, et al. Antiplasmodial sesquiterpenes from the seeds of *Salacia longipes* var. *camerunensis*. Phytochemistry. 2013;96:347-52.
121. Dastan D, Salehi P, Gohari AR, Zimmermann S, Kaiser M, Hamburger M, et al. Disesquiterpene and sesquiterpene coumarins from *Ferula pseudalliacea,* and determination of their absolute configurations. Phytochemistry. 2012;78:170-8.
122. Daengrot C, Rukachaisirikul V, Tansakul C, Thongpanchang T, Phongpaichit S, Bowornwiriyapan K, et al. Eremophilane sesquiterpenes and diphenyl thioethers from the soil fungus *Penicillium copticola* PSU-RSPG138. J Nat Prod. 2015;78:615-22.
123. Hemtasin C, Kanokmedhakul S, Kanokmedhakul K, Hahnvajanawong C, Soytong K, Prabpai S, et al. Cytotoxic pentacyclic and tetracyclic aromatic sesquiterpenes from *Phomopsis archeri*. J Nat Prod. 2011;74:609-13.
124. White AM, Pierens GK, Skinner-Adams T, Andrews KT, Bernhardt PV, Krenske EH, et al. Antimalarial isocyano and isothiocyanato sesquiterpenes with tri-and bicyclic skeletons from the nudibranch *Phyllidia ocellata*. J Nat Prod. 2015;78:1422-7.
125. Young RM, Adendorff MR, Wright AD, Davies-Coleman MT. Antiplasmodial activity: The first proof of inhibition of heme crystallization by marine isonitriles. Eur J Med Chem. 2015;93:373-80.
126. Morita H, Mori R, Deguchi J, Oshimi S, Hirasawa Y, Ekasari W, et al. Antiplasmodial decarboxyportentol acetate and 3,4-dehydrotheaspirone from *Laumoniera bruceadelpha*. J Nat Med. 2012;66:571-5.
127. Zhou B, Wu Y, Dalal S, Merino EF, Liu Q-F, Xu C-H, et al. Nanomolar antimalarial agents against chloroquine-resistant *Plasmodium falciparum* from medicinal plants and their structure–activity relationships. J Nat Prod. 2016;80:96-107.
128. Jansen O, Angenot L, Tits M, Nicolas JP, De Mol P, Nikiéma J-B, et al. Evaluation of 13 selected medicinal plants from Burkina Faso for their antiplasmodial properties. J Ethnopharmacol. 2010;130:143-50.
129. Jansen O, Tits M, Angenot L, Nicolas J-P, De Mol P, Nikiema J-B, et al. Anti-plasmodial activity of *Dicoma tomentosa* (Asteraceae) and identification of urospermal A-15-O-acetate as the main active compound. Malar J. 2012;11:289.
130. Becker JV, Van der Merwe MM, van Brummelen AC, Pillay P, Crampton BG, Mmutlane EM, et al. *In vitro* anti-plasmodial activity of *Dicoma anomala* subsp. *gerrardii* (Asteraceae): Identification of its main active constituent, structure-activity relationship studies and gene expression profiling. Malar J. 2011;10:295.
131. Du Y, Pearce KC, Dai Y, Krai P, Dalal S, Cassera MB, et al. Antiplasmodial sesquiterpenoid lactones from *Trichospira verticillata*: Structure elucidation by spectroscopic methods and comparison of experimental and calculated ECD data. J Nat Prod. 2017;80:1639-47.
132. Liu Y, Rakotondraibe LH, Brodie PJ, Wiley JD, Cassera MB, Goetz M, et al. Antiproliferative and antimalarial sesquiterpene lactones from *Piptocoma antillana* from Puerto Rico. Nat Prod Commun. 2014;9:1403.
133. Bero J, Ganfon H, Jonville M-C, Frédérich M, Gbaguidi F, DeMol P, et al. *In vitro* antiplasmodial activity of plants used in Benin in traditional medicine to treat malaria. J Ethnopharmacol. 2009;122:439-44.
134. Ganfon H, Bero J, Tchinda AT, Gbaguidi F, Gbenou J, Moudachirou M, et al. Antiparasitic activities of two sesquiterpenic lactones isolated from *Acanthospermum hispidum* DC. J Ethnopharmacol. 2012;141:411-7.
135. Toyang NJ, Krause MA, Fairhurst RM, Tane P, Bryant J, Verpoorte R. Antiplasmodial activity of sesquiterpene lactones and a sucrose ester from *Vernonia guineensis* Benth.(Asteraceae). J Ethnopharmacol. 2013;147:618-21.
136. Maas M, Hensel A, da Costa FB, Brun R, Kaiser M, Schmidt TJ. An unusual dimeric guaianolide with antiprotozoal activity and further sesquiterpene lactones from *Eupatorium perfoliatum*. Phytochemistry. 2011;72:635-44.
137. Ma G, Wu H, Chen D, Zhu N, Zhu Y, Sun Z, et al. Antimalarial and antiproliferative cassane diterpenes of *Caesalpinia sappan*. J Nat Prod. 2015;78:2364-71.
138. Nondo RS, Erasto P, Moshi MJ, Zacharia A, Masimba PJ, Kidukuli AW. *In vivo* antimalarial activity of extracts of Tanzanian medicinal plants used for the treatment of malaria. J Adv Pharm Technol Res. 2016;7:59.
139. Nondo RSO, Moshi MJ, Erasto P, Masimba PJ, Machumi F, Kidukuli AW, et al. Anti-plasmodial activity of norcaesalpin D and extracts of four medicinal plants used traditionally for treatment of malaria. BMC Complementary Altern Med. 2017;17:167.
140. Liu J, He X-F, Wang G-H, Merino EF, Yang S-P, Zhu R-X, et al. Aphadilactones A–D, four diterpenoid dimers with DGAT inhibitory and antimalarial activities from a Meliaceae plant. J Org Chem. 2013;79:599-607.
141. Zhang H, Liu J, Gan L-S, Dalal S, Cassera MB, Yue J-M. Antimalarial diterpenoid dimers of a new carbon skeleton from *Aphanamixis grandifolia*. Org Biomol Chem. 2016;14:957-62.
142. Yin J-P, Gu M, Li Y, Nan F-J. Total synthesis of aphadilactones A–D. J Org Chem. 2014;79:6294-301.
143. Palacpac NMQ, Hiramine Y, Seto S, Hiramatsu R, Horii T, Mitamura T. Evidence that *Plasmodium falciparum* diacylglycerol acyltransferase is essential for intraerythrocytic proliferation. Biochem Biophys Res Commun. 2004;321:1062-8.
144. Gachet MS, Lecaro JS, Kaiser M, Brun R, Navarrete H, Muñoz RA, et al. Assessment of anti-protozoal activity of plants traditionally used in Ecuador in the treatment of leishmaniasis. J Ethnopharmacol. 2010;128:184-97.

145. Gachet MS, Kunert O, Kaiser M, Brun R, Zehl M, Keller W, et al. Antiparasitic compounds from *Cupania cinerea* with activities against *Plasmodium falciparum* and *Trypanosoma brucei rhodesiense*. J Nat Prod. 2011;74:559-66.
146. Kumar R, Duffy S, Avery VM, Davis RA. Synthesis of antimalarial amide analogues based on the plant serrulatane diterpenoid 3,7,8-trihydroxyserrulat-14-en-19-oic acid. Bioorg Med Chem Lett. 2017;27:4091-5.
147. Zhou B, Wu Y, Dalal S, Cassera MB, Yue J-M. Euphorbesulins A–P, structurally diverse diterpenoids from *Euphorbia esula*. J Nat Prod. 2016;79:1952-61.
148. Ebrahimi SN, Zimmermann S, Zaugg J, Smiesko M, Brun R, Hamburger M. Abietane diterpenoids from *Salvia sahendica* – antiprotozoal activity and determination of their absolute configurations. Planta Med. 2013;29:150-6.
149. González MA, Clark J, Connelly M, Rivas F. Antimalarial activity of abietane ferruginol analogues possessing a phthalimide group. Bioorg Med Chem Lett. 2014;24:5234-7.
150. Chanthathamrongsiri N, Yuenyongsawad S, Wattanapiromsakul C, Plubrukarn A. Bifunctionalized amphilectane diterpenes from the sponge *Stylissa* cf. *massa*. J Nat Prod. 2012;75:789-92.
151. Avilés E, Prudhomme J, Le Roch KG, Rodríguez AD. Structures, semisyntheses, and absolute configurations of the antiplasmodial α-substituted β-lactam monamphilectines B and C from the sponge *Svenzea flava*. Tetrahedron. 2015;71:487-94.
152. Avilés E, Rodríguez AD. Monamphilectine A, a potent antimalarial β-lactam from marine sponge *Hymeniacidon* sp: Isolation, structure, semisynthesis, and bioactivity. Org Lett. 2010;12:5290-3.
153. White AM, Dao K, Vrubliauskas D, Könst ZA, Pierens GK, Mándi A, et al. Catalyst-controlled stereoselective synthesis secures the structure of the antimalarial isocyanoterpene pustulosaisonitrile-1. J Org Chem. 2017;82:13313-23.
154. Wright AD, Wang H, Gurrath M, König GM, Kocak G, Neumann G, et al. Inhibition of heme detoxification processes underlies the antimalarial activity of terpene isonitrile compounds from marine sponges. J Med Chem. 2001;44:873-85.
155. Smyrniotopoulos V, Merten C, Kaiser M, Tasdemir D. Bifurcatriol, a new antiprotozoal acyclic diterpene from the brown alga *Bifurcaria bifurcata*. Mar Drugs. 2017;15:245.
156. Hata Y, De Mieri M, Ebrahimi SN, Mokoka T, Fouche G, Kaiser M, et al. Identification of two new phenathrenones and a saponin as antiprotozoal constituents of *Drypetes gerrardii*. Phytochem Lett. 2014;10:cxxxiii-cxl.
157. Seephonkai P, Pyne SG, Willis AC, Lie W. Bioactive compounds from the roots of *Strophioblachia fimbricalyx*. J Nat Prod. 2013;76:1358-64.
158. Cai S, Risinger AL, Nair S, Peng J, Anderson TJ, Du L, et al. Identification of compounds with efficacy against malaria parasites from common North American plants. J Nat Prod. 2015;79:490-8.
159. Bickiia J, Tchouyab G, Tchouankeub J, Tsamo E. The antiplasmodial agents of the stem bark of *Entandrophragma angolense* (Meliaceae). Afr J Tradit Complement Altern Med. 2007;4:135-9.
160. Happi GM, Kouam SF, Talontsi FM, Zühlke S, Lamshöft M, Spiteller M. Minor secondary metabolites from the bark of *Entandrophragma congoense* (Meliaceae). Fitoterapia. 2015;102:35-40.
161. Happi GM, Kouam SF, Talontsi FM, Lamshöft M, Zühlke S, Bauer JO, et al. Antiplasmodial and cytotoxic triterpenoids from the bark of the Cameroonian medicinal plant *Entandrophragma congoënse*. J Nat Prod. 2015;78:604-14.
162. Greve HL, Kaiser M, Brun R, Schmidt TJ. Terpenoids from the oleo-gum-resin of *Boswellia serrata* and their antiplasmodial effects *in vitro*. Planta Med. 2017;83:1214-26.
163. Ramalhete C, da Cruz FP, Lopes D, Mulhovo S, Rosário VE, Prudêncio M, et al. Triterpenoids as inhibitors of erythrocytic and liver stages of *Plasmodium* infections. Bioorg Med Chem. 2011;19:7474-81.
164. Ramalhete C, Lopes D, Molnár J, Mulhovo S, Rosário VE, Ferreira M-JU. Karavilagenin C derivatives as antimalarials. Bioorg Med Chem. 2011;19:330-8.
165. Irungu BN, Rukunga GM, Mungai GM, Muthaura CN. *In vitro* antiplasmodial and cytotoxicity activities of 14 medicinal plants from Kenya. S Afr J Bot. 2007;73:204-7.
166. Irungu BN, Adipo N, Orwa JA, Kimani F, Heydenreich M, Midiwo JO, et al. Antiplasmodial and cytotoxic activities of the constituents of *Turraea robusta* and *Turraea nilotica*. J Ethnopharmacol. 2015;174:419-25.
167. Namukobe J, Kasenene JM, Kiremire BT, Byamukama R, Kamatenesi-Mugisha M, Krief S, et al. Traditional plants used for medicinal purposes by local communities around the Northern sector of Kibale National Park, Uganda. J Ethnopharmacol. 2011;136:236-45.
168. Namukobe J, Kiremire BT, Byamukama R, Kasenene JM, Dumontet V, Guéritte F, et al. Cycloartane triterpenes from the leaves of *Neoboutonia macrocalyx* L. Phytochemistry. 2014;102:189-96.
169. Farimani MM, Bahadori MB, Taheri S, Ebrahimi SN, Zimmermann S, Brun R, et al. Triterpenoids with rare carbon skeletons from *Salvia hydrangea*: Antiprotozoal activity and absolute configurations. J Nat Prod. 2011;74:2200-5.
170. Foubert K, Gorella T, Faizal A, Cos P, Maes L, Apers S, et al. Triterpenoid saponins from *Maesa argentea* leaves. Planta Med. 2016;82:1568-75.
171. Ma K, Ren J, Han J, Bao L, Li L, Yao Y, et al. Ganoboninketals A–C, antiplasmodial 3,4-seco-27-norlanostane triterpenes from *Ganoderma boninense* Pat. J Nat Prod. 2014;77:1847-52.
172. Banzouzi J, Soh PN, Ramos S, Toto P, Cavé A, Hemez J, et al. Samvisterin, a new natural antiplasmodial betulin derivative from *Uapaca paludosa* (Euphorbiaceae). J Ethnopharmacol. 2015;173:100-4.
173. Yim T, Kanokmedhakul K, Kanokmedhakul S, Sanmanoch W, Boonlue S. A new meroterpenoid tatenoic acid from the fungus *Neosartorya tatenoi* KKU-2NK23. Nat Prod Res. 2014;28:1847-52.
174. Sá MS, de Menezes MN, Krettli AU, Ribeiro IM, Tomassini TC, Ribeiro dos Santos R, et al. Antimalarial activity of physalins B, D, F, and G. J Nat Prod. 2011;74:2269-72.

175. Ochieng CO, Manguro LA, Owuor PO, Akala H. Voulkensin C–E, new 11-oxocassane-type diterpenoids and a steroid glycoside from *Caesalpinia volkensii* stem bark and their antiplasmodial activities. Bioorg Med Chem Lett. 2013;23:3088-95.
176. Meesala S, Gurung P, Karmodiya K, Subrayan P, Watve MG. Isolation and structure elucidation of halymeniaol, a new antimalarial sterol derivative from the red alga *Halymenia floresii*. J Asian Nat Prod Res. 2017:1-8.
177. Regalado EL, Tasdemir D, Kaiser M, Cachet N, Amade P, Thomas OP. Antiprotozoal steroidal saponins from the marine sponge *Pandaros acanthifolium*. J Nat Prod. 2010;73:1404-10.
178. Huffman MA. Current evidence for self-medication in primates: A multidisciplinary perspective. Am J Phys Anthropol. 1997;104:171-200.
179. Newton-Fisher NE. The diet of chimpanzees in the Budongo Forest Reserve, Uganda. Afr J Ecol. 1999;37:344-54.
180. Obbo C, Makanga B, Mulholland D, Coombes P, Brun R. Antiprotozoal activity of *Khaya anthotheca,* (Welv.) CDC a plant used by chimpanzees for self-medication. J Ethnopharmacol. 2013;147:220-3.
181. Kassim OO, Loyevsky M, Amonoo H, Lashley L, Ako-Nai KA, Gordeuk VR. Inhibition of in-vitro growth of *Plasmodium falciparum* by *Pseudocedrela kotschyi* extract alone and in combination with *Fagara zanthoxyloides* extract. Trans R Soc Trop Med Hyg. 2009;103:698-702.
182. Sidjui LS, Nganso YO, Toghueo RM, Wakeu BN, Dameue JT, Mkounga P, et al. Kostchyienones A and B, new antiplasmodial and cytotoxicity of limonoids from the roots of *Pseudocedrela kotschyi* (Schweinf.) Harms. Z Naturforsch C Bio Sci. 2018;73:153-60.
183. Vigneron M, Deparis X, Deharo E, Bourdy G. Antimalarial remedies in French Guiana: a knowledge attitudes and practices study. J Ethnopharmacol. 2005;98:351-60.
184. Bertania S, Bourdyb G, Landaua I, Robinsonc J, Esterred P, Deharo E. Evaluation of French Guiana traditional antimalarial remedies. J Ethnopharmacol. 2005;98:45-54.
185. Bertani S, Houel E, Stien D, Chevolot L, Jullian V, Garavito G, et al. Simalikalactone D is responsible for the antimalarial properties of an Amazonian traditional remedy made with *Quassia amara* L. (Simaroubaceae). J Ethnopharmacol. 2006;108:155-7.
186. Bertani S, Houël E, Jullian V, Bourdy G, Valentin A, Stien D, et al. New findings on simalikalactone D, an antimalarial compound from *Quassia amara* L. (Simaroubaceae). Exp Parasitol. 2012;130:341-7.
187. Mishra K, Chakraborty D, Pal A, Dey N. *Plasmodium falciparum: in vitro* interaction of quassin and neo-quassin with artesunate, a hemisuccinate derivative of artemisinin. Exp Parasitol. 2010;124:421-7.
188. Chumkaew P, Pechwang J, Srisawat T. Two new antimalarial quassinoid derivatives from the stems of *Brucea javanica*. J Nat Med. 2017;71:570-3.
189. Chumkaew P, Srisawat T. Antimalarial and cytotoxic quassinoids from the roots of *Brucea javanica*. J Asian Nat Prod Res. 2017;19:247-53.
190. Tona L, Ngimbi N, Tsakala M, Mesia K, Cimanga K, Apers S, et al. Antimalarial activity of 20 crude extracts from nine African medicinal plants used in Kinshasa, Congo. J Ethnopharmacol. 1999;68:193-203.
191. Oluwatosin A, Tolulope A, Ayokulehin K, Patricia O, Aderemi K, Catherine F, et al. Antimalarial potential of kolaviron, a biflavonoid from *Garcinia kola* seeds, against *Plasmodium berghei* infection in Swiss albino mice. Asian Pac J Trop Med. 2014;7:97-104.
192. Konziase B. Protective activity of biflavanones from *Garcinia kola* against *Plasmodium* infection. J Ethnopharmacol. 2015;172:214-8.
193. Azebaze AGB, Teinkela JEM, Nguemfo EL, Valentin A, Dongmo AB, Vardamides JC. Antiplasmodial activity of some phenolic compounds from Cameroonians *Allanblackia*. Afr Health Sci. 2015;15:835-40.
194. Bourjot M, Apel C, Martin M-T, Grellier P, Guéritte F, Litaudon M. Antiplasmodial, antitrypanosomal, and cytotoxic activities of prenylated flavonoids isolated from the stem bark of *Artocarpus styracifolius*. Planta Med. 2010;76:1600-4.
195. Zakaria I, Ahmat N, Jaafar FM, Widyawaruyanti A. Flavonoids with antiplasmodial and cytotoxic activities of *Macaranga triloba*. Fitoterapia. 2012;83:968-72.
196. Juma WP, Akala HM, Eyase FL, Muiva LM, Heydenreich M, Okalebo FA, et al. Terpurinflavone: An antiplasmodial flavone from the stem of *Tephrosia purpurea*. Phytochem Lett. 2011;4:176-8.
197. Muiva-Mutisya L, Macharia B, Heydenreich M, Koch A, Akala HM, Derese S, et al. 6α-Hydroxy-α-toxicarol and (+)-tephrodin with antiplasmodial activities from *Tephrosia* species. Phytochem Lett. 2014;10:179-83.
198. Atilaw Y, Muiva-Mutisya L, Ndakala A, Akala HM, Yeda R, Wu YJ, et al. Four prenylflavone derivatives with antiplasmodial activities from the stem of *Tephrosia purpurea* subsp. *leptostachya*. Molecules. 2017;22:1514.
199. Muiva-Mutisya LM, Atilaw Y, Heydenreich M, Koch A, Akala HM, Cheruiyot AC, et al. Antiplasmodial prenylated flavanonols from *Tephrosia subtriflora*. Nat Prod Res. 2017:1-8.
200. Atilaw Y, Duffy S, Heydenreich M, Muiva-Mutisya L, Avery VM, Erdélyi M, et al. Three chalconoids and a pterocarpene from the roots of *Tephrosia aequilata*. Molecules. 2017;22:318.
201. Frolich S, Schubert C, Bienzle U, Jenett-Siems K. *In vitro* antiplasmodial activity of prenylated chalcone derivatives of hops (*Humulus lupulus*) and their interaction with haemin. J Antimicrob Chemother. 2005;55:883-7.
202. Kaou AM, Mahiou-Leddet V, Hutter S, Aïnouddine S, Hassani S, Yahaya I, et al. Antimalarial activity of crude extracts from nine African medicinal plants. J Ethnopharmacol. 2008;116:74-83.
203. Sashidhara KV, Singh SP, Singh SV, Srivastava RK, Srivastava K, Saxena J, et al. Isolation and identification of β-hematin inhibitors from *Flacourtia indica* as promising antiplasmodial agents. Eur J Med Chem. 2013;60:497-502.

204. Abdalla MA, Laatsch H. Flavonoids from Sudanese *Albizia zygia* (Leguminosae, subfamily Mimosoideae), a plant with antimalarial potency. Afr J Tradit Complement Altern Med. 2012;9:56-8.
205. Zininga T, Ramatsui L, Makhado PB, Makumire S, Achilinou I, Hoppe H, et al. (−)-Epigallocatechin-3-gallate inhibits the chaperone activity of *Plasmodium falciparum* Hsp70 chaperones and abrogates their association with functional partners. Molecules. 2017;22:2139.
206. Sannella AR, Messori L, Casini A, Vincieri FF, Bilia AR, Majori G, et al. Antimalarial properties of green tea. Biochem Biophys Res Commun. 2007;353:177-81.
207. Chung IM, Ghimire BK, Kang EY, Moon HI. Antiplasmodial and cytotoxic activity of khellactone derivatives from *Angelica purpuraefolia* Chung. Phytother Res. 2010;24:469-71.
208. Chung IM, Seo SH, Kang EY, Park WH, Park SD, Moon HI. Antiplasmodial activity of isolated compounds from *Carpesium divaricatum*. Phytother Res. 2010;24:451-3.
209. Du Y, Abedi AK, Valenciano AL, Fernández-Murga ML, Cassera MB, Rasamison VE, et al. Isolation of the new antiplasmodial butanolide, malleastrumolide A, from *Malleastrum* sp.(Meliaceae) from Madagascar. Chem Biodiversity. 2017;14.
210. Zofou D, Tene M, Ngemenya MN, Tane P, Titanji VP. *In vitro* antiplasmodial activity and cytotoxicity of extracts of selected medicinal plants used by traditional healers of Western Cameroon. Malar Res Treat. 2011;doi:10.4061/2011/561342.
211. Zofou D, Tematio EL, Ntie-Kang F, Tene M, Ngemenya MN, Tane P, et al. New antimalarial hits from *Dacryodes edulis* (Burseraceae) - Part I: Isolation, *in vitro* activity, *in silico* "drug-likeness" and pharmacokinetic profiles. PLoS One. 2013;8:e79544.
212. Gadetskaya AV, Mohamed SM, Tarawneh AH, Mohamed NM, Ma G, Ponomarev BN, et al. Phytochemical characterization and biological activity of secondary metabolites from three *Limonium* species. Med Chem Res. 2017;26:2743-50.
213. Tangmouo JG, Ho R, Matheeussen A, Lannang AM, Komguem J, Messi BB, et al. Antimalarial activity of extract and norbergenin derivatives from the stem bark of *Diospyros sanza-minika* A. Chevalier (Ebenaceae). Phytother Res. 2010;24:1676-9.
214. Ndjonka D, Bergmann B, Agyare C, Zimbres FM, Lüersen K, Hensel A, et al. *In vitro* activity of extracts and isolated polyphenols from West African medicinal plants against *Plasmodium falciparum*. Parasitol Res. 2012;111:827-34.
215. Soh PN, Witkowski B, Olagnier D, Nicolau M-L, Garcia-Alvarez M-C, Berry A, et al. *In vitro* and *in vivo* properties of ellagic acid in malaria treatment. Antimicrob Agents Chemother. 2009;53:1100-6.
216. Gachet MS, Kunert O, Kaiser M, Brun R, Munoz RA, Bauer R, et al. Jacaranone-derived glucosidic esters from *Jacaranda glabra* and their activity against *Plasmodium falciparum*. J Nat Prod. 2010;73:553-6.
217. Latif A, Du Y, Dalal SR, Merino EF, Cassera MB, Goetz M, et al. Bioactive neolignans and other compounds from *Magnolia grandiflora* L.: Isolation and antiplasmodial activity. Chem Biodiversity. 2017.
218. Rakotondraibe LH, Graupner PR, Xiong Q, Olson M, Wiley JD, Krai P, et al. Neolignans and other metabolites from *Ocotea cymosa* from the Madagascar rain forest and their biological activities. J Nat Prod. 2015;78:431-40.
219. Ovenden SP, Cobbe M, Kissell R, Birrell GW, Chavchich M, Edstein MD. Phenolic glycosides with antimalarial activity from *Grevillea* "Poorinda Queen". J Nat Prod. 2010;74:74-8.
220. Xiao H, Rao Ravu R, Tekwani BL, Li W, Liu W-B, Jacob MR, et al. Biological evaluation of phytoconstituents from *Polygonum hydropiper*. Nat Prod Res. 2017;31:2053-7.
221. Iwatsuki M, Takada S, Mori M, Ishiyama A, Namatame M, Nishihara-Tsukashima A, et al. *In vitro* and *in vivo* antimalarial activity of puberulic acid and its new analogs, viticolins A–C, produced by *Penicillium* sp. FKI-4410. J Antibiot. 2011;64:183.
222. Nyandoro SS, Munissi JJ, Gruhonjic A, Duffy S, Pan F, Puttreddy R, et al. Polyoxygenated cyclohexenes and other constituents of *Cleistochlamys kirkii* leaves. J Nat Prod. 2016;80:114-25.
223. Kornsakulkarn J, Thongpanchang C, Chainoy R, Choowong W, Nithithanasilp S, Thongpanchang T. Bioactive metabolites from cultures of basidiomycete *Favolaschia tonkinensis*. J Nat Prod. 2010;73:759-62.
224. Lenta BN, Kamdem LM, Ngouela S, Tantangmo F, Devkota KP, Boyom FF, et al. Antiplasmodial constituents from the fruit pericarp of *Pentadesma butyracea*. Planta Med. 2011;77:377-9.
225. Zelefack F, Guilet D, Fabre N, Bayet C, Chevalley S, Ngouela S, et al. Cytotoxic and antiplasmodial xanthones from *Pentadesma butyracea*. J Nat Prod. 2009;72:954-7.
226. Upegui Y, Robledo SM, Gil Romero JF, Quiñones W, Archbold R, Torres F, et al. *In vivo* antimalarial activity of α-mangostin and the new xanthone δ-mangostin. Phytother Res. 2015;29:1195-201.
227. Focho D, Ndam W, Fonge B. Medicinal plants of Aguambu-Bamumbu in the Lebialem highlands, southwest province of Cameroon. Afr J Pharm Pharmacol. 2009;3:001-13.
228. Zofou D, Kowa TK, Wabo HK, Ngemenya MN, Tane P, Titanji VP. *Hypericum lanceolatum* (Hypericaceae) as a potential source of new anti-malarial agents: a bioassay-guided fractionation of the stem bark. Malar J. 2011;10:167.
229. Guizzunti G, Batova A, Chantarasriwong O, Dakanali M, Theodorakis EA. Subcellular localization and activity of gambogic acid. ChemBioChem. 2012;13:1191-8.
230. Ke H, Morrisey JM, Qu S, Chantarasriwong O, Mather MW, Theodorakis EA, et al. Caged *Garcinia* xanthones, a novel chemical scaffold with potent antimalarial activity. Antimicrob Agents Chemother. 2017;61:e01220-16.

231. Calcul L, Waterman C, Ma WS, Lebar MD, Harter C, Mutka T, et al. Screening mangrove endophytic fungi for antimalarial natural products. Mar Drugs. 2013;11:5036-50.
232. Harinantenaina L, Bowman JD, Brodie PJ, Slebodnick C, Callmander MW, Rakotobe E, et al. Antiproliferative and antiplasmodial dimeric phloroglucinols from *Mallotus oppositifolius* from the Madagascar dry forest. J Nat Prod. 2013;76:388-93.
233. Eaton AL, Dalal S, Cassera MB, Zhao S, Kingston DG. Synthesis and antimalarial activity of mallatojaponin C and related compounds. J Nat Prod. 2016;79:1679-83.
234. Marti G, Eparvier V, Moretti C, Prado S, Grellier P, Hue N, et al. Antiplasmodial benzophenone derivatives from the root barks of *Symphonia globulifera* (Clusiaceae). Phytochemistry. 2010;71:964-74.
235. Su Q, Dalal S, Goetz M, Cassera MB, Kingston DG. Antiplasmodial phloroglucinol derivatives from *Syncarpia glomulifera*. Bioorg Med Chem. 2016;24:2544-8.
236. Senadeera SP, Duffy S, Avery VM, Carroll AR. Antiplasmodial β-triketones from the flowers of the Australian tree *Angophora woodsiana*. Bioorg Med Chem Lett. 2017;27:2602-7.
237. Hiranrat A, Mahabusarakam W, Carroll AR, Duffy S, Avery VM. Tomentosones A and B, hexacyclic phloroglucinol derivatives from the Thai shrub *Rhodomyrtus tomentosa*. J Org Chem. 2011;77:680-3.
238. Carroll AR, Avery VM, Duffy S, Forster PI, Guymer GP. Watsonianone A–C, anti-plasmodial β-triketones from the Australian tree, *Corymbia watsoniana*. Org Biomol Chem. 2013;11:453-8.
239. Dai Y, Harinantenaina L, Bowman JD, Da Fonseca IO, Brodie PJ, Goetz M, et al. Isolation of antiplasmodial anthraquinones from *Kniphofia ensifolia*, and synthesis and structure–activity relationships of related compounds. Bioorg Med Chem. 2014;22:269-76.
240. Wube AA, Bucar F, Asres K, Gibbons S, Rattray L, Croft SL. Antimalarial compounds from *Kniphofia foliosa* roots. Phytother Res. 2005;19:472-6.
241. Abdissa N, Induli M, Akala HM, Heydenreich M, Midiwo JO, Ndakala A, et al. Knipholone cyclooxanthrone and an anthraquinone dimer with antiplasmodial activities from the roots of *Kniphofia foliosa*. Phytochem Lett. 2013;6:241-5.
242. Isaka M, Palasarn S, Tobwor P, Boonruangprapa T, Tasanathai K. Bioactive anthraquinone dimers from the leafhopper pathogenic fungus *Torrubiella* sp. BCC 28517. J Antibiot. 2012;65:571.
243. Supong K, Thawai C, Suwanborirux K, Choowong W, Supothina S, Pittayakhajonwut P. Antimalarial and antitubercular C-glycosylated benz[α]anthraquinones from the marine-derived *Streptomyces* sp. BCC45596. Phytochem Lett. 2012;5:651-6.
244. Osman CP, Ismail NH, Ahmad R, Ahmat N, Awang K, Jaafar FM. Anthraquinones with antiplasmodial activity from the roots of *Rennellia elliptica* Korth. (Rubiaceae). Molecules. 2010;15:7218-26.
245. Wanyoike G, Chhabra S, Lang'at-Thoruwa C, Omar S. Brine shrimp toxicity and antiplasmodial activity of five Kenyan medicinal plants. J Ethnopharmacol. 2004;90:129-33.
246. Endale M, Alao JP, Akala HM, Rono NK, Eyase FL, Derese S, et al. Antiplasmodial quinones from *Pentas longiflora* and *Pentas lanceolata*. Planta Med. 2012;78:31-5.
247. Tantangmo F, Lenta B, Boyom F, Ngouela S, Kaiser M, Tsamo E, et al. Antiprotozoal activities of some constituents of *Markhamia tomentosa* (Bignoniaceae). Ann Trop Med Parasitol. 2010;104:391-8.
248. Simonsen HT, Nordskjold JB, Smitt UW, Nyman U, Palpu P, Joshi P, et al. In vitro screening of Indian medicinal plants for antiplasmodial activity. J Ethnopharmacol. 2001;74:195-204.
249. Thiengsusuk A, Chaijaroenkul W, Na-Bangchang K. Antimalarial activities of medicinal plants and herbal formulations used in Thai traditional medicine. Parasitol Res. 2013;112:1475-81.
250. Sumsakul W, Plengsuriyakarn T, Chaijaroenkul W, Viyanant V, Karbwang J, Na-Bangchang K. Antimalarial activity of plumbagin *in vitro* and in animal models. BMC Complementary Altern Med. 2014;14:15.
251. Moreno E, Varughese T, Spadafora C, Arnold AE, Coley PD, Kursar TA, et al. Chemical constituents of the new endophytic fungus *Mycosphaerella* sp. nov. and their anti-parasitic activity. Nat Prod Commun. 2011;6:835.
252. Kumarihamy M, Khan SI, Jacob M, Tekwani BL, Duke SO, Ferreira D, et al. Antiprotozoal and antimicrobial compounds from the plant pathogen *Septoria pistaciarum*. J Nat Prod. 2012;75:883-9.
253. Longeon A, Copp BR, Roué M, Dubois J, Valentin A, Petek S, et al. New bioactive halenaquinone derivatives from South Pacific marine sponges of the genus *Xestospongia*. Bioorg Med Chem. 2010;18:6006-11.
254. Supong K, Sripreechasak P, Tanasupawat S, Danwisetkanjana K, Rachtawee P, Pittayakhajonwut P. Investigation on antimicrobial agents of the terrestrial *Streptomyces* sp. BCC71188. Appl Microbiol Biotechnol. 2017;101:533-43.
255. Panthama N, Kanokmedhakul S, Kanokmedhakul K, Soytong K. Cytotoxic and antimalarial azaphilones from *Chaetomium longirostre*. J Nat Prod. 2011;74:2395-9.
256. Ledoux A, St-Gelais A, Cieckiewicz E, Jansen O, Bordignon A, Illien B, et al. Antimalarial activities of alkyl cyclohexenone derivatives isolated from the leaves of *Poupartia borbonica*. J Nat Prod. 2017;80:1750-7.
257. Farokhi F, Grellier P, Clément M, Roussakis C, Loiseau PM, Genin-Seward E, et al. Antimalarial activity of axidjiferosides, new β-galactosylceramides from the African sponge *Axinyssa djiferi*. Mar Drugs. 2013;11:1304-15.
258. Ferreira MC, Cantrell CL, Wedge DE, Gonçalves VN, Jacob MR, Khan S, et al. Antimycobacterial and antimalarial activities of endophytic fungi associated with the ancient and narrowly endemic neotropical plant *Vellozia gigantea* from Brazil. Mem Inst Oswaldo Cruz. 2017;112:692-7.
259. Lane AL, Stout EP, Lin A-S, Prudhomme J, Le Roch K, Fairchild CR, et al. Antimalarial bromophycolides J− Q from the Fijian red alga *Callophycus serratus*. J Org Chem. 2009;74:2736-42.

260. Lin A-S, Stout EP, Prudhomme J, Roch KL, Fairchild CR, Franzblau SG, et al. Bioactive bromophycolides R−U from the Fijian red alga *Callophycus serratus*. J Nat Prod. 2010;73:275-8.
261. Stout EP, Prudhomme J, Le Roch K, Fairchild CR, Franzblau SG, Aalbersberg W, et al. Unusual antimalarial meroditerpenes from tropical red macroalgae. Bioorg Med Chem Lett. 2010;20:5662-5.
262. Stout EP, Cervantes S, Prudhomme J, France S, La Clair JJ, Le Roch K, et al. Bromophycolide A targets heme crystallization in the human malaria parasite *Plasmodium falciparum*. ChemMedChem. 2011;6:1572-7.
263. Shao C-L, Linington RG, Balunas MJ, Centeno A, Boudreau P, Zhang C, et al. Bastimolide A, a potent antimalarial polyhydroxy macrolide from the marine cyanobacterium *Okeania hirsuta*. J Org Chem. 2015;80:7849-55.
264. Shao C-L, Mou X-F, Cao F, Spadafora C, Glukhov E, Gerwick L, et al. Bastimolide B, an antimalarial 24-membered marine macrolide possessing a *tert*-butyl group. J Nat Prod. 2018.
265. Sirirak T, Kittiwisut S, Janma C, Yuenyongsawad S, Suwanborirux K, Plubrukarn A. Kabiramides J and K, trisoxazole macrolides from the sponge *Pachastrissa nux*. J Nat Prod. 2011;74:1288-92.
266. Sirirak T, Brecker L, Plubrukarn A. Kabiramide L, a new antiplasmodial trisoxazole macrolide from the sponge *Pachastrissa nux*. Nat Prod Res. 2013;27:1213-9.
267. Supong K, Thawai C, Choowong W, Kittiwongwattana C, Thanaboripat D, Laosinwattana C, et al. Antimicrobial compounds from endophytic *Streptomyces* sp. BCC72023 isolated from rice (*Oryza sativa* L.). Res Microbiol. 2016;167:290-8.
268. Xu L, He Z, Xue J, Chen X, Wei X. β-Resorcylic acid lactones from a *Paecilomyces* fungus. J Nat Prod. 2010;73:885-9.
269. Shao C-L, Wu H-X, Wang C-Y, Liu Q-A, Xu Y, Wei M-Y, et al. Potent antifouling resorcylic acid lactones from the gorgonian-derived fungus *Cochliobolus lunatus*. J Nat Prod. 2011;74:629-33.
270. Liu Q-A, Shao C-L, Gu Y-C, Blum M, Gan L-S, Wang K-L, et al. Antifouling and fungicidal resorcylic acid lactones from the sea anemone-derived fungus *Cochliobolus lunatus*. J Agric Food Chem. 2014;62:3183-91.
271. Zhang X-Q, Spadafora C, Pineda LM, Ng MG, Sun J-H, Wang W, et al. Discovery, semisynthesis, antiparasitic and cytotoxic evaluation of 14-membered resorcylic acidlLactones and their derivatives. Sci Rep. 2017;7:11822.
272. Tripathi A, Puddick J, Prinsep MR, Rottmann M, Tan LT. Lagunamides A and B: cytotoxic and antimalarial cyclodepsipeptides from the marine cyanobacterium *Lyngbya majuscula*. J Nat Prod. 2010;73:1810-4.
273. Tripathi A, Puddick J, Prinsep MR, Rottmann M, Chan KP, Chen DY-K, et al. Lagunamide C, a cytotoxic cyclodepsipeptide from the marine cyanobacterium *Lyngbya majuscula*. Phytochemistry. 2011;72:2369-75.
274. Raju R, Khalil ZG, Piggott AM, Blumenthal A, Gardiner DL, Skinner-Adams TS, et al. Mollemycin A: An antimalarial and antibacterial glyco-hexadepsipeptide-polyketide from an Australian marine-derived *Streptomyces* sp.(CMB-M0244). Org Lett. 2014;16:1716-9.
275. Son S, Ko S-K, Kim JW, Lee JK, Jang M, Ryoo I-J, et al. Structures and biological activities of azaphilones produced by *Penicillium* sp. KCB11A109 from a ginseng field. Phytochemistry. 2016;122:154-64.
276. Ibrahim SR, Abdallah HM, Elkhayat ES, Al Musayeib NM, Asfour HZ, Zayed MF, et al. Fusaripeptide A: New antifungal and anti-malarial cyclodepsipeptide from the endophytic fungus *Fusarium* sp. J Asian Nat Prod Res. 2018;20:75-85.
277. LaMonte GM, Almaliti J, Bibo-Verdugo B, Keller L, Zou BY, Yang J, et al. Development of a potent inhibitor of the *Plasmodium* proteasome with reduced mammalian toxicity. J Med Chem. 2017;60:6721-32.
278. Cheng KC-C, Cao S, Raveh A, MacArthur R, Dranchak P, Chlipala G, et al. Actinoramide A identified as a potent antimalarial from titration-based screening of marine natural product extracts. J Nat Prod. 2015;78:2411-22.
279. Von Bargen KW, Niehaus E-M, Bergander K, Brun R, Tudzynski B, Humpf H-U. Structure elucidation and antimalarial activity of apicidin F: an apicidin-like compound produced by *Fusarium fujikuroi*. J Nat Prod. 2013;76:2136-40.
280. Tuenter E, Foubert K, Staerk D, Apers S, Pieters L. Isolation and structure elucidation of cyclopeptide alkaloids from *Ziziphus nummularia* and *Ziziphus spina-christi* by HPLC-DAD-MS and HPLC-PDA-(HRMS)-SPE-NMR. Phytochemistry. 2017;138:163-9.
281. Tuenter E, Segers K, Kang KB, Viaene J, Sung SH, Cos P, et al. Antiplasmodial activity, cytotoxicity and structure-activity relationship study of cyclopeptide alkaloids. Molecules. 2017;22:224.
282. Yu J, Zhou B, Dalal S, Liu Q, Cassera MB, Yue J. Cipaferoids A–C, three limonoids represent two different scaffolds from *Cipadessa baccifera*. Chin J Chem. 2018;36:124-8.
283. Schulze CJ, Navarro G, Ebert D, DeRisi J, Linington RG. Salinipostins A–K, long-chain bicyclic phosphotriesters as a potent and selective antimalarial chemotype. J Org Chem. 2015;80:1312-20.
284. Stolze SC, Deu E, Kaschani F, Li N, Florea BI, Richau KH, et al. The antimalarial natural product symplostatin 4 is a nanomolar inhibitor of the food vacuole falcipains. Chem Biol. 2012;19:1546-55.
285. Olliaro P. Mode of action and mechanisms of resistance for antimalarial drugs. Pharmacol Ther. 2001;89:207-19.
286. Olliaro P, Wells T. The global portfolio of new antimalarial medicines under development. Clin Pharmacol Ther. 2009;85:584-95.
287. Rottmann M, McNamara C, Yeung BK, Lee MC, Zou B, Russell B, et al. Spiroindolones, a potent compound class for the treatment of malaria. Science. 2010;329:1175-80.
288. Kissinger JC, Brunk BP, Crabtree J, Fraunholz MJ, Gajria B, Milgram AJ, et al. The *Plasmodium* genome database. Nature. 2002;419:490.
289. López ML, Vommaro R, Zalis M, de Souza W, Blair S, Segura C. Induction of cell death on *Plasmodium falciparum* asexual blood stages by *Solanum nudum* steroids. Parasitol Int. 2010;59:217-25.

290. Tasdemir D, Topaloglu B, Perozzo R, Brun R, O'Neill R, Carballeira NM, et al. Marine natural products from the Turkish sponge *Agelas oroides* that inhibit the enoyl reductases from *Plasmodium falciparum*, *Mycobacterium tuberculosis* and *Escherichia coli*. Bioorg Med Chem. 2007;15:6834-45.
291. Kirmizibekmez H, Calis I, Perozzo R, Brun R, Donmez AA, Linden A, et al. Inhibiting activities of the secondary metabolites of *Phlomis brunneogaleata* against parasitic protozoa and plasmodial enoyl-ACP reductase, a crucial enzyme in fatty acid biosynthesis. Planta Med. 2004;70:711-7.
292. Karioti A, Skaltsa H, Linden A, Perozzo R, Brun R, Tasdemir D. Anthecularin: a novel sesquiterpene lactone from *Anthemis auriculata* with antiprotozoal activity. J Org Chem. 2007;72:8103-6.
293. Karioti A, Skaltsa H, Zhang X, Tonge PJ, Perozzo R, Kaiser M, et al. Inhibiting enoyl-ACP reductase (FabI) across pathogenic microorganisms by linear sesquiterpene lactones from *Anthemis auriculata*. Phytomedicine. 2008;15:1125-9.
294. Bankeu JJ, Khayala R, Lenta BN, Noungoué DT, Ngouela SA, Mustafa SA, et al. Isoflavone dimers and other bioactive constituents from the figs of *Ficus mucuso*. J Nat Prod. 2011;74:1370-8.
295. Lauinger IL, Vivas L, Perozzo R, Stairiker C, Tarun A, Zloh M, et al. Potential of lichen secondary metabolites against *Plasmodium* liver stage parasites with FAS-II as the potential target. J Nat Prod. 2013;76:1064-70.
296. Muhammad A, Anis I, Ali Z, Awadelkarim S, Khan A, Khalid A, et al. Methylenebissantin: A rare methylene-bridged bisflavonoid from *Dodonaea viscosa* which inhibits *Plasmodium falciparum* enoyl-ACP reductase. Bioorg Med Chem Lett. 2012;22:610-2.
297. Tasdemir D, Lack G, Brun R, Rüedi P, Scapozza L, Perozzo R. Inhibition of *Plasmodium falciparum* fatty acid biosynthesis: Evaluation of FabG, FabZ, and FabI as drug targets for flavonoids. J Med Chem. 2006;49:3345-53.
298. Singh SV, Manhas A, Kumar Y, Mishra S, Shanker K, Khan F, et al. Antimalarial activity and safety assessment of *Flueggea virosa* leaves and its major constituent with special emphasis on their mode of action. Biomed Pharmacother. 2017;89:761-71.
299. Singh DK, Cheema HS, Saxena A, Singh S, Darokar MP, Bawankule DU, et al. Fraxetin and ethyl acetate extract from *Lawsonia inermis* L. ameliorate oxidative stress in *P. berghei* infected mice by augmenting antioxidant defence system. Phytomedicine. 2017;36:262-72.
300. Wahyuono S, Simanjuntak P. Heme polymerization inhibitory activities of xanthone from *G. parvifolia* (Miq) Miq stem bark as an antimalarial agent. Asian J Chem. 2013;25:1311.
301. Singh SV, Manhas A, Singh SP, Mishra S, Tiwari N, Kumar P, et al. A phenolic glycoside from *Flacourtia indica* induces heme mediated oxidative stress in *Plasmodium falciparum* and attenuates malaria pathogenesis in mice. Phytomedicine. 2017;30:1-9.
302. Mangoyi R, Hayeshi R, Ngadjui B, Ngandeu F, Bezabih M, Abegaz B, et al. Glutathione transferase from *Plasmodium falciparum* – Interaction with malagashanine and selected plant natural products. J Enzyme Inhib Med Chem. 2010;25:854-62.
303. Skorokhod OA, Davalos-Schafler D, Gallo V, Valente E, Ulliers D, Notarpietro A, et al. Oxidative stress-mediated antimalarial activity of plakortin, a natural endoperoxide from the tropical sponge *Plakortis simplex*. Free Radical Biol Med. 2015;89:624-37.
304. Kamkumo RG, Ngoutane AM, Tchokouaha LR, Fokou PV, Madiesse EA, Legac J, et al. Compounds from *Sorindeia juglandifolia* (Anacardiaceae) exhibit potent anti-plasmodial activities *in vitro* and *in vivo*. Malar J. 2012;11:382.
305. Ishiyama A, Iwatsuki M, Yamamoto T, Miura H, Ōmura S, Otoguro K. Antimalarial tropones and their *Plasmodium falciparum* glyoxalase I (pfGLOI) inhibitory activity. J Antibiot. 2014;67:545.
306. Cockburn IL, Pesce E-R, Pryzborski JM, Davies-Coleman MT, Clark PG, Keyzers RA, et al. Screening for small molecule modulators of Hsp70 chaperone activity using protein aggregation suppression assays: inhibition of the plasmodial chaperone PfHsp70-1. Biol Chem. 2011;392:431-8.
307. Eckstein-Ludwig U, Webb R, Van Goethem I, East J, Lee A, Kimura M, et al. Artemisinins target the SERCA of *Plasmodium falciparum*. Nature. 2003;424:957.
308. Hoepfner D, McNamara CW, Lim CS, Studer C, Riedl R, Aust T, et al. Selective and specific inhibition of the *Plasmodium falciparum* lysyl-tRNA synthetase by the fungal secondary metabolite cladosporin. Cell Host Microbe. 2012;11:654-63.
309. Birkholtz L-M, Coetzer TL, Mancama D, Leroy D, Alano P. Discovering new transmission-blocking antimalarial compounds: challenges and opportunities. Trends Parasitol. 2016;32:669-81.
310. Abay SM, Lucantoni L, Dahiya N, Dori G, Dembo EG, Esposito F, et al. *Plasmodium* transmission blocking activities of *Vernonia amygdalina* extracts and isolated compounds. Malar J. 2015;14:288.
311. Moyo P, Botha ME, Nondaba S, Niemand J, Maharaj VJ, Eloff JN, et al. I*n vitro* inhibition of *Plasmodium falciparum* early and late stage gametocyte viability by extracts from eight traditionally used South African plant species. J Ethnopharmacol. 2016;185:235-42.
312. Lucantoni L, Yerbanga RS, Lupidi G, Pasqualini L, Esposito F, Habluetzel A. Transmission blocking activity of a standardized neem (*Azadirachta indica*) seed extract on the rodent malaria parasite *Plasmodium berghei* in its vector *Anopheles stephensi*. Malar J. 2010;9.
313. Yerbanga R, Lucantoni L, Ouédraogo R, Da DF, Yaméogo K, Churcher T. Transmission blocking activity of *Azadirachta indica* and *Guiera senegalensis* extracts on the sporogonic development of *Plasmodium falciparum* field isolates in *Anopheles coluzzii* mosquitoes. Parasites Vectors. 2014;7.

314. Balaich JN, Mathias DK, Torto B, Jackson BT, Tao D, Ebrahimi B, et al. The non-artemisinin sesquiterpene lactones parthenin and parthenolide block *Plasmodium falciparum* sexual stage transmission. Antimicrob Agents Chemother. 2016:AAC. 02002-15.
315. Tapanelli S, Chianese G, Lucantoni L, Yerbanga RS, Habluetzel A, Taglialatela-Scafati O. Transmission blocking effects of neem (*Azadirachta indica*) seed kernel limonoids on *Plasmodium berghei* early sporogonic development. Fitoterapia. 2016;114:122-6.
316. Jones IW, Denholm AA, Ley SV, Lovell H, Wood A, Sinden RE. Sexual development of malaria parasites is inhibited in vitro by the neem extract azadirachtin, and its semi-synthetic analogues. FEMS Microbiol Lett. 1994;120.
317. Carr G, Derbyshire ER, Caldera E, Currie CR, Clardy J. Antibiotic and antimalarial quinones from fungus-growing ant-associated *Pseudonocardia* sp. J Nat Prod. 2012;75:1806-9.
318. Almeida C, Kehraus S, Prudêncio M, König GM. Marilones A–C, phthalides from the sponge-derived fungus *Stachylidium* sp. Beilstein J Org Chem. 2011;7:1636.
319. Plouffe DM, Wree M, Du AY, Meister S, Li F, Patra K, et al. High-throughput assay and discovery of small molecules that interrupt malaria transmission. Cell Host Microbe. 2016;19:114-26.
320. Peatey CL, Spicer TP, Hodder PS, Trenholme KR, Gardiner DL. A high-throughput assay for the identification of drugs against late-stage *Plasmodium falciparum* gametocytes. Mol Biochem Parasitol. 2011;180:127-31.

CHAPTER 3: Antiplasmodial activity of *Vachellia xanthophloea* (Benth.) P.J.H. Hurter (African fever tree) and its active constituents

Nasir Tajuddeen[a], Tarryn Swart[b], Heinrich C. Hoppe[b] and Fanie R. van Heerden[a]

[a]School of Chemistry and Physics, University of KwaZulu-Natal, Private Bag X01, Scottsville 3209, Pietermaritzburg, South Africa

[b]Department of Biochemistry & Microbiology, Rhodes University, Grahamstown 6140, South Africa

Formatted for ***Journal of Ethnopharmacology***

Abstract

Ethnopharmacological relevance: *Vachellia xanthophloea* (Fabaceae) is known in Zulu as *umkhanyagude* (to be bright or to shine from afar), and in Zulu folk medicine, an emetic prepared from the powdered bark and roots is used for malaria treatment and prophylaxis. In Tanzania, the powdered stem and root bark are taken as a remedy for malaria while the root and bark decoctions are used against abdominal pains and anemia, respectively. *Vachellia xanthophloea* was reported as an antimalarial remedy in Zulu folk medicine during an interview with traditional healers in KwaZulu-Natal province of South Africa.

Aim of the study: Moderate antiplasmodial activity was previously reported for the leaf and stem bark extracts of *V. xanthophloea* against D10 *Plasmodium falciparum* strain. This study aimed to identify the phytochemicals responsible for the antiplasmodial activity of *V. xanthophloea* leaf extract.

Methods: The bioactive compounds in the leaf extract of *V. xanthophloea* were isolated using column chromatographic techniques. The structures of the phytochemicals were established using NMR, HRMS, GC-MS and UV spectroscopy. Antiplasmodial activity of *Vachellia xanthophloea* leaf extract and isolated compounds against chloroquine-sensitive 3D7 *P. falciparum* was evaluated using the parasite lactate dehydrogenase assay. Cytotoxicity against HeLa (human cervix adenocarcinoma) cells was determined using the resazurin assay.

Results: The ethyl acetate fraction of *V. xanthophloea* leaf extract displayed good in vitro antiplasmodial activity with IC_{50} = 10.6 µg/mL and was not cytotoxic. Chromatographic purification of this fraction afforded two new flavonoids and fourteen other compounds, including eight flavonoids, a phenolic ester, a furofuranlignan, a carotenoid and a fatty alcohol. Also, a mixture (1:1) of phytol and lupeol was isolated from the hexane fraction. All the compounds are reported from the leaves of the plant for the first time. Methyl gallate isolated from the ethyl acetate fraction displayed the best activity against 3D7 *P. falciparum* (IC_{50} = 1.2 µg/mL) and was not cytotoxic against HeLa cells.

Conclusion: Methyl gallate is responsible for the antiplasmodial activity of *V. xanthophloea* leaf extract. The folkloric use of *V. xanthophloea* as an antimalarial remedy could be associated with the presence of the compound.

Keywords: *V. xanthophloea*, Fabaceae, malaria, antiplasmodial, flavonoids, quercetin

3.1 Introduction

Acacia (Fabaceae) is a genus of diverse trees and shrubs that is widely distributed in Africa, Australia, Asia, and the Americas. The genus was reclassified in 2003 at the 17th International Botanical Congress, after the approval of a proposal by an Australian group of botanists. The name *Acacia* was retained for the Australian species, while the African species were grouped into two genera, *Vachellia* and *Senegalia*, based on morphological, anatomical and biochemical characteristics.[1-3] *Acacia xanthophloea* was renamed *V. xanthophloea*, based on this reclassification. *V. xanthophloea* (Benth.) P.J.H. Hurter (Fabaceae) (syn. *Acacia xanthophloea*) is known in isiZulu as *umkhanyagude* (to be bright or to shine from afar),[4] apparently due to the iconic bright yellow-green colouration of its bark, which appears powdery in some locations. *V. xanthophloea* has long been associated with malaria. Before the cause of malaria was understood, early discoverers thought that the tree caused malaria because people living and/or travelling in areas where the trees grow usually ended up with fever and thus named it 'the fever tree'.[4,5] However, this is only a coincidence as the tree mostly grows in swampy areas, which is an ideal breeding ground for mosquitoes, the vector for the malaria parasite. In Zulu folk medicine, an emetic prepared from the powdered bark and roots is used for malaria treatment and prophylaxis. In Tanzania, the powdered stem and root bark are taken as a remedy for malaria while root and bark decoctions are used against

abdominal pains and anaemia, respectively. The Luvale women in Angola and Zambia use cold root infusions from a tree purported to be *V. xanthophloea* as a vaginal wash for the relief of abdominal pain.[6,7] *V. xanthophloea* is listed among the traditional fever remedies in Zambian folkloric medicine and most fevers in Zambia are due to malaria.[8] Interviews conducted with traditional health practitioners, in Meru county at Imenti forest game reserve and Tharaka Nithi county at Gatunga in Kenya,[9] and KwaZulu-Natal province in South Africa,[10] indicated that *V. xanthophloea* is used to treat malaria. Furthermore, information from traditional healers show that the plant is used by people in South Africa to treat symptoms of tuberculosis such as fever, cough, and blood in the sputum,[11] while the Masai people in the Loitoktok district of Kenya use it against skin disorders and to relieve fatigue.[12] A decoction made from *V. xanthophloea* bark together with four other medicinal plants is used against infertility by women in Kenya while the Zulus in South Africa prepare a love charm by mixing the plant with *Lithops lesliei* (Aizoaceae).[13] Previous biological studies showed that the stem bark extract of *V. xanthophloea* inhibited the D10 strain of *P. falciparum*,[14] but no compounds were isolated. In this paper, we report on the antiplasmodial and cytotoxic activities of *V. xanthophloea* leaf extract and isolated compounds. To the best of our knowledge, this is the first report of the phytochemistry of *V. xanthophloea*.

3.2 Material and methods

3.2.1. General procedures

Optical rotations were recorded on a Bellingham and Stanley ADP440+ polarimeter. NMR spectra were obtained on Bruker AVANCE III spectrometers (400 or 500 MHz for ^{1}H and 100 or 125 MHz for ^{13}C), using a 5 mm BBOZ probe. The spectra were referenced to residual solvent peaks, δ_H 3.31 and δ_C 49.03 for CD_3OD and δ_H 7.26, δ_C 77.06 for $CDCl_3$ and δ_H 2.50, δ_C 39.53 for DMSO-d_6. Mass spectra were recorded on a TOF Waters Micromass LCT Premier mass spectrometer using ESI-ionization in negative or positive modes in MS-grade acetonitrile and methanol solutions. GC-MS analysis was performed on a Shimadzu GCMS-QP2010SE gas chromatograph-mass spectrometer. For thin-layer chromatographic analyses, pre-coated TLC silica gel 60 F_{254} (Merck) plates were used. Column chromatography was performed on Merck silica gel (230-400) mesh, and gel filtration chromatography was performed using Sephadex LH-20 (Fluka). Spots on TLC plates were observed under UV light at 254 and 365 nm, and visualised by spraying with *p*-anisaldehyde/H_2SO_4 spray reagent (0.5 mL of *p*-anisaldehyde, 10

mL of glacial acetic acid, 4 mL of concentrated H_2SO_4 acid and 85 mL of MeOH), followed by heating at 100 °C for 5 min. Hexanes used for column chromatography referred to an isomeric mixture of hexanes separated on boiling point and commercially referred to as hexane.

HPLC experiments were performed on a Shimadzu LC-20AB Prominence liquid chromatograph equipped with a binary pump, an SPD-M20A Prominence diode-array detector, and a CBM-20A communications bus module. All the analytical HPLC analyses were performed using a Phenomenex (00G-4252-B0) Luna column (5 µm, C18 (2), 100 Å, 250 x 4.6 mm), with a flow rate of 0.5 mL/min at ambient temperature and an injection volume of 10 µL. The solvents used were methanol-acetonitrile (4:3) containing 0.1% formic acid (solvent B), and H_2O containing 0.1% formic acid (solvent A)**.** A gradient elution starting with a linear gradient from 40% B to 100% B in 28 mins, followed by maintaining at 100% B for the next 5 mins, then returning to 40% B in 2 mins, was used. Before injection, the sample solution (1 mg/mL) was filtered using a PVDF membrane with a pore size of 0.45 µm.

3.2.2. Plant material and preparation of extract

The leaves of *V. xanthophloea* were collected from the University of KwaZulu-Natal (UKZN) botanical gardens, Pietermaritzburg Campus, in April 2017. The plant was identified by Ms Alison Young, the curator of the botanical gardens. A voucher specimen was prepared and deposited at the Bews herbarium, UKZN School of Life Sciences, where an accession number, (*V. xanthophloea* NU0048529) was assigned. The plant material was air-dried at room temperature in the laboratory and crushed to a coarse powder using a hammer mill. The powdered material was weighed and stored in paper bags in an aerated environment.

For the antiplasmodial bioassay, the plant material (50 g) was extracted by cold maceration with constant stirring in 500 mL of dichloromethane-methanol (1:1, v/v) for 72 hours. The extract was filtered and concentrated *in vacuo* using a rotary evaporator. *Acacia* species are notorious for tannin content. Tannins bind non-selectively to most proteins and then give false-positive results in bioassays. Therefore, the fractionation of *V. xanthophloea* crude extracts was optimized to reduce or eliminate the tannin content as described by Wall et al.[15] with a slight modification. Briefly, the crude extract of *V. xanthophloea* was reconstituted in 90% methanol and partitioned with hexanes to give a hexane fraction. The residual methanol extract was concentrated under reduced pressure, re-dissolved in distilled water, and

exhaustively partitioned with ethyl acetate. The obtained ethyl acetate fraction was concentrated to a third of the initial volume and then partitioned with a 2% NaCl solution to remove the tannins present. Finally, the residual ethyl acetate layer was dried over anhydrous $MgSO_4$, and evaporated to afford a greenish-brown solid mass.

3.2.3. Isolation of compounds from *V. xanthophloea* leaf

The leaf of *V. xanthophloea* (1000 g) was extracted as described in section 3.2.2. The resulting detannised ethyl acetate fraction (4.5 g) was subjected to silica gel column chromatography and eluted with dichloromethane, combinations of dichloromethane-ethyl acetate (1:9, 2:8, and 3:7) and ethyl acetate, to afford five fractions A-E. Fraction A (147 mg), which had an intense orange colour was purified on a silica gel column eluting with hexanes-ethyl acetate gradient (9:1, 7:3, 1:1) to give four subfractions. Purification of subfraction 1 gave (*E*)-lutein (**3.13**) (3.3 mg). Purification of subfraction two by isocratic elution with hexanes-ethyl acetate (8:2) gave a mixture (4.0 mg) of 3,7,8,2',4',5'-hexamethoxyflavone (**3.1**) and 2'-hydroxy-3,7,8,4'5'-pentamethoxyflavone (**3.2**). Attempts to separate the two compounds using silica column chromatography, Sephadex LH-20, and TLC were not successful. Subfraction three was chromatographed on Sephadex LH-20 eluting with methanol to give pinoresinol (**3.12**) (1.6 mg) and 5,7,2'-trihydroxy-3,4',5'-trimethoxyflavone (**3.3**) (0.9 mg). Repeated Sephadex LH-20 chromatographic purification of fraction B (19 mg) by eluting with methanol gave kaempferol (**3.10**) (3 mg) and impure apigenin (**3.11**) (6 mg), which was further purified on a silica gel column by isocratic elution with hexanes-ethyl acetate (7:3). Silica gel column chromatography of fraction C (52 mg) by isocratic elution with hexanes-ethyl acetate (9:1) gave 1-heptacosanol (**3.14**) (6 mg). Fraction D (340 mg) was initially purified on a Sephadex LH-20 column (eluted with methanol), and three sub-fractions were obtained from this process. Sub-fraction one was further chromatographed on a silica gel column to afford quercetin (**3.5**) (6 mg). Sub-fractions two and three were pooled together, based on the similarity of the TLC profiles, and repeatedly subjected to Sephadex LH-20 chromatography (methanol) to afford methyl gallate (**3.9**) (154 mg) and 3-*O*-methylquercetin (**3.4**) (9 mg). Repeated Sephadex LH-20 chromatography of fraction E eluting with methanol gave taxifolin (**3.6**) (7.8 mg), catechin (**3.7**) (48.2 mg) and a mixture of catechin and gallocatechin (**3.8**) (6.5 mg).

The hexane fraction obtained from the partitioning of *V. xanthophloea* crude extract was also purified by silica gel column chromatography and afforded a mixture of phytol and lupeol (**3.15**) and (**3.16**).

3.2.4. Spectroscopic and physical data of compounds:

3,7,8,2',4',5'-Hexamethoxyflavone (**3.1**): yellow solid, UV (MeOH/ACN): λ_{max} 229, 331 nm; ^{1}H NMR (500MHz, $CDCl_3$): δ_H 8.00 (1H, d, *J*=9.0 Hz, H-5), 7.32 (1H, s, H-6'), 7.03 (1H, d, *J*=9.0 Hz, H-6), 6.64 (1H, s, H-3'), 3.98 (3H, s, OCH_3), 3.97 (3H, s, OCH_3), 3.95 (3H, s, OCH_3), 3.86 (3H, s, OCH_3), 3.85 (3H, s, OCH_3), 3.80 (3H, s, OCH_3). ^{13}C NMR (125 MHz, $CDCl_3$): δ_C 173.4 (C-4), 156.1 (C-7), 155.7 (C-2), 153.6 (C-4'), 151.9 (-2'), 149.9 (C-9), 143.5 (C-5'), 138.2 (C-3), 136.8 (C-8), 121.0 (C-5), 119.6 (C-10), 110.9 (C-6'), 111.4 (C-1'), 109.8 (C-6), 97.7 (C-3'), 61.9 (OCH_3-3), 61.5 (OCH_3-8), 56.6 (OCH_3-7), 56.3 (OCH_3-2'), 56.2 (OCH_3-4'), 56.1 (OCH_3-5'). HPLC R_t: 25.919 min; HR-ESI-(+)-MS: *m/z* 403.1401 $[M+H]^+$ (Calculated for $C_{21}H_{23}O_8$, 403.1393).

2'-Hydroxy-3,7,8,4',5'-pentamethoxyflavone (**3.2**): yellow solid, UV (MeOH/ACN): λ_{max} 247, 344 nm; ^{1}H NMR (500 MHz, $CDCl_3$): δ_H 8.15 (1H, s, OH), 7.99 (1H, d, *J*=9.0 Hz, H-5), 7.06 (1H, d, *J*=9.0 Hz, H-6), 7.05 (1H, s, H-6'), 6.63 (1H, s, H-3'), 4.00 (3H, s, OCH_3), 3.99 (3H, s, OCH_3), 3.93 (3H, s, OCH_3), 3.92 (3H, s, OCH_3), 3.89 (3H, s, OCH_3). ^{13}C NMR (125 MHz, $CDCl_3$) δ_C 173.4 (C-4), 156.6 (C-7), 155.2 (C-2), 152.6 (C-4'), 151.3 (C-2'), 150.1 (C-9), 143.0 (C-5'), 141.2 (C-3), 136.8 (C-8), 121.1 (C-5), 118.8 (C-10), 114.0 (C-6'), 108.9 (C-1'), 110.1 (C-6), 102.8 (C-3'), 61.5 (OCH_3-8), 60.4 (OCH_3-3), 56.8 (OCH_3-5'), 56.7 (OCH_3-4'), 56.5 (OCH_3-7). HPLC R_t: 24.101 min; HR-ESI-(+)-MS: *m/z* 389.1248 $[M+H]^+$ (Calculated for $C_{20}H_{21}O_8$, 389.1236).

5,7,2'-Trihydroxy-3,4',5'-trimethoxyflavone (**3.3**): yellow solid, UV (MeOH/ACN): λ_{max} 256, 342 nm; ^{1}H NMR (500 MHz, CD_3OD+$CDCl_3$): δ_H 7.02 (1H, s, H-3'), 6.60 (1H, s, H-6'), 6.33 (1H, d, *J*= 2.0 Hz, H-8), 6.20 (1H, d, *J*=2.0 Hz, H-6), 3.88 (3H, s, OCH_3), 3.83 (3H, s, OCH_3), 3.73 (3H, s, OCH_3). ^{13}C (125 MHz, CD_3OD+$CDCl_3$): δ_C NMR 180.3 (C-4), 166.2 (C-7), 161.5 (C-5), 158.2 (C-9), 156.6 (C-2), 153.4 (C-4'), 151.0 (C-2'), 142.5 (C-5'), 138.6 (C-3), 113.0 (C-6'), 109.4 (C-1'), 105.8 (C-10), 101.5 (C-3'), 99.7 (C-6), 94.7 (C-8), 60.7 (OCH_3-3'), 56.4 (OCH_3-5'), 55.4 (OCH_3-4'). HPLC R_t: 26.040 min; HR-ESI-(-)-MS: *m/z* 359.0776 $[M-H]^-$ (Calculated for $C_{18}H_{15}O_8$, 359.0767).

3-*O*-Methylquercetin (**3.4**): yellow solid, UV (MeOH/ACN): λ_{max} 266, 373 nm; ^{1}H NMR (400 MHz, CD_3OD): δ_H 7.62 (1H, d, *J*=2.1 Hz, H-2'), 7.52 (1H, dd, *J*=8.5, 2.1 Hz, H-6'), 6.9 (1H, d, *J*=8.5

Hz, H-5'), 6.38 (1H, d, *J*=1.9 Hz, H-8), 6.19 (1H, d, *J*=1.9 Hz, H-6), 3.78 (3H, s, OCH_3). ^{13}C NMR (100 MHz, CD_3OD): δ_C 180.0 (C-4), 166.1 (C-7), 163.1 (C-5), 158.4 (C-9), 158.0 (C-2), 150.0 (C-4'), 146.5 (C-3'), 139.5 (C-3), 123.0 (C-6'), 122.3 (C-1'), 116.5 (C-5'), 116.4 (C-2'), 105.8 (C-10), 99.8 (C-6), 94.8 (C-8), 60.5 (OCH_3-3). HPLC R_t: 23.275 min; HR-ESI-(-)-MS: *m/z* 315.0508 $[M-H]^-$ (Calculated for $C_{16}H_{11}O_7$, 315.0505).

Quercetin (**3.5**): yellow solid, UV (MeOH/ACN): λ_{max} 254, 371 nm; ^1H NMR (400 MHz, CD_3OD): δ_H 7.73 (1H, d, *J*=1.9 Hz, H-2'), 7.63 (1H, dd, *J*=8.4, 1.9Hz, H-6'), 6.88 (1H, d, *J*=8.4 Hz, H-5'), 6.38 (1H, d, *J*=1.9 Hz, H-8), 6.18 (1H, d, *J*=1.9 Hz, H-6). ^{13}C NMR (100 MHz, CD_3OD): δ_C 177.3 (C-4), 166.0 (C-7), 162.5 (C-5), 158.3 (C-9), 148.8 (C-4'), 148.0 (C-2), 146.3 (C-3'), 137.2 (C-3), 124.2 (C-1'), 121.7 (C-6'), 116.3 (C-2'), 116.0 (C-5'), 104.5 (C-10), 99.4 (C-6), 94.5 (C-8). HPLC R_t: 22.136 min; HR-ESI-(-)-MS: *m/z* 301.0341 $[M-H]^-$ (Calculated for $C_{15}H_9O_7$, 301.0348).

(*2R,3R*)-Dihydroquercetin ((+)-taxifolin) (**3.6**): brown solid, $[\alpha]_D^{24.9}$ +34.6 (*c*=0.78, MeOH), UV (MeOH/ACN): λ_{max} 298 nm; ^1H NMR (400 MHz, CD_3OD): δ_H 6.96 (1H, d, *J*=1.86 Hz, H-2'), 6.85 (1H, dd, *J*=8.2, 1.86 Hz, H-6'), 6.8 (1H, d, *J*=8.2 Hz, H-5'), 5.92 (d, 1H, *J*=2.2 Hz, H-8), 5.88 (1H, d, *J*=2.2 Hz, H-6), 4.91 (1H, d, *J*=11.5 Hz, H-2), 4.49 (1H, d, *J*=11.5, Hz, H-3). ^{13}C (100 MHz, CD_3OD): δ_C 198.4 (C-4), 168.8 (C-5), 165.3 (C-7), 164.5 (C-9), 147.2 (C-4'), 146.3 (C-3'), 129.9 (C-1'), 120.9 (C-6'), 116.1 (C-2'), 115.9 (C-5'), 101.8 (C-10), 97.4 (C-6), 96.3 (C-8), 85.1 (C-2), 73.7 (C-3). HPLC R_t: 15.856 min; HR-ESI-(-)-MS: *m/z* 303.0517 $[M-H]^-$ (Calculated for $C_{15}H_{11}O_7$, 303.0505).

(+)-Catechin (**3.7**): brown solid, $[\alpha]_D^{24.9}$ +7.1 (*c*=0.68, MeOH), UV (MeOH/ACN): λ_{max} 279 nm; ^1H NMR (400 MHz, CD_3OD): δ_H 6.83 (1H, d, *J*=1.8 Hz, H-2'), 6.76 (1H, d, *J*=8.0, Hz, H-5'), 6.72 (1H, dd, *J*=8.0, 1.8 Hz, H-6'), 5.93 (1H, d, *J*=2.3 Hz, H-6), 5.86 (1H, d, *J*=2.3 Hz, H-8), 4.57 (1H, d, *J*=7.5 Hz, H-2), 3.98 (1H, dt, *J*=7.7, 5.3 Hz H-3), 2.85 (1H, dd, *J*=16.0, 5.5 Hz, H-4a), 2.51 (1H, dd, *J*=16.5, 8.5 Hz, H-4b). ^{13}C NMR (100 MHz, CD_3OD): δ_C 157.8 (C-7), 157.6 (C-5), 156.9 (C-9), 146.2 (C-3' and C-4'), 132.2 (C-1'), 120.1 (C-6'), 116.1 (C-5'), 115.3 (C-2'), 100.9 (C-10), 96.4 (C-6), 95.5 (C-8), 82.8 (C-2), 68.8 (C-3), 28.5 (C-4). HPLC R_t: 9.039 min; HR-ESI-(-)-MS: *m/z* 289.0706 $[M-H]^-$ (Calculated for $C_{15}H_{13}O_6$, 289.0712).

Gallocatechin (**3.8**): brown solid, UV (MeOH/ACN): λ_{max} 270 nm; ^1H NMR (400 MHz, CD_3OD): δ_H 6.41 (2H, s, H-2',6'), 5.92 (1H, d, *J*=2.3 Hz, H-6), 5.86 (1H, d, *J*=2.3 Hz, H-8), 4.53 (1H, d, *J*=7.0 Hz, H-2), 3.94 (1H, dt, *J*=7.0, 5.5 Hz, H-3), 2.81 (1H, dd, *J*= 16.0, 5.5 Hz, H-4a), 2.51 (1H, dd,

J=16.5, 8.5 Hz, H-4b). ^{13}C (100 MHz, CD_3OD): δ_C 157.8 (C-7), 157.6 (C-5), 156.9 (C-9), 146.8 (C-3' and C-5'), 134.1 (C-4'), 131.7 (C-1'), 107.3 (C-2', C-6'), 100.8 (C-10), 96.3 (C-6), 95.5 (C-8), 82.8 (C-2), 68.8 (C-3), 28.1 (C-4). HPLC R_t: 6.923 min; HR-ESI-(-)-MS: *m/z* 305.0649 $[M-H]^-$ (Calculated for $C_{15}H_{13}O_7$, 305.0661).

Methyl gallate (**3.9**): white solid, UV (MeOH/ACN): λ_{max} 271 nm; ^{1}H NMR (400 MHz, CD_3OD): δ_H 7.05 (2H, s, H-2', 6'), 3.80 (3H, s, H-OCH_3). ^{13}C NMR (100 MHz, CD_3OD): δ_C 169.05 (C=O), 146.44 (C-3 and C-5), 139.73 (C-4), 121.46 (C-1), 110.08 (C-2 and C-6), 52.29 (OCH_3). HPLC R_t: 11.149 min; HR-ESI-(-)-MS: *m/z* 183.0291 $[M-H]^-$ (Calculated for $C_8H_7O_5$, 183.0293).

Kaempferol (**3.10**): yellow solid, ^{1}H NMR (400 MHz, CD_3OD): δ_H 7.86 (2H, d, *J*=8.8 Hz, H-2',6'), 6.93 (2H, d, *J*=8.8 Hz, H-3',5'), 6.38 (1H, d, *J*=2.2 Hz, H-8), 6.17 (1H, d, *J*=2.4 Hz, H-6).

Apigenin (**3.11**): greenish yellow solid, ^{1}H NMR (400 MHz, CD_3OD): δ_H 7.88 (2H, d, *J*=8.8 Hz, H-2',6'), 6.96 (2H, d, *J*=8.8 Hz, H-3',5'), 6.62 (1H, s, H-3), 6.48 (1H, d, *J*=2.1 Hz, H-8), 6.23 (1H, d, *J*=2.1 Hz, H-6).

Pinoresinol (**3.12**): grey solid, UV (MeOH/ACN): λ_{max} 279 nm; ^{1}H NMR (400 MHz, $CDCl_3$): δ_H 6.89 (1H, d, *J*=1.7 Hz, H-2/2'), 6.88 (1H, d, *J*=8.1 Hz, H-5/5'), 6.82 (1H, dd, *J*=8.1, 1.7 Hz, H-6/6'), 5.6 (1H, s, OH), 4.74 (1H, d, *J*=4.3 Hz, H-7/7'), 4.25 (1H, dd, *J*=9.0, 7.0 Hz, H-9a/9a'), 3.9 (3H, s, OCH_3), 3.88 (1H, *J*=8.5, 3.0 Hz, H-9b/9b'), 3.1 (1H, m, H-8/8'). ^{13}C NMR (100 MHz, $CDCl_3$): δ_C 146.8 (C-3/3'), 145.3 (C-4/4'), 133.0 (C-1/1'), 119.0 (C-6/6'), 114.3 (C-5/5'), 108.7 (C-2/2'), 85.9 (C-7/7'), 71.7 (C-9/9'), 56.0 (OCH_3), 54.2 (C-8/8'). HPLC R_t: 20.707 min; HR-ESI-(-)-MS: *m/z* 357.1332 $[M-H]^-$ (Calculated for $C_{20}H_{21}O_6$, 357.1338).

(*E*)-Lutein (**3.13**): orange powder, UV (MeOH/ACN): λ_{max} 445, 472 nm; ^{1}H NMR (400 MHz, $CDCl_3$): δ_H 6.67-6.57 (4H, m, H-11, H-11', H-15, H-15'), 6.35 (1H, d, *J*=14.8 Hz, H-12, H-12'), 6.25 (2H, d, *J*=9.5 Hz, H-14, H-14'), 6.11-6.17 (5H, m, H-7, 8, 8', 10, 10'), 5.54 (1H, brs, H-4'), 5.43 (1H, dd, *J*=15.2, 9.9 Hz, H-7'), 4.25 (1H, brs, H-3'eq), 4.00 (1H, m, H-3ax), 2.41 (1H, brs, H-6'), 2.39 (1H, brs, H-4eq), 2.05 (1H, brd, H-4ax), 1.97 (9H, s, CH_3-19,20,20'), 1.91 (3H, s, CH_3-19'), 1.84 (1H, dd, *J*=13.2, 5.8 Hz, H-2'eq), 1.78 (1H, brs, H-2eq), 1.74 (3H, s, CH_3-18), 1.63 (3H, s, CH_3-18'), 1.48 (1H, brs, H-2ax), 1.37 (1H, dd, *J*=13.3, 6.7 Hz, H-2'ax), 1.07 (6H, s, CH_3-16,17), 0.99 (3H, s, H-17'), 0.84 (3H, s, 16'). ^{13}C NMR (100 MHz, $CDCl_3$): δ_C 138.6 (C-8), 137.8 (C-6, 5'), 137.6 (C-12, 12', 8'), 136.5 (C-13, 13'), 135.9 (C-9), 135.1 (C-9'), 132.6 (C-14, 14'), 131.4 (C-10),

131.0 (C-7), 130.8 (C-10'), 130.1 (C-15, 15'), 128.8 (C-7'), 126.2 (C-5), 125.0 (C-11), 124.8 (C-11'), 124.5 (C-4'), 66.0 (C-3), 65.2 (C-3'), 55.0 (C-6'), 44.7 (C-2'), 42.6 (C-4), 37.1 (C-1), 34.1 (C-1'), 30.3 (C-16), 29.7 (C-2), 29.6 (C-17'), 28.8 (C-17), 24.4 (C-16'), 22.9 (C-20'), 22.7 (C-18'), 21.7 (C-19'), 14.1 (C-18), 13.1 (C-20), 12.8 (C-19). HPLC R_t: 41.795 min; HR-ESI-(+)-MS m/z 568.4295 M^+ (Calculated for $C_{40}H_{56}O_2$, 568.4280).

1-Heptacosanol (**3.14**): White amorphous solid, ^{1}H NMR (400 MHz, $CDCl_3$) δ_H 3.64 (2H, t, *J*=6.5 Hz, H-1), 1.56 (2H, m, H-2), 1.26 (46H, brs, H-3-H26), 0.88 (3H, t, *J*=6.8 Hz, H-27). ^{13}C NMR (100 MHz, $CDCl_3$): δ_C 63.2 (C-1), 32.9 (C-2), 32.0 (C-3), 29.4-29.8 (C4-24), 25.8 (C-25), 22.7 (C-26), 14.2 (C-27).

3.2.5. Antimalarial assay

3.2.5.1. The parasites

Malaria parasites (*Plasmodium falciparum* strain 3D7) were maintained in RPMI 1640 medium containing 2 mM L-glutamine and 25 mM Hepes (Lonza). The medium was further supplemented with 5% Albumax II, 20 mM glucose, 0.65 mM hypoxanthine, 60 µg/mL gentamycin and 2-4% haematocrit human red blood cells. The parasites were cultured at 37 ^oC under an atmosphere of 5% CO_2, 5% O_2, 90% N_2 in a sealed T75 culture flask.[16]

3.2.5.2. Assessment of in vitro antiplasmodial activity

The extracts and pure compounds were initially screened in duplicate at a single concentration of 50 µg/mL, followed by 10 µg/mL. Compounds showing less than 50% viability without cytotoxicity at 10 µg/mL were screened for an IC_{50} value. For IC_{50} screening, extracts and compounds were tested in a concentration range starting from 100 µg/mL and extended by 3-fold serial dilution. Compounds and extracts were tested in triplicates, and standard deviations (SD) were derived, where applicable. Parasite viability was determined by measuring the activity of parasite lactate dehydrogenase (pLDH) as described by Makler et al.[17]. Serial dilutions of the extracts and compounds were added to in vitro cultures of *P. falciparum* (strain 3D7) in 96-well plates (1% haematocrit, 2% parasitaemia). After 48 hours of incubation, 20 µL of culture was removed from each well and combined with 125 µL of a mixture of Malstat (0.18 M lactic acid, 0.13 mM 3-acetylpyridine adenine dinucleotide, 0.16% Triton X-100, 44 mM Tris, pH 9) and NBT/PES (0.39 mM nitro blue tetrazolium, 0.05 mM phenazine ethosulfate) solutions in a fresh 96-well plate. The purple product formed, which

indicates the presence of pLDH, was quantified in a Spectramax M3 microplate reader (Abs_{620}). The Abs_{620} reading in each well is an indication of the pLDH activity, and hence the number of parasites present. The % parasite viability, as indicated by the pLDH activity in treated wells relative to untreated controls, was calculated for each compound/extract. The parasitized RBCs in the absence of test compounds were taken as untreated control with 100% viability. For each compound, percentage viability was plotted against Log of compound concentration and the IC_{50} value (50% inhibitory concentration) was obtained from the resulting dose-response curve by non-linear regression. Chloroquine was used as a positive control drug (IC_{50} values range from 0.01-0.05 µM).

3.2.5.3. In vitro cytotoxicity assay

HeLa (human cervix adenocarcinoma) cells (Cellonex, South Africa) were plated in 96-well plates at a density of $2x10^4$ cells per well in medium consisting of DMEM supplemented with 10% fetal bovine serum and penicillin/streptomycin/amphotericin B antibiotics. After an overnight incubation at 37°C in a humidified 5% CO_2 incubator, test samples were added to a final concentration of 50 µg/ml or 10 µg/ml to the cells in triplicate wells, bringing the total medium volume per well to 200 µl, and incubation continued for 24 hours. Twenty µl resazurin stock solution (0.6 mM resazurin in phosphate-buffered saline) was added to each well and, after a 4 hour incubation, fluorescence (Exc_{560}/Emm_{590}) was measured in a Spectramax M3 plate reader. After subtracting background readings obtained from empty wells, the fluorescence values were used to calculate percentage cell viability in treated wells relative to wells containing untreated control cells.

3.3 Results and discussion

3.3.1. Chemistry

The ethyl acetate fraction displayed good antiplasmodial activity and was not cytotoxic. The extract was subsequently subjected to various chromatographic purification techniques to afford sixteen compounds. The structures of the compounds were elucidated by analyses of the NMR and mass spectral data (compiled in Appendix A) and by comparison with literature data. The structures of the isolated compounds from the leaves of *V. xanthophloea* are given in **Fig. 3.1**.

Compound **3.1** was isolated as a pale yellow amorphous solid. It was assigned a molecular formula of $C_{21}H_{22}O_8$ based on the pseudo-molecular ion $[M+H]^+$ at *m/z* 403.1401 (Calculated for $C_{21}H_{23}O_8$ 403.1393) observed in the HR-ESI-(+)-MS (**Plate 3.1**), suggesting eleven degrees of unsaturation. The ^{1}H NMR spectrum of **3.1** (**Plate 3.3**) revealed a pair of *ortho*-coupled aromatic doublets at δ_H 8.00 (1H, d, *J*=9.0 Hz, H-5) and δ_H 7.03 (1H, d, *J*=9.0 Hz, H-6). These ^{1}H NMR data is typical of H-5 and H-6 of 5-deoxyflavones with oxygenation at position 7, and fall within the ranges for chemical shifts of H-5 (δ_H 7.9-8.2 ppm) and H-6 (δ_H 6.7-7.1 ppm).[18] In addition, two aromatic singlets at δ_H 7.32 (1H, s, H-6'), and δ_H 6.64 (1H, s, H-3') and six aromatic methoxy singlets at δ_H 3.98 (3H, s, OCH_3), 3.97 (3H, s, OCH_3), 3.95 (3H, s, OCH_3), 3.86 (3H, s, OCH_3), 3.85 (3H, s, OCH_3) and δ_H 3.80 (3H, s, OCH_3) were observed in the ^{1}H NMR spectrum. The ^{13}C and DEPT spectra of **3.1** (**Plate 3.4**) showed 14 aromatic signals of which eight are oxygenated, in addition to six methoxy carbons at δ_C 56.1-61.9 and a carbonyl carbon at δ_C 173.4. All protonated carbons were assigned based on HSQC (**Plate 3.5**) cross-peaks. These ^{13}C NMR data suggest that **3.1** is a polymethoxylated flavonoid and is in agreement with the assigned molecular formula $C_{21}H_{23}O_8$.

The appearance of the two aromatic protons at δ_H 7.32 and δ_H 6.64 as singlets suggests that the two protons are isolated from each other and could be assigned to two *para*-substituted protons on ring B. Alternatively, one of the signals could be assigned to C-3 of a flavonoid, and the other signal placed on the ring B. The absence of a correlation in the HMBC spectrum (**Plate 3.6**) between any of the singlet protons and the carbonyl at C-4, supports the assignment of two protons on aromatic ring B. The assignment of the two singlets at positions H-3' and H-6' was further supported by the HMBC correlations between H-3' and H-6' with C-1' and that of only H-6' with C-2. The placement of the two protons that resonate as doublets at δ_H 8.00 and δ_H 7.03 in *ortho* positions at H-5 and H-6 on ring A was supported by COSY (**Plate 3.7**) correlation between H-5 and H-6. The assignment of H-5 and H-6 was confirmed by the long-range HMBC correlations of H-5 with C-4 and C-9, and that of H-6 with C-10. Five of the methoxy groups were located at C-7, C-8, C-2', C-4' and C5', based on HMBC correlations of δ_H 3.98 with δ_C 156.1 (C-7), δ_H 3.95 with δ_C 136.8 (C-8), δ_H 3.96 with δ_C 151.9 (C-2'), δ_H 3.93 with δ_C 153.6 (C-4') and δ_H 3.92 with δ_C 143.5 (C-5'). The sixth methoxy group was placed at C-3, based on the downfield chemical shift of C-3 (δ_C 138.2), and HMBC correlation between δ_H 3.89 and δ_C 138.2. The above NMR data indicated that **3.1** is a 5-

deoxyflavonoid with 3,7,8,2',4',5'-hexasubstitution pattern and the structure was assigned as 3,7,8,2',4',5'-hexamethoxyflavone **3.1** (**Fig. 3.1**), a new natural product.

Compound **3.2** was isolated in a mixture (approximately 1:1 based, on NMR integration) with **3.1,** and the HR-ESI-(+)-MS (**Plate 3.2**) showed a pseudo-molecular ion $[M+H]^+$ at *m/z* 389.1248 (calculated for $C_{20}H_{21}O_8$ 389.1236), suggesting a molecular formula of $C_{20}H_{20}O_8$. The ^1H and ^{13}C NMR spectra (**Plate 3.3 and 3.4**) of **3.2** were similar to those of compound **3.1**. However, compound **3.2** has one less methoxy signal compared to **3.1,** in addition to the appearance of a proton singlet at δ_H 8.15 (1H, s, OH). Analysis of the HSQC spectrum (**Plate 3.5**) of **3.2** showed that this proton was not attached to any carbon atom, indicating that it is a hydroxy proton. An examination of the HMBC spectrum (**Plate 3.6**) showed a cross-peak between the hydroxy proton and δ_C 151.3 (C-2'), suggesting that the methoxy at C-2' of compound **3.1** was replaced by a hydroxy group. A comparison of the NMR data of **3.2** with literature[19,20] showed that the compound was 2'-hydroxy-3,7,8,4'5'-pentamethoxyflavone **3.2** (**Fig. 3.1**). The compound was previously only reported from *Mimosa diplotricha* and *Parkia clappertoniana*,[19,20] both part of the Fabaceae.

Compound **3.3** was isolated as a yellow solid and assigned a molecular formula of $C_{18}H_{16}O_8$ based on pseudo-molecular ion $[M-H]^-$ at *m/z* 359.0776 (calculated for $C_{18}H_{15}O_8$ 359.0767) observed in the HR-ESI-(-)-MS (**Plate 3.8**). The ^1H NMR spectrum (**Plate 3.9**) showed signals for a pair of *meta*-coupled aromatic doublets at δ_H 6.33 (1H, d, *J*= 2.0 Hz, H-8) and δ_H 6.20 (1H, d, *J*=2.0 Hz, H-6), assignable to a flavonoid phloroglucinol ring A, two aromatic singlets at δ_H 7.02 (1H, s, H-3') and δ_H 6.60 (1H, s, H-6'), and three methoxy singlets at δ_H 3.88 (3H, s, OCH_3), δ_H 3.83 (3H, s, OCH_3) and δ_H 3.73 (3H, s, OCH_3). The COSY spectrum (**Plate 3.10**) showed the expected correlation between δ_H 6.20 (H-6) and δ_H 6.33 (H-8). The ^{13}C spectrum (**Plate 3.11**) showed a total of 18 resonances between δ_C 180.3 and δ_C 55.4, including a carbonyl at δ_C 180.3, eight oxygenated aromatic carbons between δ_C 166.2 and δ_C 139.4, and three methoxy carbons between δ_C 60.7 and δ_C 55.4, suggesting a trimethoxylated flavonoid nucleus. All the protonated carbons were assigned based on HSQC (**Plate 3.12**) cross-peaks. The HMBC spectrum (**Plate 3.13**) did not show a correlation between any of the two aromatic singlets in the ^1H NMR spectrum and the carbonyl carbon, thereby precluding a proton on C-3. It follows that both singlets must be assigned to ring B at *para* positions relative to each other. The observed HMBC correlations between δ_H 7.02 (H-3') and δ_H 6.60 (H6') with δ_C 153.4 (C-4'), δ_C

151.0 (C-2'), δ_C 142.5 (C-5') and δ_C 156.6 (C-2), confirmed the assignment. Two methoxy groups were placed at C-4' and C-5', based on the HMBC correlations between the singlet at δ_H 3.88 and δ_C 153.4 (C-4'), and between the singlet at δ_H 3.83 and δ_C 142.5 (C-5'). The third methoxy group was assigned to C-3 based on the downfield chemical shift of C-3 (δ_C 138.6), and HMBC correlation of the singlet at δ_H 3.73 with δ_C 138.6. Based on the above analysis, the structure of **3.3** was assigned as 5,7,2'-trihydroxy-3,4',5'-trimethoxyflavone **3.3** (**Fig. 3.1**), a new natural product.

Compound **3.4** was isolated as a yellow amorphous solid and the molecular formula was determined to be $C_{16}H_{12}O_7$ based on the pseudo-molecular ion $[M-H]^-$ at *m/z* 315.0508 (calculated for $C_{16}H_{11}O_7$ 315.0505) observed in the HR-ESI-(-)-MS (**Plate 3.14**). The aromatic region of the ^{1}H NMR spectrum (**Plate 3.15**) showed signals typical of the ABX spin pattern of a 1,3,4-trisubstituted benzene ring [δ_H 7.62 (1H, d, *J*=2.1 Hz, H-2'), 7.52 (1H, dd, *J*=8.5, 2.1 Hz, H-6'), 6.90 (1H, d, *J*=8.5 Hz, H-5')], which were assigned to a 3',4'-disubstituted flavonoid ring B. The other two signals typified the AX spin pattern of a 1,2,3,5-tetrasubstituted benzene ring [δ_H 6.38 (1H, d, *J*=1.9 Hz, H-8), 6.19 (1H, d, *J*=1.9 Hz, H-6)] and were assigned to a flavonoid phloroglucinol-type ring A. A methoxy proton signal was also observed in the ^{1}H NMR spectrum at δ_H 3.78 (3H, s, OCH_3). The ^{13}C and DEPT spectra (**Plate 3.16**) revealed 14 signals typical of a flavonoid nucleus of which seven are oxygenated, in addition to one carbonyl and one methoxy resonance. The attachment of the methoxy group at C-3 of the flavonoid nucleus was confirmed by the HMBC (**Plate 3.17**) cross peak of δ_H 3.78 with δ_C 139.8 (C-3) and the observed NOESY (**Plate 3.18**) interaction between OCH_3 protons (δ_H 3.78) and H-2' and 6' (δ_H 7.62 and 7.52). All the protonated carbons were assigned based on HSQC (**Plate 3.19**) cross-peaks. A comparison of the above data with those reported in the literature[21] allowed us to assign the structure as 3-*O*-methylquercetin (**3.4**) (**Fig. 3.1**).

The molecular formula of compound **3.5**, a yellow solid, was established as $C_{15}H_{10}O_7$, based on the pseudo-molecular ion $[M-H]^-$ at *m/z* 301.0341 (calculated for $C_{15}H_9O_7$ 301.0348) observed in the HR-ESI-(-)-MS (**Plate 3.20**). The NMR spectra (**Plate 3.21-3.24**) of **3.5** is similar to those of compound **3.4**, except for the absence of one methoxy signal and the upfield shift in the resonance of C-3 by 2.3 ppm, indicating demethoxylation of C-3. Co-TLC with a known sample of quercetin showed that the Rf value was the same. The structure of **3.5** as quercetin

(**3.5**) (**Fig. 3.1**) was confirmed by comparing the NMR data of **3.5** with literature data for quercetin.[22,23]

Compound **3.6**, a brown amorphous solid, showed a pseudo-molecular ion $[M-H]^-$ at *m/z* 303.0517 (calculated $C_{15}H_{11}O_7$ for 303.0505) in the HR-ESI-(-)-MS (**Plate 3.25**), suggesting a molecular formula of $C_{15}H_{12}O_7$. The ^1H NMR spectrum (**Plate 3.26**) of **3.6** displayed aromatic signals assignable to a flavonoid nucleus with a spin system characteristic of an ABX-type ring B [δ_H 6.96 (1H, d, *J*=1.86 Hz, H-2'), 6.85 (1H, dd, *J*=8.2, 1.86 Hz, H-6'), 6.8 (1H, d, *J*=8.2 Hz, H-5')] and an AX-type A [δ_H 5.92 (d, 1H, *J*=2.2 Hz, H-8), 5.88 (1H, d, *J*=2.2 Hz, H-6)], similar to compound **3.5**. Also, a pair of oxymethine doublets at δ_H 4.91 (1H, d, *J*=11.5 Hz, H-2) and δ_H 4.49 (1H, d, *J*=11.5, Hz, H-3) in the ^1H NMR spectrum, suggested a reduction of the C-2/C-3 double bond in **3.5**. The appearance of the aromatic proton signals of **3.6** at higher fields compared to **3.5** further indicated that **3.6** was a dihydroflavonol.[18] A 1,2-diaxial coupling between the C-2 and C-3 protons is apparent from a *J* values of 11.5 Hz, suggesting the relative configuration at C-2/C-3 to be *trans*, typical of naturally occurring dihydroflavonols. The absolute configuration was assigned as (*2R,3R*) based on the positive sign of the specific rotation (+34.6), as found in naturally occurring (+)-(2,3)-*trans*-taxifolin. The ^{13}C and DEPT (**Plate 3.27**) spectra revealed resonances for a carbonyl, 12 aromatic carbons, and two oxygenated methine carbons. The 15 signals were assigned to the dihydroflavonol nucleus by analyzing the HSQC and HMBC spectra (**Plate 3.28 and 3.29**). A comparison of the above NMR data with the literature showed close agreement between the data for **3.6** and dihydroquercetin,[24] and co-TLC of **3.6** with a known sample of dihydroquercetin (**3.6**) showed identical Rf values (**Fig. 3.1**).

Compound **3.7,** a brown powder, has a molecular formula of $C_{15}H_{14}O_6$, based on the pseudo-molecular ion $[M-H]^-$ at *m/z* 289.0706 (calculated for $C_{15}H_{13}O_6$ 289.0712) observed in the HR-ESI-(-)-MS (**Plate 3.30**). The ^1H NMR spectrum (**Plate 3.31**) displayed signals for five aromatic protons which were assigned to an ABX-type ring B [δ_H 6.83 (1H, d, *J*=1.8 Hz, H-2'), 6.76 (1H, d, *J*=8.0, Hz, H-5'), 6.72 (1H, dd, *J*=8.0, 1.8 Hz, H-6') and an AX-type ring A [δ_H 5.93 (1H, d, *J*=2.3 Hz, H-6), 5.86 (1H, d, *J*=2.3 Hz, H-8)]. An oxymethine doublet at δ_H 4.57 (1H, d, *J*=7.5 Hz, H-2), a multiplet at δ_H 3.98 (1H, m, H-3) and a pair of methylene doublet of doublets at δ_H 2.85 (1H, dd, *J*= 16.0, 5.5 Hz, H-4a) and δ_H 2.51 (1H, dd, *J*=16.5, 8.5 Hz, H-4b) were also observed on the ^1H NMR spectrum. The signals were respectively assigned to the protons on C-2, C-3 and C-4

positions of a flavan-3-ol. The large values of $J_{(3,4\beta)}$ (8.4 Hz) and $J_{(3,4\alpha)}$ (5.5 Hz) suggested that **3.7** is catechin. The ^{13}C NMR and DEPT spectra (**Plate 3.32**) displayed 15 resonances including 12 aromatic carbons, a methylene, and two oxygenated methine carbons. The presence of three signals in the ^{13}C spectrum around δ_C 157 is typical of C-5, C-7, and C-9 of catechin. The carbon signals were assigned by analyses of the HSQC and HMBC spectra (**Plate 3.33 and 3.34**). The structure was confirmed to be catechin (**3.7**) (**Fig. 3.1**) after comparing the NMR data with those reported in the literature.[25,26]

Compound **3.8** was isolated in a mixture (1:2 based on NMR integration) with **3.7**. The HR-ESI-(-)-MS (**Plate 3.35**) showed a pseudo-molecular ion $[M-H]^-$ at *m/z* 305.0649 (calculated for $C_{15}H_{13}O_7$ 305.0661), indicating a molecular formula of $C_{15}H_{14}O_7$. A comparison of the ^1H NMR spectrum (**Plate 3.36**) with that of compound **3.7** showed close similarity, except for the disappearance of the ABX spin pattern of ring B and the appearance of a singlet at δ_H 6.4 (2H, s, H-2',6'). Two new carbon signals were also observed on the ^{13}C NMR spectrum (**Plate 3.37**) of **3.7** at δ_C 146.9 (C-3',5') and δ_C 107.3 (C-2', 6'). These NMR data suggested an increase in the oxidation level of ring B of **3.8,** as found in gallocatechin. A comparison of the NMR data of **3.8** with those reported in the literature for gallocatechin showed close agreement.[26] Therefore, the compound was assigned as gallocatechin (**3.8**) (**Fig. 3.1**).

Compound **3.9** was isolated as a white crystalline solid and assigned a molecular formula of $C_8H_8O_5$ based on the observed pseudo-molecular ion $[M-H]^-$ at *m/z* 183.0291 (calculated for $C_8H_7O_5$ 183.0293) in the HR-ESI-(-)-MS (**Plate 3.38**). The ^1H NMR spectrum (**Plate 3.39**) showed only two resonances, an aromatic singlet at δ_H 7.05 (2H, s, H-2', 6') and an oxygenated methyl at δ_H 3.80 (3H, s, OCH_3), suggesting that the compound is a phenolic acid derivative. The ^{13}C and DEPT spectra (**Plate 3.40**) revealed four aromatic carbon resonances of which two are oxygenated, in addition to an ester carbonyl (δ_C 169.05) and a methoxy carbon. The HMBC (**Plate 3.41**) cross peak observed between the methoxy protons (δ_H 3.80) and the carbonyl carbon suggested that **3.9** was the methyl ester of gallic acid. The other peaks were assigned by analysing the HSQC (**Plate 3.42**) and HMBC spectra. The compound was confirmed to be methyl gallate (**3.9**) (**Fig. 3.1**) by comparison of the NMR data with the literature values.[27]

Compound **3.10** was isolated as a yellow solid. The ^1H NMR spectrum (**Plate 3.43**) revealed resonances for a AA'XX' spin system of a 4'-substituted flavonoid ring B [δ_H 8.11 (2H, d, *J*=8.8

Hz, H-2',6'), 6.93 (2H, d, *J*=8.8 Hz, H-3',5')] and an AX-type ring A [δ_H 6.38 (1H, d, *J*=2.2 Hz, H-8), 6.17 (1H, d, *J*=2.4 Hz, H-6)], typical of kaempferol. After comparing the ^{1}H NMR data with those reported in the literature for kaempferol,[28] the structure of the compound was assigned as kaempferol (**3.10**) (**Fig. 3.1**).

Compound **3.11** was isolated as a pale yellow solid. The ^{1}H NMR spectrum (**Plate 3.44**) revealed similar spin systems to those of **3.10,** but with an additional aromatic singlet at δ_H 6.62 (1H, s, H-3), suggesting that **3.11** is a flavone. The proton NMR data of **3.11** closely matched those reported in the literature for apigenin (**3.11**)[29] (**Fig. 3.1**), thus confirming the structure of the compound.

Compound **3.12** was obtained as an amorphous white powder with a molecular formula of $C_{20}H_{22}O_6$, based on a pseudo-molecular ion $[M-H]^-$ observed at m/z 357.1332 (calculated for $C_{20}H_{21}O_6$ 357.1338) in the HR-ESI-(-)-MS (**Plate 3.45**). The ^{1}H NMR spectrum (**Plate 3.46**) revealed three aromatic proton signals assignable to a 1,3,4-trisubstituted benzene ring with an ABC spin pattern [δ_H 6.89 (2H, d, *J*=1.7 Hz, H-2/2'), 6.88 (2H, d, *J*=8.1, H-5/5'), 6.82 (2H, dd, *J*=8.1, 1.7 Hz, H-6/6')]. Further information from the ^{1}H NMR spectrum is the presence of, an oxymethine doublet at δ_H 4.74 (2H, d, *J*=4.3 Hz, H-7/7'), two oxymethylene doublet of doublets at δ_H 4.25 (2H, dd, *J*=9.0, 7.0 Hz, H-9a/9a') and δ_H 3.88 (2H, *J*=8.5, 3.0 Hz H-9b/9b'), a methine multiplet at δ_H 3.1 (2H, m, H-8/8'), a methoxy singlet at δ_H 3.9 (6H, s, OCH_3) and a singlet due to exchangeable hydroxy proton at δ_H 5.6 (2H, s, OH). The ^{13}C and DEPT spectra (**Plate 3.47**) showed ten carbon resonances, including six aromatic carbons, of which two are oxygenated, an oxygenated methine, an oxygenated methylene, a methine, and a methoxy carbon. Considering the molecular mass of compound **3.12**, the symmetrical nature of the structure becomes apparent. All protonated carbons were assigned by analysing the HSQC spectrum (**Plate 3.48**). Analysis of the COSY spectrum (**Plate 3.49**) showed correlations between the methine resonance at δ_H 3.1 and oxymethine at δ_H 4.74 and oxymethylene at δ_H 4.25, and a correlation between the two oxymethylene protons δ_H 4.25 and δ_H 3.88, thereby revealing a 3,7-dioxobicyclo[3.3.0]octane moiety. The above analysis suggests that compound **3.12** is a symmetrical furofurano lignan with a methoxy group on each aromatic ring. This was further supported by the HMBC (**Plate 3.50**) correlations of δ_H 4.74 (H-7/7') with the aromatic carbon resonating at δ_C 133.0 (C-1/1'), and δ_H 6.98 (C-2/2'), δ_H 6.82 (C-6/6') with δ_C 85.93 (C-7/7'), indicating the attachment of the aromatic rings to the furofuran moiety. The

attachment of the methoxy group to position C-3/3' was confirmed by the HMBC correlation between δ_H 3.9 and δ_C 146.8 (C-3'). The HMBC cross-peaks between the hydroxy proton δ_H 5.6 ppm and carbon resonances at δ_C 145.3 (C-4/4'), δ_C 146.8 (C-3/3') and δ_C 114.3 (C-5/5') confirmed that the aromatic ring is hydroxylated at position 4/4'. Naturally occurring furofuran lignans are isolated predominantly with a *cis*-orientation for the ring junction protons (H-8/H-8') due to geometric constraint.[30] The relative stereochemistry of **3.12** was assigned as H-7/H-8 *trans*, H-7'/H-8' *trans* or 7α,8α,7α',8α', based on the small value of $J_{7,8}$ (4.3 Hz), the small value of the difference in the chemical shifts ($\Delta_{\delta H}$) of the diastereotopic protons 9α/9β ($\Delta_{\delta H}$=0.4), and lack of a difference in the chemical shifts of H-7, H-8, H9 and H-7', H-8', H9'.[31] Based on the above NMR data and after comparing with literature values,[32] compound **3.12** was identified as pinoresinol (**3.12**) (**Fig. 3.1**).

(*E*)-lutein **3.13**[33-35] and 1-heptacosanol **3.14**[36] were also isolated from the ethyl acetate fraction, and the structures were identified by comparing the ^{1}H and ^{13}C NMR data with the literature values, in addition to GC-MS for 1-heptacosanol. Similarly, a mixture of phytol **3.15**[37] and lupeol **3.16**[38] was isolated from the hexane fraction, and the structures were determined by comparing the ^{1}H NMR with literature data and GC-MS.

Most of the compounds isolated from the leaves of *V. xanthophloea* in this study are flavonoids, and are reported from the plant for the first time. Some of the flavonoids and flavonoid glycosides have been isolated from other *Vachellia* species (syn. *Acacia*). Apigenin and quercetin have been reported from the leaves of *Acacia tortilis* (now *Vachellia tortilis* (Forssk.) Gallaso & Banfi).[39] Glycosides of apigenin, quercetin and kaempferol were isolated from the leaves of *A. pennata* (now *Senegalia pennata* (L.) Maslin) and shown to have anti-inflammatory activity.[40] However, to the best of our knowledge, this is the first report of polymethoxylated flavonoids from a *Vachellia* species. The isolation of methyl gallate from *V. xanthophloea* is consistent with the phytochemistry of the *Vachellia*. Several phenolic acid derivatives have been isolated from species of *Vachellia*, methyl gallate was reported in *A. nilotica* (now *Vachellia nilotica* (L.) P.J.H. Hurter & Mabb. subsp. *kraussiana* (Benth) Kyal. & Boatwr.)[41] and *A. farnesiana* (now *Vachellia farnesiana*),[42] ethyl gallate was isolated from *A. nilotica* (now *V. nilotica*),[41] and benzoic acid derivatives were isolated from *A. confusa*.[43] Lignans are not common in the *Vachellia*, and *Senegalia* genera,[44] and, in fact, the isolation

of pinoresinol from *V. xanthophloea* is the first report of a lignan from a *Vachellia* or *Senegalia* species.

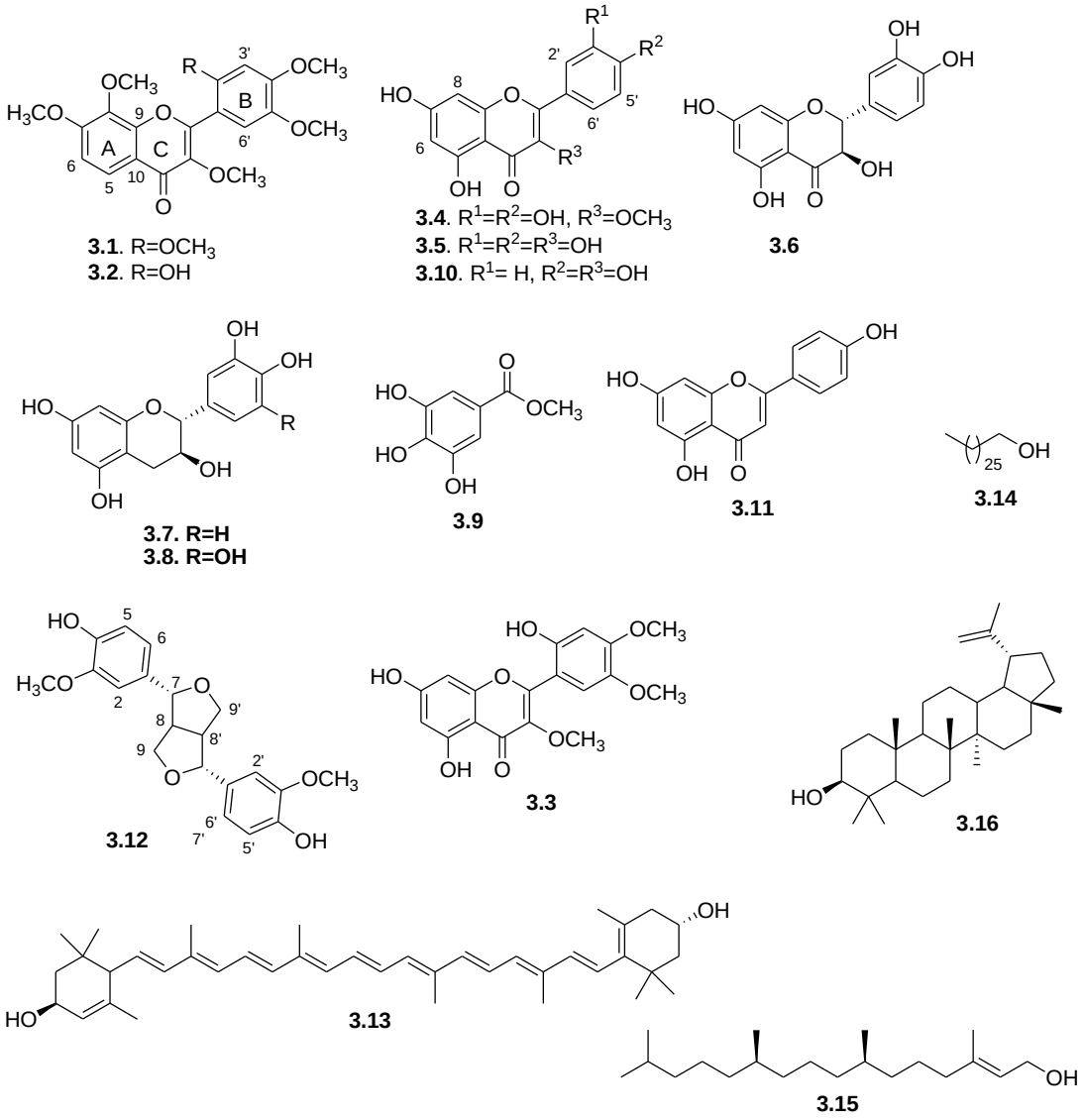

Fig. 3.1: Structures of the isolated compounds from *V. xanthophloea*

3.3.2. Biological activity

The antiplasmodial and cytotoxic activities of the extract and isolated compounds against the chloroquine sensitive 3D7 strain of *P. falciparum* and HeLa cells are summarised in **Tables 3.1 and 3.2**. The ethyl acetate extract showed good antiplasmodial activity and was not cytotoxic. Among the isolated compounds, methyl gallate (**3.9**) showed the best antiparasitic activity (IC_{50} 1.2 µg/mL). Although it was cytotoxic to HeLa cells at 50 µg/mL, at 10 µg/mL HeLa cell viability was reduced by 30%, suggesting a degree of selectivity for 3D7 parasites. The

flavonoids inhibited parasite viability at a high concentration of 50 µg/mL but the compounds were equally cytotoxic. The antiplasmodial activity and cytotoxicity were lost at a lower concentration of 10 µg/mL. Considering that the leaf extract was not cytotoxic, it is possible that the coexistence of all the compounds in the mixture act in ways that mitigate cytotoxicity. But it is worthy to note that when a mixture of methyl gallate (**3.9**) and 3-*O*-methylquercetin (**3.4**) were tested, the antiplasmodial activity of methyl gallate was lowered.

Methyl gallate was previously reported to show good selective antiplasmodial activity against the 3D7 and Dd2 parasite strains.[45] The compound presented a good pharmacokinetic profile and satisfied the Lipinski rule of drug-likeness in an in silico prediction. It was also shown to act in synergy with quinine, and on late-stage parasite schizonts and trophozoites.[45] Methyl gallate could be considered as a good antimalarial hit compound and is worthy of further development. Common dietary flavonoids such as kaempferol, apigenin, quercetin, myricetin, luteonin and glycosides have been shown to possess moderate to weak antiplasmodial activity.[46,47] In this study, most of the flavonoids showed cytotoxicity to HeLa cells at the concentration in which the activity against the malaria parasite was significant, suggesting that the antiplasmodial activity might be due to general toxicity.

Table 3.1: In vitro antiplasmodial activity of the extract and some isolated compounds

Compound	IC_{50} (µg/mL)	50 µg/mL	10 µg/mL
		Viability % ± SD	Viability % ± SD
V. xanthophloea	10.6	-	-
Methyl gallate **3.9**	1.2 ± 0.07	17.7 ± 1.5	26.9 ± 0.7
3-*O*-methylquercetin **3.4**	Nd	21.9 ± 1.5	82.9 ± 3.0
Mixture of compound **3.1** and **3.2**	Nd	14.1 ± 0.7	73.0 ± 0.7
Kaempferol	25.0	-	-
Dihydroquercetin **3.6**	27.6		
Mixture of **3.4** and **3.9**	4.6	-	-
Chloroquine	0.014 µM		

Table 3.2: In vitro cytotoxic activity of the extract and some isolated compounds

Compound	50 µg/mL	10 µg/mL
	Viability % ± SD	Viability % ± SD
V. xanthophloea	*41%	#98%
Methyl gallate **3.9**	2.0 ± 0.2	68.6 ± 2.0
3-*O*-methylquercetin **3.4**	4.5 ± 0.1	57.9 ± 5.2
Mixture of compound **3.1** and **3.2**	7.1 ± 0.4	63.1 ± 4.3
Emetine standard	IC_{50} = 0.033 µM	IC_{50} = 0.04 µM

% cell viability at 33 µg/mL, * % cell viability at 100 µg/mL

3.4. Conclusion

The chemical investigation of *V. xanthophloea* leaf has resulted in the isolation of two new flavonoids and 14 known compounds. To the best of our knowledge, this is the first report on the chemical constituents of *V. xanthophloea*, despite its widespread use. Methyl gallate is responsible for the antiplasmodial activity observed for the plant extract.

Acknowledgment

The authors are grateful to Dr Christina Potgieter of Bews Herbarium, School of Life Sciences, University of KwaZulu-Natal for helping with the preparation of plant voucher specimens and Ms Alison young for identifying the plant material. NT is grateful to the University of KwaZulu-Natal for the award of a doctoral scholarship. Antimalarial and cytotoxicity evaluations were supported by Rhodes University (Sandisa Imbewu grant) and the South African Medical Research Council. FRVH acknowledges the National Research Foundation (South Africa) Grant [number 98345] for financial support.

Conflict of interest

The authors declare that they have no conflict of interest.

References

1. Boatwright, J. S.; Van der Bank, M.; Maurin, O., Name changes in African *Acacia* species: plant name changes. *Veld & Flora* **2014,** 100, (1), 33.
2. Haddad, W., Classification and nomenclature of the genus *Acacia* (Leguminosae), with emphasis on Africa. *Dendron* **2011,** 43, 34-43.

3. Kyalangalilwa, B.; Boatwright, J. S.; Daru, B. H.; Maurin, O.; Van der Bank, M., Phylogenetic position and revised classification of *Acacia* sl (Fabaceae: Mimosoideae) in Africa, including new combinations in *Vachellia* and *Senegalia*. *Botanical Journal of the Linnean Society* **2013,** 172, (4), 500-523.
4. Pooley, E., *Complete Field Guide to Trees of Natal, Zululand & Transkei*. Natal Flora Publications Trust: 1993.
5. Coates Palgrave, K., Drummond, R., *Trees of Southern Africa*. C. Struik Publishers, Cape Town: 1977.
6. Hutchings, A., *Zulu Medicinal Plants: an Inventory*. University of Natal Press: 1996; p 124.
7. Watt, J. M., Breyer-Brandwijk, M.G., *The Medicinal and Poisonous Plants of Southern and Eastern Africa*. E. and S. Livingstone LTD., London: 1962; p 552.
8. Fowler, D. G., *Zambian Plants Used as Traditional Fever Cures*. University of Chicago Press: 2011; p 5.
9. Muthaura, C. N.; Keriko, J. M.; Mutai, C.; Yenesew, A.; Gathirwa, J. W.; Irungu, B. N.; Nyangacha, R.; Mungai, G. M.; Derese, S., Antiplasmodial potential of traditional phytotherapy of some remedies used in treatment of malaria in Meru-Tharaka Nithi County of Kenya. *Journal of Ethnopharmacology* **2015,** 175, 315-323.
10. Nandkumar, N.; Ojewole, J. A. O., Studies on the antiplasmodial properties of some South African medicinal plants used as antimalarial remedies in Zulu folk medicine. *Methods and Findings in Experimental and Clinical Pharmacology* **2002,** 24, (7), 397-401.
11. Lall, N.; Meyer, J. J. M., In vitro inhibition of drug-resistant and drug-sensitive strains of *Mycobacterium tuberculosis* by ethnobotanically selected South African plants. *Journal of Ethnopharmacology* **1999,** 66, (3), 347-354.
12. Muthee, J. K.; Gakuya, D. W.; Mbaria, J. M.; Kareru, P. G.; Mulei, C. M.; Njonge, F. K., Ethnobotanical study of anthelmintic and other medicinal plants traditionally used in Loitoktok district of Kenya. *Journal of Ethnopharmacology* **2011,** 135, (1), 15-21.
13. Smith, G. F.; Crouch, N. R., Mesembs in the muthimarket: *Lithops lesliei* as an ethnomedicinal plant. *British Cactus & Succulent Journal* **1999,** 17, (3), 133-137.

14. Prozesky, E. A.; Meyer, J. J. M.; Louw, A. I., In vitro antiplasmodial activity and cytotoxicity of ethnobotanically selected South African plants. *Journal of Ethnopharmacology* **2001,** 76, (3), 239-245.

15. Wall, M. E.; Wani, M. C.; Brown, D. M.; Fullas, F.; Olwald, J. B.; Josephson, F. F.; Thornton, N. M.; Pezzuto, J. M.; Beecher, C. W. W.; Farnsworth, N. R.; Cordell, G. A.; Kinghorn, A. D., Effect of tannins on screening of plant extracts for enzyme inhibitory activity and techniques for their removal. *Phytomedicine* **1996,** 3, (3), 281-285.

16. Trager, W.; Jensen, J. B., Human malaria parasites in continuous culture. *Science* **1976,** 193, (4254), 673-675.

17. Makler, M. T.; Ries, J. M.; Williams, J. A.; Bancroft, J. E.; Piper, R. C.; Gibbins, B. L.; Hinrichs, D. J., Parasite lactate-dehydrogenase as an assay for *plasmodium-falciparum* drug-sensitivity. *American Journal of Tropical Medicine and Hygiene* **1993,** 48, (6), 739-741.

18. Mabry, T., Markham, K., Thomas, M., *The Systematic Identification of Flavonoids*. Springer-Verlag, New York: 1970.

19. Lin, L.-C.; Chiou, C. T.; Cheng, J. J., 5-Deoxyflavones with cytotoxic activity from *Mimosa diplotricha*. *Journal of Natural Products* **2011,** 74, (9), 2001-2004.

20. Lemmich, E.; Adewunmi, C. O.; Furu, P.; Kristensen, A.; Larsen, L.; Olsen, C. E., 5-Deoxyflavones from *Parkia clappertoniana*. *Phytochemistry* **1996,** 42, (4), 1011-1013.

21. Krenn, L.; Miron, A.; Pemp, E.; Petr, U.; Kopp, B., Flavonoids from *Achillea nobilis* L. *Zeitschrift für Naturforschung C* **2003,** 58, (1-2), 11-16.

22. Lallemand, J.; Duteil, M., ^{13}C NMR spectra of quercetin and rutin. *Organic Magnetic Resonance* **1977,** 9, (3), 179-180.

23. Peng, Z. F.; Strack, D.; Baumert, A.; Subramaniam, R.; Goh, N. K.; Chia, T. F.; Tan, S. N.; Chia, L. S., Antioxidant flavonoids from leaves of *Polygonum hydropiper* L. *Phytochemistry* **2003,** 62, (2), 219-228.

24. Agrawal, P.; Agarwal, S.; Rastogi, R.; Österdahal, B.-G., Dihydroflavanonols from *Cedrus deodara*, A ^{13}C NMR study. *Planta Medica* **1981,** 43, (09), 82-85.

25. Houel, E.; Nardella, F.; Jullian, V.; Valentin, A.; Vonthron-Senecheau, C.; Villa, P.; Obrecht, A.; Kaiser, M.; Bourreau, E.; Odonne, G.; Fleury, M.; Bourdy, G.; Eparvier, V.; Deharo, E.; Stien, D., Wayanin and guaijaverin, two active metabolites found in a *Psidium acutangulum* Mart. ex DC (syn. *P. persoonii* McVaugh) (Myrtaceae)

antimalarial decoction from the Wayana Amerindians. *Journal of Ethnopharmacology* **2016,** 187, 241-248.

26. Davis, A. L.; Cai, Y.; Davies, A. P.; Lewis, J. R., H-1 and C-13 NMR assignments of some green tea polyphenols. *Magnetic Resonance in Chemistry* **1996,** 34, (11), 887-890.
27. Ma, X. F.; Wu, L. H.; Ito, Y.; Tian, W. X., Application of preparative high-speed counter-current chromatography for separation of methyl gallate from *Acer truncatum* Bunge. *Journal of Chromatography A* **2005,** 1076, (1-2), 212-215.
28. Tajuddeen, N.; Sallau, M. S.; Musa, A. M.; Habila, D. J.; Yahaya, S. M., Flavonoids with antimicrobial activity from the stem bark of *Commiphora pedunculata* (Kotschy & Peyr.) Engl. *Natural Product Research* **2014,** 28, (21), 1915-1918.
29. Teles, Y. C. F.; Rebello Horta, C. C.; Agra, M. d. F.; Siheri, W.; Boyd, M.; Igoli, J. O.; Gray, A. I.; Vanderlei de Souza, M. d. F., New sulphated flavonoids from *Wissadula periplocifolia* (L.) C. Presl (Malvaceae). *Molecules* **2015,** 20, (11), 20161-20172.
30. Lu, Y.; Xue, Y.; Liu, J.; Yao, G.; Li, D.; Sun, B.; Zhang, J.; Liu, Y.; Qi, C.; Xiang, M.; Luo, Z.; Du, G.; Zhang, Y., (+/-)-Acortatarinowins A-F, norlignan, neolignan, and lignan enantiomers from *Acorus tatarinowii*. *Journal of Natural Products* **2015,** 78, (9), 2205-2214.
31. Xu, W.-H.; Zhao, P.; Wang, M.; Liang, Q., Naturally occurring furofuran lignans: structural diversity and biological activities. *Natural Product Research* **2019,** 33, (9), 1357-1373.
32. Cowan, S.; Stewart, M.; Abbiw, D. K.; Latif, Z.; Sarker, S. D.; Nash, R. J., Lignans from *Strophanthus gratus*. *Fitoterapia* **2001,** 72, (1), 80-82.
33. Khachik, F.; Englert, G.; Daitch, C. E.; Beecher, G. R.; Tonucci, L. H.; Lusby, W. R., Isolation and structural elucidation of the geometrical-isomers of lutein and zeaxanthin in extracts from human plasma. *Journal of Chromatography-Biomedical Applications* **1992,** 582, (1-2), 153-166.
34. Moss, G., Carbon-13 NMR spectra of carotenoids. *Pure and Applied Chemistry* **1976,** 47, (2-3), 97-102.
35. Dachtler, M.; Glaser, T.; Kohler, K.; Albert, K., Combined HPLC− MS and HPLC− NMR on-line coupling for the separation and determination of lutein and zeaxanthin stereoisomers in spinach and in retina. *Analytical Chemistry* **2001,** 73, (3), 667-674.

36. Koay, Y. C.; Wong, K. C.; Osman, H.; Eldeen, I. M. S.; Asmawi, M. Z., Chemical constituents and biological activities of *Strobilanthes crispus L*. *Records of Natural Products* **2013,** 7, (1), 59-64.

37. Pongprayoon, U.; Baeckström, P.; Jacobsson, U.; Lindström, M.; Bohlin, L., Antispasmodic activity of β-damascenone and E-phytol isolated from *Ipomoea pes-caprae*. *Planta Medica* **1992,** 58, (01), 19-21.

38. Burns, D.; Reynolds, W. F.; Buchanan, G.; Reese, P. B.; Enriquez, R. G., Assignment of ^{1}H and ^{13}C spectra and investigation of hindered side-chain rotation in lupeol derivatives. *Magnetic Resonance in Chemistry* **2000,** 38, (7), 488-493.

39. Muhaisen, H. M. H.; Ilyas, M.; Mushfiq, M.; Parveen, M.; Basudan, O. A., Flavonoids from *Acacia tortilis*. *Journal of Chemical Research* **2002**, (6), 276-278.

40. Dongmo, A. B.; Miyamoto, T.; Yoshikawa, K.; Arihara, S.; Lacaille-Dubois, M.-A., Flavonoids from *Acacia pennata* and their cyclooxygenase (COX-1 and COX-2) inhibitory activities. *Planta Medica* **2007,** 73, (11), 1202-1207.

41. Kalaivani, T.; Rajasekaran, C.; Mathew, L., Free radical scavenging, cytotoxic, and haemolytic activities of an active antioxidant compound ethyl gallate from leaves of *Acacia nilotica* (L.) Wild. Ex. Delile subsp. *indica* (Benth.) Brenan. *Journal of Food Science* **2011,** 76, (6), T144-T149.

42. Sanchez, E.; Heredia, N.; Camacho-Corona, M. d. R.; Garcia, S., Isolation, characterization and mode of antimicrobial action against *Vibrio cholerae* of methyl gallate isolated from *Acacia farnesiana*. *Journal of Applied Microbiology* **2013,** 115, (6), 1307-1316.

43. Tung, Y.-T.; Wu, J.-H.; Kuo, Y.-H.; Chang, S.-T., Antioxidant activities of natural phenolic compounds from *Acacia confusa* bark. *Bioresource Technology* **2007,** 98, (5), 1120-1123.

44. Seigler, D. S., Phytochemistry of *Acacia* - sensu lato. *Biochemical Systematics and Ecology* **2003,** 31, (8), 845-873.

45. Zofou, D.; Tematio, E. L.; Ntie-Kang, F.; Tene, M.; Ngemenya, M. N.; Tane, P.; Titanji, V. P. K., New antimalarial hits from *Dacryodes edulis* (Burseraceae) - Part I: Isolation, in vitro activity, in silico "drug-likeness" and pharmacokinetic profiles. *Plos One* **2013,** 8, (11).

46. Ganesh, D.; Fuehrer, H.-P.; Starzengrueber, P.; Swoboda, P.; Khan, W. A.; Reismann, J. A. B.; Mueller, M. S. K.; Chiba, P.; Noedl, H., Antiplasmodial activity of flavonol quercetin and its analogues in *Plasmodium falciparum*: evidence from clinical isolates in Bangladesh and standardized parasite clones. *Parasitology Research* **2012,** 110, (6), 2289-2295.

47. Lehane, A. M.; Saliba, K. J., Common dietary flavonoids inhibit the growth of the intraerythrocytic malaria parasite. *BMC Research Notes* **2008,** 1, 26-26.

CHAPTER 4: Phytochemical and antiplasmodial studies of *Ozoroa obovata* (Oliv.) R. & A. Fern. var. *obovata*

Nasir Tajuddeen[a], Tarryn Swart[b], Heinrich C. Hoppe[b] and Fanie R. van Heerden[a]

[a]School of Chemistry and Physics, University of KwaZulu-Natal, Private Bag X01, Scottsville 3209, Pietermaritzburg, South Africa

[b]Department of Biochemistry & Microbiology, Rhodes University, Grahamstown 6140, South Africa

Formatted for ***Journal of Ethnopharmacology***

Abstract

Ethnopharmacological relevance: An ethnobotanical survey of medicinal plants in Ghana showed that a decoction of the leaves and twigs of *Ozoroa insignis* is effective against malaria. Some species of *Ozoroa* have shown good in vitro antiplasmodial activity. *Ozoroa obovata* is found in KwaZulu-Natal and has not been investigated for its phytochemical and antiplasmodial activity.

Aim of the study: This project aimed to study the phytochemical and antiplasmodial properties of *O. obovata*.

Methods: The plant leaf extract was investigated for inhibitory activity against 3D7 *P. falciparum* using the parasite lactate dehydrogenase (pLDH) assay and cytotoxicity against HeLa cells using the resazurin assay. The bioactive compounds were isolated using chromatographic techniques and the structures of the isolated were established using spectroscopic and spectrometric techniques.

Results: The plant leaf extract displayed antiplasmodial activity at 50 µg/mL but was also cytotoxic. Chromatographic purification of the extract led to the isolation of two biflavonoids, four flavonoid glycosides, a steroid glycoside, and a megastigmene derivative. These compounds are being reported in *O. obovata* for the first time. The compounds displayed non-selective antiplasmodial activity at 50 µg/mL but the activity was substantially reduced at 10 µg/mL.

Conclusion: The leaf extract of *O. obovata* contains compounds with antiplasmodial activity, but the extract and compounds are also cytotoxic.

Keywords: *Ozoroa obovata*, Anacardiaceae, malaria, antiplasmodial, biflavonoids, flavonoid glycosides

4.1. Introduction

The genus *Ozoroa* Del. is part of the Anacardiaceae, also known as the cashew family, a family of flowering plants that consist of approximately 83 genera and 860 species. Some Anacardiaceae species are trees that produce edible fruits, e.g. mango and cashew, whereas others produce a milky sap that may be a skin irritant.[1] Several *Ozoroa* species are used by traditional healers in Africa for medicinal purpose. In a survey on plants used by the people of the Wechiau community in Ghana to treat malaria, it was found that a decoction of the leaves and twigs of *O. insignis* is used for treating malaria.[2] The *in vitro* antiplasmodial activities of *O. insignis* Del. roots, *O. sphaerocarpa* R. & A. Fern. (whole plant), and *O. engleri* R. & A. Fern. stem bark have been demonstrated.[3-5] Prozesky et al. have also reported potent antiplasmodial activity for the dichloromethane stem bark extract of *O. engleri* (IC_{50} = 1.7 µg/mL).[4]

Ozoroa obovata (Oliv.) R. & A. Fern. var. *obovata* is a multi-branched shrub that is distributed in southern Africa from the south of Mozambique to northern KwaZulu-Natal. The tree is found in coastal dune bush, in several types of forest, and on the islands off the coast of Mozambique.[1] A decoction made by boiling the roots of *O. obovata*, *Tabernaemontana elegans* and *Artabotrys brachypetalus* is mixed with the powdered roots of *Securinega virosa* and used as a remedy for sexual impotence in Mozambique.[6] Traditional herbalists in Mozambique make a panacea by boiling the mixed roots of *O. obovata*, *T. elegans*, *Artabotrys brachypetalus*, *Maclura africana*, *Fagara humilis*, *Cissampelos hirta*, and *Ximenia caffra*.[6] In East Africa, a decoction of the root and bark of *O. obovata* is drunk three times daily as a remedy for dysentery.[7] Zulu traditional healers use the root of *O. obovata* in medicinal preparations and the bark for the treatment of dysentery and acute inflammation of the chest.[8] Interviews with rural dwellers in northern Maputaland in South Africa indicated that *O. obovata* is among the ethnobotanical plants used against respiratory infections. The antimicrobial activity of the plant leaves against respiratory pathogens was subsequently

demonstrated.[9] Screening for biological activities have shown that some species of *Ozoroa* have cytotoxic,[10] anthelminthic,[11] and antimicrobial activity,[12] and inhibit topoisomerase[13] and 15-lipoxygenase.[12] These biological activities could be ascribed to the presence of bioactive compounds that have been isolated from *Ozoroa* species. Phytochemical investigation of the *Ozoroa* genus has led to the isolation of a wide array of bioactive compounds including, triterpenoids,[14,15] flavonoids,[15] alkylanacardic acids, alkylphenols,[16-18] and ceramides.[19] The rich phytochemical profile and associated interesting biological activities of the *Ozoroa* genus makes it attractive for natural product drug discovery. The phytochemical and biological activities of *O. obovata* have received little attention. Therefore, as part of a program aimed at finding antiplasmodial compounds from South African medicinal plants, the leaves of *O. obovata* was investigated.

4.2. Material and methods

4.2.1. General procedures

The same as section 3.2.1 in chapter 3

The same as section 3.2.2 in chapter 3

4.2.2. The plant material and preparation of extracts

The leaves of *O. obovata* were collected from the University of KwaZulu-Natal (UKZN) arboretum on the Pietermaritzburg Campus, in March 2019. The tree was identified by Ms Alison Young, the curator of the University of KwaZulu-Natal (UKZN) botanical gardens. A voucher specimen was prepared and deposited at the Bews herbarium, UKZN School of Life Sciences, where it was assigned an accession number (NU0087105). The leaves were air dried at room temperature in the laboratory and crushed to a coarse powder using a hammer mill. The powdered plant material was stored in paper bags in a ventilated environment.

For antiplasmodial bioassay, the powdered plant leaves (50 g) was extracted by cold maceration with constant stirring in 500 mL of dichloromethane-methanol (1:1, v/v) for 72 hours. The extract was filtered and concentrated under reduced pressure using a rotary evaporator to give a green solid mass. A portion of the crude extract (50 mg) was dissolved in a minimal amount of methanol, loaded on a polyamide (1.0 g) packed column and eluted

three times with methanol (6 mL each). The eluates were combined, evaporated to dryness, weighed, and stored in a refrigerator until needed for the assay.

4.2.3. Extraction and Isolation

The powdered leaves of *O. obovata* (900 g) were extracted as described in section 4.2.2, but without passing through a polyamide column. From the resulting crude extract, 40.0 g was subjected to VLC using 200 g of silica and 800 mL each of five solvent systems; hexanes-dichloromethane (9:1), dichloromethane-ethyl acetate (20:1), 100% ethyl acetate, ethyl acetate-methanol (5:1), and 100% methanol. Five fractions A-E were collected. The fractions weighed 2.2, 10.4, 10.3, 5.1, and 10.3 g, respectively. Fraction A composed of oily material and was not further purified. Fraction C (6.5 g) was chromatographed over silica gel column eluting with gradients of chloroform-ethyl acetate (9:1, 8:2, 4:6) and ethyl acetate-methanol (9:1 and 8:2) before finally washing the column with 100% methanol to afford six subfractions (sb-Fr1-6) by pooling together eluates with similar TLC profiles. Sb-Fr1-3 mostly composed of pigments and were therefore ignored. Sb-Fr4 and 5 were further pooled together after initially reducing the pigments in sb-Fr4 (0.5 g) by subjecting it to silica gel column chromatography using an isocratic elution with chloroform-ethyl acetate (1:1). The combined Sb-Fr4 and 5 (1.77 g) were chromatographed over silica gel eluting with gradients of chloroform-ethyl acetate (1:1, 3:7) and ethyl acetate-methanol (8:2) to afford three subfractions (sb-fr1a-1c) and some pigments. Purification of sb-fr1a (150 mg) using Sephadex LH-20 eluting with methanol afforded amentoflavone (**4.2**) (31.4 mg) and robustaflavone (**4.1**) (10.8 mg). Silica gel column chromatography of sb-fr1b (200 mg) by isocratic elution with chloroform-methanol (7:1) gave three minor fractions (m-fr1a-c). Chromatography of m-fr1a (39.2 mg) over Sephadex LH-20 led to the isolation of quercetin 3-*O*-arabinofuranoside (**4.3**) (25.9 mg) and kaempferol 3-*O*-arabinofuranoside (**4.5**) (1.7 mg). Purification of m-fr1b (102 mg) over silica gel by isocratic elution with chloroform-methanol (14:1) gave β-sitosterol 3-*O*-β-D-glucoside (**4.7**) (5.6 mg) and (*3S,5R,6R,7E,9S*)-3,5,6,9-tetrahydroxymegastigman-7-ene (**4.8**) (4.8 mg). Sephadex LH-20 purification of mfr-1c (17.4 mg) gave quercetin 3-*O*-α-L-rhamnoside (**4.4**) (11.8 mg). Purification of sb-fr1c (500 mg) over silica gel by isocratic elution with chloroform-methanol (14:1) gave myricetin 3-*O*-α-L-rhamnoside (**4.6**) (4.7 mg). Subfraction 6 was mostly composed of very polar material adjudged to be sugars based on ^{1}H

NMR and so was not further purified. Fraction D and E were soluble only in water but insoluble in methanol, ethyl acetate or chloroform and were ignored.

4.2.4. Spectroscopic and physical data of compounds

Robustaflavone (**4.1**): yellow powder, UV (MeOH/ACN): λ_{max} 268, 337 nm; ^{1}H NMR (400 MHz, CD_3OD): δ_H 7.93 (1H, d, *J*=2.0 Hz, H-2'), 7.88 (1H, dd, *J*=8.5, 2.0 Hz, H-6'), 7.51 (2H, d, *J*=8.7 Hz, H-2''',6'''), 7.11 (1H, d, *J*=8.5 Hz, H-5'), 6.71 (2H, d, *J*=8.7 Hz, H-3''',5'''), 6.59 (1H, s, H-3), 6.58 (1H, s, H-3''), 6.40 (1H, d, *J*=1.8 Hz, H-8), 6.37 (1H, s, H-8''), 6.18 (1H, d, *J*=1.8 Hz, H-6). ^{13}C NMR (100 MHz, CD_3OD): δ_C 184.2 (C-4), 183.8 (C-4''), 166.4 (C-2''), 166.0 (C-2), 165.9 (C-7), 163.6 (C-7''), 163.2 (C-5), 162.5 (C-5'',4'''), 161.0 (C-4'), 159.4 (C-9), 156.5 (C-9''), 132.8 (C-2'), 129.3 (C-2''',6'''), 128.9 (C-6'), 123.2 (C-1',1'''), 121.6 (C-3'), 117.4 (C-5'), 116.8 (C-3''',5'''), 105.4 (C-6'',10,10''), 104.0 (C-3), 103.4 (C-3''), 100.2 (C-6), 100.0 (C-8''), 95.1 (C-8). HPLC R_t: 24.339 min; HR-ESI-(-)-MS: *m/z* 537.0818 $[M-H]^-$ (Calculated for $C_{30}H_{17}O_{10}$, 537.0822).

Amentoflavone (**4.2**): yellow solid, UV (MeOH/ACN): λ_{max} 268, 338 nm; ^{1}H NMR (400 MHz, CD_3OD): δ_H 8.24 (1H, d, *J*=2.3 Hz, H-2'), 7.87 (1H, dd, *J*=8.7, 2.3 Hz, H-6'), 7.65 (2H, d, *J*=8.8 Hz, H-2''',6'''), 7.08 (1H, d, *J*=8.7 Hz, H-5'), 6.60 (2H, d, *J*=8.8 Hz, H-3''',5'''), 6.58 (2H, s, H-3,3''), 6.24 (1H, brs, H-6''), 6.12 (2H, brs, H-8,6). ^{13}C NMR (100 MHz, CD_3OD): δ_C 183.9 (C-4''), 183.6 (C-4), 167.5 (C-7''), 166.5 (C-2''), 165.4 (C-2), 163.7 (C-4'), 162.9 (C-7), 162.5 (C-5'',4'''), 162.2 (C-5), 159.4 (C-9), 156.6 (C-9''), 132.7 (C-2'), 129.3 (C-2''',6'''), 127.6 (C-6'), 124.7 (C-1'), 123.2 (C-1'''), 121.5 (C-3'), 120.6 (C-5'), 116.8 (C-3''',5'''), 108.5 (C-8''), 104.7 (C-10), 103.9 (C-10''), 103.4 (C-3,6''), 103.0 (C-3''), 100.6 (C-6), 95.4 (C-8). HPLC R_t: 24.256 min; HR-ESI-(-)-MS: *m/z* 537.0811 $[M-H]^-$ (Calculated for $C_{30}H_{17}O_{10}$, 537.0822).

Quercetin 3-*O*- α-L-arabinofuranoside (avicularin) (**4.3**): yellow solid, $[\alpha]_D^{29}$ -115.6 (*c*=0.65, MeOH) UV (MeOH/ACN): λ_{max} 255, 353 nm; ^{1}H NMR (400 MHz, CD_3OD): δ_H 7.53 (1H, d, *J*=2.0 Hz, H-2'), 7.49 (1H, dd, *J*=8.3, 2.0 Hz, H-6'), 6.90 (1H, d, *J*=8.3 Hz, H-5'), 6.39 (1H, d, *J*=2.1 Hz, H-8), 6.21 (1H, d, *J*=2.0 Hz, H-6), 5.5 (1H, s, H-1''), 4.33 (1H, dd, *J*=2.9, 0.9 Hz, H-2''), 3.91 (1H, dd, *J*=5.2, 2.9 Hz, H-3''), 3.87 (1H, t, *J*=4.4 Hz, H-4''), 3.51 (2H, m, H-5''). ^{13}C NMR (100 MHz, CD_3OD): δ_C 180.0 (C-4), 166.3 (C-7), 163.1 (C-5), 159.4 (C-2), 158.6 (C-9), 149.9 (C-4'), 146.4 (C-3'), 134.9 (C-3), 123.1 (C-1'), 122.9 (C-6'), 116.9 (C-2'), 116.5 (C-5'), 109.6 (C-1''), 105.6 (C-10), 99.9 (C-6), 94.9 (C-8), 88.1 (C-4''), 83.3 (C-2''), 78.7 (C-3''), 62.6 (C-5''). HPLC R_t: 14.641 min; HR-ESI-(-)-MS: *m/z* 433.0779 $[M-H]^-$ (Calculated for $C_{20}H_{17}O_{11}$, 433.0771).

Quercetin 3-*O*-α-L-rhamnoside (quercitrin) (**4.4**): yellow solid, $[\alpha]_D^{29}$ -136.93 (*c*=1.1, MeOH), UV (MeOH/ACN): λ_{max} 260, 354 nm; ^{1}H NMR (400 MHz, CD_3OD): δ_H 7.34 (1H, d, *J*=2.0 Hz, H-2'), 7.30 (1H, dd, *J*=8.5, 2.0 Hz, H-6'), 6.87 (1H, d, *J*=8.5 Hz, H-5'), 6.36 (1H, d, *J*=2.0 Hz, H-8), 6.19 (1H, d, *J*=2.0 Hz, H-6), 5.35 (1H, d, *J*=1.2 Hz, H-1''), 4.22 (1H, dd, *J*=3.2, 1.7 Hz, H-2''), 3.75 (1H, dd, *J*=9.2, 3.2 Hz, H-3''), 3.45 (1H, m, H-5''), 3.34 (1H, d, *J*=9.4 Hz, H-4''), 0.94 (3H, d, *J*=6.2 Hz, H-6''). ^{13}C NMR (100 MHz, CD_3OD): δ_C 179.6 (C-4), 165.9 (C-7), 163.2 (C-5), 159.3 (C-2), 158.5 (C-9), 149.8 (C-3'), 146.4 (C-4'), 136.2 (C-3), 123.0 (C-1'), 122.9 (C-6'), 117.0 (C-2'), 116.4 (C-5'), 105.9 (C-10), 103.5 (C-1''), 99.8 (C6-), 94.8 (C-8), 73.3 (C-4''), 72.1 (C-3''), 72.0 (C-2''), 71.9 (C-5''), 17.7 (C-6''). HPLC R_t: 14.699 min; HR-ESI-(-)-MS: *m/z* 433.0779 $[M-H]^-$ (Calculated for $C_{21}H_{19}O_{11}$, 447.0927).

Kaempferol 3-*O*-arabinofuranoside (juglanin) (**4.5**): yellow powder, $[\alpha]_D^{29}$ -98.93 (*c*=0.07, MeOH), UV (MeOH/ACN): λ_{max} 264, 347 nm; ^{1}H NMR (400 MHz, CD_3OD): δ_H 7.96 (2H, d, *J*=8.8 Hz, H-2',6'), 6.92 (2H, d, *J*=8.8 Hz, H-3',5'), 6.40 (1H, d, *J*=2.0 Hz, H-8), 6.20 (1H, d, *J*=2.0 Hz, H-6), 5.48 (1H, s, H-1''), 4.31 (1H, dd, *J*=2.9, 0.9 Hz, H-2''), 3.90 (1H, dd, *J*=4.8, 2.7 Hz, H-3''), 3.81 (1H, dd, *J*=8.9, 4.4 Hz, H-4''), 3.48 (2H, m, H-5''). ^{13}C NMR (100 MHz, CD_3OD): δ_C 179.9 (C-4), 166.6 (C-7), 163.1 (C-5), 161.6 (C-4'), 159.3 (C-2), 158.6 (C-9), 134.9 (C-3), 132.0 (C-2',6'), 122.8 (C-1'), 116.5 (C-3',5'), 109.7 (C-1'), 105.5 (C-10), 100.1 (C-6), 94.9 (C-8), 88.0 (C-4''), 83.9 (C-2''), 78.7 (C-3''), 62.5 (C-5''). HPLC R_t: 16.707 min; HR-ESI-(-)-MS: *m/z* 417.0818 $[M-H]^-$ (Calculated for $C_{20}H_{17}O_{10}$, 417.0822).

Myricetin 3-*O*-α-L-rhamnoside (myricetrin) (**4.6**): yellow solid, $[\alpha]_D^{29}$ -179.76 (*c*=0.47, MeOH), ^{1}H NMR (500 MHz, CD_3OD): δ_H 6.95 (2H, s, H-2',6'), 6.35 (1H, d, *J*=2.5 Hz, H-8), 6.20 (1H, d, *J*=2.5 Hz, H-6), 5.31 (1H, d, *J*=1.3 Hz, H-1''), 4.22 (1H, dd, *J*=3.3, 1.7 Hz, H-2''), 3.78 (1H, dd, *J*=10.5, 4.3 Hz, H-3''), 3.47 (1H, m, H-5''), 3.35 (1H, d, *J*=9.5 Hz, H-4''), 0.96 (3H, d, *J*=6.2 Hz, H-6''). ^{13}C NMR (125 MHz, CD_3OD): δ_C 179.5 (C-4), 165.8 (C-7), 163.2 (C-5), 159.4 (C-2), 158.5 (C-9), 146.9 (C-3', 5'), 137.9 (C-4'), 136.3 (C-3), 121.9 (C-1'), 109.7 (C-2', 6'), 105.8 (C-10), 103.6 (C-1''), 99.9 (C-6), 94.8 (C-8), 73.4 (C-4''), 72.2 (C-3''), 72.1 (C-5''), 72.0 (C-2''), 17.7 (C-6''). HR-ESI-(-)-MS: *m/z* 463.0881 $[M-H]^-$ (Calculated for $C_{21}H_{19}O_{12}$, 463.0877).

β-Sitosterol 3-*O*-β-D-glucoside (**4.7**): white amorphous solid, ^{1}H NMR (500 MHz, DMSO-*d*$_6$): δ_H 5.32 (1H, d, *J*=4.9 Hz, H-6), 4.83-4.86 (3H, d, *J*=4.8 Hz, OH-2',3',4'), 4.41 (1H, t, *J*=5.7 Hz, OH-6), 4.21 (1H, d, *J*=7.7 Hz, H-1'), 3.64 (1H, m, H-6'a), 3.45 (1H, m, H-3), 3.40 (1H, m, H-6b'), 3.12 (H,

m, H-3'), 3.09 (1H, m, H-5'), 3.05 (1H, m, H-4'), 3.01 (1H, m, H-2'), 2.35 (1H, m, H-4a), 2.12 (1H, dt, *J*=1.9, 13.4 Hz, H-4b), 1.94-0.97 (overlapped aglycone CH_2 and CH signals), 0.95 (3H, s, H-19), 0.90 (3H, d, *J*=6.5 Hz, H-21), 0.82 (3H, t, *J*=7.2 Hz, H-29), 0.80 (3H, d, *J*=7.0 Hz, H-27), 0.79 (3H, d, *J*=6.9 Hz, H-26), 0.64 (3H, s, H-18). ^{13}C NMR (125 MHz, DMSO-d_6): δ_C 140.5 (C-5), 121.2 (C-6), 100.8 (C-1'), 77.0 (C-3), 76.8 (C-3'), 76.7 (C-5'), 73.5 (C-2'), 70.1 (C-4'), 61.6 (C-6'), 56.2 (C-14), 55.4 (C-17), 49.6 (C-9), 45.2 (C-24), 41.9 (C-13), 39.2 (12), 38.3 (C-4), 36.8 (C-1), 36.2 (C-10), 35.5 (C-20), 33.3 (C-22), 31.5 (C-8), 31.4 (C-7), 29.3 (C-2), 28.7 (C-25), 27.8 (C-16), 25.5 (C-23), 23.8 (C-15), 22.6 (C-28), 20.6 (C-11), 19.7 (C-27), 19.1 (C-19), 18.9 (C-26), 18.6 (C-21), 11.8 (C-29), 11.7 (C-18) HR-ESI-(-)-MS: *m/z* 621.4362 $[M+HCOOH-H]^-$ (Calculated for $C_{36}H_{61}O_8$, 621.4366).

(*3S,5R,6R,7E,9S*)-3,5,6,9-Tetrahydroxymegastigman-7-ene (**4.8**): colourless oil, $[\alpha]_D^{29}$ -17.31 (*c*=0.48, MeOH), ^{1}H NMR (400 MHz, CD_3OD): δ_H 6.07 (1H, dd, *J*=15.9, 1.0 Hz, H-7), 5.78 (1H, dd, *J*=15.9, 6.2 Hz, H-8), 4.34 (1H, qd, *J*=6.5, 1.0 Hz, H-9), 4.06 (1H, m, H-3), 1.76 (2H, m, H-4), 1.64 (1H, t, *J*=12.0 Hz, H-2ax), 1.45 (1H, ddd, *J*=12.2, 4.0, 1.9 Hz, H-2eq), 1.27 (3H, d, *J*=6.4 Hz, H-10), 1.22 (3H, s, H-11), 1.10 (3H, s, H-13), 0.87 (3H, s, H-12). ^{13}C NMR (100 MHz, CD_3OD): δ_C 136.1 (C-8), 131.1 (C-7), 79.0 (C-6), 77.8 (C-5), 69.5 (C-9), 65.3 (C-3), 46.5 (C-2), 45.7 (C-4), 40.7 (C-1), 27.5 (C-12), 27.0 (C-13), 26.2 (C-11), 24.1 (C-10) HR-ESI-(+)-MS: *m/z* 267.1572 $[M+Na]^+$ (Calculated for $C_{13}H_{24}O_4Na$, 267.1572).

4.2.5. Antimalarial assay

4.2.5.1. The parasites

The same as section 3.2.5.1 in chapter 3

4.2.5.2. Assessment of in vitro antiplasmodial activity

The same as section 3.2.5.2 in chapter 3

4.2.5.3. In vitro cytotoxicity assay

The same as section 3.2.5.3 in chapter 3

4.3. Results and discussion

4.3.1. Chemistry

The leaf extract of *O. obovata* exhibited antiplasmodial activity but it was also cytotoxic. Chromatographic purification of this extract afforded eight bioactive compounds, including two biflavonoids, four flavonoid glycosides, a sterol glycoside, and a megastigmane derivative. The structures of the compounds (**Fig. 4.1**) were determined by analysis of the NMR and mass spectral data (Appendix B).

Compound **4.1** was isolated as a yellow powder and assigned a molecular formula of $C_{30}H_{18}O_{10}$ based on a pseudo-molecular ion $[M-H]^-$ at *m/z* 537.0818 (Calculated for $C_{30}H_{17}O_{10}$ 537.0822) in its HR-ESI-(-)-MS (**Plate 4.1**). The ^1H NMR spectrum (**Plate 4.2**) showed signals for 12 aromatic protons assignable to an ABX type spin system at δ_H 7.93 (1H, d, *J*=2.0 Hz, H-2'), δ_H 7.88 (1H, dd, *J*=8.5, 2.0 Hz, H-6'), δ_H 7.11 (1H, d, *J*=8.5 Hz, H-5'), an AA'XX' spin system at δ_H 7.51 (2H, d, *J*=8.7 Hz, H-2''',6'''), δ_H 6.71 (2H, d, *J*=8.7 Hz, H-3''',5''') and an AX type spin system at δ_H 6.40 (1H, d, *J*=1.8 Hz, H-8), δ_H 6.18 (1H, d, *J*=1.8 Hz, H-6), in addition to three singlets at δ_H 6.59 (1H, s, H-3), 6.58 (1H, s, H-3'') and δ_H 6.37 (1H, s, H-8''). Taking cognisance of the MS and the ^1H NMR data, it is obvious that compound **4.1** is a biflavonoid. This deduction was supported by the ^{13}C and DEPT spectra (**Plate 4.3**) which revealed 26 carbon resonances including two carbonyls between δ_C 184.2 and δ_C 95.1 ppm. The ^1H and ^{13}C NMR signals were assigned to two apigenin units by analysis of the HMBC (**Plate 4.4**) and HSQC spectra (**Plate 4.5**). The HSQC facilitated the assignment of all protonated carbons and the HMBC was useful in assigning the quaternary carbons. Some of the important HMBC correlations observed include δ_H 6.37 (H-8'')/ δ_C 162.5 (C-5''), δ_H 7.51 (H-2''',6''')/ δ_C 162.5 (C-4'''), δ_H 7.51 (H-2''',6'''), 6.59, 6.58 (H-3,3'') and δ_H 7.93 (H-2')/ δ_C 166.4, δ_C 166.0 (C-2'',2), δ_H 7.11 (H-5')/ δ_C 121.6 (C-3'), δ_H 6.59, 6.58 (H-3,3'')/ δ_C 123.2 (C-1',1'''), δ_H 6.4 (H-8), 6.18 (H-6), 6.37 (H-8''), 6.59, 6.58 (H-3,3'')/ δ_C 105.4 (C-10,10''). It is clear from the ABX splitting pattern observed in the ^1H NMR spectrum that one of the flavonoid ring B is substituted at C-3'. Similarly, the presence of only two *meta*-coupled protons resonances at δ_H 6.4 and δ_H 6.18 ppm (H-8 and 6, respectively) and one isolated proton at δ_H 6.37 ppm shows that the phloroglucinol ring A of the second flavonoid unit is substituted at either C-6'' or C-8''. Considering that for flavonoids with a 5,7-dihydroxy substituent, the H-6 proton consistently appears upfield compared to H-8,[20] the singlet at δ_H 6.37 was assigned to H-8'', implying that the ring A is substituted at C-6''. Thus

compound **4.1** has a C3'-C6'' interflavonoid linkage between the two apigenin units as found in robustaflavone. This interflavonoid linkage was further supported by the HMBC correlation of δ_H 7.93 (H-2') and a quaternary carbon at δ_C 105.4 (C-6''). Based on the above analysis and after comparing the NMR data with the literature,[21,22] compound **4.1** was assigned as robustaflavone (**4.1**) (**Fig. 4.1**).

Compound **4.2** was isolated as a yellow solid and the HR-ESI-(-)-MS (**Plate 4.6**) showed the same *m/z* and molecular formula as compound **4.1**, indicating that the two compounds are isomers. The NMR data (**Plate 4.7-4.10**) of compound **4.2** were similar to those of **4.1**, but the physical appearance, Rf values and HPLC retention times (R_t) were different. A close examination of the ^{1}H NMR spectrum showed that some of the signals have shifted relative to the chemical shifts observed for compound **4.1**. The phloroglucinol ring signals were particularly useful in elucidating the structure of **4.2**. Unlike in the case of robustaflavone above, compound **4.2** showed two signals for H-6,6'' and only one isolated signal for H-8, indicating that the position of linkage is C-8'' as opposed to C-6'' in compound **4.1**. Thus, compound **4.2** is composed of two apigenin units with a C-3'-C-8'' interflavonoid linkage, as found in amentoflavone. Comparison of the NMR data with the literature data for amentoflavone[21,22](**4.2**) confirmed the structure of compound **4.2** (**Fig. 4.1**). Many biflavonoids show atropisomerism as a result of restricted rotation. However, in both robustaflavone (**4.1**) and amentoflavone (**4.2**), the steric hindrance is not enough to cause restricted rotation and, therefore, these two compounds are not chiral.

Compound **4.3**, which was obtained as a yellow powder, showed a pseudo-molecular ion $[M-H]^-$ at *m/z* 433.0779 (Calculated for $C_{20}H_{17}O_{11}$ 433.0771) in the HR-ESI-(-)-MS (**Plate 4.11**), suggesting a molecular formula of $C_{20}H_{18}O_{11}$. The aromatic region of the ^{1}H NMR spectrum (**Plate 4.12**) of **4.3** displayed signals of an ABX spin system at δ_H 7.53 (1H, d, *J*=2.0 Hz, H-2'), δ_H 7.49 (1H, dd, *J*=8.3, 2.06 Hz, H-6'), and δ_H 6.90 (1H, d, *J*=8.3 Hz, H-5'), and an AX system resonating at δ_H 6.39 (1H, d, *J*=2.1 Hz, H-8) and δ_H 6.21 (1H, d, *J*=2.0 Hz, H-6), characteristic of a derivative of quercetin. This deduction was supported by the ^{13}C and DEPT (**Plate 4.13**) spectra of **4.3**, which showed 15 carbon resonances including a carbonyl at δ_C 180.0 and seven oxygenated carbon resonances (δ_C 166.3-134.9), assignable to a quercetin nucleus. The HMBC (**Plate 4.14**) correlations of δ_H 6.21/ δ_C 163.1 (H-6/C-5), δ_H 6.21/ δ_C 105.6 (H-6/C-10), δ_H 6.39/ δ_C 158.6 (H-8/C-9), δ_H 7.53,7.46/ δ_C 159.4 (H-2',6'/C-2), δ_H 7.53,6.9/ δ_C 146.4 (H-2',5'/C-3'),

and δ_H 7.53,7.46,6.9/ δ_C 149.9 (H-2',5',6'/C-4') facilitated the assignment of the quaternary carbons. The oxygenated methine singlet at δ_H 5.5 (1H, s, H-1''), three other oxymethine resonances between δ_H 3.87 and 4.33, and a two-proton oxymethylene multiplet at δ_H 3.51 suggest the presence of a pentose sugar. The singlet at δ_H 5.5 ppm was assigned to the anomeric proton. The relatively small values of the coupling constants of the sugar protons indicate that the sugar is a furanose. The point of attachment of the sugar to the aglycone was established by the observed HMBC cross peak between the anomeric proton δ_H 5.5 (H-1'') and δ_C 134.9 (C-3). All other protonated carbons were assigned by analysis of HSQC cross-peaks (**Plate 4.15**). The sugar NMR data resembled those of arabinofuranose and a comparison of the NMR data of **4.3** with those reported in the literature for quercetin 3-*O*-α-D-arabinofuranoside[23,24] (**4.3**) (**Fig. 4.1**) established the identity of the compound.

Compound **4.4** was also isolated as a yellow powder. Its molecular formula was established to be $C_{21}H_{20}O_{11}$, based on the pseudo-molecular ion $[M-H]^-$ at *m/z* 433.0779 (Calculated for $C_{21}H_{19}O_{11}$ 447.0927) in the HR-ESI-(-)-MS (**Plate 4.16**). The NMR data (**Plate 4.17-4.20**) of **4.4** revealed signals consistent with the presence of a quercetin derivative. Also, a doublet at δ_H 5.35 (1H, d, *J*=1.2 Hz, H-1''), four oxymethine protons between δ_H 4.22 and 3.34 and a methyl doublet at δ_H 0.94 (3H, d, *J*=6.2 Hz, H-6'') suggested the presence of a rhamnose sugar moiety. The HMBC cross peak observed between the anomeric proton and δ_C 136.2 (C-3) confirmed the attachment of the rhamnosyl unit to position 3 of the quercetin nucleus. The structure of **4.4** was thus assigned as quercetin 3-*O*-α-L-rhamnoside (**4.4**) (**Fig. 4.1**), after comparing its spectroscopic data with published literature values.[25]

Compound **4.5** was obtained as a yellow powder and assigned a molecular formula of $C_{20}H_{18}O_{10}$ based on the pseudo-molecular ion $[M-H]^-$ at *m/z* 417.0818 (calculated for $C_{20}H_{17}O_{10}$ 417.0822) in the HR-ESI-(-)-MS (**Plate 4.21**). The ^{1}H NMR spectrum (**Plate 4.22**) revealed resonances for a 1,4-disubstituted benzene ring with an AA'XX' spin system at δ_H 7.96 (2H, d, *J*=8.8 Hz, H-2',6') and δ_H 6.92 (2H, d, *J*=8.8 Hz, H-3',5'), and another benzene ring possessing an AX spin system at δ_H 6.40 (1H, d, *J*=2.0 Hz, H-8) and δ_H 6.20 (1H, d, *J*=2.0 Hz, H-6), consistent with a kaempferol derivative. This deduction was confirmed by the ^{13}C and DEPT spectra (**Plate 4.23**), which revealed 13 resonances assignable to a kaempferol nucleus, including a carbonyl at δ_C 179.9 (C-4) and six oxygenated quaternary carbons at δ_C 166.6-134.7. The quaternary carbons were assigned unambiguously by analysis of the HMBC

spectrum (**Plate 4.24**). The NMR spectra further showed resonances for a pentose sugar, consisting of an oxymethine singlet at δ_H 5.48 (1H, s, H-1''), three other oxymethines resonances at δ_H 4.31-3.81, an oxymethylene resonating at δ_H 3.48 and the associated carbon resonances. The relatively small values of the sugar protons coupling constants indicate that the sugar is a furanose. The singlet at δ_H 5.48 was assigned to a sugar anomeric proton in an α-linkage with the flavonoid unit. The attachment of the sugar unit to C-3 of the flavonoid was established by the HMBC cross-peak between δ_H 5.48 (1H, s, H-1'') and δ_C 134.9 (C-3). All the protonated carbons were assigned based on HSQC correlations (**Plate 4.25**). The NMR data of the sugar moiety closely matched those of arabinofuranose. Comparing the NMR data of **4.5** with the literature showed close similarity with kaempferol 3-*O*- α-D-arabinofuranoside (**4.5**) (**Fig. 4.1**) thus establishing the structure.[24,26,27]

Compound **4.6** was isolated as a yellow amorphous solid. It was assigned a molecular formula of $C_{21}H_{20}O_{12}$ based on pseudo-molecular ion $[M-H]^-$ peak at *m/z* 463.0881 (calculated for $C_{21}H_{19}O_{12}$ 463.0877) observed in the HR-ESI-(-)-MS (**Plate 4.26**). The aromatic regions of the ^{1}H NMR spectrum (**Plate 4.27**) of **4.6** showed a singlet aromatic proton resonance at δ_H 6.95 (2H, s, H-2',6') and a pair of meta coupled doublets at δ_H 6.35 (1H, d, *J*=2.5 Hz, H-8), δ_H 6.20 (1H, d, *J*=2.5 Hz, H-6) consistent with the presence of myricetin aglycone. This deduction was supported by the ^{13}C and DEPT NMR data (**Plate 4.28**) which revealed a carbonyl signal at δ_C 179.3 and 12 other aromatic resonances, of which eight are oxygenated between δ_C 166.3 and δ_C 64.8. The assignment of the ^{1}H and ^{13}C resonances to the flavonoid rings were facilitated by HMBC correlations (**Plate 4.29**). Further, an anomeric proton at δ_H 5.31 (1H, d, *J*=1.3 Hz, H-1''), a sharp methyl doublet at δ_H 0.96 (3H, d, *J*=6.2 Hz, H-6''), and four other oxygenated methine resonances between δ_H 3.35 and 4.22 in the ^{1}H NMR spectrum suggested the presence of a rhamnosyl moiety. The connectivity of the sugar to the aglycone at position 3 was established by the HMBC cross peak observed between the anomeric proton δ_H 5.31 (H-1'') and δ_H 136.3 (C-3). All the other protonated carbons were assigned by analysis of the HSQC spectrum (**Plate 4.30**). Based on these NMR analyses and after comparison of the data with those reported in the literature, the structure of compound **4.6** was confirmed to be myricetin 3-*O*-α-L-rhamnoside (**4.6**) (**Fig. 4.1**).[25,28]

Compound **4.7** was isolated as a white amorphous solid. Its molecular formula was assigned as $C_{35}H_{60}O_6$ from the pseudo-molecular ion $[M+HCOOH-H]^-$ observed at *m/z* 621.4362

(calculated for $C_{36}H_{61}O_8$ 621.4366) in the negative HR-ESI-(-)-MS (**Plate 4.31**). The ^{1}H NMR spectrum (**Plate 4.32**) showed resonances for two tertiary methyl singlets at δ_H 0.95 (3H, s, H-19) and δ_H 0.64 (3H, s, H-18), a primary methyl triplet at δ_H 0.82 (3H, t, *J*=7.2 Hz, H-29), and three secondary methyl doublets resonating at δ_H 0.90 (3H, d, *J*=6.5 Hz, H-21), δ_H 0.80 (3H, d, *J*=7.0 Hz, H-27), and δ_H 0.79 (3H, d, *J*=6.9 Hz, H-26), in addition to an olefinic doublet at δ_H 5.32 (1H, d, *J*=4.9 Hz, H-6) and a multiplet due to an oxymethine proton at δ_H 3.45 (1H, m, H-3). These ^{1}H NMR signals are characteristic of a Δ^5-3β-hydroxy sterol having a ten carbon atoms saturated side chain that ends with an isopropyl group.[29] This deduction was supported by the ^{13}C and DEPT spectra (**Plate 4.33**) which showed resonances for two olefinic carbons at δ_C 140.5 (C-5) and δ_C 121.2 (C-6), six methyls between δ_C 19.7 and δ_C 11.7 and an oxygenated methine carbon at δ_C 77.0, suggesting a β-sitosterol derivative. The ^{1}H NMR spectrum in DMSO-*d*$_6$ further revealed resonances for four hydroxyl protons including three doublets at δ_H 4.83-4.86 and a triplet at δ_H 4.41, suggesting the presence of a sugar moiety. The appearance of an anomeric proton doublet resonance at δ_H 4.21 (1H, d, *J*=7.7 Hz, H-1'), four oxymethine signals between δ_H 3.01 and δ_H 3.12, and resonances for an oxymethylene at δ_H 3.64 and 3.40 and the associated ^{13}C resonances confirmed the presence of the sugar unit. The sugar carbon signals between δ_C 76.8 and δ_C 61.6 as well as an anomeric proton and carbon suggest that the sugar is a β-glucose.[30] The large coupling constant of the anomeric proton (*J*=7.7 Hz) indicates a 1,2-diaxial coupling between H-1 and H-2 of the sugar and was assigned to a glucosyl moeity with a β-glycosidic linkage with the aglycone. The attachment of the sugar to C-3 of the steroid nucleus was confirmed by the HMBC cross peak (**Plate 4.34**) between the anomeric proton δ_H 4.21 and δ_C 77.0 (C-3). All the other protonated carbons were assigned by HSQC correlations (**Plate 4.35**) and comparison with literature data.[30] Therefore, compound **4.7** was confirmed to be β-sitosterol 3-*O*-β-D-glucoside (**4.7**) (**Fig. 4.1**).

Compound **4.8** was obtained as a colourless oil. Its molecular formula was determined to be $C_{13}H_{24}O_4$ based on pseudo-molecular ion $[M+Na]^+$ at *m/z* 267.1572 (Calculated for $C_{13}H_{24}O_4Na$ 267.1572) in the positive HR-ESI-(+)-MS (**Plate 4.36**). The ^{1}H NMR (**Plate 4.37**) of **4.8** showed signals for three tertiary methyl groups at δ_H 1.22 (3H, s, H-11), δ_H 1.10 (3H, s, H-13) and δ_H 0.87 (3H, s, H-12), one secondary methyl doublet at δ_H 1.27 (3H, d, *J*=6.4 Hz, H-10), two oxymethine multiplets at δ_H 4.34 (1H, qd, *J*=6.5, 1.0 Hz, H-9) and δ_H 4.06 (1H, m, H-3), a pair of trans coupled alkene doublet of doublets at δ_H 6.07 (1H, dd, *J*=15.9, 1.0 Hz, H-7) and δ_H

5.78 (1H, dd, *J*=15.9, 6.2 Hz, H-8), as well as two methylene groups at δ_H 1.76 (2H, m, H-4), δ_H 1.64 (1H, t, *J*=12.0 Hz, H-2ax) and δ_H 1.45 (1H, ddd, *J*=12.2, 4.0, 1.9 Hz, H-2eq). The ^{13}C and DEPT spectra (**Plate 4.38**) revealed the presence of 13 carbons, including two olefinic carbons at δ_C 136.1 and 131.1, two oxygenated methines at δ_C 69.5 and 65.3, three quaternary carbons of which two are oxygenated at δ_C 79.0, 77.8 and δ_C 40.7, two methylenes and four methyls between δ_C 46.5 and 24.1. The COSY spectrum (**Plate 4.39**) showed connectivity between the two olefinic protons δ_H 6.07//5.78 (H-7 and 8) and the oxymethine at δ_H 4.34 (H-9), which in turn showed COSY correlation with the methyl doublet at δ_H 1.27 (H-10), thereby establishing an unsaturated four carbon atoms chain. The presence of a *gem*-dimethyl fragment was established by the HMBC correlations (**Plate 4.40**) of the two singlet methyls at δ_H 0.87 (H-12) and 1.10 (H-11) with carbons δ_C 40.7 (C-1), 46.5 (C-2) and δ_C 79.0 (C-6). The COSY correlation of the oxymethine at δ_H 4.06 (H-3) with the two methylene groups at δ_H 1.76 (H-4) and δ_H 1.64//1.45 ($H2_{ax,\ eq}$) revealed a three-carbon fragment which together with the two oxygenated quaternary carbons and the gem dimethyl fragment constitute a cyclohexane ring. The attachment of the side chain to the monocyclic ring at C-6 was established by the HMBC correlations of the olefinic protons at δ_H 6.07 (H-7), 5.78 (H-8) with the oxymethine carbon at δ_C 79.0 (C-6). All the protonated carbons were assigned based on HSQC (**Plate 4.41**) cross-peaks and the ^1H and ^{13}C assignments were supported by other observed HMBC correlations. Therefore compound **4.8** was deduced to be a megastigman-7-ene derivative with four attached hydroxyl groups at C-3, C-5, C-6, and C-9. The relative stereochemistry of the hydroxyl group at C-3 was established as equatorial based on the coupling constants of H-2 (H_{ax} *J*=12.0 Hz, H_{eq} *J*=12.2, 4.0, 1.9 Hz). The tertiary methyl at C-5 and the side chain at C-6 were assumed to take an equatorial orientation based on NOESY (**Plate 4.42**) cross-peaks between H-13 (1.10) and H-8 (δ_H 5.78), H-7 (δ_H 6.07). Based on the above analyses and after comparing its spectral data with the literature,[31,32] the structure of **4.8** was established as (*3S,5R,6R,7E,9S*)-3,5,6,9-tetrahydroxymegastigman-7-ene (**4.8**) (**Fig. 4.1**).

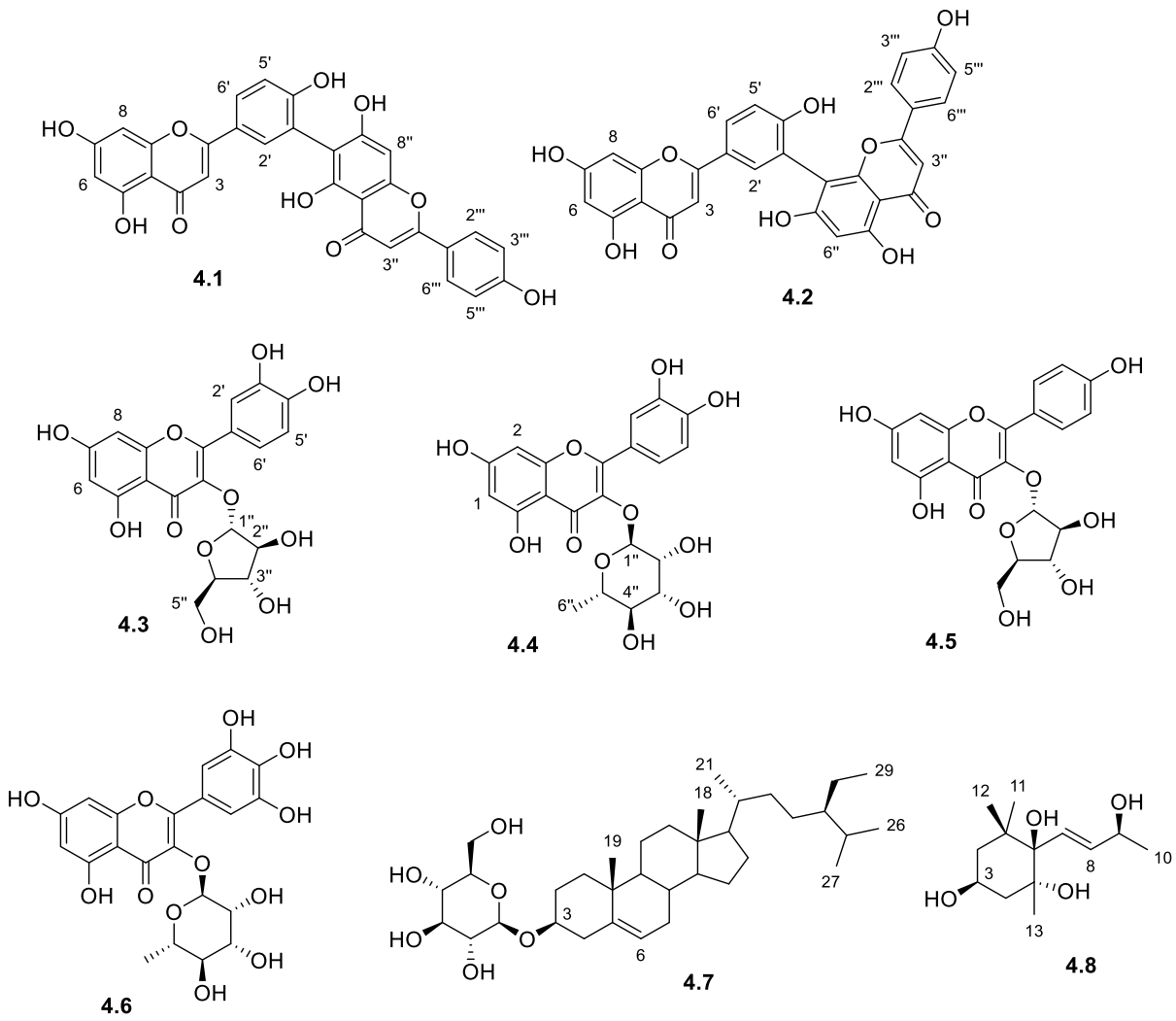

Fig. 4.1: Structures of the isolated compounds from *O.obovata*

Previous chemical investigations of the *Ozoroa* genus have focused on the root, root bark and stem bark, and resulted in the isolation of mainly cardanols, alkaylanarcadic acids and triterpenoids.[14-18] Amentoflavone was previously reported in only one species of *Ozoroa*, *O. sphaerocarpa*,[33] but robustaflavone is reported from the *Ozoroa* genus here for the first time. To the best of our knowledge, this is only the second report of the isolation biflavonoids, and the first report of the isolation of flavonoid glycosides from the *Ozoroa* genus. However, biflavonoids and flavonoid glycosides have been reported from within the Anacardiaceae.[34-39] Most of these biflavonoids and glycosides were reported from the leaves, consistent with our findings on the phytochemistry of *O. obovata* leaves. The biflavonoids reported in the Anacardiaceae are mostly flavone and flavanone dimers having C-C and C-O-C interflavonoid linkages. The two dimers isolated in this study have a C-C interflavanyl linkage between two

flavone units. The flavonoid glycosides of the Anacardiaceae are mostly derived from kaempferol, quercetin and myricetin, glycosides of all the three flavonoids were isolated from *O. obovata* in this study. The presence of these compounds could play a chemotaxonomic significance in genus.

4.3.2. Biological activity

The antiplasmodial and cytotoxic activities of the leaf extract and isolated compounds from *O. obovata* are presented in Table 4.1. The extract and compounds all displayed non-selective antiplasmodial activities at 50 µg/mL. Cytotoxicity was also observed against HeLa cells at the same concentration. The activities were lost at a lower concentration of 10 µg/mL, indicating that the compounds were generally toxic to cells. Antiplasmodial activity was previously reported for amentoflavone[40] and some other biflavonoids.[41] Similar to our result, amentoflavone displayed unselective activity and was only 2-fold more selective towards *P. falciparum* compared to HeLa cells.[40] No report on the antiplasmodial activity of robustaflavone could be found in the literature. Therefore, this is the first report of the antiplasmodial activity of robustaflavone. As was already mentioned in chapter 3, flavonoids including flavonoid glycosides have been reported to possess antiplasmodial activity. However, flavonoids have generally displayed a wide array of biological activities due to the ability for nonspecific inhibition of various biological targets.[42]

Table 4.1: In vitro antiplasmodial and cytotoxic activity of the extract and isolated compounds

Compound	Viability% ±SD (50 µg/mL)		Viability% ±SD (10 µg/mL)	
	3D7	HeLa	3D7	HeLa
O. obovata	4.65 ± 0.97	3.02 ± 1.11	68.86 ± 0.00	68.14 ± 0.31
Compound **4.2**	9.64 ± 0.24	9.32 ± 0.44	72.42 ± 1.22	86.21 ± 2.66
Compound **4.1**	10.33 ± 0.24	6.32 ± 0.30	75.88 ± 1.22	86.01 ± 2.46
Compound **4.3**	21.00 ± 2.68	5.84 ± 0.03	83.85 ± 2.72	77.24 ± 3.51
Compound **4.4**	16.18 ± 2.19	1.35 ± 0.14	66.84 ± 2.58	71.31 ± 4.66
Compound **4.5**	16.52 ± 2.19	2.83 ± 0.48	73.57 ± 2.31	71.84 ± 1.31
Compound **4.6**	18.93 ± 0.73	2.52 ± 0.57	77.90 ± 2.99	70.08 ± 2.40
Chloroquine			IC_{50} = 0.014 µM	
Emetin				IC_{50} = 0.04 µM

4.4. Conclusion

Eight bioactive compounds were isolated from the leaves of *O. obovata* for the first time. The extract and isolated compounds displayed non-selective antiplasmodial activity. Considering the use of the plant leaves in traditional medicine, the cytotoxicity of the extract and isolated compounds against noncancerous cells needs to be investigated to further ascertain the selectivity.

Acknowledgment

The authors are grateful to Dr Christina Potgieter of Bews Herbarium, School of Life Sciences, University of KwaZulu-Natal for helping with the preparation of plant voucher specimens and Ms Alison young for identifying the plant material. NT is grateful to the University of KwaZulu-Natal for the award of a doctoral scholarship. FRVH acknowledges the National Research Foundation (South Africa) Grant [number 98345] for financial support. Antimalarial and cytotoxicity evaluations were supported by Rhodes University (Sandisa Imbewu grant) and the South African Medical Research Council.

Conflict of interest

The authors declare that they have no conflict of interest.

References

1. Coates Palgrave, K., Drummond, R., *Trees of Southern Africa*. C. Struik Publishers, Cape Town: 1977.
2. Asase, A.; Oteng-Yeboah, A. A.; Odamtten, G. T.; Simmonds, M. S. J., Ethnobotanical study of some Ghanaian anti-malarial plants. *Journal of Ethnopharmacology* **2005,** 99, (2), 273-279.
3. Mokoka, T. A.; Xolani, P. K.; Zimmermann, S.; Hata, Y.; Adams, M.; Kaiser, M.; Moodley, N.; Maharaj, V.; Koorbanally, N. A.; Hamburger, M.; Brun, R.; Fouche, G., Antiprotozoal screening of 60 South African plants, and the identification of the antitrypanosomal germacranolides schkuhrin I and II. *Planta Medica* **2013,** 79, (14), 1380-1384.

4. Prozesky, E. A.; Meyer, J. J. M.; Louw, A. I., In vitro antiplasmodial activity and cytotoxicity of ethnobotanically selected South African plants. *Journal of Ethnopharmacology* **2001,** 76, (3), 239-245.
5. Weenen, H.; Nkunya, M. H. H.; Bray, D. H.; Mwasumbi, L. B.; Kinabo, L. S.; Kilimali, V., Antimalarial activity of Tanzanian medicinal-plants. *Planta Medica* **1990,** 56, (4), 368-370.
6. Jansen, P.; Mendes, O., *Plantas medicinais seu uso Tradicional em Mocambique. Tomo 2*. In Instituto Nacional do Licro e do Disco: 1988; p 120, 199.
7. Kokwaro, J. O., *Medicinal Plants of East Africa*. East African Literature Bureau: 1976; p 22.
8. Hutchings, A., *Zulu Medicinal Plants: an Inventory*. University of Natal Press: 1996; p 180.
9. York, T.; van Vuuren, S. F.; de Wet, H., An antimicrobial evaluation of plants used for the treatment of respiratory infections in rural Maputaland, KwaZulu-Natal, South Africa. *Journal of Ethnopharmacology* **2012,** 144, (1), 118-127.
10. Rea, A. I.; Schmidt, J. M.; Setzer, W. N.; Sibanda, S.; Taylor, C.; Gwebu, E. T., Cytotoxic activity of *Ozoroa insignis* from Zimbabwe. *Fitoterapia* **2003,** 74, (7-8), 732-735.
11. Molgaard, P.; Nielsen, S. B.; Rasmussen, D. E.; Drummond, R. B.; Makaza, N.; Andreassen, J., Anthelmintic screening of Zimbabwean plants traditionally used against schistosomiasis. *Journal of Ethnopharmacology* **2001,** 74, (3), 257-264.
12. Ahmed, A. S.; McGaw, L. J.; Moodley, N.; Naidoo, V.; Eloff, J. N., Cytotoxic, antimicrobial, antioxidant, antilipoxygenase activities and phenolic composition of *Ozoroa* and *Searsia* species (Anacardiaceae) used in South African traditional medicine for treating diarrhoea. *South African Journal of Botany* **2014,** 95, 9-18.
13. Wall, M. E.; Wani, M. C.; Brown, D. M.; Fullas, F.; Olwald, J. B.; Josephson, F. F.; Thornton, N. M.; Pezzuto, J. M.; Beecher, C. W. W.; Farnsworth, N. R.; Cordell, G. A.; Kinghorn, A. D., Effect of tannins on screening of plant extracts for enzyme inhibitory activity and techniques for their removal. *Phytomedicine* **1996,** 3, (3), 281-285.
14. Liu, Y.; Abreu, P., Tirucallane triterpenes from the roots of *Ozoroa insignis*. *Phytochemistry* **2006,** 67, (13), 1309-1315.

15. Ng'ang'a, M. M.; Hussain, H.; Chhabra, S.; Langat-Thoruwa, C.; Krohn, K., Chemical constituents from the root bark of *Ozoroa insignis*. *Biochemical Systematics and Ecology* **2009,** 37, (2), 116-119.

16. Liu, Y.; Abreu, P. J. M., Long chain alkyl and alkenyl phenols from the roots of *Ozoroa insignis*. *Journal of the Brazilian Chemical Society* **2006,** 17, (3), 527-532.

17. Christelle, T. D.; Hussain, H.; Dongo, E.; Hermine, J.-M. B.; Ahmed, I.; Krohn, K., Two new alkylanacardic acids, ozorcardic A and B, from *Ozoroa pulcherrima*. *Natural Product Communications* **2011,** 6, (8), 1133-1134.

18. Christelle, T. D.; Hussain, H.; Dongo, E.; Hermine, J.-M. B.; Ahmed, I.; Krohn, K., Ozocardic A: a new alkylanacardic acid from *Ozoroa pulcherrima*. *Journal of Asian Natural Products Research* **2011,** 13, (1), 84-87.

19. Dongmo, C. T.; Hussain, H.; Boukeng, H. J.-M.; Saleem, M.; Abbas, G.; Farooq, M.; Wadaan, M. A. M.; Dongo, E.; Al-Harrasi, A., Ozoromide: a new ceramide from the stem bark of *Ozoroa pulcherrima*. *Chemistry of Natural Compounds* **2017,** 53, (5), 923-925.

20. Mabry, T., Markham, K., Thomas, M., *The Systematic Identification of Flavonoids*. Springer-Verlag, New York: 1970.

21. Markham, K. R.; Sheppard, C.; Geiger, H., C-13 NMR of flavonoids .4. C-13 NMR-studies of some naturally-occurring amentoflavone and hinokiflavone biflavonoids. *Phytochemistry* **1987,** 26, (12), 3335-3337.

22. Geiger, H.; Seeger, T.; Hahn, H.; Zinsmeister, H. D.; Markham, K. R.; Wong, H., H-1-NMR assignments in biflavonoid spectra by proton-detected C-H correlation. *Zeitschrift Fur Naturforschung C-A Journal of Biosciences* **1993,** 48, (11-12), 821-826.

23. Houel, E.; Nardella, F.; Jullian, V.; Valentin, A.; Vonthron-Senecheau, C.; Villa, P.; Obrecht, A.; Kaiser, M.; Bourreau, E.; Odonne, G.; Fleury, M.; Bourdy, G.; Eparvier, V.; Deharo, E.; Stien, D., Wayanin and guaijaverin, two active metabolites found in a *Psidium acutangulum* Mart. ex DC (syn. *P. persoonii* McVaugh) (Myrtaceae) antimalarial decoction from the Wayana Amerindians. *Journal of Ethnopharmacology* **2016,** 187, 241-248.

24. Da Silva Sa, F. A.; Marciano de Paula, J. A.; dos Santos, P. A.; Ribeiro Oliveira, L. d. A.; Ribeiro Oliveira, G. d. A.; Liao, L. M.; de Paula, J. R.; Rodrigues Silva, M. d. R.,

Phytochemical analysis and antimicrobial activity of *Myrcia tomentosa* (Aubl.) DC. leaves. *Molecules* **2017,** 22, (7), 1100.

25. Fossen, T.; Larsen, A.; Kiremirec, B. T.; Andersen, O. M., Flavonoids from blue flowers of *Nymphaea caerulea*. *Phytochemistry* **1999,** 51, (8), 1133-1137.
26. Xiao, Z. P.; Wu, H. K.; Wu, T.; Shi, H.; Hang, B.; Aisa, H. A., Kaempferol and quercetin flavonoids from *Rosa rugosa*. *Chemistry of Natural Compounds* **2006,** 42, (6), 736-737.
27. Kil, H. W.; Rho, T.; Yoon, K. D., Phytochemical study of aerial parts of *Leea asiatica*. *Molecules* **2019,** 24, (9).
28. Madikizela, B.; Aderogba, M. A.; Van Staden, J., Isolation and characterization of antimicrobial constituents of *Searsia chirindensis* L. (Anacardiaceae) leaf extracts. *Journal of Ethnopharmacology* **2013,** 150, (2), 609-613.
29. De Rosa, S.; De Giulio, A.; Tommonaro, G., Triterpenoids and sterol glucoside from cell cultures of *Lycopersicon esculentum*. *Phytochemistry* **1997,** 44, (5), 861-864.
30. Faizi, S.; Ali, M.; Saleem, R.; Bibi, S., Complete ^{1}H and ^{13}C NMR assignments of stigma-5-en-3-O-β-glucoside and its acetyl derivative. *Magnetic Resonance in Chemistry* **2001,** 39, (7), 399-405.
31. Takeda, Y.; Okada, Y.; Masuda, T.; Hirata, E.; Shinzato, T.; Takushi, A.; Yu, Q.; Otsuka, H., New megastigmane and tetraketide from the leaves of *Euscaphis japonica*. *Chemical & Pharmaceutical Bulletin* **2000,** 48, (5), 752-754.
32. Hou, Y.-z.; Chen, K.-k.; Deng, X.-l.; Fu, Z.-l.; Chen, D.-f.; Wang, Q., Anti-complementary constituents of *Anchusa italica*. *Natural Product Research* **2017,** 31, (21), 2572-2574.
33. Sibandze, G.; Stapleton, P.; Gibbons, S., Efflux inhibitors from Swazi medicinal plants. *Planta Medica* **2016,** 82, (S 01), S1-S381.
34. Cardoso, M. P.; Lima, L. S.; David, J. P.; Moreira, B. O.; Santos, E. O.; David, J. M.; Alves, C. Q., A new biflavonoid from *Schinopsis brasiliensis* (Anacardiaceae). *Journal of the Brazilian Chemical Society* **2015,** 26, (7), 1527-1531.
35. Lin, Y. M.; Flavin, M. T.; Schure, R.; Chen, F. C.; Sidwell, R.; Barnard, D. L.; Huffman, J. H.; Kern, E. R., Antiviral activities of biflavonoids. *Planta Medica* **1999,** 65, (2), 120-125.
36. Weniger, B.; Vonthron-Senecheau, C.; Arango, G. J.; Kaiser, M.; Brun, R.; Anton, R., A bioactive biflavonoid from *Campnosperma panamense*. *Fitoterapia* **2004,** 75, (7-8), 764-767.

37. Okoth, D. A.; Chenia, H. Y.; Koorbanally, N. A., Antibacterial and antioxidant activities of flavonoids from *Lannea alata* (Engl.) Engl. (Anacardiaceae). *Phytochemistry Letters* **2013,** 6, (3), 476-481.

38. Schulze-Kaysers, N.; Feuereisen, M. M.; Schieber, A., Phenolic compounds in edible species of the Anacardiaceae family - a review. *Rsc Advances* **2015,** 5, (89), 73301-73314.

39. Braca, A.; Politi, M.; Sanogo, R.; Sanou, H.; Morelli, I.; Pizza, C.; De Tommasi, N., Chemical composition and antioxidant activity of phenolic compounds from wild and cultivated *Sclerocarya birrea* (Anacardiaceae) leaves. *Journal of Agricultural and Food Chemistry* **2003,** 51, (23), 6689-6695.

40. Cai, S.; Risinger, A. L.; Nair, S.; Peng, J.; Anderson, T. J. C.; Du, L.; Powell, D. R.; Mooberry, S. L.; Cichewicz, R. H., Identification of compounds with efficacy against malaria parasites from common North American plants. *Journal of Natural Products* **2016,** 79, (3), 490-498.

41. Konziase, B., Protective activity of biflavanones from *Garcinia kola* against *Plasmodium* infection. *Journal of Ethnopharmacology* **2015,** 172, 214-218.

42. Duan, D.; Doak, A. K.; Nedyalkova, L.; Shoichet, B. K., Colloidal aggregation and the in vitro activity of traditional Chinese medicines. *ACS Chemical Biology* **2015,** 10, (4), 978-988.

CHAPTER 5: Phytochemical and antiplasmodial investigation of *Euclea natalensis* A.DC. subsp. *natalensis* leaves

Nasir Tajuddeen[a], Tarryn Swart[b], Heinrich C. Hoppe[b] and Fanie R. van Heerden[a]

[a]School of Chemistry and Physics, University of KwaZulu-Natal, Private Bag X01, Scottsville 3209, Pietermaritzburg, South Africa

[b]Department of Biochemistry & Microbiology, Rhodes University, Grahamstown 6140, South Africa

Formatted for ***South African Journal of Botany***

Abstract

Ethnopharmacological relevance: *E. natalensis* is used ethnomedically to treat a range of illnesses including malaria. Traditional healers surveyed in Zimbabwe reported that *E. natalensis* is effective against malaria.

Aim of the study: Previous studies indicate that extracts from the plant root and root bark have antiplasmodial activity but the plant leaves have not been investigated for its phytochemical composition and antiplasmodial activity. Therefore, this study was designed to investigate the phytochemical and antiplasmodial properties of *E. natalensis* leaves.

Methods: The plant leaves were investigated for inhibitory activity against 3D7 *P. falciparum* using the parasite lactate dehydrogenase (pLDH) assay. The cytotoxicity against Vero cells was evaluated using the MTT assay and cytotoxicity against HeLa cells was determined using the resazurin assay. The bioactive compounds were isolated using chromatographic techniques and the structures of the isolated were established using spectroscopic and spectrometric techniques.

Results: The dichloromethane-methanol (1:1) extract of *E. natalensis* leaves inhibited the in vitro viability of *P. falciparum* with IC_{50}=25.6 µg/mL and was not cytotoxic against Vero cells. Chromatographic purification of the extracts led to the isolation of six known flavonoid glycosides, four triterpenoids, and a coumarin. This is the first report of the isolation of the compounds from *E. natalensis*.The flavonoid glycosides suppressed parasite viability by more than 70% at 50 µg/mL, but were also cytotoxic against HeLa cells. The activities were reduced substantially at a lower concentration of 10 µg/mL for all the compounds.

Conclusion: Naphthoquinones which are among the predominant phytochemicals in root and root bark of *E. natalensis* are absent in the leaves. The isolated bioactive compounds showed nonselective antiplasmodial activity. However, the presence of the isolated compounds could account for the antiplasmodial activity of the extract and explains the folkloric use of the plant in traditional medicine.

Keywords: *Euclea natalensis*, Ebenaceae, antiplasmodial, malaria, flavonoid glycosides, ethnobotany

5.1. Introduction

Euclea natalensis A. DC. (Ebenaceae) is a shrub that is widely distributed in tropical and sub-tropical parts of Africa including the east coast of South Africa.[1,2] There are six subspecies found in a variety of habitats, with *E. natalensis* A. DC. subsp. *natalensis* being the most common subspecies in the province of KwaZulu-Natal.[3] *E. natalensis* is used in traditional medicine preparations alone or in combination with other medicinal plants for the treatment of various ailments in east and southern Africa. In South Africa, Zulu traditional healers prepare a decoction from several plants, including the roots of *E. natalensis*, as a remedy for swelling. The root bark is used as an enema in South Africa and the root as an emetic for stomach disturbances in east Africa. The powdered bark is applied topically on abnormal growth and is also used against schistosomiasis.[4,5] In Mozambique, a decoction is made by boiling a mixture of the leaves of *E. natalensis* and *Tabernaemontana elegans*, and used to shower in the morning and afternoon as a remedy for malaria.[6] Traditional healers in Chipinge district in Zimbabwe reported in a survey that the root of *E. natalensis* is used to cure malaria.[7] The efficacy of the root and stem extracts against *P. falciparum* D10 and K1 strains was demonstrated by Clarkson et al.[8] and Mokoka et al.[9], who reported good inhibitory activity for these extracts. Previous phytochemical studies on *E. natalensis* have focused on the root and root bark, probably because those are the parts frequently prescribed by traditional healers. These studies have shown that naphthoquinones, in addition to triterpenoids and phenolic compounds, are the most abundant phytochemicals present.[10-12] Naphthoquinones show a range of biological activities that include antiplasmodial activity.[13,14] Atovaquone is an example of a naphthoquinone that, in combination with proguanil, is used for the treatment and prevention of malaria. However, harvesting the roots is an unsustainable way to utilize

trees as this could lead to the death of the plants. Using the plant leaves for medicinal purposes is more sustainable because leaves grow fast and harvesting leaves will not kill the plant. The leaf infusion of *E. natalensis* is drunk to relieve menstrual cramps and remedy abnormal menstrual cycle. *E. natalensis* leaves are also used to relieve chest and cardiac pains.[15] Despite the widespread use of *E. natalensis* for medicinal purposes, no previous attempt at investigating the phytochemical properties of the plant leaves was found in the literature. Therefore, in our search for antiplasmodial compounds from medicinal plants, we investigated the leaves of *E. natalensis* for antiplasmodial activity against 3D7 *P. falciparum*. The leaf extract showed moderate antiplasmodial activity, and this paper reports on the phytochemical and antiplasmodial investigation of *E. natalensis* leaves.

5.2. Material and methods

5.2.1. General procedure

The same as section 3.2.1 in chapter 3

5.2.2. Plant material and preparation of extracts for bioassays

Euclea natalensis whole plant was collected at Highstakes airfield, Cato Ridge, KwaZulu-Natal (29;45'57.14S 30;34'39.26E) in February 2018. The plant was identified by Ms Alison Young, the curator of the University of KwaZulu-Natal (UKZN) botanical gardens. A voucher specimen was prepared by Ms Young, who assigned an accession number, (*E. natalensis* 2976). The leaves were separated from the other plant parts, air-dried at room temperature in the laboratory and crushed to a coarse powder, using a hammer mill. The powdered plant material was stored in paper bags in a ventilated environment.

For the bioassays, the powdered plant leaves (50 g) was extracted at room temperature by maceration with constant stirring in 500 mL of dichloromethane-methanol (1:1, v/v) for 72 hours. The extract was filtered and concentrated *in vacuo* using a rotary evaporator to give a green paste which was weighed, and stored in a refrigerator until needed for the assay.

5.2.3. Extraction and Isolation of compounds

The powdered leaves of *E. natalensis* (850 g) were extracted as described in section 5.2.3.2. From the resulting crude extract, 40.0 g was subjected to VLC using 200 g of silica and 800 mL each of five solvent systems, hexanes-dichloromethane (9:1), dichloromethane-ethyl acetate

(20:1), 100% ethyl acetate, ethyl acetate-methanol (5:1), and 100% methanol. Five fractions A-E, weighing 1.2, 8.0, 5.5, 11.7, and 6.5 g, respectively, were collected. Fraction D (8.0 g) was adsorbed onto silica and subjected to silica gel column chromatography using gradient elution with dichloromethane-ethyl acetate (8:2 and 6:4), ethyl acetate-methanol (4:1, 3:1 and 3:2) and finally 100% methanol, to afford five subfraction (sb-Fr1-5) by pooling together eluates with similar TLC profiles. Further silica gel column chromatography of sb-Fr1 (0.5 g) by gradient elution with mixtures of hexanes-ethyl acetate (9:1, 6:4,3:7) afforded oleanolic acid (**5.7**) (27.3 mg) and scopoletin (**5.8**) (3.5 mg). Subfraction 2 (0.2 g) was subjected to silica gel column chromatography eluting with dichloromethane-ethyl acetate gradients (8:2, 1:1, 3:7) followed by purification of the resulting subfractions (Fr1a-Fr3a) on a Sephadex LH-20 column eluting with methanol to afford myricetin 3-*O*-arabinopyranoside (**5.1**) (11.1 mg) and quercetin 3-*O*-arabinofuranoside (**5.3**) (6.7 mg). Subfraction 3 (175 mg), showing two major spots on TLC, was subjected to repeated chromatography on a Sephadex LH-20 column eluting with methanol to give a mixture of quercetin 3-*O*-arabinopyranoside (**5.4**) and quercetin 3-*O*-α-L-rhamnoside (**5.5**) (10.5 mg). Subfraction 4 (52.5 mg) showing one major spot on TLC was initially subjected to purification by silica gel column chromatography with isocratic elution using dichloromethane-methanol (7:1) followed by repeated Sephadex LH-20 purification to give a mixture of quercetin 3-*O*-β-D-glucoside (**5.6**) and myricetin 3-*O*-α-L-rhamnoside (**5.2**) (5.7 mg). Based on ^{1}H NMR evidence, subfraction 5 (0.97 g) contained a complex mixture of sugars and was not purified further.

The VLC fraction C was chromatographed on a silica gel column eluting with gradients of dichloromethane-ethylacetate (9:1, 8:2 and 6:4) to give four fractions. Three of the fractions were composed of oily material and pigments. The fourth fraction appeared as a major spot on TLC and was further purified by isocratic elution on a silica gel column to afford lupeol (**5.9**) (26.8 mg) and a mixture of α-amyrin (**5.10**) and β-amyrin (**5.11**) (8.1 mg).

5.2.4. Spectroscopic and physical data of compounds

Myricetin 3-*O*-α-L-arabinopyranoside (**5.1**): yellow solid, $[\alpha]_D^{29}$ -21.64 (*c*=0.08, MeOH), UV (MeOH/ACN): λ_{max} 255, 358 nm; ^{1}H NMR (400 MHz, CD_3OD): δ_H 7.31 (2H, s, H-2',6'), 6.36 (1H, d, *J*=2.0 Hz, H-8), 6.18 (1H, d, *J*=2.0 Hz, H-6), 5.15 (1H, d, *J*=6.7 Hz, H-1''), 3.90 (1H, dd, *J*=8.4, 6.7 Hz, H-2''), 3.86 (1H, dd, *J*=11.9, 3.5 Hz, H-5''), 3.83 (1H, m, H-4''), 3.65 (1H, dd, *J*=8.5, 3.2

Hz, H-3''), 3.47 (1H, d, *J*=10.9 Hz, H-5''). ^{13}C NMR (100 MHz, CD_3OD): δ_C 179.3 (C-4), 167.3 (C-7), 163.0 (C-5), 158.5 (C-9,2), 146.5 (C-3', 5'), 138.2 (C-4'), 135.8 (C-3), 121.8 (C-1'), 109.9 (C-2', 6'), 105.3 (C-10), 104.9 (C-1''), 100.3 (C-6), 95.0 (C-8), 74.3 (C-3''), 73.0 (C-2''), 69.2 (C-4''), 67.1 (C-5''). HPLC R_t: 12.009 min; HR-ESI-(-)-MS: *m/z* 449.0732 $[M-H]^-$ (Calculated for $C_{20}H_{17}O_{12}$, 449.0720).

Myricetin 3-*O*-α-L-rhamnoside (myricitrin) (**5.2**): yellow solid, $[\alpha]_D^{29}$ -179.76 (*c*=0.47, MeOH), UV (MeOH/ACN): λ_{max} 257, 351 nm; ^{1}H NMR (500 MHz, CD_3OD): δ_H 6.95 (2H, s, H-2',6'), 6.35 (1H, d, *J*=2.5 Hz, H-8), 6.19 (1H, d, *J*=2.5 Hz, H-6), 5.31 (1H, d, *J*=1.3 Hz, H-1''), 4.22 (1H, dd, *J*=3.3, 1.7 Hz, H-2''), 3.78 (1H, dd, *J*=10.5, 4.3 Hz, H-3''), 3.47 (1H, m, H-5''), 3.35 (1H, d, *J*=9.5 Hz, H-4''), 0.96 (3H, d, *J*=6.2 Hz, H-6''). ^{13}C NMR (125 MHz, CD_3OD) δ_C 179.5 (C-4), 166.3 (C-7), 163.2 (C-5), 159.4 (C-2), 158.5 (C-9), 146.9 (C-3', 5'), 137.9 (C-4'), 136.3 (C-3), 121.9 (C-1'), 109.7 (C-2', 6'), 105.8 (C-10), 103.6 (C-1''), 99.9 (C-6), 94.8 (C-8), 73.4 (C-4''), 72.2 (C-3''), 72.1 (C-5''), 72.0 (C-2''), 17.7 (C-6''). HPLC R_t: 12.244 min; HR-ESI-(-)-MS: *m/z* 463.0881 $[M-H]^-$ (Calculated for $C_{21}H_{19}O_{12}$, 463.0877).

Quercetin 3-*O*-α-L-arabinofuranoside (avicularin) (**5.3**): yellow solid, $[\alpha]_D^{29}$ -115.6 (*c*=0.65, MeOH), UV (MeOH/ACN): λ_{max} 255, 353 nm; ^{1}H NMR (400 MHz, CD_3OD): δ_H 7.53 (1H, d, *J*=2.0 Hz, H-2'), 7.49 (1H, dd, *J*=8.3, 2.06 Hz, H-6'), 6.90 (1H, d, *J*=8.3 Hz, H-5'), 6.39 (1H, d, *J*=2.1 Hz, H-8), 6.21 (1H, d, *J*=2.0 Hz, H-6), 5.5 (1H, s, H-1''), 4.33 (1H, dd, *J*=2.9, 0.9 Hz, H-2''), 3.91 (1H, dd, *J*=5.2, 2.9 Hz, H-3''), 3.87 (1H, t, *J*=4.4 Hz, H-4''), 3.51 (2H, m, H-5''). ^{13}C NMR (100 MHz, CD_3OD): δ_C 180.0 (C-4), 166.3 (C-7), 163.1 (C-5), 159.4 (C-2), 158.6 (C-9), 149.9 (C-4'), 146.4 (C-3'), 134.9 (C-3), 123.1 (C-1'), 122.9 (C-6'), 116.9 (C-2'), 116.5 (C-5'), 109.6 (C-1''), 105.6 (C-10), 99.9 (C-6), 94.9 (C-8), 88.1 (C-4''), 83.3 (C-2''), 78.7 (C-3''), 62.6 (C-5''). HPLC R_t: 14.460 min; HR-ESI-(-)-MS: *m/z* 433.0779 $[M-H]^-$ (Calculated for $C_{20}H_{17}O_{11}$, 433.0771).

Quercetin 3-*O*-α-L-arabinopyranoside (guaijaverin) (**5.4**): yellow solid, $[\alpha]_D^{29}$ -54.07 (*c*=0.5, MeOH), UV (MeOH/ACN): λ_{max} 255, 355 nm; ^{1}H NMR (400 MHz, CD_3OD): δ_H 7.74 (1H, d, *J*=2.1 Hz, H-2'), 7.57 (1H, dd, *J*=8.5, 2.1 Hz, H-6'), 6.88 (1H, d, *J*=8.3 Hz, H-5'), 6.39 (1H, d, *J*=1.9 Hz, H-8), 6.20 (1H, d, *J*=1.9 Hz, H-6), 5.16 (1H. d, *J*=6.5 Hz, H-1''), 3.90 (1H, dd, *J*=8.4, 6.5 Hz, H-2''), 3.81-3.84 (2H, m, H-4'',5''), 3.65 (1H, dd, *J*=8.4, 3.1 Hz, H-3''), 3.44 (1H, m, H-5''). ^{13}C NMR (100 MHz, CD_3OD): δ_C 179.4 (C-4), 166.5 (C-7), 163.0 (C-5), 158.7 (C-2), 158.5 (C-9), 150.0 (C-4'), 145.9 (C-3'), 135.6 (C-3), 123.1 (C-1'), 122.9 (C-6'), 117.5 (C-2'), 116.4 (C-5'), 105.5 (C-10),

104.7 (C-1''), 100.0 (C-6), 94.8 (C-8), 74.2 (C-3''), 72.8 (C-2''), 69.1 (C-4''), 66.9 (C-5''). HPLC R_t: 14.030 min; HR-ESI-(-)-MS: *m/z* 433.0775 $[M-H]^-$ (Calculated for $C_{20}H_{17}O_{11}$, 433.0771).

Quercetin 3-*O*-α-L-rhamnoside (quercitrin) (**5.5**): yellow solid, $[\alpha]_D^{29}$ -136.93 (*c*=1.1, MeOH), UV (MeOH/ACN): λ_{max} 255, 350 nm; ^{1}H NMR (400 MHz, CD_3OD): δ_H 7.34 (1H, d, *J*=2.0 Hz, H-2'), 7.30 (1H, dd, *J*=8.5, 2.0 Hz, H-6'), 6.87 (1H, d, *J*=8.5 Hz, H-5'), 6.36 (1H, d, *J*=2.0 Hz, H-8), 6.19 (1H, d, *J*=2.0 Hz, H-6), 5.35 (1H, d, *J*=1.2 Hz, H-1''), 4.22 (1H, dd, *J*=3.2, 1.7 Hz, H-2''), 3.75 (1H, dd, *J*=9.2, 3.2 Hz, H-3''), 3.45 (1H, m, H-5''), 3.34 (1H, d, *J*=9.4 Hz, H-4''), 0.96 (3H, d, *J*=6.2 Hz, H-6''). ^{13}C NMR (100 MHz, CD_3OD): δ_C 179.6 (C-4), 165.9 (C-7), 163.2 (C-5), 159.3 (C-2), 158.5 (C-9), 149.8 (C-3'), 146.4 (C-4'), 136.2 (C-3), 123.0 (C-1'), 122.9 (C-6'), 117.0 (C-2'), 116.4 (C-5'), 105.9 (C-10), 103.5 (C-1''), 99.8 (C6-), 94.8 (C-8), 73.3 (C-4''), 72.1 (C-3''), 72.0 (C-2''), 71.9 (C-5''), 17.7 (C-6''). HPLC R_t: 14.668 min; HR-ESI-(-)-MS: *m/z* 433.0779 $[M-H]^-$ (Calculated for $C_{21}H_{19}O_{11}$, 447.0927).

Quercetin 3-*O*-β-D-glucoside (isoquercitrin) (**5.6**): yellow solid, $[\alpha]_D^{29}$ -32.70 (*c*=0.18, MeOH), UV (MeOH/ACN): λ_{max} 255, 355 nm; ^{1}H NMR (400 MHz, CD_3OD): δ_H 7.84 (1H, d, *J*=2.2 Hz, H-2'), 7.59 (1H, dd, *J*=8.5, 2.2 Hz, H-6'), 6.86 (1H, d, *J*=8.5 Hz, H-5'), 6.39 (1H, d, *J*=2.1 Hz, H-8), 6.19 (1H, d, *J*=2.1 Hz, H-6), 5.14 (1H, d, *J*=7.8 Hz, H-1''), 3.85 (1H, m, Hz, H-4''), 3.83 (1H, d, *J*= 7.8 Hz, H-2''), 3.64 (1H, d, *J*=11.1, 6.0 Hz, H-6''), 3.56 (2H, m, H-6''), 3.53 (1H, m, H-3''), 3.46 (1H, m, H-5''). ^{13}C NMR (100 MHz, CD_3OD): δ_C 179.6 (C-4), 166.6 (C-7), 163.2 (C-5), 158.8 (C-2), 158.5 (C-9), 149.9 (C-4'), 145.8 (C-3'), 135.7 (C-3), 122.9 (C-6'), 121.9 (C-1'), 117.8 (C-2'), 116.1 (C-5'), 105.8 (C-10), 105.5 (C-1''), 100.1 (C-6), 94.9 (C-8), 77.2 (C-5''), 75.1 (C-3''), 73.2 (C-2''), 70.0 (C-4''), 61.9 (C-6''). HPLC R_t: 12.608 min; HR-ESI-(-)-MS: *m/z* 463.0881 $[M-H]^-$ (Calculated for $C_{21}H_{19}O_{12}$, 463.0877).

Oleanolic acid (**5.7**): white solid, ^{1}H NMR (500 MHz, CD_3OD + $CDCl_3$): δ_H 5.23 (1H, t, *J*=3.4 Hz, H-12), 3.15 (1H, dd, *J*=11.3, 5.1 Hz, H-3), 2.82 (1H, dd, *J*=13.8, 4.0 Hz, H-18), 1.97 (1H, m, H-16), 1.89 (1H, m, H-11a,11b), 1.74 (1H, m, H-22), 1.69 (1H, m, H-15), 1.64 (1H, brs, H-19), 1.61-1.58 (3H, m, H-16,2,1), 1.56 (2H, m, H-2, 22), 1.54-1.51 (3H, m, H-2,6,9), 1.45 (1H, m, H-7), 1.39 (1H, m, H-6), 1.35 (1H, m, H-21), 1.28 (1H, m, H-7), 1.19 (1H, m, H-21), 1.13 (3H, s, H-27), 1.1 (1H, m, H-19), 1.08 (1H, m, H-15), 0.96 (3H, s, H-23), 0.93 (1H, m, H-1), 0.91 (6H, s, H-25, 29), 0.88 (3H, s, H-30), 0.79 (3H, s, H-26), 0.76 (3H, s, H-24), 0.72 (1H, d, *J*=11.7 Hz, H-5). ^{13}C NMR (125 MHz, CD_3OD + $CDCl_3$): δ_C 181.6 (C-28), 144.7 (C-13), 123.2 (C-12), 79.4 (C-3), 56.2

(C-5), 47.2 (C-9), 46.8 (C-17), 42.5 (C-19), 42.2 (C-14), 40.1 (C-18), 39.5 (C-8,4), 39.4 (C-1), 37.8 (C-10), 34.6 (C-21), 33.6 (C-29), 33.5 (C-7), 33.4 (C-22), 31.3 (C-20), 28.6(C-23), 28.5 (C-15), 27.6 (C-2), 26.4 (C-27), 24.2 (C-30), 23.9 (C-11), 23.8 (C-16), 19.1 (C-6), 17.5 (C-26), 16.1 (C-24), 15.8 (C-25). HR-ESI-(-)-MS: *m/z* 455.3538 $[M-H]^-$ (Calculated for $C_{30}H_{47}O_3$, 455.3525).

Scopoletin (**5.8**): white solid, ^1H NMR (500 MHz, $CDCl_3$): δ_H 7.59 (1H, d, *J*=9.4 Hz, H-4), 6.9 (1H, s, H-5), 6.8 (1H, s, H-8), 6.27 (1H, d, *J*=9.4 Hz, H-3), 6.11 (1H, s, OH), 3.95 (3H, s, OCH_3). ^{13}C NMR (125 MHz, $CDCl_3$): δ_C 161.6 (C-2), 150.5 (C-9), 149.8 (C-7), 143.4 (C-4,6), 113.7 (C-3), 111.6 (C-10), 107.7 (C-5), 103.4 (C-8), 56.6 (OCH_3-6). HR-ESI-(-)-MS: *m/z* 191.0346 $[M-H]^-$ (Calculated for $C_{10}H_8O_4$, 191.0344).

Lupeol (**5.9**): white solid ^1H NMR (500 MHz, $CDCl_3$): δ_H 4.68 (1H, d, *J*=2.3 Hz, H-29b), 4.56 (1H, dd, *J*=2.3, 1.3 Hz, H-29a), 3.18 (1H, dd, *J*=11.4, 4.8 Hz, H-3), 2.38 (1H, m, H-19), 1.92 (1H, m, H-21b), 1.68 (3H, s, H-30), 1.65-1.05 (overlapped signals), 1.03 (3H, s, H-26), 0.97 (3H, s, H-23), 0.94 (3H, s, H-27), 0.83 (3H, s, H-25), 0.79 (3H, s, H-28), 0.76 (3H, s, H-24), 068 (1H, d, *J*=9.3 Hz, H-5). ^{13}C NMR (125 MHz, $CDCl_3$): δ_C 150.9 (C-20), 109.3 (C-29), 79.0 (C-3), 55.3 (C-5), 50.5 (C-9), 48.4 (C-18), 48.0 (C-19), 43.0 (C-17), 42.9 (C-14), 40.9 (C-8), 40.0 (C-22), 38.9 (C-4), 38.7 (C-1), 38.1 (C-13), 37.2 (C-10), 35.6 (C-16), 34.3 (C-7), 29.9 (C-21), 28.0 (C-23), 27.5 (C-15), 27.4 (C-2), 25.2 (C-12), 21.0 (C-11), 19.3 (C-30), 18.3 (C-6), 18.0 (C-28), 16.1 (C-25), 16.0 (C-26), 15.4 (C-24), 14.6 (C-27). GCMS R_t: 26.92 min. EIMS: 189 (40%), 205 (50%), 218 (100%), 424 (40%).

α-Amyrin (**5.10**): white solid, ^1H NMR (500 MHz, $CDCl_3$): δ_H 5.13 (1H, t, *J*=3.6 Hz, H-12), 3.21 (1H, m, H-3), 1.07 (3H, s, H-27), 1.01 (3H, s, H-26), 0.99 (3H, s, H-23), 0.95 (3H, s, H-25), 0.91 (3H, d, *J*=5.8 Hz, H-30), 0.80 (3H, d, *J*=5.6 Hz, H-29), 0.80 (3H, s, H-28), 0.79 (3H, s, H24). ^{13}C NMR (125 MHz, $CDCl_3$): δ_C 139.6 (C-13), 124.5 (C-12), 79.1, (C-3), 59.1 (C-18), 55.2 (C-5), 47.8 (C-9), 42.1 (C-14), 41.6 (C-22), 40.1 (C-8), 39.7 (C-19), 39.6 (C-20), 38.9 (C-4), 38.6 (C-1), 36.9 (C-10), 33.8 (C-17), 33.0 (C-7), 31.3 (C-21), 28.8 (C-15), 28.1 (C-23, 28), 27.3 (C-2), 26.6 (C-16), 23.4 (C-27), 23.3 (C-11), 21.4 (C-30), 18.4 (C-6), 17.5 (C-29), 16.8 (C-26), 15.7 (C-25), 15.6 (C-24). GCMS R_t: 27.35 min. EIMS: 189 (20%), 203 (20%), 218 (100%), 426 (10%).

β-Amyrin (**5.11**): white solid, ^1H NMR (500 MHz, $CDCl_3$): δ_H 5.18 (1H, t, *J*=3.5 Hz, H-12), 3.23 (1H, m, H-3), 1.13 (3H, s, H-27), 0.99 (3H, s, H-23), 0.97 (3H, s, H-26), 0.94 (3H, s, H-25), 0.87 (6H, s, H-29, 30), 0.83 (3H, s, H-28), 0.79 (3H, s, H-24). ^{13}C (125 MHz, $CDCl_3$): δ_C 145.2 (C-13), 121.8 (C-12), 79.1 (C-3), 55.2 (C-5), 47.7 (C-9), 47.3 (C-18), 46.9 (C-19), 41.8 (C-14), 38.8 (C-4,

8), 38.6 (C-1), 37.2 (C-22), 37.0 (C-10), 34.8 (C-21), 33.3 (C-29), 32.7 (C-7), 32.5 (C-17), 31.1 (C-20), 28.4 (C-28), 28.2 (C-23), 27.3 (C-2), 27.0 (C-16), 26.2 (C-15), 26.0 (C-27), 23.7 (C-30), 23.6 (C-11), 18.5 (C-6), 16.9 (C-26), 15.6 (C-25), 15.5 (C-24). GCMS R_t: 26.724 min. EIMS: 189 (20%), 203 (60%), 218 (100%), 426 (10%).

5.2.5. Antimalarial assay

5.2.5.1. The parasites

The same as section 3.2.5.1 in chapter 3

5.2.5.2. Assessment of in vitro antiplasmodial activity

The same as section 3.2.5.2 in chapter 3

5.2.5.3. In vitro cytotoxicity

The cytotoxicity against HeLa cells is the same as section 3.2.5.3 in chapter 3. For cytotoxicity against Vero cells, the extract was evaluated using the MTT assay in 96-well microtitre plates. Cell suspensions were prepared from confluent monolayer cultures and harvested. Thereafter, 1×10^4 cells in 200 µL of minimal essential medium (MEM, Whitehead Scientific, South Africa), supplemented with 0.1% gentamicin (Virbac) and 5% foetal calf serum (Highveld Biological), were inoculated into each well. After 24 hours of incubation at 37 ^oC and 5% CO_2, cells were treated with dilutions of the extracts and positive control (doxorubicin chloride, Pfizer Laboratories), and incubated further for 48 hours. Then, 30 µL of MTT (Sigma, stock solution of 5 mg/ml in PBS) was added to each well and further incubated for 4 hours. The resulting MTT formazan crystals were dissolved by adding 50 µL of DMSO to each well after removal of the medium. The amount of MTT reduction was detected by recording the absorbance at 540 nm using a microplate reader (Chromate 4300) and the IC_{50}s were calculated from the plotted regression curves.[16]

5.3. Results and discussion

The dichloromethane-methanol (1:1) extract of *E. natalensis* inhibited the in vitro growth of *P. falciparum* 3D7 (IC_{50} = 25.6 µg/mL) and was not cytotoxic against Vero cells. The extract was subjected to chromatographic purification, which afforded six flavonoid glycosides, four triterpenoids and a coumarin. The structures were established by analysis of the NMR and mass spectra (Appendix C).

5.3.1 Chemistry

The structures of the isolated compounds are given in **Fig. 5.1**.

Compound **5.1** was isolated as a yellow crystalline solid and assigned a molecular formula of $C_{20}H_{18}O_{12}$ based on the pseudo-molecular ion $[M-H]^-$ (*m/z* 449.0732) observed in the HR-ESI-(-)-MS (**Plate 5.1**) (Calculated for $C_{20}H_{17}O_{12}$ 449.0720). The ^1H NMR spectrum (**Plate 5.2**) of **5.1** revealed a two-proton aromatic singlet at δ_H 7.31 (2H, s, H-2',6') and a pair of aromatic AX spin-type doublets at δ_H 6.36 (1H, d, *J*=2.05 Hz, H-8) and δ_H 6.18 (1H, d, *J*=2.05 Hz, H-6), consistent with a myricetin nucleus. This deduction was supported by the ^{13}C NMR and DEPT spectra (**Plate 5.3**), which showed the presence of a carbonyl at δ_C 179.3 and 12 other aromatic resonances, of which eight are oxygenated (δ_C 167.3-135.8). Assignments of the quaternary carbons were achieved by analysis of the HMBC spectrum (**Plate 5.4**). Important HMBC crosspeaks include δ_H 6.18/ δ_C 163.0 (H-6/C-5), δ_H 6.18/ δ_C 105.3 (H-6/C-10), δ_H 6.38/ δ_C 158.5 (H-8/C-9), δ_H 7.31/ δ_C 158.5 (H-2',6'/C-2) and δ_H 7.31/ δ_C 121.8 (H-2',6'/C-1'). Also observed in the ^1H NMR spectrum are a doublet at δ_H 5.15 (1H, d, *J*=6.7 Hz, H-1''), three oxymethine and two oxymethylene resonances between δ_H 3.47 and 3.9 ppm, suggesting a pentose sugar moiety. This deduction was supported by the appearance of three oxymethine carbons at δ_C 69.2-74.3, an oxymethylene carbon at δ_C 67.1 and an anomeric carbon at δ_C 104.9. The COSY (**Plate 5.5**) correlations of δ_H 5.15/ δ_H 3.9 (H-1''/H-2''), δ_H 3.9/ δ_H 3.65 (H-2''/H-3''), δ_H 3.83/ δ_H 3.65 (H-4''/H-3'') and δ_H 3.86/ δ_H 3.83 (H-4''/H-5'') facilitated the assignment of the sugar protons. The relatively large coupling constants of the sugar protons indicate that the sugar is a pyranose. The doublet at δ_H 5.15 ppm is assignable to the sugar anomeric proton with a 1,2-diaxial coupling (*J*=6.4 Hz) between H-1 and H-2 of the sugar. The attachment of the sugar unit to position 3 of the aglycone was confirmed by the HMBC correlation of the anomeric proton δ_H 5.15 (H-1'') with δ_C 135.8 (C-3) of the flavonoid. All the protonated carbons of compound **5.1** were assigned based on HSQC (**Plate 5.6**) cross peaks. The sugar NMR data closely match those of arabinopyranoside and a comparison of the NMR data of compound **5.1** with those reported in the literature for myrecitin 3-*O*-arabinopyranoside showed good agreement.[17,18] Therefore, the structure of **5.1** was confirmed to be myrecitin 3-*O*-α-L-arabinopyranoside (**5.1**) (**Fig. 5.1**).

Compound **5.2** was isolated as a yellow amorphous solid. It was assigned a molecular formula of $C_{21}H_{20}O_{12}$, based on a pseudo-molecular ion $[M-H]^-$ peak at *m/z* 463.0881 (calculated for $C_{21}H_{19}O_{12}$ 463.0877) observed in the HR-ESI-(-)-MS (**Plate 5.7**). The aromatic regions of the NMR spectra (**Plate 5.8-5.11**) of **5.2** resembled those of compound **5.1**, suggesting the presence of a myricetin aglycone. Further, an anomeric proton at δ_H 5.31 (1H, d, *J*=1.3 Hz, H-1''), a sharp methyl doublet at δ_H 0.96 (3H, d, *J*=6.2 Hz, H-6'') and four other oxygenated methine resonances between δ_H 3.35 and δ_H 4.22 suggested the presence of a rhamnosyl moiety in an α-linkage with the flavonoid nucleus. The connectivity of the sugar to the aglycone at position 3 was established by the HMBC (**Plate 5.11**) cross peak observed between the anomeric proton δ_H 5.31 (H-1'') and δ_C 136.3 (C-3). Based on these NMR analyses and after comparison of the data with those reported in the literature, the identity of compound **5.2** was assigned as myricetin 3-*O*-α-L-rhamnoside (**5.2**) (**Fig. 5.1**).[17,19]

Compound **5.3,** which was obtained as a yellow powder, showed a pseudomolecular ion peak $[M-H]^-$ at *m/z* 433.0779 (Calculated for $C_{20}H_{17}O_{11}$ 433.0771) in the HR-ESI-(-)-MS (**Plate 5.12**), suggesting a molecular formula of $C_{20}H_{18}O_{11}$. The aromatic region of the ^{1}H NMR spectrum (**Plate 5.13**) displayed signals characteristic of an ABX spin system at δ_H 7.53 (1H, d, *J*=2.0 Hz, H-2'), δ_H 7.49 (1H, dd, *J*=8.3, 2.06 Hz, H-6') and δ_H 6.90 (1H, d, *J*=8.3 Hz, H-5'), as well as an AX system at δ_H 6.39 (1H, d, *J*=2.1 Hz, H-8), δ_H 6.21 (1H, d, *J*=2.0 Hz, H-6), as found in a quercetin derivative. This deduction was supported by the ^{13}C and DEPT (**Plate 5.14**) spectra of **5.3**, which showed 15 carbon resonances including a carbonyl at δ_C 180.0 and seven oxygenated carbon resonances (δ_C 166.3-134.9), assignable to a quercetin nucleus. The HMBC (**Plate 5.15**) correlations of δ_H 6.21/ δ_C 163.1 (H-6/C-5), δ_H 6.21/ δ_C 105.6 (H-6/C-10), δ_C 6.39/ δ_C 158.6 (H-8/C-9), δ_H 7.53,7.49/ δ_C 159.4 (H-2',6'/C-2), δ_H 7.53,6.9/ δ_C 146.4 (H-2',5'/C-3') and δ_H 7.53,7.46,6.9/ δ_C 149.9 (H-2',6',5'/C-4') facilitated the assignment of the quaternary carbons. The oxygenated methine singlet at δ_H 5.5 (1H, s, H-1''), three oxymethine resonances between δ_H 3.87 and δ_H 4.33, and an oxymethylene multiplet at δ_H 3.51 suggested the presence of a pentose sugar. The singlet at δ_H 5.5 was assigned to a sugar anomeric proton in an α-linkage with the flavonoid unit. The relatively small coupling constants values of the sugar protons indicate that the sugar is a furanose. The point of attachment of the sugar to the aglycone was established by the observed HMBC cross peak between the anomeric proton signals at δ_H 5.5 (H-1'') and δ_C 134.9 (C-3). All other protonated carbons were assigned by analysis of

HSQC cross peaks (**Plate 5.16**). The sugar NMR data resembled those of arabinofuranose and a comparison of the NMR data of **5.3** with those reported in the literature showed close similarity with quercetin 3-*O*-α-L-arabinofuranoside[20,21] (**Fig. 5.1**), thus establishing the identity of the compound.

Compound **5.4** and **5.5** were isolated as a yellow mixture (1:1 based on ^{1}H NMR integration) and attempts to separate them were unsuccessful. However, analysis of the NMR and MS data facilitated unambiguous identification. Moreover, both compounds were also isolated as single compounds from *Ozoroa obovata* for compound **5.5** (chapter 4) and *Pappea capensis* (chapter 6) for compound **5.4**. The spectroscopic data of the individual compounds matched those of the mixture. Compound **5.4** was assigned a molecular formula of $C_{20}H_{18}O_{11}$, based on the pseudo-molecular ion $[M-H]^-$ at *m/z* 433.0775 (Calculated for $C_{20}H_{17}O_{11}$ 433.0771) observed in the HR-ESI-(-)-MS (**Plate 5.17**). The NMR data (**Plate 5.19-5.22**) of **5.4** showed close resemblance to those of **5.3**, and together with the MS data, suggests that the two compounds are closely related isomers. However, the two compounds had different Rf values on TLC using the same solvent systems. A closer analysis of the NMR data showed subtle differences in the chemical shifts of some of the aromatic protons as well as the sugar proton multiplicities. The aromatic protons at H-2' and H-6' of ring B were slightly shifted downfield (0.21 and 0.08 ppm, respectively) compared to **5.3**. The anomeric at proton δ_H 5.16 (1H, d, *J*=6.5 Hz, H-1''), unlike that of **5.3**, was slightly shifted upfield and appeared as a sharp doublet with a coupling constant *J*=6.5 Hz. This suggests a 1,2-diaxial coupling of the anomeric proton H-1'' with sugar H-2''. Examination of the coupling constants of the sugar protons showed that it is in the pyranose form as found in arabinopyranoside. The HMBC correlation of the anomeric proton δ_H 5.16 (H-1'') with δ_C 135.6 (C-3) confirmed the point of sugar attachment to the quercetin nucleus. Thus the structure of compound **5.4** was assigned as quercetin 3-*O*-α-L-arabinopyranoside[20,21] (**5.4**) (**Fig. 5.1**).

Compound **5.5** was assigned a molecular formula of $C_{21}H_{20}O_{11}$, based on pseudo-molecular ion $[M-H]^-$ at *m/z* 433.0779 (Calculated for $C_{21}H_{19}O_{11}$ 447.0927) on the HR-ESI-(-)-MS (**Plate 5.18**). The NMR data (**Plate 5.19-5.22**) of **5.5** revealed signals consistent with the presence of a quercetin derivative. Also, a doublet at δ_H 5.35 (1H, d, *J*=1.2 Hz, H-1''), four oxymethines between δ_H 4.22 and δ_H 3.34 and a methyl doublet at δ_H 0.94 (3H, d, *J*=6.2 Hz, H-6'') suggested the presence of a rhamnose sugar moiety. The HMBC cross peak observed between the

anomeric proton and δ_C 136.2 (C-3) confirmed the attachment of the rhamnosyl unit to position 3 of the quercetin nucleus. The identity of **5.5** was confirmed to be quercetin 3-*O*-α-L-rhamnoside (**5.5**) (**Fig. 5.1**) after comparing the spectral data with published literature data.[19]

Compound **5.2** and **5.6** are isomeric (molecular formula of $C_{21}H_{20}O_{12}$) and were also isolated as a yellow mixture (1:1 based on ^{1}H NMR integration). Attempts to separate them were not successful. However, analysis of the NMR and MS data facilitated unambiguous identification. Moreover, compound **5.2** was also isolated as a single compound from *Ozoroa obovata* (chapter 4), and compound **5.6** was also isolated as a single compound from *Gardenia thunbergia* (chapter 7). Compound **5.6** was assigned a molecular formula of $C_{21}H_{20}O_{12}$, based on pseudo-molecular ion $[M-H]^-$ at *m/z* 463.0881 (Calculated for $C_{21}H_{19}O_{11}$ 463.0877) on it HR-ESI-(-)-MS (**Plate 5.7**). The NMR data (**Plate 5.8-5.11**) of **5.6** also showed resonances consistent with a quercetin aglycone. The presence of a sugar unit was indicated by the doublet at δ_H 5.14 (1H, d, *J*=7.8 Hz, H-1'') assignable to a 1,2 diaxial coupled anomeric proton based on *J* value of 7.8 Hz. The other sugar protons including four oxymethines between δ_H 3.85 and δ_H 3.46 and two oxymethylenes at δ_H 3.56 and δ_H 3.64 were similar to those of glucopyranose. This deduction was supported by the ^{13}C NMR signals at δ_C 105.5 and between δ_C 77.2 and δ_C 61.9. The attachment of the sugar to position 3 of the flavonoid aglycone was established by the HMBC correlation of δ_H 5.14 (H-1'') with δ_C 135.7 (C-3). Therefore, the structure of **5.6** was determined as quercetin 3-*O*-β-D-glucoside (**5.6**) (**Fig. 5.1**) and this was confirmed after comparison with literature data.[22,23]

Compound **5.7** was obtained as a pale-white amorphous powder. The pseudo-molecular ion $[M-H]^-$ at *m/z* 455.3538 in the HR-ESI-(-)-MS (**Plate 5.23**) allowed the determination of the molecular formula to be $C_{30}H_{48}O_3$ (Calculated for $C_{30}H_{47}O_3$ 455.3525). The ^{1}H NMR spectrum (**Plate 5.24**) displayed resonances for a characteristic olefinic proton triplet at δ_H 5.23 (1H, t, *J*=3.4 Hz, H-12) and 7 tertiary methyl groups at δ_H 0.96 (3H, s, H-23), 0.93 (1H, m, H-1), 0.91 (6H, s, H-25, 29), 0.88 (3H, s, H-30), 0.79 (3H, s, H-26) and δ_H 0.76 (3H, s, H-24). These ^{1}H NMR resonances together with ^{13}C and DEPT resonances (**Plate 5.25**) for two olefinic carbons at δ_C 144.7 (C-13) and δ_C 123.2 (C-12), and seven methyls at δ_C 33.6 (C-29), 28.6(C-23), 26.4 (C-27), 24.2 (C-30), 17.5 (C-26), 16.1 (C-24), δ_C 15.8 (C-25), suggest the presence of an olean-12-ene skeleton. The NMR data also revealed the presence of an oxygenated methine group at δ_H

3.15 (1H, dd, *J*=11.3, 5.1 Hz, H-3), which showed HSQC correlation (**Plate 5.26**) with carbon at δ_C 79.4 (C-3), a carboxylic acid resonance at δ_C 181.6 (C-28), and overlapped proton resonances for methine and methylene protons, consistent with the structure of oleanolic acid (**Fig. 5.1**). A comparison of the NMR data of **5.7** with those reported in the literature for oleanolic acid[24,25] (**5.7**) showed good agreement and confirmed the structure of the compound.

Compound **5.8** was isolated as a brown solid and assigned the molecular formula $C_{10}H_8O_4$ (calculated for $C_{10}H_7O_4$ 191.0344) based on pseudo-molecular ion $[M-H]^-$ at *m/z* 191.0346 in the HR-ESI-(-)-MS (**Plate 5.28**). The ^{1}H NMR spectrum (**Plate 5.29**) of **5.8** showed resonances characteristic of an α,β-unsaturated carbonyl system with a *cis* configuration of the alkene protons resonating at δ_H 7.59 (1H, d, *J*=9.4 Hz, H-4) and δ_H 6.27 (1H, d, *J*=9.4 Hz, H-3), in addition to two aromatic singlets at δ_H 6.9 (1H, s, H-5), and δ_H 6.8 (1H, s, H-8), an exchangeable hydroxyl singlet at δ_H 6.11 (1H, s, OH), and a methoxy singlet at δ_H 3.95 (3H, s, OCH_3) consistent with the structure of scopoletin. This assignment was supported by the ^{13}C NMR data (**Plate 5.30**) of **5.8** which showed resonances characteristic of an ester carbonyl at δ_C 161.6 (C-2), two olefinic carbons at δ_C 143.4 (C-4) and δ_C 113.7 (C-3), six aromatic carbons of which three are oxygenated at δ_C 150.5-103.4 and a methoxy carbon resonance at δ_C 56.6. A comparison of these NMR data with the literature[26] showed close agreement with the resonances of scopoletin (**5.8**) (**Fig. 5.1**), thus confirming the structure.

Purification of the dichloromethane-ethyl acetate (20:1) extract of *E. natalensis* using silica gel column chromatography afforded lupeol (**5.9**) and a mixture (1:2 from ^{1}H NMR integration) of α-amyrin (**5.10**) and β-amyrin (**5.11**). The structures were confirmed by GCMS analysis and comparison of the ^{1}H and ^{13}C NMR data with those reported in the literature.

The EIMS (**Plate 5.31**) of **5.9** showed a base peak at *m/z* 218, resulting from the fragmentation of C8-C14 bond to yield the C*DE fragment (*m/z* 218)[27] and a molecular ion peak at *m/z* 424, suggesting a molecular formula of $C_{30}H_{50}O$. The ^{1}H NMR spectrum (**Plate 5.32**) of **5.9** showed signals characteristic of lupene-type exocyclic double bond at δ_H 4.68 (1H, d, *J*=2.3 Hz, H-29b) and δ_H 4.56 (1H, dd, *J*=2.3, 1.3 Hz, H-29a), in addition to an oxymethine resonance at δ_H 3.18 (1H, dd, *J*=11.4, 4.8 Hz, H-3) and seven methyl singlets between δ_H 1.68-0.76 characteristic of lupeol. The ^{13}C spectrum (**Plate 5.33**) showed 30 carbon resonances and confirmed the

presence of an exocyclic double bond δ_C 150.9 (C-20), δ_C 109.3 (C-29), a carbinol group δ_C 79.0 (C-3) and seven tertiary methyls. After Comparing the NMR data with those reported in the literature[28,29] for lupeol, the structure of **5.9** was assigned as lupeol (**5.9**) (**Fig. 5.1**).

Compound **5.10** and **5.11** were isolated as a white powder in a mixture (1:2). The EIMS (**Plate 5.34** and **5.35**) showed a base peak at *m/z* 218, resulting from a retro Diels-Alder fragmentation of the C8-C14 and C9-C11 bonds to yield the C*DE fragment ion[30] and a molecular ion peak at *m/z* 426, suggesting a molecular formula of $C_{30}H_{50}O$. The ^{1}H NMR spectrum (**Plate 5.36**) showed a duplication of signals in a ratio of approximately 1:2 (α:β). Two characteristic olefinic triplets at δ_H 5.13 (1H, t, *J*=3.6 Hz) and δ_H 5.18 (1H, t, *J*=3.5 Hz), assignable to H-12 of the pentacyclic oleanane and ursane skeleton of α- and β-amyrin respectively, were observed on the ^{1}H NMR spectrum. The spectrum also showed signals for two oxymethines at δ_H 3.23 (1H, m, H-3) and δ_H 3.21 (1H, m, H-3). Sixteen methyls, of which two were secondary methyls at δ_H 0.91 (3H, d, *J*=5.8 Hz, H-30) and δ_H 0.80 (3H, d, *J*=5.6 Hz, H-29), and the remaining methyl proton resonances between δ_H 0.79 and 1.13 were tertiary, consistent with a mixture of α and β-amyrin, were also observed on the ^{1}H NMR spectrum. This deduction was confirmed by the ^{13}C NMR spectrum (**Plate 5.37**) which showed four olefinic resonances at δ_C 139.6, 145.2 (C-13, α and β), δ_C 124.5, 121.8 (C-12, α and β) and two oxymethine carbons at δ_C 79.1 (C-3). The other carbon resonances where assigned by comparing with literature data for α-amyrin **(5.10**) (**Fig. 5.1**)[31,32] and β-amyrin (**5.11**) (**Fig. 5.1**)[29,32].

Plants belonging to the *Euclea* genus are renowned for the naphthoquinone content of the root and root bark. However, the leaf extracts yielded mostly flavonoids, flavonoid glycosides and pentacyclic triterpenoids. Glycosides of quercetin and myricetin have been isolated from leaves of *E. crispa* subsp. *crispa*.[33] The aerial parts of *E. divinorum* afforded glycosides of quercetin, myricetin and dihydrokaempferol.[34] Also, lupene-, oleanane- and ursane-type triterpenoid have been isolated from other *Euclea* species.[10,35] This is the first report of the isolation of flavonoid glycosides and triterpenoids from the leaves of *E. natalensis*. The isolation of flavonoid glycosides and triterpenoids, and the absence of naphthoquinones in the leaves of *E. natalensis* is in agreement with the phytochemistry of other *Euclea* species.

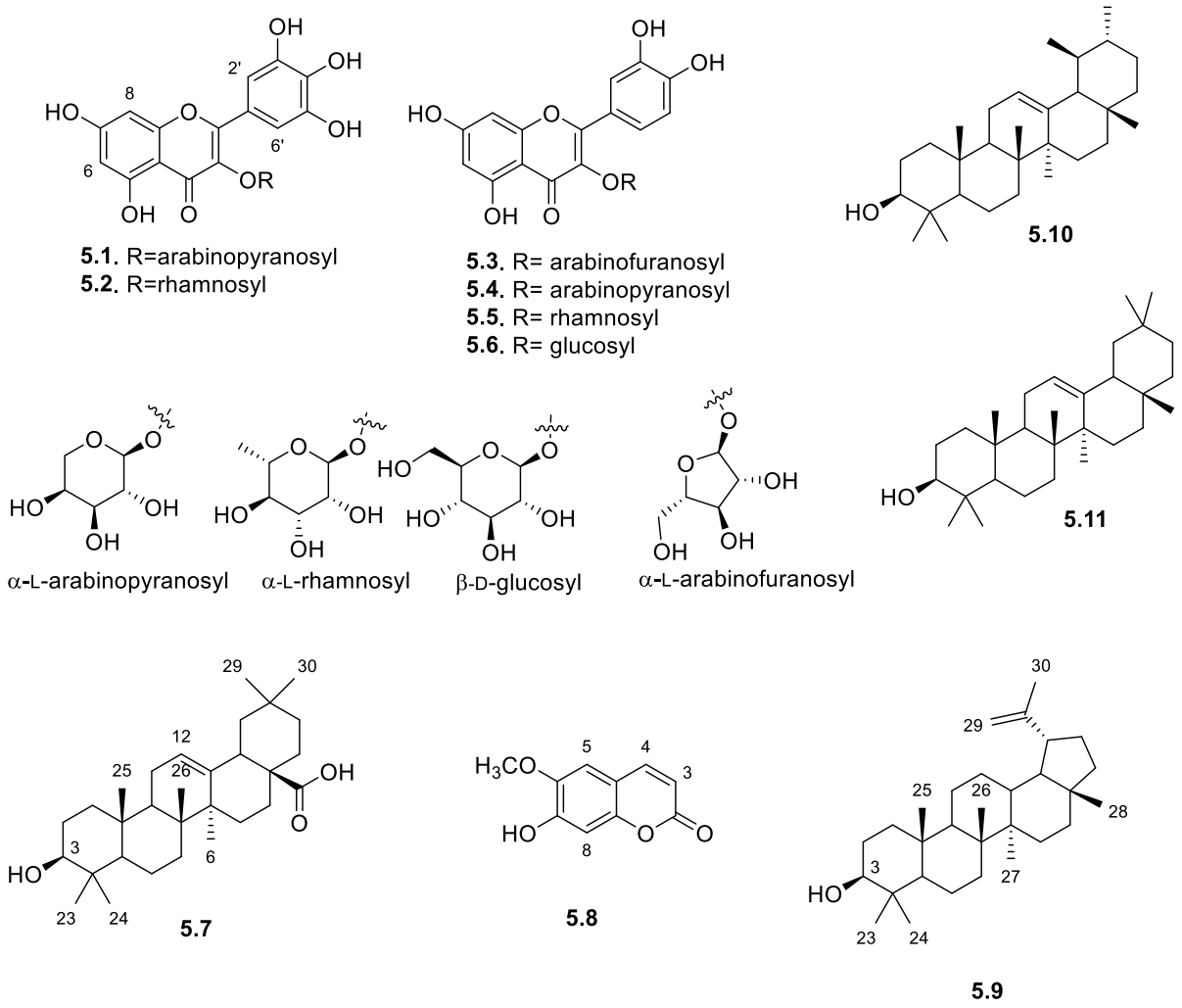

Fig. 5.1: Structures of the isolated compounds from *E. natalensis*

5.3.2. Biological activity

The leaf extract of *E. natalensis* showed moderate inhibitory activity against *P. falciparum* with IC_{50} = 25.4 µg/mL and was not cytotoxic against monkey kidney Vero cells (**Table 5.1**). Purification of the extract afforded six flavonoid glycosides and four ubiquitous triterpenoids. The flavonoid glycosides displayed strong antiplasmodial activity at a concentration of 50 µg/mL, reducing parasite viability to 21% or less (**Table 5.1**), but were also cytotoxic against a cancerous HeLa cell line at this concentration. At a lower concentration of 10 µg/mL, the antiplasmodial and cytotoxic activities were lost, suggesting that the observed activity was not selective. Since the leaf extract was not cytotoxic to non-cancerous Vero cells, it is possible that there is some selectivity in the bioactivity of the extract and isolated compounds. Guaijaverin (**5.4**), avicularin (**5.3**), quercitrin (**5.5**), myricitrin (**5.2**), and isoquercitrin (**5.6**) have been reported to have varying levels of antiplasmodial activity.[20,36,37] Guaijaverin, avicularin

and quercitrin were also reported not to be cytotoxic against noncancerous Vero cells,[20] indicating that perhaps, there is a degree of selectivity in the activity of these compounds. Myricitrin and isoquercitrin have been identified as inhibitors of β-hematin formation in an in vitro assay, at low mM concentrations.[37] Myricetin 3-*O*-arabinopyranoside has not been previously assayed for antiplasmodial activity. Therefore, its antiplasmodial activity is being reported here for the first time. As was stated in chapters 3 and 4, flavonoids and flavonoid glycosides have been shown to possess a variety of biological activities, including antiplasmodial activity. However, the nonspecific binding to biological targets remains an obstacle to harnessing the potential of flavonoids in antiplasmodial drug discovery. The tested compounds in this study are all glycosides of quercetin and myricetin, with sugars attached to the flavonoid at position 3. The type of sugar and degree of oxygenation of the flavonoid had negligible influence on the activities of the compounds.

Table 5.1: In vitro antiplasmodial and cytotoxic activity of the extract and isolated compounds

Compound	Viability% ±SD (50 µg/mL)		Viability% ±SD (10 µg/mL)	
	3D7	HeLa	3D7	HeLa
*E. natalensis**	-	-	IC_{50} = 25.4 µg/mL	-
Compound **5.1**	13.9 ± 1.5	11.9 ± 0.2	64.6 ± 0.8	77.3 ± 1.2
Myricitrin (**5.2**)	18.9 ± 0.7	2.5 ± 0.6	77.9 ± 3.0	70.1 ± 2.4
Avicularin (**5.3)**	21.0 ± 2.7	5.8 ± 0.03	83.9 ± 2.7	77.2 ± 3.5
Guaijaverin (**5.4**)	19.1 ± 0.5	2.8 ± 0.1	68.4 ± 3.4	72.4 ± 5.4
Quercitrin (**5.5**)	16.2 ± 2.2	1.4 ± 0.1	66.8 ± 2.6	71.3 ± 4.5
Isoquercitrin (**5.6**)	18.4 ± 2.9	1.9 ± 0.6	58.7 ± 2.0	64.8 ± 2.2
Mixture of **5.4** and **5.5**	19.1 ± 1.0	6.4 ± 0.5	69.2 ± 2.6	70.8 ± 2.1
Chloroquine	-	-	IC_{50} = 0.014 µM	-
Emetine	-	-	-	IC_{50} = 0.04 µM

* Cytotoxicity against Vero cells, IC_{50} = 403.7 µg/mL

5.4. Conclusion

The leaf extract of *E. natalensis* displayed moderate antiplasmodial activity and was not cytotoxic against non-cancerous Vero cells. Purification of the active extract afforded six flavonoid glycosides and four common triterpenoids. The glycosides inhibited the viability of *P. falciparum* and were cytotoxic to cancerous HeLa cells, suggesting that the activity is not selective. However, the presence of the isolated compounds in the leaf extract of *E. natalensis*

could account for the antiplasmodial activity of the extract and explains the folkloric use of the plant in traditional medicine.

Acknowledgment

The authors are grateful to Ms Alison Young for assisting with the collection and identification of the plant material and preparation of voucher specimen. NT is grateful to the University of KwaZulu-Natal for the award of a doctoral scholarship. Antimalarial and HeLa cell cytotoxicity assays were supported by Rhodes University (Sandisa Imbewu grant) and the South African Medical Research Council. FRVH acknowledges the National Research Foundation (South Africa) Grant [number 98345] for financial support.

Conflict of interest

The authors declare that they have no conflict of interest.

References

1. Van Wyk, B. E.; Gericke, N., *People's Plants: a Guide to Useful Plants of Southern Africa*. Briza Publications: 2000.
2. Coates Palgrave, K., Drummond, R., *Trees of Southern Africa*. C. Struik Publishers, Cape Town: 1977.
3. Boon, R., *Pooley's Trees of Eastern South Africa a Complete Guide*. Flora and Fauna Publications Trust: 2010; p 468.
4. Hutchings, A., *Zulu Medicinal Plants: an Inventory*. University of Natal Press: 1996; p 232-233.
5. Kokwaro, J. O., *Medicinal Plants of East Africa*. East African Literature Bureau: 1976; p 84.
6. Jansen, P.; Mendes, O., *Plantas medicinais seu uso Tradicional em Mocambique. Tomo 2*. In Instituto Nacional do Licro e do Disco: 1988; p 120.
7. Ngarivhume, T.; van't Klooster, C. I. E. A.; de Jong, J. T. V. M.; Van der Westhuizen, J. H., Medicinal plants used by traditional healers for the treatment of malaria in the Chipinge district in Zimbabwe. *Journal of Ethnopharmacology* **2015,** 159, 224-237.
8. Clarkson, C.; Maharaj, V. J.; Crouch, N. R.; Grace, W. M.; Pillay, P.; Matsabisa, M. G.; Bhagwandin, N.; Smith, P. J.; Folb, P. I., In vitro antiplasmodial activity of medicinal

plants native to or naturalised in South Africa. *Journal of Ethnopharmacology* **2004,** 92, (2-3), 177-191.

9. Mokoka, T. A.; Xolani, P. K.; Zimmermann, S.; Hata, Y.; Adams, M.; Kaiser, M.; Moodley, N.; Maharaj, V.; Koorbanally, N. A.; Hamburger, M.; Brun, R.; Fouche, G., Antiprotozoal screening of 60 South African plants, and the identification of the antitrypanosomal germacranolides schkuhrin I and II. *Planta Medica* **2013,** 79, (14), 1380-1384.
10. Weigenand, O.; Hussein, A. A.; Lall, N.; Meyer, J. J. M., Antibacterial activity of naphthoquinones and triterpenoids from *Euclea natalensis* root bark. *Journal of Natural Products* **2004,** 67, (11), 1936-1938.
11. Lall, N.; Weiganand, O.; Hussein, A. A.; Meyer, J. J. M., Antifungal activity of naphthoquinones and triterpenes isolated from the root bark of *Euclea natalensis*. *South African Journal of Botany* **2006,** 72, (4), 579-583.
12. Lall, N.; Meyer, J. J. M.; Wang, Y.; Bapela, N. B.; van Rensburg, C. E. J.; Fourie, B.; Franzblau, S. G., Characterization of intracellular activity of antitubercular constituents from the roots of *Euclea natalensis*. *Pharmaceutical Biology* **2005,** 43, (4), 353-357.
13. Onegi, B.; Kraft, C.; Kohler, I.; Freund, M.; Jenett-Siems, K.; Siems, K.; Beyer, G.; Melzig, M. F.; Bienzle, U.; Eich, E., Herbal remedies traditionally used against malaria Part 6 - Antiplasmodial activity of napthoquinones and one anthraquinone from *Stereospermum kunthianum*. *Phytochemistry* **2002,** 60, (1), 39-44.
14. Likhitwitayawuid, K.; Kaewamatawong, R.; Ruangrungsi, N.; Krungkrai, J., Antimalarial naphthoquinones from *Nepenthes thorelii*. *Planta Medica* **1998,** 64, (3), 237-241.
15. Neuwinger, H. D., *African Traditional Medicine: A Dictionary of Plant Use and Applications. With Supplement: Search System for Diseases*. Medpharm: 2000; p 213.
16. Mosmann, T., Rapid colorimetric assay for cellular growth and survival - application to proliferation and cyto-toxicity assays. *Journal of Immunological Methods* **1983,** 65, (1-2), 55-63.
17. Madikizela, B.; Aderogba, M. A.; Van Staden, J., Isolation and characterization of antimicrobial constituents of *Searsia chirindensis* L. (Anacardiaceae) leaf extracts. *Journal of Ethnopharmacology* **2013,** 150, (2), 609-613.
18. Kadota, S.; Takamori, Y.; Nyein, K. N.; Kikuchi, T.; Tanaka, K.; Ekimoto, H., Constituents of the leaves of *Woodfordia fruticosa* Kurz .I. Isolation, structure, and proton and carbon-13 nuclear magnetic resonance signal assignments of woodfruticosin

(woodfordin-C), an inhibitor of deoxyribonucleic-acid topoisomerase-II. *Chemical & Pharmaceutical Bulletin* **1990,** 38, (10), 2687-2697.

19. Fossen, T.; Larsen, A.; Kiremirec, B. T.; Andersen, O. M., Flavonoids from blue flowers of *Nymphaea caerulea*. *Phytochemistry* **1999,** 51, (8), 1133-1137.
20. Houel, E.; Nardella, F.; Jullian, V.; Valentin, A.; Vonthron-Senecheau, C.; Villa, P.; Obrecht, A.; Kaiser, M.; Bourreau, E.; Odonne, G.; Fleury, M.; Bourdy, G.; Eparvier, V.; Deharo, E.; Stien, D., Wayanin and guaijaverin, two active metabolites found in a *Psidium acutangulum* Mart. ex DC (syn. *P. persoonii* McVaugh) (Myrtaceae) antimalarial decoction from the Wayana Amerindians. *Journal of Ethnopharmacology* **2016,** 187, 241-248.
21. Da Silva Sa, F. A.; Marciano de Paula, J. A.; dos Santos, P. A.; Ribeiro Oliveira, L. d. A.; Ribeiro Oliveira, G. d. A.; Liao, L. M.; de Paula, J. R.; Rodrigues Silva, M. d. R., Phytochemical analysis and antimicrobial activity of *Myrcia tomentosa* (Aubl.) DC. leaves. *Molecules* **2017,** 22, (7), 1100.
22. Lee, S.; Park, H.-S.; Notsu, Y.; Ban, H. S.; Kim, Y. P.; Ishihara, K.; Hirasawa, N.; Jung, S. H.; Lee, Y. S.; Lim, S. S.; Park, E.-H.; Shin, K. H.; Seyama, T.; Hong, J.; Ohuchi, K., Effects of hyperin, isoquercitrin and quercetin on lipopolysaccharide-induced nitrite production in rat peritoneal macrophages. *Phytotherapy Research* **2008,** 22, (11), 1552-1556.
23. Fernandez, J.; Reyes, R.; Ponce, H.; Oropeza, M.; VanCalsteren, M. R.; Jankowski, C.; Campos, M. G., Isoquercitrin from *Argemone platyceras* inhibits carbachol and leukotriene D-4-induced contraction in guinea-pig airways. *European Journal of Pharmacology* **2005,** 522, (1-3), 108-115.
24. Seebacher, W.; Simic, N.; Weis, R.; Saf, R.; Kunert, O., Complete assignments of ^{1}H and ^{13}C NMR resonances of oleanolic acid, 18α-oleanolic acid, ursolic acid and their 11-oxo derivatives. *Magnetic Resonance in Chemistry* **2003,** 41, (8), 636-638.
25. Dais, P.; Plessel, R.; Williamson, K.; Hatzakis, E., Complete H-1 and C-13 NMR assignment and P-31 NMR determination of pentacyclic triterpenic acids. *Analytical Methods* **2017,** 9, (6), 949-957.
26. Lee, J.; Kim, N. H.; Nam, J. W.; Lee, Y. M.; Jang, D. S.; Kim, Y. S.; Nam, S. H.; Seo, E.-K.; Yang, M. S.; Kim, J. S., Scopoletin from the flower buds of *Magnolia fargesii* inhibits

protein glycation, aldose reductase, and cataractogenesis ex vivo. *Archives of Pharmacal Research* **2010,** 33, (9), 1317-1323.

27. Santos, P. F. P.; Gomes, L. N. L. F.; Mazzei, J. L.; Fontao, A. P. A.; Sampaio, A. L. F.; Siani, A. C.; Valente, L. M. M., Polyphenol and triterpenoid constituents of *Eugenia orida* DC. (Myrtaceae) leaves and their antioxidant and cytotoxic potential. *Quimica Nova* **2018,** 41, (10), 1140-1149.
28. Burns, D.; Reynolds, W. F.; Buchanan, G.; Reese, P. B.; Enriquez, R. G., Assignment of H-1 and C-13 spectra and investigation of hindered side-chain rotation in lupeol derivatives. *Magnetic Resonance in Chemistry* **2000,** 38, (7), 488-493.
29. Mahato, S. B.; Kundu, A. P., C-13 nmr-spectra of pentacyclic triterpenoid - A compilation and some salient features. *Phytochemistry* **1994,** 37, (6), 1517-1575.
30. Talapatra, S. K.; Talapatra, B., Triterpenes (C 30). In *Chemistry of Plant Natural Products*, Springer: 2015; pp 517-552.
31. Miranda, R. R. S. d.; Silva, G. D. d. F.; Duarte, L. P.; Fortes, I. C. P.; Filho, S. V., Structural determination of 3β-stearyloxy-urs-12-ene from *Maytenus salicifolia* by 1D and 2D NMR and quantitative 13C NMR spectroscopy. *Magnetic Resonance in Chemistry* **2006,** 44, (2), 127-131.
32. Morita, M.; Shibuya, M.; Kushiro, T.; Masuda, K.; Ebizuka, Y., Molecular cloning and functional expression of triterpene synthases from pea (*Pisum sativum*) - New alpha-amyrin-producing enzyme is a multifunctional triterpene synthase. *European Journal of Biochemistry* **2000,** 267, (12), 3453-3460.
33. Pretorius, J. C.; Magama, S.; Zietsman, P. C., Purification and identification of antibacterial compounds from *Euclea crispa* subsp *crispa* (Ebenaceae) leaves. *South African Journal of Botany* **2003,** 69, (4), 579-586.
34. Dagne, E.; Alemua, M.; Sterner, O., Flavonoids from *Euclea divinorum*. *Bulletin of the Chemical Society of Ethiopia* **1993,** 7, (2), 87-92.
35. Orzalesi, G.; Mezzetti, T.; Rossi, C.; Bellavita, V., Pentacyclic triterpenoids from *Euclea kellau*. *Planta Medica* **1970,** 19, (1), 30-36.
36. Ganesh, D.; Fuehrer, H.-P.; Starzengrueber, P.; Swoboda, P.; Khan, W. A.; Reismann, J. A. B.; Mueller, M. S. K.; Chiba, P.; Noedl, H., Antiplasmodial activity of flavonol quercetin and its analogues in *Plasmodium falciparum*: evidence from clinical isolates

in Bangladesh and standardized parasite clones. *Parasitology Research* **2012,** 110, (6), 2289-2295.

37. Vargas, S.; Ioset, K. N.; Hay, A. E.; Ioset, J. R.; Wittlin, S.; Hostettmann, K., Screening medicinal plants for the detection of novel antimalarial products applying the inhibition of beta-hematin formation. *Journal of Pharmaceutical and Biomedical Analysis* **2011,** 56, (5), 880-886.

CHAPTER 6: Phytochemical and antiplasmodial studies of *Pappea capensis* (Eckl. & Zeyh.) leaves

Nasir Tajuddeen[a], Tarryn Swart[b], Heinrich C. Hoppe[b] and Fanie R. van Heerden[a]

[a]School of Chemistry and Physics, University of KwaZulu-Natal, Private Bag X01, Scottsville 3209, Pietermaritzburg, South Africa

[b]Department of Biochemistry & Microbiology, Rhodes University, Grahamstown 6140, South Africa

Formatted for ***Journal of Ethnopharmacology***

Abstract

Ethnopharmacological relevance: Results from the studies of plant-use by traditional healers indicate that the Masai and Kikuyu people in Kenya, the Venda people in South Africa, and the Gumuz people of Ethiopia use *Pappea capensis* for the treatment of malaria. Previous investigation also showed that the leaf extract of *P. capensis* inhibited the in vitro growth of *P. falciparum*.

Aim of the study: The present study aimed to investigate the phytochemical and antiplasmodial properties of *P. capensis* leaf extract.

Methods: The plant leaves were investigated for inhibitory activity against 3D7 *P. falciparum* using the parasite lactate dehydrogenase (pLDH) assay and cytotoxicity against Vero and HeLa cells using the MTT assay. The bioactive compounds were isolated using chromatographic techniques and the structures of the isolated were established using spectroscopic and spectrometric techniques.

Results: The leaf extract of *P. capensis* inhibited the viability of *P. falciparum* by more than 80% at 50 µg/mL, but it was also cytotoxic against HeLa cells at the same concentration. Chromatographic purification of the extract led to the isolation of four flavonoid glycosides and epicatechin. The compounds displayed similar activity pattern with the extract against *P. falciparum* and HeLa cells.

Conclusion: The results from this study suggest that the widespread use of *P. capensis* in traditional medicine for the treatment of malaria might have some merits. However, more

selectivity studies are needed to determine whether the leaf extract is cytotoxic against noncancerous cells.

Keywords: *Pappea capensis*, Sapindaceae, flavonoids, flavonoid glycosides, malaria, antiplasmodial

6.1. Introduction

Pappea capensis Eckl. & Zeyh. (Sapindaceae) is a small to medium-sized tree with a dense crown. It is the only species of the *Pappea* genus and is dominant in several types of sub-tropical thickets. The tree is endemic to Africa and is mostly found in open woodland, on the edge of riverine areas, on termite mounds, and among rocks.[1,2] The bark is smooth with a pale grey to brownish colour and the leaves vary in size, with those from arid areas being smaller than those from wetter climates. *P. capensis*, also known as the jacket-plum or wild-plum tree, produces pleasantly flavoured edible fruits, which can be made into a jelly, an alcoholic beverage, or vinegar. The seed oil with a golden yellow colour is edible, has a mild purgative effect, and is used topically against baldness and ringworm.[1,3] Zulu traditional healers use the bark and roots for medicinal purposes while unspecified parts are used medicinally for calves.[3] The Ndebele people use an infusion from the leaves for curing painful eyes and the root infusions are given to cattle as an enema or orally for purging.[1,3] The Swahili moisten the root bark with water and use it against chest problems. Masai warriors take a decoction or infusion from the bark as a blood tonic, aphrodisiac and to gain courage. The bark is used for the treatment of venereal diseases and as a protective charm in Botswana, and the leaf is used for nose bleeding.[3] The outcome from studies of medicinal plant-use by the Masai of Kenya,[4] Gumuz people of Mandura Woreda in Ethiopia[5] and the Kikuyus of Kenya[6] show that *P. capensis* is frequently used to treat malaria. In an informal interview with Venda people living in Mutale Municipality in Limpopo province, it was claimed that *P. capensis* is effective against malaria and related symptoms.[7] In previous biological studies, the extracts of *P. capensis* leaves, twigs and roots showed moderate antiplasmodial activity against NF54 *P. falciparum*[7,8] while the inner bark extract was not active against *P. falciparum* D6 strain.[4] The leaf extract of *P. capensis* was also shown to possess anti-inflammatory, anti-oxidant and antimicrobial activities.[9,10] Previous phytochemical investigation of the ethyl acetate leaf extract led to the isolation of epicatechin and quercitrin.[10] However, despite the widespread use of different

parts of *P. capensis* in the treatment of various diseases including malaria, the antiplasmodial activity of the plant leaves has not been investigated previously. Therefore, in search of antiplasmodial compounds from South African medicinal plants, the leaves of *P. capensis* was investigated for antiplasmodial activity and the presence of bioactive compounds.

6.2. Material and methods

6.2.1. General procedures

The same as section 3.2.1 in chapter 3

6.2.2. HPLC and HPLC conditions

HPLC experiment was performed on a Shimadzu LC-20AB Prominence liquid chromatograph equipped with a binary pump, an SPD-M20A Prominence diode-array detector, a SIL-20A Prominence autosampler, and a CBM-20A communications bus module. Analytical HPLC analysis was performed using a Phenomenex (00G-4252-B0) Luna column (5 µm, C18 (2), 100 Å, (250 x 4.6 mm)), the flow rate was 0.5 mL/min with isocratic elution at 23 °C and an injection volume of 10 µL. The mobile phase used was 40% methanol-acetonitrile (4:3) containing 0.1% formic acid (solvent B) and H_2O containing with 0.1% formic acid (solvent A). The sample solution (1 mg/mL) was filtered using a PVDF membrane with a pore size of 0.45 µm before injection. Semi-preparative HPLC was performed on a Phenomenex (00G-4252-N0) Luna column (5 µm C18 (2) 100 Å, (250 x 10 mm)), the flow rate was 2.1 mL/min with isocratic elution at 23 °C and an injection volume of 150 µL. The solvents used were 37% methanol-acetonitrile (4:3) containing 0.1% formic acid (solvent B) and H_2O containing 0.1% formic acid (solvent A). Before injection, the sample solutions (10 mg/mL) were filtered using a PVDF membrane with a pore size of 0.45 µm. HPLC grade acetonitrile and methanol were used and the detector was set to read wavelengths from 230-750 nm.

6.2.3. Plant material and preparation of extract for bioassay

The leaves of *P. capensis* were collected from the University of KwaZulu-Natal (UKZN) botanical gardens Pietermaritzburg Campus, in March 2019. The leaves were identified by Ms Alison Young, the curator at the University of KwaZulu-Natal (UKZN) botanical gardens. A voucher specimen was prepared and deposited at the Bews herbarium, UKZN School of life Sciences where it was assigned an accession number, (NU0087106). The leaves were air-dried

at room temperature in the laboratory and crushed to a coarse powder using a hammer mill. The powdered plant material was weighed and stored in paper bags in a ventilated environment.

For the biological assays, the powdered plant leaves (50 g) was extracted by cold maceration with constant stirring in 500 mL of dichloromethane-methanol (1:1, v/v) for 72 hours. The extract was filtered and concentrated under reduced pressure using a rotary evaporator to give a green solid mass. A portion of the crude extract (50 mg) was dissolved in minimal amount of methanol, loaded on a polyamide (1.0 g) packed column and eluted three times with methanol (6 mL each). The eluates were combined, evaporated to dryness, weighed, and stored in a refrigerator until needed for the assay.

6.2.4. Isolation of compounds from the leaves of *P. capensis*

The powdered leaves of *P. capensis* (950 g) were extracted as described in section 6.2.3, but without passing through a polyamide column. From the resulting crude extract, 40.0 g was subjected to VLC using 200 g of silica and 800 mL each of five solvent systems, including hexanes-dichloromethane (9:1), dichloromethane-ethyl acetate (20:1), 100% ethyl acetate, ethyl acetate-methanol (5:1), and 100% methanol to give five fractions (A-E). Fractions A (324.8 mg) and B (5.0 g) were composed of fatty material and pigments respectively, and were ignored. Fraction C (5.2 g) was chromatographed over silica gel packed column and eluted with gradients of dichloromethane-ethyl acetate (8:2, 1:1, 2:8) and ethyl acetate-methanol (8:2) before finally washing the column with 100% methanol, to afford four subfractions (sb-Fr1-4) by pooling together eluates with similar TLC profiles. Sb-fr1-3 mostly composed of pigments and oils, and were ignored. Silica gel column chromatography of sb-fr4 (1.2 g) by isocratic elution with hexanes-ethyl acetate (1:3) afforded epicatechin (**6.1**) (128.7 mg) and a yellow residue (550 mg) which was further purified over silica gel column followed by chromatography over Sephadex LH-20 to afford quercetin 3-*O*-arabinopyranoside (**6.2**) (33.2 mg), and a yellow residue (120 mg) with one major and two other minor spots on TLC. Attempts to separate the yellow residue using silica gel and Sephadex LH-20 chromatography were not successful. Further semipreparative HPLC purification of the yellow residue by isocratic elution over 60 minutes using 37% methanol-acetonitrile (4:3, 0.1% formic acid) and 63% H_2O (0.1% formic acid) at a flow rate of 2.1 mL/min gave quercetin 3-*O*-β-D-glucoside

(**6.5**) (0.9 mg), quercetin 3-*O*-arabinopyranoside (**6.2**), quercetin 3-*O*-α-L-rhamnoside (**6.3**) (1.2 mg) and kaempferol 3-*O*-arabinopyranoside (**6.4**) (0.9 mg). Fractions D (15.15 g) and E (11.8 g) contained a sticky grey solid mass that dissolved only in water, but was insoluble in methanol, ethyl acetate, and chloroform, and so was not further investigated.

6.2.5. Spectroscopic and physical data of compounds

Epicatechin (**6.1**): brown powder, $[\alpha]_D^{29}$ -42.12 (*c*=1.2, MeOH), ^{1}H NMR (500 MHz, CD_3OD): δ_H 6.98 (1H, d, *J*=2.0 Hz, H-2'), 6.80 (1H, dd, *J*=8.3, 2.0 Hz, H-6'), 6.76 (1H, d, *J*=8.3 Hz, H-5'), 5.95 (1H, d, *J*=2.3 Hz, H-8), 5.93 (1H, d, *J*=2.3 Hz, H-6), 4.82 (1H, m, H-2), 4.18 (1H, m, H-3), 2.86 (1H, dd, *J*=16.6, 4.5 Hz, H-4a), 2.74 (1H, dd, *J*=16.8, 2.8 Hz, H-4b). ^{13}C NMR (125 MHz, CD_3OD): δ_C 157.9 (C-5), 157.6 (C-7), 157.3 (C-9), 145.9 (C-3'), 145.7 (C-4'), 132.2 (C-1'), 119.4 (C-6'), 115.9 (C-5'), 115.3 (C-2'), 100.1 (C-10), 96.4 (C-6), 95.9 (C-8), 79.8 (C-2), 67.4 (C-3), 29.2 (C-4). HR-ESI-(-)-MS: *m/z* 289.0705 $[M-H]^-$ (Calculated for $C_{15}H_{13}O_6$, 289.0712).

Quercetin 3-*O*-α-L-arabinopyranoside (guaijaverin) (**6.2**): yellow solid, $[\alpha]_D^{29}$ -54.07 (*c*=0.5, MeOH), UV (MeOH/ACN): λ_{max} 255, 355 nm; ^{1}H NMR (400 MHz, CD_3OD) δ_H 7.74 (1H, d, *J*=2.1 Hz, H-2'), 7.57 (1H, dd, *J*=8.5, 2.1 Hz, H-6'), 6.88 (1H, d, *J*=8.3 Hz, H-5'), 6.39 (1H, d, *J*=1.9 Hz, H-8), 6.20 (1H, d, *J*=1.9 Hz, H-6), 5.16 (1H. d, *J*=6.5 Hz, H-1''), 3.90 (1H, dd, *J*=8.4, 6.5 Hz, H-2''), 3.81-3.84 (2H, m, H-4'',5''), 3.65 (1H, dd, *J*=8.4, 3.1 Hz, H-3''), 3.44 (1H, m, H-5''). ^{13}C NMR (100 MHz, CD_3OD) δ_C 179.5 (C-4), 166.1 (C-7), 163.0 (C-5), 158.7 (C-2), 158.5 (C-9), 150.0 (C-4'), 146.0 (C-3'), 135.6 (C-3), 123.1 (C-1'), 122.9 (C-6'), 117.5 (C-2'), 116.2 (C-5'), 105.6 (C-10), 104.7 (C-1''), 100.0 (C-6), 94.8 (C-8), 74.1 (C-3''), 72.9 (C-2''), 69.1 (C-4''), 66.9 (C-5''). HPLC R_t: 25.334 min; HR-ESI-(-)-MS: *m/z* 433.0775 $[M-H]^-$ (Calculated for $C_{20}H_{17}O_{11}$, 433.0771).

Quercetin 3-*O*-α-L-rhamnoside (quercitrin) (**6.3**): yellow solid, $[\alpha]_D^{29}$ -136.93 (*c*=1.1, MeOH), UV (MeOH/ACN): λ_{max} 255, 350 nm; ^{1}H NMR (400 MHz, CD_3OD): δ_H 7.34 (1H, d, *J*=2.0 Hz, H-2'), 7.30 (1H, dd, *J*=8.5, 2.0 Hz, H-6'), 6.87 (1H, d, *J*=8.5 Hz, H-5'), 6.36 (1H, d, *J*=2.0 Hz, H-8), 6.19 (1H, d, *J*=2.0 Hz, H-6), 5.35 (1H, d, *J*=1.2 Hz, H-1''), 4.22 (1H, dd, *J*=3.2, 1.7 Hz, H-2''), 3.75 (1H, dd, *J*=9.2, 3.2 Hz, H-3''), 3.45 (1H, m, H-5''), 3.34 (1H, d, *J*=9.4 Hz, H-4''), 0.94 (3H, d, *J*=6.2 Hz, H-6''). ^{13}C NMR (100 MHz, CD_3OD): δ_C 179.6 (C-4), 165.9 (C-7), 163.2 (C-5), 159.3 (C-2), 158.5 (C-9), 149.8 (C-3'), 146.4 (C-4'), 136.2 (C-3), 123.0 (C-1'), 122.9 (C-6'), 117.0 (C-2'), 116.4 (C-5'), 105.9 (C-10), 103.5 (C-1''), 99.8 (C6-), 94.8 (C-8), 73.3 (C-4''), 72.1 (C-3''), 72.0 (C-2''),

71.9 (C-5''), 17.7 (C-6''). HPLC R_t: 29.504 min; HR-ESI-(-)-MS: *m/z* 433.0779 $[M-H]^-$ (Calculated for $C_{21}H_{19}O11$, 447.0927).

Kaempferol 3-*O*-α-L-arabinopyranoside (juglalin) (**6.4**): yellow solid, UV (MeOH/ACN): λ_{max} 265, 347 nm; ^1H NMR (500 MHz, CD_3OD): δ_H 8.06 (2H, d, *J*=8.0 Hz, H-2',6'), 6.89 (2H, d, *J*= 8.0 Hz, H-3',5'), 6.41 (1H, brs, H-8), 6.21 (1H, brs, H-6), 5.13 (1H, d, *J*=5.6 Hz, H-1''), 3.89 (1H, t, *J*=6.7, H-2''), 3.79-3.76 (1H, brs, H-4'',5a''), 3.63 (1H, brs, H-3''), 3.40 (1H, d, *J*=11.2 Hz, H-5b''). ^{13}C NMR (125 MHz, CD_3OD): δ_C 179.6 (C-4), 166.2 (C-7), 163.1 (C-5), 161.6 (C-4'), 158.9 (C-2), 158.5 (C-9), 135.6 (C-3), 132.3 (C-2',6'), 122.7 (C-1'), 116.3 (C-3',5'), 105.6 (C-10), 104.4 (C-1''), 100.0 (C-6), 94.8 (C-8), 74.0 (C-3''), 72.7 (C-2''), 68.9 (C-4''), 66.7 (C-5''). HPLC R_t: 34.737 min; HR-ESI-(-)-MS: *m/z* 417.0829 $[M-H]^-$ (Calculated for $C_{20}H_{17}O_{10}$, 417.0822).

Quercetin 3-*O*-β-D-glucoside (isoquercitrin) (**6.5**): yellow solid, $[\alpha]_D^{29}$ -32.70 (*c*=0.18, MeOH), UV (MeOH/ACN): λ_{max} 255, 355 nm; ^1H NMR (500 MHz, CD_3OD): δ_H 7.70 (1H, d, *J*=2.1 Hz, H-2'), 7.59 (1H, dd, *J*=8.5, 2.1 Hz, H-6'), 6.87 (1H, d, *J*=8.5 Hz, H-5'), 6.4 (1H, brs, H-8), 6.21 (1H, d, *J*=2.0 Hz, H-6), 5.24 (1H, d, *J*=7.6 Hz, H-1''), 3.71-3.42 (undefined sugar protons). ^{13}C NMR (500 MHz, CD_3OD): δ_C 179.6 (C-4), 166.4 (C-7), 161.6 (C-5), 158.6 (C-2), 158.2 (C-9), 150.4 (C-4'), 145.7 (C-3'), 135.2 (C-3), 122.6 (C-6'), 121.9 (C-1'), 117.4 (C-2'), 116.0 (C-5'), 105.8 (C-10), 105.2 (C-1''), 100.1 (C-6), 94.4 (C-8), 77.7 (C-5''), 75.5 (C-3''), 71.0 (C-2''), 70.0 (C-4''), 62.0 (C-6''). HPLC R_t: 20.216 min; HR-ESI-(-)-MS: *m/z* 463.0881 $[M-H]^-$ (Calculated for $C_{21}H_{19}O_{12}$, 463.0877).

6.2.6. Antimalarial assay

6.2.6.1. The parasites

The same as section 3.2.5.1 in chapter 3

6.2.6.2. Assessment of in vitro antiplasmodial activity

The same as section 3.2.5.2 in chapter 3

6.2.6.3. In vitro cytotoxicity assay

The same as section 3.2.5.3 in chapter 3

6.3. Results and discussion

6.3.1 Chemistry

Investigation of the dichloromethane-methanol (1:1) extract of the leaves of *P. capensis* resulted in the isolation of five known flavonoids, of which four are glycosides. The compounds were identified by analysing the spectroscopic data (compiled in Appendix D) and comparison with literature data. The structures of the isolated compounds are presented in **Fig. 6.1**

Compound **6.1** was isolated as a brown solid and assigned a molecular formula of $C_{15}H_{14}O_6$ based on pseudo-molecular ion $[M-H]^-$ at *m/z* 289.0705 (calculated for $C_{15}H_{13}O_6$ 289.0712) observed in the HR-ESI-(-)-MS (**Plate 6.1**). The five aromatic signals in the ^{1}H NMR spectrum (**Plate 6.2**) of compound **6.1** were assigned to an AMX-type ring B [δ_H 6.98 (1H, d, *J*=2.0 Hz, H-2'), 6.80 (1H, dd, *J*=8.3, 2.0 Hz, H-6'), 6.76 (1H, d, *J*=8.3 Hz, H-5')] and an AB-type ring A [δ_H 5.95 (1H, d, *J*=2.3 Hz, H-8), 5.93 (1H, d, *J*=2.3 Hz, H-6)]. The ^{1}H NMR spectrum also showed signals for two oxymethines at δ_H 4.82 (1H, m, H-2) and 4.18 (1H, m, H-3), and two methylene protons at δ_H 2.86 (1H, dd, *J*=16.6, 4.5 Hz, H-4a) and δ_C 2.74 (1H, dd, *J*=16.8, 2.8 Hz, H-4b), indicating that **6.1** has a flavan-3-ol nucleus. This was supported by the ^{13}C and DEPT NMR spectra (**Plate 6.3**) which showed 15 carbon resonances including a methylene at δ_C 29.2 (C-4), two oxymethines at δ_C 79.8 (C-2), 67.4 (C-3) and 12 aromatic carbons (δ_C 157.9-95.9), of which five are oxygenated. The small values of $J_{3,4\beta}$ (4.5 Hz) and $J_{3,4\alpha}$ (2.8 Hz) observed in the ^{1}H NMR spectrum suggest that **6.1** is epicatechin. The appearance of three signals around δ_C 157 in the ^{13}C spectrum of **6.1** is characteristic of C-5, C-7 and C-9 of epicatechin. All the protonated carbons were assigned based on HSQC cross-peaks (**Plate 6.4**) and the quaternary carbons were assigned by analysis of the HMBC spectrum (**Plate 6.5**). Comparing the NMR data of **6.1** with the literature data for epicatechin (**6.1**) confirmed the structure (**Fig. 6.1**).[11,12]

Compound **6.2**, obtained as a yellow powder, showed a pseudo-molecular ion peak $[M-H]^-$ at *m/z* 433.0767 (Calculated for $C_{20}H_{17}O_{11}$ 433.0771) in the HR-ESI-(-)-MS (**Plate 6.6**), suggesting a molecular formula of $C_{20}H_{18}O_{11}$. The aromatic region of the ^{1}H NMR spectrum (**Plate 6.7**) of **6.2** displayed signals for an AMX spin system at δ_H 7.74 (1H, d, *J*=2.1 Hz, H-2'), 7.57 (1H, dd, *J*=8.5, 2.1 Hz, H-6'), and δ_H 6.88 (1H, d, *J*=8.3 Hz, H-5') and an AX spin system at δ_H 6.39 (1H, d, *J*=1.9 Hz, H-8), 6.20 (1H, d, *J*=1.9 Hz, H-6), as found in a derivative of quercetin. This

deduction was supported by the ^{13}C and DEPT (**Plate 6.8**) spectra which showed 15 carbon resonances including a carbonyl at δ_C 179.9 and seven oxygenated carbon resonances (δ_C 166.1-135.6), assignable to a quercetin nucleus. The observed HMBC (**Plate 6.9**) correlations between δ_H 6.20 and δ_C 163.0 (H-6/C-5), δ_H 6.20 and δ_C 105.6 (H-6/C-10), δ_H 6.39 and δ_C 158.5 (H-8/C-9), δ_H 7.74, 7.57 and δ_C 158.7 (H-2',6'/C-2), δ_H 7.74, 6.88 and δ_C 146.0 (H-2',5'/C-3'), and δ_H 7.74, 7.57, 6.88 and δ_C 150.0 (H-2',6',5'/C-4'), facilitated the assignment of the quaternary carbons. The ^1H NMR spectrum of **6.2** also showed signals for an anomeric doublet at δ_H 5.16 (1H, d, J=6.5 Hz, H-1''), three oxymethine and two oxymethylene resonances between δ_H 3.44 and 3.9 ppm, suggesting the presence of a pentose sugar. This deduction was supported by the appearance of an anomeric carbon at δ_C 104.7, three oxymethine carbons at δ_C 69.1-74.1 and an oxymethylene carbon at δ_C 66.9. The relatively large coupling constants of the sugar protons indicate that the sugar is a pyranose. The anomeric proton with a 1,2-diaxial coupling (*J*=6.4 Hz) was assigned to a sugar moiety in a β-linkage with the flavonoid aglycone. The attachment of the sugar unit to position 3 of the aglycone was confirmed by the HMBC correlation of the anomeric proton resonating at δ_H 5.16 (H-1'') with δ_C 135.6 (C-3) of the flavonoid. All the protonated carbons of compound **6.2** were assigned based on HSQC (**Plate 6.10**) cross-peaks. The sugar NMR data closely match those of an arabinopyranoside, and a comparison of the NMR data of compound **6.2** with those reported in the literature for quercetin 3-*O*-α-L-arabinopyranoside (**6.2**) (**Fig. 6.1**) showed good agreement, thus confirming the structure.[13,14]

Compound **6.3** was also isolated as a yellow powder. The molecular formula was established to be $C_{21}H_{20}O_{11}$ based on a pseudo-molecular ion $[M-H]^-$ at *m/z* 433.0779 (calculated for $C_{21}H_{19}O_{11}$ 447.0927) observed in the HR-ESI-(-)-MS (**Plate 6.11**). The NMR data (**Plate 6.12-6.15**) of **6.3** revealed signals consistent with the presence of a quercetin derivative similar to compound **6.2** above. Also, a doublet at δ_H 5.35 (1H, d, *J*=1.2 Hz, H-1''), four oxymethines between δ_H 4.22 and 3.34 and a methyl doublet at δ_H 0.94 (3H, d, *J*=6.2 Hz, H-6'') suggested the presence of a rhamnose sugar moiety. The HMBC cross peak observed between the anomeric proton and δ_C 136.2 (C-3) confirmed the attachment of the rhamnosyl unit to position 3 of the quercetin nucleus. The structure of **6.3** was confirmed to be quercetin 3-*O*-α-L-rhamnoside (**6.3**) (**Fig. 6.1**) after comparing its spectroscopic data with published literature data for quercetin 3-*O*-α-L-rhamnoside.[15]

Compound **6.4** was assigned a molecular formula of $C_{20}H_{18}O_{10}$ based on pseudo-molecular ion peak $[M-H]^-$ at *m/z* 417.0829 (calculated for $C_{20}H_{17}O_{10}$ 417.0822) observed in the HR-ESI-(-)-MS (**Plate 6.16**). The ^1H NMR spectrum (**Plate 6.17**) of compound **6.4** showed resonances for a 1,4-disubstituted benzene ring with an AA'XX' spin system at [δ_H 8.06 (2H, d, *J*=8.0 Hz, H-2',6'), 6.89 (2H, d, *J*=8.0 Hz, H-3',5')], and another benzene ring possessing an AX spin system at δ_H 6.41 (1H, brs, H-8) and δ_H 6.21 (1H, brs, H-6), consistent with a kaempferol derivative. The ^{13}C and DEPT spectra (**Plate 6.18**) which revealed 13 resonances assignable to a kaempferol nucleus, including a carbonyl at δ_C 179.6 (C-4) and six oxygenated quaternary carbons at δ_C 166.2-135.6, supported the presence of a kaempferol nucleus. The quaternary carbons were unambiguously assigned based on HMBC cross-peaks (**Plate 6.19**). The sugar region of compound **6.4** was similar to that of **6.2**, indicating that the sugar was arabinopyranoside. The attachment of the sugar unit at position 3 of the flavonoid nucleus was deduced from the upfield shift in the ^{13}C NMR spectrum of the signal of C-3 by 1.0 ppm and the accompanying downfield shift (so-called *ortho*-effect) of *ortho*-related C-2 by 12.1 ppm.[16,17] The structure of compound **6.4** was assigned as kaempferol 3-*O*-α-L-arabinopyranoside (**6.4**) (**Fig. 6.1**) after comparison of the NMR data with those reported in the literature for kaempferol 3-*O*-α-L-arabinopyranoside showed close agreement.[18,19]

Compound **6.5** which was isolated as a yellow solid, was assigned a molecular formula of $C_{21}H_{20}O_{12}$ based on a pseudo-molecular ion $[M-H]^-$ at *m/z* 463.0881 (Calculated for $C_{21}H_{19}O_{12}$ 463.0877) observed in the HR-ESI-(-)-MS (**Plate 6.21**). The NMR data (**Plate 6.22-6.25**) of **6.5** showed resonances consistent with a quercetin derivative. The presence of a sugar unit was indicated by the anomeric doublet at δ_H 5.24 (1H, d, *J*=7.6 Hz, H-1''). The other sugar protons between δ_H 3.71-3.42 appeared as a complex multiplet and were assigned to glucopyranose. This deduction was supported by the ^{13}C NMR signals at δ_C 105.2 and between δ_C 77.7 and 62.0 which are characteristic of glucose. The attachment of the sugar to position 3 of the flavonoid aglycone was established by the HMBC correlation between δ_H 5.24 (H-1'') and δ_C 135.2 (C-3). Therefore, the structure of **6.5** was assigned as quercetin 3-*O*-β-D-glucoside (**6.5**) (**Fig.6.1**), and this was confirmed after comparison of the NMR data with literature data.[20,21]

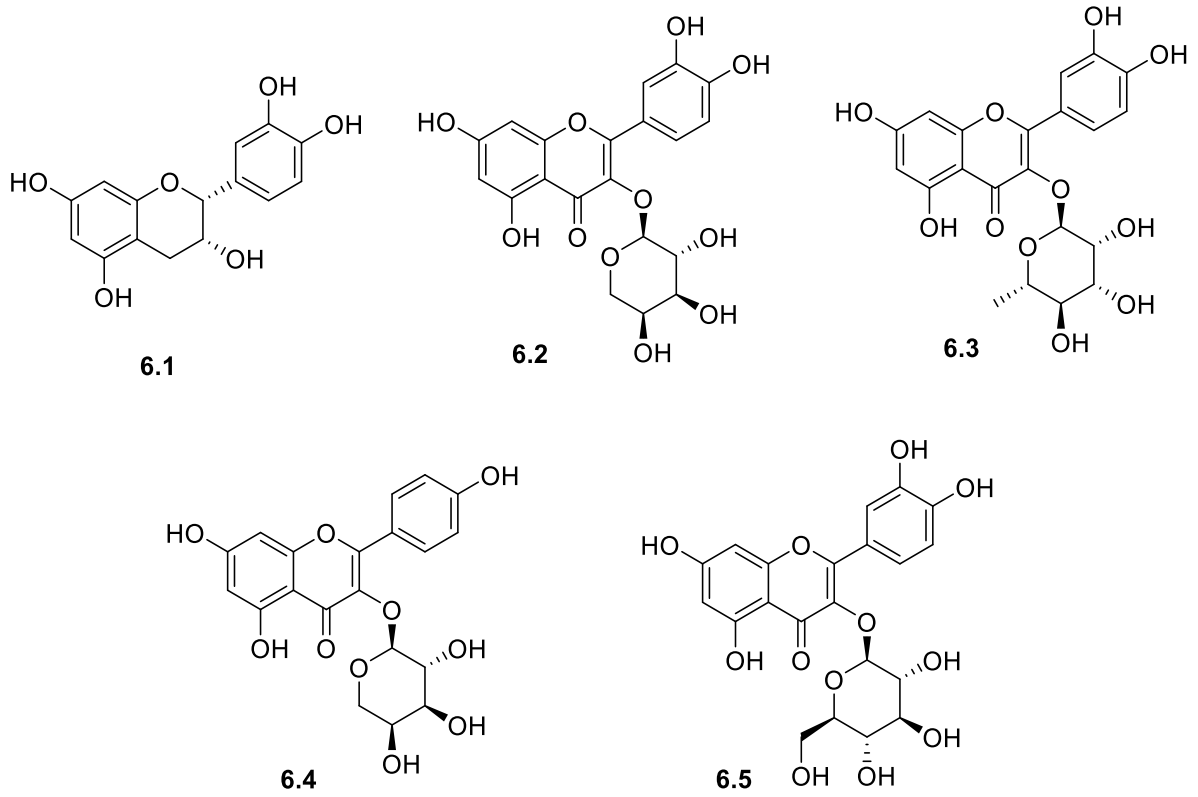

Fig. 6.1: Structures of the isolated compounds from *P. capensis*

P. capensis is the only species in the genus *Pappea*. Epicatechin (**6.1**) and quercitrin were previously isolated from the plant leaves.[10] This is the first report of the isolation of quercetin 3-*O*-arabinopyranoside (**6.2**), kaempferol 3-*O*-arabinopyranoside (**6.4**) and quercetin 3-*O*-β-D-glucoside (**6.5**) from the plant leaves. Chemosystematics of the Sapindaceae shows that the family is rich in flavonoids.[22,23] The leaves of plants belonging to the Sapindaceae have been reported to contain flavones, flavonols, including *O*- and *C*-glycosides, and proanthocyanidins.[22,24] In this study, four of the isolated flavonoids from the leaves of *P. capensis* are flavonol *O*-glucosides, whereas epicatechin is a monomer of some proanthocyanidin.

6.3.2. Biological activity

The in vitro antiplasmodial activity of the leaf extract of *P. capensis* and the isolated flavonoid glycosides are presented in **Table 6.1**. The extract and isolated compounds inhibited the viability of *P. falciparum* by more than 80% at 50 µg/mL. However, there was a significant drop in antiplasmodial activity at a lower concentration of 10 µg/mL. None of the isolated compounds or extract showed 50% inhibition of *P. falciparum* at 10 µg/mL. The extract and

compounds were also evaluated for cytotoxicity against HeLa cells. The pattern of antiproliferative activity against HeLa cells was similar to the antiplasmodial activity, indicating that the activity was not selective. The antiplasmodial activity of flavonoids and flavonoid glycosides has been discussed in chapters 3, 4 and 5.

Table 6.1: In vitro antiplasmodial and cytotoxic activity of the extract and isolated compounds

Compound	Viability% ±SD (50 µg/mL)		Viability% ±SD (10 µg/mL)	
	3D7	HeLa	3D7	HeLa
P. capensis	12.1 ± 0.2	1.9 ± 0.2	93.1 ± 3.8	71.4 ± 6.1
Compound **6.4**	18.1 ± 1.0	3.1 ± 0.1	83.1 ± 3.5	70.9 ± 3.7
Compound **6.2**	19.1 ± 0.5	2.8 ± 0.1	68.4 ± 3.4	72.4 ± 5.4
Compound **6.3**	16.2 ± 2.2	1.4 ± 0.1	66.8 ± 2.6	71.3 ± 4.5
Compound **6.5**	18.4 ± 2.9	1.9 ± 0.6	58.7 ± 1.9	64.8 ± 2.2
Chloroquine	-	-	IC_{50} = 0.014 µM	-
Emetine	-	-	-	IC_{50} = 0.04 µM

6.4. Conclusion

The leaf extract of *P. capensis* displayed antiplasmodial activity against *P. falciparum* at a concentration at which it was also cytotoxic to cancerous HeLa cells. Investigation of the extract afforded four flavonoid glycosides for the first time. The glycosides showed similar activity to the extract. However, the reported use of *P. capensis* leaves in traditional medicine suggests that there might be some other compounds present in the extract that act to mitigate the cytotoxicity.

Acknowledgment

The authors are grateful to Dr Christina Potgieter of Bews Herbarium, School of Life Sciences, University of KwaZulu-Natal for helping with the preparation of plant voucher specimens and Ms. Alison young for identifying the plant material. NT is grateful to the University of KwaZulu-Natal for the award of a doctoral scholarship. FRVH acknowledges the National Research Foundation (South Africa) Grant [number 98345] for financial support. Antimalarial and cytotoxicity evaluations were supported by Rhodes University (Sandisa Imbewu grant) and the South African Medical Research Council.

Conflict of interest

The authors declare that they have no conflict of interest.

References

1. Coates Palgrave, K., Drummond, R., *Trees of Southern Africa*. C. Struik Publishers, Cape Town: 2002; p 652.
2. Cowling, R.; Proches, S.; Vlok, J. H. J., On the origin of southern African subtropical thicket vegetation. *South African Journal of Botany* **2005,** 71, (1), 1-23.
3. Hutchings, A., *Zulu Medicinal Plants: an Inventory*. University of Natal Press: 1996; p 189.
4. Koch, A.; Tamez, P.; Pezzuto, J.; Soejarto, D., Evaluation of plants used for antimalarial treatment by the Maasai of Kenya. *Journal of Ethnopharmacology* **2005,** 101, (1-3), 95-99.
5. Asnake, S.; Teklehaymanot, T.; Hymete, A.; Erko, B.; Giday, M., Antimalarial medicinal plants used by Gumuz people of Mandura Woreda, Benishangul-Gumuz Regional State, Ethiopia. *Indian Journal of Traditional Knowledge* **2016,** 15, (4), 546-552.
6. Njoroge, G. N.; Bussmann, R. W., Diversity and utilization of antimalarial ethnophytotherapeutic remedies among the Kikuyus (Central Kenya). *Journal of Ethnobiology and Ethnomedicine* **2006,** 2.
7. Bapela, M. J.; Meyer, J. J. M.; Kaiser, M., In vitro antiplasmodial screening of ethnopharmacologically selected South African plant species used for the treatment of malaria. *Journal of Ethnopharmacology* **2014,** 156, 370-373.
8. Mokoka, T. A.; Xolani, P. K.; Zimmermann, S.; Hata, Y.; Adams, M.; Kaiser, M.; Moodley, N.; Maharaj, V.; Koorbanally, N. A.; Hamburger, M.; Brun, R.; Fouche, G., Antiprotozoal screening of 60 South African plants, and the identification of the antitrypanosomal germacranolides schkuhrin I and II. *Planta Medica* **2013,** 79, (14), 1380-1384.
9. Mulaudzi, R. B.; Ndhlala, A. R.; Kulkarni, M. G.; Finnie, J. F.; Van Staden, J., Anti-inflammatory and mutagenic evaluation of medicinal plants used by Venda people against venereal and related diseases. *Journal of Ethnopharmacology* **2013,** 146, (1), 173-179.

10. Pendota, S. C.; Aderogba, M. A.; Moyo, M.; McGaw, L. J.; Mulaudzi, R. B.; Van Staden, J., Antimicrobial, antioxidant and cytotoxicity of isolated compounds from leaves of *Pappea capensis*. *South African Journal of Botany* **2017,** 108, 272-277.
11. Davis, A. L.; Cai, Y.; Davies, A. P.; Lewis, J. R., H-1 and C-13 NMR assignments of some green tea polyphenols. *Magnetic Resonance in Chemistry* **1996,** 34, (11), 887-890.
12. Tajuddeen, N.; Sallau, M. S.; Musa, A. M.; Yahaya, S. M.; Habila, J. D.; Ismail, A. M., A novel antimicrobial flavonoid from the stem bark of *Commiphora pedunculata* (Kotschy & Peyr.) Engl. *Natural Product Research* **2016,** 30, (10), 1109-1115.
13. Houel, E.; Nardella, F.; Jullian, V.; Valentin, A.; Vonthron-Senecheau, C.; Villa, P.; Obrecht, A.; Kaiser, M.; Bourreau, E.; Odonne, G.; Fleury, M.; Bourdy, G.; Eparvier, V.; Deharo, E.; Stien, D., Wayanin and guaijaverin, two active metabolites found in a *Psidium acutangulum* Mart. ex DC (syn. *P. persoonii* McVaugh) (Myrtaceae) antimalarial decoction from the Wayana Amerindians. *Journal of Ethnopharmacology* **2016,** 187, 241-248.
14. Da Silva Sa, F. A.; Marciano de Paula, J. A.; dos Santos, P. A.; Ribeiro Oliveira, L. d. A.; Ribeiro Oliveira, G. d. A.; Liao, L. M.; de Paula, J. R.; Rodrigues Silva, M. d. R., Phytochemical analysis and antimicrobial activity of *Myrcia tomentosa* (Aubl.) DC. leaves. *Molecules* **2017,** 22, (7), 1100.
15. Fossen, T.; Larsen, A.; Kiremirec, B. T.; Andersen, O. M., Flavonoids from blue flowers of *Nymphaea caerulea*. *Phytochemistry* **1999,** 51, (8), 1133-1137.
16. Markham, K. R.; Ternai, B., C-13 nmr of flavonoids .2. Flavonoids other then flavone and flavonol aglycones. *Tetrahedron* **1976,** 32, (21), 2607-2612.
17. Markham, K. R.; Ternai, B.; Stanley, R.; Geiger, H.; Mabry, T. J., C-13 NMR-studies of flavonoids .3. Naturally occurring flavonoid glycosides and their acylated derivatives. *Tetrahedron* **1978,** 34, (9), 1389-1397.
18. Kim, S.-J.; Cho, J.-Y.; Wee, J.-H.; Jang, M.-Y.; Kim, C.; Rim, Y.-S.; Shin, S.-C.; Ma, S.-J.; Moon, J.-H.; Park, K.-H., Isolation and characterization of antioxidative compounds from the aerial parts of *Angelica keiskei*. *Food Science and Biotechnology* **2005,** 14, (1), 58-63.
19. Vasange, M.; Liu, B. L.; Welch, C. J.; Rolfsen, W. C.; Bohlin, L., The flavonoid constituents of two *Polypodium* species (Calaguala) and their effect on the elastase release in human neutrophils. *Planta Medica* **1997,** 63, (6), 511-517.

20. Lee, S.; Park, H.-S.; Notsu, Y.; Ban, H. S.; Kim, Y. P.; Ishihara, K.; Hirasawa, N.; Jung, S. H.; Lee, Y. S.; Lim, S. S.; Park, E.-H.; Shin, K. H.; Seyama, T.; Hong, J.; Ohuchi, K., Effects of hyperin, isoquercitrin and quercetin on lipopolysaccharide-induced nitrite production in rat peritoneal macrophages. *Phytotherapy Research* **2008,** 22, (11), 1552-1556.

21. Fernandez, J.; Reyes, R.; Ponce, H.; Oropeza, M.; VanCalsteren, M. R.; Jankowski, C.; Campos, M. G., Isoquercitrin from *Argemone platyceras* inhibits carbachol and leukotriene D-4-induced contraction in guinea-pig airways. *European Journal of Pharmacology* **2005,** 522, (1-3), 108-115.

22. Umadevi, I.; Daniel, M., Chemosystematics of the Sapindaceae. *Feddes Repertorium* **1991,** 102, (7-8), 607-612.

23. Silva, F. L.; Moreno, P. R. H.; Braz-Filho, R.; Tavares, J. F.; Barbosa-Filho, J. M., Chemical constituents of *Cardiospermum corindum* L. and their distribution in Sapindaceae. *Biochemical Systematics and Ecology* **2014,** 57, 137-140.

24. Lima Cardoso, C. A.; Coelho, R. G.; Honda, N. K.; Pott, A.; Pavan, F. R.; Fujimura Leite, C. Q., Phenolic compounds and antioxidant, antimicrobial and antimycobacterial activities of *Serjania erecta* Radlk. (Sapindaceae). *Brazilian Journal of Pharmaceutical Sciences* **2013,** 49, (4), 775-782.

CHAPTER 7: Phytochemical and antiplasmodial investigation of *Gardenia thunbergia* L.f. leaves

Nasir Tajuddeen[a], Tarryn Swart[b], Heinrich C. Hoppe[b] and Fanie R. van Heerden[a]

[a]School of Chemistry and Physics, University of KwaZulu-Natal, Private Bag X01, Scottsville 3209, Pietermaritzburg, South Africa

[b]Department of Biochemistry & Microbiology, Rhodes University, Grahamstown 6140, South Africa

Formatted for ***Journal of Ethnopharmacology***

Abstract

Ethnopharmacological relevance: In a survey among traditional healers in KwaZulu-Natal, South Africa, *Gardenia thunbergia* L.f. was listed as a treatment for malaria.

Aim of study: Although preliminary results in the literature indicated that the methanol extract from *G. thunbergia* has antiplasmodial activity, the chemical constituents in the plant have not been identified. Therefore, this project aimed to investigate the phytochemical and antiplasmodial properties of *G. thunbergia*.

Methods: The plant leaf extract and isolated compounds were investigated for inhibitory activity against 3D7 *P. falciparum* using the parasite lactate dehydrogenase (pLDH) assay and cytotoxicity against HeLa cells using the resazurin assay. The bioactive compounds were isolated using chromatographic techniques, and the structures of the isolated compounds were established using spectroscopic and spectrometric techniques.

Results: The methanol leaf extract of *G. thunbergia* inhibited *P. falciparum* at 50 µg/mL (>80% inhibition) and was not cytotoxic against HeLa cells. Chromatographic purification of the extracts led to the isolation of nine compounds including a new triterpenoid saponin and two known flavonoid glycosides. The saponin and flavonoid glycosides displayed non-selective antiplasmodial activity at 50 µg/mL, but the activities were diminished at 10 µg/mL.

Conclusion: A new saponin has been isolated from *G. thunbergia*. The presence of the isolated compounds in the leaf extract of *G. thunbergia* could account for the folkloric use of the plant in treating malaria.

Keywords: Malaria, antiplasmodial, *Gardenia thunbergia*, Rubiaceae, saponin, flavonoid glycosides, traditional medicine

7.1. Introduction

Gardenia thunbergia L. f. is a small tree or shrub that grows in coastal thickets and evergreen forests.[1] It belongs to the Rubiaceae, an angiosperm family that consists of approximately 637 genera and 13,000 species, making it the fourth-largest family in terms of diversity among the angiosperms.[2,3] The family is reputed for producing diverse bioactive molecules including anthraquinones, di- and triterpenoids, iridoids, indole alkaloids, flavonoids, and other phenolic derivatives.[3] These phytochemicals have been documented to have important biological and pharmacological properties. The presence of these bioactive compounds could be responsible for the widespread use of the Rubiaceae plants in the treatment of a variety of diseases in traditional medicine. Some famous genera of the Rubiaceae include the South American *Cinchona,* also called the quinine tree, and *Coffea*. Quinine, the first antimalarial drug, was isolated from the bark of a *Cinchona* species. Coffee made from roasted *Coffea Arabica* L. or *Coffea robusta* L. Linden beans is one of the most widely consumed beverages. In South Africa, the Rubiacaea is the largest tree family[1] and several species belonging to the family are used in traditional medicine. One of these speciesis *G. thunbergia*, which is found in a strip along the east coast of South Africa from the north of KwaZulu-Natal to near Grahamstown in the Eastern Cape. The Zulu people in South Africa prepare emetics from the root and root bark against fever and stomach upsets.[4,5] In some other parts of Africa, the roots are widely used as a remedy for leprosy-induced skin lesions. The leaf and root infusions are used for treating syphilis while the latex is taken as a purgative.[5] A survey showed that traditional healers in KwaZulu-Natal use *G. thunbergia* for the treatment of malaria.[6] The methanol extract of *G. thunbergia* (plant part not given) was previously reported to inhibit the in vitro growth of D10 *P. falciparum* (IC_{50}=4.36 µg/ml) and was not cytotoxic against cancerous and noncancerous cells.[6] However, the chemical constituents of *G. thunbergia* have not been previously reported. In search of antiplasmodial compounds from South African medicinal plants, we investigated the phytochemical and antiplasmodial properties of *G. thunbergia* leaves and report here for the first time the isolation of bioactive compounds from the leaf extract.

7.2. Material and methods

7.2.1. General procedures

The same as section 3.2.1 in chapter 3.

7.2.2. Plant material and preparation of extracts for bioassays

The leaves of *Gardenia thunbergia* L. f. were collected from the University of KwaZulu-Natal (UKZN) botanical gardens, Pietermaritzburg Campus in January 2018. The plant was identified by Ms Alison Young, the curator at the University of KwaZulu-Natal (UKZN) botanical gardens. A voucher specimen was prepared and deposited at the Bews herbarium, UKZN School of life Sciences where it was assigned an accession number, (*G. thunbergia* NU0080890). The leaves were air-dried at room temperature in the laboratory and crushed to a coarse powder using a hammer mill. The powdered plant material was weighed and stored in paper bags in a ventilated environment.

For the bioassays, the powdered plant leaves (50 g) were extracted by maceration with constant stirring in 500 mL of dichloromethane-methanol (1:1, v/v) for 72 hours. The extract was filtered and concentrated under reduced pressure using a rotary evaporator to give a green solid mass which was weighed and stored in a refrigerator until needed for the assay. Similarly, the plant leaf (50 g) was extracted with 100% methanol (500 mL). The extract was filtered and concentrated under reduced pressure using a rotary evaporator to give a green solid mass. A portion of the crude extract (50 mg) was dissolved in a minimal amount of methanol, loaded on a column packed with polyamide (1.0 g) and eluted three times with methanol (6 mL each). The eluates were combined, evaporated to dryness, weighed, and stored in a refrigerator until needed for the assay.

7.2.3. Isolation of compounds from *G. thunbergia* leaves

The powdered leaves of *G. thunbergia* (900 g) were extracted as described in section 7.2.3.2. The resulting crude extract (57.3 g) was suspended in 10% methanol and successively partitioned with hexanes, dichloromethane, and ethyl acetate to give three fractions. The dichloromethane fraction (2.0 g) was chromatographed over silica gel and eluted with a gradient of hexanes-ethyl acetate (8:2, 7:3, 3:7, 100% ethyl acetate) and 100% methanol to give 46 fractions that were pooled together into four subfractions (sb-FrA-D), based on the

TLC profiles. Silica gel column chromatography of sb-FrA (135 mg) using gradient mixtures of hexanes-ethyl acetate gave lupeol (**7.7**) (5.9 mg) and a mixture of β-sitosterol (**7.8**) and stigmasterol (**7.9**) (5.4 mg). Purification of sb-FrC (56 mg) by centrifugal thin-layer chromatography on a Chromatotron™ afforded scopoletin (**7.6**) (4.5 mg), and loliolide (**7.4**) and (*3S,5R,6S,7E*)-5,6-epoxy-3-hydroxymegastigman-7-en-9-one (**7.5**) as a (1:1) mixture (11.3 mg). The ethyl acetate fraction (2.2 g) was chromatographed on a silica gel column eluting with a gradient of chloroform-ethyl acetate (8:2, 6:4, 1:9), ethyl acetate-methanol (9:1, 7:3, 1:1), and finally 100% methanol to give 57 fractions which were pooled together, based on the similarity in the TLC profiles, into four subfraction (sb-Fr1-4). Purification of sb-Fr2 (35 mg) over Sephadex LH-20 eluted with methanol gave kaempferol 3-*O*-β-D-glucoside (**7.2**) (8.5 mg) and quercetin 3-*O*-β-D-glucoside (**7.3**) (3.6 mg). Repeated Sephadex LH-20 chromatography of sb-Fr3 (150 mg) eluted with methanol gave 3-*O*-[α-L-rhamnopyranosyl-(1→2)-β-D-glucopyranosyl] oleanolic acid 28-*O*-β-D-glucopyranosyl ester (**7.1**) (11.7 mg).

7.2.4. Spectroscopic and physical data of compounds

3-*O*-[α-Rhamnopyranosyl-(1→2)-β-glucopyranosyl]oleanolic acid 28-*O*-β-glucopyranosyl ester (**7.1**): White solid, $[\alpha]_D^{29}$ -39.57 (*c*=0.21, MeOH), ^{1}H NMR (500 MHz, CD_3OD): δ_H 5.38 (1H, d, *J*=8.2 Hz, H-1 Glc B), 5.25 (1H, t, *J*=3.5, H-12), 5.18 (1H, d, *J*=1.4 Hz, H-1 Rham), 4.36 (1H, d, *J*=7.9 Hz, H-1 Glc A), 4.11 (dd, *J*=9.5, 6.2 Hz, H-5 Rham), 3.93 (dd, *J*=1.6, 3.1 Hz, H-2 Rham), 3.72 (dd, *J*=3.4, 9.5 Hz, H-3 Rham), 3.36 (m, H-4 Rham), 3.33-3.82 (overlapped glucosyl protons), 3.17 (1H, d, *J*=10.8 Hz, H-3), 2.85 (1H, dd, *J*=13.8, 3.9 Hz, H-18), 2.05 (1H, m, H-16b), 1.94-1.28 (overlapped aglycone CH_2 and CH signals), 1.24 (3H, d, *J*=6.2 Hz, H-6 Rham), 1.15 (3H, s, H-27), 1.05 (3H, s, H-23), 0.94 (3H, s, H-25), 0.93 (3H, s, H-30), 0.91 (3H, s, H-29), 0.84 (3H, s, H-24), 0.80 (3H, s, H-26). ^{13}C NMR (125 MHz, CD_3OD): δ_C 178.2 (C-28), 144.9 (C-13), 123.8 (C-14), 106.5 (C-1 Glc A), 102.4 (C-1 Rham), 95.7 (C-1 Glc B), 90.7 (C-3), 83.6 (C-2, Glc A), 78.7 (C-5 Glc B), 78.3 (C-5 Glc A), 76.1 (C-3 Glc B), 74.2 (C-4 Glc B), 73.9 (C-4 Rham), 72.3 (C-2 Rham), 72.5 (C-4 Glc A) 72.4 (C-3 Rham), 71.4 (C-3 Glc A), 71.2 (C-2 Glc B), 69.8 (C-5 Rham), 65.1 (C-6 Glc A), 62.4 (C-6 Glc B), 57.0 (C-5), 49.1 (C-9), 48.1 (C-17), 47.2 (C-19), 42.9 (C-14), 42.6 (C-18), 40.7 (C-8), 40.1 (C-4), 39.8 (C-1), 37.9 (C-10), 34.9 (C-21), 33.9 (C-7), 33.5 (C-29), 33.1 (C-22), 31.5 (C-20), 28.9 (C-15), 28.6 (C-23), 26.9 (C-2), 26.3 (C-27), 24.6 (C-11), 24.0 (C-16), 23.9 (C-30), 19.3 (C-6), 17.9 (C-6 Rham), 17.7 (C-26), 17.0 (C-24), 16.0 (C-25).

Kaempferol 3-*O*-β-D-glucoside (astragalin) (**7.2**): yellow solid, $[\alpha]_D^{29}$ -12.92 (*c*=0.375, MeOH), ^{1}H NMR (400 MHz, CD_3OD): δ_H 8.08 (2H, d, *J*=8.8 Hz, H-2',6'), 6.88 (2H, d, *J*= 8.8 Hz, H-3',5'), 6.40 (1H, d, *J*=2.1 Hz, H-8), 6.20 (1H, d, *J*=2.1 Hz, H-6), 5.13 (1H, d, *J*=7.8 Hz, H-1''), 3.82 (1H, d, *J*=2.9 Hz, H-4''), 3.78 (1H, dd, *J*=10.0, 7.8 Hz, H-2''), 3.62 (1H, dd, *J*=11.4, 6.0 Hz, H-6''), 3.53 (1H, dd, *J*=8.0, 4.8 Hz, H-3''), 3.49 (1H, m, H-6''), 3.43 (1H, t, J= 7.2 Hz, H-5''). ^{13}C NMR (100 MHz, CD_3OD): δ_C 179.7 (C-4), 166.3 (C-7), 163.1 (C-5), 161.6 (C-4'), 159.1 (C-2), 158.6 (C-9), 135.6 (C-3), 132.4 (C-2',6'), 122.7 (C-1'), 116.1 (C-3',5'), 105.6 (C-10), 105.1 (C-1''), 100.0 (C-6), 94.8 (C-8), 77.1 (C-5''), 75.0 (C-3''), 73.0 (C-2''), 70.0 (C-4''),62.0 (C-6''). HR-ESI-(+)-MS *m/z* 474.1083 $[M+Na]^+$ (Calculated for $C_{21}{}^1H_{17}{}^2H_3O_{11}Na$, 474.1092)

Quercetin 3-*O*-β-D-glucoside (**7.3**): yellow solid, $[\alpha]_D^{29}$ -32.70 (*c*=0.18, MeOH), ^{1}H NMR (500 MHz, CD_3OD): δ_H 7.84 (1H, d, *J*=2.2 Hz, H-2'), 7.59 (1H, dd, *J*=8.5, 2.2 Hz, H-6'), 6.86 (1H, d, *J*=8.5 Hz, H-5'), 6.39 (1H, d, *J*=2.1 Hz, H-8), 6.19 (1H, d, *J*=2.1 Hz, H-6), 5.14 (1H, d, *J*=7.8 Hz, H-1''), 3.82 (1H, d, *J*=2.9 Hz, H-4''), 3.78 (1H, dd, *J*=10.0, 7.8 Hz, H-2''), 3.62 (1H, dd, *J*=11.1, 6.0 Hz, H-6''), 3.53 (1H, dd, *J*=8.0, 4.8 Hz, H-3''), 3.49 (1H, m, H-6''), 3.43 (1H, t, J= 7.2 Hz, H-5''). ^{13}C NMR (100 MHz, CD_3OD): δ_C 179.6 (C-4), 166.6 (C-7), 163.2 (C-5), 158.8 (C-2), 158.5 (C-9), 149.9 (C-4'), 145.8 (C-3'), 135.7 (C-3), 122.9 (C-6'), 122.9 (C-1'), 117.8 (C-2'), 116.1 (C-5'), 105.8 (C-10), 105.5 (C-1''), 100.1 (C-6), 94.9 (C-8), 77.2 (C-5''), 75.1 (C-3''), 73.2 (C-2''), 70.0 (C-4''), 61.9 (C-6''). HR-ESI-(-)-MS *m/z* 463.0881 $[M-H]^-$ (Calculated for $C_{21}H_{19}O_{12}$, 463.0877).

Loliolide (**7.4**): ^{1}H NMR (400 MHz, CD_3OD): δ_H 5.74 (1H, s, H-7), 4.21 (1H, m, *J*=6.9, 3.6 Hz, H-3), 2.42 (1H, dt, *J*=13.8, 2.5 Hz, H-4a), 1.98 (1H, dt, *J*=14.4, 2.4 Hz, H-2a), 1.78 (1H, dd, *J*=13.0, 2.5 Hz, H-4b), 1.76 (3H, s, H-11), 1.53 (1H, dd, *J*=14.4, 3.7 Hz, H-2b), 1.46 (3H, s, H-9), 1.27 (3H, s, H-10). ^{13}C NMR (100 MHz, CD_3OD): δ_C 185.7 (C-8), 174.4 (C-6), 113.3 (C-7), 88.9 (C-5), 67.2 (C-3), 47.6 (C-2), 46.4 (C-4), 37.1 (C-1), 31.0 (C-10), 27.4 (C-11), 27.0 (C-9). HR-ESI-(+)-MS *m/z* 219.0998 $[M+Na]^+$ (Calculated for $C_{11}H_{16}O_3Na$, 219.0997).

(*3S,5R,6S,7E*)-5,6-Epoxy-3-hydroxymegastigman-7-en-9-one (**7.5**): ^{1}H NMR (400 MHz, CD_3OD): δ_H 7.16 (1H, d, *J*=15.4 Hz, H-7), 6.18 (1H, d, *J*=15.4 Hz, H-8), 3.77 (1H, m, H-3), 2.29 (1H, m, H-4a), 2.28 (3H, s, H-10), 1.66 (1H, dd, *J*=14.4, 9.1 Hz, H-4b), 1.58 (1H, dd, *J*=12.8, 5.1 Hz, H-2a), 1.29 (1H, m, H-2b), 1.19 (3H, s, H-13), 1.17 (3H, s, H-11), 0.96 (3H, s, H-12). ^{13}C NMR (100 MHz, CD_3OD): δ_C 200.2 (C-9), 145.3 (C-7), 133.8 (C-8), 70.8 (C-6), 68.7 (C-5), 64.3 (C-3), 48.0 (C-2), 41.3 (C-4), 36.1 (C-1), 30.7 (C-11), 29.7 (C-10), 25.1 (C-12), 20.0 (C-13)

Scopoletin (**7.6**): white solid, ^{1}H NMR (500 MHz, $CDCl_3$): δ_H 7.59 (1H, d, *J*=9.4 Hz, H-4), 6.9 (1H, s, H-5), 6.8 (1H, s, H-8), 6.27 (1H, d, *J*=9.4 Hz, H-3), 6.11 (1H, s, H-OH), 3.95 (3H, s, H-OCH_3). ^{13}C NMR (125 MHz, $CDCl_3$): δ_C 161.6 (C-2), 150.5 (C-9), 149.8 (C-7), 143.4 (C-4,6), 113.7 (C-3), 111.6 (C-10), 107.7 (C-5), 103.4 (C-8), 56.6 (OCH_3-6). HR-ESI-(-)-MS *m/z* 191.0346 $[M-H]^-$ (Calculated for $C_{10}H_8O_4$, 191.0344).

Lupeol (**7.7**)**:** white solid ^{1}H NMR (500 MHz, $CDCl_3$): δ_H 4.68 (1H, d, *J*=2.3 Hz, H-29b), 4.56 (1H, dd, *J*=2.3, 1.3 Hz, H-29a), 3.18 (1H, dd, *J*=11.4, 4.8 Hz, H-3), 2.38 (1H, m, H-19), 1.92 (1H, m, H-21b), 1.68 (3H, s, H-30), 1.65-1.05 (overlapped signals), 1.03 (3H, s, H-26), 0.97 (3H, s, H-23), 0.94 (3H, s, H-27), 0.83 (3H, s, H-25), 0.79 (3H, s, H-28), 0.76 (3H, s, H-24), 068 (1H, d, *J*=9.3 Hz, H-5). ^{13}C NMR (125 MHz, $CDCl_3$): δ_C 150.9 (C-20), 109.3 (C-29), 79.0 (C-3), 55.3 (C-5), 50.5 (C-9), 48.4 (C-18), 48.0 (C-19), 43.0 (C-17), 42.9 (C-14), 40.9 (C-8), 40.0 (C-22), 38.9 (C-4), 38.7 (C-1), 38.1 (C-13), 37.2 (C-10), 35.6 (C-16), 34.3 (C-7), 29.9 (C-21), 28.0 (C-23), 27.5 (C-15), 27.4 (C-2), 25.2 (C-12), 21.0 (C-11), 19.3 (C-30), 18.3 (C-6), 18.0 (C-28), 16.1 (C-25), 16.0 (C-26), 15.4 (C-24), 14.6 (C-27). GCMS R_t: 26.92 min. EIMS: 189 (40%), 205 (50%), 218 (100%), 424 (40%, M^+).

β-Sitosterol (**7.8**): white solid, ^{1}H NMR (400 MHz, $CDCl_3$): δ_H 5.35 (d, *J*=4.9 Hz, H-6), 3.52 (m, H-3), 2.35-0.6 (overlapped signals), 1.00 (s, H-19), 0.92 (d, *J*=6.5 Hz, H-21), 0.82 (t, *J*=7.2 Hz, H-29), 0.80 (d, *J*=7.0 Hz, H-26, 27), 0.68 (s, H-18). ^{13}C NMR (100 MHz, $CDCl_3$): δ_C 140.8 (C-5), 121.7 (C-6), 71.8 (C-3), 56.9 (C-14), 56.1 (C-17), 50.2 (C-9), 45.9 (C-24), 42.3 (C-4, 13), 39.8 (C-12), 37.3 (C-1), 36.5 (C-10), 36.2 (C-20), 34.0 (C-22), 31.9 (C-7, 8), 31.7 (C-2), 29.2 (C-25), 28.2 (C-16), 26.1 (C-23), 24.3 (C-15), 23.1 (C-28), 21.1 (C-11), 19.8 (C-26), 19.4 (C-19), 19.0 (C-27), 18.8 (C-21), 12.2 (C-29), 11.9 (C-18). GCMS R_t: 26.19 min. EIMS: 255 (50%), 273 (40%), 303 (60%), 329 (70%), 381 (50%), 396 (60%), 414 (80%, M^+).

Stigmasterol (**7.9**): white solid, ^{1}H NMR (400 MHz, $CDCl_3$): δ_H 5.35 (d, *J*=4.9 Hz, H-6), 5.15 (dd, *J*=8.3, 15.0 Hz, H-22), 5.02 (dd, *J*=8.3, 15.0 Hz, H-23), 3.52 (m, H-3), 2.35-0.6 (overlapped signals), 1.00 (s, H-19), 0.92 (d, *J*=6.5 Hz, H-21), 0.82 (t, *J*=7.2 Hz, H-29), 0.80 (d, *J*=7.0 Hz, H-26, 27), 0.68 (s, H-18). ^{13}C NMR (100 MHz, $CDCl_3$): δ_C 140.8 (C-5), 138.3 (C-22), 129.3 (C-23), 121.7 (C-6), 71.8 (C-3), 56.8 (C-14), 56.0 (C-17), 51.2 (C-24), 50.2 (C-9), 42.3 (C-4, 13), 40.5 (C-20), 39.7 (C-12), 37.3 (C-1), 36.5 (C-10), 31.9 (C-7, 8, 25), 31.7 (C-2), 28.9 (C-16), 25.4 (C-28), 24.4 (C-15), 21.2 (C-26), 21.1 (C-11, 21), 19.4 (C-19), 19.0 (C-27), 12.2 (C-29), 12.1 (C-18).

GCMS R_t: 25.48 min. EIMS: 213 (30%), 255 (60%), 271 (50%), 314 (20%), 351 (30%), 369 (20%), 394 (10%), 412 (60%, M^+).

7.2.5. Antimalarial assay

7.2.5.1. The parasites

The same as section 3.2.5.1 in chapter 3

7.2.5.2. Assessment of in vitro antiplasmodial activity

The same as section 3.2.5.2 in chapter 3.

7.2.5.3. In vitro cytotoxicity assay

The same as section 3.2.5.3 in chapter 3.

7.3. Results and discussion

Investigation of the dichloromethane-methanol (1:1, v/v) extract of the leaves of *G. thunbergia* afforded nine compounds, including a saponin, and two flavonoid glycosides. The structures of the compounds were assigned by analysing the spectroscopic data (Appendix E) and comparison with published literature data.

7.3.1 Chemistry

The structures of the isolated compounds are presented in **Fig. 7.1**.

Compound **7.1** was obtained as a white solid. The NMR data (**Plate 7.1-7.5**) revealed resonances characteristic of a pentacyclic triterpenoid derivative, with seven tertiary methyl protons at δ_H 1.15 (3H, s, H-27), 1.05 (3H, s, H-23), 0.94 (3H, s, H-25), 0.93 (3H, s, H-30), 0.91 (3H, s, H-29), 0.84 (3H, s, H-24), and δ_H 0.80 (3H, s, H-26), and corresponding ^{13}C resonances at δ_C 33.5 (C-29), 28.6 (C-23), 26.3 (C-27), 23.9 (C-30), 17.7 (C-26), 17.0 (C-24), and δ_H 16.0 (C-25). These resonances, and an olefinic proton resonance at δ_H 5.25 (1H, t, *J*=3.5, H-12) with associated ^{13}C signals at δ_C 144.9 (C-13), δ_C 123.8 (C-14), an oxymethine proton at δ_H 3.17 (1H, dd, *J*=10.8 Hz, H-3), and a ^{13}C signal for a carboxylic acid group at δ_C 178.2 (C-28) suggested the presence of an oleanolic acid derivative.[7] The NMR data of **7.1** further revealed three anomeric proton resonances at δ_H 5.38 (1H, d, *J*=8.2 Hz, H-1 Glc B), δ_H 5.18 (1H, d, *J*=1.4 Hz, H-1 Rham), δ_H 4.36 (1H, d, *J*=7.9 Hz, H-1 Glc A) and a resonance for a methyl doublet at δ_H

1.24 (3H, d, *J*=6.2 Hz, Rham-CH_3), and the associated carbon resonances at δ_C 106.5 (C-1 Glc A), δ_C 102.6 (C-1 Rham), δ_C 95.7 (C-1 Glc B) and δ_C 17.9 (C-6 Rham), indicating the presence of three sugar units. The anomeric doublet with a small *J* value (1.4 Hz) and methyl doublet were assigned to a rhamnosyl unit. The other rhamnosyl signals were successfully assigned by analysis of the COSY and HSQC spectra**.** The presence of two oxymethylene carbon signals at δ_C 65.1 and 62.6 suggested the presence of two hexose sugars**.** The two anomeric proton doublets with the large *J* values (> 7 Hz) indicating diaxial coupling of H-1 and H-2, were assigned to two β-linked glucosyl units. The other glucosyl proton signals were overlapped and could not be differentiated in the COSY spectra. However, the identities of the two sugars were confirmed as glucosyl by comparison of the ^{13}C NMR resonances with those reported in the literature for a glucosyl moiety.[8,9] The connectivities of the sugar units were assigned based on COSY and HMBC correlations, and comparison of chemical shift values with the literature. The attachment of a glucosyl unit to C-28 was established from the HMBC correlation between anomeric proton resonating at δ_H 5.38 (1H, d, H-1 Glc B) and δ_C 178.2 (C-28). The HMBC correlation between δ_H 5.17 (1H, d, H-1 Rham) and a downfield oxymethine signal at 83.6 (C-2 Glc A) suggested that the rhamnosyl unit was attached to C-2 of the second glucosyl unit to give a disaccharide (α-rhamnopyranosyl (1→2)-β-glucopyranosyl). The disaccharide was confirmed by comparison of the ^{13}C signals with those reported in the literature for similar disaccharides with a (1→2) linkage.[8,9] The significant downfield shift in the signal for the oxygenated methine carbon at C-3 to δ_C 90.7 (instead of δ_C 78.2 in oleanolic acid) suggested the attachment of the disaccharide unit at C-3 and was confirmed by the HMBC correlations between δ_H 4.36 (1H, d, H-1 Glc A) and δ_C 90.7 (C-3), and δ_H 3.17 (1H, d, H-3) and δ_C 106.5 (C-1 Glc A). A comparison of the NMR data of **7.1** with those reported in the literature for other oleanolic acid triglycosides showed good agreement with 3-*O*-[α-L-rhamnopyranosyl-(1→4)-β-D-glucopyranosyl]oleanolic acid 28-*O*-β-D-glucopyranosyl ester.[10] The points of difference were the chemical shift for the rhamnosyl anomeric protons (δ_H 4.86 for literature compound and δ_H 5.17 for compound **7.1**, and the carbon atom to which the rhamnosyl anomeric protons were attached based on HMBC correlation (δ_C 79.56 for literature compound and 83.6 for compound **7.1**. Based on this evidence, the structure of

compound **7.1** was established to be 3-*O*-[α-L-rhamnopyranosyl-(1→2)-β-D-glucopyranosyl]oleanolic acid 28-*O*-β-D-glucopyranosyl ester (**Fig. 7.1**), a new natural product.

Compound **7.2** was isolated as a yellow amorphous solid and assigned a molecular formula of $C_{21}H_{20}O_{11}$ based on a pseudo-molecular ion $[M+Na]^+$ at *m/z* 474.1083 (Calculated for $C_{21}{}^1H_{17}{}^2H_3O_{11}Na$, 474.1092) observed in the HR-ESI-(+)-MS (**Plate 7.6**). The ^1H NMR spectrum (**Plate 7.7**) revealed resonances characteristic of a disubstituted benzene ring with an AA'XX' spin pattern at δ_H 8.08 (2H, d, *J*=8.8 Hz, H-2',6') and δ_H 6.88 (2H, d, *J*= 8.8 Hz, H-3',5'), and another ring with an AX-type spin system at δ_H 6.40 (1H, d, *J*=2.1 Hz, H-8) and δ_H 6.20 (1H, d, *J*=2.1 Hz, H-6), consistent with a kaempferol derivative. This deduction was supported by the ^{13}C and DEPT spectra (**Plate 7.8**) which revealed the presence of a carbonyl at δ_C 179.7 (C-4) in addition to 12 other carbon resonances, of which six are oxygenated between δ_C 94.8 and δ_C 166.3. The ^1H NMR also showed resonances for an anomeric doublet at δ_H 5.13 (1H, d, *J*=7.8 Hz, H-1''), four oxymethines with *J* values >7 Hz suggesting axial couplings at δ_H 3.82 to 3.43 and two oxymethylenes at δ_H 3.62 (1H, dd, *J*=11.4, 6.0 Hz, H-6'') and δ_H 3.49 (1H, m, H-6''). The corresponding sugar carbon resonances appeared between δ_C 77.1 and 62.0. These sugar resonances suggest the presence of a glucosyl moiety. The protonated and quaternary carbons were assigned based on HSQC (**Plate 7.9**) and HMBC (**Plate 7.10**) correlations. The attachment of the sugar unit to C-3 of the aglycone was established based on the HMBC correlation of δ_H 5.13 (1H, d, *J*=7.8 Hz, H-1'') with δ_H 135.6 (C-3). Based on the above analyses and after comparing the NMR data of **7.2** with the literature,[11,12] the structure was confirmed to be kaempferol 3-*O*-β-D-glucoside (**7.2**) (**Fig. 7.1**).

Compound **7.3** which was obtained as a yellow solid, showed a pseudo-molecular ion $[M-H]^-$ at *m/z* 463.0881 (Calculated for $C_{21}H_{19}O_{22}$ 463.0877) in the HR-ESI-(-)-MS (**Plate 7.11**), suggesting a molecular formula of $C_{21}H_{20}O_{12}$. The NMR spectra (**Plate 7.12-15**) of **7.3** showed resonances consistent with the presence of a quercetin aglycone. Also, the sugar region of the NMR spectra was similar to that of compound **7.2**, suggesting the presence of a glucosyl moiety. The attachment of the sugar to C-3 was confirmed by the HMBC correlation of the anomeric proton resonance at δ_H 5.14 (H-1'') with a carbon signal at δ_C 135.7 (C-3). After comparing the NMR data with the literature,[13,14] the structure of compound **7.3** was confirmed to be quercetin 3-*O*-β-D-glucoside (**7.3**) (**Fig. 7.1**).

Compound **7.4** was isolated as an amorphous solid mixture with **7.5** and analysis of the NMR spectra allowed unambiguous identification of the two compounds. Compound **7.4** was assigned a molecular formula of $C_{11}H_{16}O_3$ based on a pseudo-molecular ion $[M+Na]^+$ at *m/z* 219.0998 (calculated for $C_{11}H_{16}O_3Na$ 219.0997) in the HR-ESI-(+)-MS (**Plate 7.16**). The ^1H NMR spectrum (**Plate 7.17**) of **7.4** showed signals for a singlet olefinic proton at δ_H 5.75 (1H, s, H-7), an oxymethine multiplet at δ_H 4.21 (1H, m, *J*=6.9, 3.6 Hz, H-3), two sets of methylene protons at δ_H 2.42 (1H, dt, *J*=13.8, 2.5 Hz, H-4), 1.78 (1H, dd, *J*=13.0, 2.5 Hz, H-4) and δ_H 1.98 (1H, dt, *J*=14.4, 2.4 Hz, H-2), 1.53 (1H, dd, *J*=14.4, 3.7 Hz, H-2) and three tertiary methyl signals at δ_H 1.76 (3H, s, H-11), 1.46 (3H, s, H-9) and δ_H 1.27 (3H, s, H-10). The ^{13}C and DEPT spectra (**Plate 7.18**) revealed 11 carbon signals, including a lactone carbonyl at δ_C 185.7 (C-8), two olefinic carbons (δ_C 174.4 and 113.3), and an oxymethine carbon at δ_C 67.2. The remaining carbon signals could be assigned to two quaternary carbons (δ_C 88.9 and δ_C 37.1) of which one is oxygenated, two methylene carbons and three methyl carbons. All the protonated carbons were assigned by analyszing the HSQC spectrum (**Plate 7.19**). The COSY (**Plate 7.20**) correlations between δ_H 4.21 (H-3) and δ_H 2.42/1.76 (H-4), and δ_H 4.21 and δ_H 1.98/1.53 (H-2) indicated that the protons are within the same spin system and suggested the presence of a cyclohexane ring. The presence of a second ring fused to the cyclohexane ring was indicated by the singlet nature of the olefinic proton, which showed HMBC (**Plate 7.21**) correlation with the carbonyl and the quaternary carbon at δ_C 88.9, thus establishing a five-membered lactone ring. The relative configuration of the C-3 hydroxy was determined to be equatorial, based on the diaxial coupling patterns of H-2 ($J_{ax,ax}$=14.7 Hz) and H-4 ($J_{ax,ax}$=13.7 Hz) with H-3. The NMR data of **7.4** is consistent with the structure of loliolide, and a comparison with literature showed close agreement.[15,16] Therefore, the structure of the compound was assigned as loliolide (**7.4**) (**Fig. 7.1**).

The ^1H NMR spectrum (**Plate 7.17**) of **7.5** showed a pair of *trans*-coupled olefinic doublets at δ_H 7.16 (1H, d, *J*=15.4 Hz, H-7) and δ_H 6.18 (1H, d, *J*=15.4 Hz, H-8), an oxymethine multiplet at δ_H 3.77 (1H, m, H-3), and a set of methylene pairs at δ_H 2.29 (1H, m, H-4a), δ_H 1.66 (1H, dd, *J*=14.4, 9.1 Hz, H-4b), and δ_H 1.58 (1H, dd, *J*=12.8, 5.1 Hz, H-2a), δ_H 1.29 (1H, m, H-2b). The remaining signals were assigned as an acetyl methyl at δ_H 2.28 (3H, s, H-10) and three tertiary methyls at δ_H 1.19 (3H, s, H-13), δ_H 1.17 (3H, s, H-11) and δ_H 0.96 (3H, s, H-12). The ^{13}C and DEPT spectra (**Plate 7.18**) showed the presence of 13 carbons including a carbonyl resonance

at δ_C 200.2 (C-10), two olefinic methine resonances at δ_C 145.3 and δ_C 133.8, and an oxymethine carbon at δ_C 64.3 (C-3). The remaining signals were assigned to four methyl carbons, two methylene carbons and three quaternary carbons, of which two are oxygenated. All the protonated carbons were assigned based on HSQC (**Plate 7.19**) correlations. The COSY (**Plate 7.20**) correlation between δ_H 7.16 and δ_H 6.18 (the two *trans*-alkene protons), and the mutual HMBC (**Plate 7.21**) cross-peaks of the acetyl methyl δ_H 2.28 and δ_H 7.16 (H-7) with the carbonyl signal at δ_C 200.2 (C-9) established the presence of an α,β-unsaturated ketone chain. The presence of a *gem*-dimethyl moiety was revealed by the long-range HMBC cross-peaks of the two singlet methyl resonances at δ_H 0.96 (H-12) and δ_H 1.17 (H-11) with δ_C 36.1 (C-1), δ_C 48.0 (C-2) and δ_C 70.8 (C-6). The *gem*-dimethyl unit and the two unprotonated carbons at δ_C 68.7 (C-5) and δ_C 70.8 (C-6) complete the monocyclic six-membered ring identified by the COSY correlations of δ_H 3.77 (H-3) with both δ_H 2.29/1.66 (H-4) and δ_H 1.58/1.29 (H-2). The attachment of the unsaturated side chain to the ring was established by the mutual HMBC correlations of δ_H 7.18 (H-7) and δ_H 6.18 (H-8) with the oxygenated quaternary carbon resonating at δ_C 70.8 (C-6). The relative configuration of the hydroxy group at C-3 was established as equatorial based on the diaxial couplings of H-2 ($J_{ax,ax}$=12.8 Hz) and H-4 ($J_{ax,ax}$=14.4 Hz) with H-3. After comparison with literature data,[17,18] the structure of compound **7.5** was confirmed to be (*3S,5R,6S,7E*)-5,6-Epoxy-3-hydroxymegastigman-7-en-9-one (**7.5**) (**Fig. 7.1**).

Compound **7.6** was isolated as a brown solid and assigned the molecular formula $C_{10}H_8O_4$, based on pseudo-molecular ion $[M-H]^-$ at *m/z* 191.0346 (calculated for $C_{10}H_7O_4$, 191.0344) in the HR-ESI-(-)-MS (**Plate 7.22**). The ^{1}H NMR spectrum (**Plate 7.23**) showed resonances characteristic of an α,β-unsaturated carbonyl system with a *cis*-configuration of the alkene protons at δ_H 7.59 (1H, d, *J*=9.4 Hz, H-4) and δ_H 6.27 (1H, d, *J*=9.4 Hz, H-3), two aromatic singlets at δ_H 6.9 (1H, s, H-5), and δ_H 6.8 (1H, s, H-8), a hydroxy singlet at δ_H 6.11 (1H, s, OH), and a methoxy singlet signal at δ_H 3.95 (3H, s, OCH_3), consistent with the structure of scopoletin. This deduction was supported by the ^{13}C NMR data (**Plate 7.24**) of **7.6** which showed the presence of a coumarin lactone carbonyl resonance at δ_C 161.6 (C-2), two olefinic carbons signals at δ_C 143.4 (C-4) and δ_C 113.7 (C-3), six aromatic carbons of which three are oxygenated at δ_C 150.5-103.4 and a methoxy carbon resonance at δ_C 56.6. A comparison of

these NMR data with the literature data for scopoletin[19] showed close agreement. Therefore, compound **7.6** was confirmed to be scopoletin (**7.6**) (**Fig. 7.1**).

Compound **7.7** was isolated as a white amorphous solid. The EIMS (**Plate 7.25**) showed a base peak at *m/z* 218, resulting from the fragmentation of C8-C14 bond to give the C*DE fragment[20] (*m/z* 218) and a molecular ion peak at *m/z* 424, suggesting a molecular formula of $C_{30}H_{50}O$. The ^{1}H NMR spectrum (**Plate 7.26**) showed signals characteristic of lupene-type exocyclic double bond at δ_H 4.68 (1H, d, *J*=2.3 Hz, H-29b) and δ_H 4.56 (1H, dd, *J*=2.3, 1.3 Hz, H-29a), and an oxymethine resonance at δ_H 3.18 (1H, dd, *J*=11.4, 4.8 Hz, H-3), and seven methyl singlet resonances between δ_H 1.68-0.76, characteristic of lupeol. The ^{13}C spectrum (**Plate 7.27**) showed 30 carbon resonances and confirmed the presence of an exocyclic double bond with resonances appearing at δ_C 150.9 (C-20), δ_C 109.3 (C-29), an oxymethine group δ_C 79.0 (C-3) and seven tertiary methyls. Comparing the NMR data of 7 with the literature[21,22] showed close agreement with the structure of lupeol (**7.7**) (**Fig. 7.1**).

Compound **7.8** and **7.9** were isolated as a mixture in a ratio of 2:1 based on ^{1}H NMR integration. GCMS analysis with matching to a NIST library indicated that the mixture consisted of β-sitosterol (major component) and stigmasterol (minor component). The EIMS (**Plate 7.28 and 7.29**) showed molecular ion peaks at *m/z* 414 and 412 consistent with $C_{29}H_{50}O$ and $C_{29}H_{48}O$ for β-sitosterol and stigmasterol, respectively. The ^{1}H NMR spectrum (**Plate 7.30**) of the mixture showed resonances for two tertiary methyl singlets at δ_H 1.0 (3H, s, H-19) and δ_H 0.68 (s, H-18), a primary methyl triplet at δ_H 0.82 (3H, t, *J*=7.2 Hz, H-29), and three secondary methyl doublets at δ_H 0.92 (3H, d, *J*=6.5 Hz, H-21) and δ_H 0.80 (6H, d, *J*=7.0 Hz, H-26, 27), an olefinic doublet signal at δ_H 5.32 (1H, d, *J*=4.9 Hz, H-6), and a multiplet due to an oxymethine proton resonance at δ_H 3.45 (1H, m, H-3). The resonances for the two olefinic protons in the side chain of stigmasterol appeared as a pair of doublet of doublets at δ_H 5.15 (dd, *J*=8.3, 15.0 Hz, H-22) and δ_H 5.02 (dd, *J*=8.3, 15.0 Hz, H-23). Most of the carbon signals in the ^{13}C NMR spectrum (**Plate 7.31**) overlapped for the two compounds, except for C-22 and C-23, which is the major point of difference between these two compounds. All the carbon signals closely matched the literature values[23,24] for β-sitosterol (**7.8**) and stigmasterol (**7.9**) (**Fig. 7.1**) and confirmed the structures of the two compounds.

Iridoids, indole alkaloids, and anthraquinones are the primary chemical markers of the Rubiaceae, with restricted distribution across specific subfamilies.[3] The Rubiaceae is divided into the Ixoroideae, Cinchonoideae and Rubioideae subfamilies, with iridoids considered to be the chemotaxonomic marker of the Ixoroideae. Anthraquinones predominate of the Rubioideae, whereas indole alkaloids are the major chemical markers of the Cinchonoideae.[3] *Gardenia* belongs to the Ixoroideae. However, in this study, iridioids were not found in the leaves of *G. thunbergia*. Considering that different plant organs can have different phytochemical compositions, other parts of the plants, such as the bark, roots, flowers, and fruits should be investigated for the presence of the iridoid chemical marker. Although considered a chemotaxonomical markers, most of the iridoids that have been reported in *Gardenia* were found in the fruits and flowers of *Gardenia jasminoides*.[3,25-27] The phytochemical investigation of other *Gardenia* species have resulted in the isolation of flavonoids (*Gardenia thailandica*,[28] *G. lucida*,[29] *G. gummifera*,[29] *G. fructus*,[30] *G. jasminoides*[31]), triterpenoids (*Gardenia thailandica*,[28] *G. saxatilis*,[32] *G. collinsae*,[33] G. *jasminoides*[31]), sesquiterpenoids (*G. sootepensis*[34]), coumarins (G. *jasminoides*[31]) and phenolic derivatives (*G. fructus*[30] and G. *jasminoides*[31]). Flavonoids and triterpenoids are reported in most species of *Gardenia* and are present widely in the Rubiaceae.[3] Therefore, the isolation of triterpene and flavonoid glycosides and the absence of iridoids in the leaves of *G. thunbergia* in this study is in agreement with the phytochemistry of other *Gardenia* species and perhaps iridoids are not good markers for this genus.

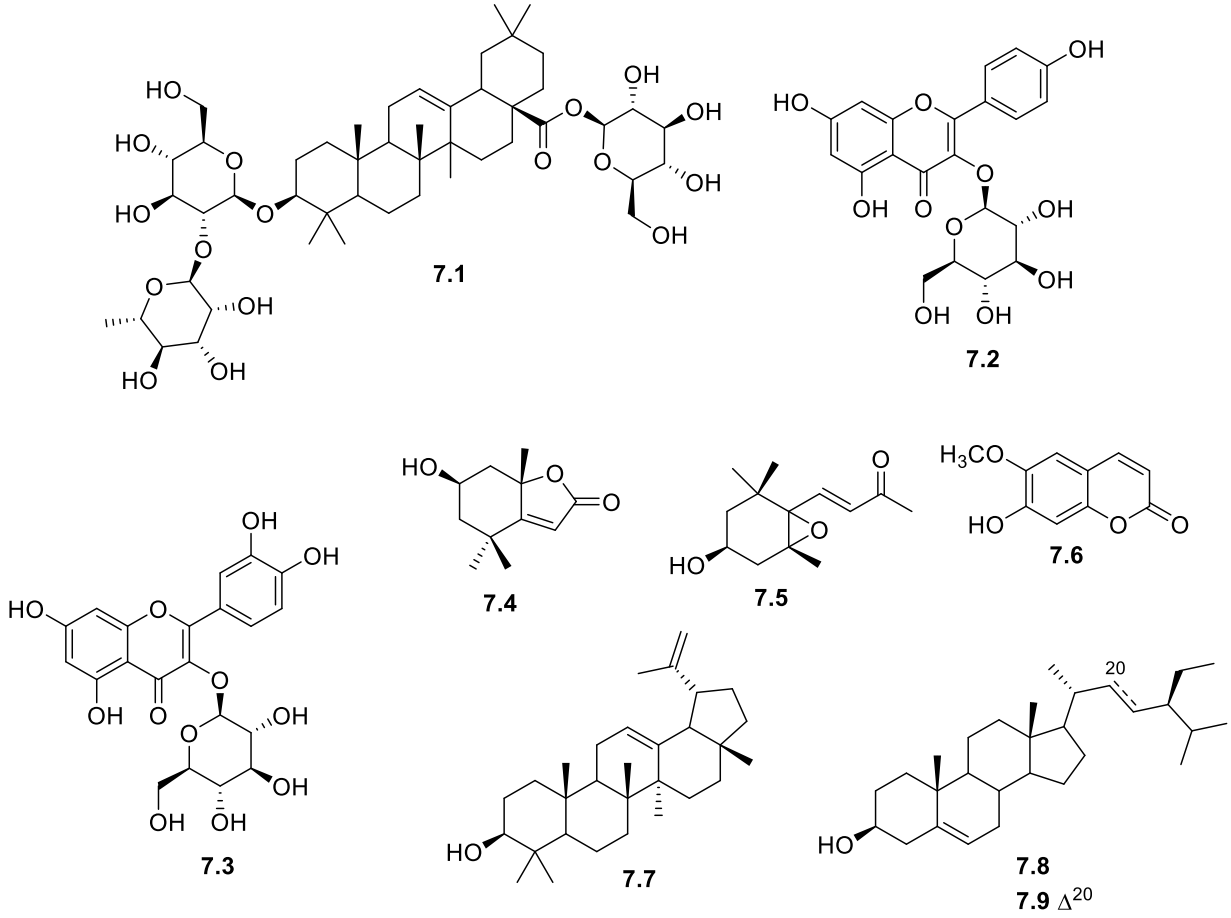

Fig. 7.1: Structures of the isolated compounds from *G. thunbergia*

7.3.2. Biological activity

The methanol extract of the leaves of *G. thunbergia* displayed significant antiplasmodial activity (>80% inhibition) at 50 µg/mL and was not cytotoxic against HeLa cells (Table 7.1). The antiplasmodial activity decreased at a lower concentration of 10 µg/mL. It is noteworthy that a DCM-MeOH (1:1) extract of the leaves did not show antiplasmodial activity, suggesting that the active compounds in the plant extract are polar. Purification of the leaf extract afforded nine compounds including a triterpenoid saponin and two flavonoid glycosides. The saponin and flavonoid glycosides inhibited *P. falciparum* by more than 80% at 50 µg/mL, but were also cytotoxic against HeLa cells. The antiplasmodial activity of flavonoid glycosides has been discussed in chapters 4-6. Previous studies have shown that saponins display nonselective antiprotozoal activity, including antiplasmodial activity.[35-37] The lack of selectivity is observed when the antiplasmodial activity is reported alongside the cytotoxicity

data.[35-37] Considering that the extract was not cytotoxic against cancerous and noncancerous cell lines, it is possible that other compounds in the extract mitigate the cytotoxicity.

Table 7.1: In vitro antiplasmodial and cytotoxic activity of the extract and isolated compounds

Compound	Viability% ±SD (50 µg/mL)		Viability% ±SD (10 µg/mL)	
	3D7	HeLa	3D7	HeLa
G. thunbergia	17.9 ± 2.7	80.7 ± 0.9	79.5 ± 4.2	86.7 ± 3.6
Compound **7.1**	15.5 ± 2.7	2.1 ± 0.4	66.8 ± 4.4	70.0 ± 4.8
Compound **7.2**	17.9 ± 0.7	3.3 ± 0.5	57.4 ± 1.0	75.0 ± 5.1
Compound **7.3**	18.4 ± 2.9	1.9 ± 0.6	58.7 ± 1.9	64.8 ± 2.2
Chloroquine	-	-	IC_{50} = 0.014 µM	-
Emetine	-	-	-	IC_{50} = 0.04 µM

7.4. Conclusion

The methanol leaf extract of *G. thunbergia* displayed significant antiplasmodial activity without being cytotoxic. Investigation of the leaves resulted in the isolation of nine compounds, including a new triterpenoid saponin and two flavonoid glycoside for the first time. The saponin and flavonoid glycosides showed a non-selective antiplasmodial activity and could account for the use of the plant in traditional medicine for treatment of malaria.

Acknowledgment

The authors are grateful to Dr Christina Potgieter of Bews Herbarium, School of Life Sciences, University of KwaZulu-Natal for helping with the preparation of plant voucher specimens and Ms Alison young for identifying the plant material. NT is grateful to the University of KwaZulu-Natal for the award of a doctoral scholarship. Antimalarial and HeLa cell cytotoxicity assays were supported by Rhodes University (Sandisa Imbewu grant) and the South African Medical Research Council. FRVH acknowledges the National Research Foundation (South Africa) Grant [number 98345] for financial support.

Conflict of interest

The authors declare that they have no conflict of interest.

References

1. Coates Palgrave, K., Drummond, R., *Trees of Southern Africa*. C. Struik Publishers, Cape Town: 1977.
2. Mongrand, S.; Badoc, A.; Patouille, B.; Lacomblez, C.; Chavent, M.; Bessoule, J. J., Chemotaxonomy of the Rubiaceae family based on leaf fatty acid composition. *Phytochemistry* **2005,** 66, (5), 549-559.
3. Martins, D.; Nunez, C. V., Secondary metabolites from Rubiaceae species. *Molecules* **2015,** 20, (7), 13422-13495.
4. Watt, J. M., Breyer-Brandwijk, M.G., *The Medicinal and Poisonous Plants of Southern and Eastern Africa*. E. and S. Livingstone LTD., London: 1962.
5. Hutchings, A., *Zulu Medicinal Plants: an Inventory*. University of Natal Press: 1996.
6. Nethengwe, M.; Opoku, A.; Dludla, P.; Madida, K.; Shonhai, A.; Smith, P.; Singh, M., Larvicidal, antipyretic and antiplasmodial activity of some Zulu medicinal plants. *Journal of Medicinal Plants Research* **2012,** 6, (7), 1255-1262.
7. Seebacher, W.; Simic, N.; Weis, R.; Saf, R.; Kunert, O., Complete assignments of ^{1}H and ^{13}C NMR resonances of oleanolic acid, 18α-oleanolic acid, ursolic acid and their 11-oxo derivatives. *Magnetic Resonance in Chemistry* **2003,** 41, (8), 636-638.
8. Kuroda, M.; Mimaki, Y.; Sashida, Y.; Hirano, T.; Oka, K.; Dobashi, A.; Li, H.-y.; Harada, N., Novel cholestane glycosides from the bulbs of *Ornithogalum saundersiae* and their cytostatic activity on leukemia HL-60 and MOLT-4 cells. *Tetrahedron* **1997,** 53, (34), 11549-11562.
9. Chen, Q.-W.; Zhang, X.; Gong, T.; Gao, W.; Yuan, S.; Zhang, P.-C.; Kong, J.-Q., Structure and bioactivity of cholestane glycosides from the bulbs of *Ornithogalum saundersiae* Baker. *Phytochemistry* **2019,** 164, 206-214.
10. Achouri, A.; Derbre, S.; Medjroubi, K.; Laouer, H.; Seraphin, D.; Akkal, S., Two new triterpenoid saponins from the leaves of *Bupleurum lancifolium* (Apiaceae). *Natural Product Research* **2017,** 31, (19), 2286-2293.
11. Ganbaatar, C.; Gruner, M.; Tunsag, J.; Batsuren, D.; Ganpurev, B.; Chuluunnyam, L.; Sodbayar, B.; Schmidt, A. W.; Knoelker, H.-J., Chemical constituents isolated from *Zygophyllum melongena* Bunge growing in Mongolia. *Natural Product Research* **2016,** 30, (14), 1661-1664.

12. Chludil, H. D.; Corbino, G. B.; Leicach, S. R., Soil quality effects on *Chenopodium album* flavonoid content and antioxidant potential. *Journal of Agricultural and Food Chemistry* **2008,** 56, (13), 5050-5056.

13. Fernandez, J.; Reyes, R.; Ponce, H.; Oropeza, M.; VanCalsteren, M. R.; Jankowski, C.; Campos, M. G., Isoquercitrin from *Argemone platyceras* inhibits carbachol and leukotriene D-4-induced contraction in guinea-pig airways. *European Journal of Pharmacology* **2005,** 522, (1-3), 108-115.

14. Lee, S.; Park, H.-S.; Notsu, Y.; Ban, H. S.; Kim, Y. P.; Ishihara, K.; Hirasawa, N.; Jung, S. H.; Lee, Y. S.; Lim, S. S.; Park, E.-H.; Shin, K. H.; Seyama, T.; Hong, J.; Ohuchi, K., Effects of hyperin, isoquercitrin and quercetin on lipopolysaccharide-induced nitrite production in rat peritoneal macrophages. *Phytotherapy Research* **2008,** 22, (11), 1552-1556.

15. Tanaka, R.; Matsunaga, S., Loliolide and olean-12-en-3β,9α,11-α-triol from *Euphorbia supina*. *Phytochemistry* **1989,** 28, (6), 1699-1702.

16. Hiraga, Y.; Taino, K.; Kurokawa, M.; Takagi, R.; Ohkata, K., (-)-Loliolide and other germination inhibitory active constituents in *Equisetum arvense*. *Natural Product Letters* **1997,** 10, (3), 181-186.

17. Kim, K. H.; Lee, K. H.; Choi, S. U.; Kim, Y. H.; Lee, K. R., Terpene and phenolic constituents of *Lactuca indica* L. *Archives of Pharmacal Research* **2008,** 31, (8), 983-988.

18. D'Abrosca, B.; DellaGreca, M.; Fiorentino, A.; Monaco, P.; Oriano, P.; Temussi, F., Structure elucidation and phytotoxicity of C-13 nor-isoprenoids from *Cestrum parqui*. *Phytochemistry* **2004,** 65, (4), 497-505.

19. Lee, J.; Kim, N. H.; Nam, J. W.; Lee, Y. M.; Jang, D. S.; Kim, Y. S.; Nam, S. H.; Seo, E.-K.; Yang, M. S.; Kim, J. S., Scopoletin from the flower buds of *Magnolia fargesii* inhibits protein glycation, aldose reductase, and cataractogenesis ex vivo. *Archives of Pharmacal Research* **2010,** 33, (9), 1317-1323.

20. Santos, P. F. P.; Gomes, L. N. L. F.; Mazzei, J. L.; Fontao, A. P. A.; Sampaio, A. L. F.; Siani, A. C.; Valente, L. M. M., Polyphenol and triterpenoid constituents of *Eugenia orida* DC. (Myrtaceae) leaves and their antioxidant and cytotoxic potential. *Quimica Nova* **2018,** 41, (10), 1140-1149.

21. Burns, D.; Reynolds, W. F.; Buchanan, G.; Reese, P. B.; Enriquez, R. G., Assignment of H-1 and C-13 spectra and investigation of hindered side-chain rotation in lupeol derivatives. *Magnetic Resonance in Chemistry* **2000,** 38, (7), 488-493.
22. Mahato, S. B.; Kundu, A. P., C-13 nmr-spectra of pentacyclic triterpenoid - A compilation and some salient features. *Phytochemistry* **1994,** 37, (6), 1517-1575.
23. Jamaluddin, F.; Mohamed, S.; Lajis, M. N., Hypoglycaemic effect of *Parkia speciosa* seeds due to the synergistic action of β-sitosterol and stigmasterol. *Food Chemistry* **1994,** 49, (4), 339-345.
24. Suttiarporn, P.; Chumpolsri, W.; Mahatheeranont, S.; Luangkamin, S.; Teepsawang, S.; Leardkamolkarn, V., Structures of phytosterols and triterpenoids with potential anti-cancer activity in bran of black non-glutinous rice. *Nutrients* **2015,** 7, (3), 1672-1687.
25. Fu, X. M.; Chou, G. X.; Wang, Z. T., Iridoid glycosides from *Gardenia jasminoides* Ellis. *Helvetica Chimica Acta* **2008,** 91, (4), 646-653.
26. Yu, Y.; Xie, Z.-l.; Gao, H.; Ma, W.-w.; Dai, Y.; Wang, Y.; Zhong, Y.; Yao, X.-s., Bioactive iridoid glucosides from the fruit of *Gardenia jasminoides*. *Journal of Natural Products* **2009,** 72, (8), 1459-1464.
27. Ragasa, C. Y.; Pimenta, L. E. N.; Rideout, J. A., Iridoids from *Gardenia jasminoides*. *Natural Product Research* **2007,** 21, (12), 1078-1084.
28. Tuchinda, P.; Saiai, A.; Pohmakotr, M.; Yoosook, C.; Kasisit, J.; Napaswat, C.; Santisuk, T.; Reutrakul, V., Anti-HIV-1 cycloartanes from leaves and twigs of *Gardenia thailandica*. *Planta Medica* **2004,** 70, (04), 366-370.
29. Kunert, O.; Sreekanth, G.; Babu, G. S.; Rao, B. V. R. A.; Radhakishan, M.; Kumar, B. R.; Saf, R.; Rao, A. V. N. A.; Schuehly, W., Cycloartane triterpenes from Dikamali, the gum resin of *Gardenia gummifera* and *Gardenia lucida*. *Chemistry & Biodiversity* **2009,** 6, (8), 1185-1192.
30. Wu, X.; Zhou, Y.; Yin, F.; Mao, C.; Li, L.; Cai, B.; Lu, T., Quality control and producing areas differentiation of *Gardeniae Fructus* for eight bioactive constituents by HPLC–DAD–ESI/MS. *Phytomedicine* **2014,** 21, (4), 551-559.
31. Yang, L.; Peng, K.; Zhao, S.; Zhao, F.; Chen, L.; Qiu, F., 2-Methyl-l-erythritol glycosides from *Gardenia jasminoides*. *Fitoterapia* **2013,** 89, 126-130.

32. Suksamrarn, A.; Tanachatchairatana, T.; Kanokmedhakul, S., Antiplasmodial triterpenes from twigs of *Gardenia saxatilis*. *Journal of Ethnopharmacology* **2003,** 88, (2-3), 275-277.

33. Nuanyai, T.; Sappapan, R.; Vilaivan, T.; Pudhom, K., Dammarane triterpenes from the apical buds of *Gardenia collinsae*. *Phytochemistry Letters* **2011,** 4, (2), 183-186.

34. Rukachaisirikul, V.; Naovanit, S.-a.; Taylor, W. C.; Bubb, W. A.; Dampawan, P., A sesquiterpene from *Gardenia sootepensis*. *Phytochemistry* **1998,** 48, (1), 197-200.

35. Traore, F.; Faure, R.; Ollivier, E.; Gasquet, M.; Azas, N.; Debrauwer, L.; Keita, A.; Timon-David, P.; Balansard, G., Structure and antiprotozoal activity of triterpenoid saponins from *Glinus oppositifolius*. *Planta Medica* **2000,** 66, (4), 368-371.

36. Mostafa, A. E.; El-Hela, A. A.; Mohammad, A.-E. I.; Cutler, S. J.; Ross, S. A., New triterpenoidal saponins from *Koelreuteria paniculata*. *Phytochemistry Letters* **2016,** 17, 213-218.

37. Foubert, K.; Gorella, T.; Faizal, A.; Cos, P.; Maes, L.; Apers, S.; Geelen, D.; Pieters, L., Triterpenoid saponins from *Maesa argentea* leaves. *Planta Medica* **2016,** 82, (18), 1568-1575.

Chapter 8: Conclusion and recommendations

Medicinal plants and an ethnopharmacology approach have played a significant role in the discovery of the most important antimalarial compounds. A review of the antimalarial natural products reported between 2010 and 2017 as described in chapter 2 shows that majority of the compounds were discovered by investigating plants that are used in traditional medicine for the treatment of malaria. In the search for antiplasmodial compounds from South African plants, the work in this thesis described the phytochemistry and antiplasmodial activities of five plants that are used in traditional medicine to treat malaria or fever. Prior to this study, the phytochemistry of *Vachellia xanthophloea* (Benth.) P.J.H.Hurter, *Ozoroa obovata* (Oliv.) R. & A. Fern., *Gardenia thunbergia* L.f., and the leaves of *Euclea natalensis* A.DC. have not been examined, whereas only two compounds were previously reported from the leaves of *Pappea capensis* Eckl. & Zeyh. Overall, 39 different compounds were isolated from the five plants, and some of the compounds were obtained from more than one plant species. All the structures were elucidated based on spectroscopic experiments. Three compounds were new natural products, i.e. two flavonoids isolated from *V. xanthophloea*, 3,7,8,2',4',5'-hexamethoxyflavone (**3.1**) and 5,7,2'-trihydroxy-3,4',5'-trimethoxyflavone (**3.3**), and a saponin from *G. thunbergia*, 3-*O*-[α-L-rhamnopyranosyl-(1→2)-β-D-glucopyranosyl]oleanolic acid 28-*O*-β-D-glucopyranosyl ester (**7.1**).

The antiplasmodial activity of *V. xanthophloea* against the D10 strain of *P. falciparum* has been reported previously. This project has examined the activity of the plant leaf extract against the 3D7 strain for the first time. The ethyl acetate fraction of the leaf extract showed good antiplasmodial activity and was not cytotoxic. Phytochemical investigation of the active fraction of the leaves of *V. xanthophloea* led to the isolation of 16 compounds, including 10 flavonoids (including two new polymethoxy flavones), a phenolic ester and a furofuran lignan. Methyl gallate, isolated from the ethyl acetate fraction, was found to be responsible for the antiplasmodial activity. The compound displayed good selective antiplasmodial activity, better than the ethyl acetate fraction and is worthy of further exploration. The isolation of flavonoids and a phenolic ester from the leaves of *V. xanthophloea* is consistent with the phytochemistry of other *Vachellia* (*Acacia*) species.

No previous studies on the antiplasmodial activity or phytochemistry of *Ozoroa obovata* could be found in the literature. Thus, this study represents the first investigation of the chemical constituents and antiplasmodial activity of *O. obovata*. The leaf extract of *O. obovata* showed nonselective antiplasmodial activity against the 3D7 parasite strain. The plant leaf extract afforded eight compounds, two biflavonoids, four flavonoid glycosides, a steroid glycoside, and a megastigmane derivative. The biflavonoids and flavonoid glycosides inhibited the viability of *P. falciparum* but were also cytotoxic against a cancerous HeLa cell line. Previous chemical investigations of the *Ozoroa* genus have focused on the root, and root bark, and stem bark, and resulted in the isolation of triterpenoids, alkyl phenols, and alkylanarcardic acids. The isolation of flavonoid glycosides from a species of *Ozoroa* is being reported for the first time, although biflavonoids and flavonoids glycosides have been reported from the Anacardiaceae family.

The root and root bark of *Euclea natalensis* are renowned for the presence of naphthoquinones and various biological activities. The antiplasmodial activity of the root and stem extracts against the K1 and D10 strains of *P. falciparum* has been reported. This project investigated the antiplasmodial activity and chemical constituents of the leaves of *E. natalensis* for the first time. Moderate activity was observed against the 3D7 strain without cytotoxicity against noncancerous cells. Purification of the active extract led to the isolation of six flavonoid glycosides and four triterpenoids. The flavonoid glycosides inhibited *P. falciparum* parasites and were cytotoxic against cancerous cells. This is the first report of the isolation of flavonoid glycosides from *E. natalensis*. Previous investigations on the leaves of other *Euclea* species also found flavonoids and flavonoid glycosides. Naphthoquinones were not found in the leaf extract, and it could be deduced that flavonoid glycosides are predominant in the leaf extract of *Euclea natalensis*, whereas the root and bark are rich in naphthoquinones.

The antiplasmodial activity of the leaves of *Pappea capensis* was previously investigated, and the extract inhibited *P. falciparum* NF54. This project investigated the activity of the leaf extract against the 3D7 parasite strain, and the extract displayed good inhibition of the parasite, but it was also cytotoxic against cancerous HeLa cells. Phytochemical investigation of the leaf extract resulted in the isolation of five flavonoids, of which four are glycosides. The flavonoid glycosides displayed nonselective antiplasmodial activity. Epicatechin and

quercitrin were reported from the leaves in an earlier investigation, while guaijaverin, juglalin and isoquercitrin are reported in *P. capensis* here for the first time.

Gardenia thunbergia is used in traditional medicine in different parts of Africa for the treatment of various diseases, including malaria. Previous antiplasmodial studies of the methanol extract of the plant showed strong activity against the D10 strain, without cytotoxicity against human hepatocellular carcinoma and embryonic kidney cells, but the phytochemistry has not been investigated. In this project, the methanol extract of the leaves was found to inhibit 3D7 *P. falciparum* without cytotoxicity against cancerous HeLa cells. Purification of the leaf extract yielded nine compounds, including a saponin and two flavonoid glycosides. The saponin and flavonoid glycosides inhibited *P. falciparum* parasites but were also cytotoxic against HeLa cells at the active concentrations. Triterpenes and flavonoids have also been reported as the major phytochemicals in other *Gardenia* species. Iridoids, which are considered as a chemical marker for this genus, were not isolated from *G. thunbergia* in this study.

This project has resulted in the isolation of compounds belonging to different phytochemical classes from five ethnobotanically selected South *African* plants. Most of the compounds belonged to the flavonoid and triterpenoid classes and is consistent with the reported phytochemical constitution of other studied plants with antiplasmodial activity. Comparing the antiplasmodial activity of the extracts and isolated compounds, the leaf extract of *V. xanthophloea* and methyl gallate which was isolated from the leaf extract of *V. xanthophloea* had the most promising activity. The leaf extract of *V. xanthophloea* could be developed into a viable antiplasmodial herbal product. Similarly, methyl gallate could be considered as an antiplasmodial hit compound. There is a conflicting account on the reported antiplasmodial activity and selectivity of flavonoids against different strains of *P. falciparum*. Reports of potent and selective, to weak and unselective flavonoids against *P. falciparum* can be found in the literature. Antiplasmodial activity has been reported for prenylated, methoxylated, glycosylated and common dietary flavonoids. The discrepancy in the antiplasmodial activity profile of flavonoids might be due to the different assay methods and type of cancer cells. The apparent lack of selectivity in the antiplasmodial activity of flavonoids has been a limiting factor in the further development of this class of compounds as antimalarial agents. Considering the abundance of flavonoids in dietary sources and how easily the flavonoids

could be harnessed to combat malaria if the efficacy is proven, a detailed structure-activity relationship study on the antimalarial activity of flavonoids would be worthwhile. Most of the triterpenoids isolated in this project were among the most commonly encountered triterpenoids and were not assayed for antiplasmodial activity. Nevertheless, antiplasmodial activity has been reported for some of these triterpenoids, such as oleanolic acid and lupeol.

Traditional health practitioners have long argued that the natural remedies prescribed by them are only fully efficacious as extracts and or mixtures of extracts, or only when the remedy is prepared under special conditions, some of which may not be open to scientific validation. The long experience in the use of herbal and other natural products for the treatment of diseases by the traditional health practitioners is reflected in the varied combination of ingredients in their remedies. It has been shown that an infusion of *Artemisia annua* used in Traditional Chinese Medicine to treat malaria contains only about 20% artemisinin, and a substantially lower dose is required to attain a similar effect as artemisinin. The infusion of *Artemisia annua* contains flavonoids which are inactive against the malaria parasite alone but have been shown to potentiate the activity of artemisinin in combination. It has been postulated that some of the ingredients in a prescription serve to enhance the potency of the main drug or eliminate toxicity. The activity observed for some of the assayed extracts and compounds in this project should be viewed from the perspective of the traditional health practitioner outlined above. The fact that some extracts show selective activity, while the individual components are nonselective in their activity lends credence to these claims. Therefore, the goal of natural product drug discovery should not only be the isolation of the active compounds in an extract.

Recommendations for future research

This project investigated the phytochemical constituents of the leaves of five plants used in traditional medicine for the treatment of malaria. Two these plants, *Ozoroa obovata* and *Gardenia thunbergia*, have not been investigated at all for their chemical composition. The compounds present in these other plant parts should be investigated.

Some of the extracts and compounds isolated in this project such as *Vachellia xanthophloea*, *G. thunbergia*, *O. obovata*, and methyl gallate have shown promising antiplasmodial activity in in vitro investigation against the 3D7 parasite. The good activity should be further

investigated against a panel of *P. falciparum* parasites and in in vivo studies in order to validate the potency. Also, structure-activity studies should be conducted on methyl gallate and the flavonoids in order to gain further understanding of the activity and assist in the possible development of more potent and less toxic analogues.

The cytotoxicity displayed by some of the plant extracts and isolated compounds suggests that more toxicity studies need to be conducted on these natural products considering that people already use of some of these plants in traditional medicine.

APPENDIX A. HRESIMS AND NMR SPECTRA OF COMPOUNDS DESCRIBED IN CHAPTER 3

Elemental Composition Report Page 1

Single Mass Analysis
Tolerance = 5.0 PPM / DBE: min = -1.5, max = 50.0
Element prediction: Off
Number of isotope peaks used for i-FIT = 3

Monoisotopic Mass, Even Electron Ions
2 formula(e) evaluated with 1 results within limits (all results (up to 1000) for each mass)
Elements Used:
C: 20-25 H: 20-25 O: 5-10
NT-V 2_5 12 (0.387) Cm (1:58)
TOF MS ES+

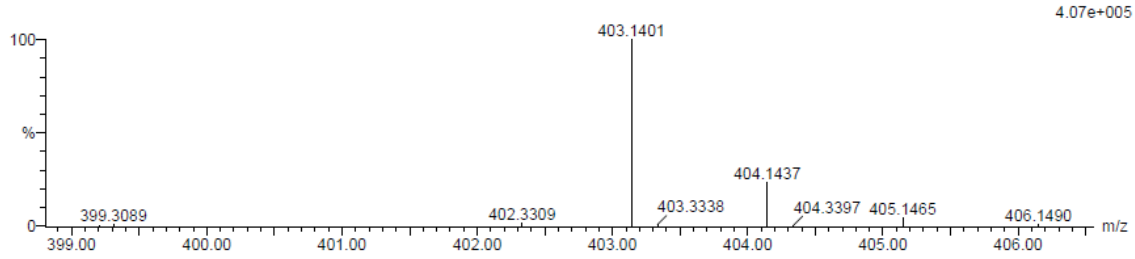

Minimum:				-1.5			
Maximum:		5.0	5.0	50.0			
Mass	Calc. Mass	mDa	PPM	DBE	i-FIT	i-FIT (Norm)	Formula
403.1401	403.1393	0.8	2.0	10.5	47.1	0.0	C21 H23 O8

Plate 3.1: HRESIMS of 3,7,8,2',4',5'-hexamethoxyflavone (3.1).

Elemental Composition Report Page 1

Single Mass Analysis
Tolerance = 5.0 PPM / DBE: min = -1.5, max = 50.0
Element prediction: Off
Number of isotope peaks used for i-FIT = 3

Monoisotopic Mass, Even Electron Ions
4 formula(e) evaluated with 1 results within limits (all results (up to 1000) for each mass)
Elements Used:
C: 20-25 H: 20-25 O: 5-10
NT-V 2_5 12 (0.387) Cm (1:58)
TOF MS ES+

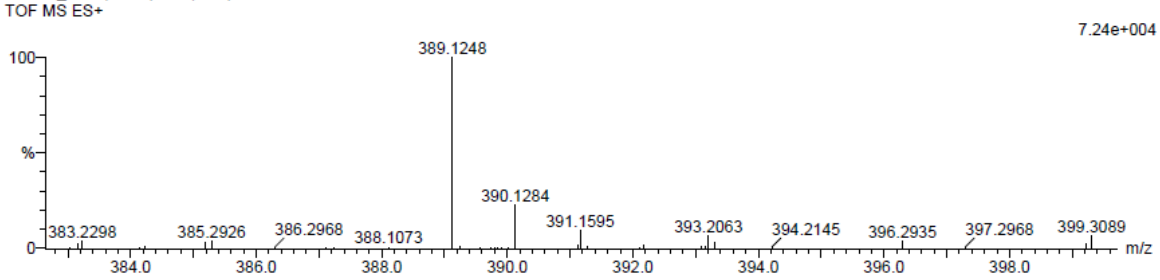

Minimum:				-1.5			
Maximum:		5.0	5.0	50.0			
Mass	Calc. Mass	mDa	PPM	DBE	i-FIT	i-FIT (Norm)	Formula
389.1248	389.1236	1.2	3.1	10.5	136.4	0.0	C20 H21 O8

Plate 3.2: HRESIMS of 2'-hydroxy-3,7,8,4',5'-pentamethoxyflavone (3.2).

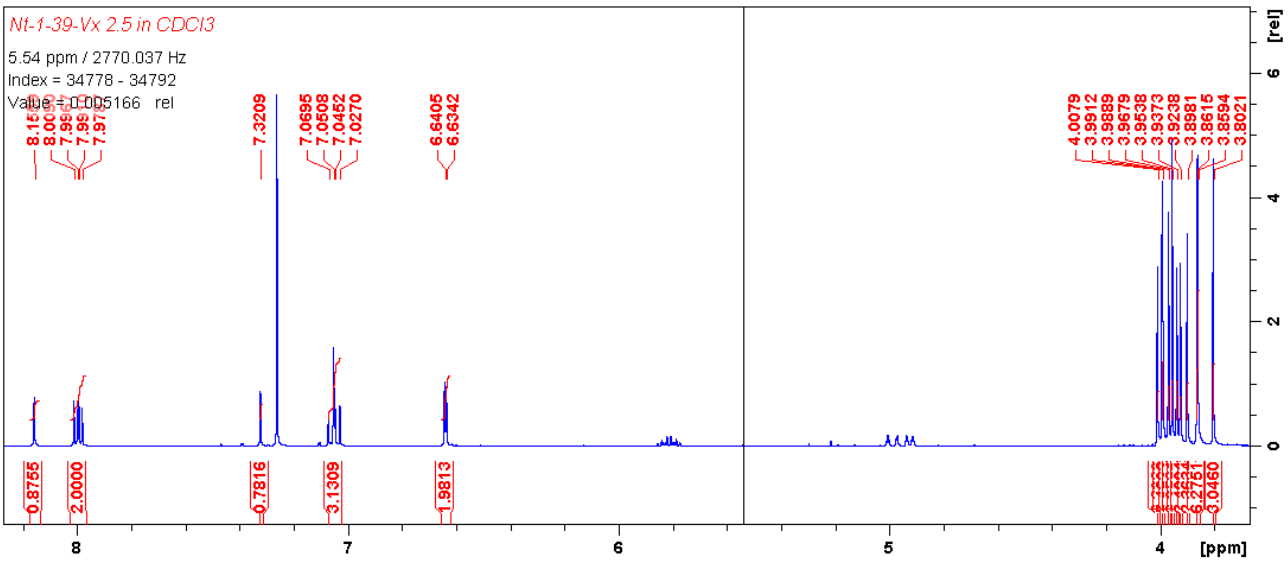

^{1}H NMR (500 MHz, $CDCl_3$) spectrum of 3,7,8,2',4',5'-hexamethoxyflavone (3.1) and 2'-hydroxy-3,7,8,4',5'-pentamethoxyflavone (3.2).

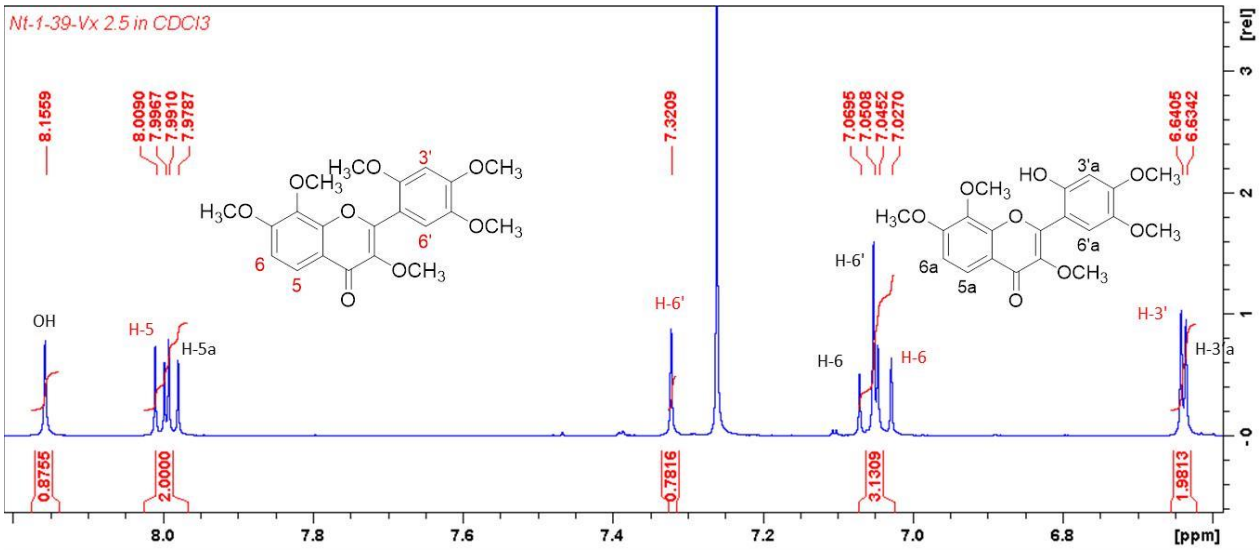

Plate 3.3: Expansion of ^{1}H NMR (500 MHz, $CDCl_3$) spectrum of 3,7,8,2',4',5'-hexamethoxyflavone (3.1) and 2'-hydroxy-3,7,8,4',5'-pentamethoxyflavone (3.2).

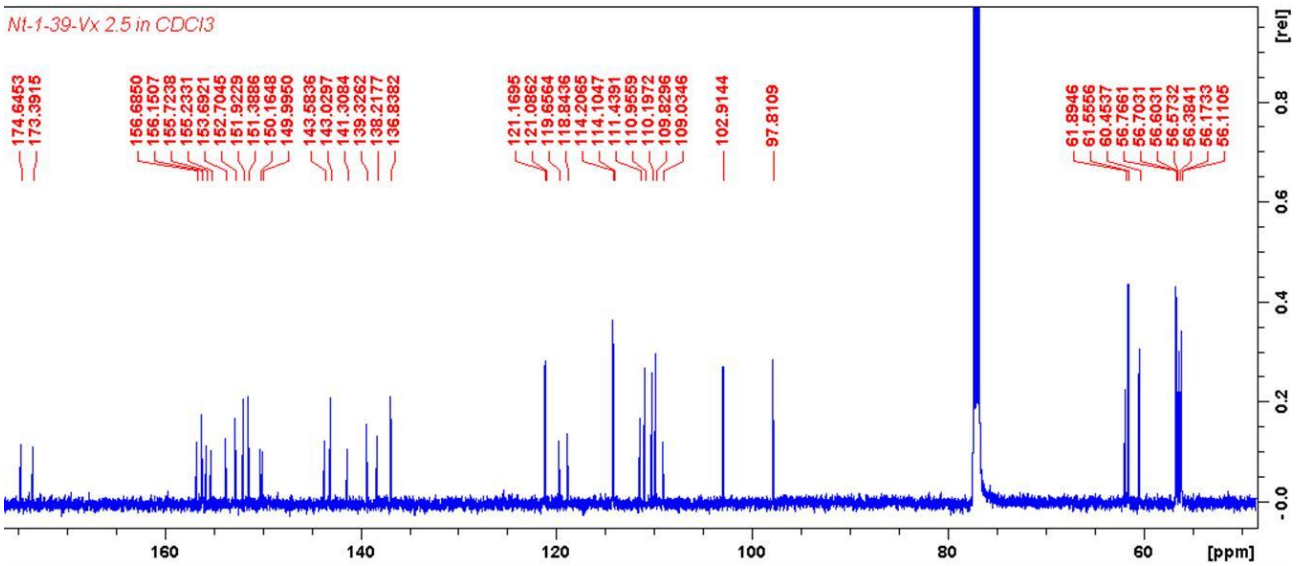

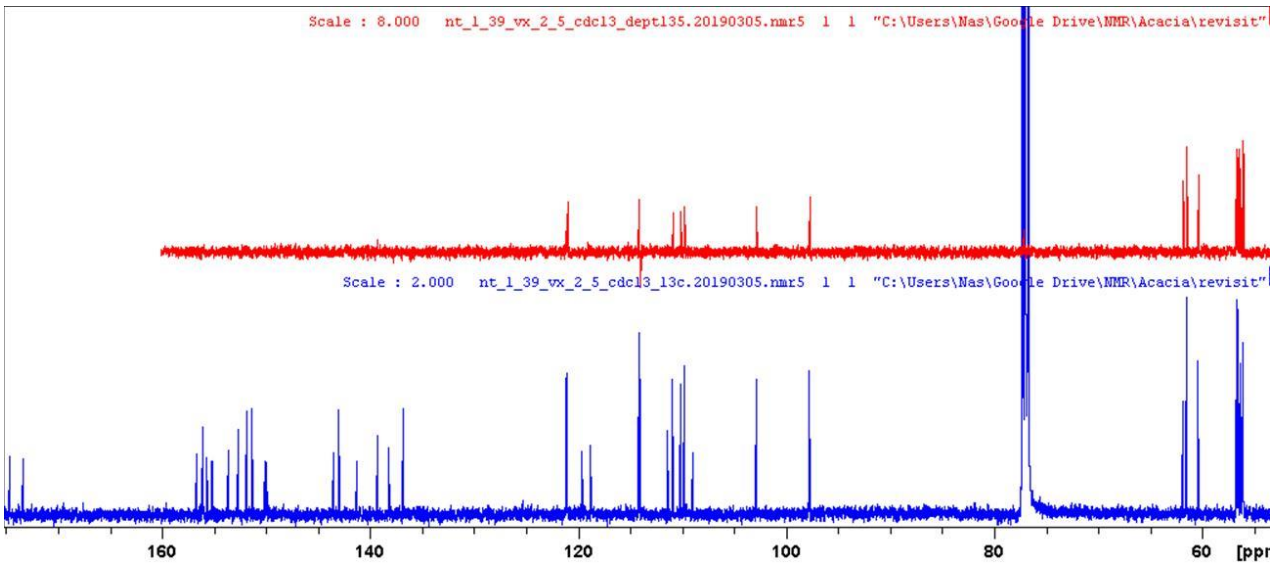

Plate 3.4: ^{13}C and DEPT (125 MHz, $CDCl_3$) spectra of 3,7,8,2',4',5'-hexamethoxyflavone (3.1) and 2'-hydroxy-3,7,8,4',5'-pentamethoxyflavone (3.2).

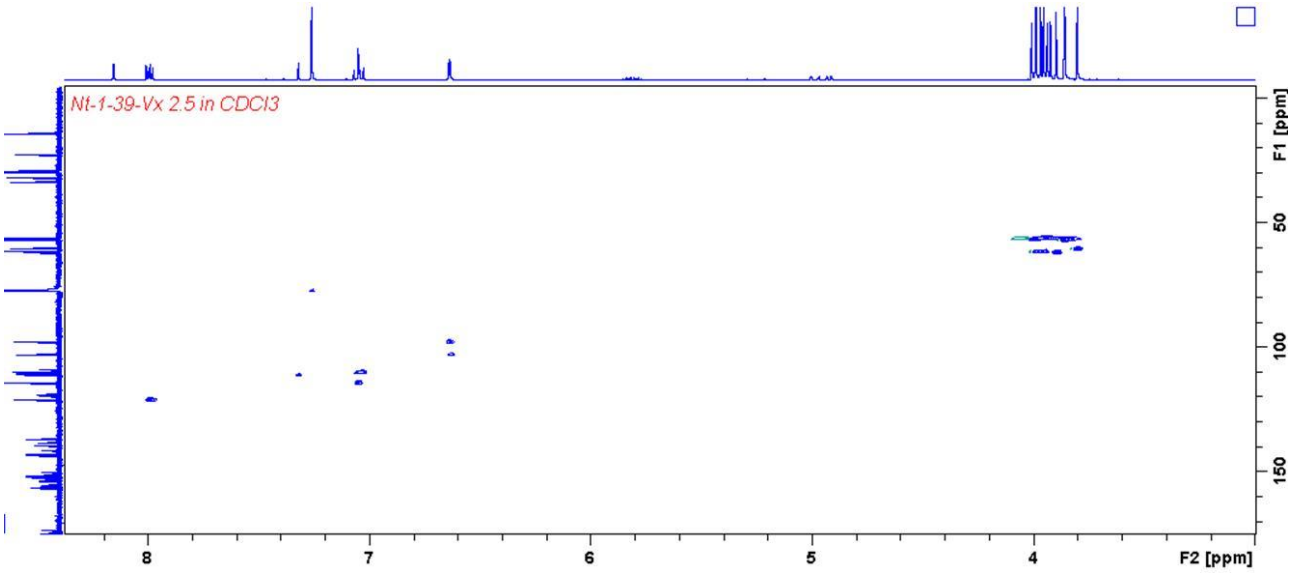

Plate 3.5: HSQC (500 MHz/125 MHz, $CDCl_3$) spectrum of 3,7,8,2',4',5'-hexamethoxyflavone (3.1) and 2'-hydroxy-3,7,8,4',5'-pentamethoxyflavone (3.2).

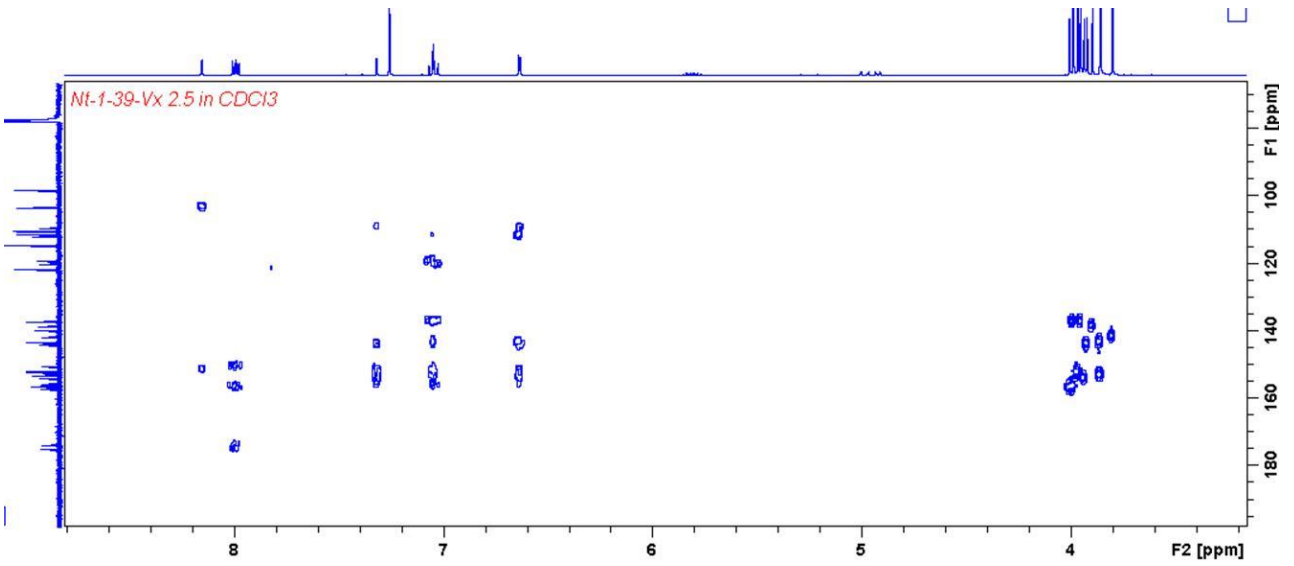

Plate 3.6: HMBC (500 MHz/125 MHz, $CDCl_3$) spectrum of 3,7,8,2',4',5'-hexamethoxyflavone (3.1) and 2'-hydroxy-3,7,8,4',5'-pentamethoxyflavone (3.2).

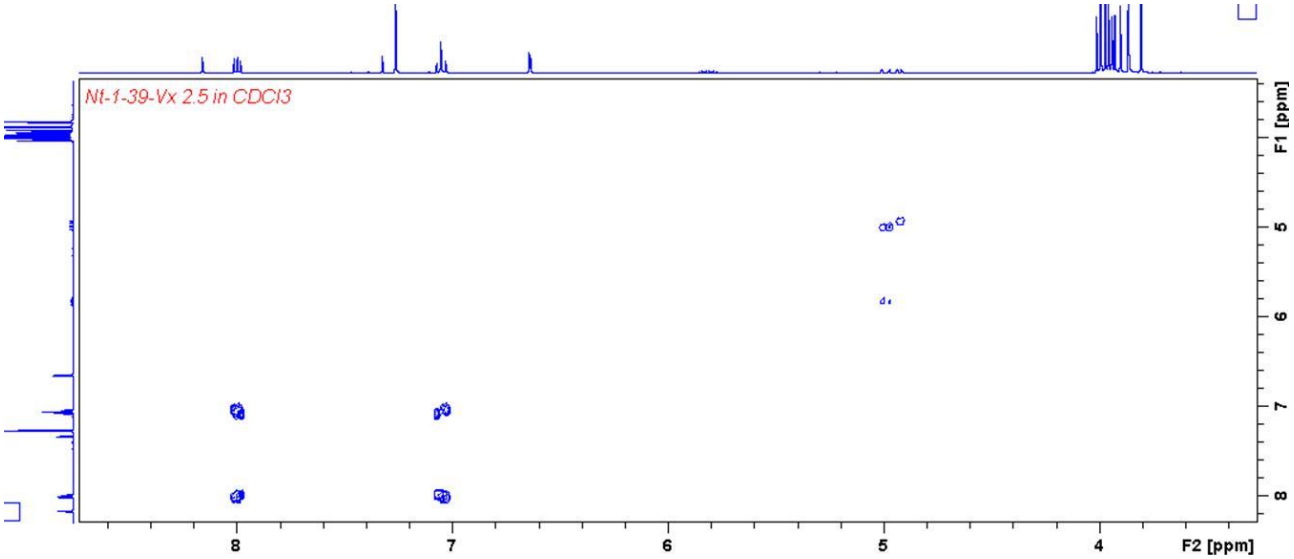

Plate 3.7: COSY (500 MHz/125 MHz, $CDCl_3$) spectrum of 3,7,8,2',4',5'-hexamethoxyflavone and 2'-hydroxy-3,7,8,4',5'-pentamethoxyflavone (3.1 and 3.2).

Elemental Composition Report Page 1

Single Mass Analysis
Tolerance = 5.0 PPM / DBE: min = -1.5, max = 100.0
Element prediction: Off
Number of isotope peaks used for i-FIT = 3

Monoisotopic Mass, Even Electron Ions
14 formula(e) evaluated with 1 results within limits (all results (up to 1000) for each mass)
Elements Used:
C: 15-30 H: 15-30 O: 0-10
Vx 2,7b2 32 (1.046) Cm (1:61)
TOF MS ES-

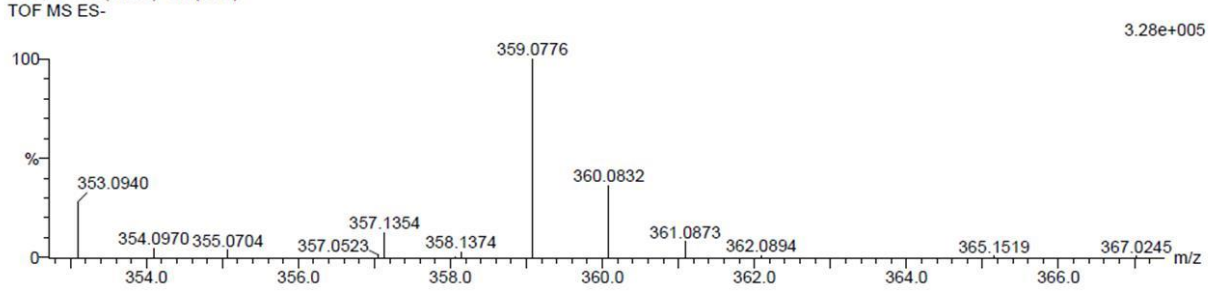

Minimum:				-1.5			
Maximum:		5.0	5.0	100.0			
Mass	Calc. Mass	mDa	PPM	DBE	i-FIT	i-FIT (Norm)	Formula
359.0776	359.0767	0.9	2.5	11.5	33.9	0.0	C18 H15 O8

Plate 3.8: HRESIMS of 5,7,2'-trihydroxy-3,4',5'-trimethoxyflavone (3.3).

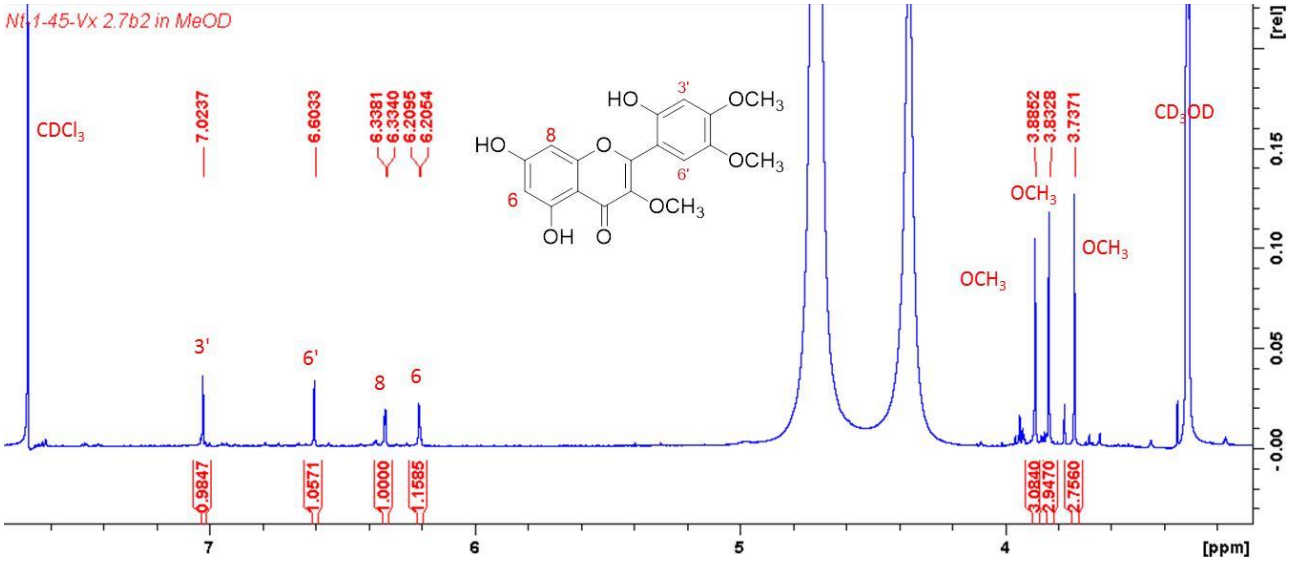

Plate 3.9: ^{1}H NMR (400 MHz, CD_3OD) spectrum of 5,7,2'-trihydroxy-3,4',5'-trimethoxyflavone (3.3).

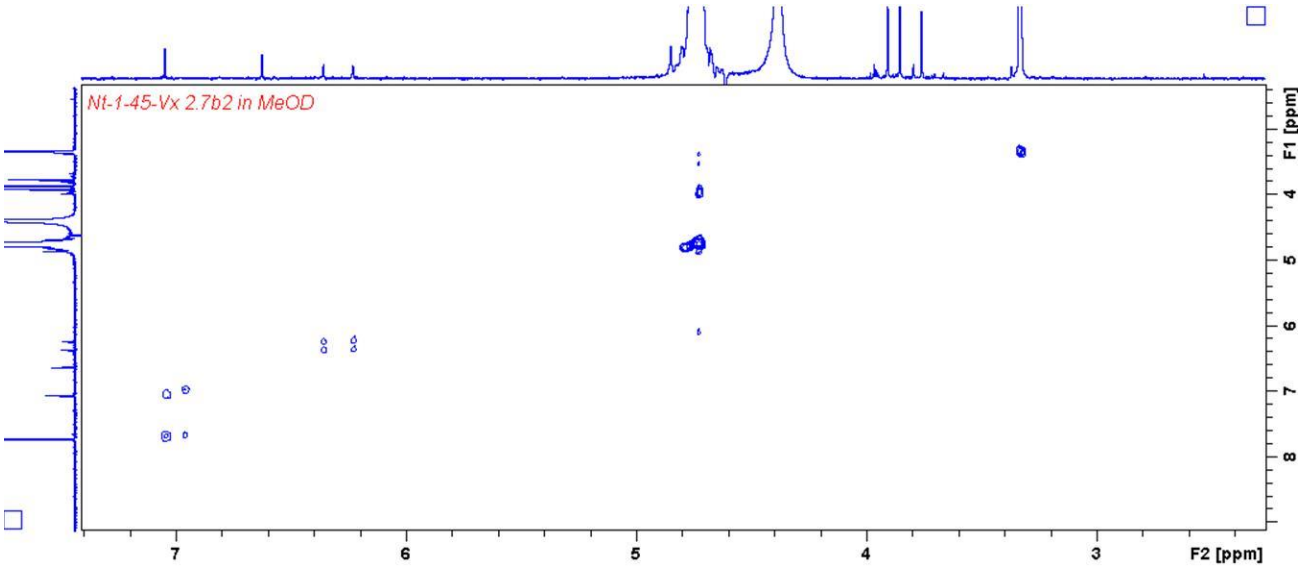

Plate 3.10: COSY (400 MHz, CD_3OD) spectrum of 5,7,2'-trihydroxy-3,4',5'-trimethoxyflavone (3.3).

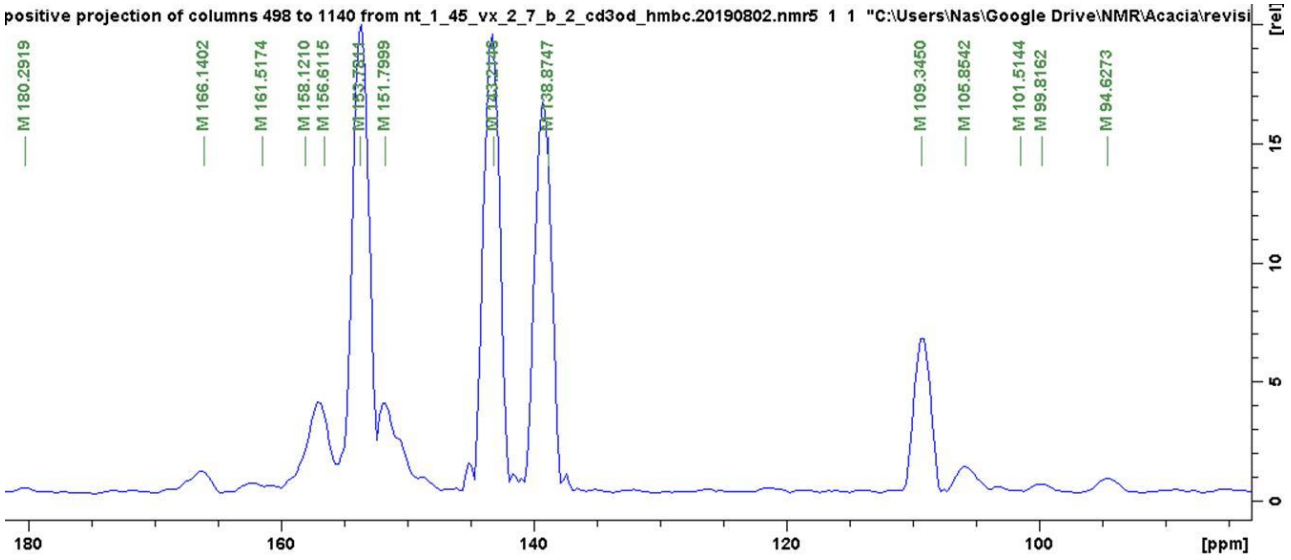

^{13}C NMR (100 MHz, CD_3OD) spectrum (positive projection from HMBC) of 5,7,2'-trihydroxy-3,4',5'-trimethoxyflavone (3.3).

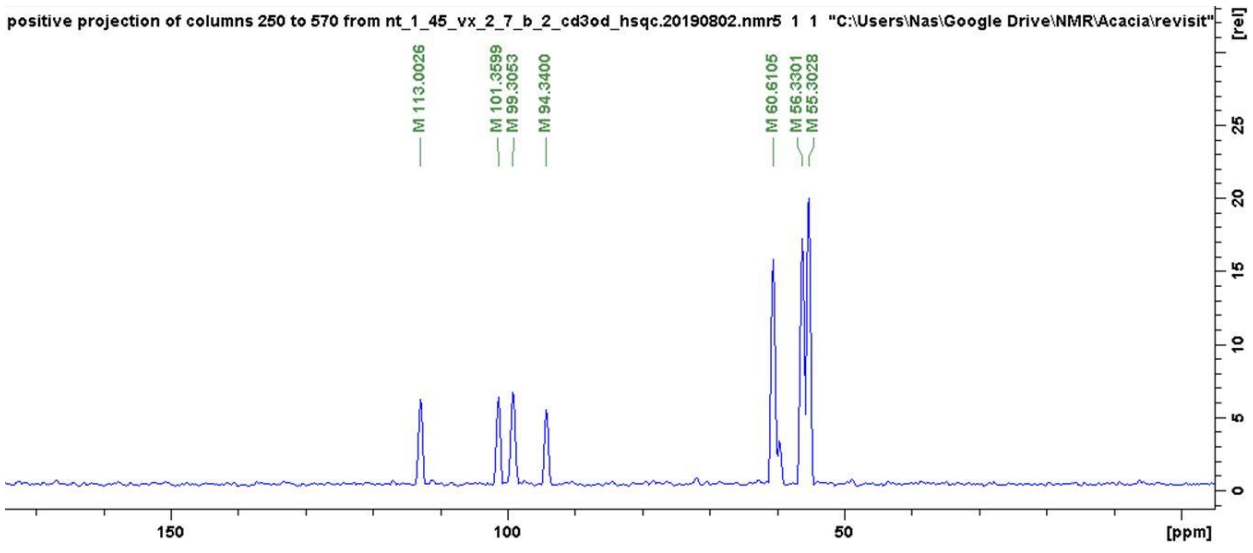

Plate 3.11: ^{13}C NMR (100 MHz, CD_3OD) spectrum (positive projection from HSQC) of 5,7,2'-trihydroxy-3,4',5'-trimethoxyflavone (3.3).

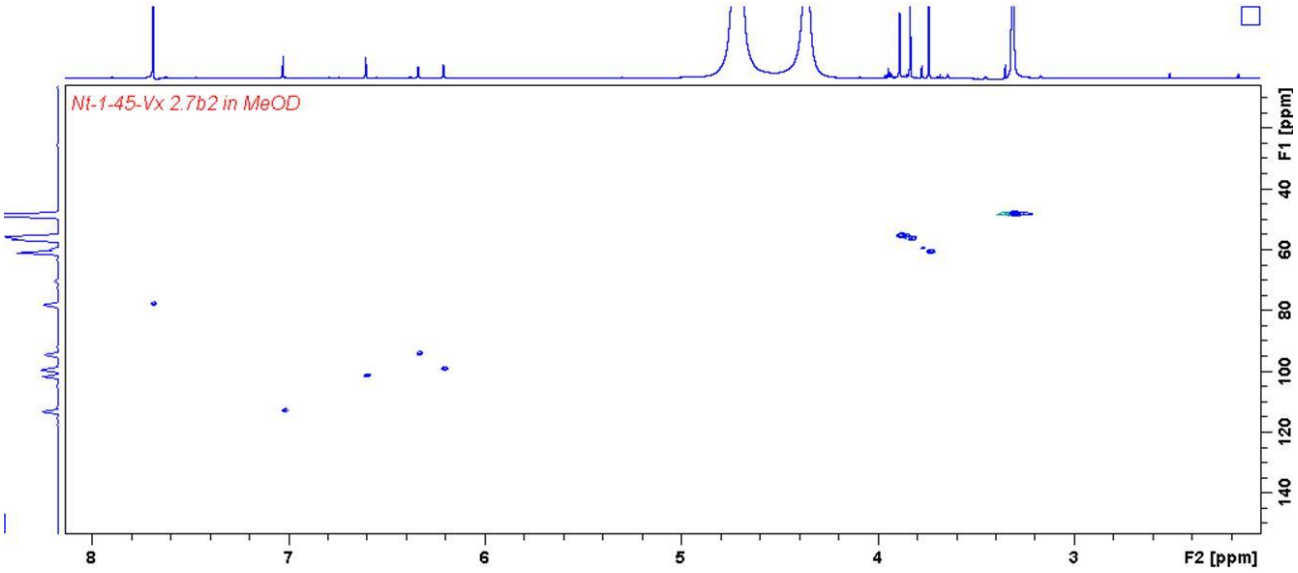

Plate 3.12: HSQC (400 MHz/100 MHz, CD_3OD) spectrum of 5,7,2'-trihydroxy-3,4',5'-trimethoxyflavone (3.3).

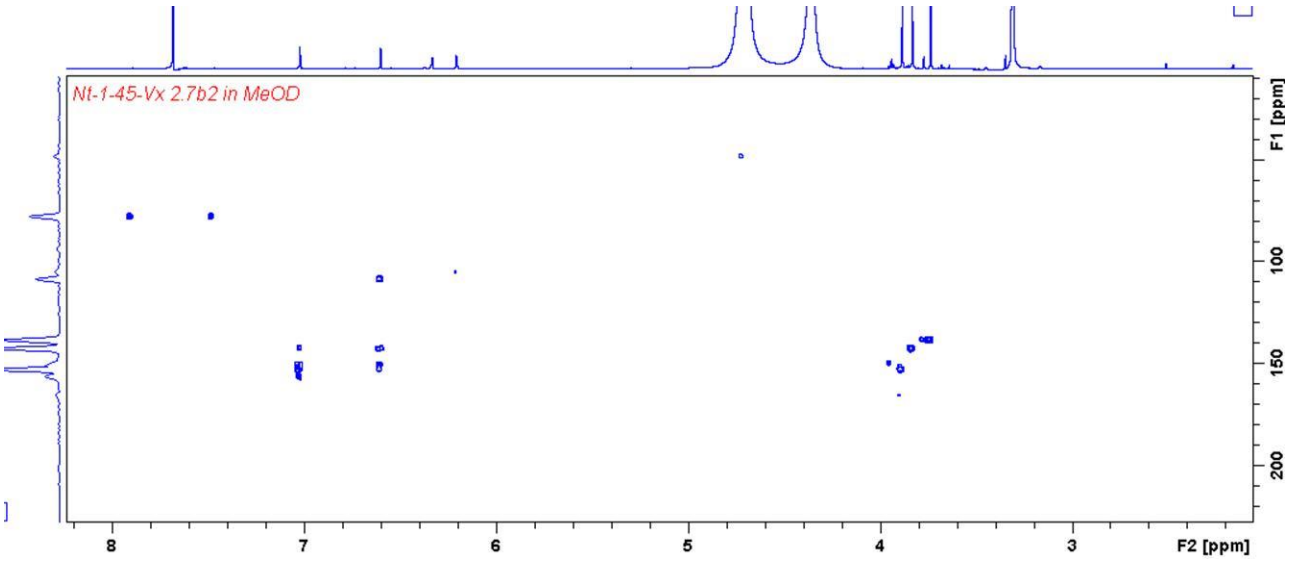

Plate 3.13: HMBC (400 MHz/100 MHz, CD_3OD) spectrum of 5,7,2'-trihydroxy-3,4',5'-trimethoxyflavone (3.3).

Elemental Composition Report Page 1

Single Mass Analysis
Tolerance = 5.0 PPM / DBE: min = -1.5, max = 50.0
Element prediction: Off
Number of isotope peaks used for i-FIT = 3

Monoisotopic Mass, Even Electron Ions
7 formula(e) evaluated with 1 results within limits (all results (up to 1000) for each mass)
Elements Used:
C: 15-20 H: 10-15 O: 0-10
VX 2_3a 8 (0.237) Cm (1:61)
TOF MS ES-

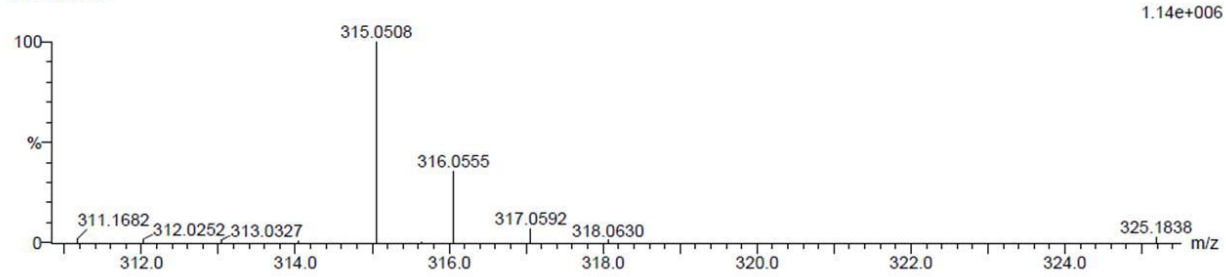

Minimum:				-1.5			
Maximum:		5.0	5.0	50.0			
Mass	Calc. Mass	mDa	PPM	DBE	i-FIT	i-FIT (Norm)	Formula
315.0508	315.0505	0.3	1.0	11.5	53.0	0.0	C16 H11 O7

Plate 3.14: HRESIMS of 3-*O*-methylquercetin (3.4).

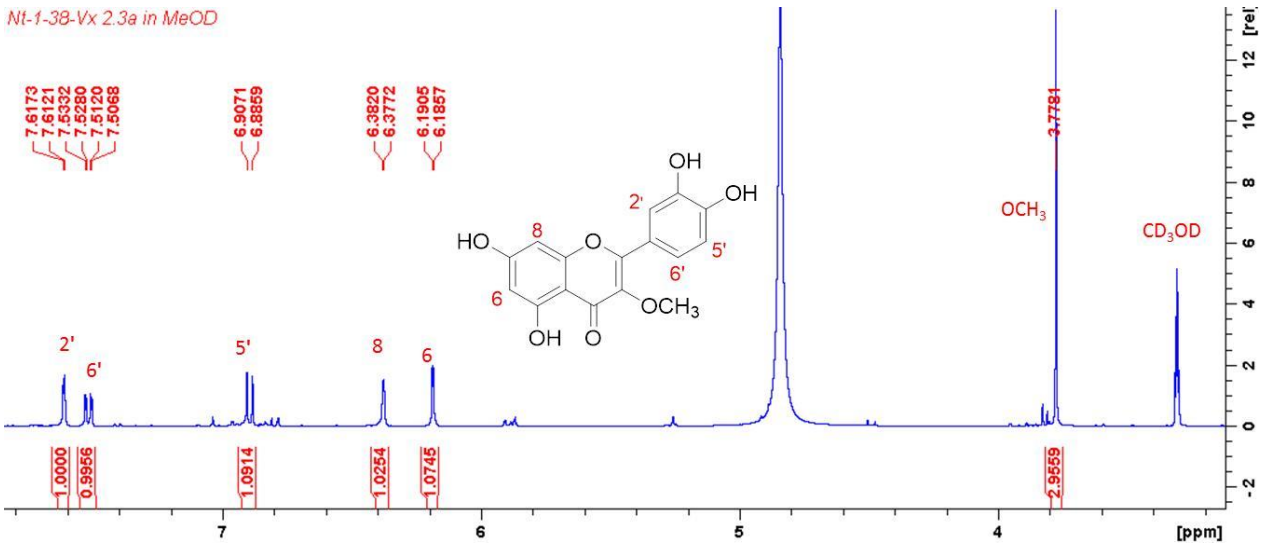

Plate 3. 15: ^{1}H NMR (500 MHz, CD_3OD) spectrum of 3-*O*-methylquercetin (3.4).

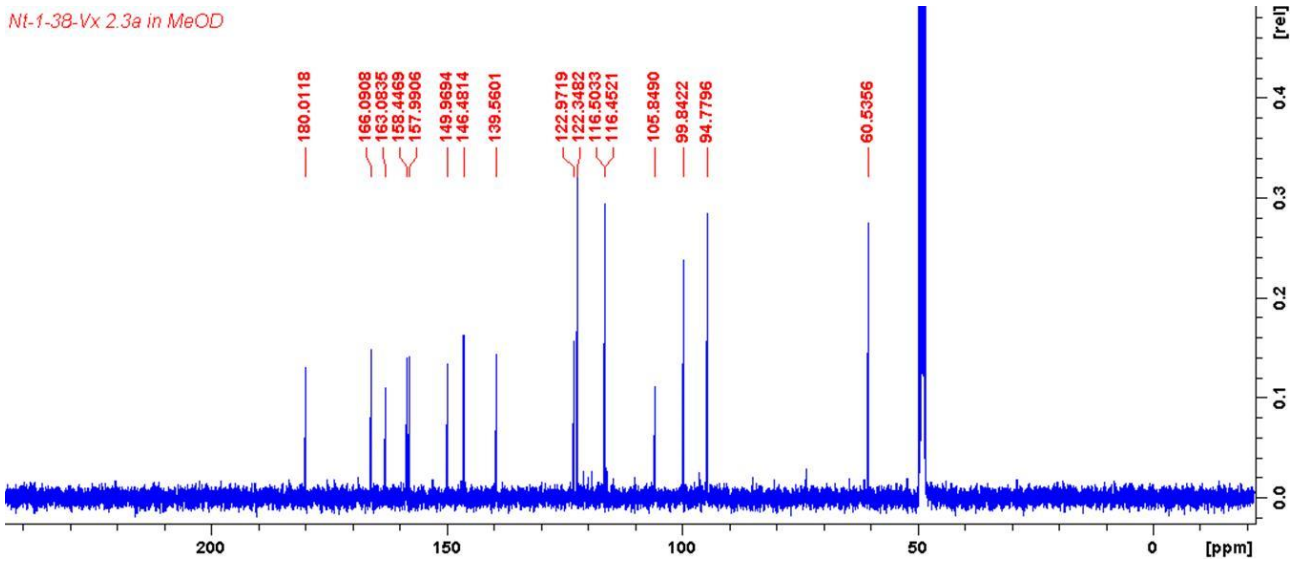

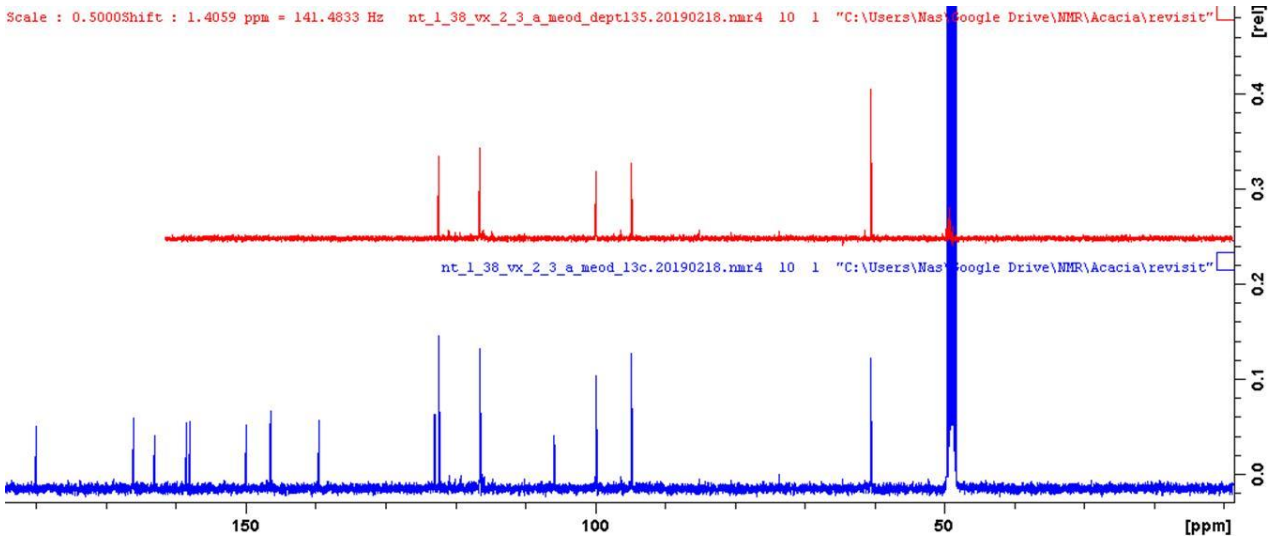

Plate 3.16: ^{13}C and DEPT (125 MHz, CD_3OD) spectra of 3-*O*-methylquercetin (3.4).

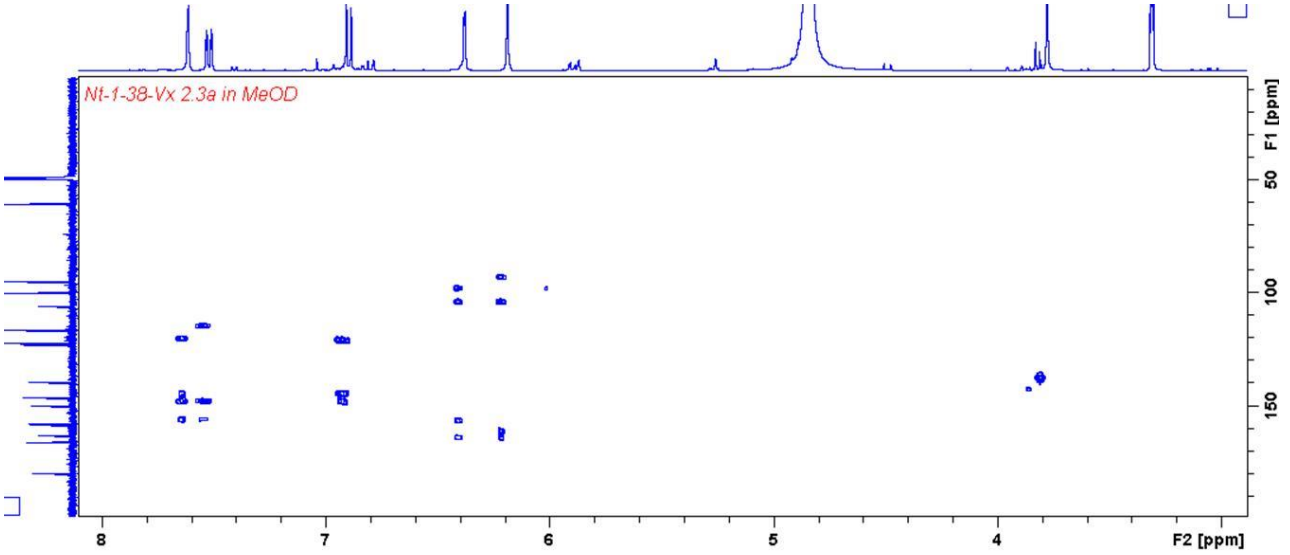

Plate 3.17: HMBC (500 MHz/125 MHz, CD_3OD) spectrum of 3-*O*-methylquercetin (3.4).

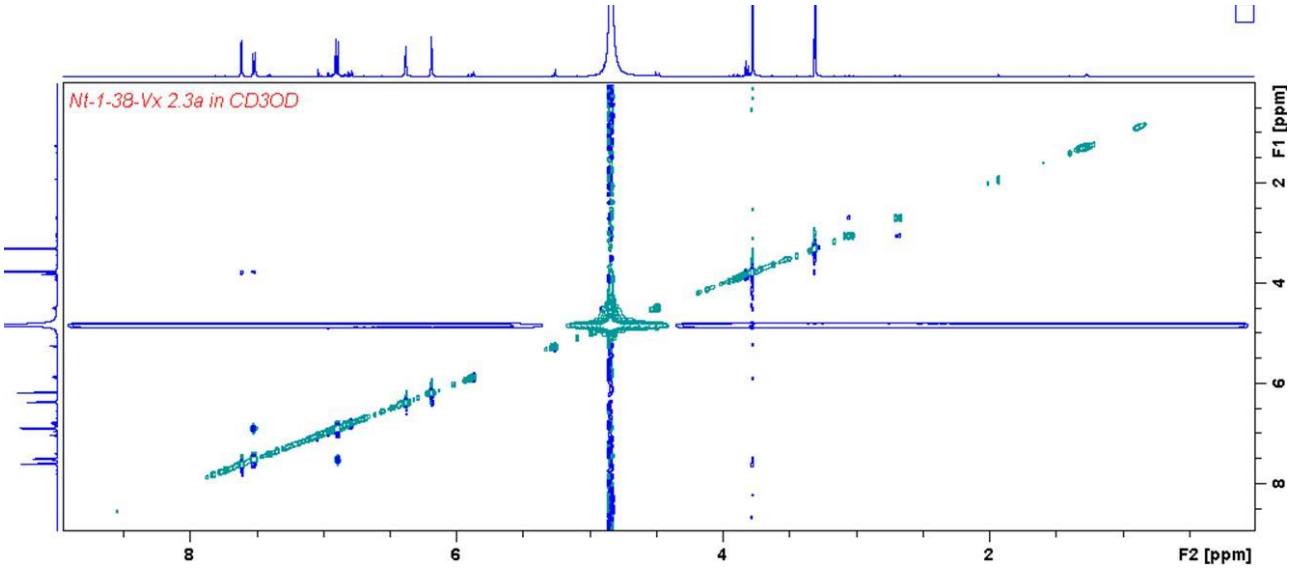

Plate 3.18: NOESY (500 MHz, CD_3OD) spectrum of 3-*O*-methylquercetin (3.4).

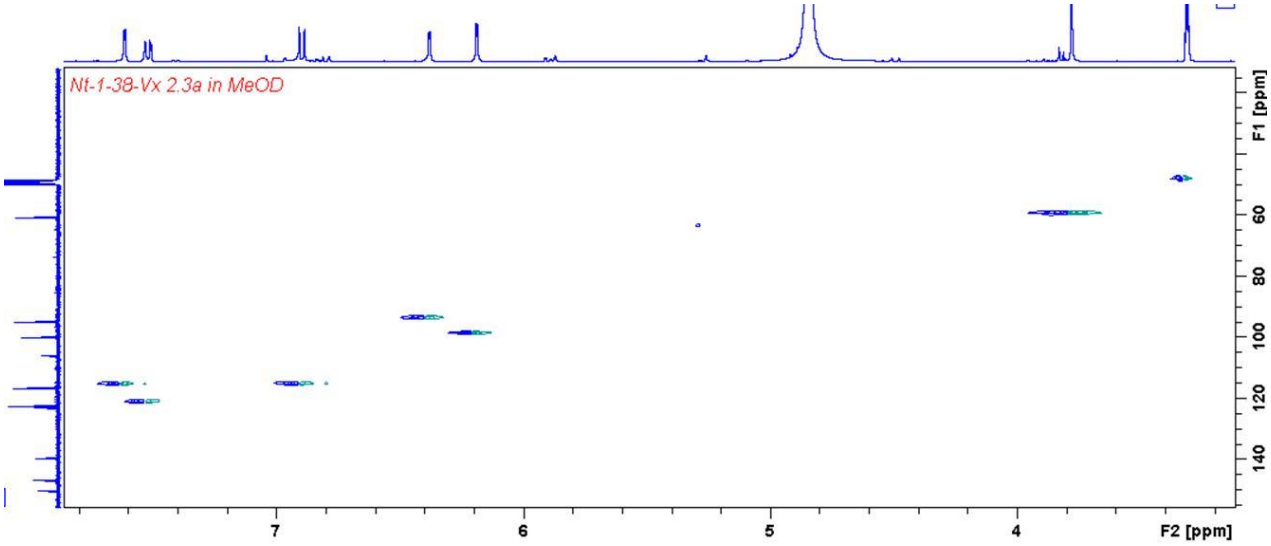

Plate 3.19: HSQC (500 MHz/125 MHz, CD_3OD) spectrum of 3-*O*-methylquercetin (3.4).

Elemental Composition Report **Page 1**

Single Mass Analysis
Tolerance = 5.0 PPM / DBE: min = -1.5, max = 50.0
Element prediction: Off
Number of isotope peaks used for i-FIT = 3

Monoisotopic Mass, Even Electron Ions
8 formula(e) evaluated with 1 results within limits (all results (up to 1000) for each mass)
Elements Used:
C: 10-15 H: 5-10 O: 0-10
VX 2_2 36 (1.181) Cm (1:61)
TOF MS ES-

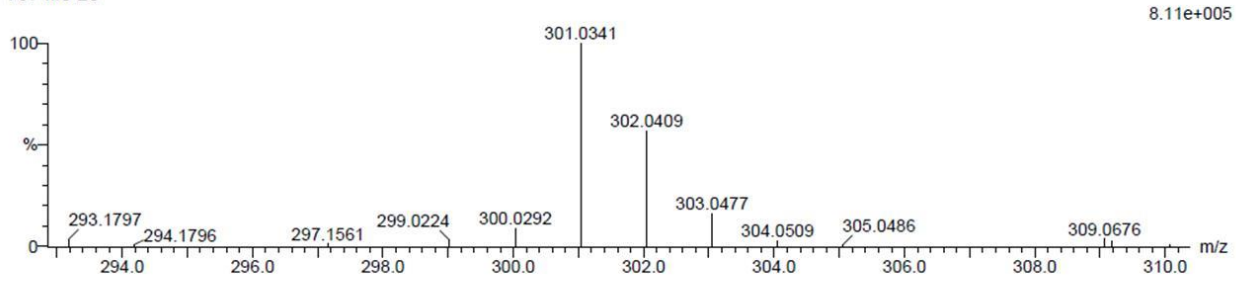

Minimum:				-1.5			
Maximum:		5.0	5.0	50.0			
Mass	Calc. Mass	mDa	PPM	DBE	i-FIT	i-FIT (Norm)	Formula
301.0341	301.0348	-0.7	-2.3	11.5	43.0	0.0	C15 H9 O7

Plate 3.20: HRESIMS of quercetin (3.5).

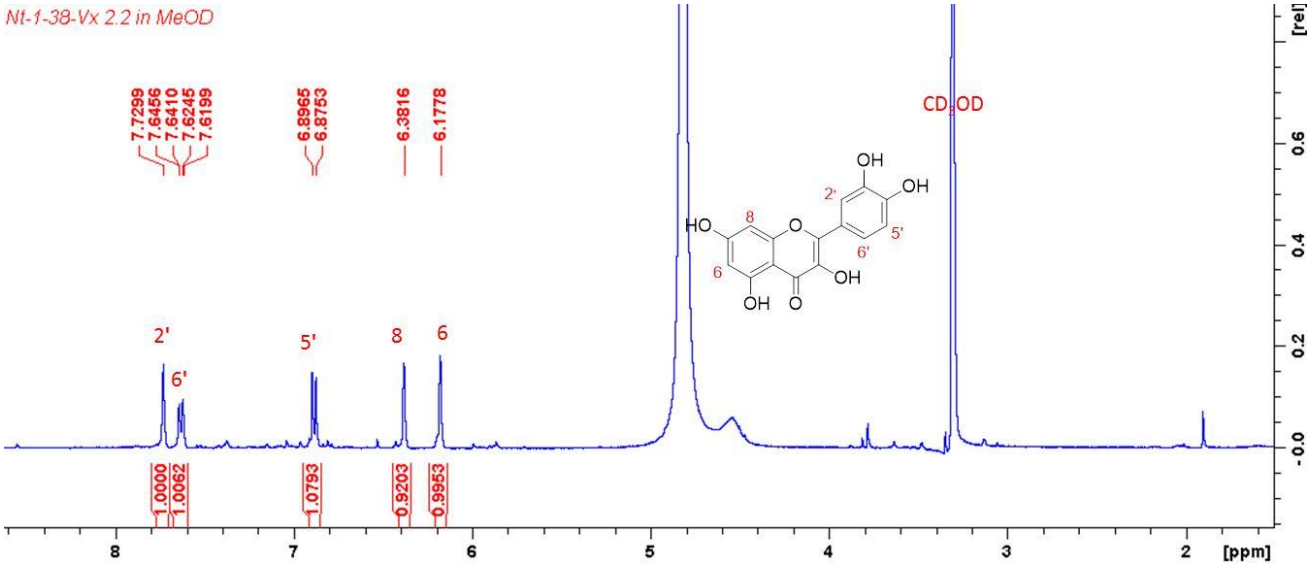

Plate 3.21: ^{1}H NMR (400 MHz, CD_3OD) spectrum of quercetin (3.5).

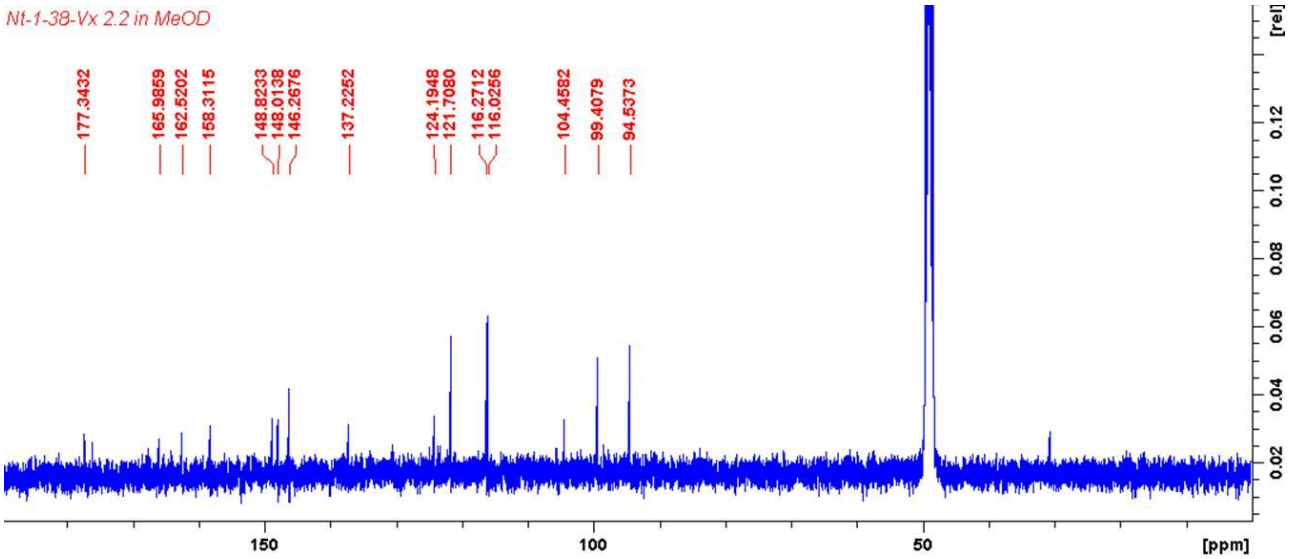

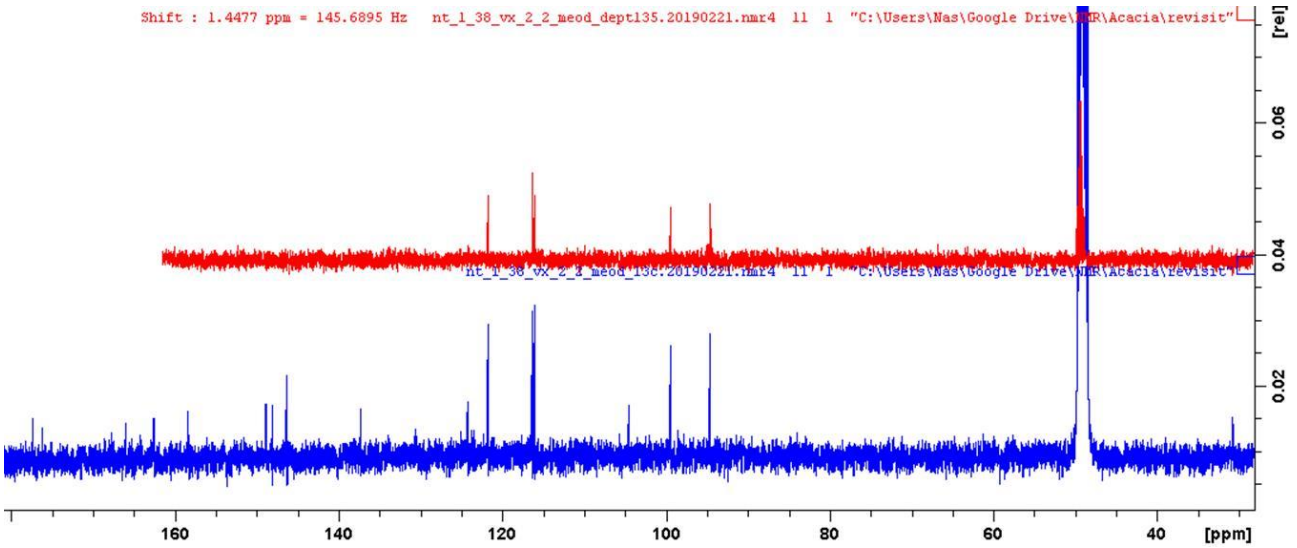

Plate 3.22: ^{13}C and DEPT (100 MHz, CD_3OD) spectra of quercetin (3.5).

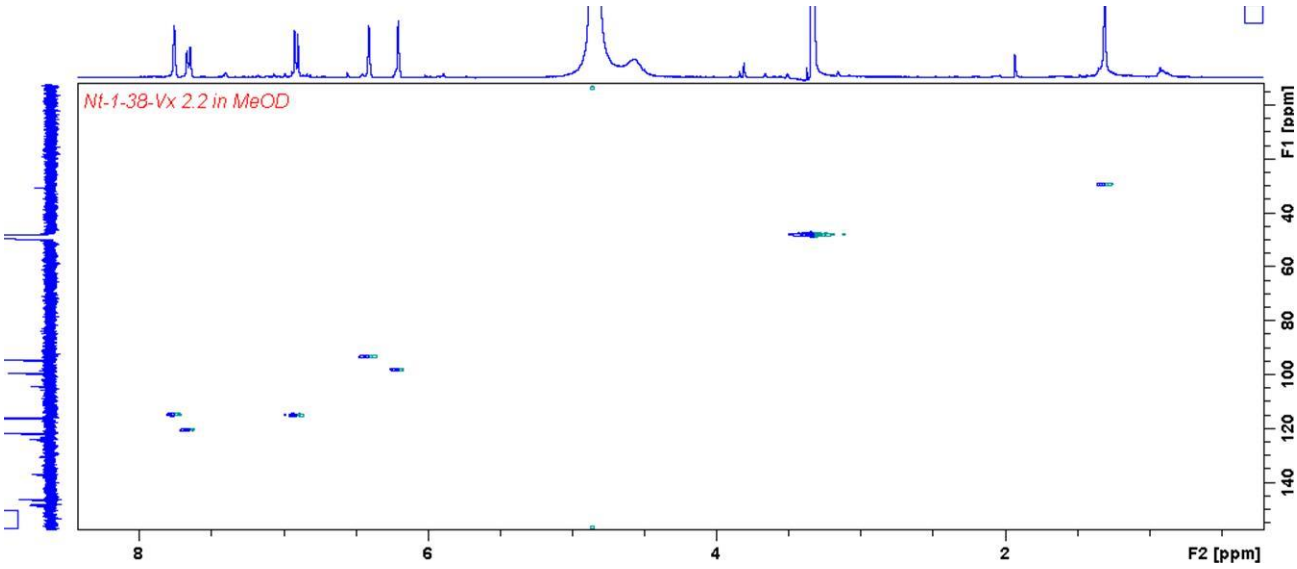

Plate 3.23: HSQC (400 MHz/100 MHz, CD_3OD) spectrum of quercetin (3.5).

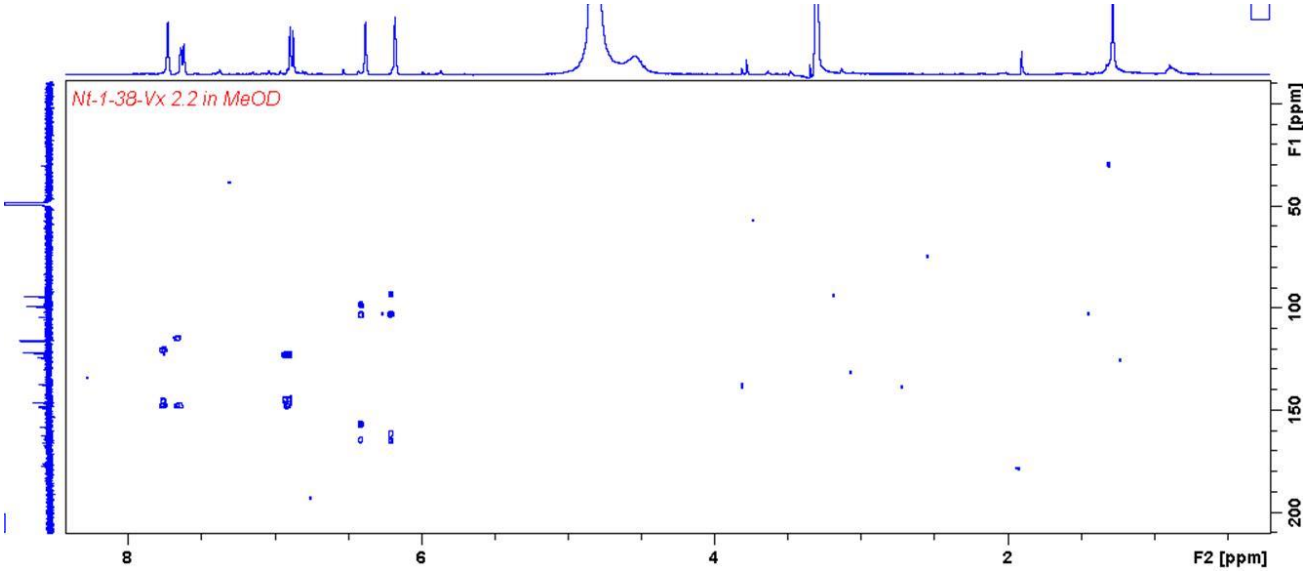

Plate 3.24: HMBC (400 MHz/100 MHz, CD_3OD) spectrum of quercetin (3.5).

Elemental Composition Report **Page 1**

Single Mass Analysis
Tolerance = 5.0 PPM / DBE: min = -1.5, max = 50.0
Element prediction: Off
Number of isotope peaks used for i-FIT = 3

Monoisotopic Mass, Even Electron Ions
4 formula(e) evaluated with 1 results within limits (all results (up to 1000) for each mass)
Elements Used:
C: 15-20 H: 10-15 O: 5-10
NT-1-VX 2_1 57 (1.967) Cm (1:58)
TOF MS ES-

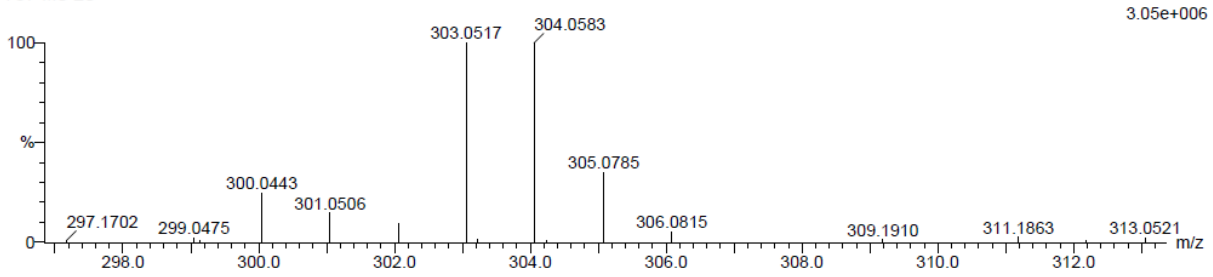

Minimum:				-1.5			
Maximum:		5.0	5.0	50.0			
Mass	Calc. Mass	mDa	PPM	DBE	i-FIT	i-FIT (Norm)	Formula
303.0517	303.0505	1.2	4.0	10.5	93.8	0.0	C15 H11 O7

Plate 3.25: HRESIMS of dihydroquercetin (3.6).

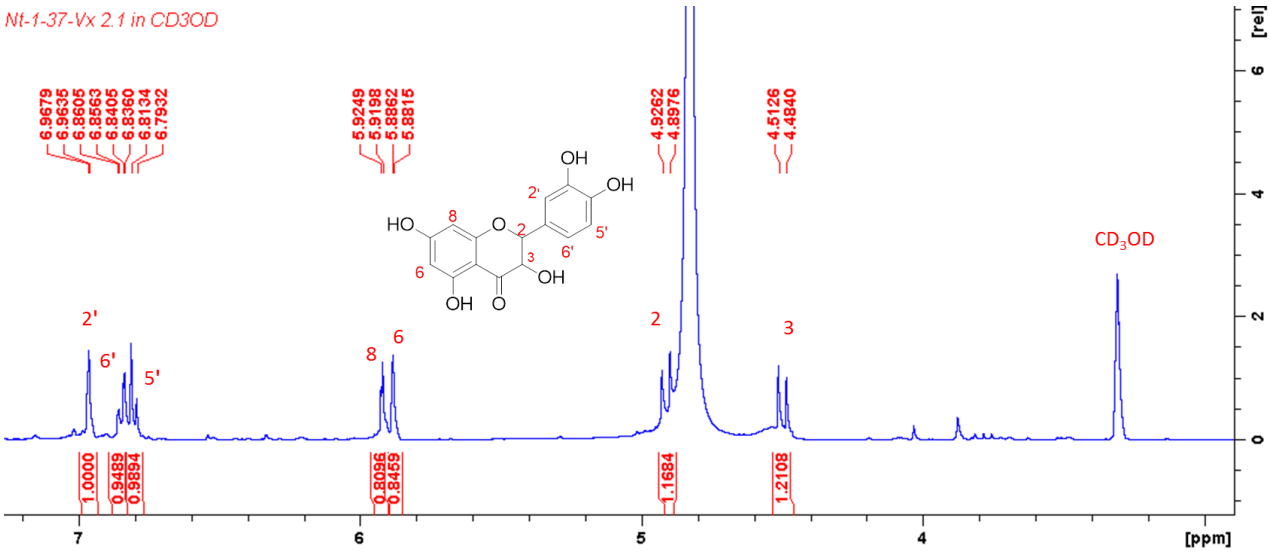

Plate 3.26: ^{1}H NMR (400 MHz, CD_3OD) spectrum of dihydroquercetin (3.6).

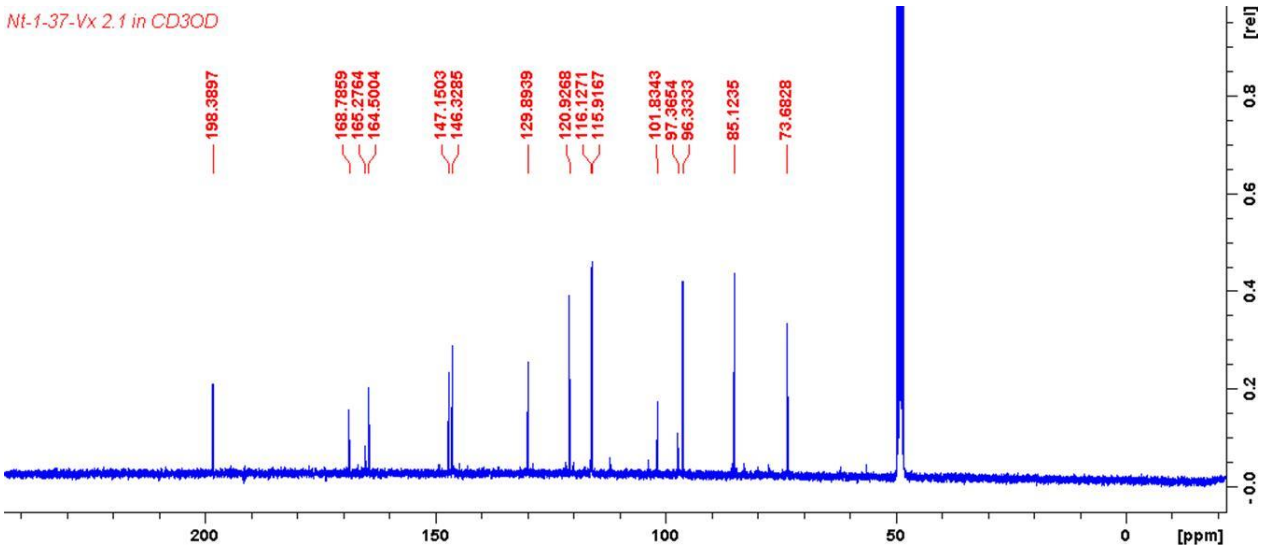

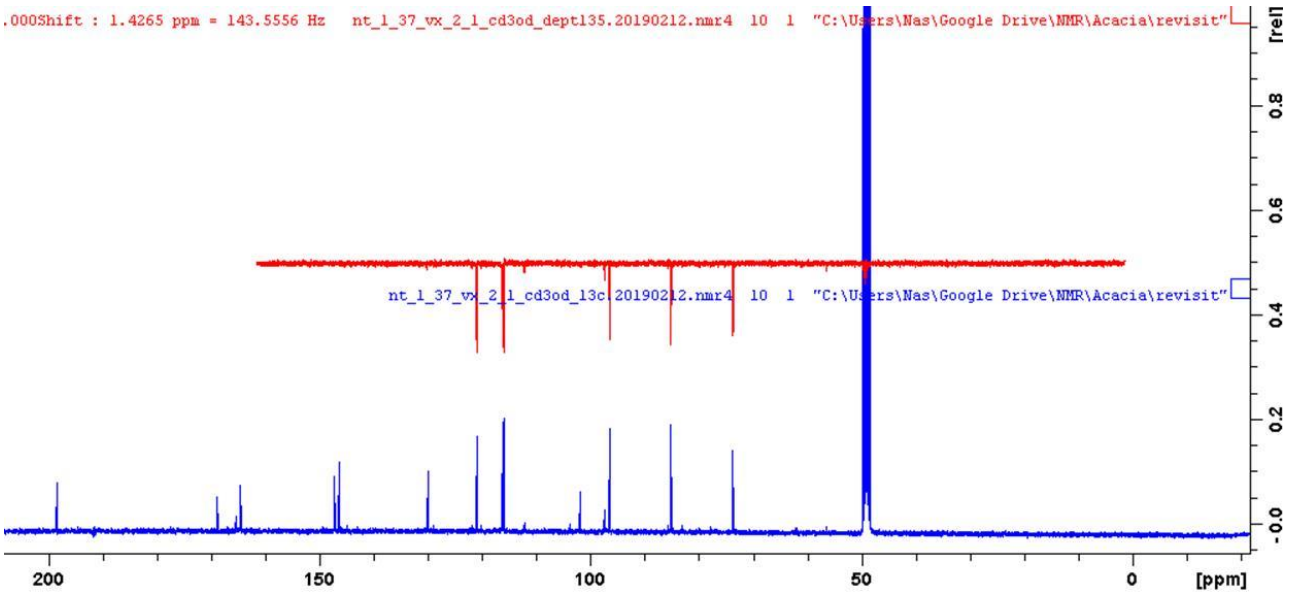

Plate 3.27: ^{13}C and DEPT (100 MHz, CD_3OD) spectra of dihydroquercetin (3.6).

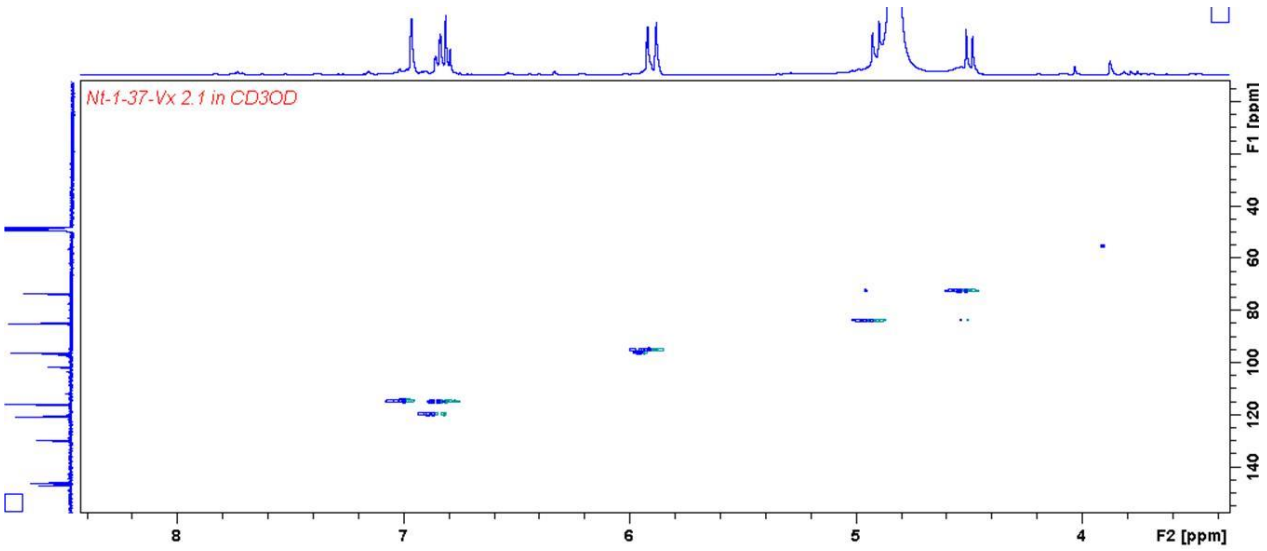

Plate 3.28: HSQC (400 MHz/100 MHz, CD_3OD) spectrum of dihydroquercetin (3.6).

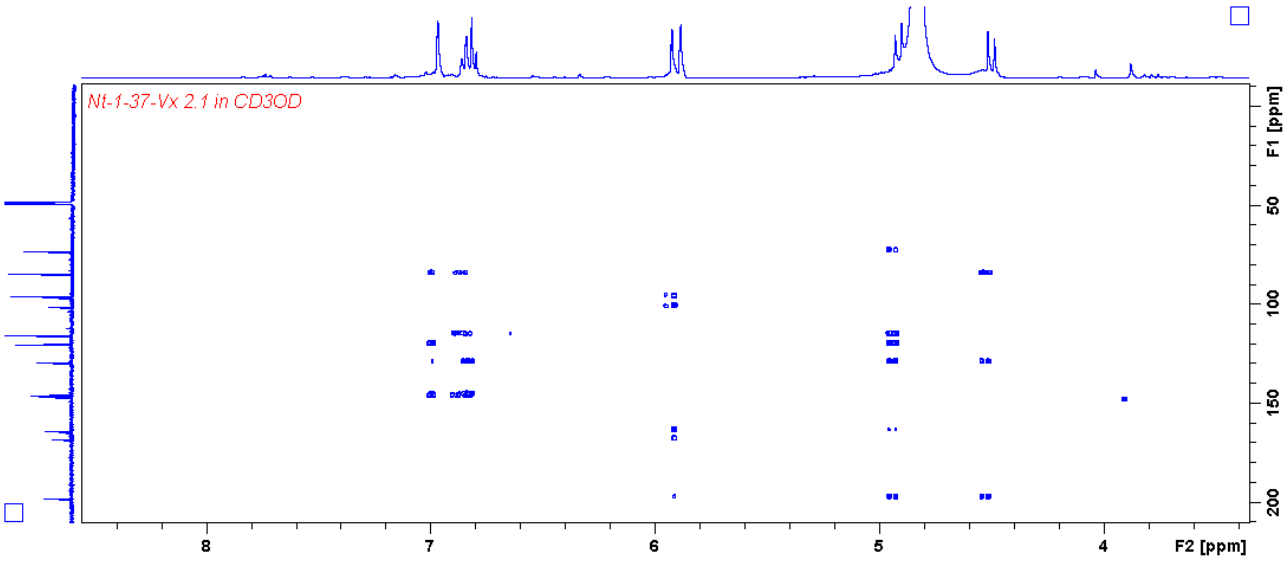

Plate 3.29: HMBC (400 MHz/100 MHz, CD_3OD) spectrum of dihydroquercetin (3.6).

Elemental Composition Report Page 1

Single Mass Analysis
Tolerance = 5.0 PPM / DBE: min = -1.5, max = 100.0
Element prediction: Off
Number of isotope peaks used for i-FIT = 3

Monoisotopic Mass, Even Electron Ions
2 formula(e) evaluated with 1 results within limits (all results (up to 1000) for each mass)
Elements Used:
C: 10-15 H: 10-15 O: 5-10
VX 2_9 3 (0.068) Cm (1:61)
TOF MS ES-

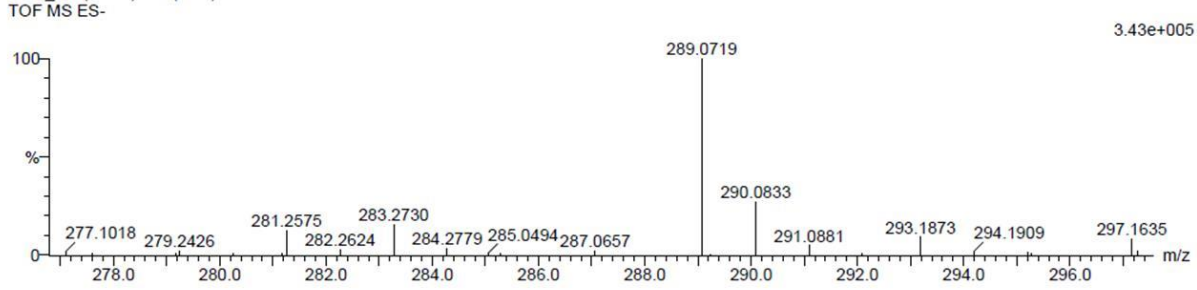

Minimum:				-1.5			
Maximum:		5.0	5.0	100.0			
Mass	Calc. Mass	mDa	PPM	DBE	i-FIT	i-FIT (Norm)	Formula
289.0719	289.0712	0.7	2.4	9.5	50.4	0.0	C15 H13 O6

Plate 3.30: HRESIMS of catechin (3.7).

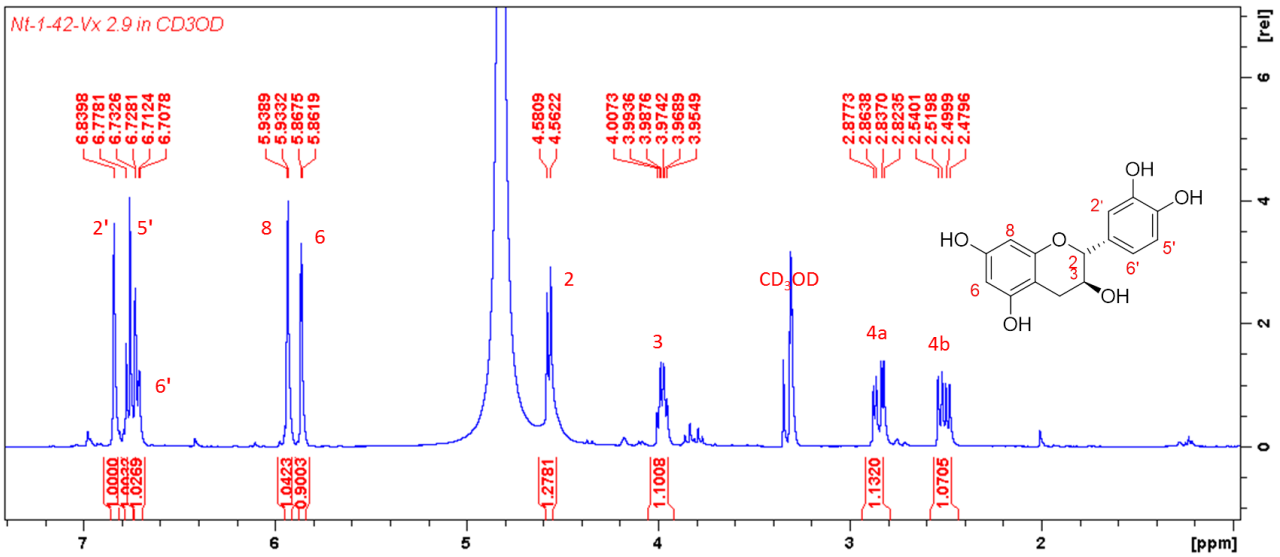

Plate 3.31: ^{1}H NMR (400 MHz, CD_3OD) spectrum of catechin (3.7).

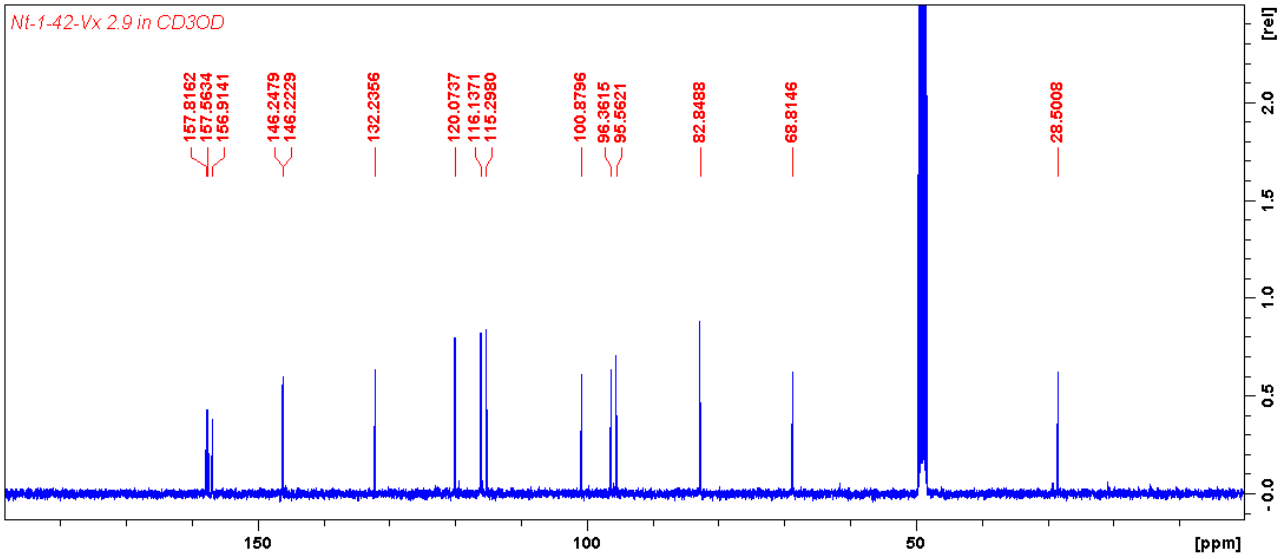

Plate 3.32: ^{13}C NMR (100 MHz, CD_3OD) spectra of catechin (3.7).

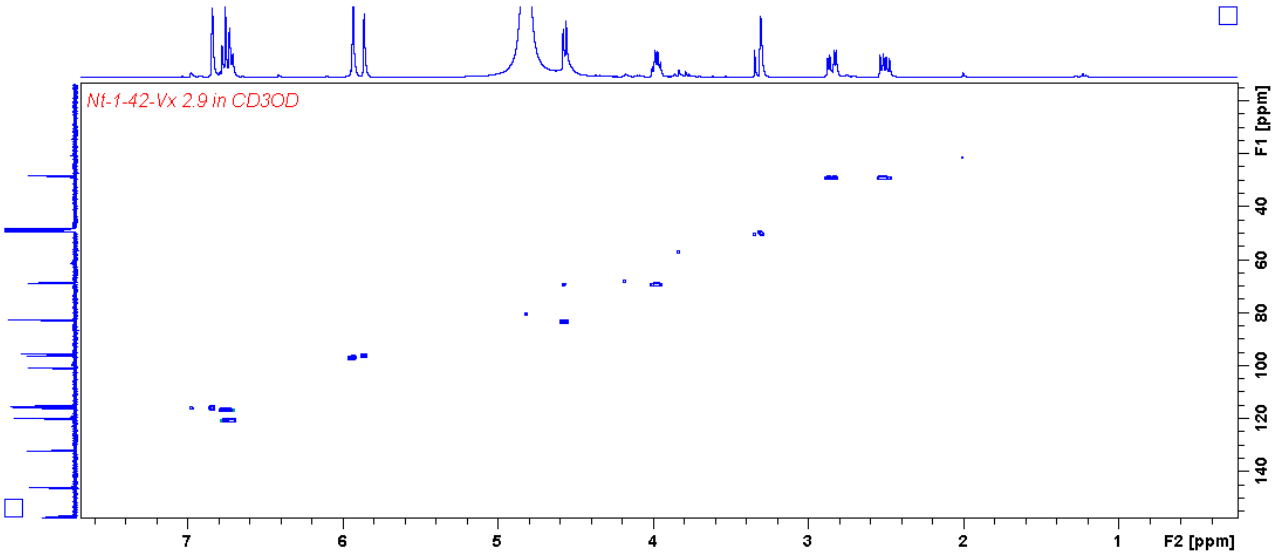

Plate 3.33: HSQC (400 MHz/100 MHz, CD_3OD) spectrum of catechin (3.7).

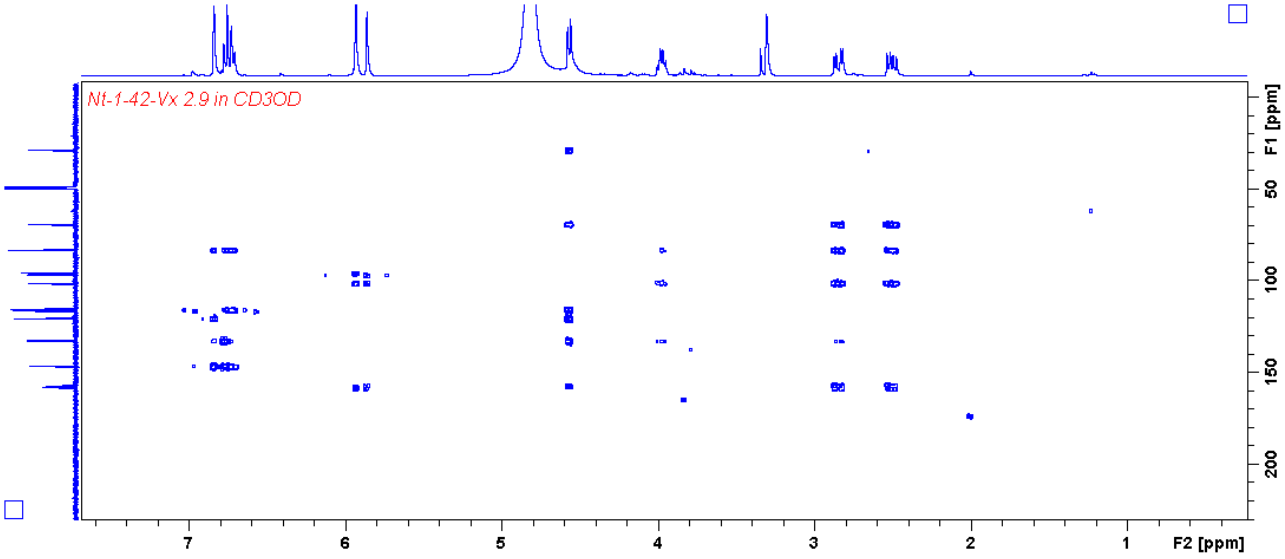

Plate 3.34: HMBC (400 MHz/100 MHz, CD_3OD) spectrum of catechin (3.7).

Elemental Composition Report Page 1

Single Mass Analysis
Tolerance = 5.0 PPM / DBE: min = -1.5, max = 100.0
Element prediction: Off
Number of isotope peaks used for i-FIT = 3

Monoisotopic Mass, Even Electron Ions
2 formula(e) evaluated with 1 results within limits (all results (up to 1000) for each mass)
Elements Used:
C: 10-15 H: 10-15 O: 5-10
Vx 2_9a 59 (1.956) Cm (1:61)
TOF MS ES-

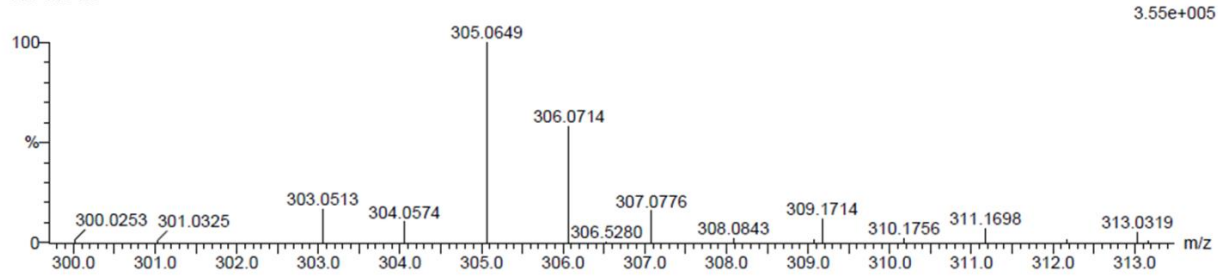

Minimum:				-1.5			
Maximum:		5.0	5.0	100.0			
Mass	Calc. Mass	mDa	PPM	DBE	i-FIT	i-FIT (Norm)	Formula
305.0649	305.0661	-1.2	-3.9	9.5	54.0	0.0	C15 H13 O7

Plate 3.35: HRESIMS of gallocatechin (3.8).

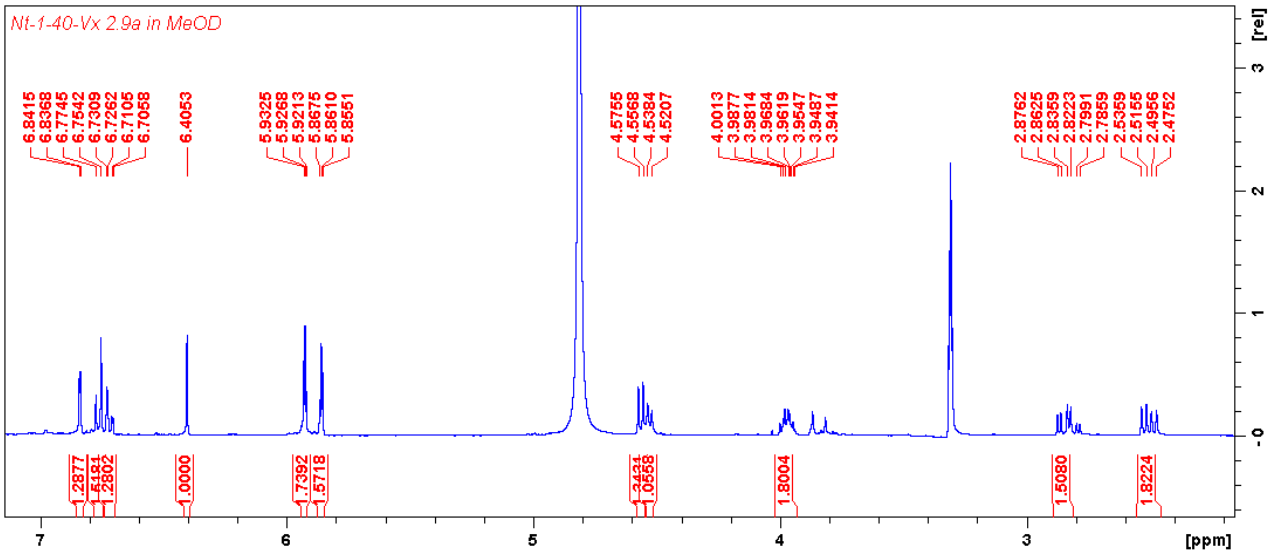

^{1}H NMR (400 MHz, CD_3OD) spectrum of gallocatechin 3.8 and catechin (3.7).

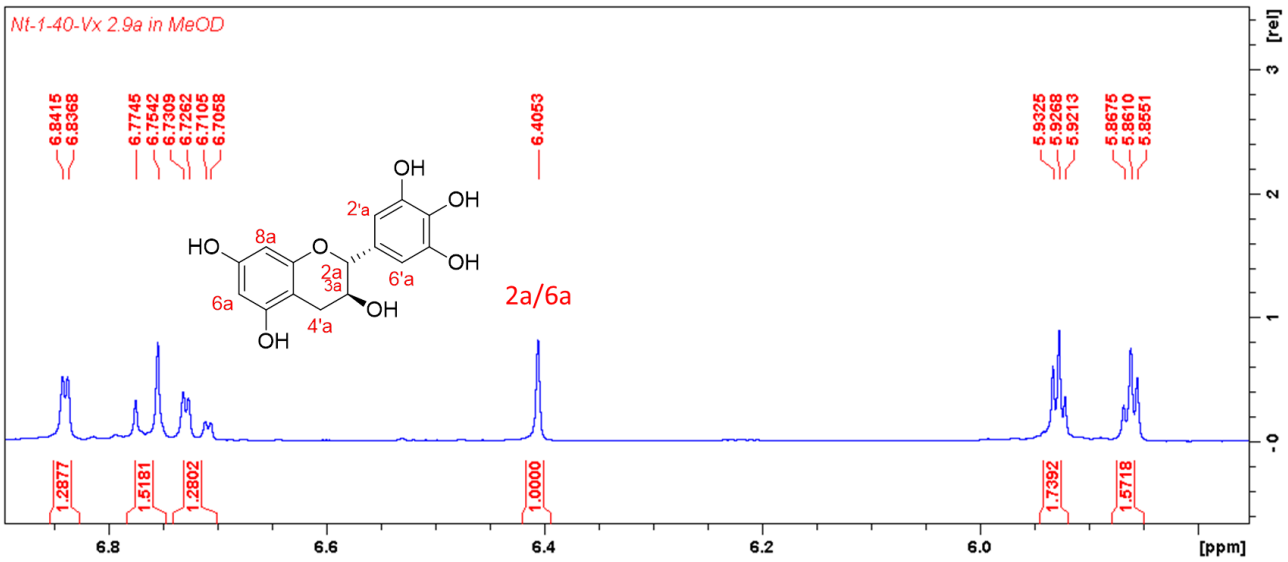

Plate 3.36: ^{1}H NMR (400 MHz, CD_3OD) spectrum (expansion of aromatic region) of gallocatechin (3.8) and catechin (3.7).

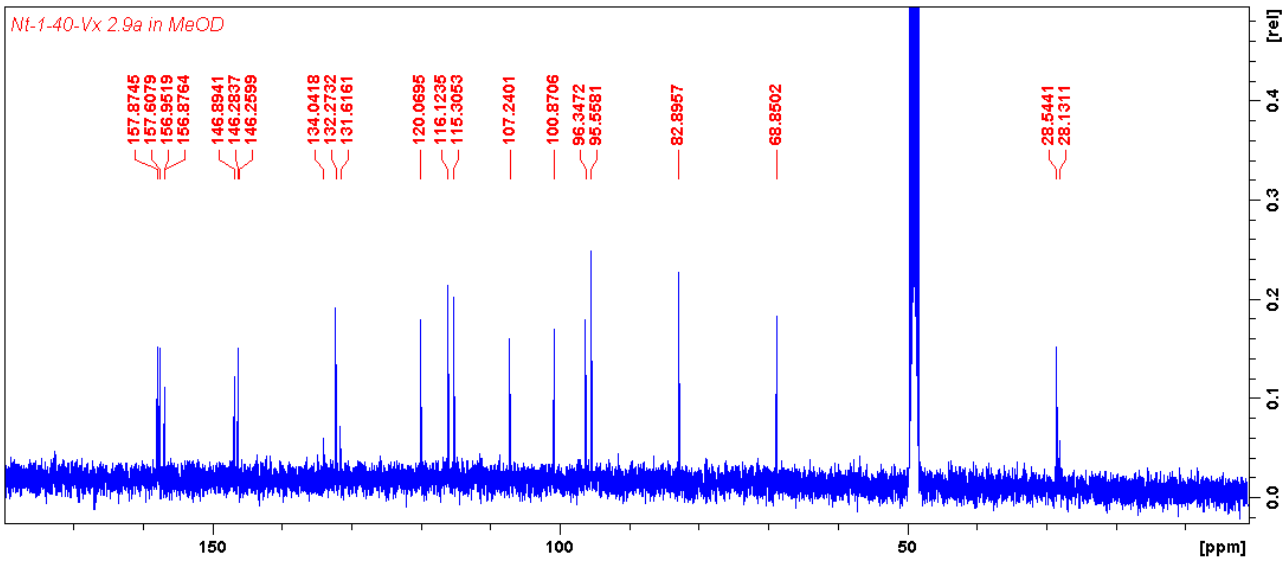

Plate 3.37: ^{13}C NMR (100 MHz, CD_3OD) spectrum of gallocatechin (3.8) and catechin (3.7).

Elemental Composition Report **Page 1**

Single Mass Analysis
Tolerance = 5.0 PPM / DBE: min = -1.5, max = 50.0
Element prediction: Off
Number of isotope peaks used for i-FIT = 3

Monoisotopic Mass, Even Electron Ions
3 formula(e) evaluated with 1 results within limits (all results (up to 1000) for each mass)
Elements Used:
C: 5-10 H: 5-10 O: 0-5
NT-1-VX 2_4 57 (1.967) Cm (1:58)
TOF MS ES-

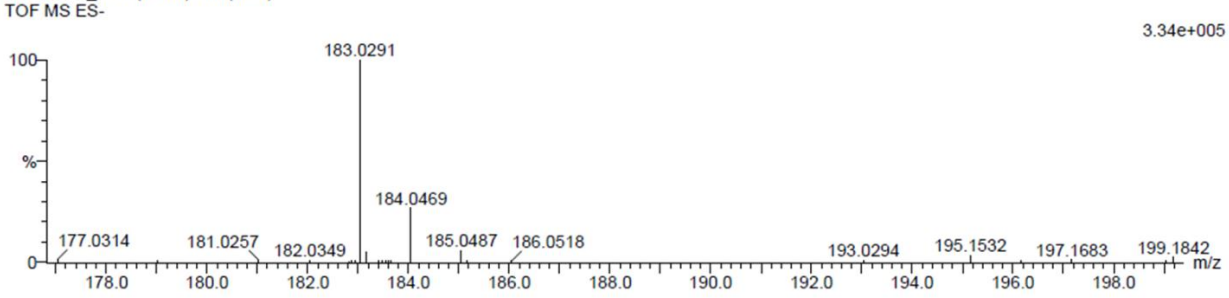

Minimum:				-1.5			
Maximum:		5.0	5.0	50.0			
Mass	Calc. Mass	mDa	PPM	DBE	i-FIT	i-FIT (Norm)	Formula
183.0291	183.0293	-0.2	-1.1	5.5	147.3	0.0	C8 H7 O5

Plate 3.38: HRESIMS of methyl gallate (3.9).

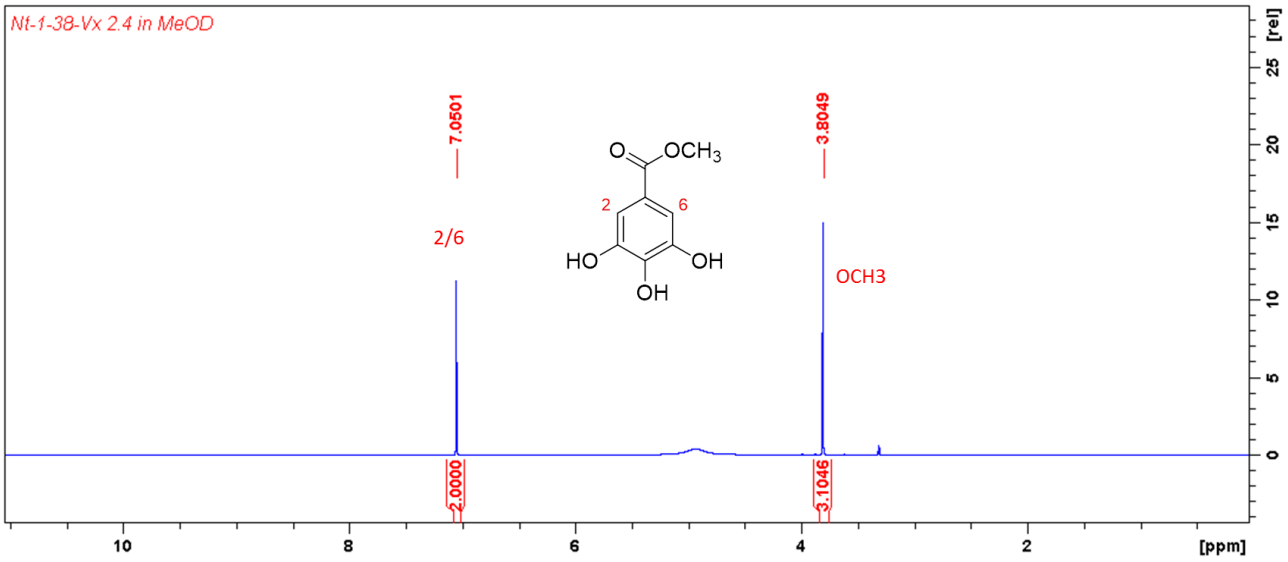

Plate 3.39: ^{1}H NMR (400 MHz, CD_3OD) spectrum of methyl gallate (3.9).

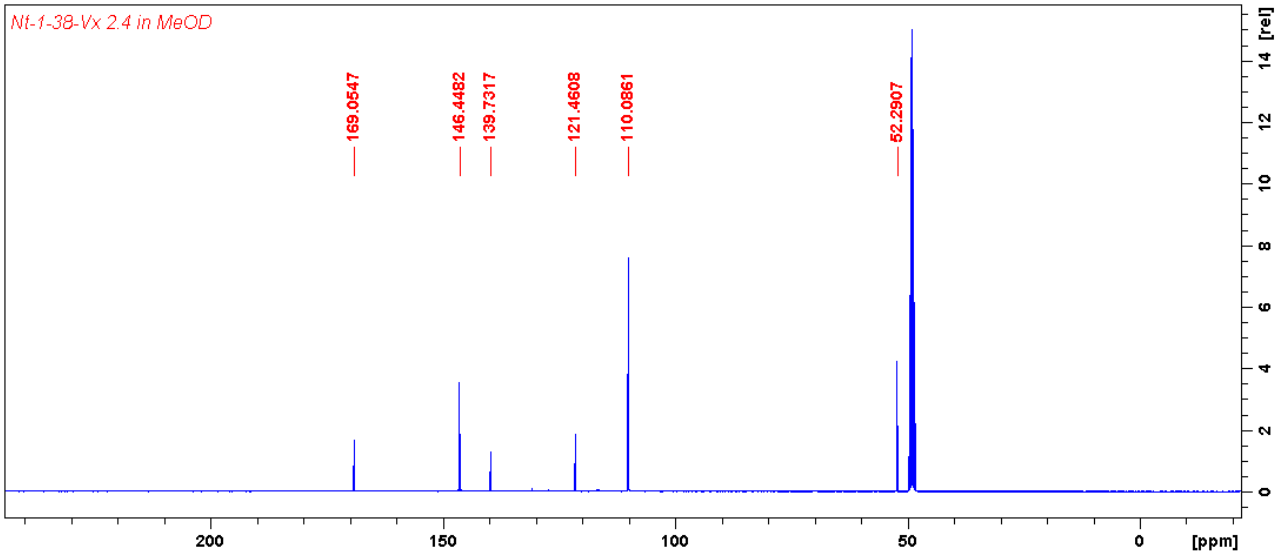

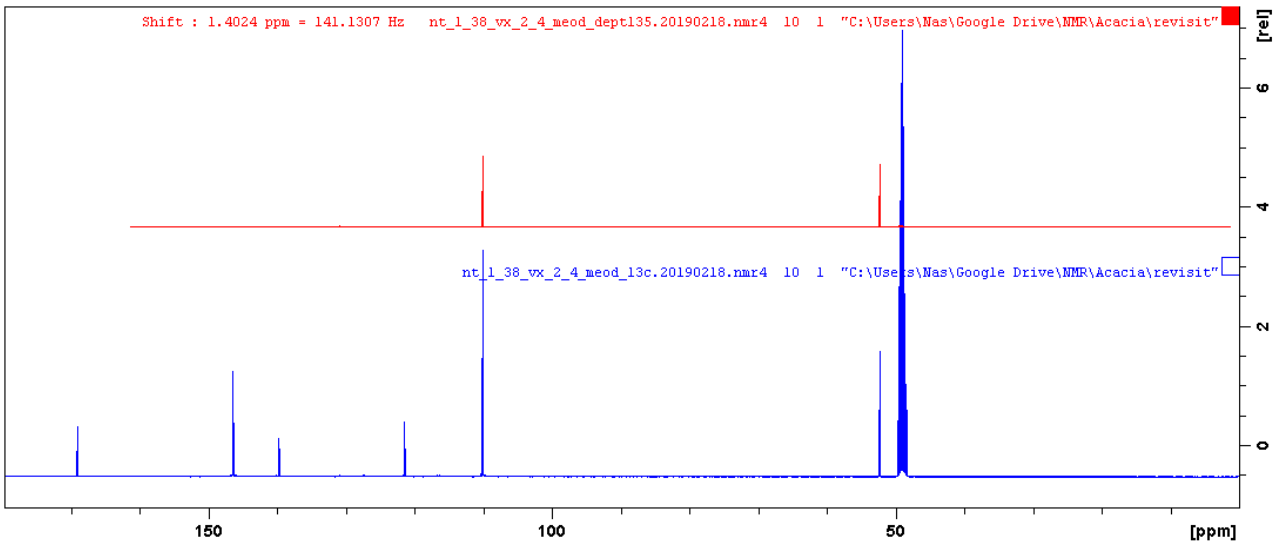

Plate 3.40: ^{13}C and DEPT (100 MHz, CD_3OD) spectra of methyl gallate (3.9).

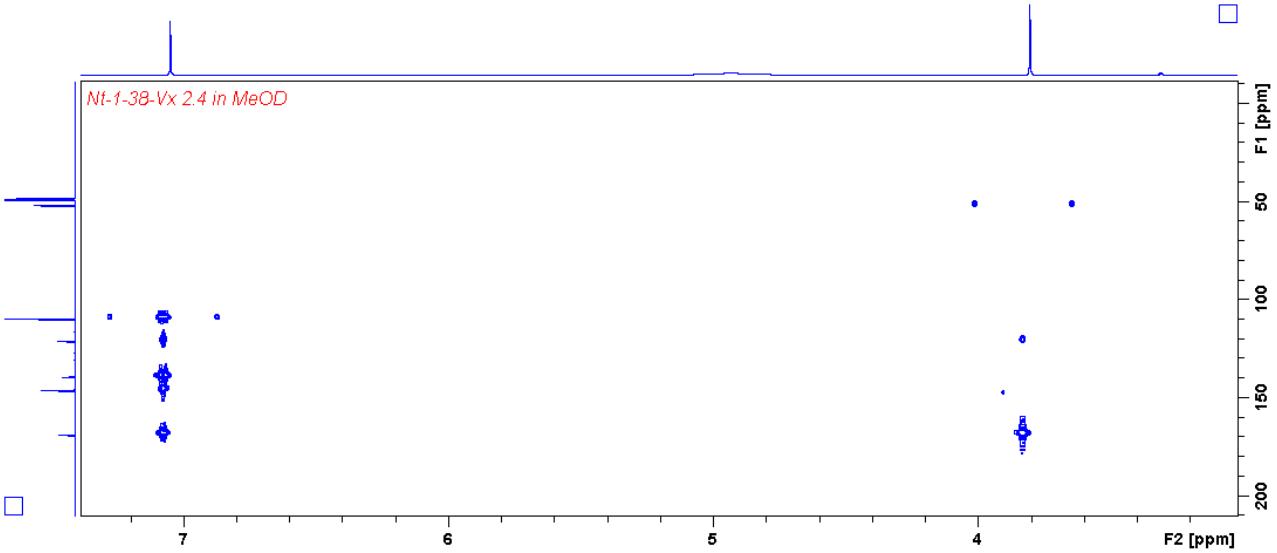

Plate 3.41: HMBC (400 MHz/100 MHz, CD_3OD) spectrum of methyl gallate (3.9).

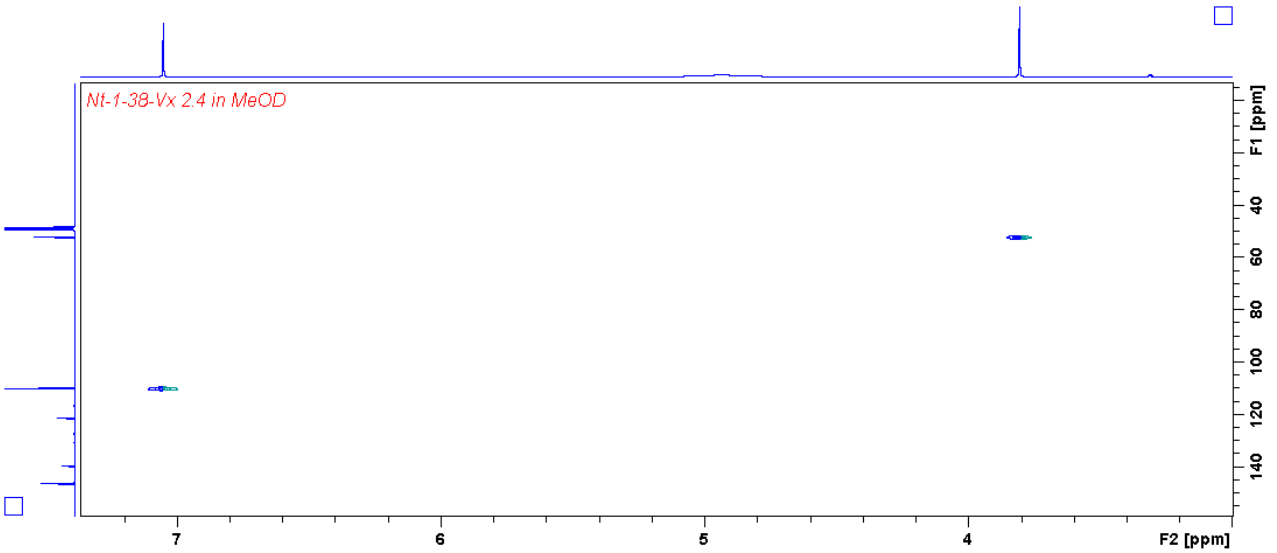

Plate 3.42: HSQC (400 MHz/100 MHz, CD_3OD) spectrum of methyl gallate (3.9).

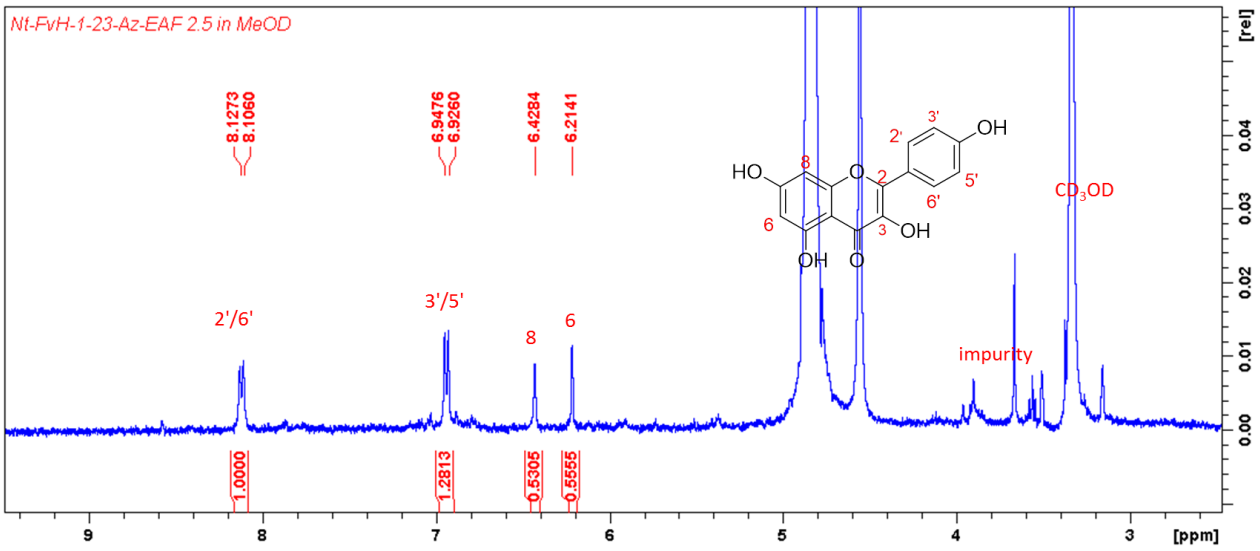

Plate 3. 43: ^{1}H NMR (400 MHz, CD_3OD) spectrum of kaempferol (3.10).

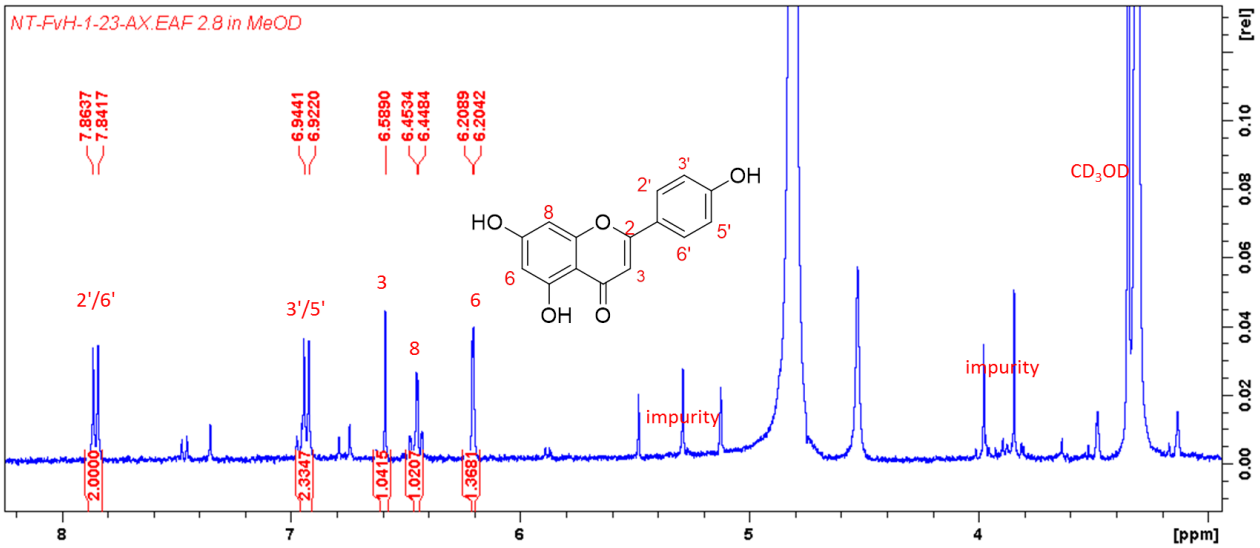

Plate 3. 44: ^{1}H NMR (400 MHz, CD_3OD) spectrum of apigenin (3.11).

Elemental Composition Report **Page 1**

Single Mass Analysis
Tolerance = 5.0 PPM / DBE: min = -1.5, max = 100.0
Element prediction: Off
Number of isotope peaks used for i-FIT = 3

Monoisotopic Mass, Even Electron Ions
5 formula(e) evaluated with 1 results within limits (all results (up to 1000) for each mass)
Elements Used:
C: 20-25 H: 20-25 O: 5-10
Vx 2,7b1 47 (1.552) Cm (1:61)
TOF MS ES-

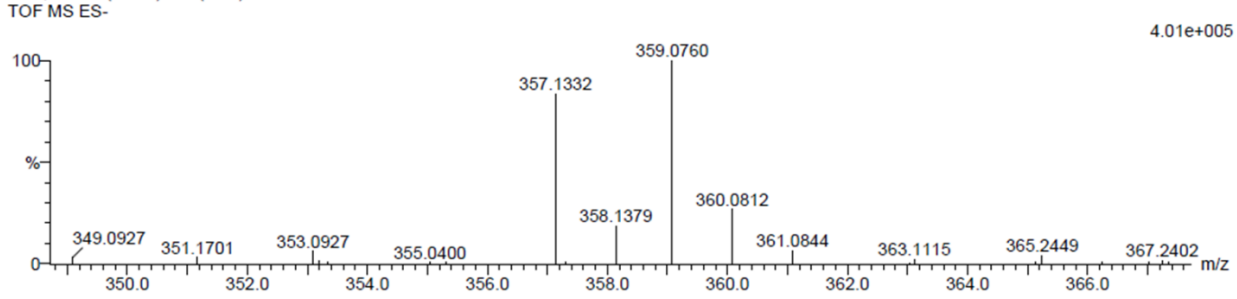

Minimum:				-1.5			
Maximum:		5.0	5.0	100.0			
Mass	Calc. Mass	mDa	PPM	DBE	i-FIT	i-FIT (Norm)	Formula
357.1332	357.1338	-0.6	-1.7	10.5	66.3	0.0	C20 H21 O6

Plate 3.45: HRESIMS of pinoresinol (3.12).

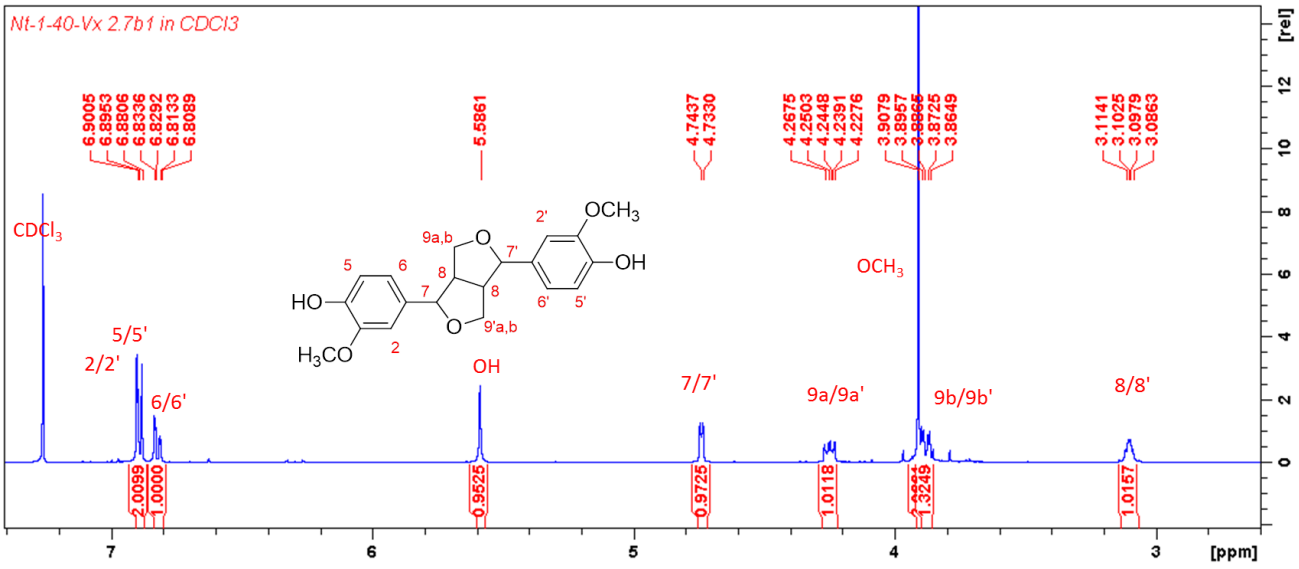

Plate 3.46: ^{1}H NMR (400 MHz, $CDCl_3$) spectrum of pinoresinol (3.12).

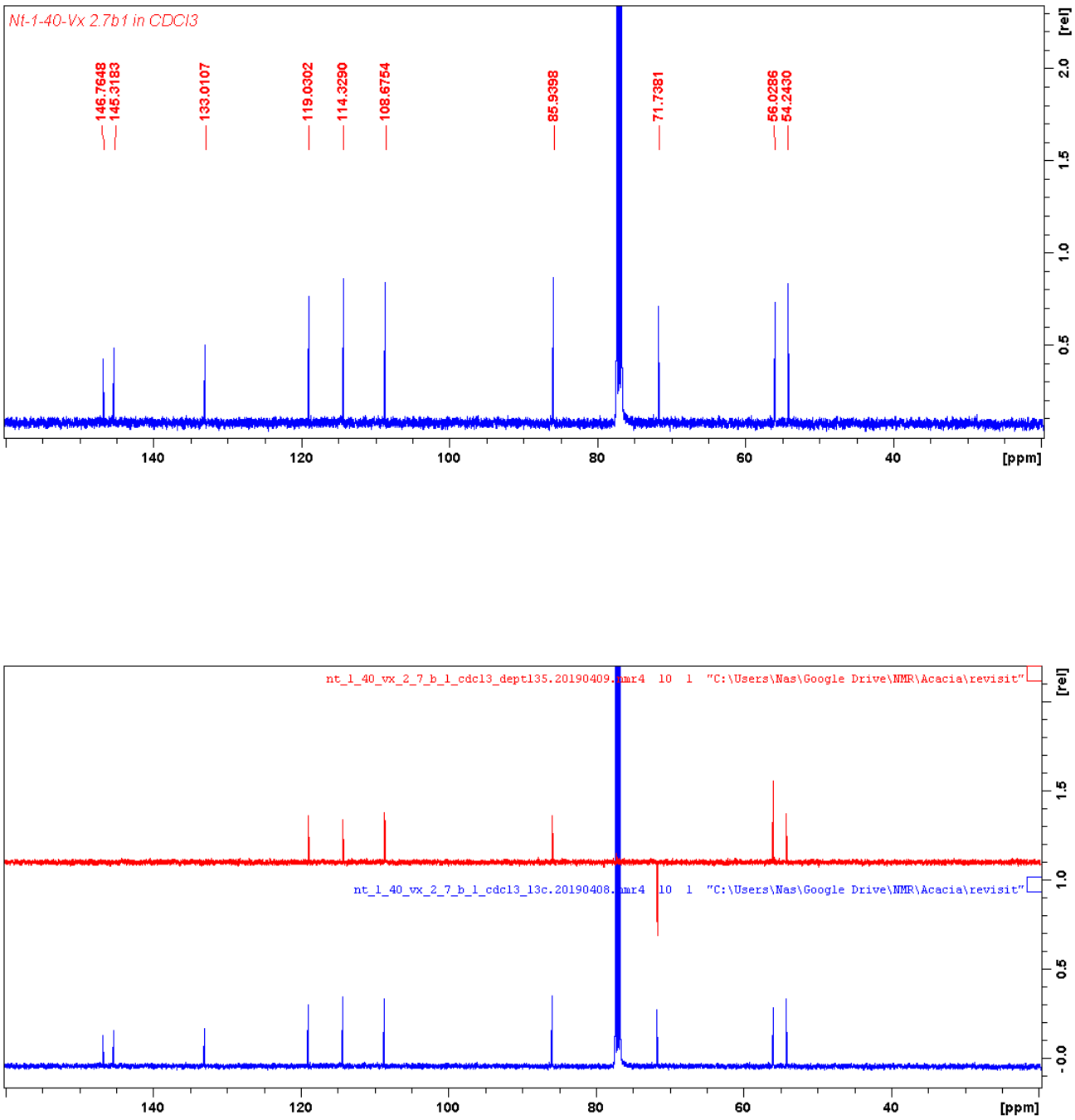

Plate 3.47: ^{13}C and DEPT (100 MHz, $CDCl_3$) spectra of pinoresinol (3.12).

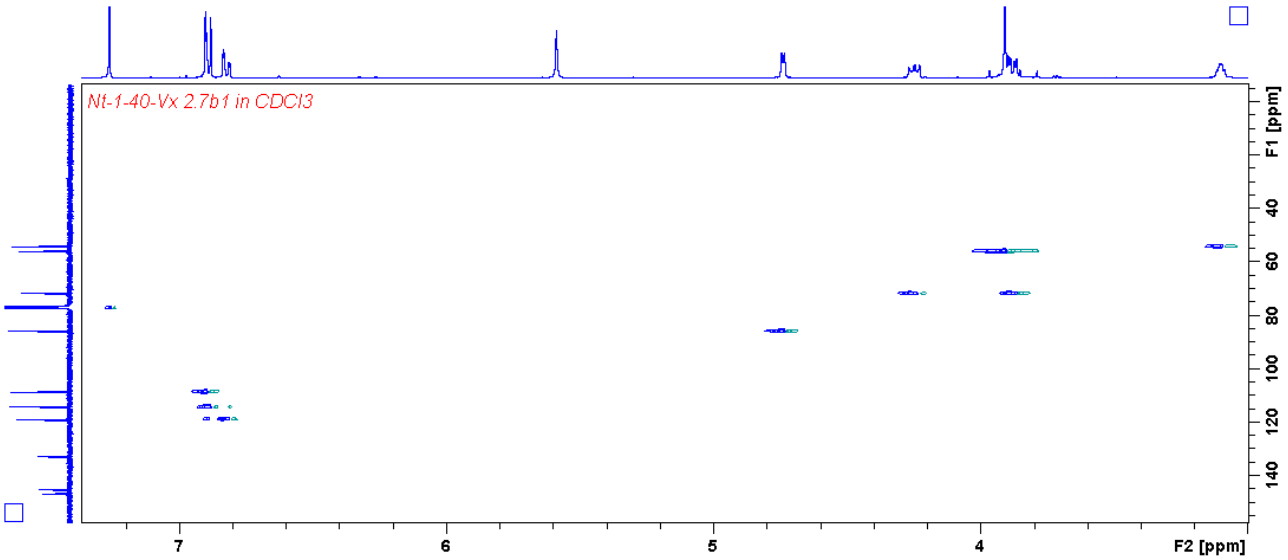

Plate 3.48: HSQC (400 MHz/100 MHz, $CDCl_3$) spectrum of pinoresinol (3.12).

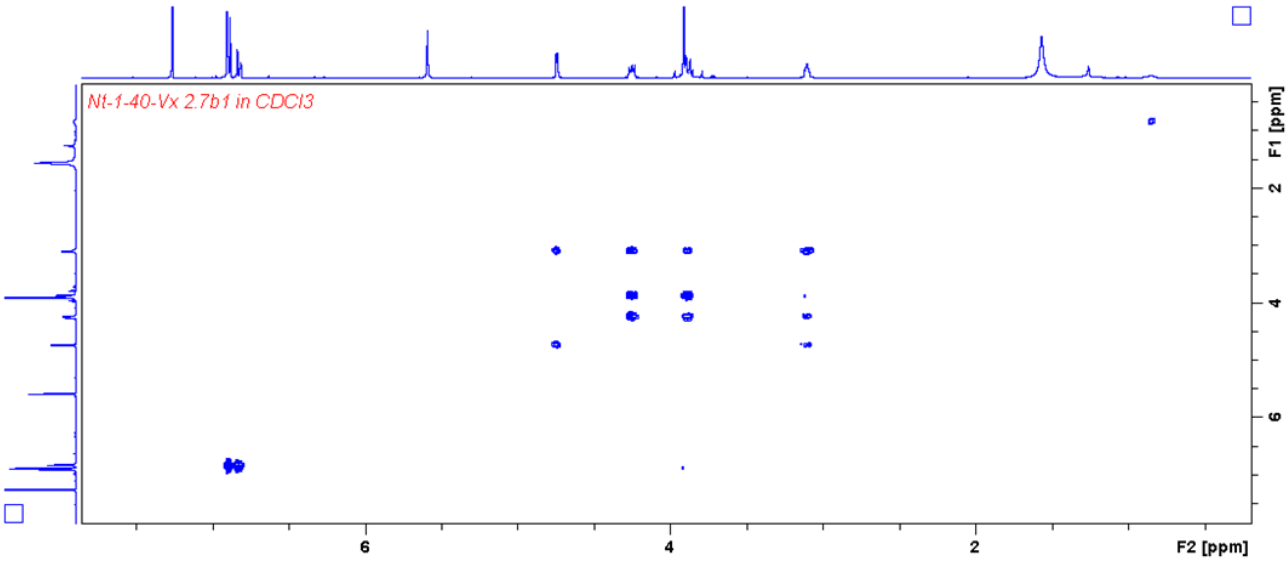

Plate 3.49: COSY (400 MHz/100 MHz, $CDCl_3$) spectrum of pinoresinol (3.12).

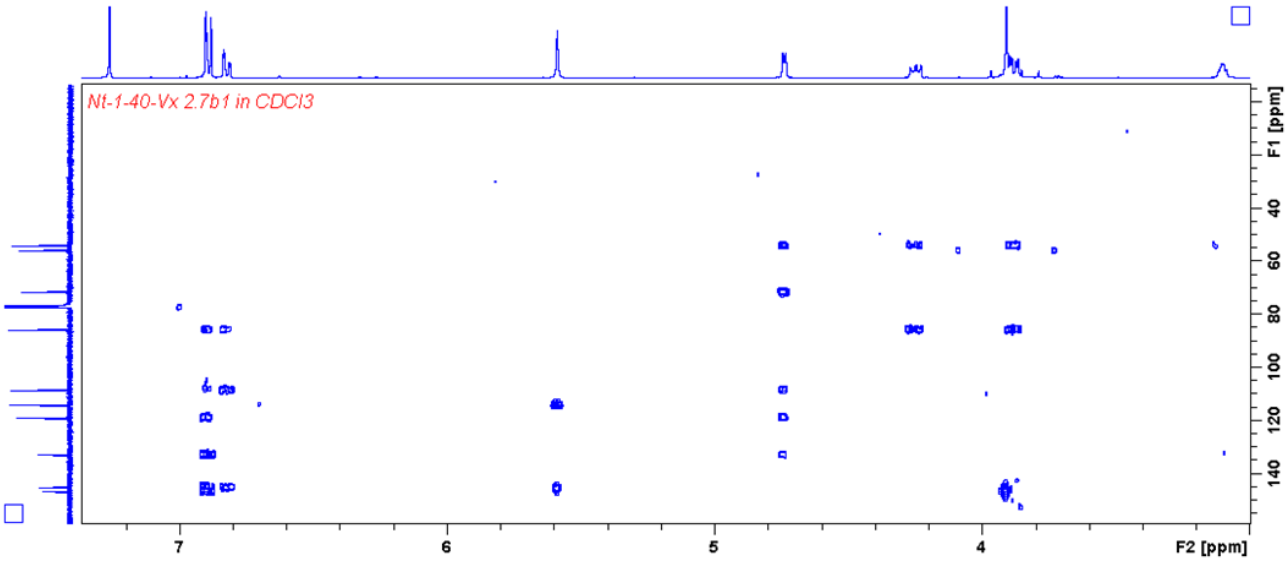

Plate 3.50: HMBC (400 MHz/100 MHz, $CDCl_3$) spectrum of pinoresinol (3.12).

Elemental Composition Report Page 1

Single Mass Analysis
Tolerance = 5.0 PPM / DBE: min = -1.5, max = 50.0
Element prediction: Off
Number of isotope peaks used for i-FIT = 3

Monoisotopic Mass, Odd and Even Electron Ions
2 formula(e) evaluated with 1 results within limits (all results (up to 1000) for each mass)
Elements Used:
C: 40-45 H: 55-60 O: 0-5
VX 2_6 32 (1.047) Cm (1:61)
TOF MS ES+

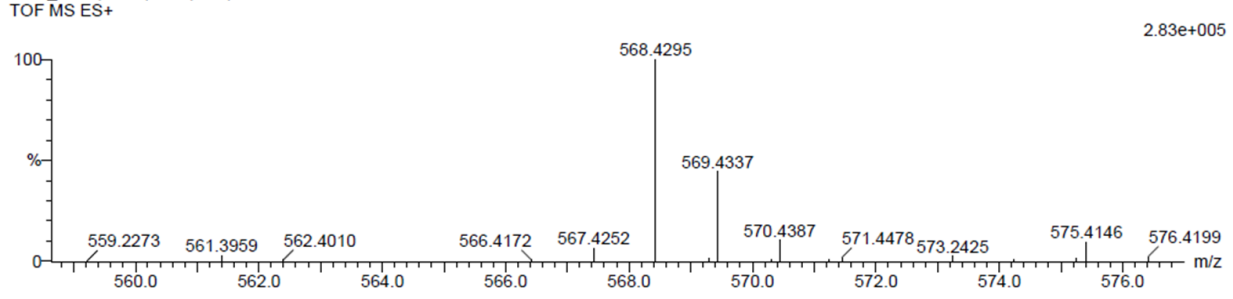

Minimum:				-1.5			
Maximum:		5.0	5.0	50.0			
Mass	Calc. Mass	mDa	PPM	DBE	i-FIT	i-FIT (Norm)	Formula
568.4295	568.4280	1.5	2.6	13.0	49.2	0.0	C40 H56 O2

Plate 3.51: HRESIMS of (*E*)-lutein (3.13).

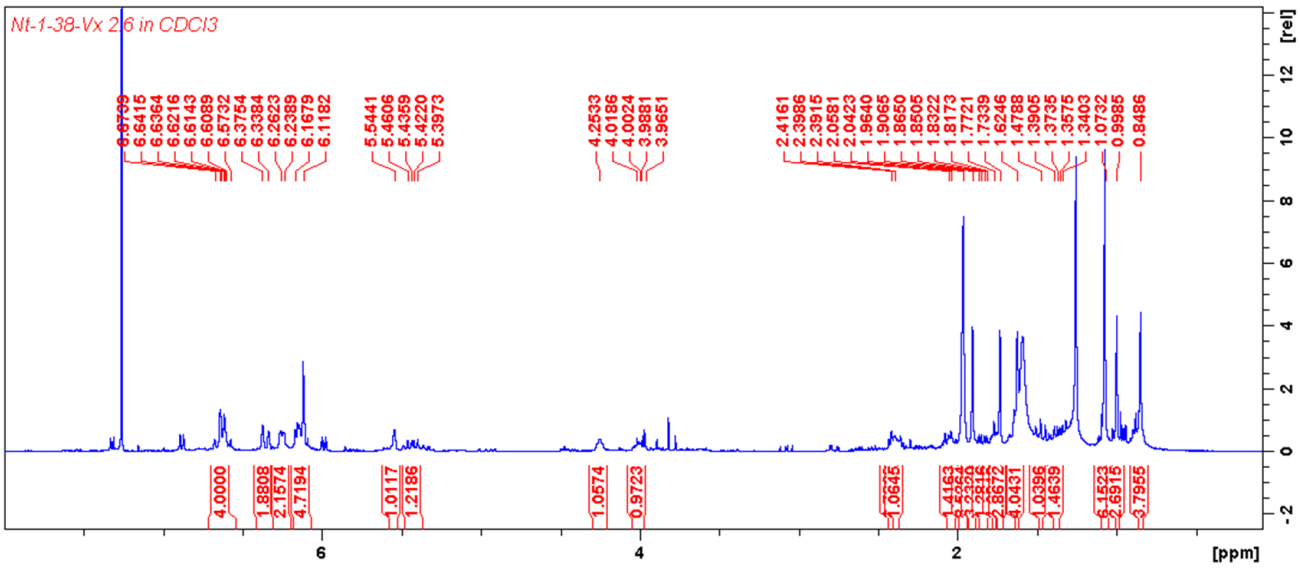

^{1}H NMR (400 MHz, $CDCl_3$) spectrum of (*E*)-lutein (3.13).

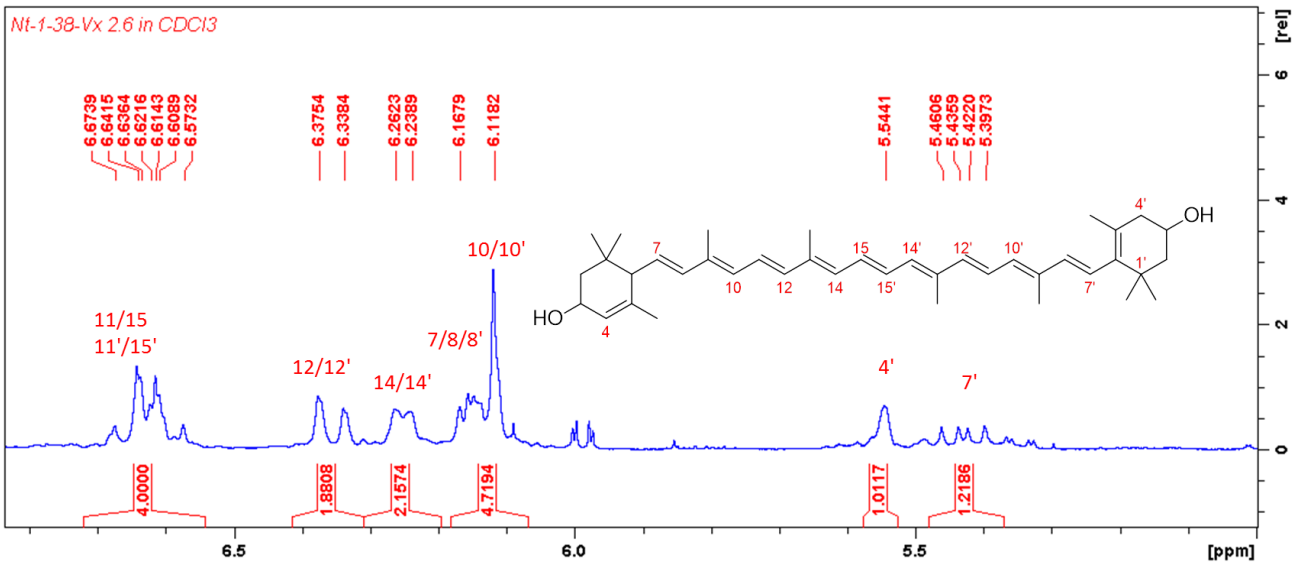

Plate 3.52: Expansion of ^{1}H (400 MHz, $CDCl_3$) spectrum of (*E*)-lutein (3.13).

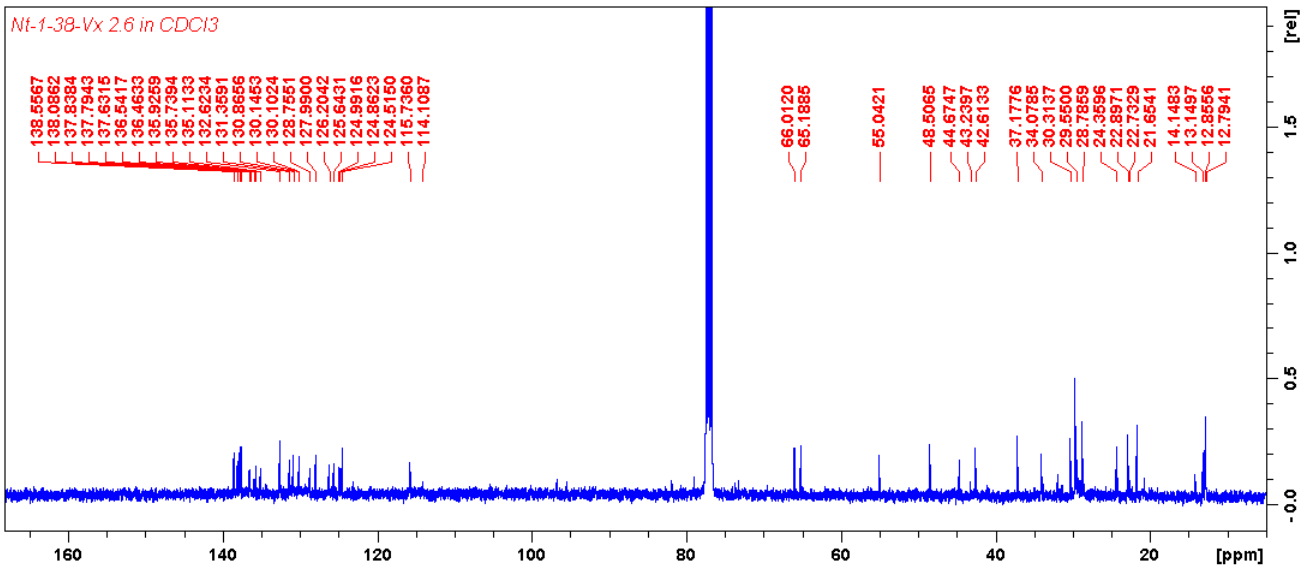

Plate 3.53: ^{13}C NMR (100 MHz, $CDCl_3$) spectrum of (*E*)-lutein (3.13).

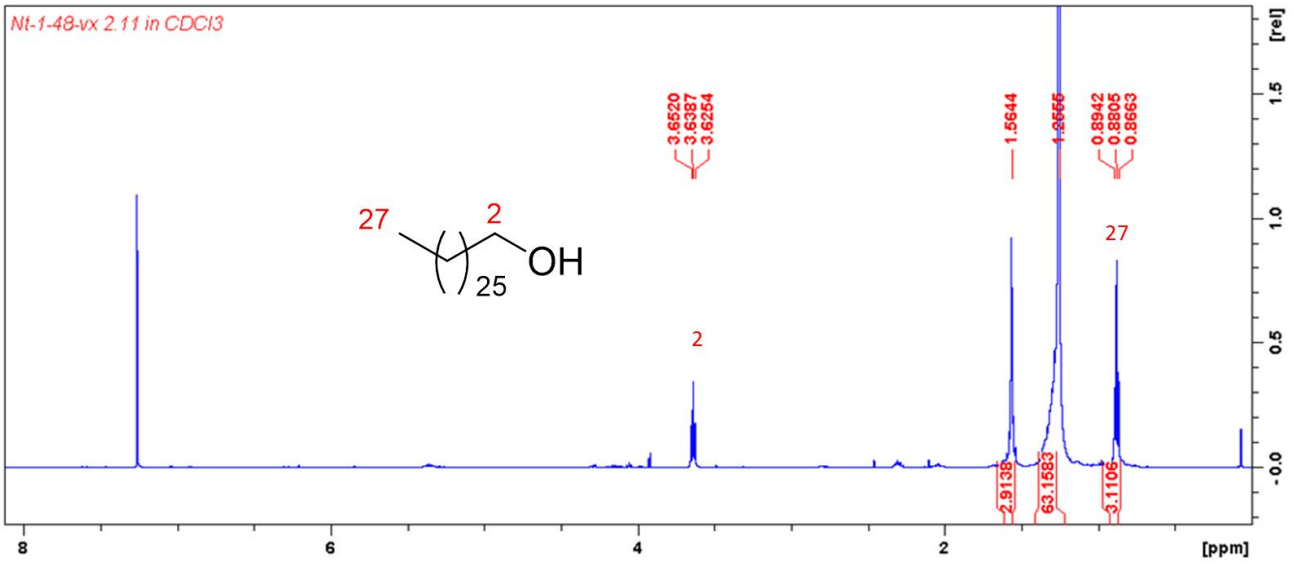

Plate 3.54: ^{1}H NMR (500 MHz, $CDCl_3$) spectrum of 1-heptacosanol (3.14).

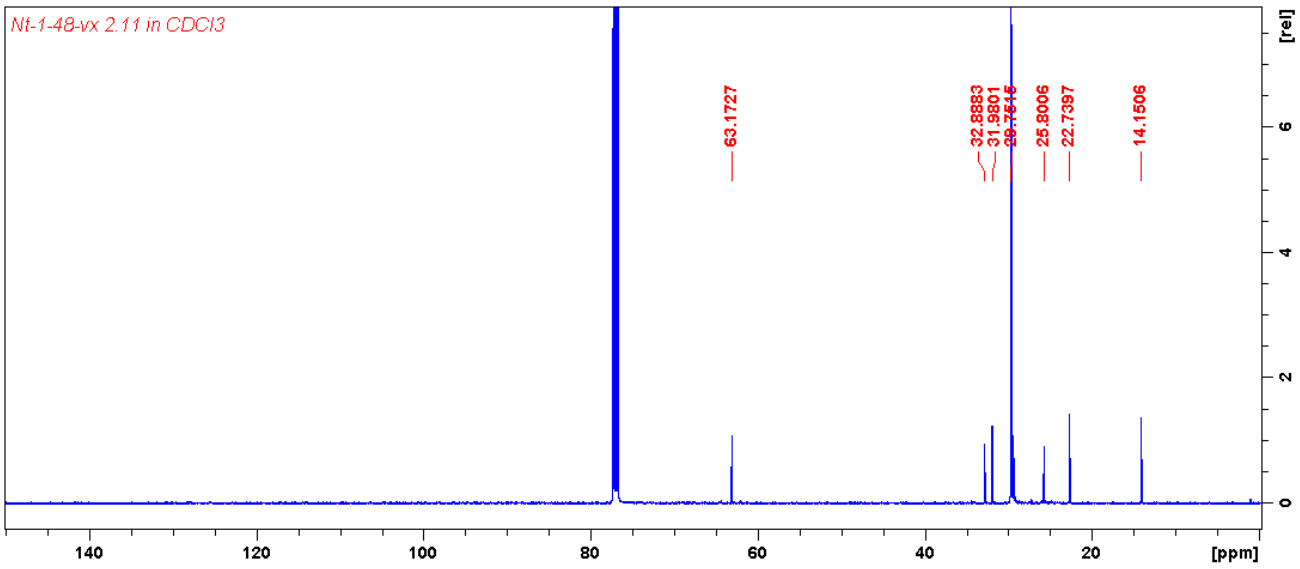

Plate 3.55: ^{13}C NMR (125 MHz, $CDCl_3$) spectrum of 1-heptacosanol (3.14).

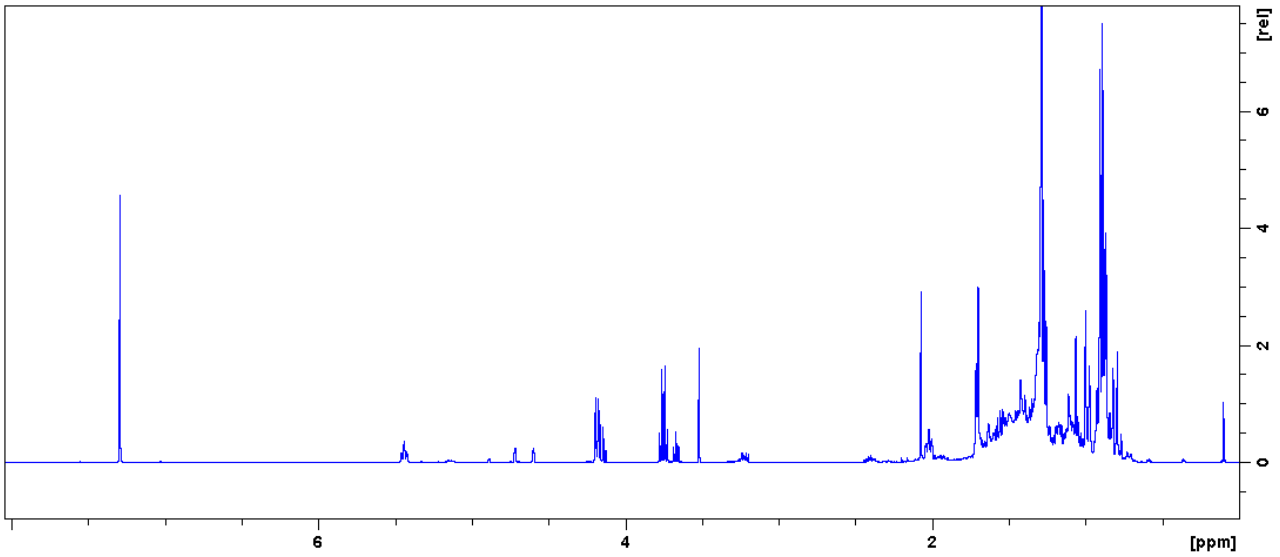

Plate 3. 56: ^{1}H NMR (400 MHz, $CDCl_3$) spectrum of phytol 3.15 and lupeol (3.16).

APPENDIX B. HRESIMS AND NMR SPECTRA OF COMPOUNDS DESCRIBED IN CHAPTER 4

Elemental Composition Report Page 1

Single Mass Analysis
Tolerance = 5.0 PPM / DBE: min = -1.5, max = 100.0
Element prediction: Off
Number of isotope peaks used for i-FIT = 3

Monoisotopic Mass, Even Electron Ions
2 formula(e) evaluated with 1 results within limits (all results (up to 1000) for each mass)
Elements Used:
C: 25-30 H: 15-20 O: 5-10
ob 1,1a 13 (0.405) Cm (1:61)
TOF MS ES-

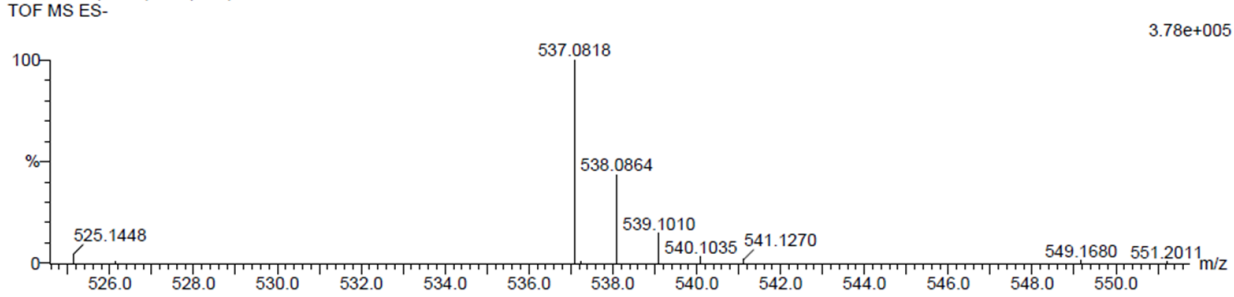

Minimum:				-1.5			
Maximum:		5.0	5.0	100.0			
Mass	Calc. Mass	mDa	PPM	DBE	i-FIT	i-FIT (Norm)	Formula
537.0818	537.0822	-0.4	-0.7	22.5	53.6	0.0	C30 H17 O10

Plate 4.1: HRESIMS of robustaflavone (4.1).

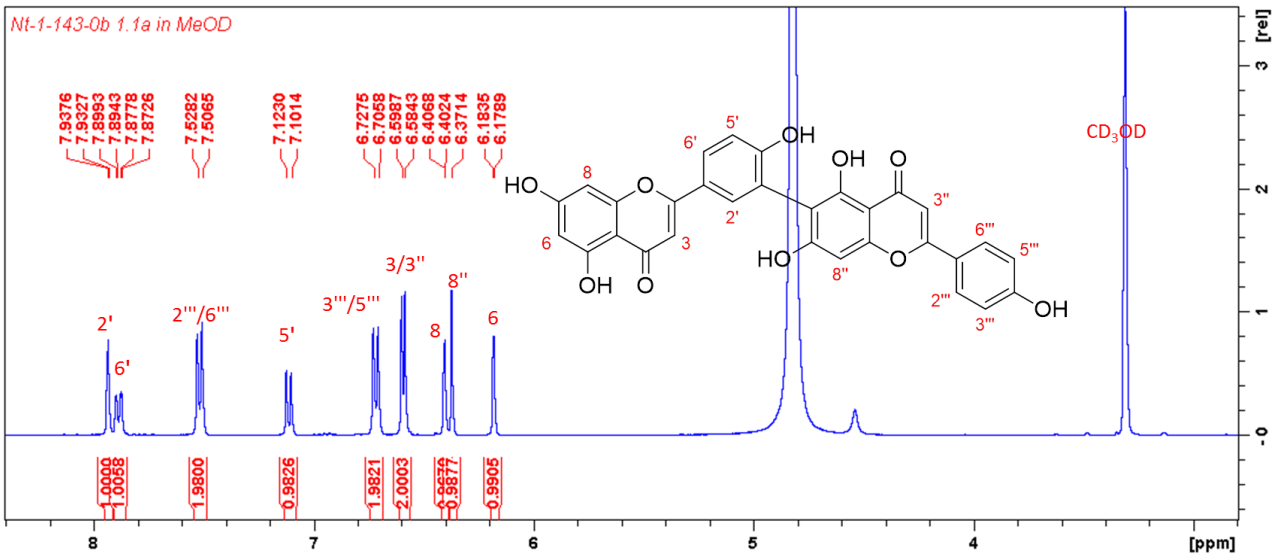

Plate 4.2: ^{1}H NMR (400 MHz, CD_3OD) spectrum of robustaflavone (4.1).

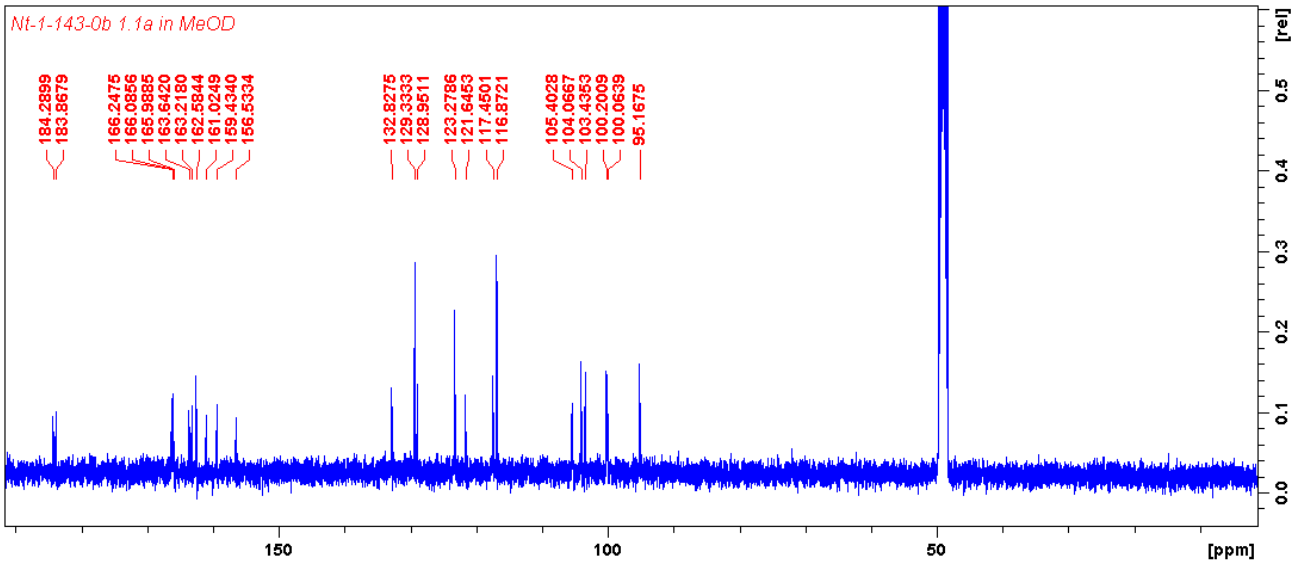

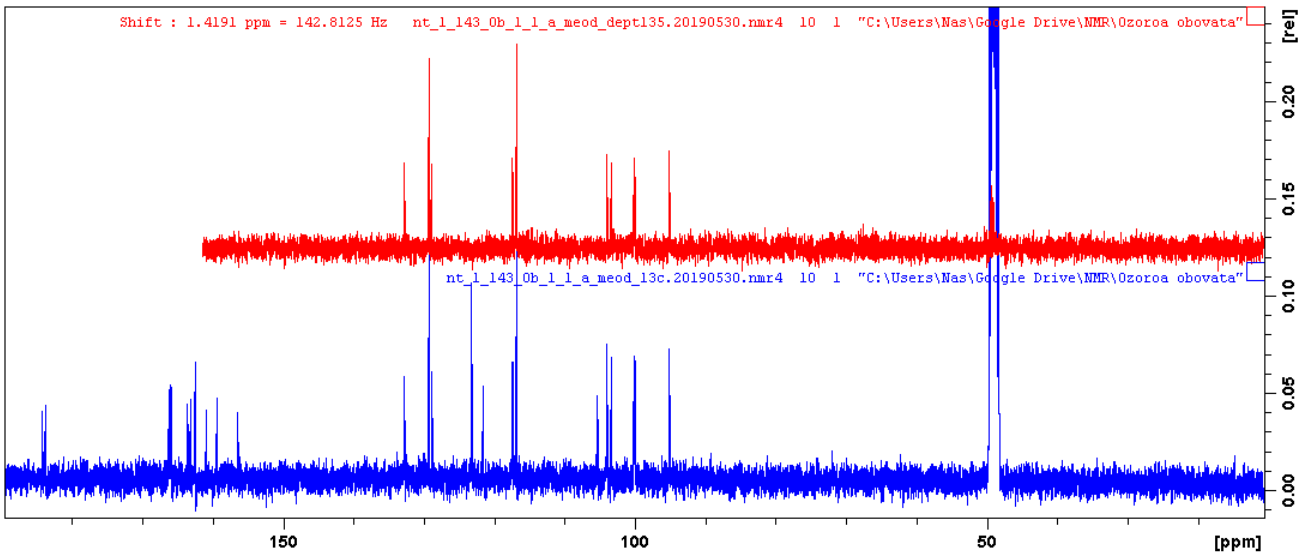

Plate 4.3: ^{13}C and DEPT (100 MHz, CD_3OD) spectra of robustaflavone (4.1).

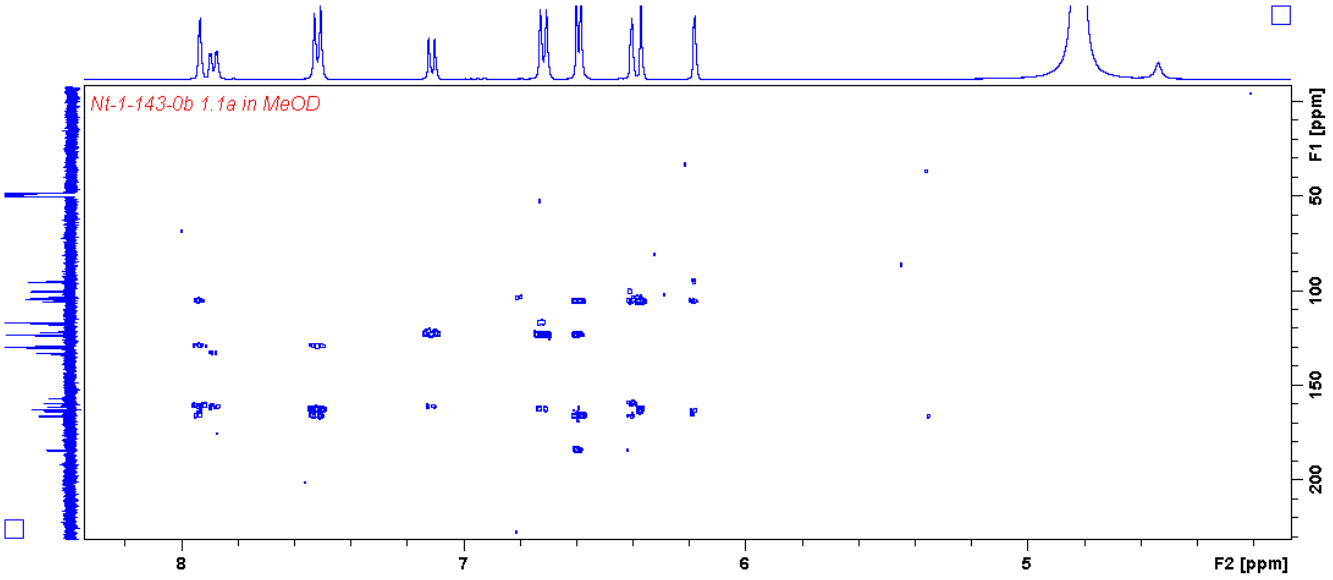

Plate 4.4: HMBC (400 MHz/100 MHz, CD_3OD) spectrum of robustaflavone (4.1).

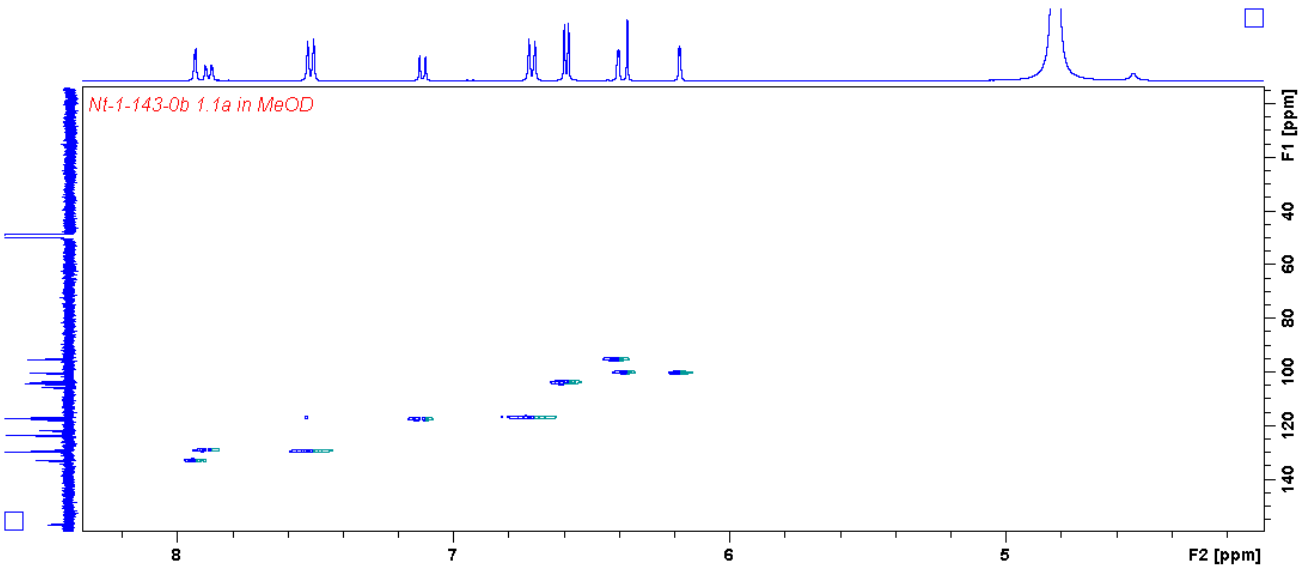

Plate 4.5: HSQC (400 MHz/100 MHz, CD_3OD) spectrum of robustaflavone (4.1).

Elemental Composition Report **Page 1**

Single Mass Analysis
Tolerance = 5.0 PPM / DBE: min = -1.5, max = 100.0
Element prediction: Off
Number of isotope peaks used for i-FIT = 3

Monoisotopic Mass, Even Electron Ions
2 formula(e) evaluated with 1 results within limits (all results (up to 1000) for each mass)
Elements Used:
C: 25-30 H: 15-20 O: 5-10
ob 1,1b 53 (1.755) Cm (1:61)
TOF MS ES-

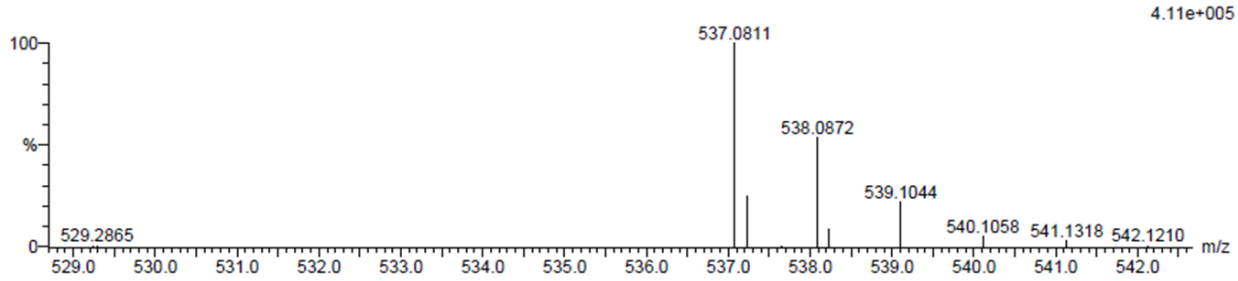

Minimum:				-1.5			
Maximum:		5.0	5.0	100.0			
Mass	Calc. Mass	mDa	PPM	DBE	i-FIT	i-FIT (Norm)	Formula
537.0811	537.0822	-1.1	-2.0	22.5	100.2	0.0	C30 H17 O10

Plate 4.6: HRESIMS of amentoflavone (4.2).

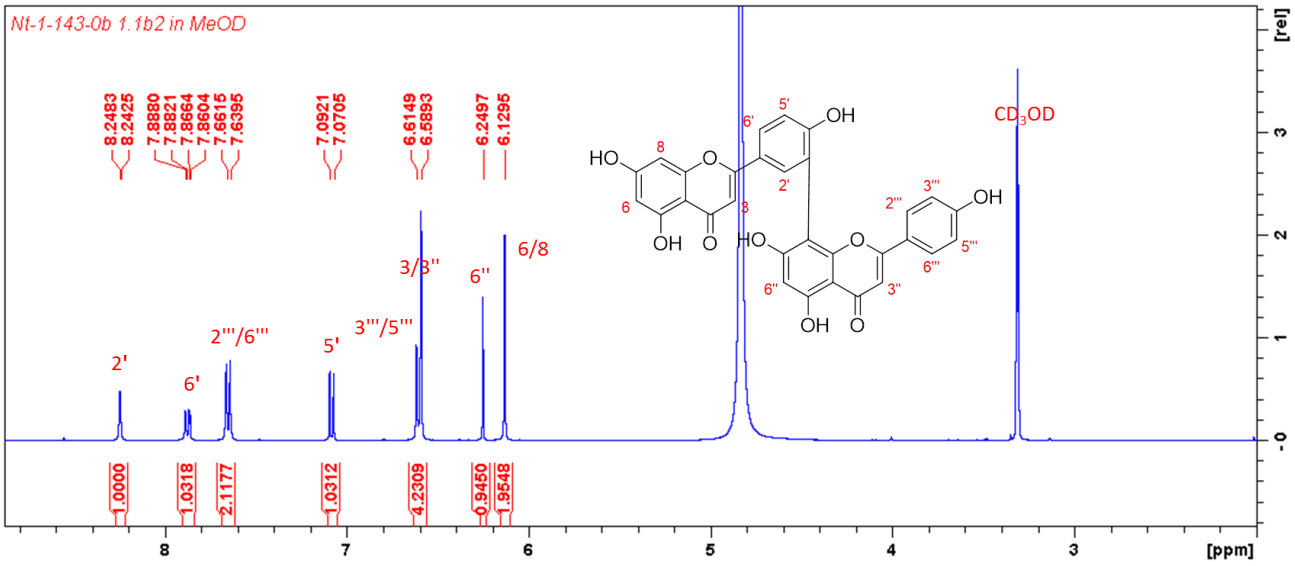

Plate 4.7: ^{1}H NMR (400 MHz, CD_3OD) spectrum of amentoflavone (4.2).

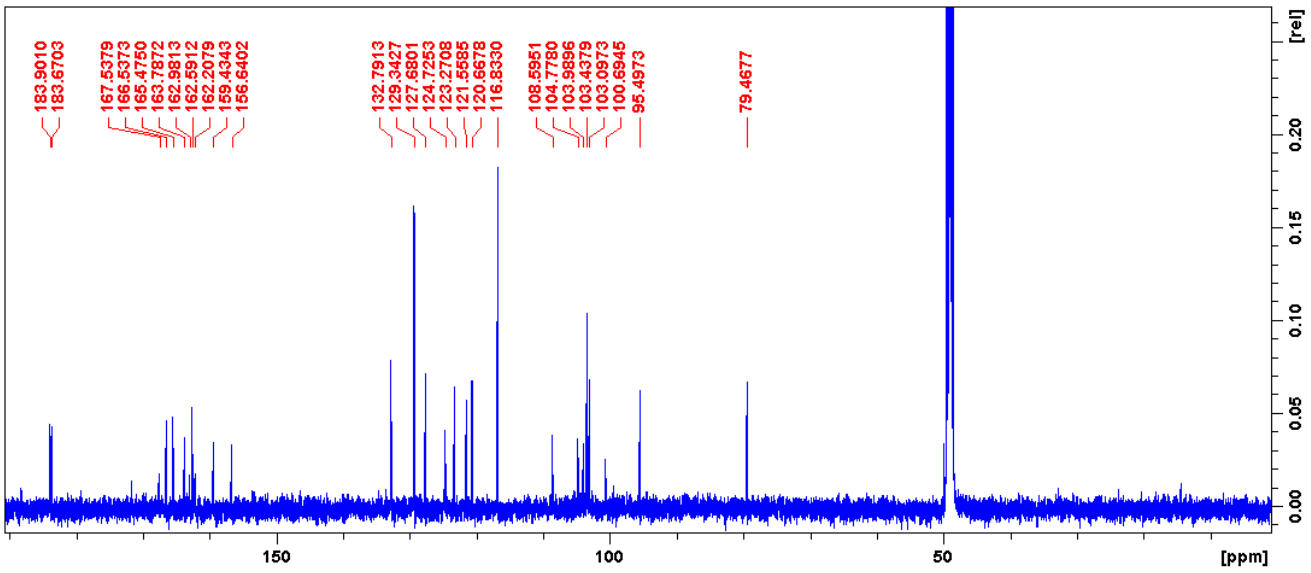

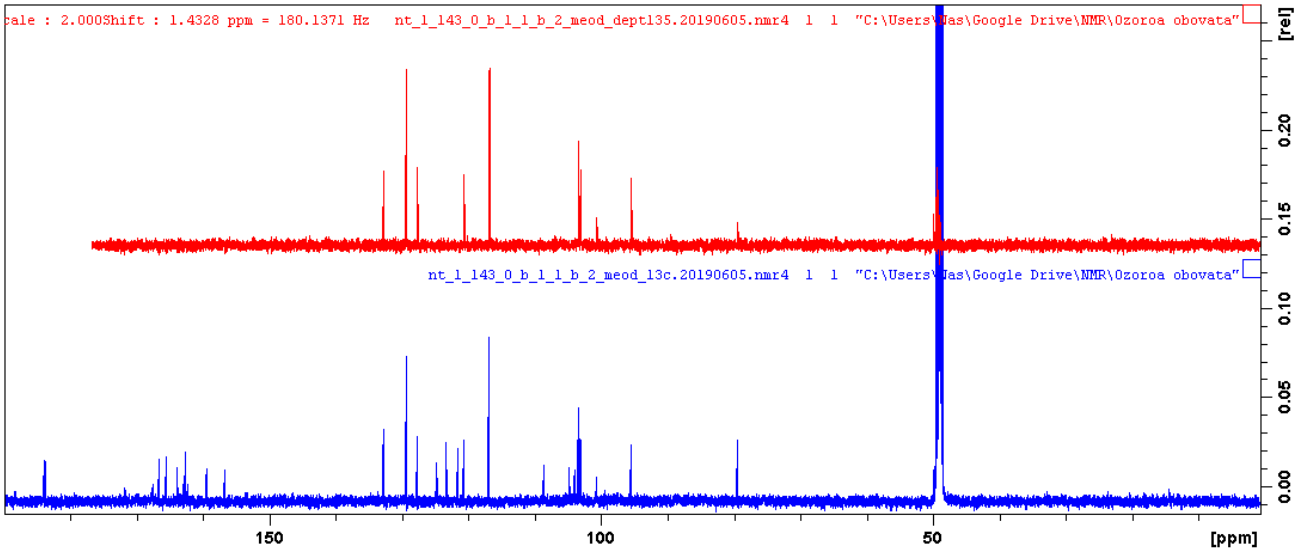

Plate 4.8: ^{13}C and DEPT (100 MHz, CD_3OD) spectra of amentoflavone (4.2).

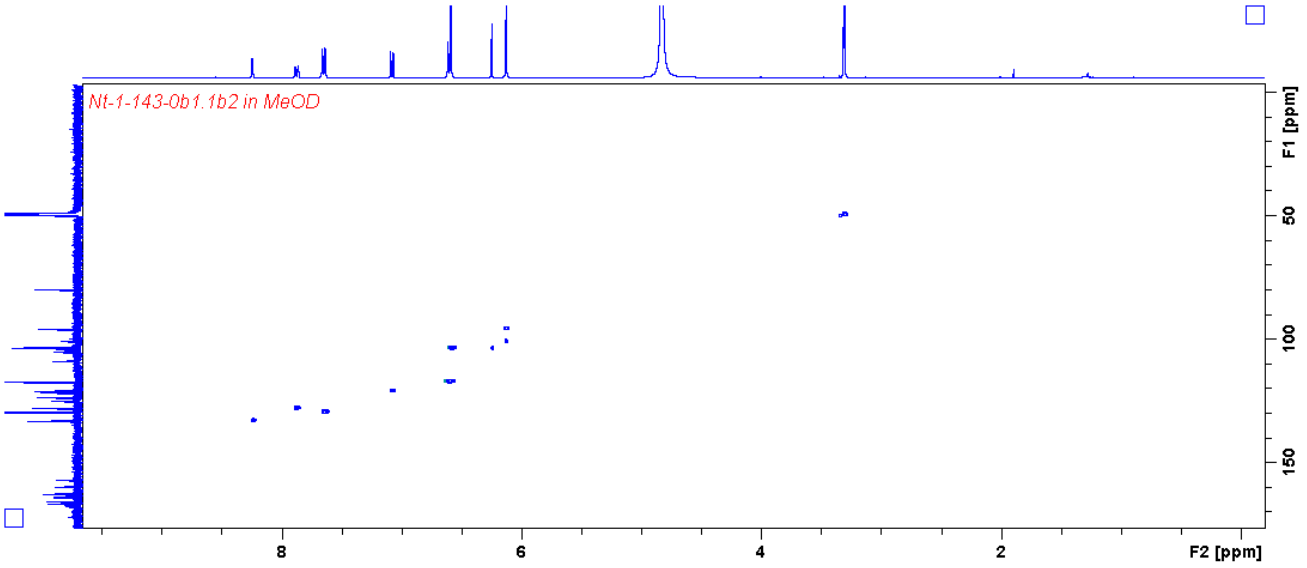

Plate 4.9: HSQC (400 MHz/100 MHz, CD_3OD) spectrum of amentoflavone (4.2).

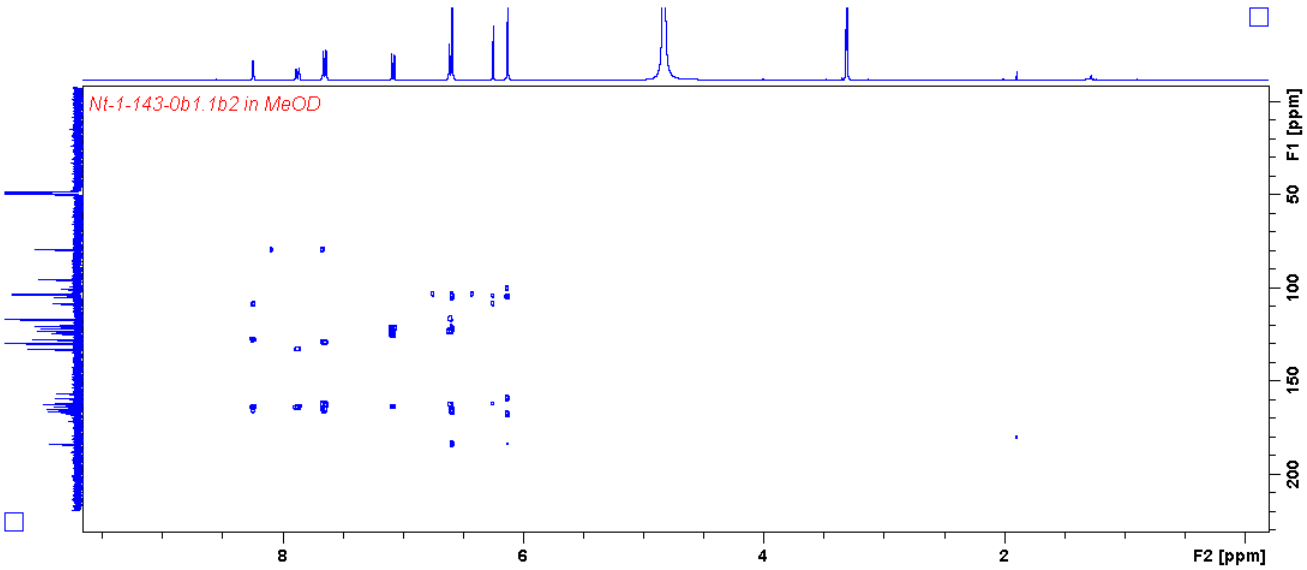

Plate 4.10: HMBC (400 MHz/100 MHz, CD_3OD) spectrum of amentoflavone (4.2).

Elemental Composition Report Page 1

Single Mass Analysis
Tolerance = 5.0 PPM / DBE: min = -1.5, max = 50.0
Element prediction: Off
Number of isotope peaks used for i-FIT = 3

Monoisotopic Mass, Even Electron Ions
4 formula(e) evaluated with 1 results within limits (all results (up to 1000) for each mass)
Elements Used:
C: 20-25 H: 15-20 O: 10-15
Nt-1-En 1_6b 60 (1.991) Cm (1:61)
TOF MS ES-

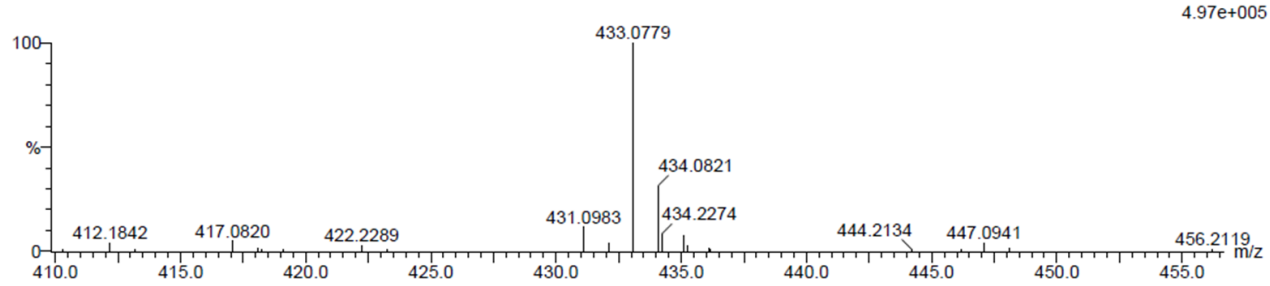

Minimum:				-1.5			
Maximum:		5.0	5.0	50.0			
Mass	Calc. Mass	mDa	PPM	DBE	i-FIT	i-FIT (Norm)	Formula
433.0779	433.0771	0.8	1.8	12.5	69.5	0.0	C20 H17 O11

Plate 4.11: HRESIMS of quercetin 3-*O*-arabinofuranoside (4.3).

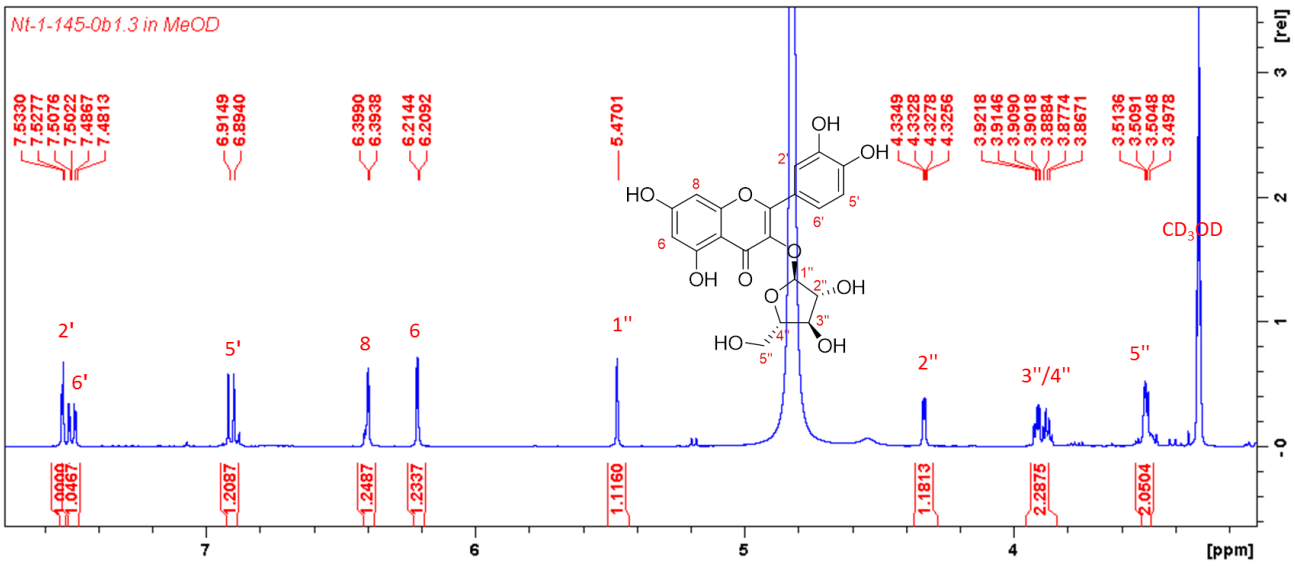

Plate 4.12: ^{1}H NMR (400 MHz, CD_3OD) spectrum of quercetin 3-*O*-arabinofuranoside (4.3).

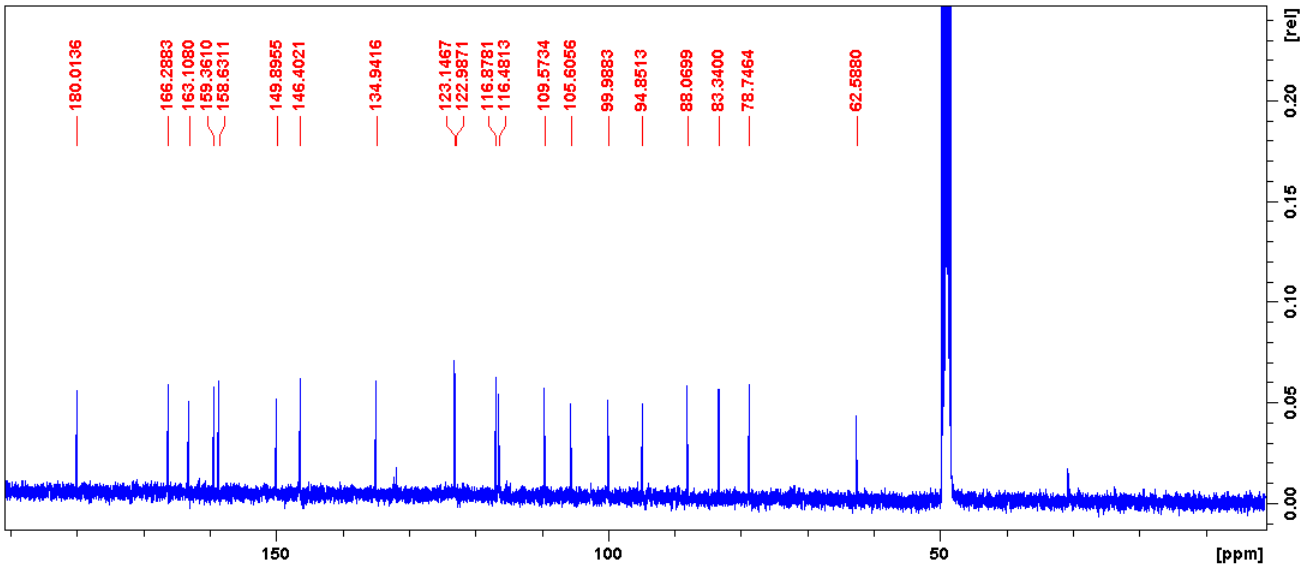

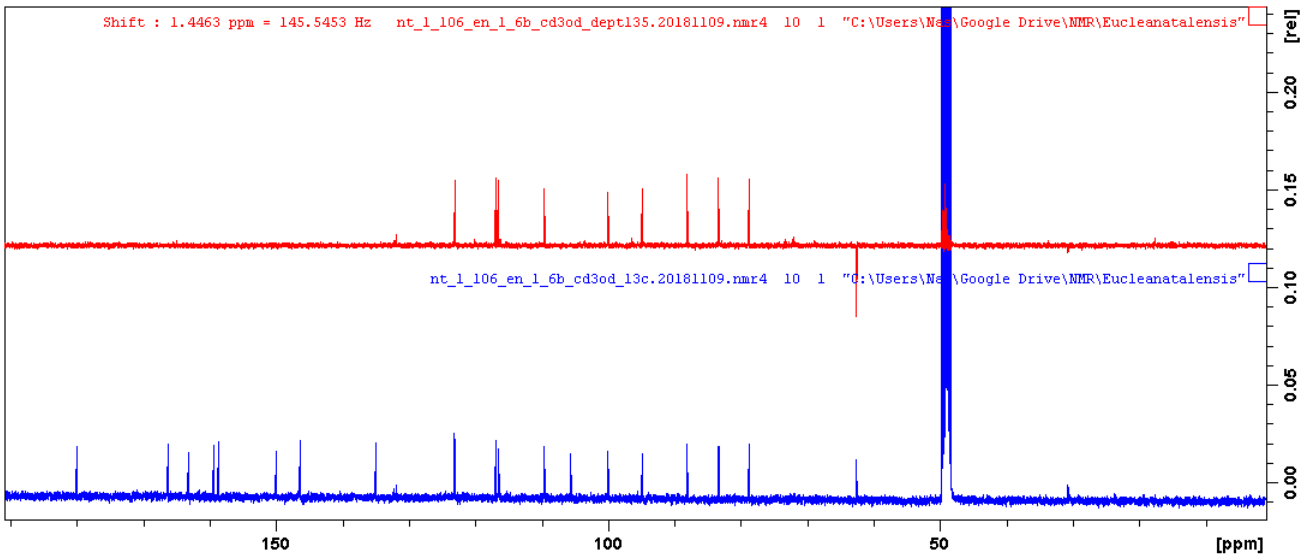

Plate 4.13: ^{13}C and DEPT NMR (100 MHz, CD_3OD) spectra of quercetin 3-*O*-arabinofuranoside (4.3).

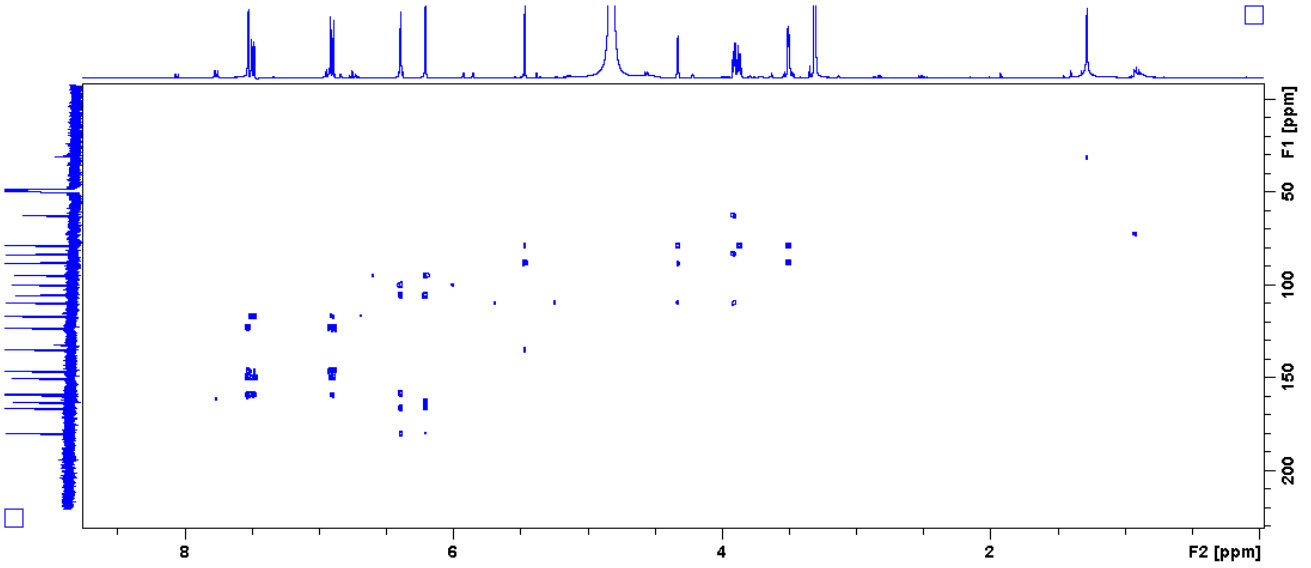

Plate 4.14: HMBC (400 MHz, CD_3OD) spectrum of quercetin 3-*O*-arabinofuranoside (4.3).

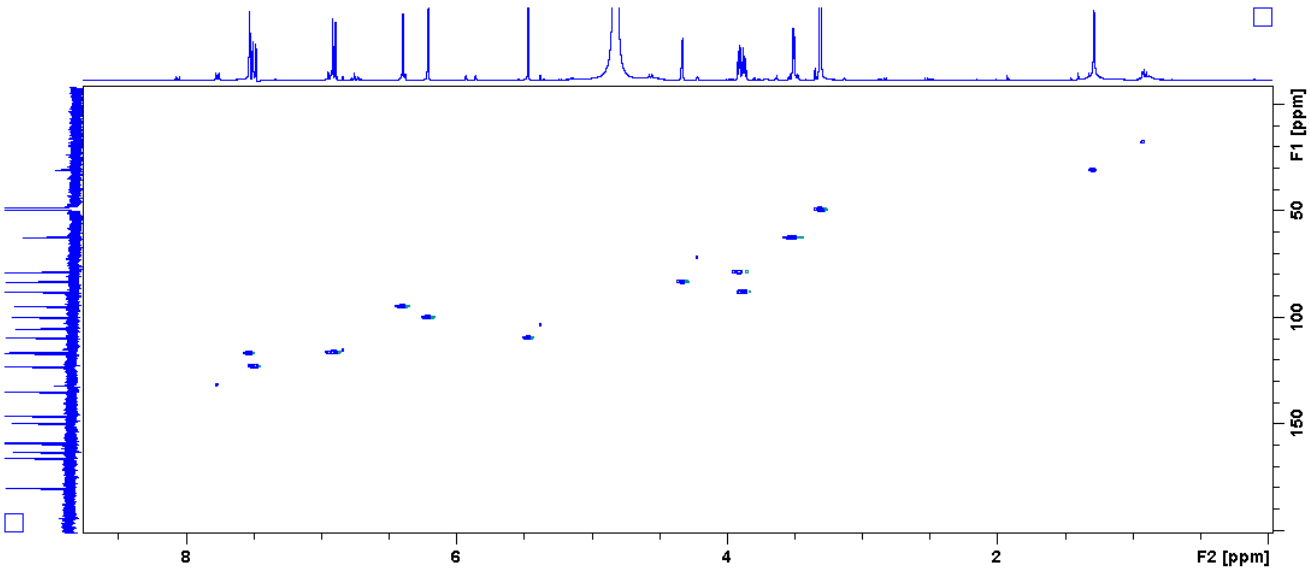

Plate 4.15: HSQC (400 MHz/100 MHz, CD_3OD) spectrum of quercetin 3-*O*-arabinofuranoside (4.3).

Elemental Composition Report Page 1

Single Mass Analysis
Tolerance = 5.0 PPM / DBE: min = -1.5, max = 100.0
Element prediction: Off
Number of isotope peaks used for i-FIT = 3

Monoisotopic Mass, Even Electron Ions
4 formula(e) evaluated with 1 results within limits (all results (up to 1000) for each mass)
Elements Used:
C: 20-25 H: 15-20 O: 10-15
Nt-1-ob1_6 15 (0.472) Cm (1:61)
TOF MS ES-

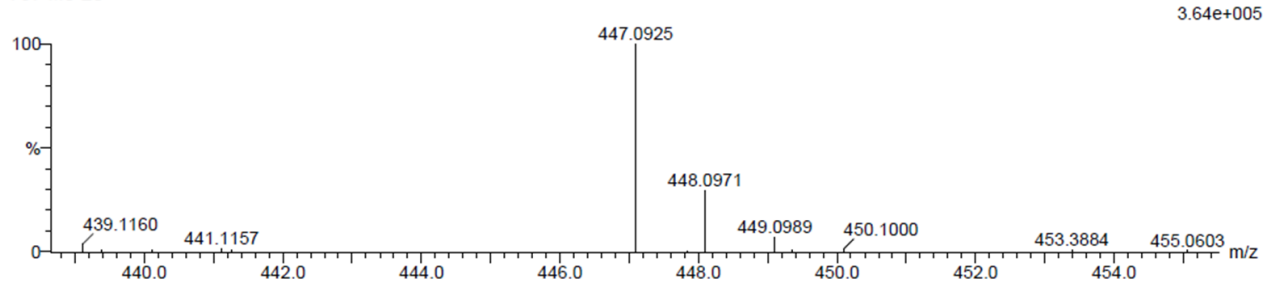

Minimum:				-1.5			
Maximum:		5.0	5.0	100.0			
Mass	Calc. Mass	mDa	PPM	DBE	i-FIT	i-FIT (Norm)	Formula
447.0925	447.0927	-0.2	-0.4	12.5	53.6	0.0	C21 H19 O11

Plate 4.16: HRESIMS of quercetin 3-*O*-rhamnopyranoside (4.4).

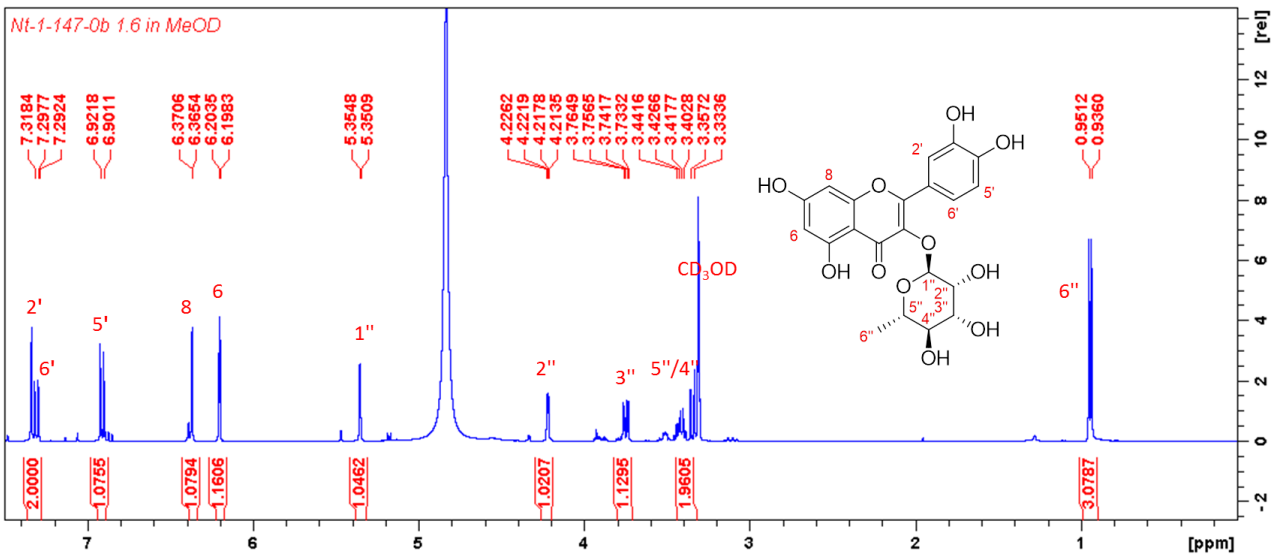

Plate 4.17: ^{1}H NMR (400 MHz, CD_3OD) spectrum of quercetin 3-*O*-rhamnopyranoside (4.4).

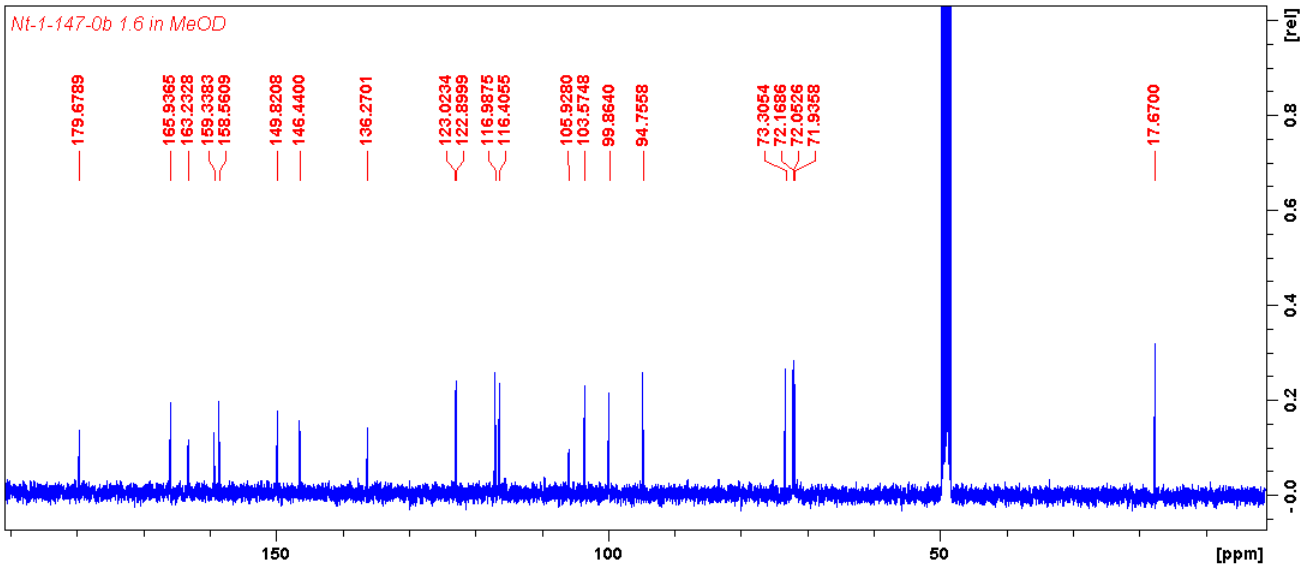

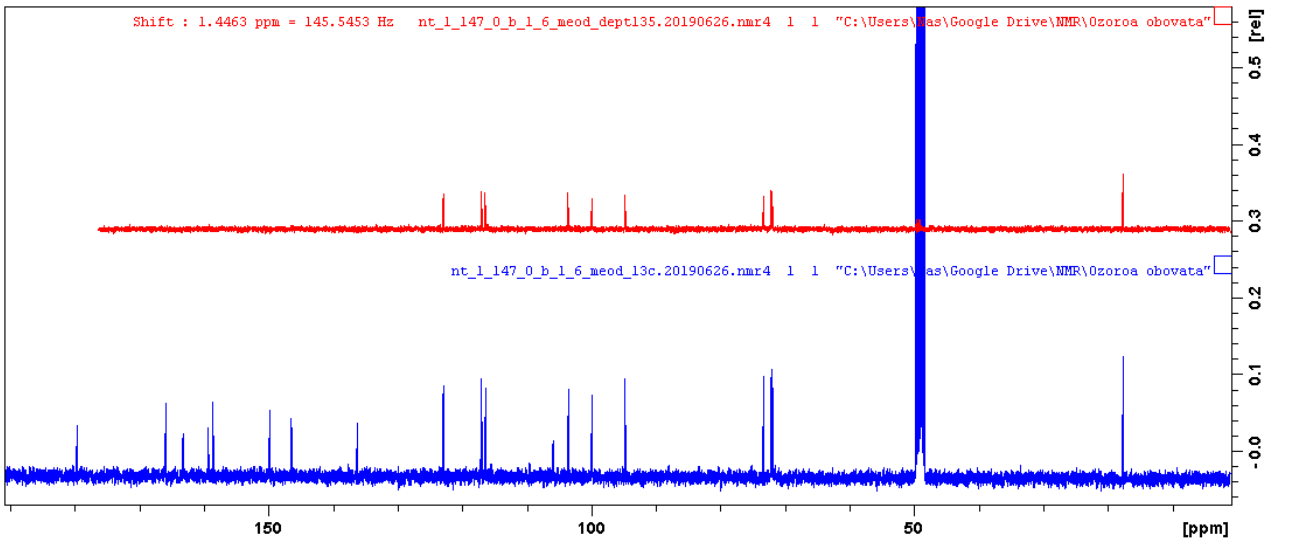

Plate 4.18: ^{13}C and DEPT NMR (100 MHz, CD_3OD) spectra of quercetin 3-*O*-rhamnopyranoside (4.4).

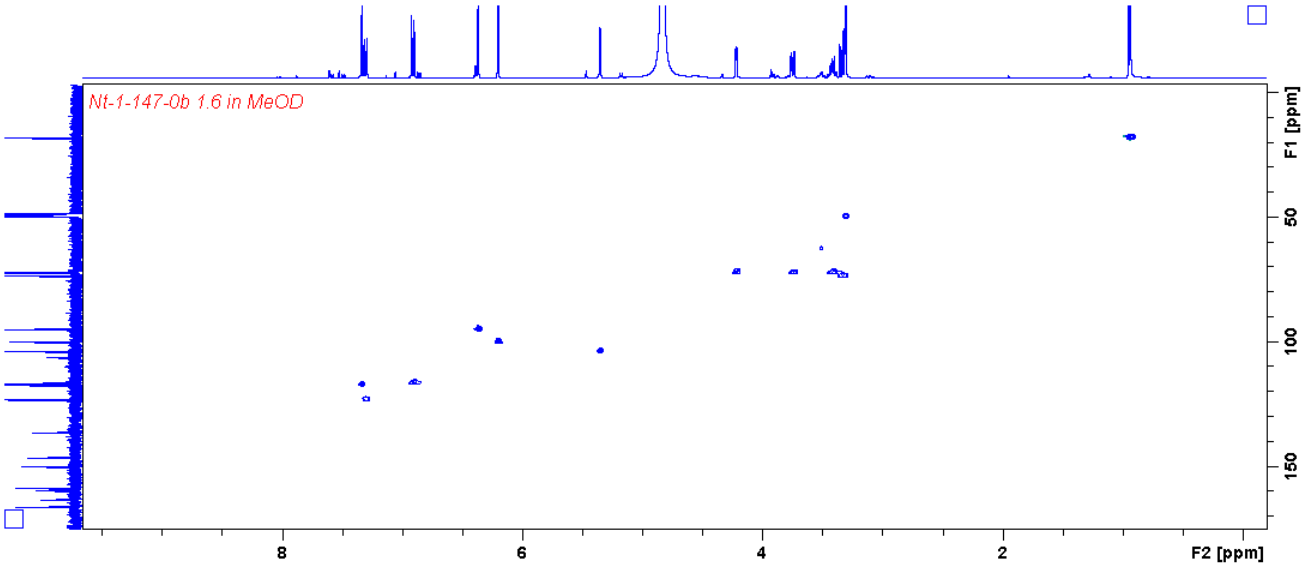

Plate 4.19: HSQC (400 MHz/100 MHz, CD_3OD) spectrum of quercetin 3-*O*-rhamnopyranoside (4.4).

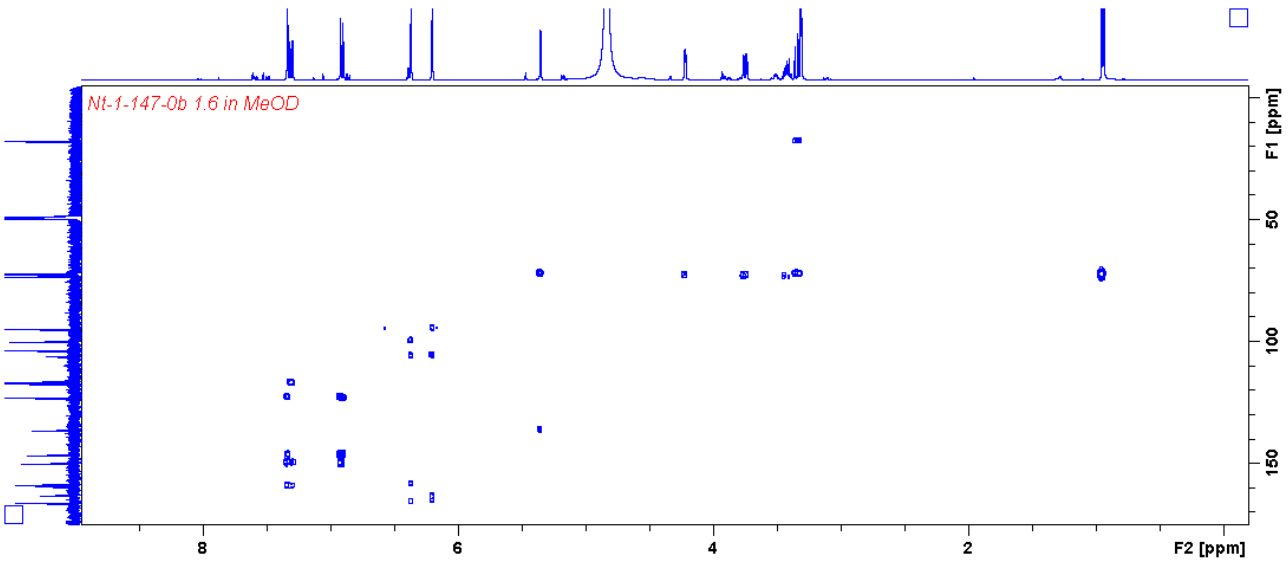

Plate 4.20: HMBC (400 MHz/100 MHz, CD_3OD) spectrum of quercetin 3-*O*-rhamnopyranoside (4.4).

Elemental Composition Report Page 1

Single Mass Analysis
Tolerance = 5.0 PPM / DBE: min = -1.5, max = 100.0
Element prediction: Off
Number of isotope peaks used for i-FIT = 3

Monoisotopic Mass, Even Electron Ions
5 formula(e) evaluated with 1 results within limits (all results (up to 1000) for each mass)
Elements Used:
C: 20-25 H: 15-20 O: 10-15
Nt-1-ob1_2 61 (2.024) Cm (1:61)
TOF MS ES-

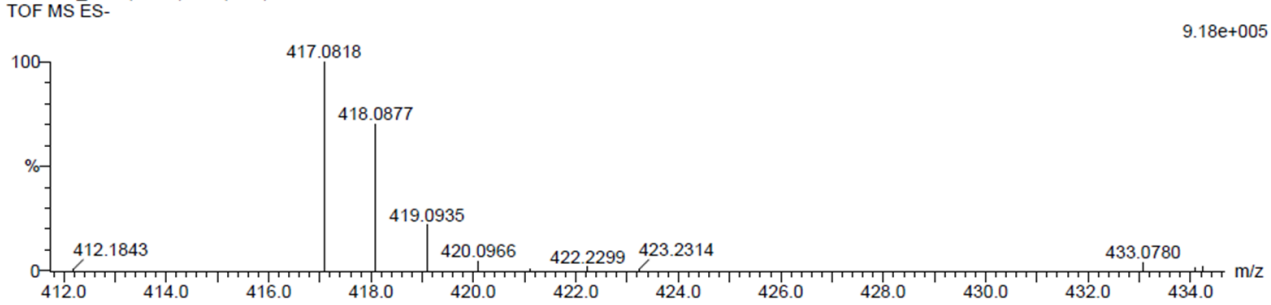

Minimum:				-1.5			
Maximum:		5.0	5.0	100.0			
Mass	Calc. Mass	mDa	PPM	DBE	i-FIT	i-FIT (Norm)	Formula
417.0818	417.0822	-0.4	-1.0	12.5	42.5	0.0	C20 H17 O10

Plate 4.21: HRESIMS of Kaempferol 3-*O*-arabinofuranoside (4.5).

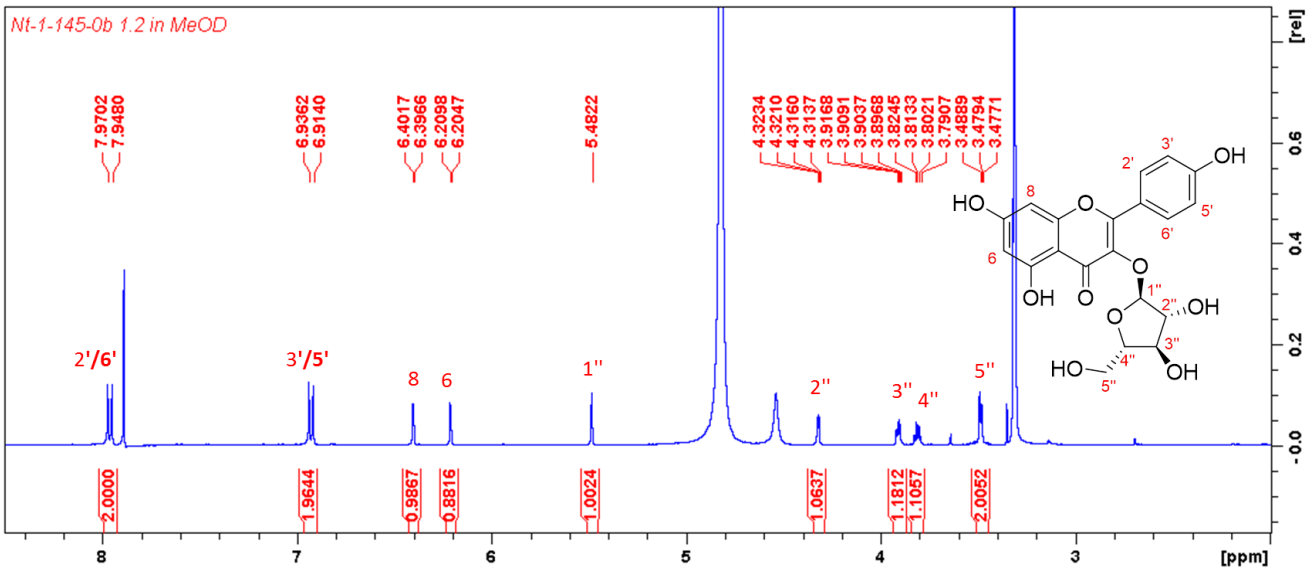

Plate 4.22: ^{1}H NMR (400 MHz, CD_3OD) spectrum of Kaempferol 3-*O*-arabinofuranoside (4.5).

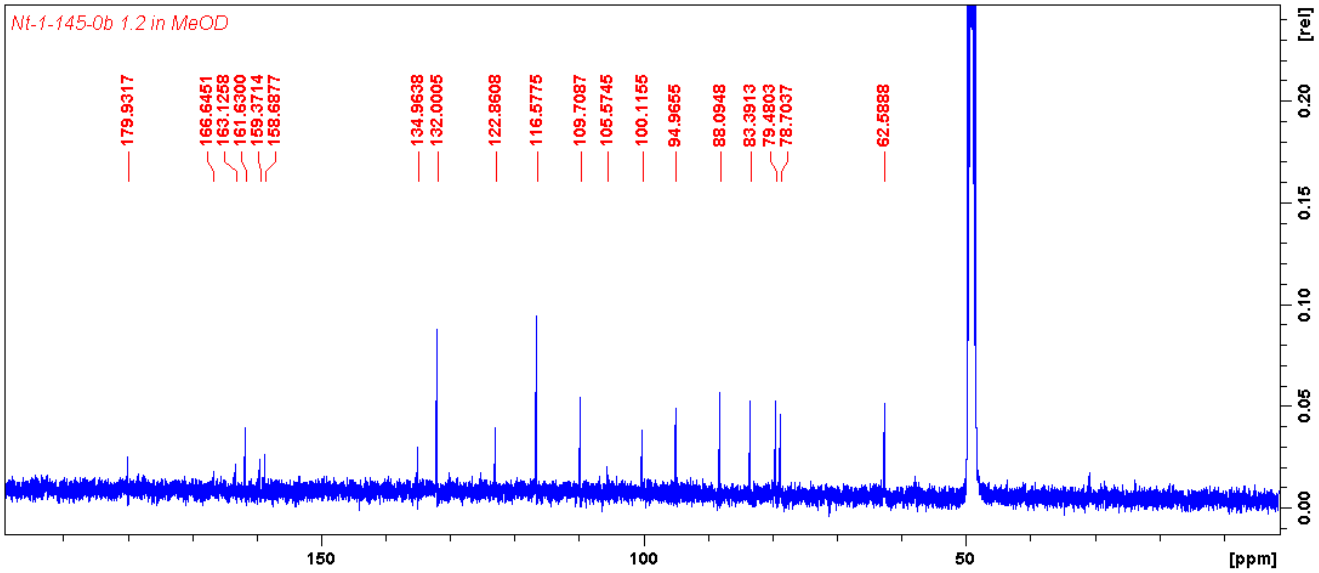

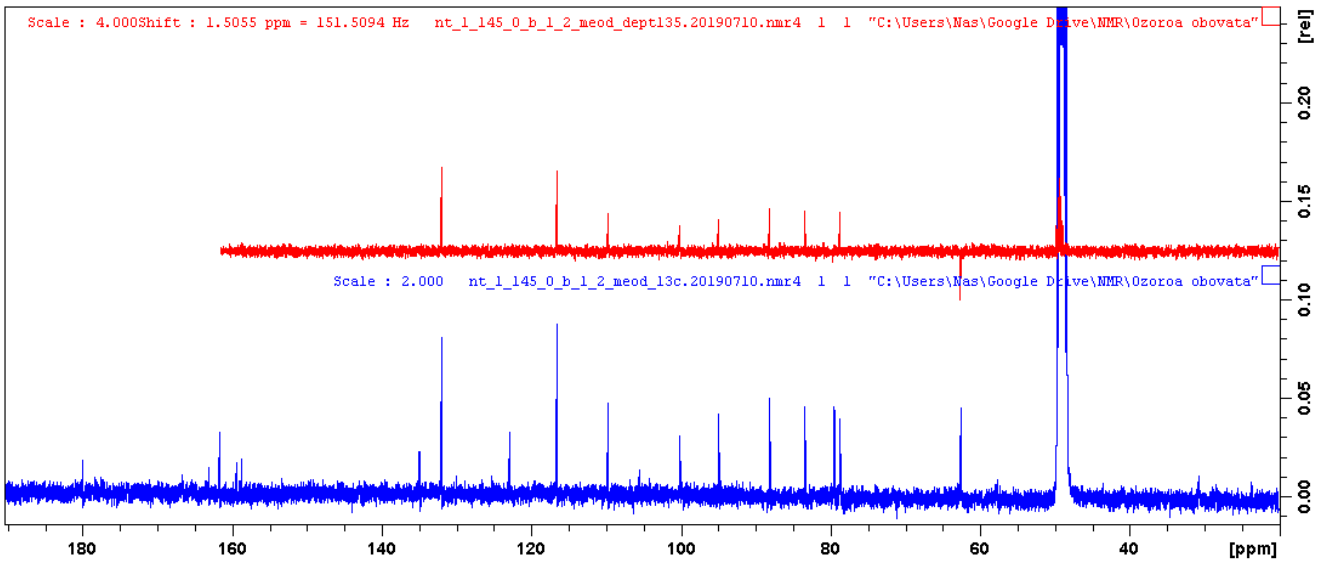

Plate 4.23: ^{13}C and DEPT (100 MHz, CD_3OD) spectra of Kaempferol 3-*O*-arabinofuranoside (4.5).

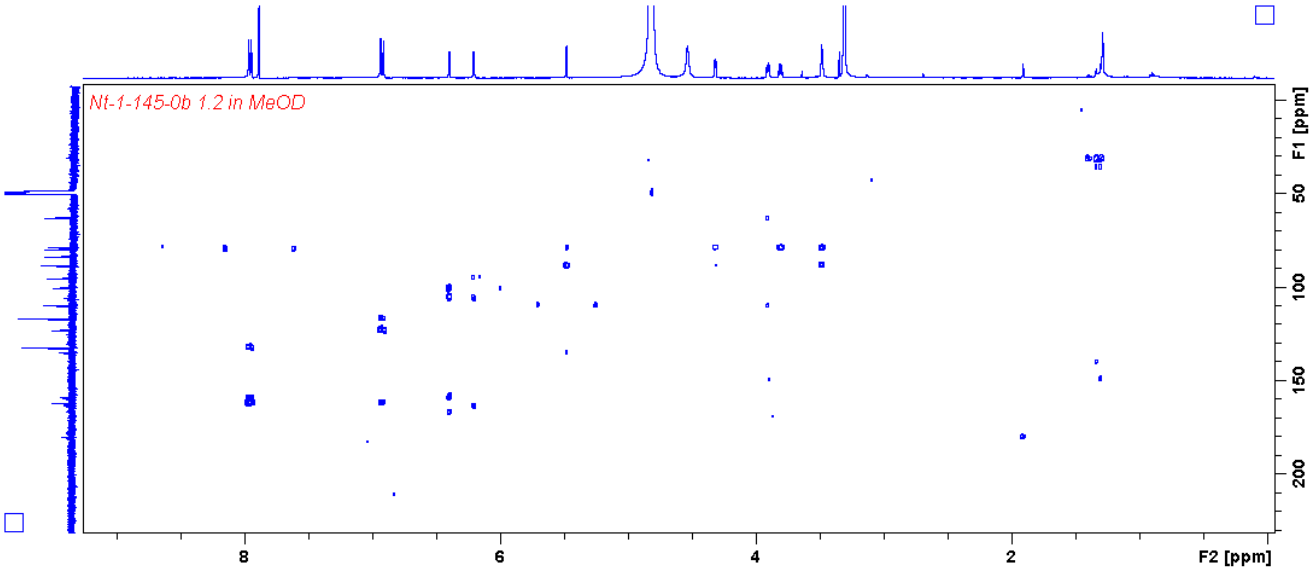

Plate 4.24: HMBC (400 MHz/100 MHz, CD_3OD) spectrum of Kaempferol 3-*O*-arabinofuranoside (4.5).

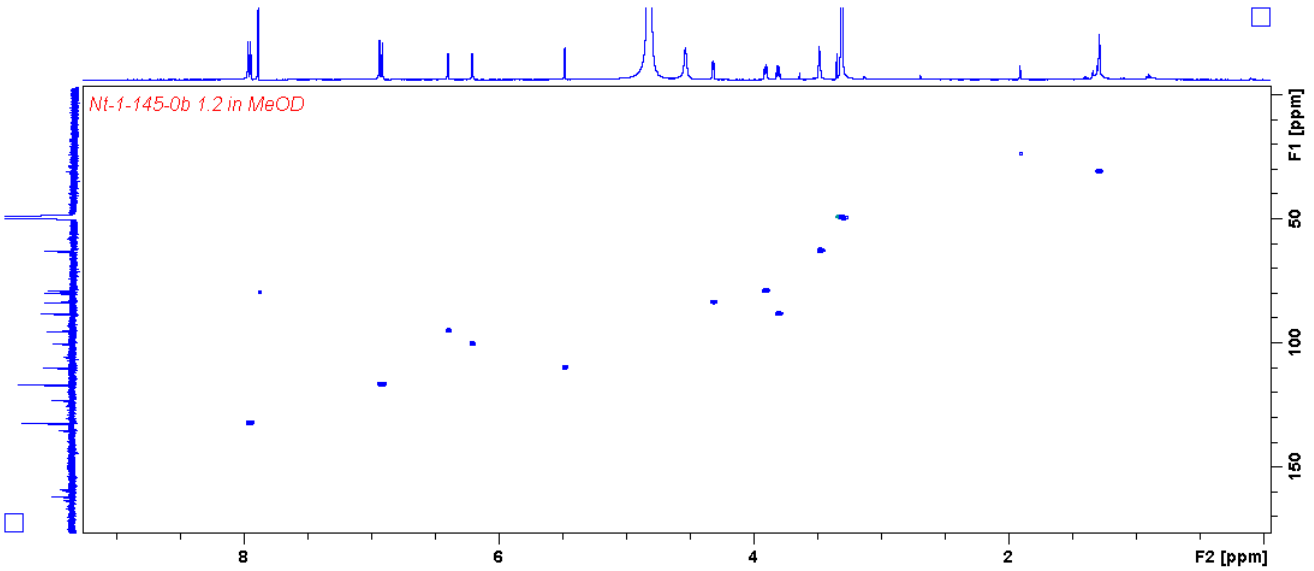

Plate 4.25: HSQC (400 MHz/100 MHz, CD_3OD) spectrum of Kaempferol 3-*O*-arabinofuranoside (4.5).

Elemental Composition Report **Page 1**

Single Mass Analysis
Tolerance = 5.0 PPM / DBE: min = -1.5, max = 50.0
Element prediction: Off
Number of isotope peaks used for i-FIT = 3

Monoisotopic Mass, Even Electron Ions
4 formula(e) evaluated with 1 results within limits (all results (up to 1000) for each mass)
Elements Used:
C: 20-25 H: 15-20 O: 10-15
Nt-1-En 1_6d1 52 (1.792) Cm (1:58)
TOF MS ES-

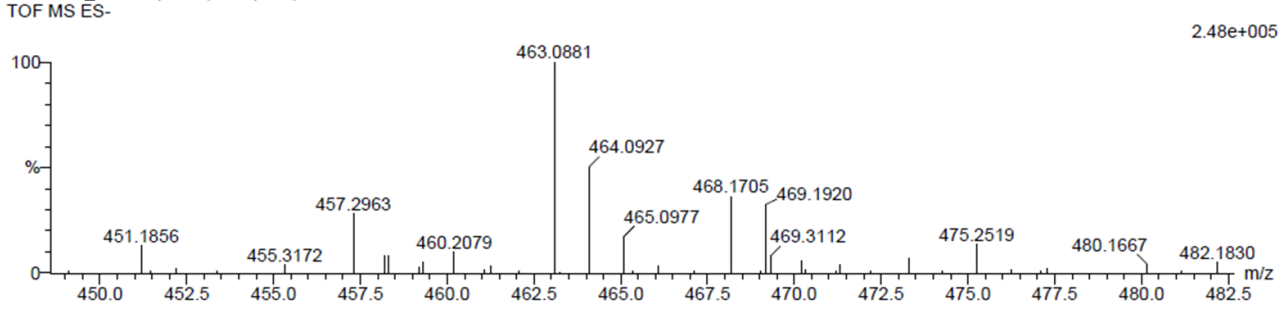

Minimum:				-1.5			
Maximum:		5.0	5.0	50.0			
Mass	Calc. Mass	mDa	PPM	DBE	i-FIT	i-FIT (Norm)	Formula
463.0881	463.0877	0.4	0.9	12.5	62.0	0.0	C21 H19 O12

Plate 4.26: HRESIMS of myricetin 3-*O*-rhamnopyranoside (4.6).

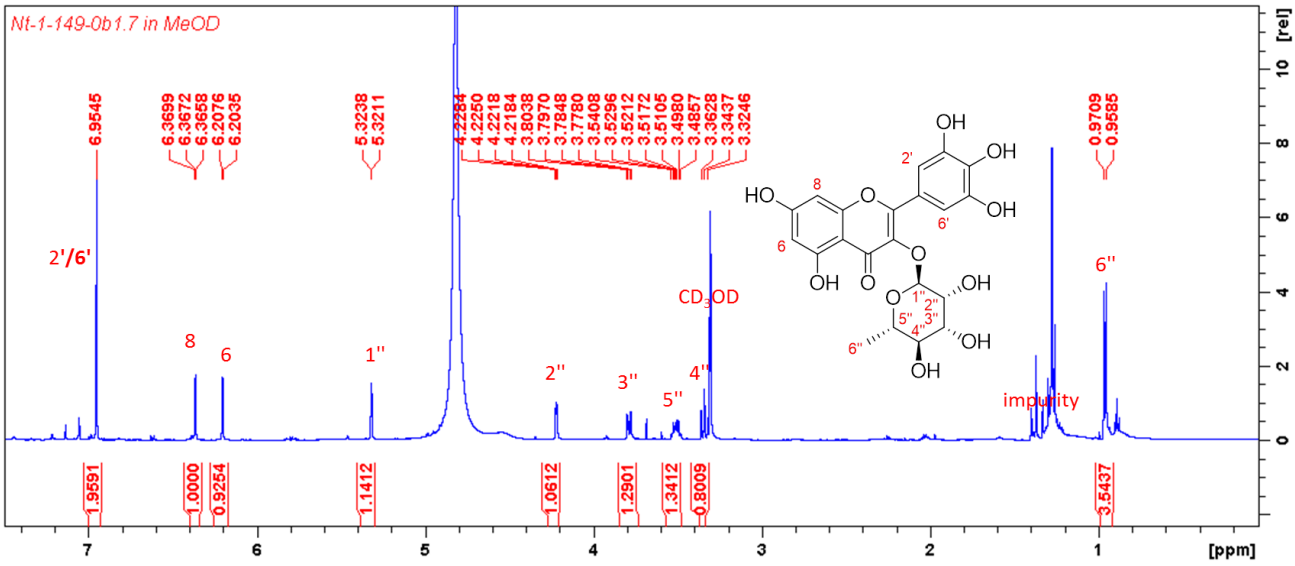

Plate 4.27: ^{1}H NMR (500 MHz, CD_3OD) spectrum of myricetin 3-*O*-rhamnopyranoside (4.6).

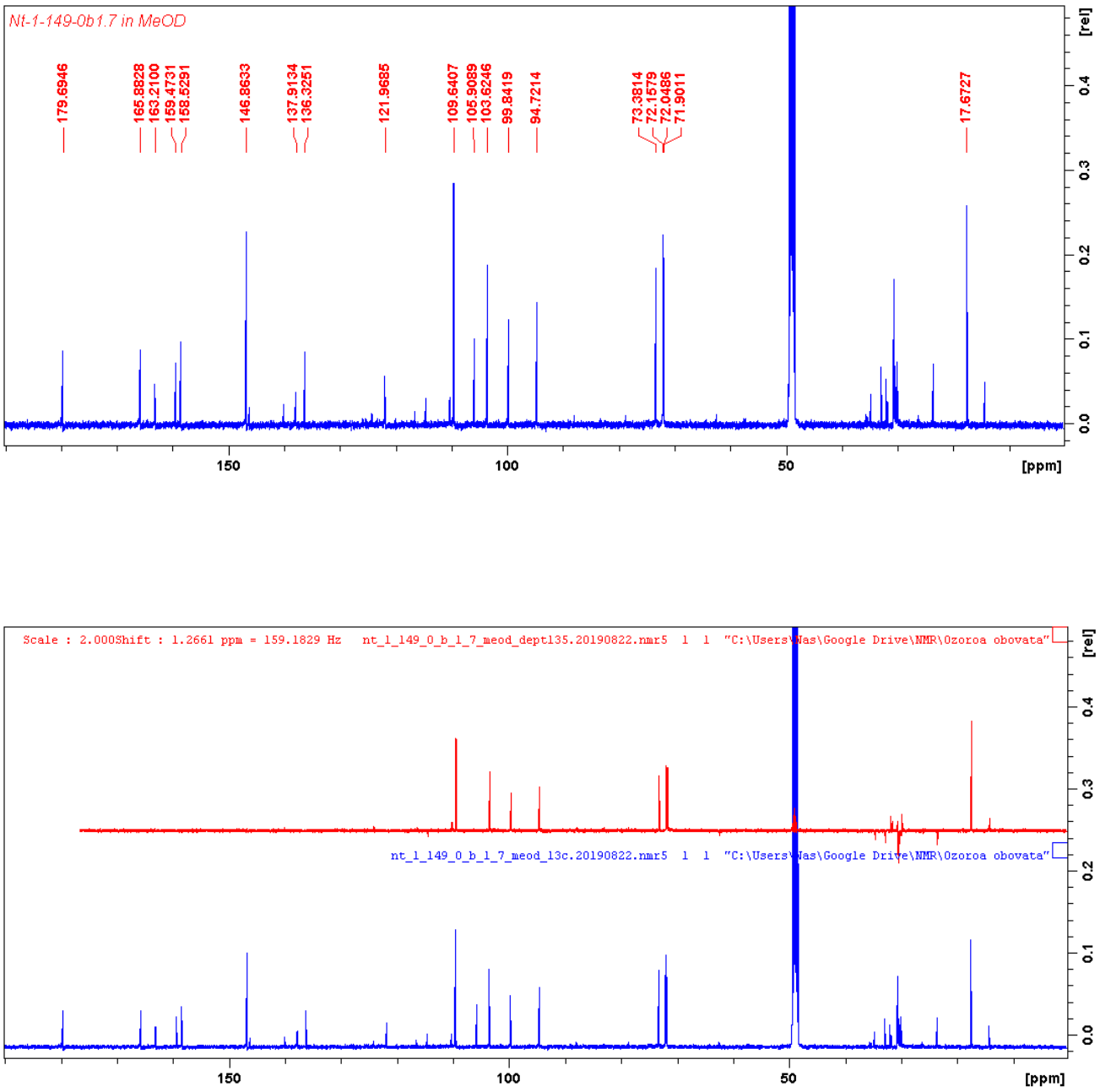

Plate 4.28: ^{13}C and DEPT (125 MHz, CD_3OD) spectra of myricetin 3-*O*-rhamnopyranoside (4.6).

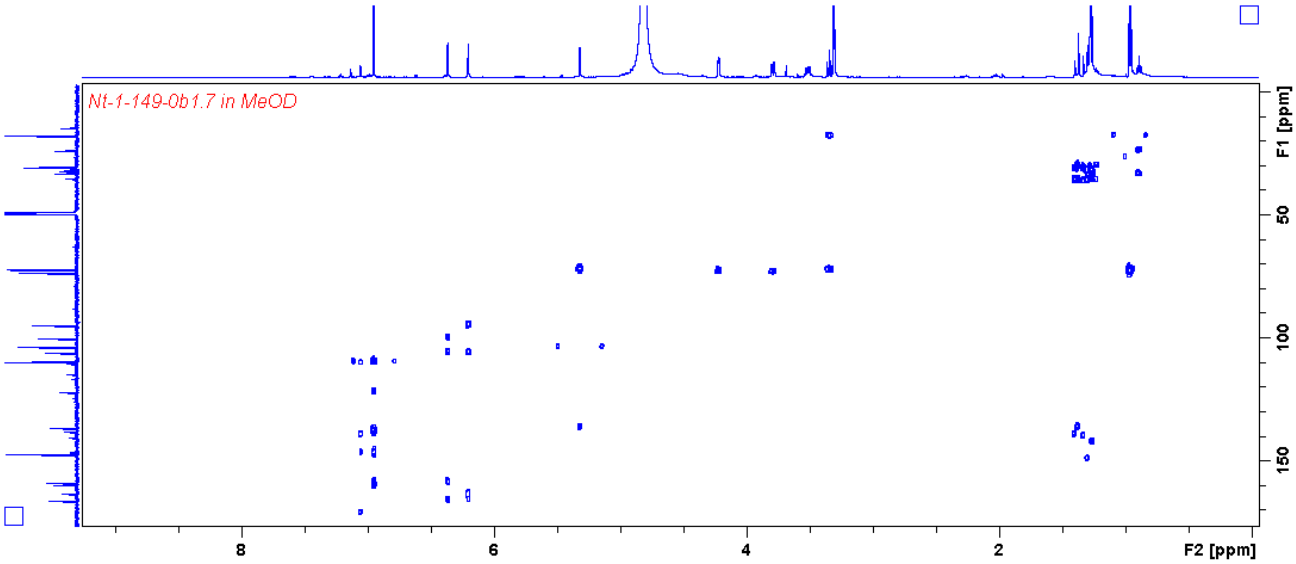

Plate 4.29: HMBC (500 MHz/125 MHz, CD_3OD) spectrum of myricetin 3-*O*-rhamnopyranoside (4.6).

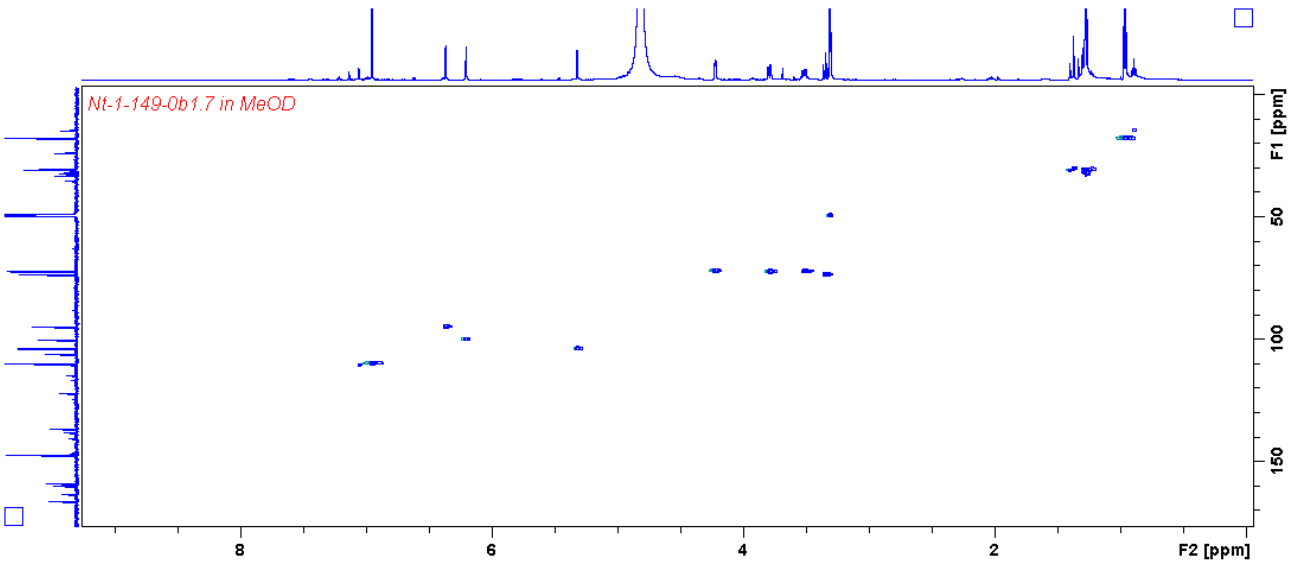

Plate 4.30: HSQC (500 MHz/125 MHz, CD_3OD) spectrum of myricetin 3-*O*-rhamnopyranoside (4.6).

Elemental Composition Report Page 1

Single Mass Analysis
Tolerance = 5.0 PPM / DBE: min = -1.5, max = 100.0
Element prediction: Off
Number of isotope peaks used for i-FIT = 3

Monoisotopic Mass, Even Electron Ions
5 formula(e) evaluated with 1 results within limits (all results (up to 1000) for each mass)
Elements Used:
C: 35-40 H: 55-65 O: 5-10
Nt-1-ob1_5 lrms 39 (0.648) Cm (1:60)
TOF MS ES-

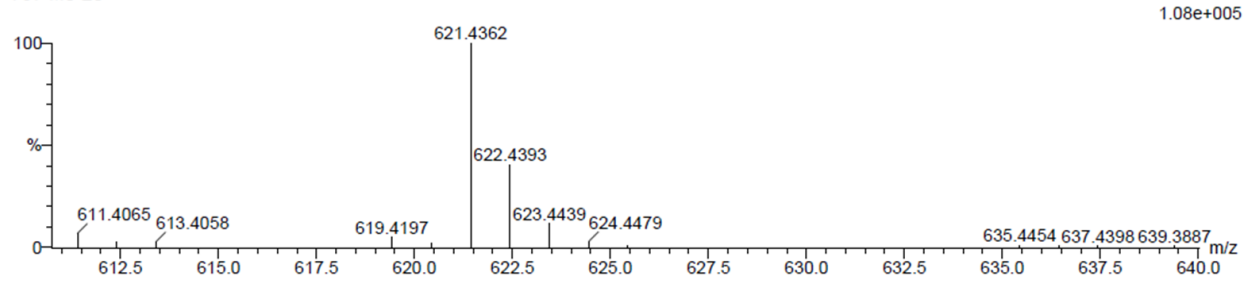

Minimum:				-1.5			
Maximum:		5.0	5.0	100.0			
Mass	Calc. Mass	mDa	PPM	DBE	i-FIT	i-FIT (Norm)	Formula
621.4362	621.4366	-0.4	-0.6	6.5	19.2	0.0	C36 H61 O8

Plate 4.31: HRESIMS of β-sitosterol 3-*O*-glucoside (4.7).

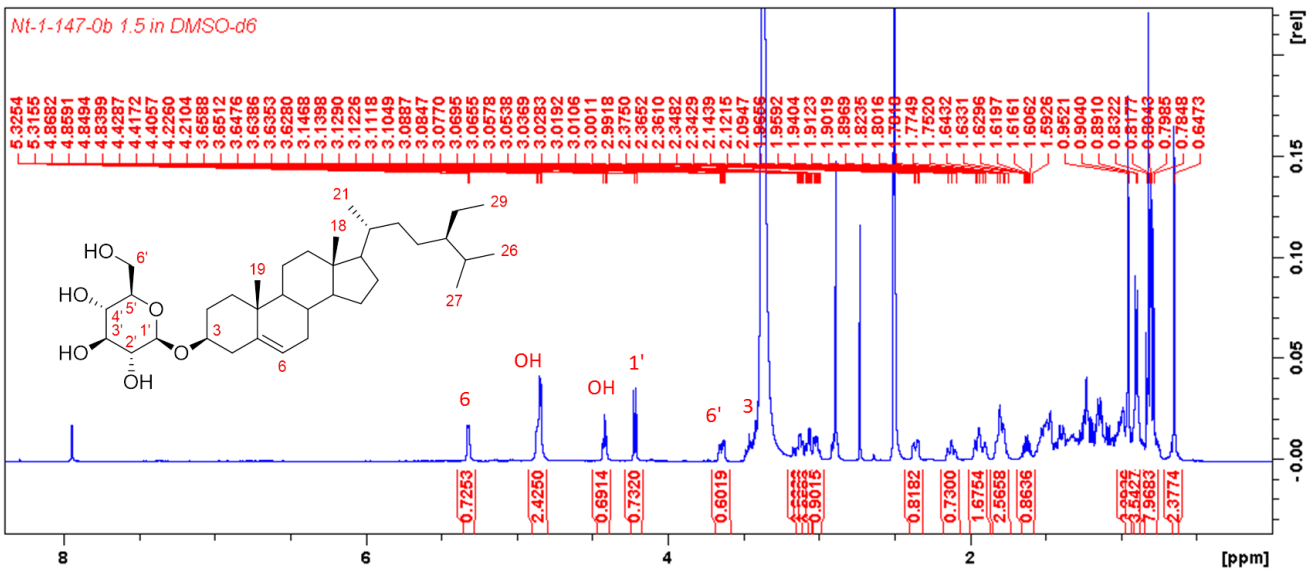

^{1}H NMR (500 MHz, DMSO-d_6) spectrum of β-sitosterol 3-*O*-glucoside (4.7).

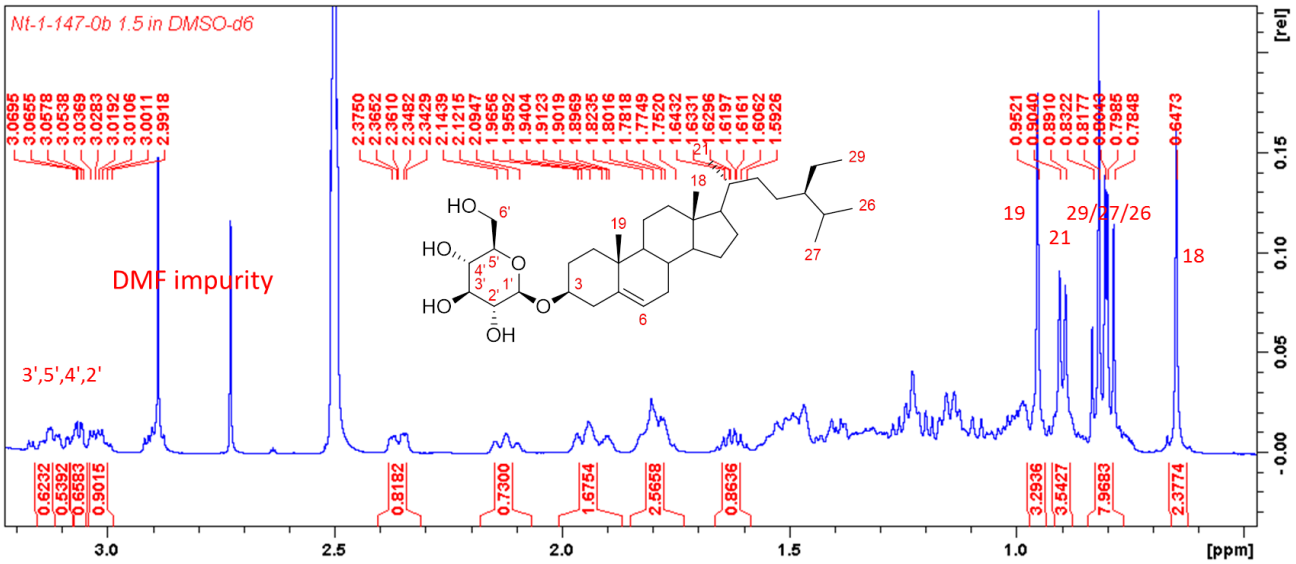

Plate 4.32: Expansion of ^{1}H NMR (500 MHz, DMSO-d_6) spectrum of β-sitosterol 3-*O*-glucoside (4.7).

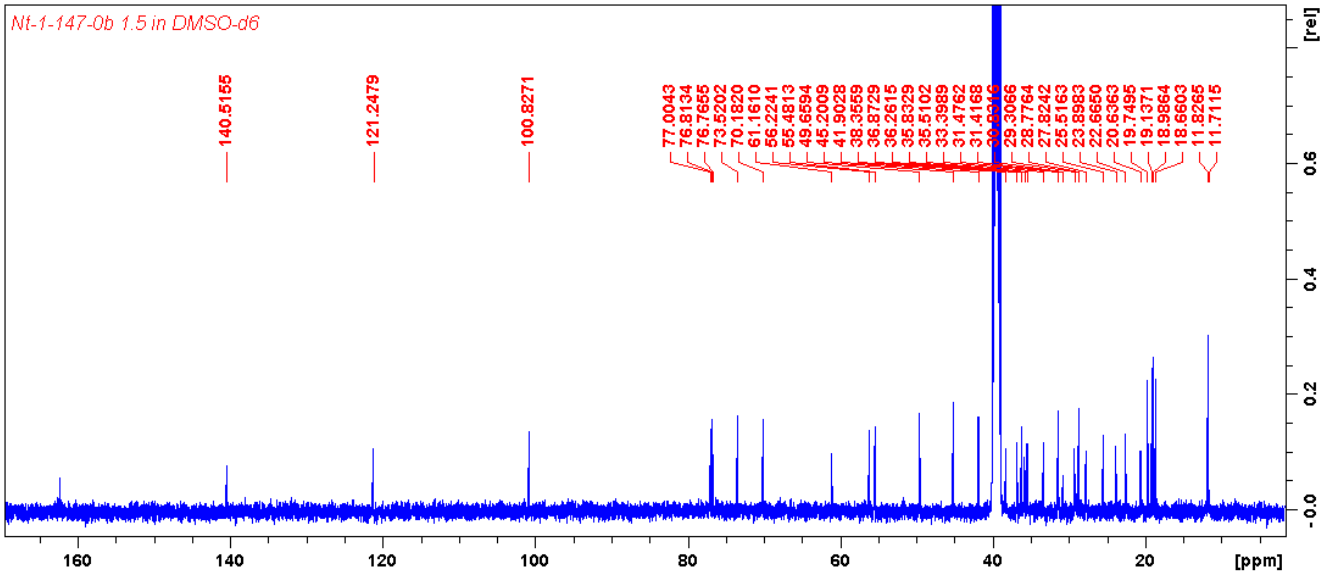

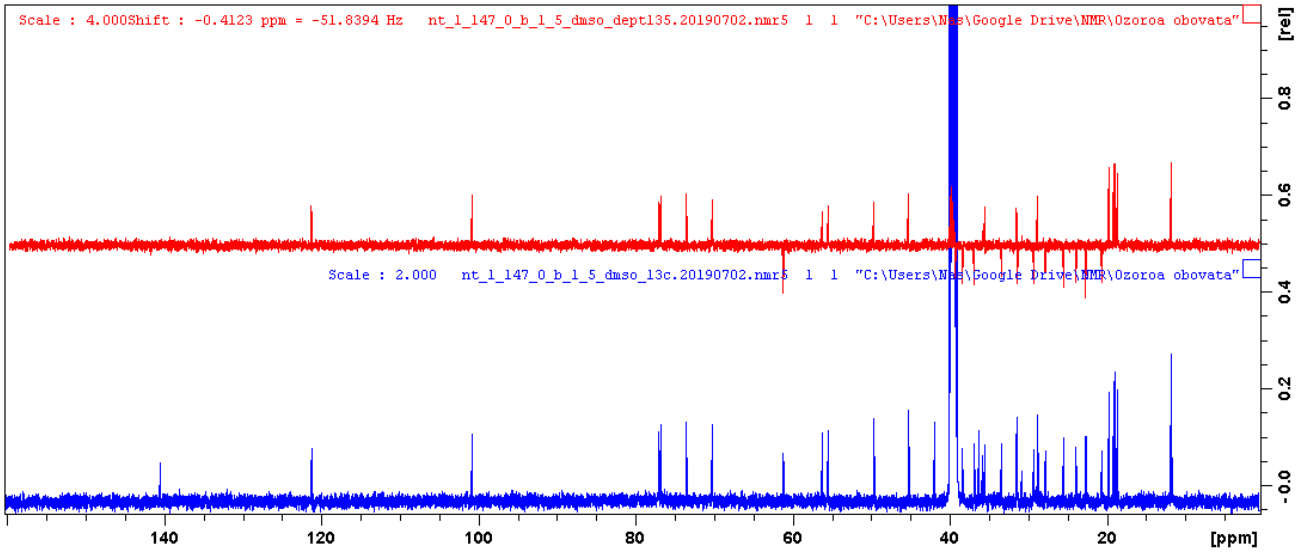

Plate 4.33: ^{13}C and DEPT (125 MHz, DMSO-d_6) spectra of β-sitosterol 3-*O*-glucoside (4.7).

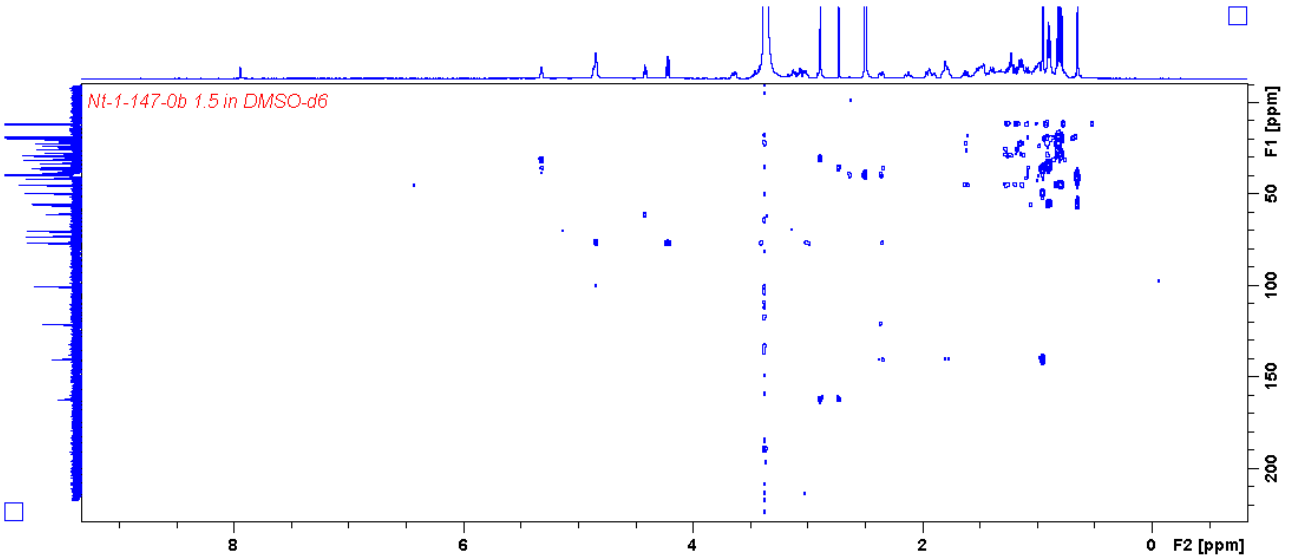

Plate 4.34: HMBC (500 MHz/125 MHz, DMSO-d_6) spectrum of β-sitosterol 3-*O*-glucoside (4.7).

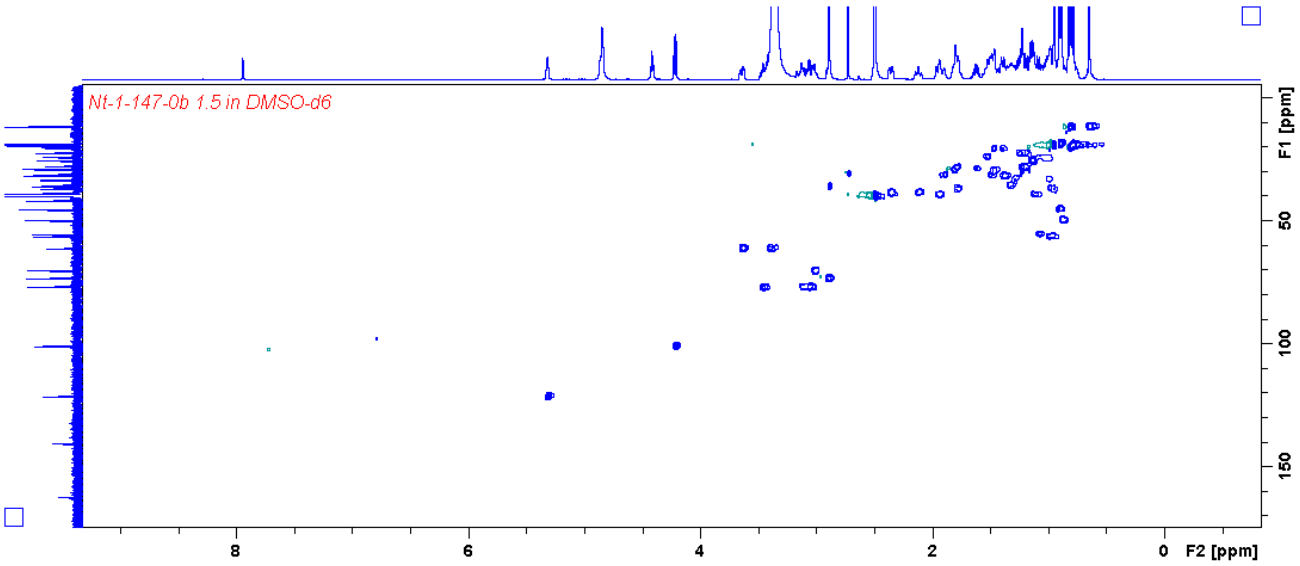

Plate 4.35: HSQC (500 MHz/125 MHz, DMSO-d_6) spectrum of β-sitosterol 3-*O*-glucoside (4.7).

Elemental Composition Report **Page 1**

Single Mass Analysis
Tolerance = 5.0 PPM / DBE: min = -1.5, max = 100.0
Element prediction: Off
Number of isotope peaks used for i-FIT = 3

Monoisotopic Mass, Even Electron Ions
3 formula(e) evaluated with 1 results within limits (all results (up to 1000) for each mass)
Elements Used:
C: 10-15 H: 20-25 O: 0-5 Na: 1-1

Nt-1-ob1_4 47 (1.552) Cm (1:61)
TOF MS ES+

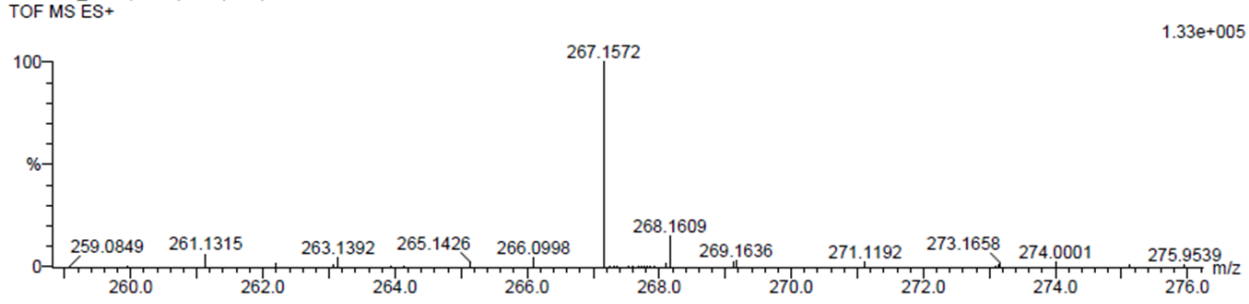

Minimum:				-1.5			
Maximum:		5.0	5.0	100.0			
Mass	Calc. Mass	mDa	PPM	DBE	i-FIT	i-FIT (Norm)	Formula
267.1572	267.1572	0.0	0.0	1.5	185.4	0.0	C13 H24 O4 Na

Plate 4.36: HRESIMS of (*3S,5R,6R,7E,9S*)-3,5,6,9-tetrahydroxymegastigman-7-ene (4.8).

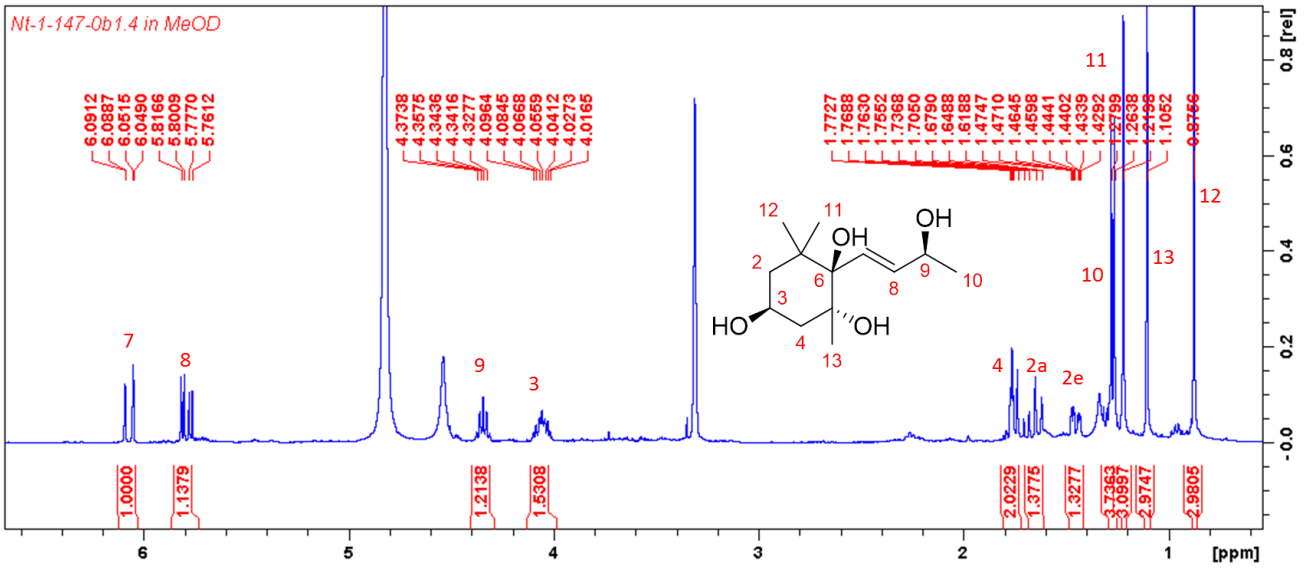

Plate 4.37: ^{1}H NMR (400 MHz, CD_3OD) spectrum of (*3S,5R,6R,7E,9S*)-3,5,6,9-tetrahydroxymegastigman-7-ene (4.8).

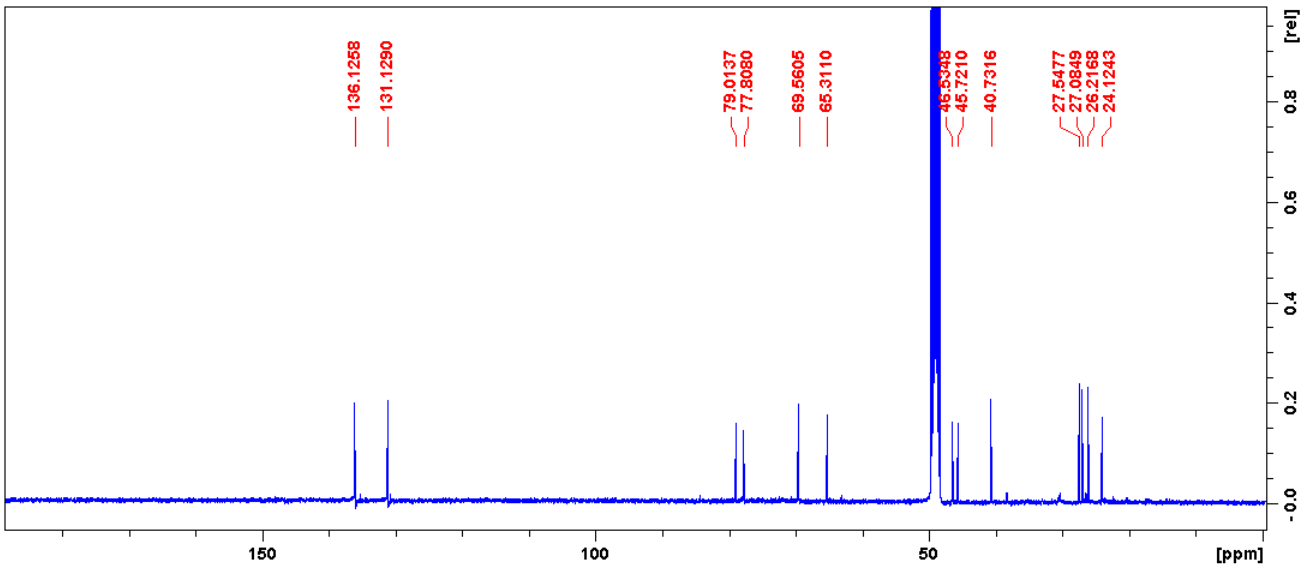

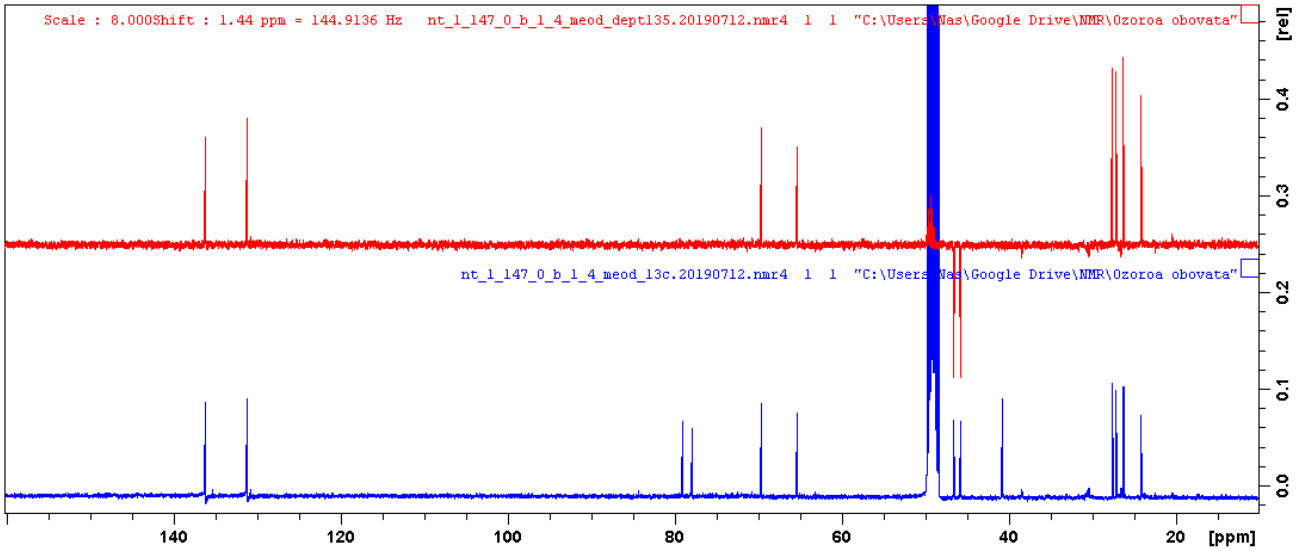

Plate 4.38: ^{13}C and DEPT (100 MHz, CD_3OD) spectra of (*3S,5R,6R,7E,9S*)-3,5,6,9-tetrahydroxymegastigman-7-ene (4.8).

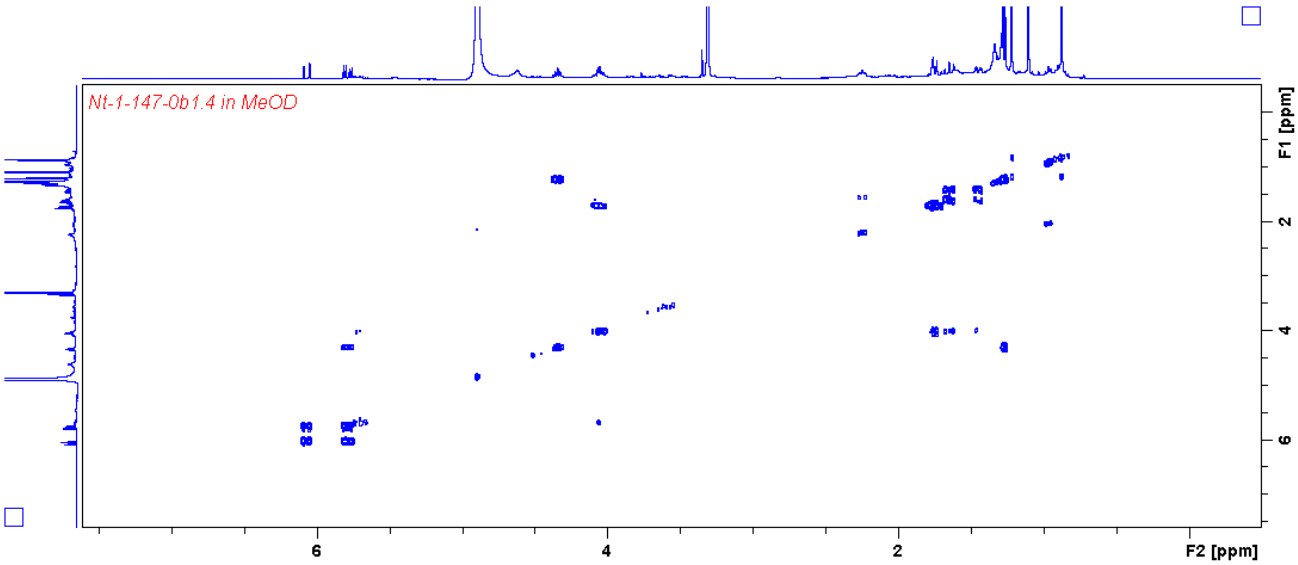

Plate 4.39: COSY (400 MHz, CD_3OD) spectrum of (*3S,5R,6R,7E,9S*)-3,5,6,9-tetrahydroxymegastigman-7-ene (4.8).

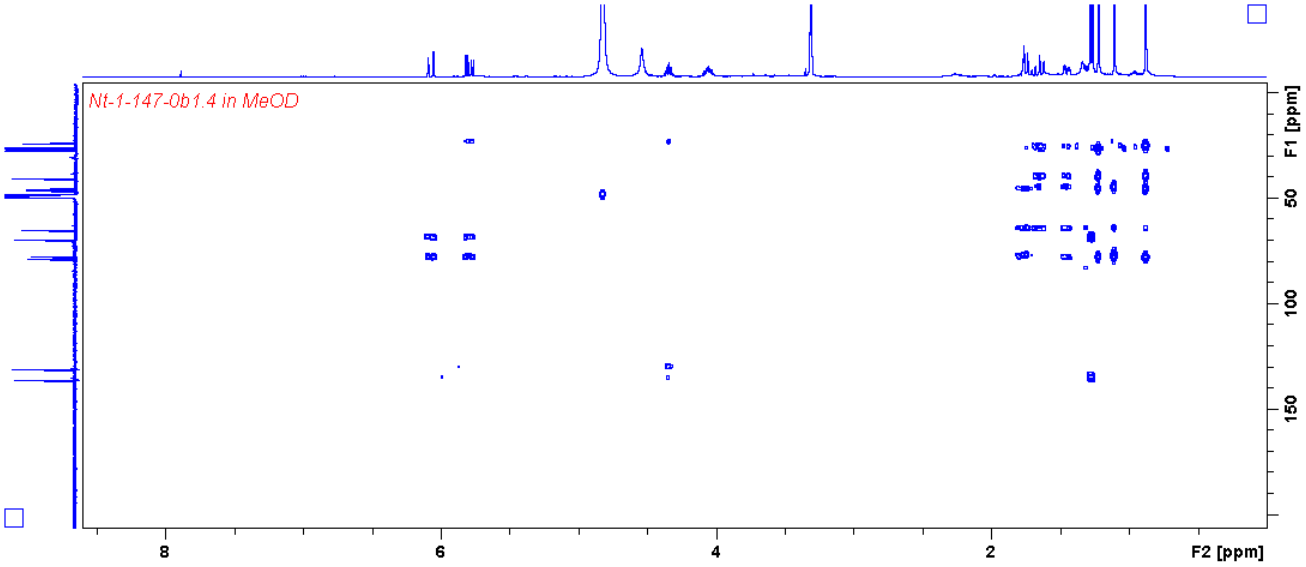

Plate 4.40: HMBC (400 MHz, CD_3OD) spectrum of (*3S,5R,6R,7E,9S*)-3,5,6,9-tetrahydroxymegastigman-7-ene (4.8).

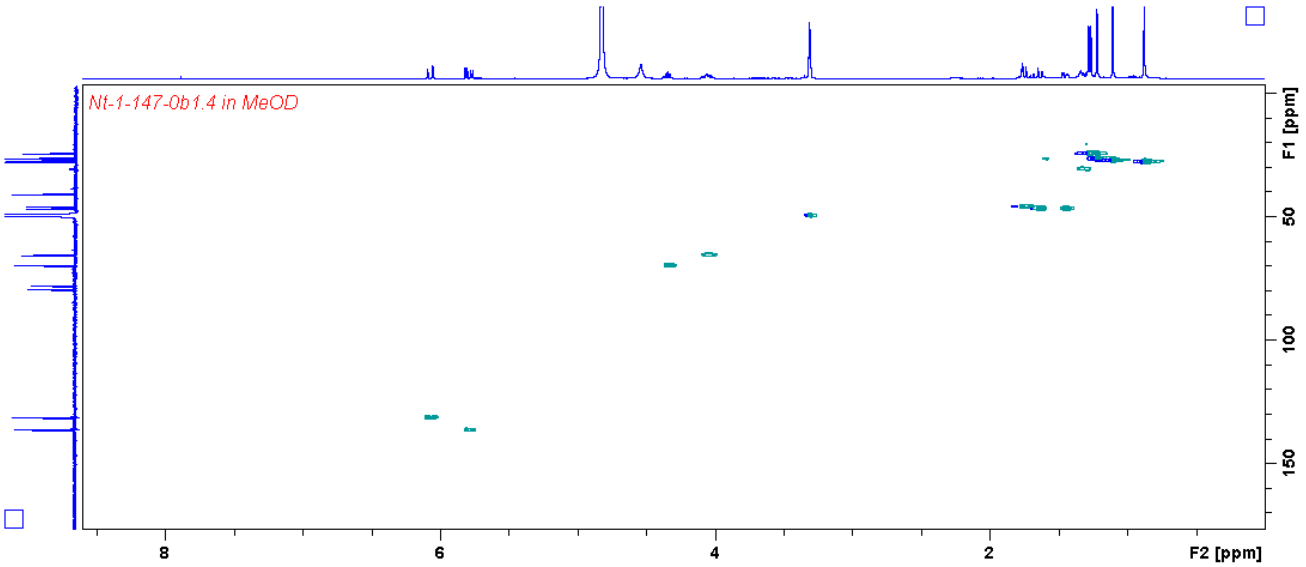

Plate 4.41: HMBC (400 MHz, CD_3OD) spectrum of (*3S,5R,6R,7E,9S*)-3,5,6,9-tetrahydroxymegastigman-7-ene (4.8).

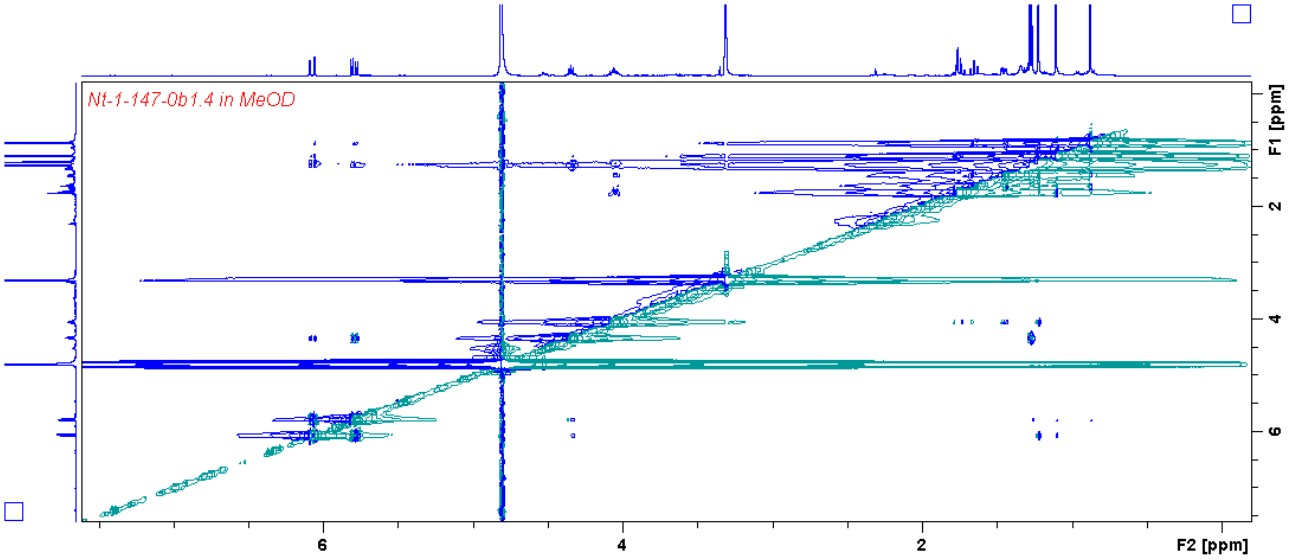

Plate 4.42: NOESY (400 MHz, CD_3OD) spectrum of (*3S,5R,6R,7E,9S*)-3,5,6,9-tetrahydroxymegastigman-7-ene (4.8).

APPENDIX C. HRESIMS AND NMR SPECTRA OF COMPOUNDS DESCRIBED IN CHAPTER 5

Elemental Composition Report Page 1

Single Mass Analysis
Tolerance = 5.0 PPM / DBE: min = -1.5, max = 50.0
Element prediction: Off
Number of isotope peaks used for i-FIT = 3

Monoisotopic Mass, Even Electron Ions
3 formula(e) evaluated with 1 results within limits (all results (up to 1000) for each mass)
Elements Used:
C: 20-25 H: 15-20 O: 10-15
Nt-1-En 1_6a 9 (0.270) Cm (1:61)
TOF MS ES-

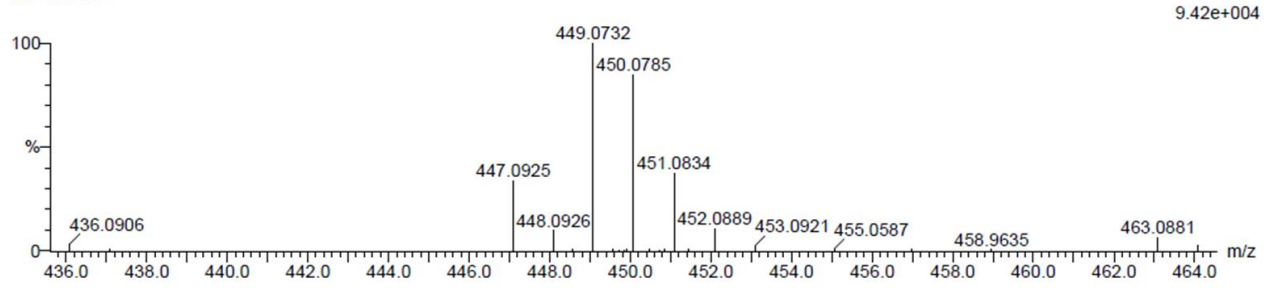

Minimum:				-1.5			
Maximum:		5.0	5.0	50.0			
Mass	Calc. Mass	mDa	PPM	DBE	i-FIT	i-FIT (Norm)	Formula
449.0732	449.0720	1.2	2.7	12.5	128.4	0.0	C20 H17 O12

Plate 5.1: HRESIMS of myricetin 3-*O*-arabinopyranoside (5.1).

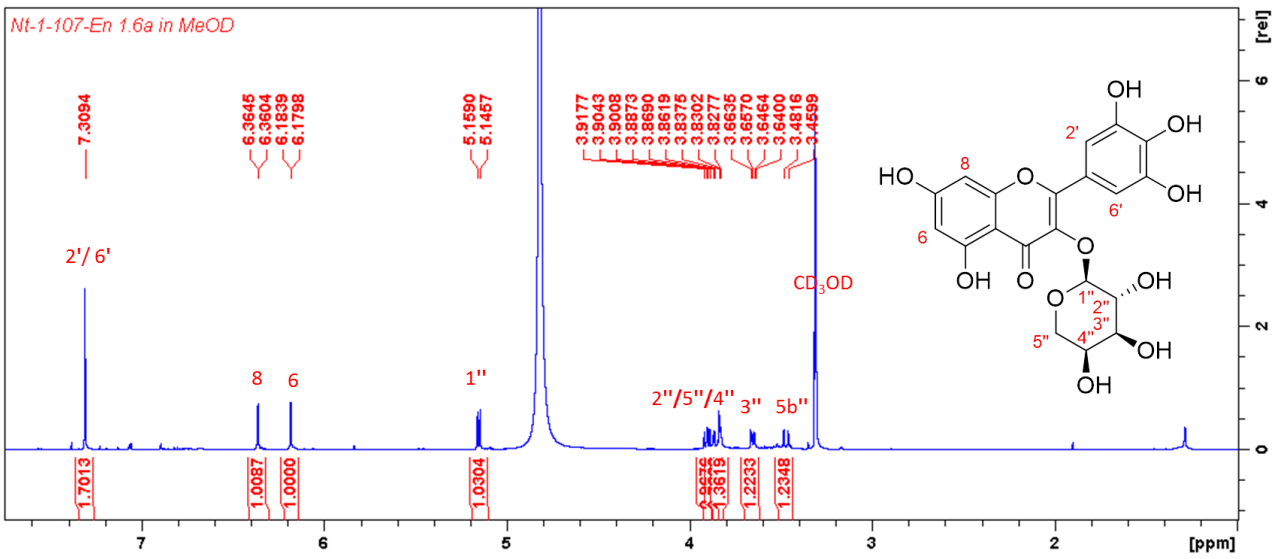

Plate 5.2: ^{1}H NMR (500 MHz, CD_3OD) spectrum of myricetin 3-*O*-arabinopyranoside (5.1).

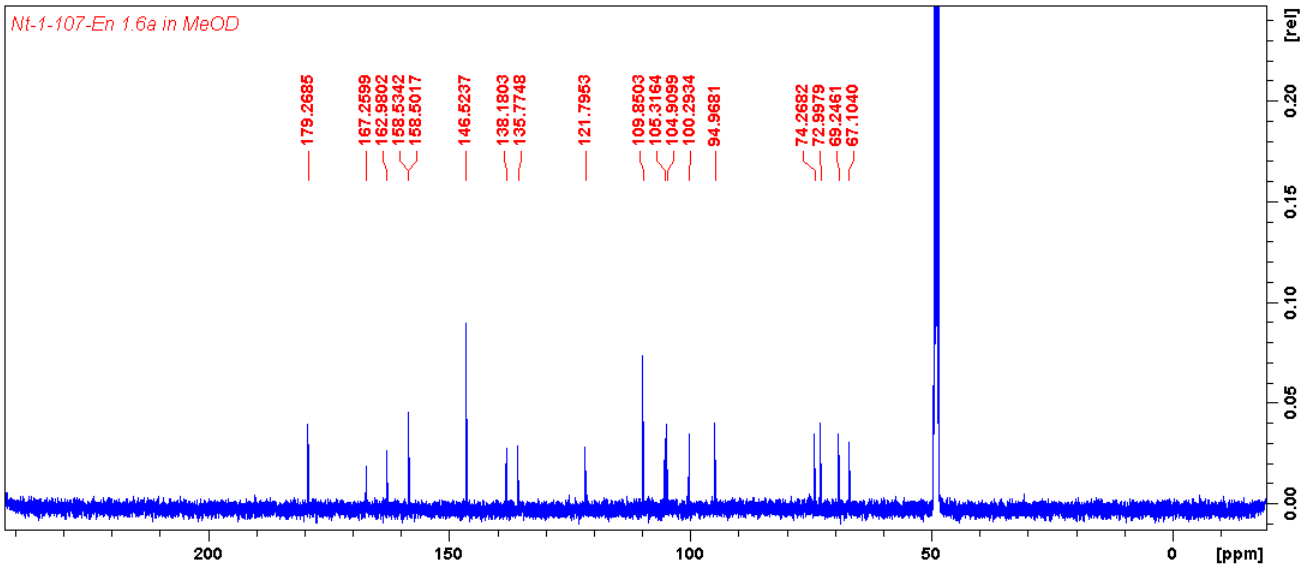

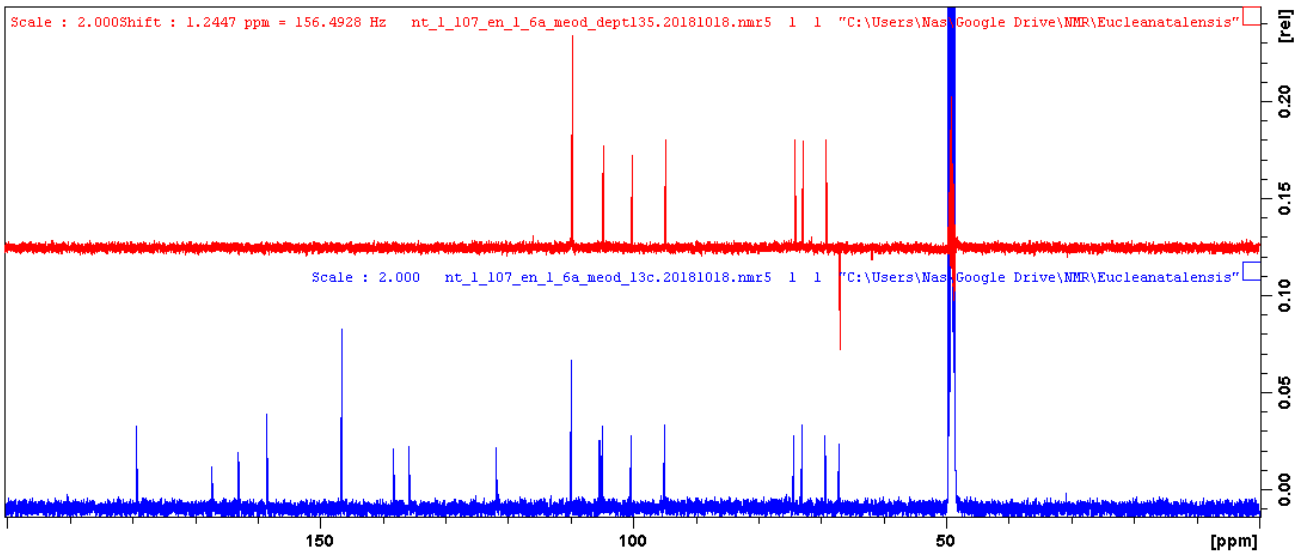

Plate 5.3: ^{13}C and DEPT (125 MHz, CD_3OD) spectra of myricetin 3-*O*-arabinopyranoside (5.1).

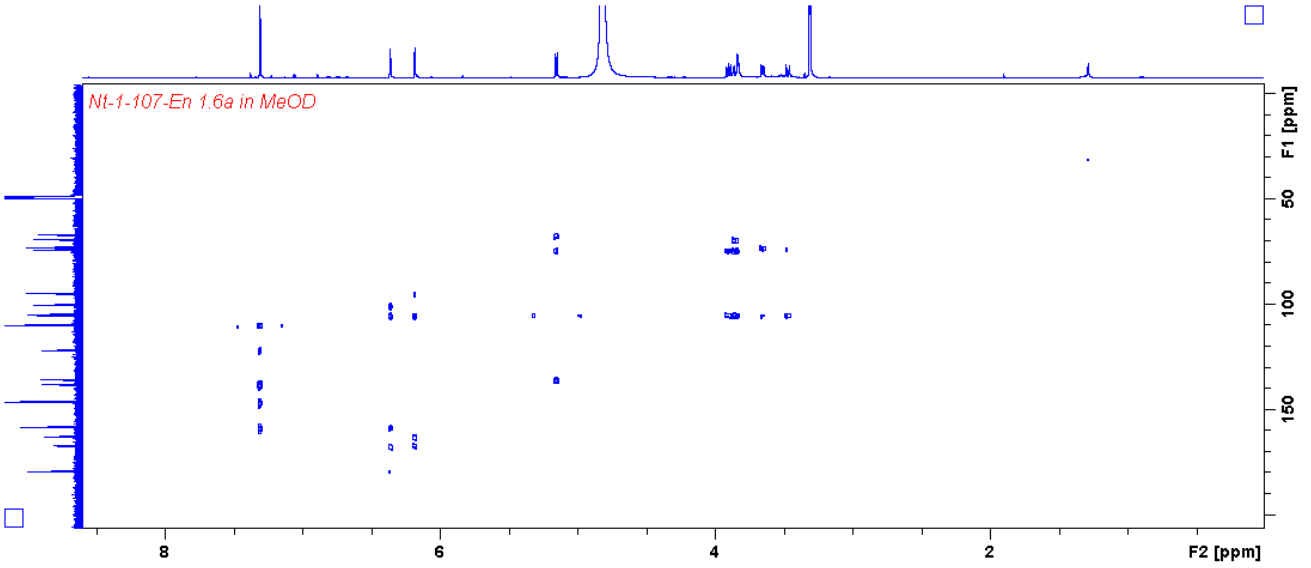

Plate 5.4: HMBC (500 MHz/125 MHz, CD_3OD) spectrum of myricetin 3-*O*-arabinopyranoside (5.1).

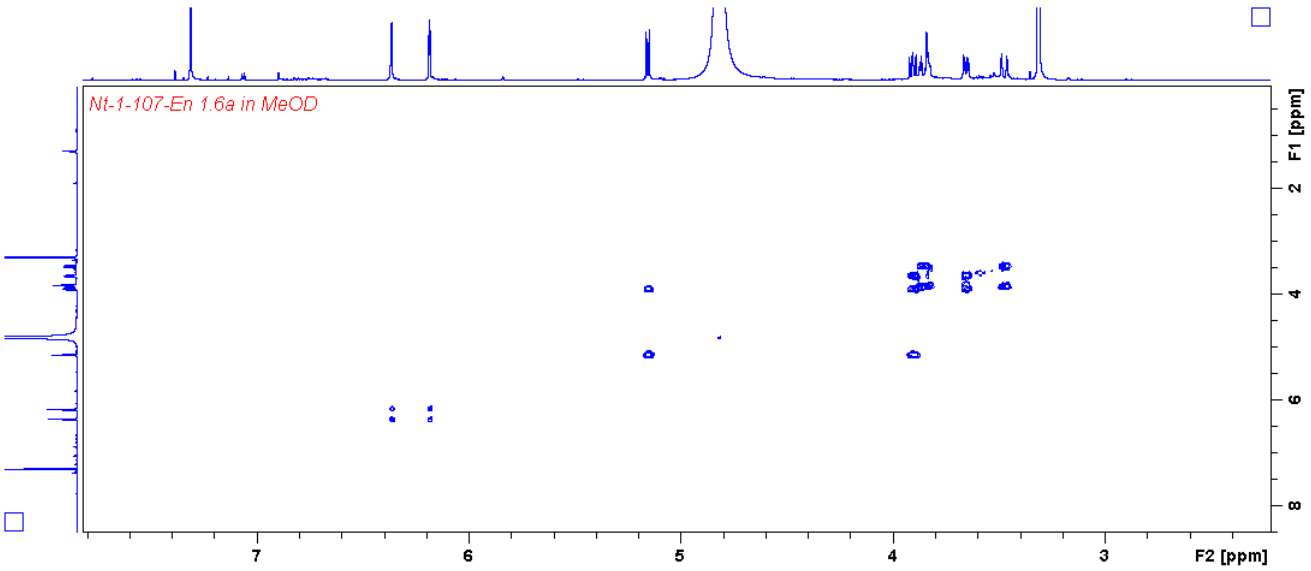

Plate 5.5: COSY (500 MHz, CD_3OD) spectrum of myricetin 3-*O*-arabinopyranoside (5.1).

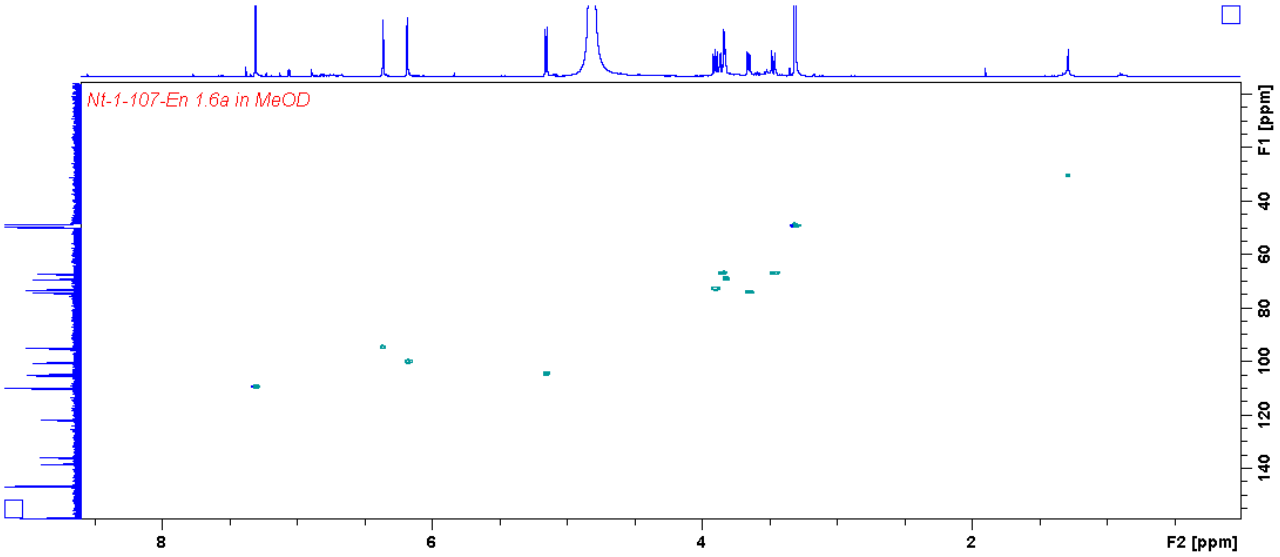

Plate 5.6: HSQC (500 MHz/125 MHz, CD_3OD) spectrum of myricetin 3-*O*-arabinopyranoside (5.1).

Elemental Composition Report Page 1

Single Mass Analysis
Tolerance = 5.0 PPM / DBE: min = -1.5, max = 50.0
Element prediction: Off
Number of isotope peaks used for i-FIT = 3

Monoisotopic Mass, Even Electron Ions
4 formula(e) evaluated with 1 results within limits (all results (up to 1000) for each mass)
Elements Used:
C: 20-25 H: 15-20 O: 10-15
Nt-1-En 1_6d1 52 (1.792) Cm (1:58)
TOF MS ES-

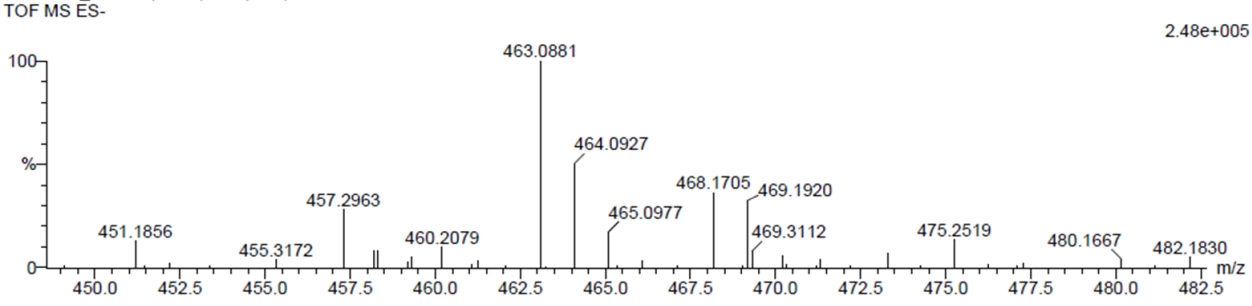

Minimum:				-1.5			
Maximum:		5.0	5.0	50.0			
Mass	Calc. Mass	mDa	PPM	DBE	i-FIT	i-FIT (Norm)	Formula
463.0881	463.0877	0.4	0.9	12.5	62.0	0.0	C21 H19 O12

Plate 5.7: HRESIMS of myricetin 3-*O*-rhamnopyranoside 5.2 and quercetin 3-*O*-glucoside (5.6).

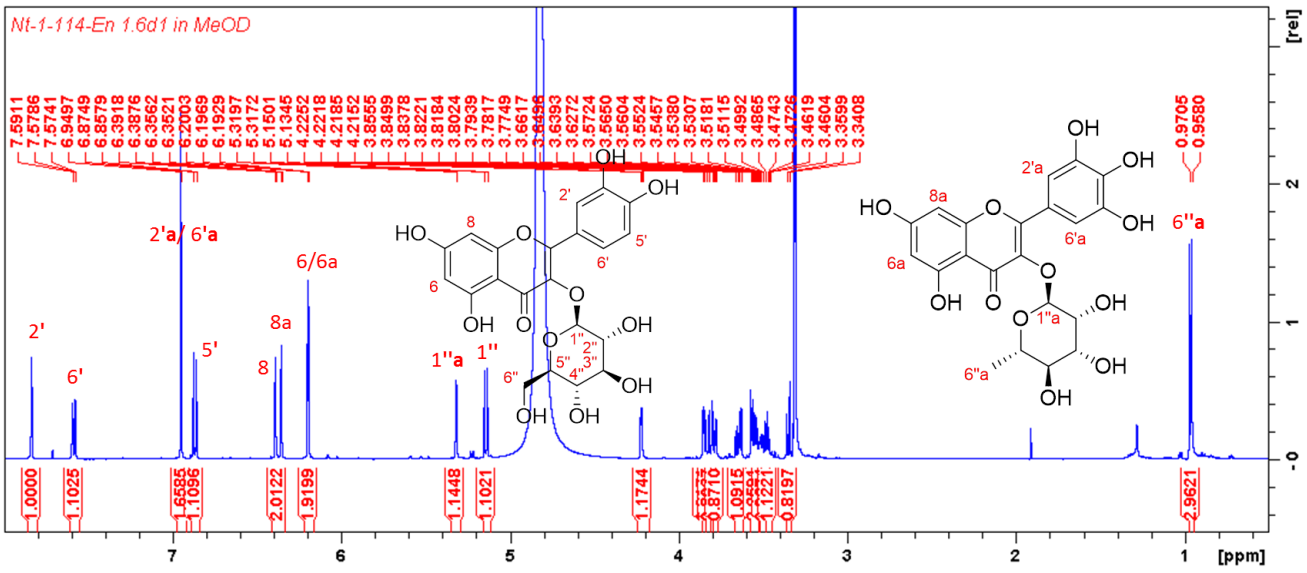

Plate 5.8: ^{1}H NMR (500 MHz, CD_3OD) spectrum of myricetin 3-*O*-rhamnopyranoside 5.2 and quercetin 3-*O*-glucoside (5.6).

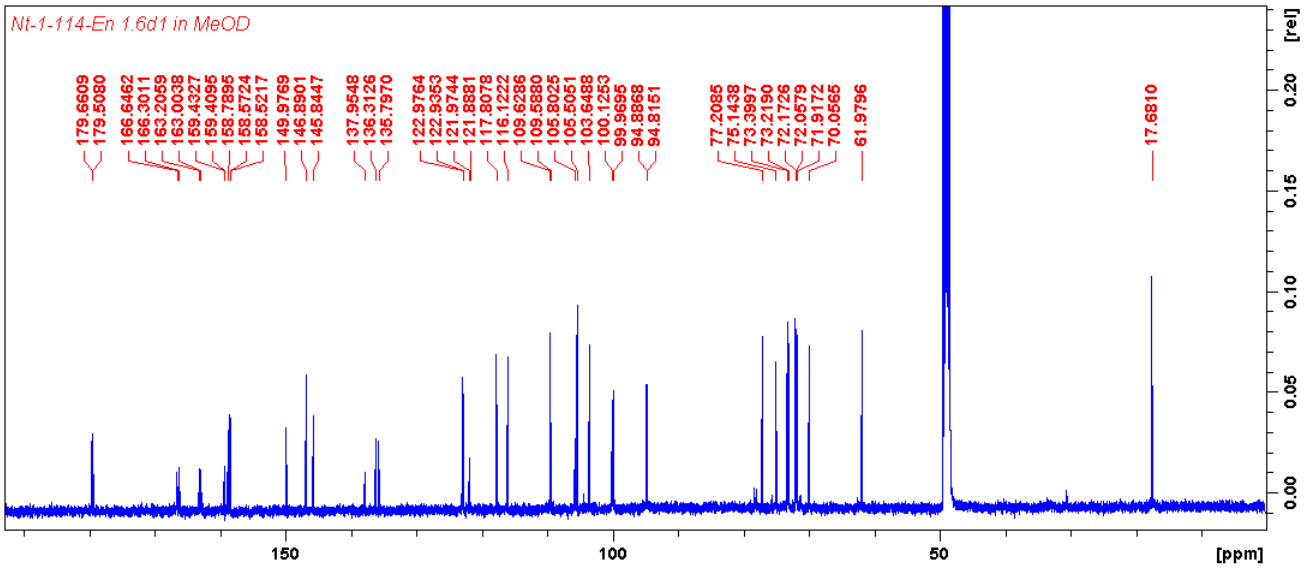

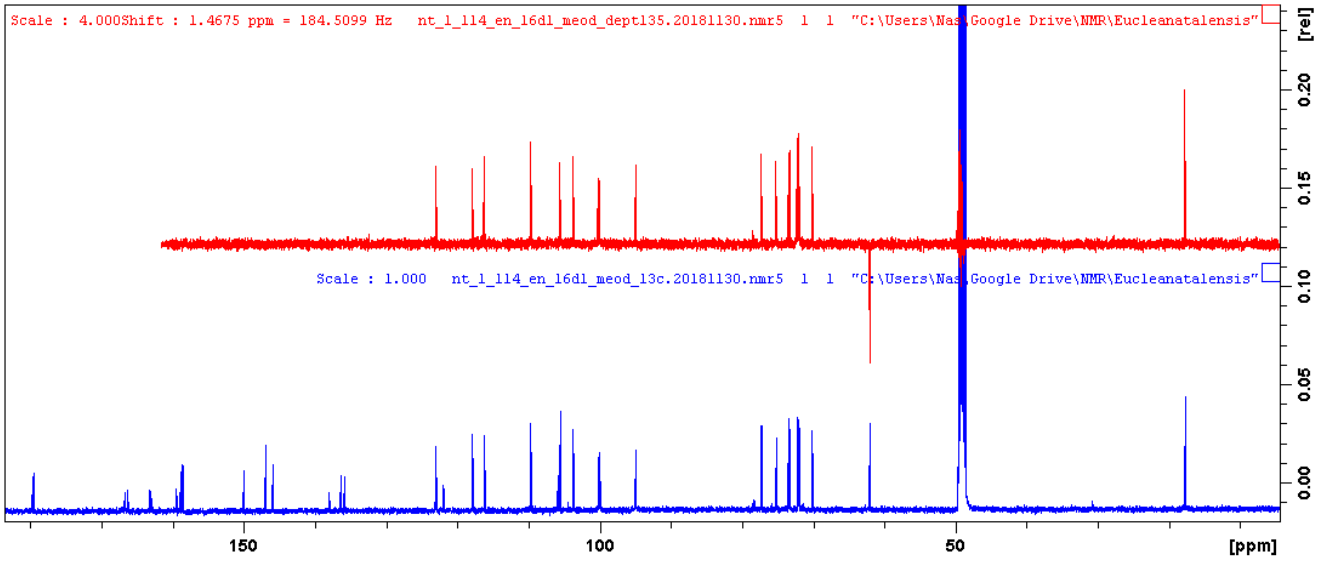

Plate 5.9: ^{13}C and DEPT (125 MHz, CD_3OD) spectra of myricetin 3-*O*-rhamnopyranoside 5.2 and quercetin 3-*O*-glucoside (5.6).

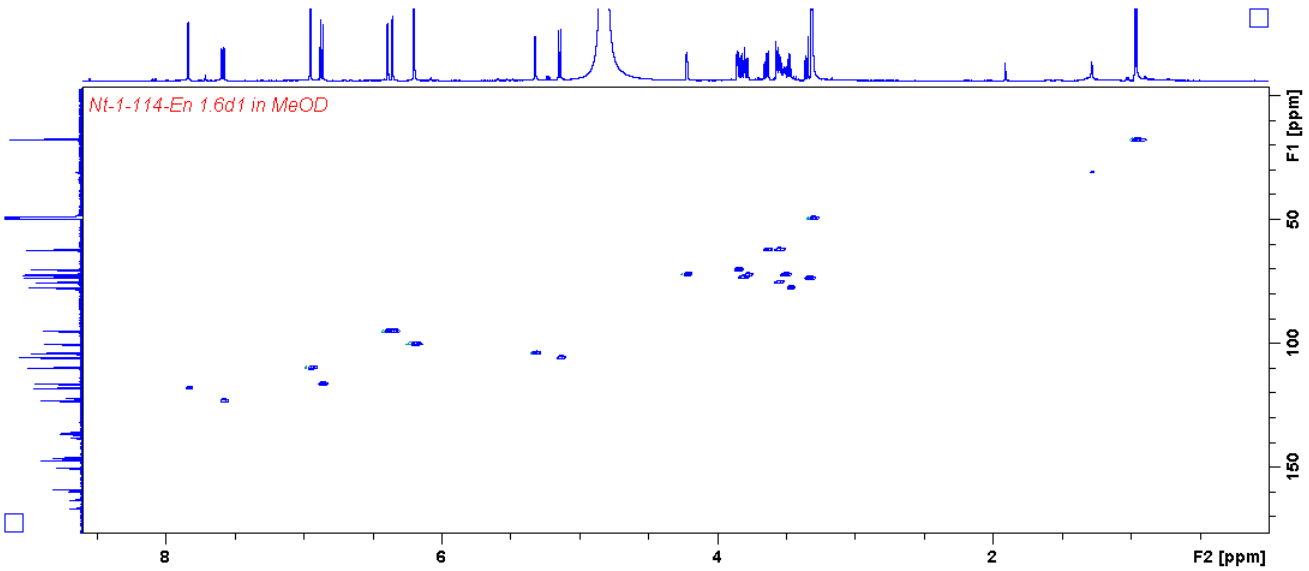

Plate 5.10: HSQC (500 MHz/125 MHz, CD_3OD) spectrum of myricetin 3-*O*-rhamnopyranoside 5.2 and quercetin 3-*O*-glucoside (5.6).

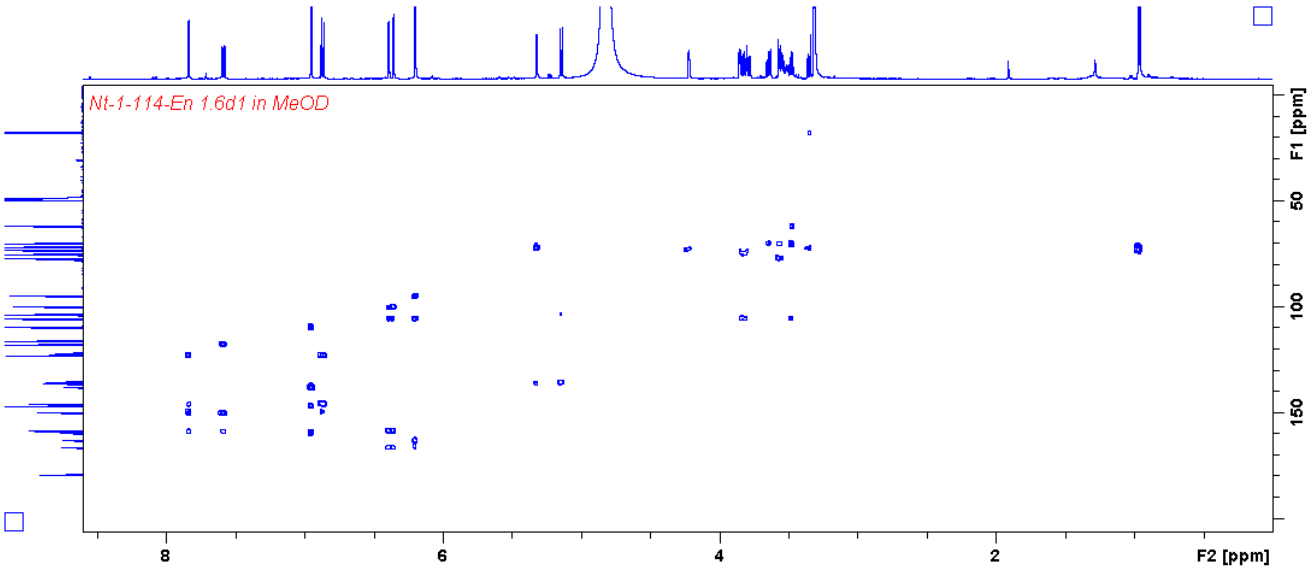

Plate 5.11: HMBC (500 MHz/125 MHz, CD_3OD) spectrum of myricetin 3-*O*-rhamnopyranoside 5.2 and quercetin 3-*O*-glucoside (5.6).

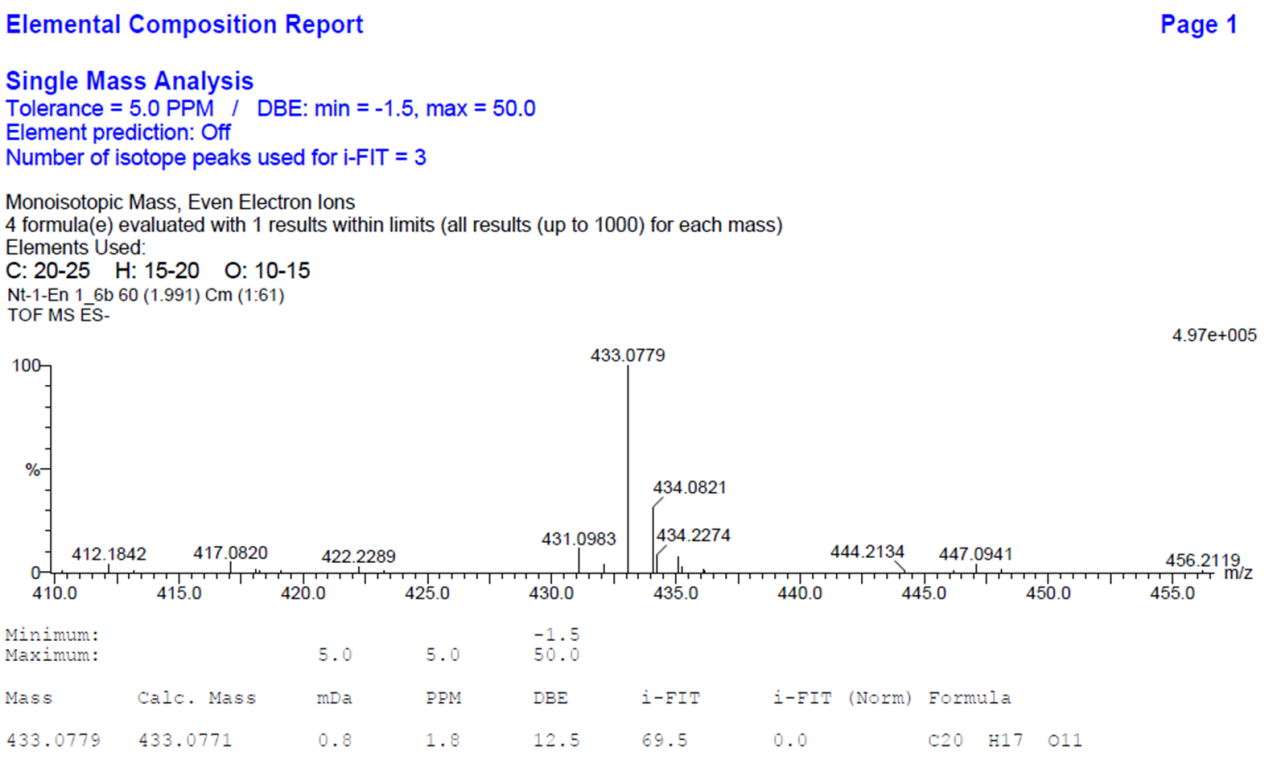

Plate 5.12: HRESIMS of quercetin 3-*O*-arabinofuranoside (5.3).

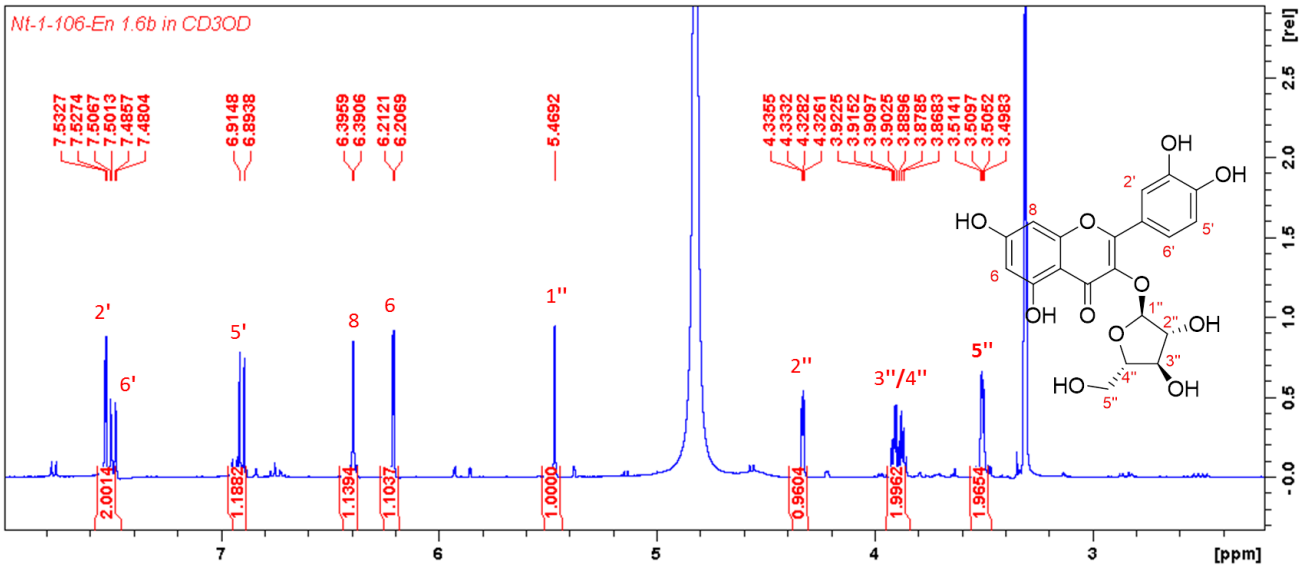

Plate 5.13: ^{1}H NMR (400 MHz, CD_3OD) spectrum of quercetin 3-*O*-arabinofuranoside (5.3).

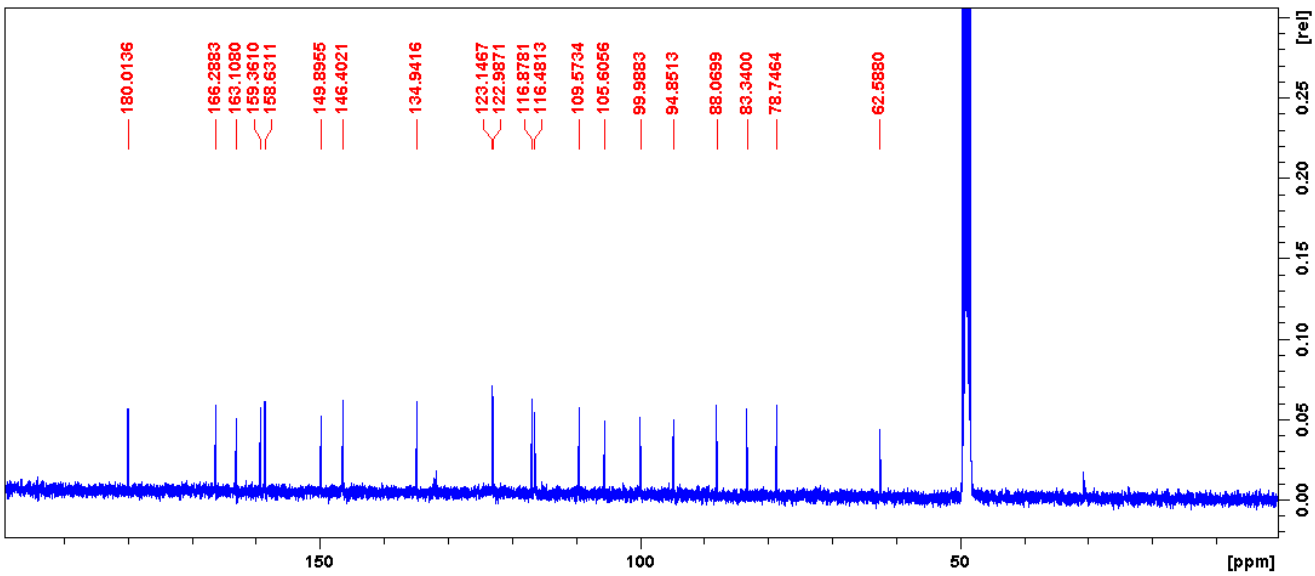

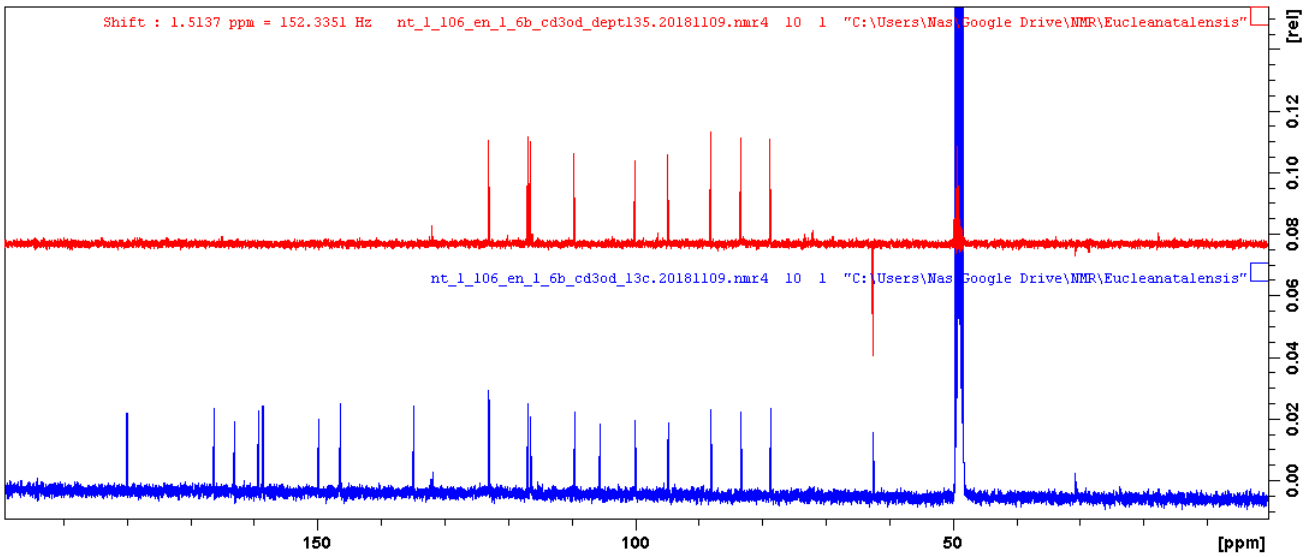

Plate 5.14: ^{13}C and DEPT (100 MHz, CD_3OD) spectra of quercetin 3-*O*-arabinofuranoside (5.3).

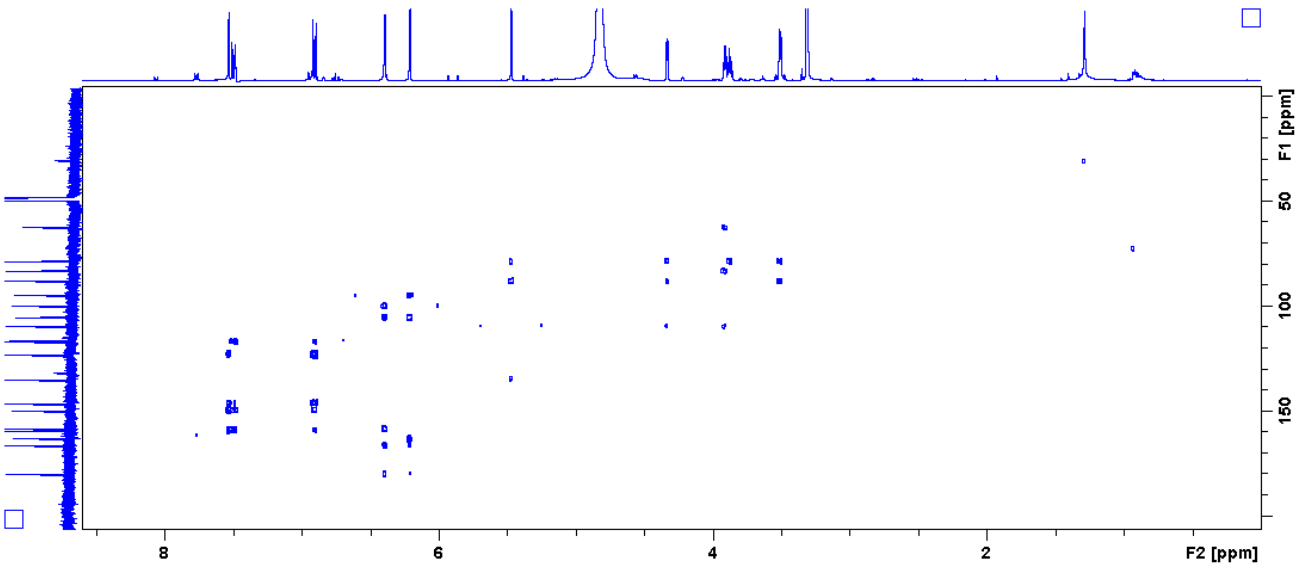

Plate 5.15: HMBC (400 MHz/100 MHz, CD_3OD) spectrum of quercetin 3-*O*-arabinofuranoside (5.3).

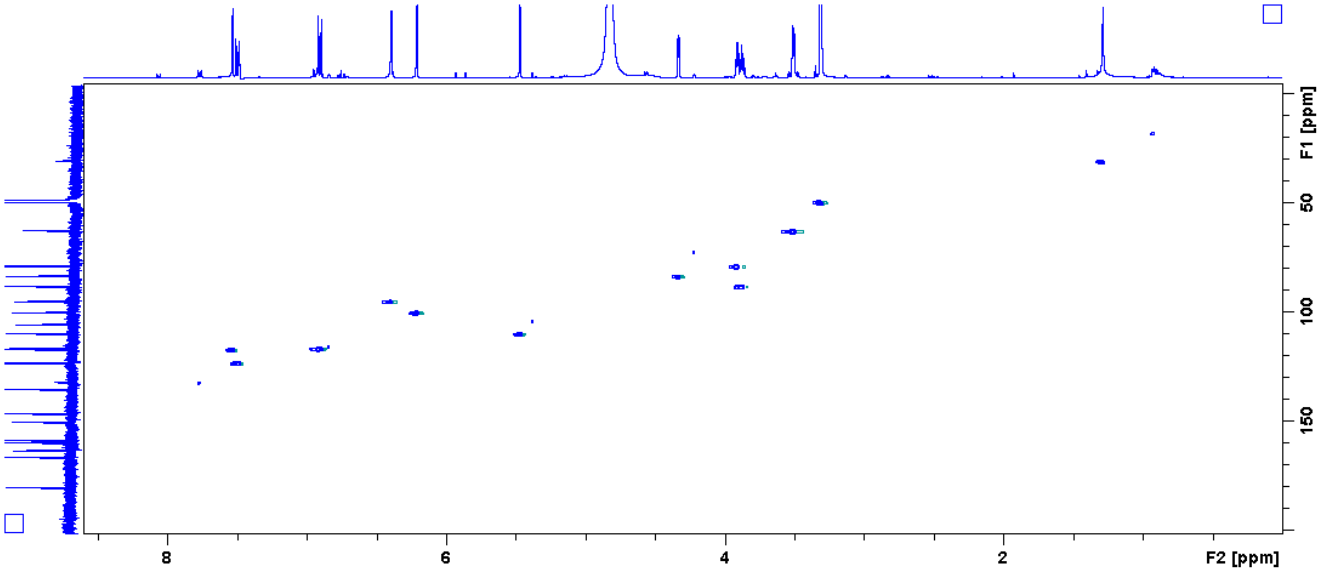

Plate 5.16: HSQC (400 MHz/100 MHz, CD_3OD) spectrum of quercetin 3-*O*-arabinofuranoside (5.3).

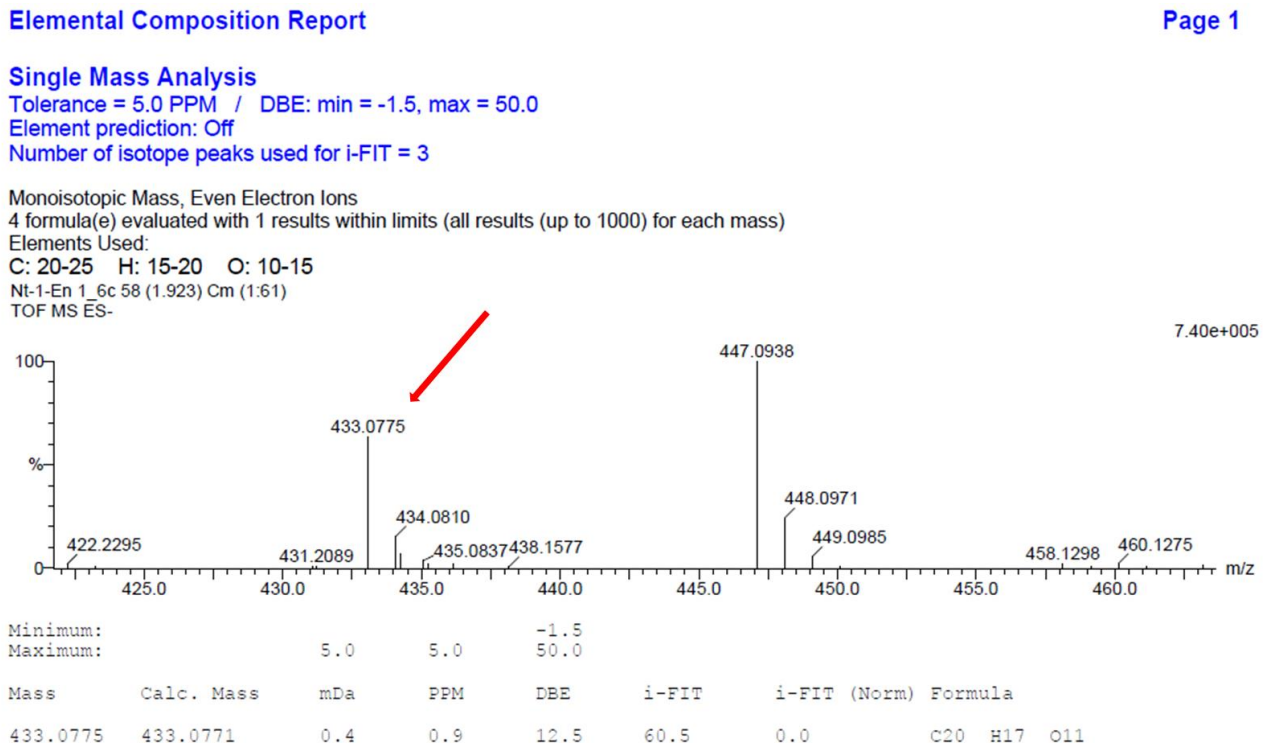

Plate 5.17: HRESIMS of quercetin 3-*O*-arabinopyranoside (5.4).

Elemental Composition Report Page 1

Single Mass Analysis
Tolerance = 5.0 PPM / DBE: min = -1.5, max = 50.0
Element prediction: Off
Number of isotope peaks used for i-FIT = 3

Monoisotopic Mass, Even Electron Ions
4 formula(e) evaluated with 1 results within limits (all results (up to 1000) for each mass)
Elements Used:
C: 20-25 H: 15-20 O: 10-15
Nt-1-En 1_6c 58 (1.923) Cm (1:61)
TOF MS ES-

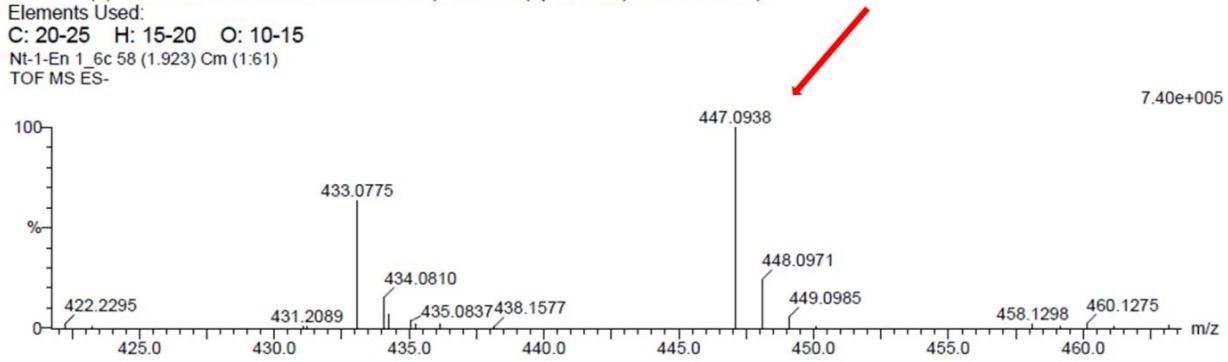

Minimum:				-1.5			
Maximum:		5.0	5.0	50.0			
Mass	Calc. Mass	mDa	PPM	DBE	i-FIT	i-FIT (Norm)	Formula
447.0938	447.0927	1.1	2.5	12.5	17.8	0.0	C21 H19 O11

Plate 5.18: HRESIMS of quercetin 3-*O*-rhamnopyranoside (5.5).

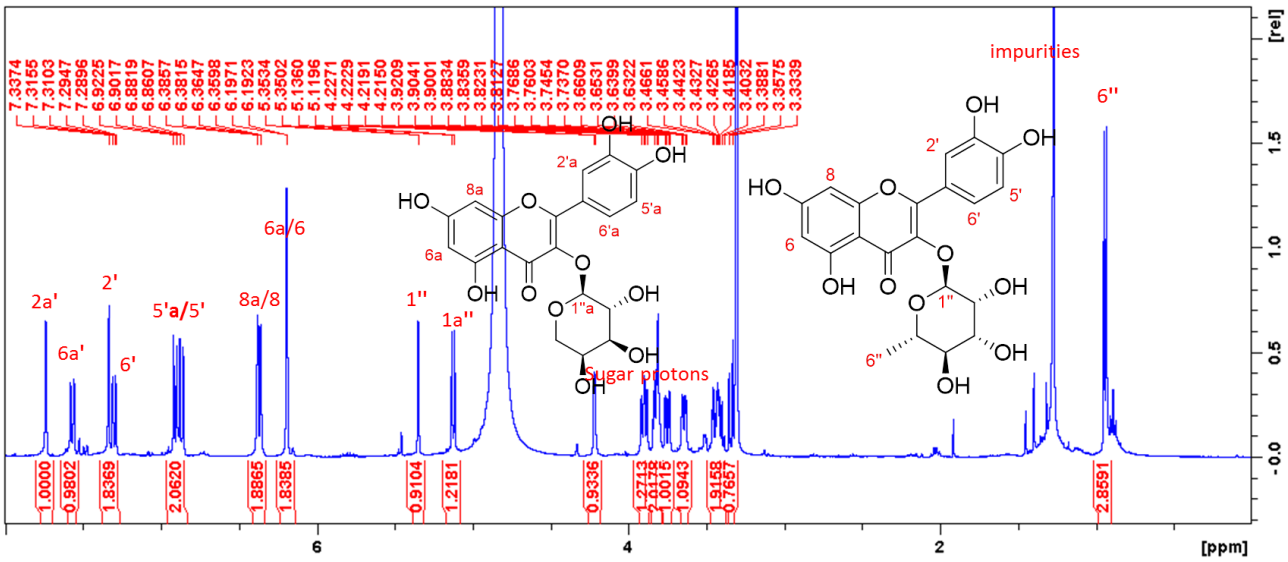

Plate 5.19: ^{1}H NMR (400 MHz, CD_3OD) spectrum of quercetin 3-*O*-arabinopyranoside (5.4). and quercetin 3-*O*- rhamnopyranoside (5.5).

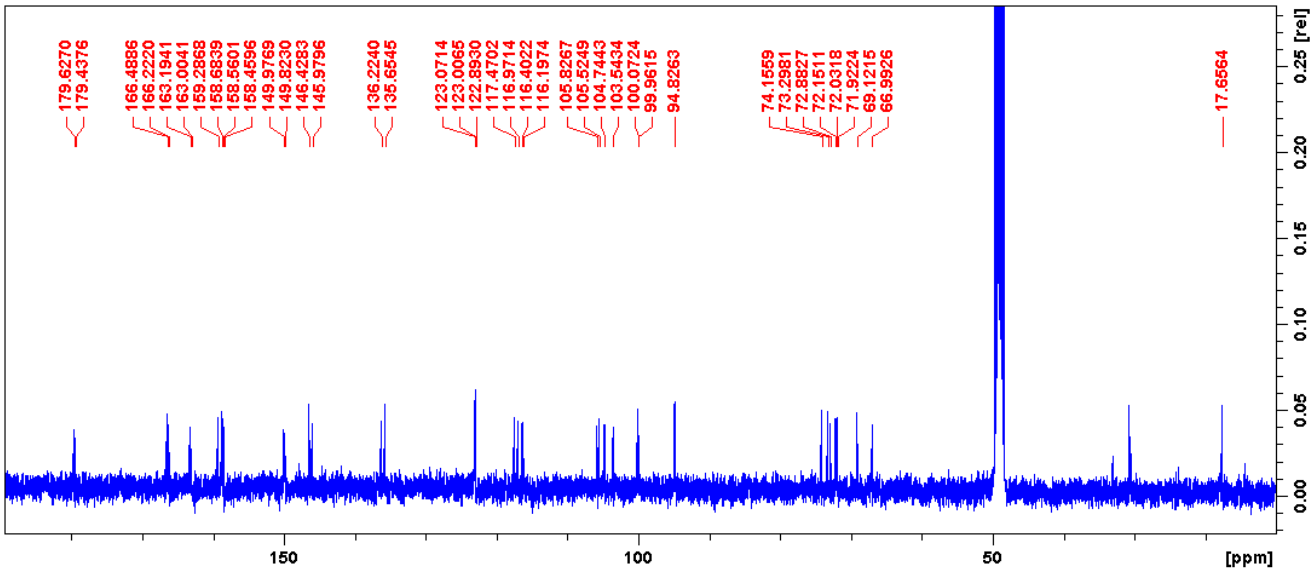

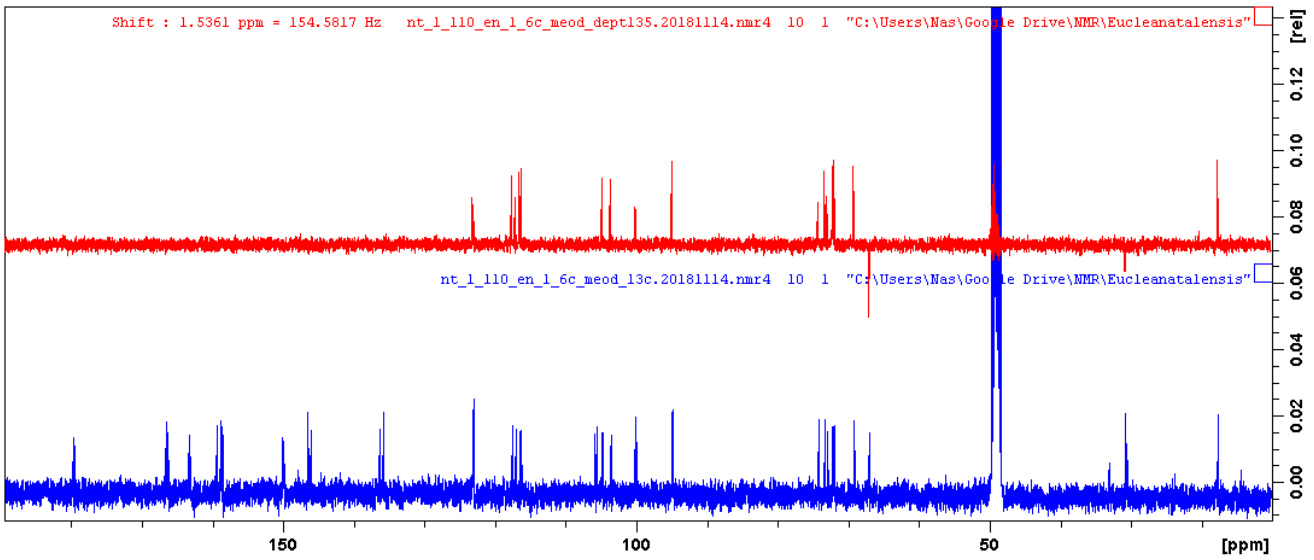

Plate 5.20: ^{13}C and DEPT (100 MHz, CD_3OD) spectra of quercetin 3-*O*-arabinopyranoside (5.4) and quercetin 3-*O*-rhamnopyranoside (5.5).

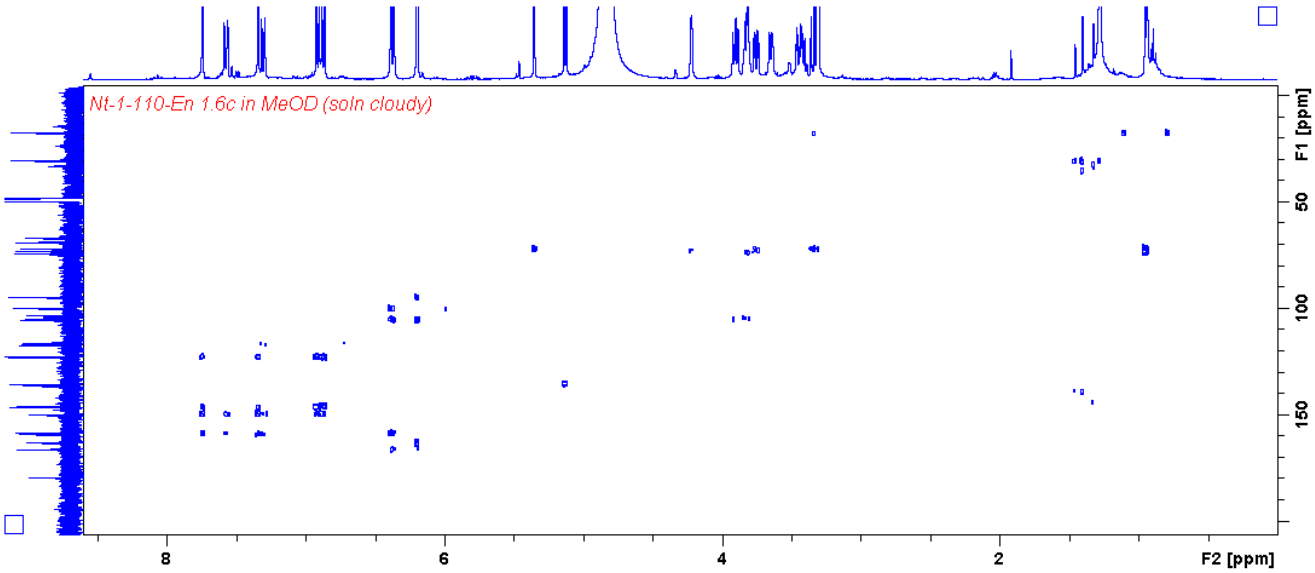

Plate 5.21: HMBC (400 MHz/100 MHz, CD_3OD) spectrum of quercetin 3-*O*-arabinopyranoside (5.4) and quercetin 3-*O*-rhamnopyranoside (5.5).

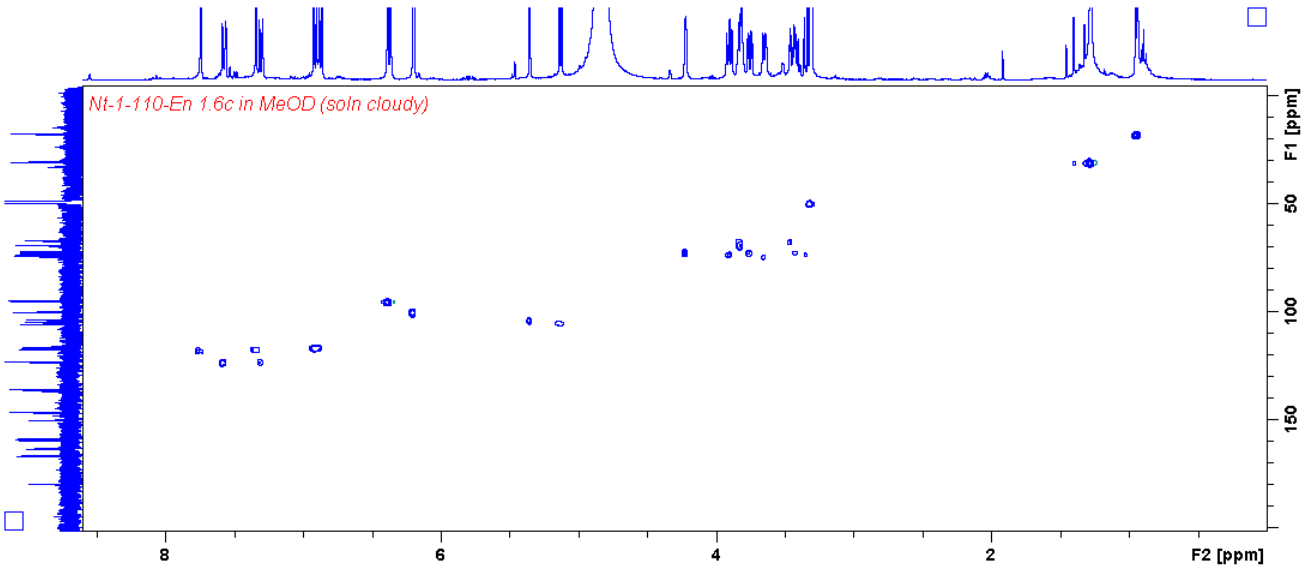

Plate 5.22: HSQC (400 MHz/100 MHz, CD_3OD) spectrum of quercetin 3-*O*-arabinopyranoside 5.4 and quercetin 3-*O*-rhamnopyranoside (5.5).

Elemental Composition Report **Page 1**

Single Mass Analysis
Tolerance = 5.0 PPM / DBE: min = -1.5, max = 50.0
Element prediction: Off
Number of isotope peaks used for i-FIT = 3

Monoisotopic Mass, Even Electron Ions
2 formula(e) evaluated with 1 results within limits (all results (up to 1000) for each mass)
Elements Used:
C: 30-35 H: 45-50 O: 0-5
en 1_1 60 (1.990) Cm (1:61)
TOF MS ES-

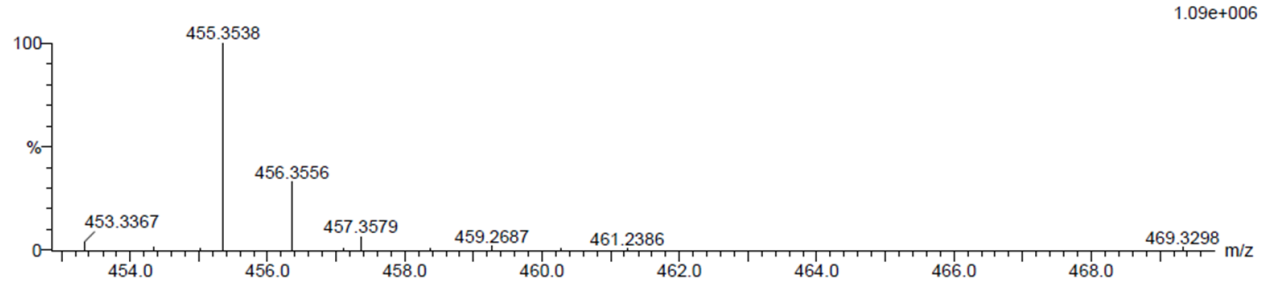

Minimum:		5.0	5.0	-1.5			
Maximum:				50.0			
Mass	Calc. Mass	mDa	PPM	DBE	i-FIT	i-FIT (Norm)	Formula
455.3538	455.3525	1.3	2.9	7.5	41.5	0.0	C30 H47 O3

Plate 5.23: HRESIMS of oleanolic acid (5.7).

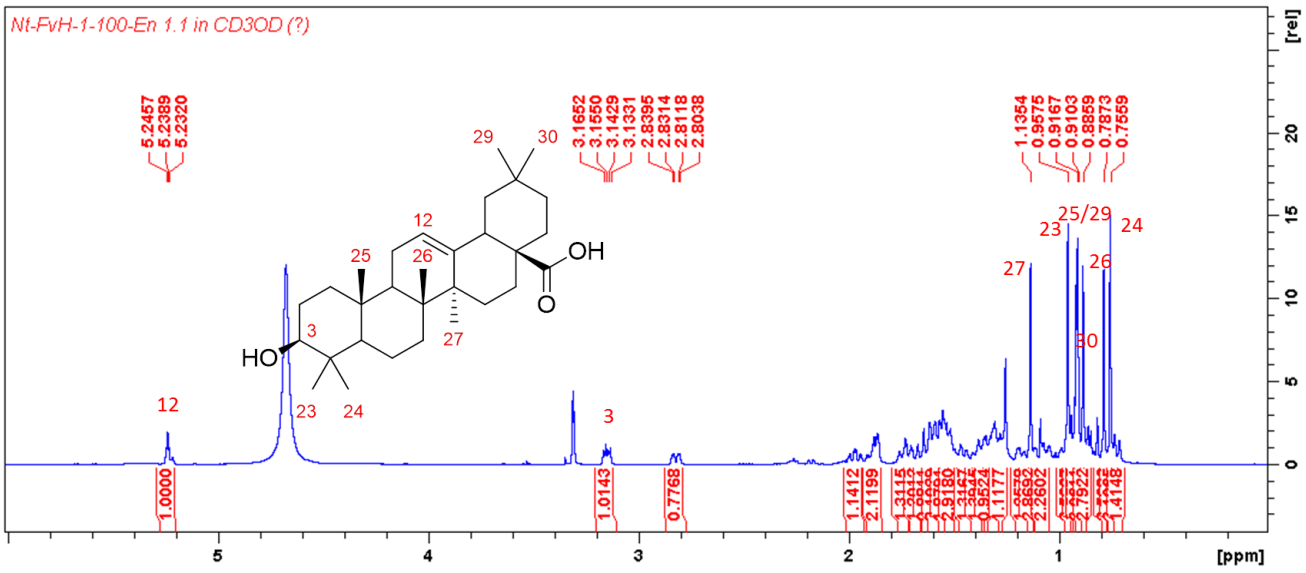

Plate 5.24: ^{1}H NMR (500 MHz, $CD_3OD+CDCl_3$) spectrum of oleanolic acid (5.7).

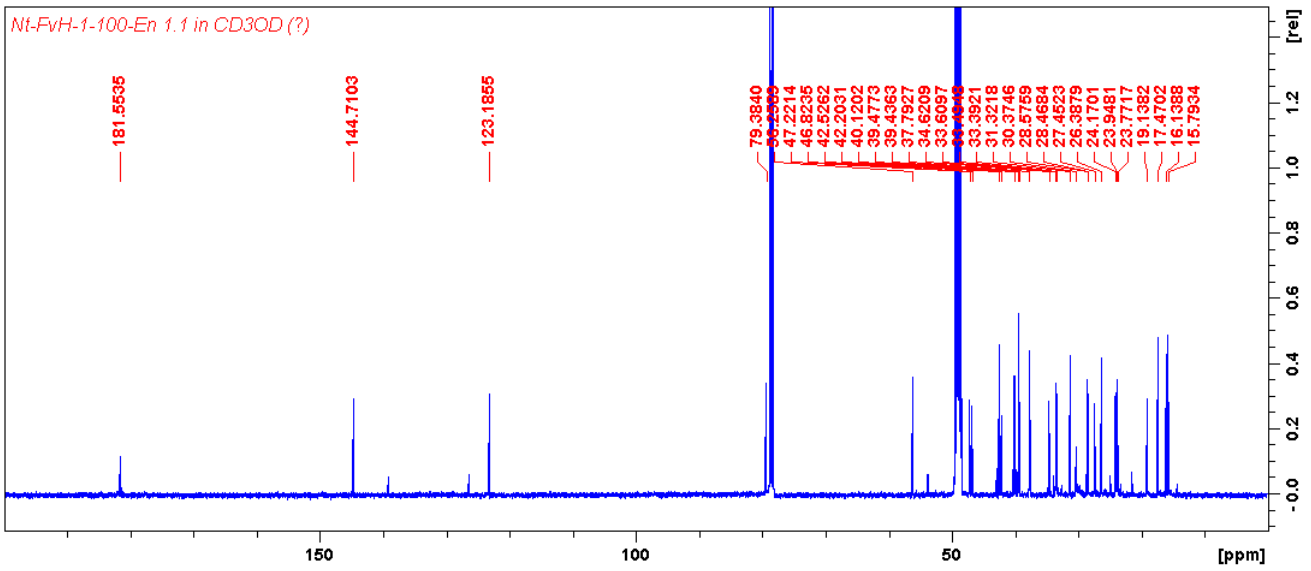

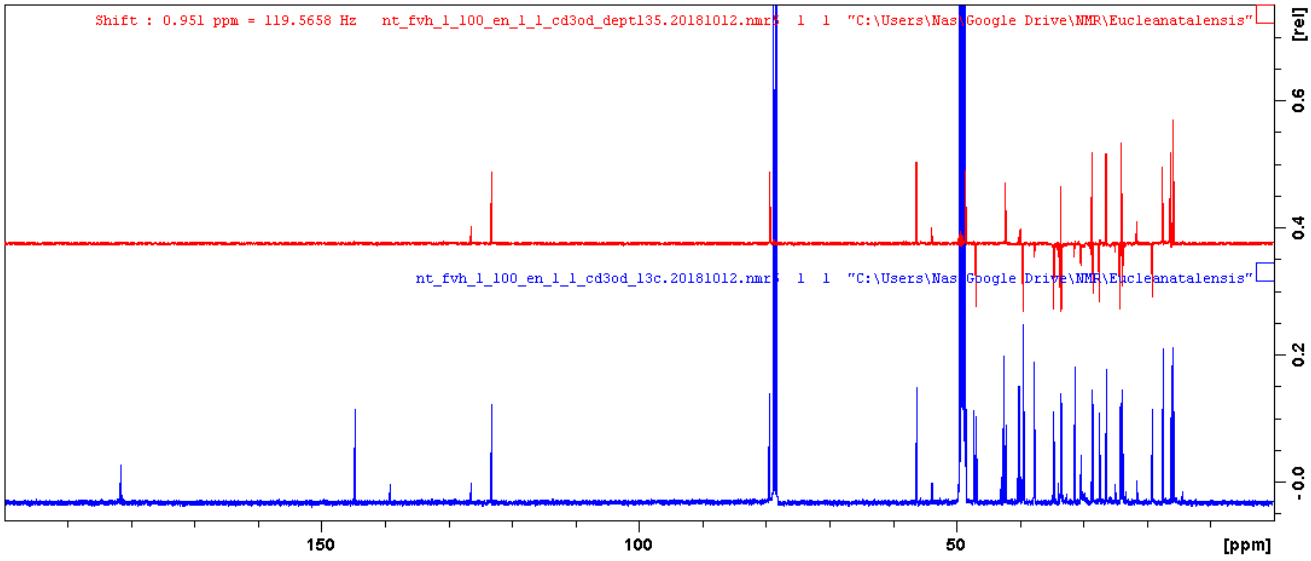

Plate 5.25: ^{13}C and DEPT (125 MHz, $CD_3OD+CDCl_3$) spectra of oleanolic acid (5.7).

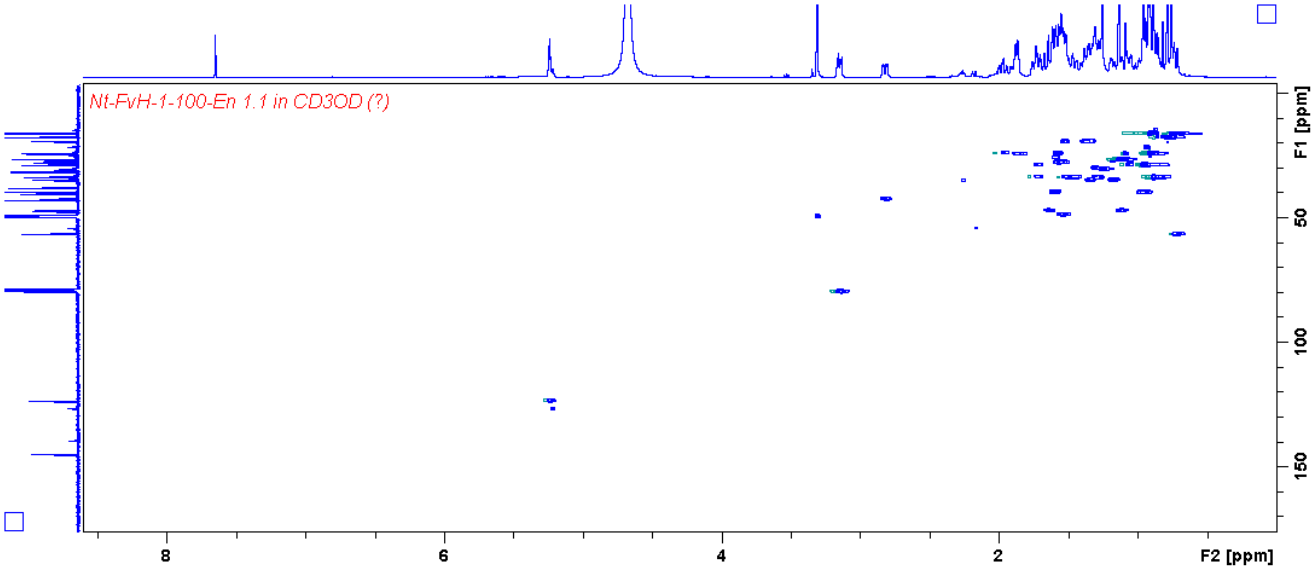

Plate 5.26: HSQC (500 MHz/125 MHz, $CD_3OD+CDCl_3$) spectrum of oleanolic acid (5.7).

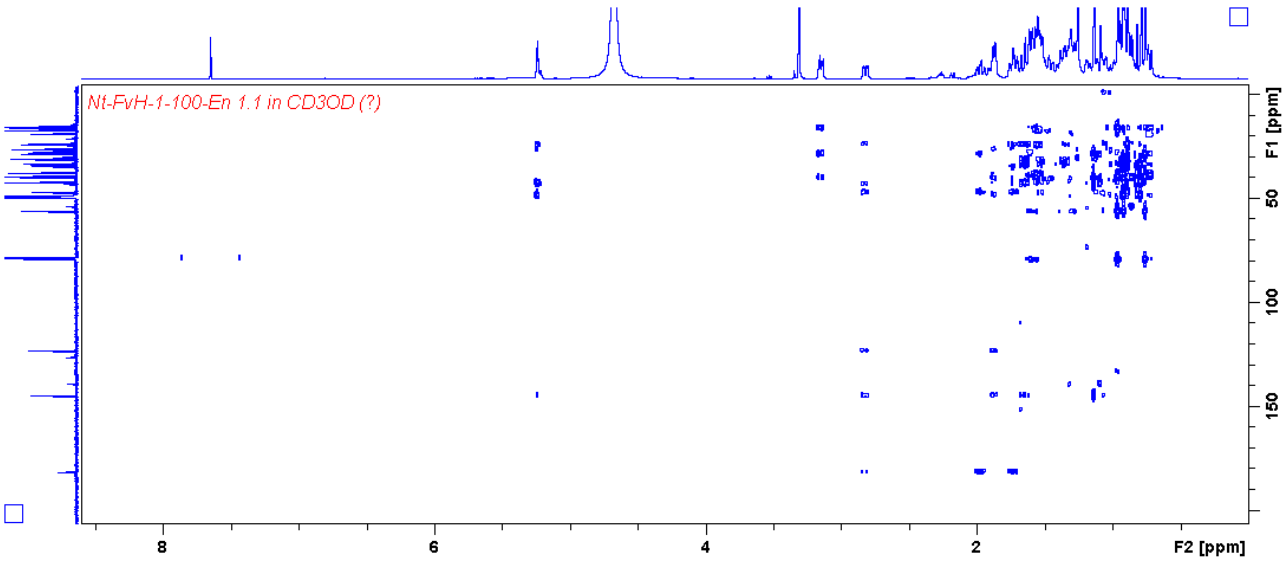

Plate 5.27: HMBC (500 MHz/125 MHz, $CD_3OD+CDCl_3$) spectrum of oleanolic acid (5.7).

Elemental Composition Report **Page 1**

Single Mass Analysis
Tolerance = 5.0 PPM / DBE: min = -1.5, max = 100.0
Element prediction: Off
Number of isotope peaks used for i-FIT = 3

Monoisotopic Mass, Even Electron Ions
3 formula(e) evaluated with 1 results within limits (all results (up to 1000) for each mass)
Elements Used:
C: 10-15 H: 5-10 O: 0-5
Nt-1-en1_2 34 (1.112) Cm (1:61)
TOF MS ES-

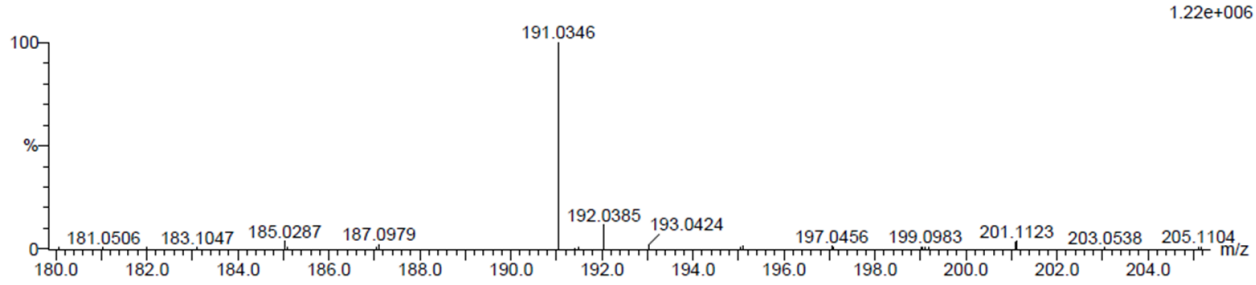

Minimum:				-1.5			
Maximum:		5.0	5.0	100.0			
Mass	Calc. Mass	mDa	PPM	DBE	i-FIT	i-FIT (Norm)	Formula
191.0346	191.0344	0.2	1.0	7.5	61.0	0.0	C10 H7 O4

Plate 5.28: HRESIMS of scopoletin (5.8).

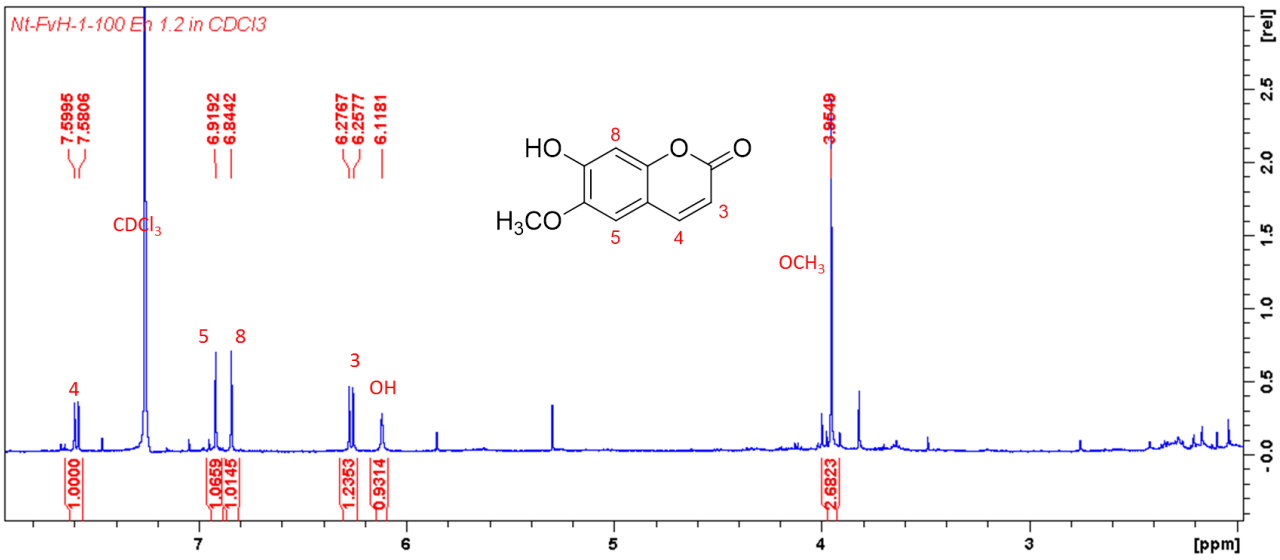

Plate 5.29: ^{1}H NMR (500 MHz, $CDCl_3$) spectrum of scopoletin (5.8).

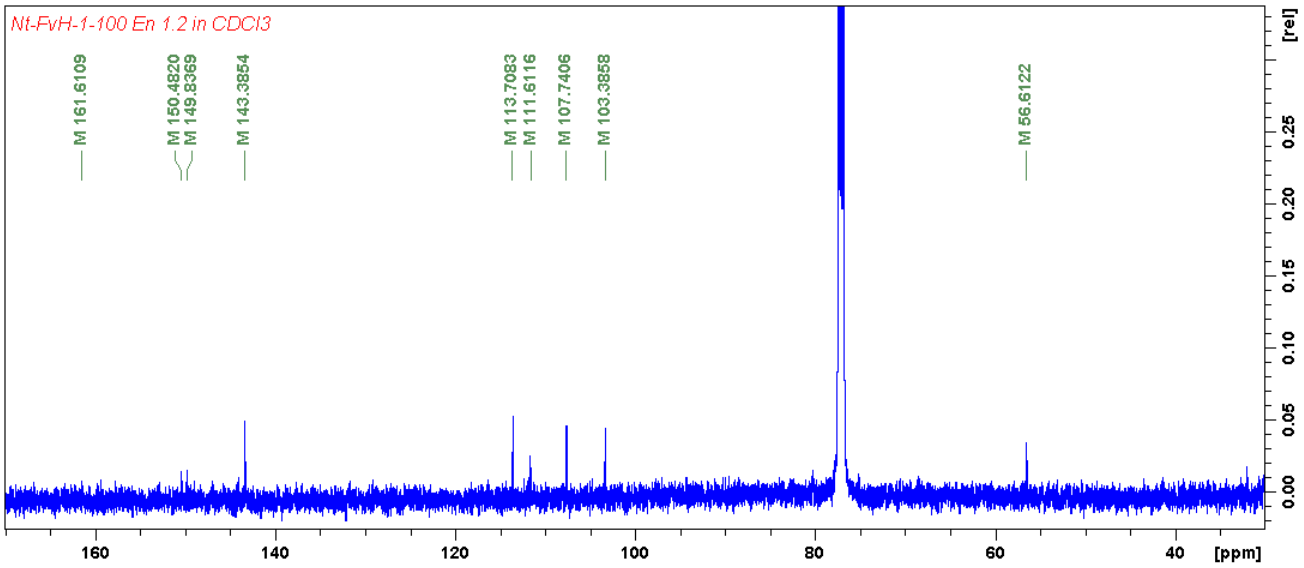

Plate 5.30: ^{13}C NMR (125 MHz, $CDCl_3$) spectrum of scopoletin (5.8).

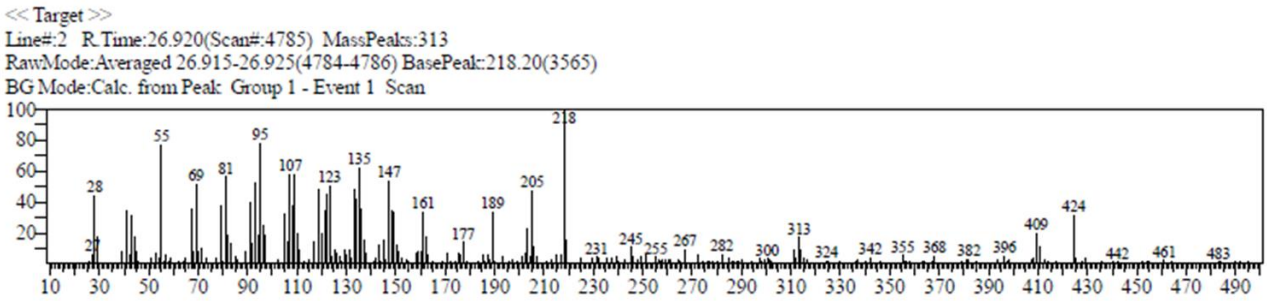

Plate 5.31: EIMS of lupeol (5.9).

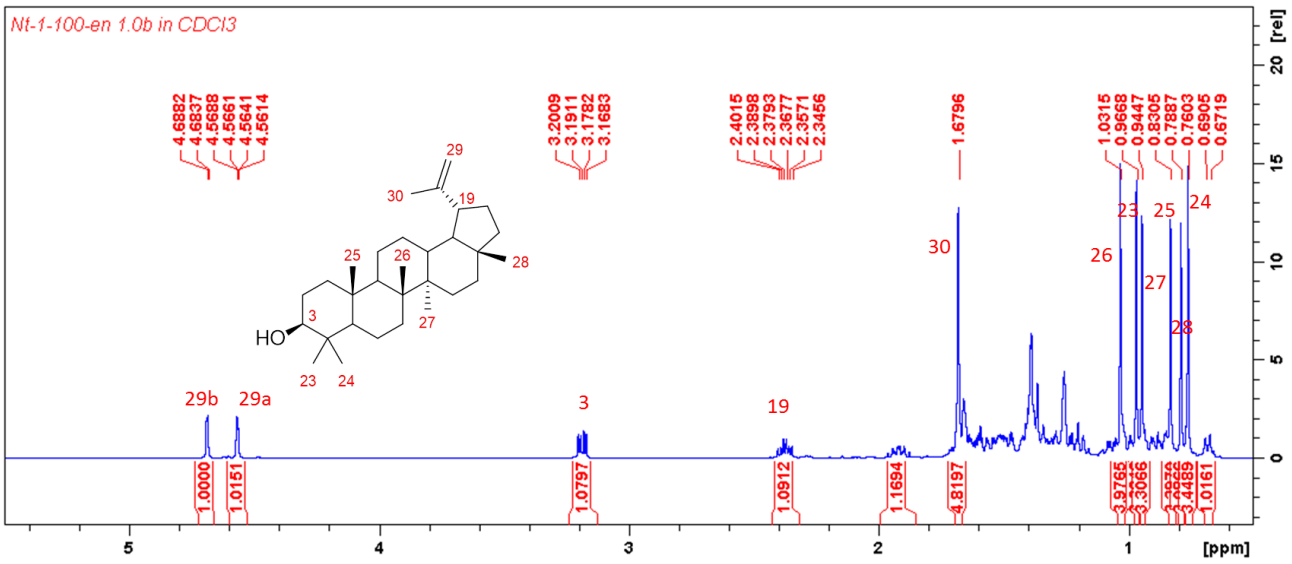

Plate 5.32: ^{1}H NMR (500 MHz, $CDCl_3$) spectrum of lupeol (5.9).

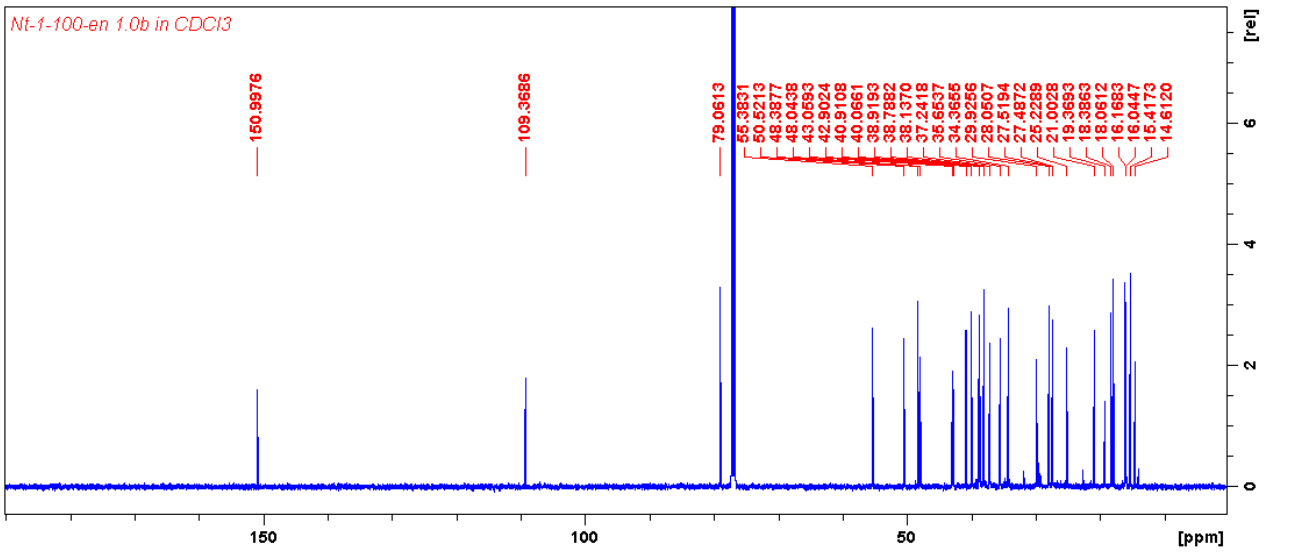

Plate 5.33: ^{13}C NMR (125 MHz, $CDCl_3$) spectrum of lupeol (5.9).

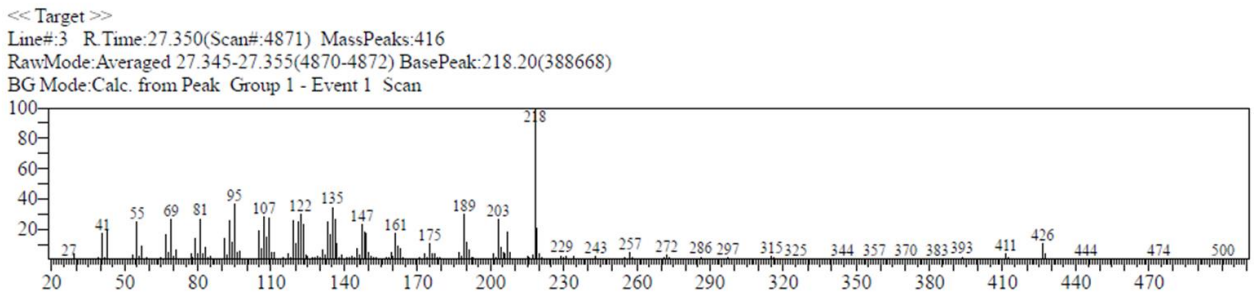

Plate 5.34: EIMS of α-amyrin (5.10).

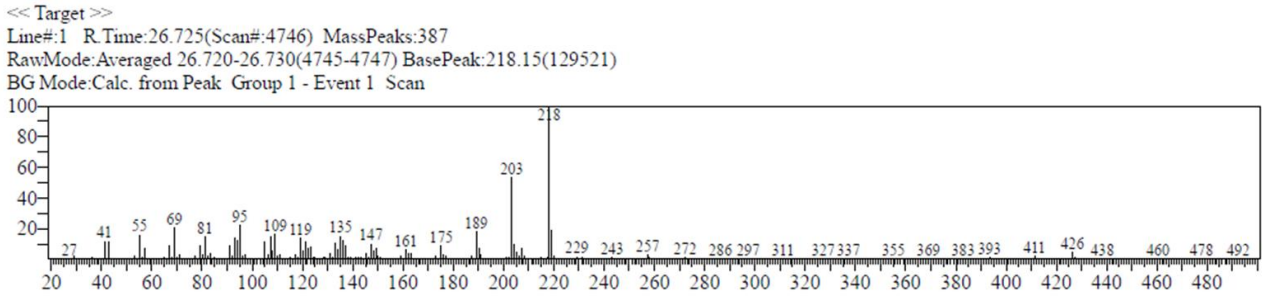

Plate 5.35: EIMS of β-amyrin (5.11).

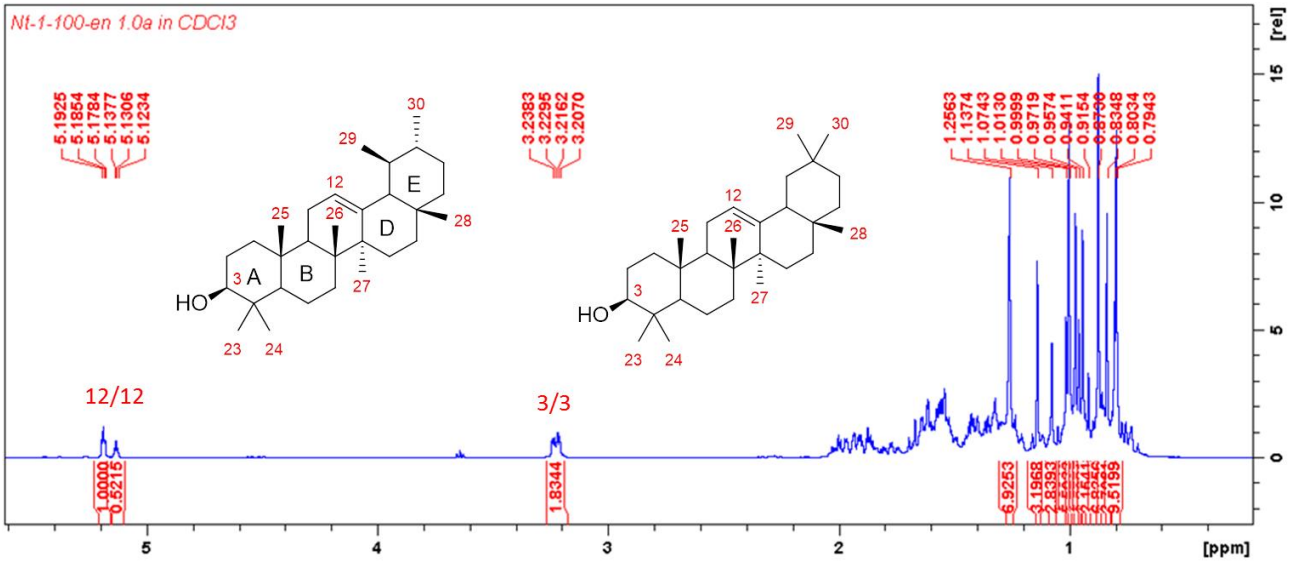

Plate 5.36: ^{1}H NMR (500 MHz, $CDCl_3$) spectrum of α-amyrin 5.10 and β-amyrin (5.11).

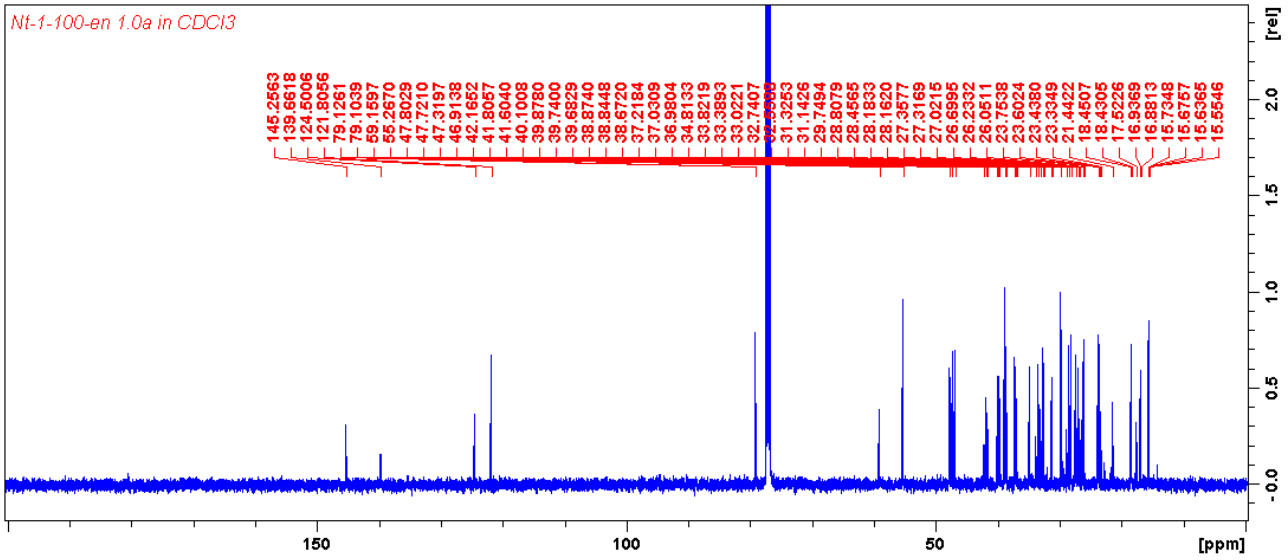

Plate 5.37: ^{13}C NMR (125 MHz, $CDCl_3$) spectrum of α-amyrin 5.10 and β-amyrin (5.11).

APPENDIX D. HRESIMS AND NMR SPECTRA OF COMPOUNDS DESCRIBED IN CHAPTER 6

Elemental Composition Report Page 1

Single Mass Analysis
Tolerance = 5.0 PPM / DBE: min = -1.5, max = 100.0
Element prediction: Off
Number of isotope peaks used for i-FIT = 3

Monoisotopic Mass, Even Electron Ions
4 formula(e) evaluated with 1 results within limits (all results (up to 1000) for each mass)
Elements Used:
C: 15-20 H: 10-15 O: 5-10
PC 1,0 18 (0.573) Cm (1:60)
TOF MS ES-

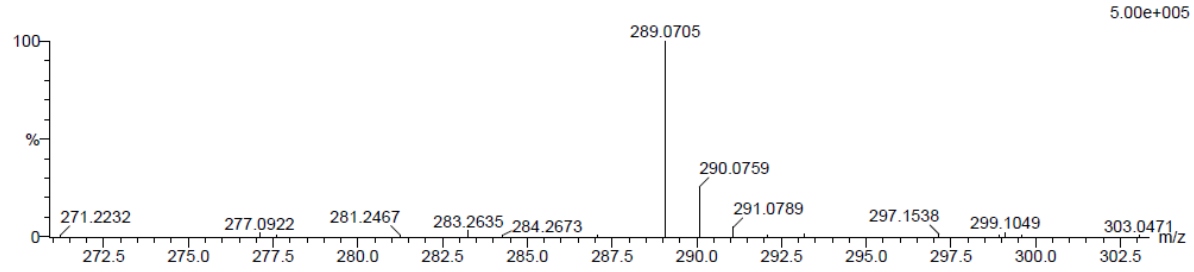

Minimum:				-1.5			
Maximum:		5.0	5.0	100.0			
Mass	Calc. Mass	mDa	PPM	DBE	i-FIT	i-FIT (Norm)	Formula
289.0705	289.0712	-0.7	-2.4	9.5	31.5	0.0	C15 H13 O6

Plate 6.1: HRESIMS of epicatechin (6.1).

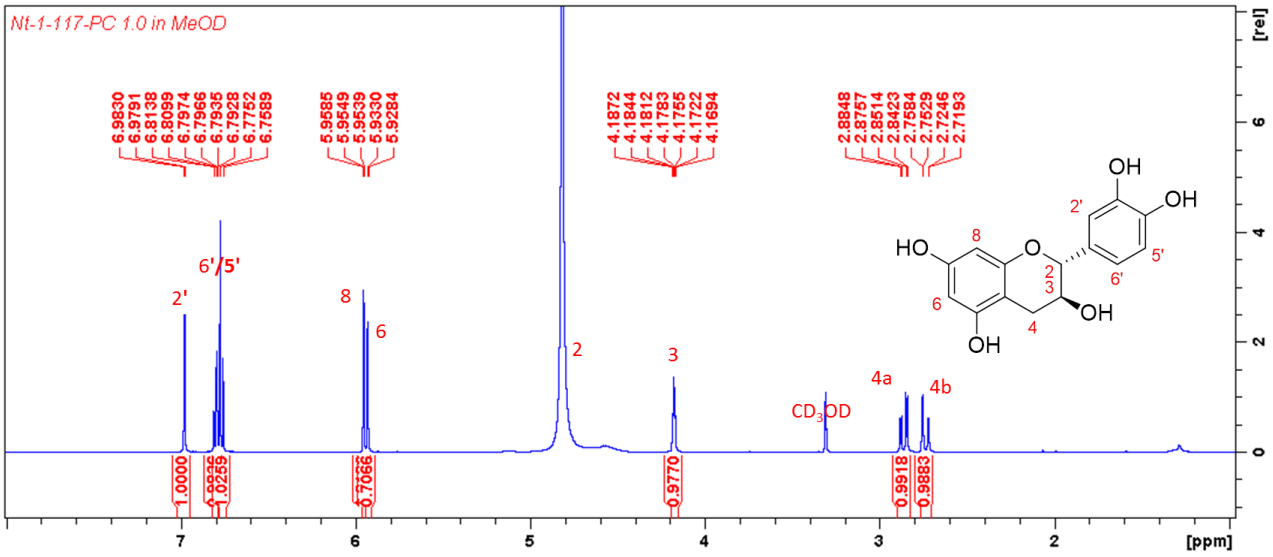

Plate 6.2: ^{1}H NMR (500 MHz, CD_3OD) spectrum of epicatechin (6.1).

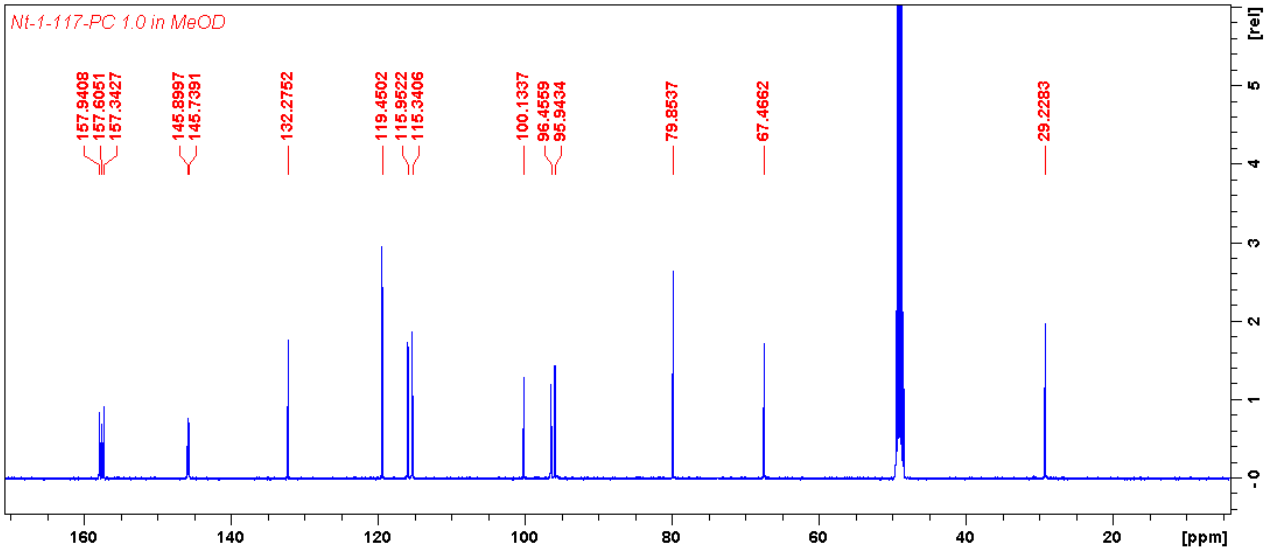

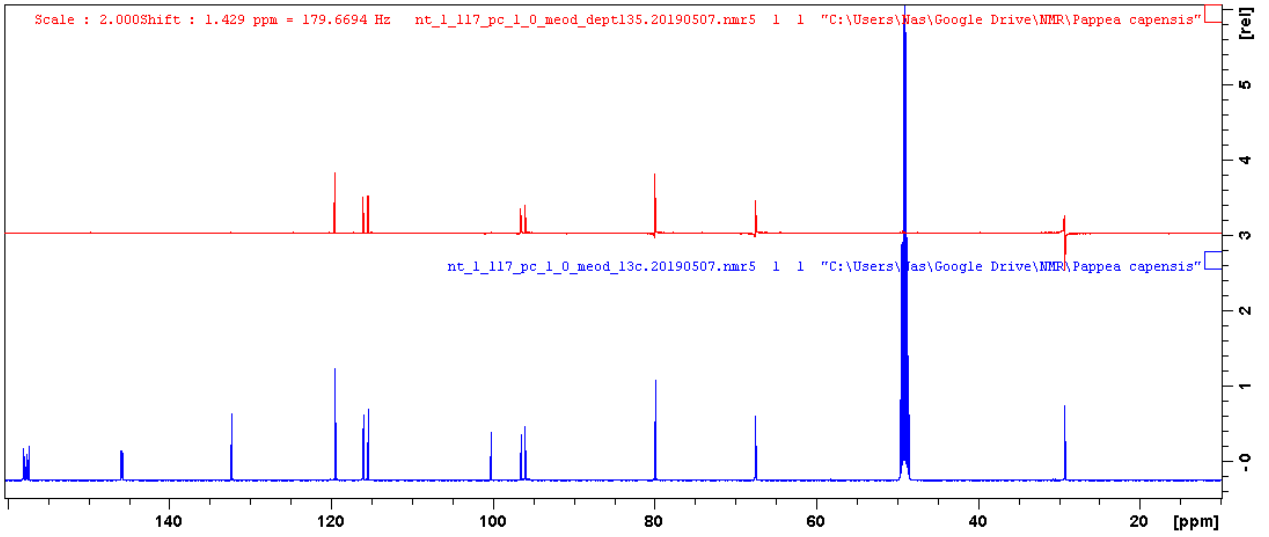

Plate 6.3: ^{13}C and DEPT (125 MHz, CD_3OD) spectra of epicatechin (6.1).

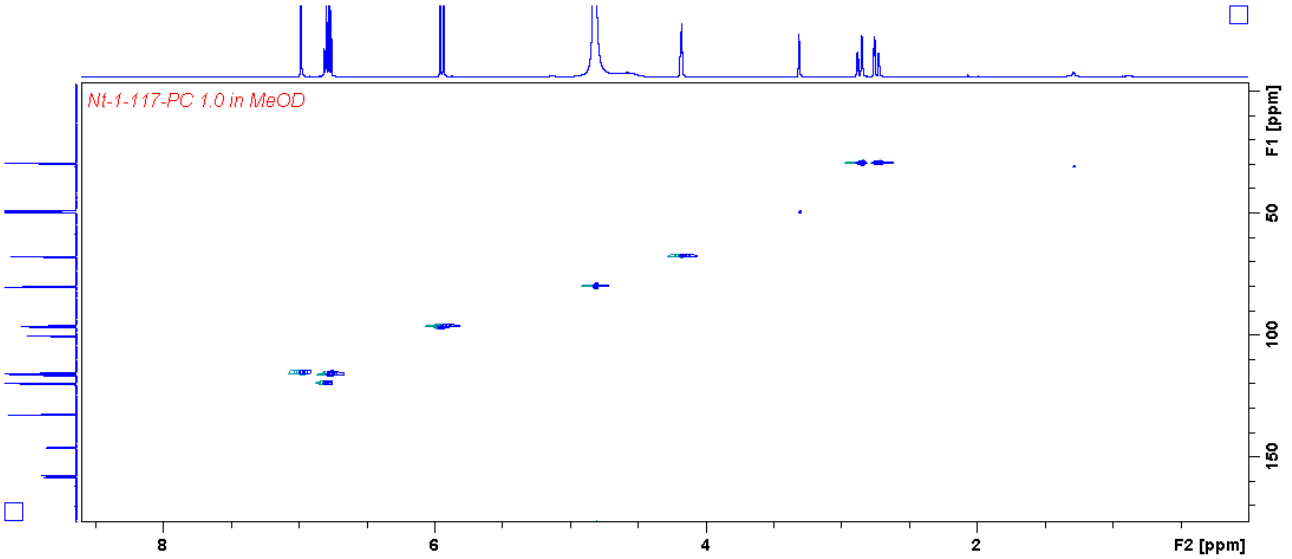

Plate 6.4: HSQC (500 MHz/125 MHz, CD_3OD) spectrum of epicatechin (6.1).

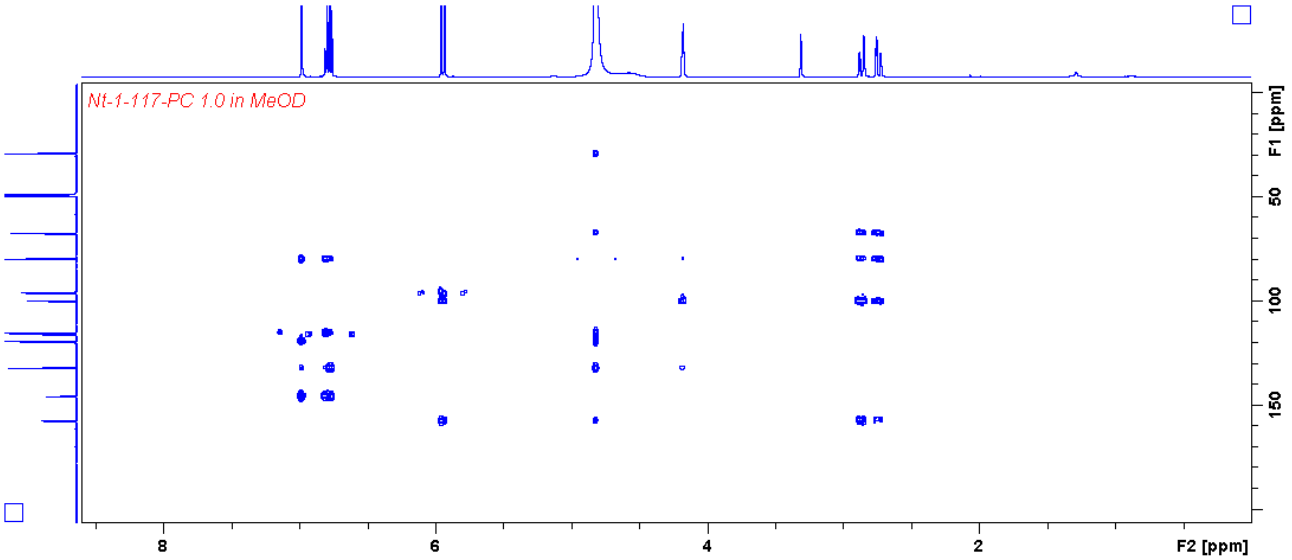

Plate 6.5: HMBC (500 MHz/125 MHz, CD_3OD) spectrum of epicatechin (6.1).

Elemental Composition Report Page 1

Single Mass Analysis
Tolerance = 5.0 PPM / DBE: min = -1.5, max = 100.0
Element prediction: Off
Number of isotope peaks used for i-FIT = 3

Monoisotopic Mass, Even Electron Ions
4 formula(e) evaluated with 1 results within limits (all results (up to 1000) for each mass)
Elements Used:
C: 20-25 H: 15-20 O: 10-15
Nt-1-PC1,1b 52 (1.720) Cm (1:61)
TOF MS ES-

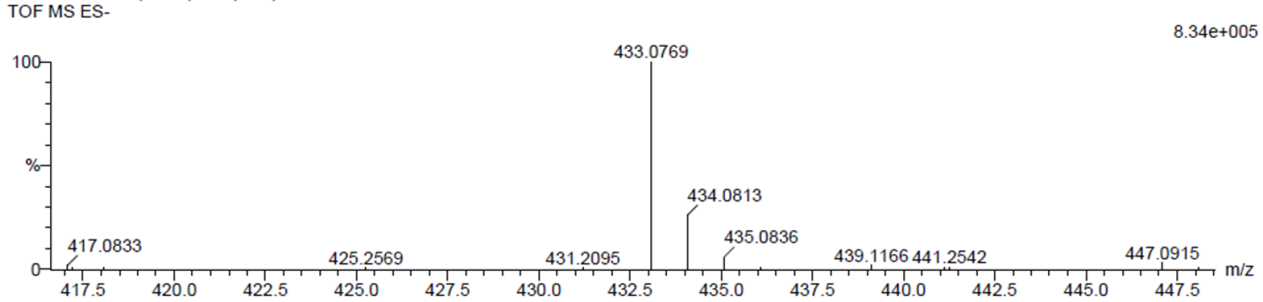

Minimum:				-1.5			
Maximum:		5.0	5.0	100.0			
Mass	Calc. Mass	mDa	PPM	DBE	i-FIT	i-FIT (Norm)	Formula
433.0769	433.0771	-0.2	-0.5	12.5	25.4	0.0	C20 H17 O11

Plate 6.6: HRESIMS of quercetin 3-*O*-arabinopyranoside (6.2).

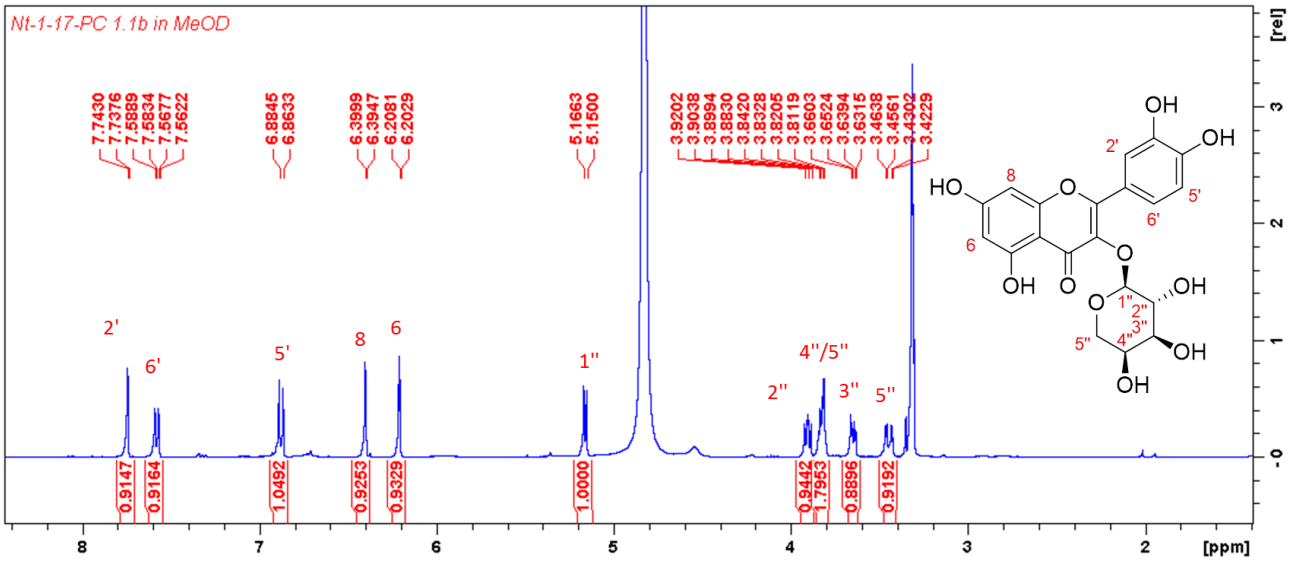

Plate 6.7: ^{1}H NMR (400 MHz, CD_3OD) spectrum of quercetin 3-*O*-arabinopyranoside (6.2).

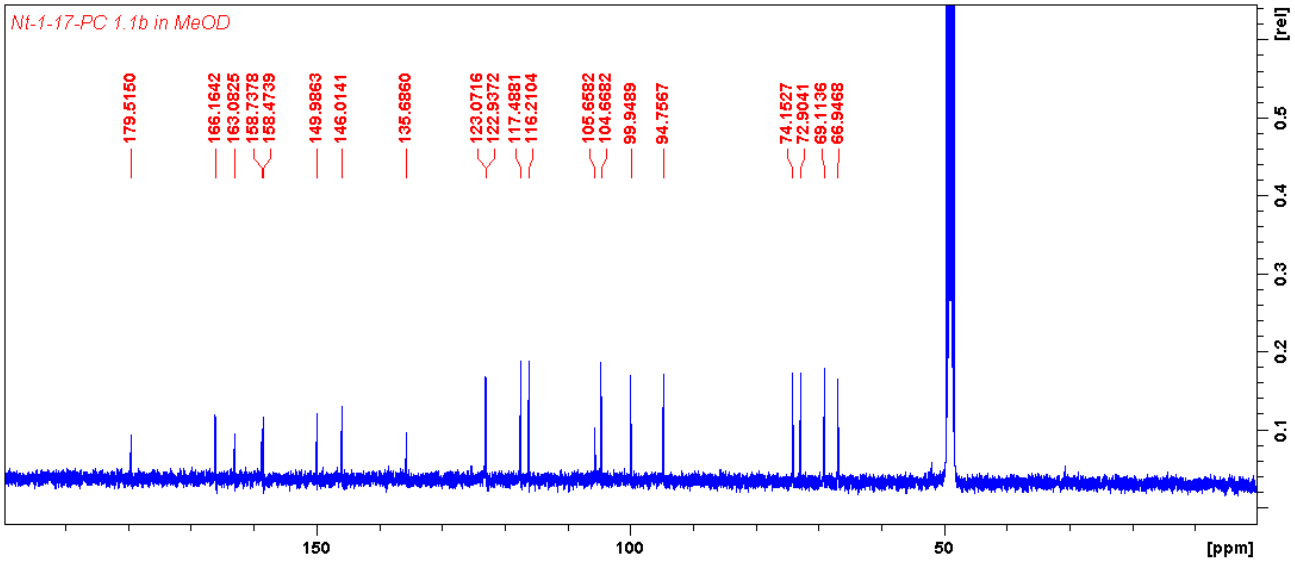

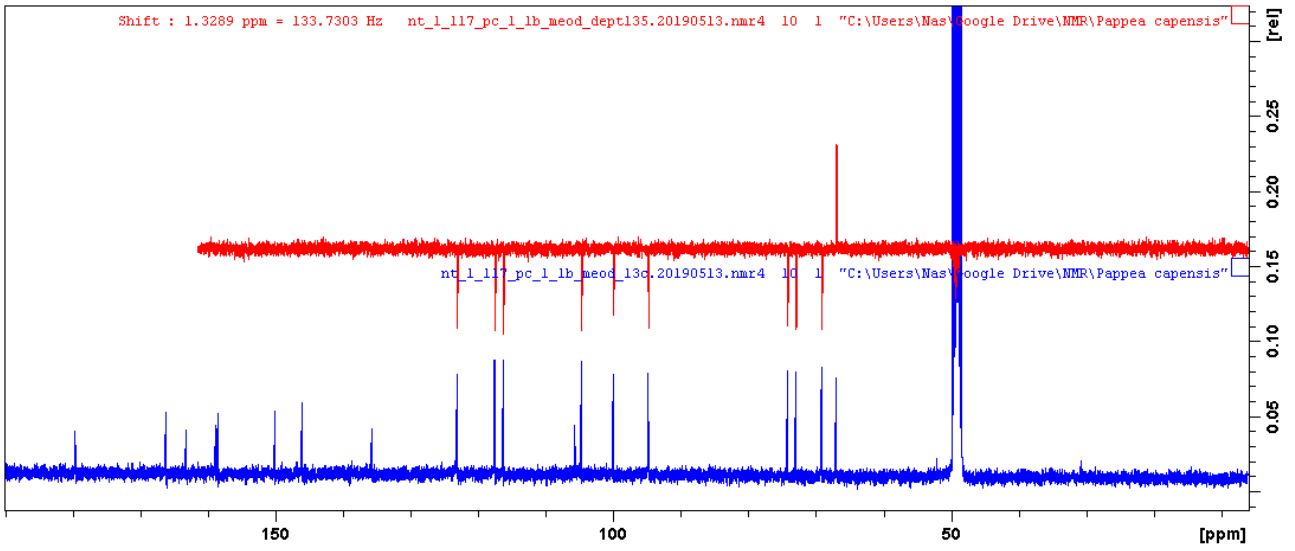

Plate 6.8: ^{13}C and DEPT (100 MHz, CD_3OD) spectra of quercetin 3-*O*-arabinopyranoside (6.2).

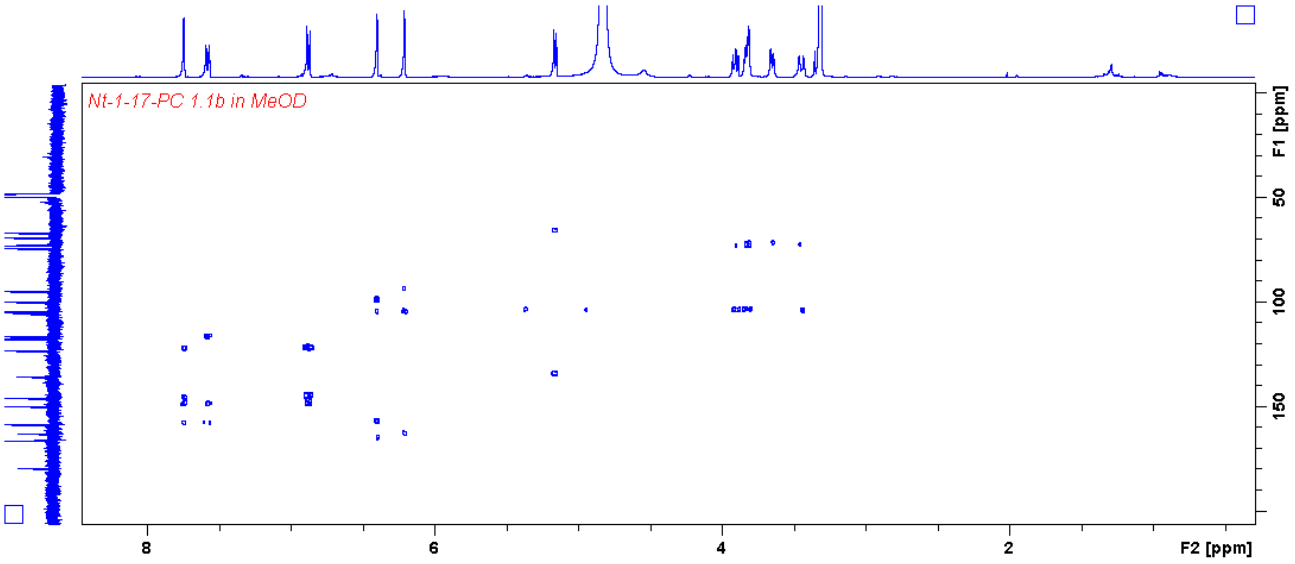

Plate 6.9: HMBC (400 MHz/100 MHz, CD_3OD) spectrum of quercetin 3-*O*-arabinopyranoside (6.2).

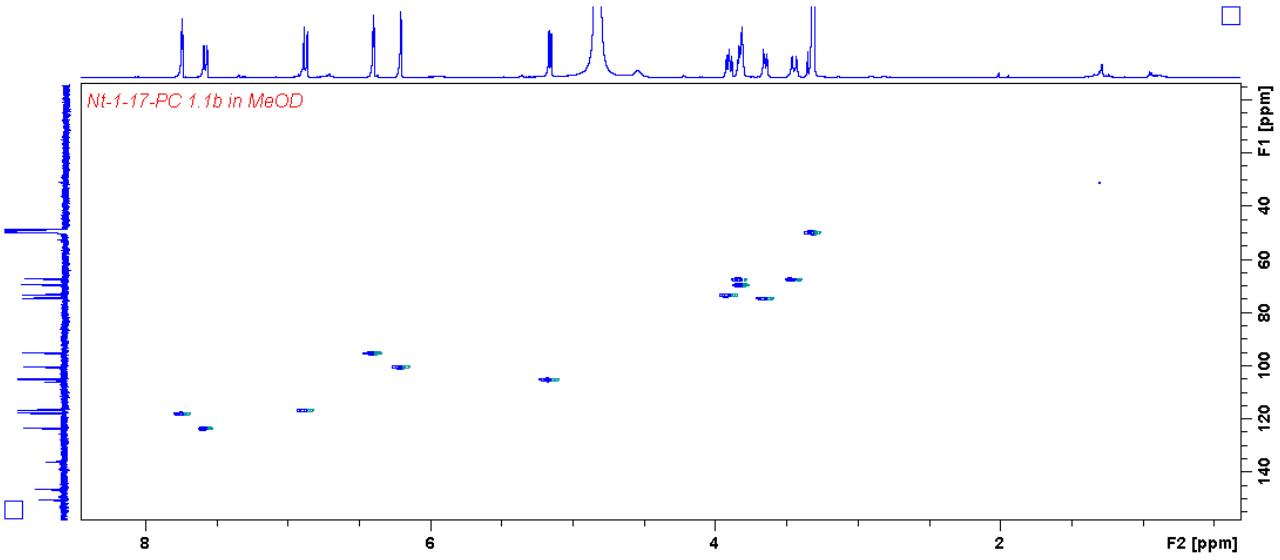

Plate 6.10: HSQC (400 MHz/100 MHz, CD_3OD) spectrum of quercetin 3-*O*-arabinopyranoside (6.2).

Elemental Composition Report **Page 1**

Single Mass Analysis
Tolerance = 5.0 PPM / DBE: min = -1.5, max = 100.0
Element prediction: Off
Number of isotope peaks used for i-FIT = 3

Monoisotopic Mass, Even Electron Ions
4 formula(e) evaluated with 1 results within limits (all results (up to 1000) for each mass)
Elements Used:
C: 20-25 H: 15-20 O: 10-15
Nt-1-ob1_6 15 (0.472) Cm (1:61)
TOF MS ES-

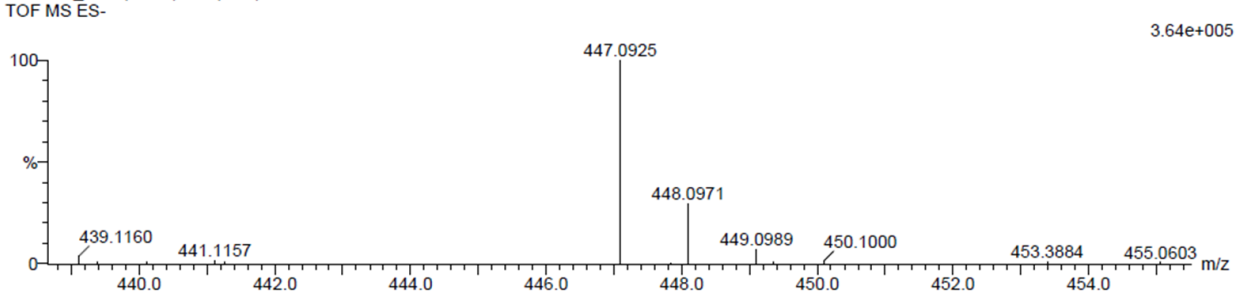

Minimum:				-1.5			
Maximum:		5.0	5.0	100.0			
Mass	Calc. Mass	mDa	PPM	DBE	i-FIT	i-FIT (Norm)	Formula
447.0925	447.0927	-0.2	-0.4	12.5	53.6	0.0	C21 H19 O11

Plate 6.11: HRESIMS of quercetin 3-*O*-rhamnoside (6.3).

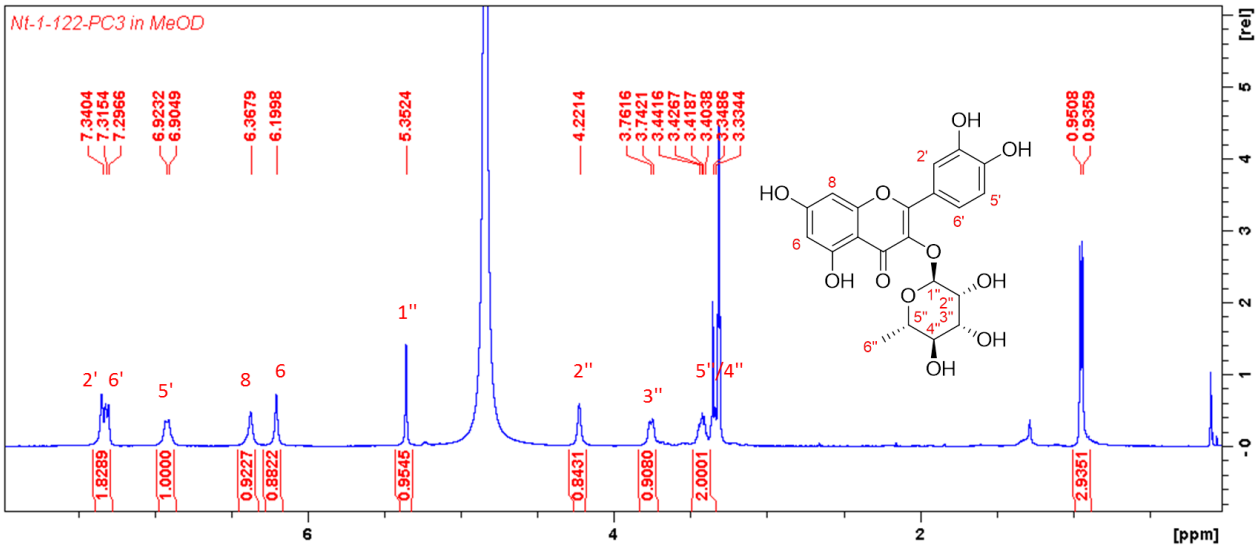

Plate 6.12: ^{1}H NMR (400 MHz, CD_3OD) spectrum of quercetin 3-*O*-rhamnoside (6.3).

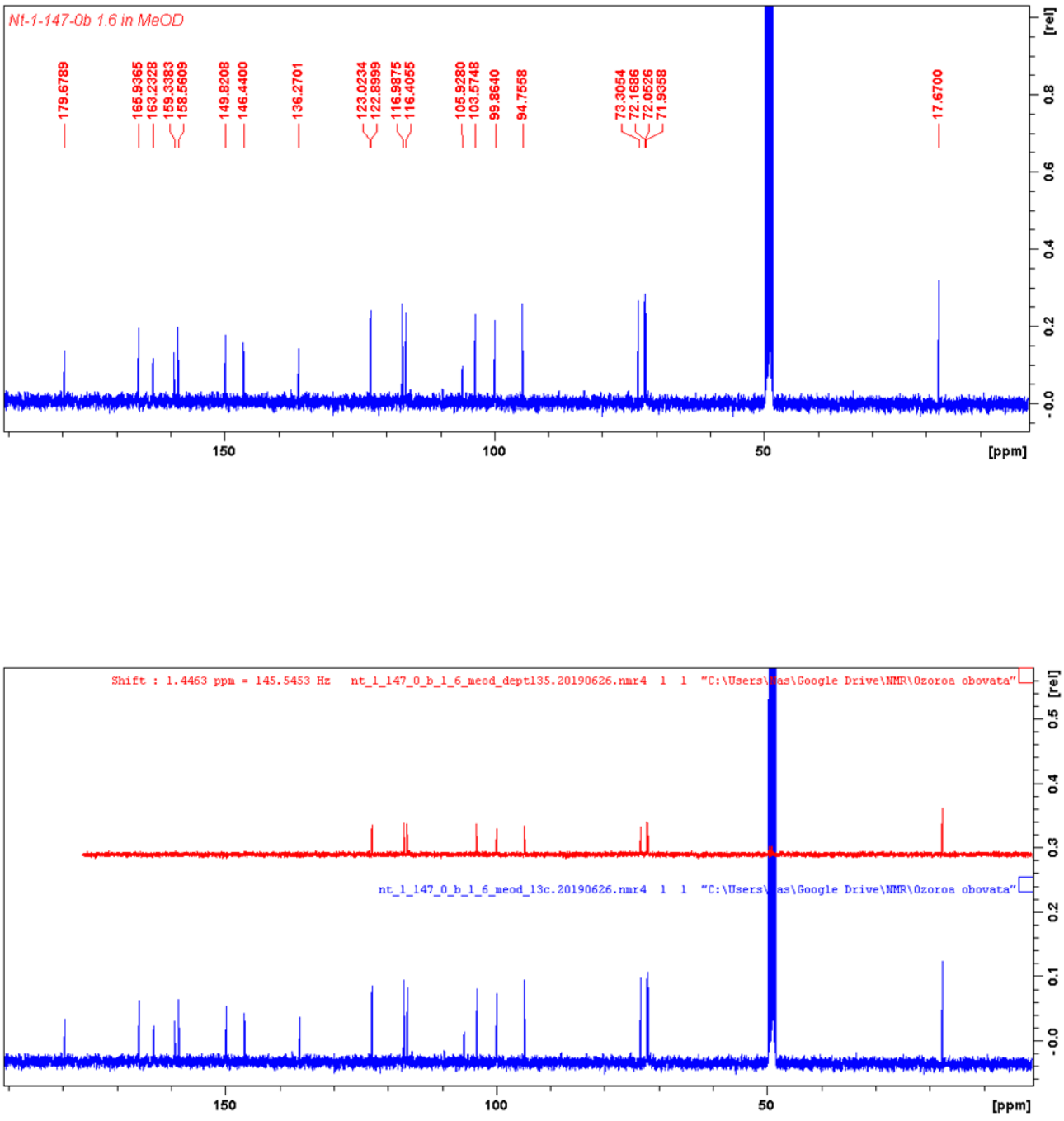

Plate 6.13: ^{13}C and DEPT (100 MHz, CD_3OD) spectra of quercetin 3-*O*-rhamnoside (6.3).

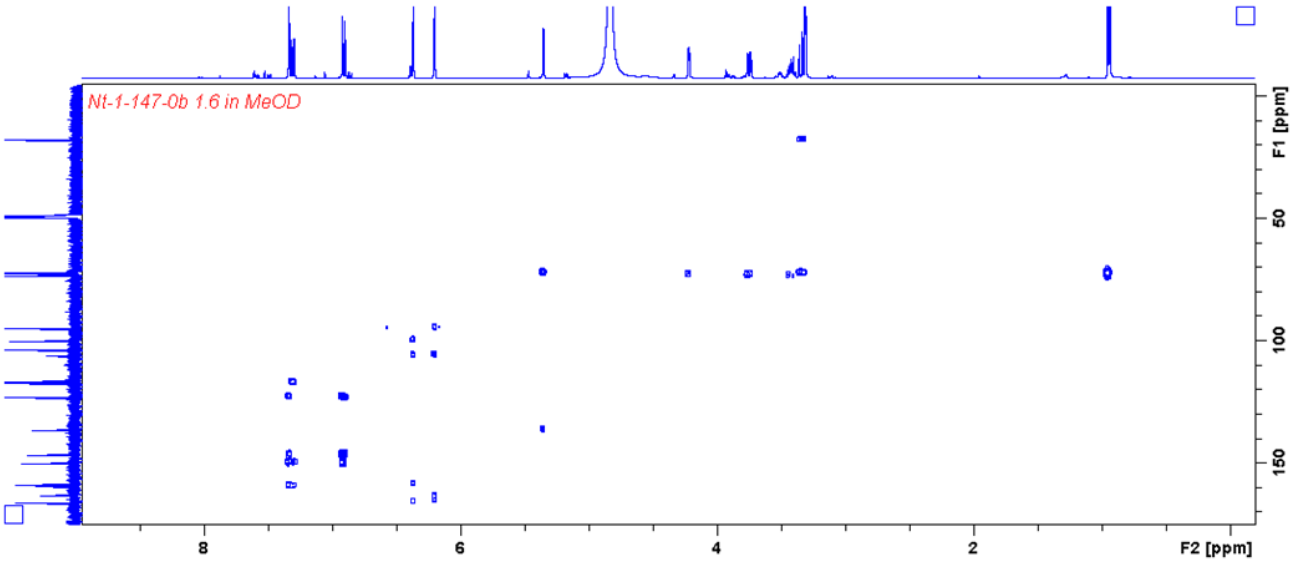

Plate 6.14: HMBC (400 MHz/100 MHz, CD_3OD) spectrum of quercetin 3-*O*-rhamnoside (6.3).

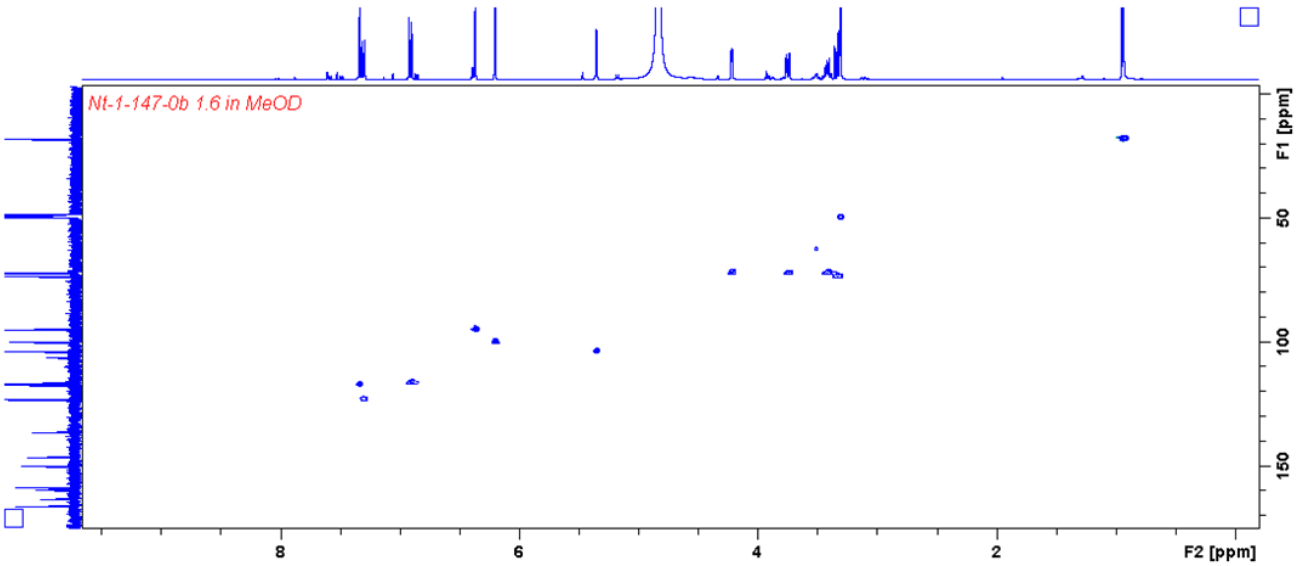

Plate 6.15: HSQC (400 MHz/100 MHz, CD_3OD) spectrum of quercetin 3-*O*-rhamnoside (6.3).

Elemental Composition Report Page 1

Single Mass Analysis
Tolerance = 5.0 PPM / DBE: min = -1.5, max = 100.0
Element prediction: Off
Number of isotope peaks used for i-FIT = 3

Monoisotopic Mass, Even Electron Ions
1 formula(e) evaluated with 1 results within limits (all results (up to 1000) for each mass)
Elements Used:
C: 19-22 H: 16-19 O: 9-11
Nt_1_PC4 57 (1.889) Cm (1:61)
TOF MS ES-

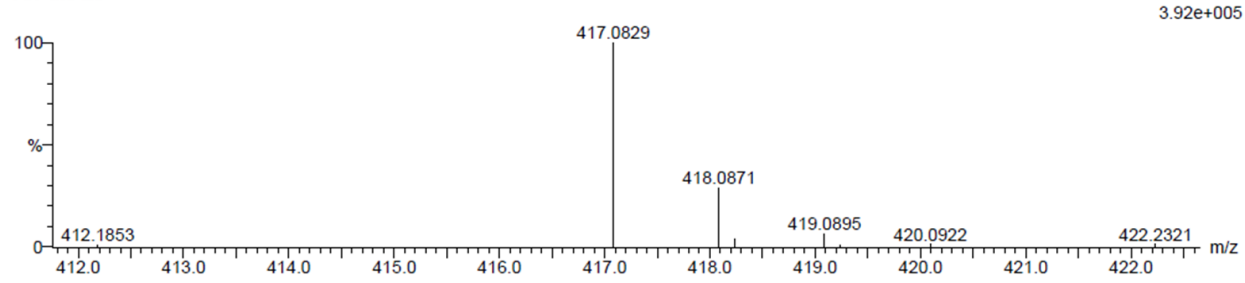

Minimum:				-1.5			
Maximum:		5.0	5.0	100.0			
Mass	Calc. Mass	mDa	PPM	DBE	i-FIT	i-FIT (Norm)	Formula
417.0829	417.0822	0.7	1.7	12.5	61.7	0.0	C20 H17 O10

Plate 6.16: HRESIMS of kaempferol 3-*O*-arabinopyranoside (6.4).

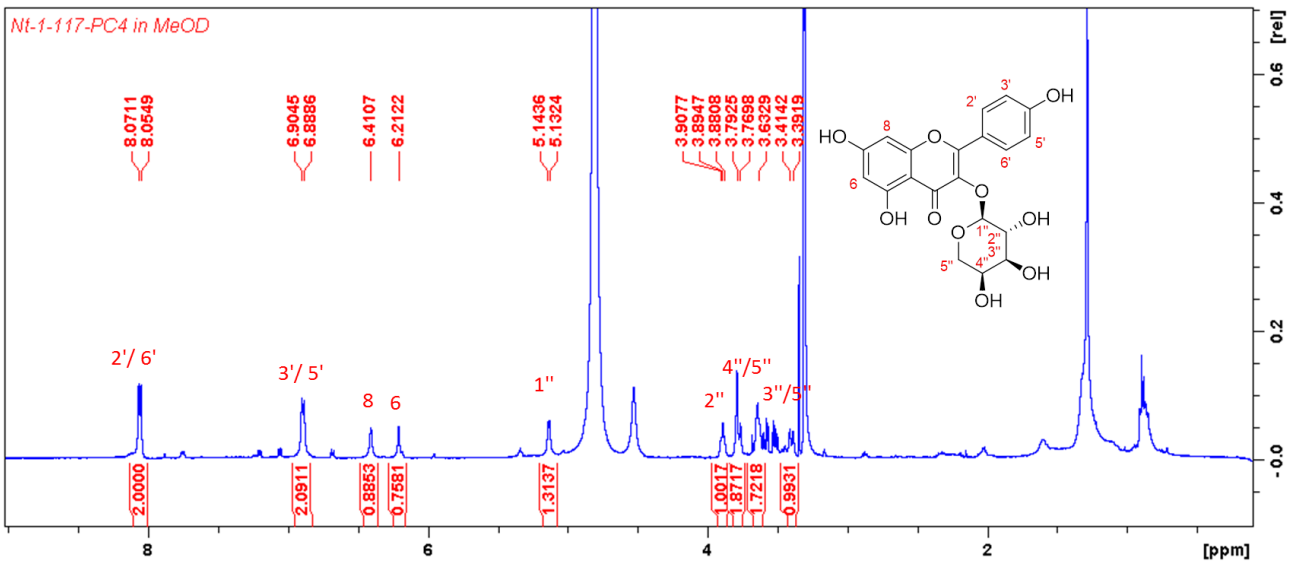

Plate 6.17: ^{1}H NMR (500 MHz, CD_3OD) spectrum of kaempferol 3-*O*-arabinopyranoside (6.4).

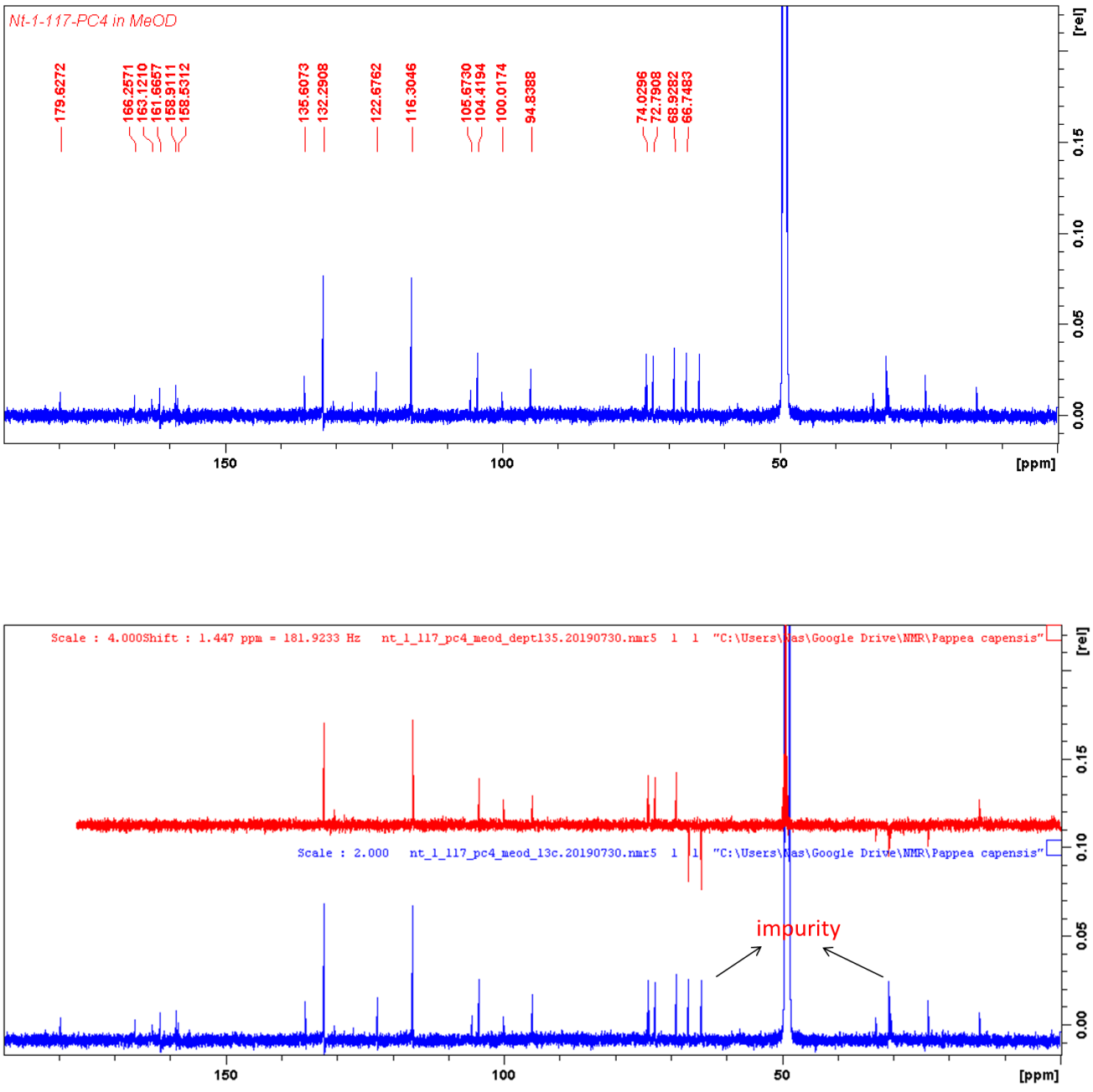

Plate 6.18: ^{13}C and DEPT (125 MHz, CD_3OD) spectra of kaempferol 3-*O*-arabinopyranoside (6.4).

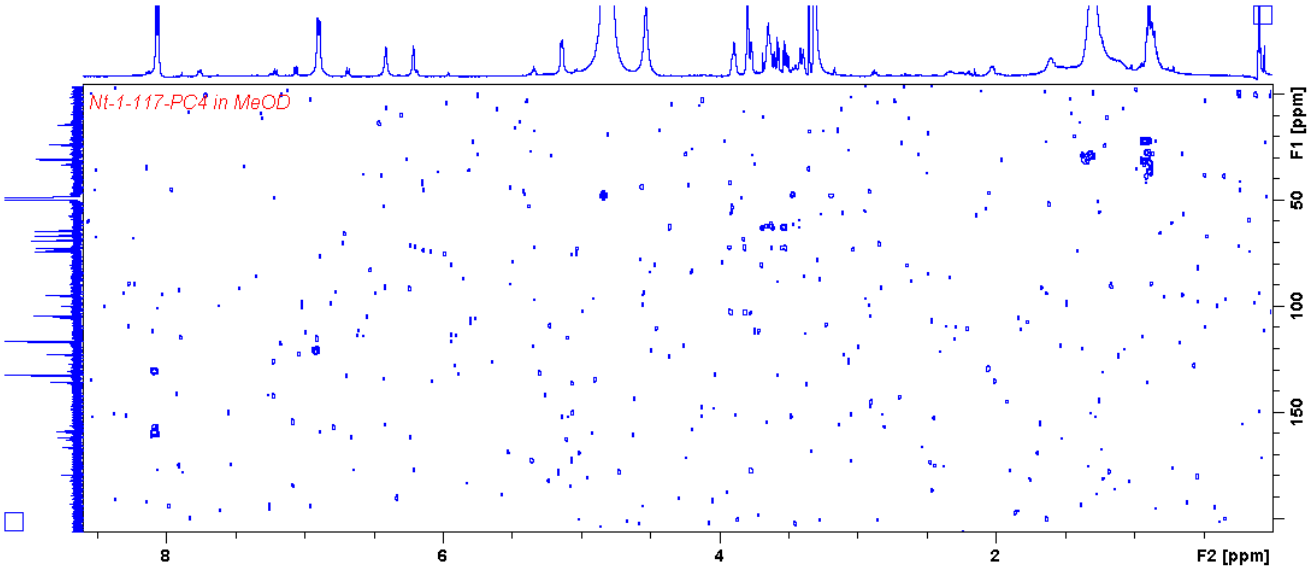

Plate 6.19: HMBC (500 MHz/125 MHz, CD_3OD) spectrum of kaempferol 3-*O*-arabinopyranoside (6.4).

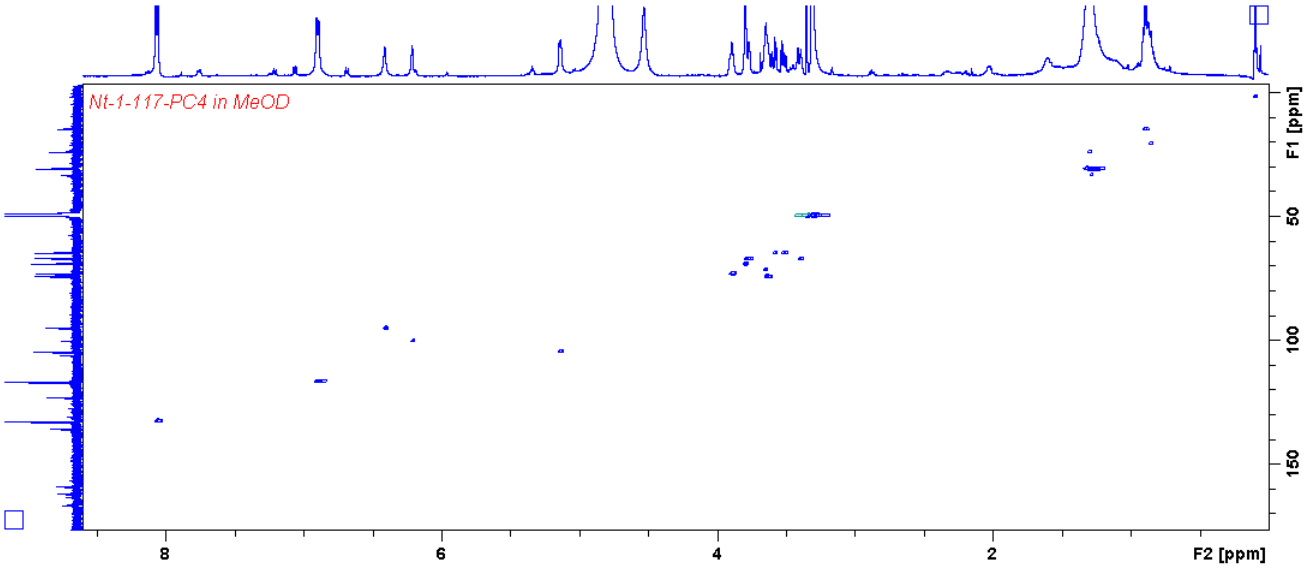

Plate 6.20: HSQC (500 MHz/125 MHz, CD_3OD) spectrum of kaempferol 3-*O*-arabinopyranoside (6.4).

Elemental Composition Report Page 1

Single Mass Analysis
Tolerance = 5.0 PPM / DBE: min = -1.5, max = 100.0
Element prediction: Off
Number of isotope peaks used for i-FIT = 3

Monoisotopic Mass, Even Electron Ions
1 formula(e) evaluated with 1 results within limits (all results (up to 1000) for each mass)
Elements Used:
C: 20-22 H: 18-20 O: 11-13
Nt-1-PC1 59 (1.957) Cm (1:61)
TOF MS ES-

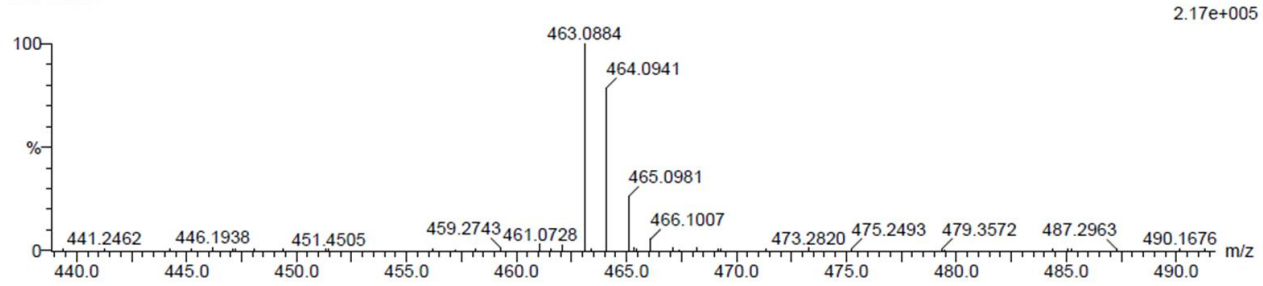

Minimum:				-1.5			
Maximum:		5.0	5.0	100.0			
Mass	Calc. Mass	mDa	PPM	DBE	i-FIT	i-FIT (Norm)	Formula
463.0884	463.0877	0.7	1.5	12.5	79.8	0.0	C21 H19 O12

Plate 6.21: HRESIMS of quercetin 3-*O*-glucopyranoside (6.5).

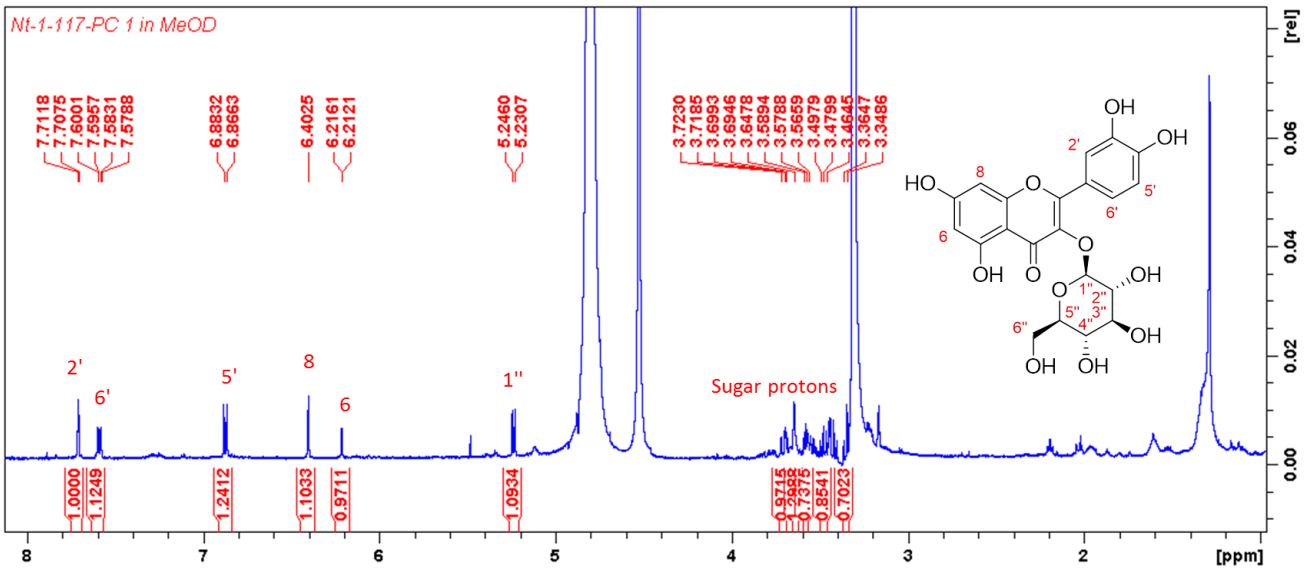

Plate 6.22: ^{1}H NMR (500 MHz, CD_3OD) spectrum of quercetin 3-*O*-glucopyranoside (6.5).

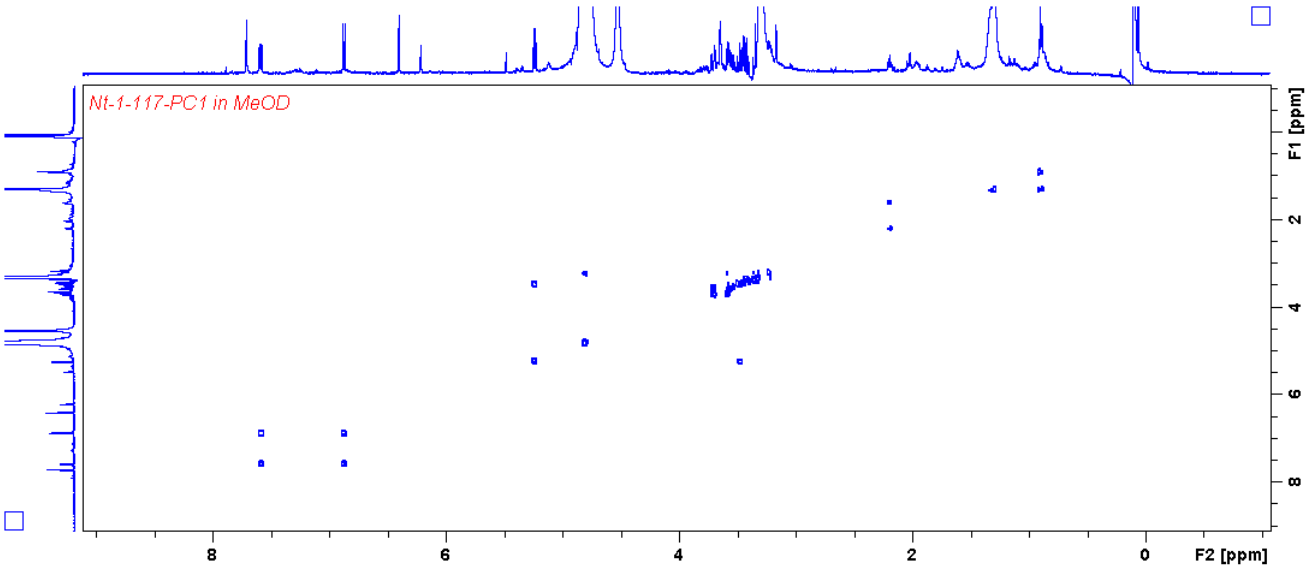

Plate 6.23: H-H COSY (500 MHz, CD_3OD) of quercetin 3-*O*-glucopyranoside (6.5).

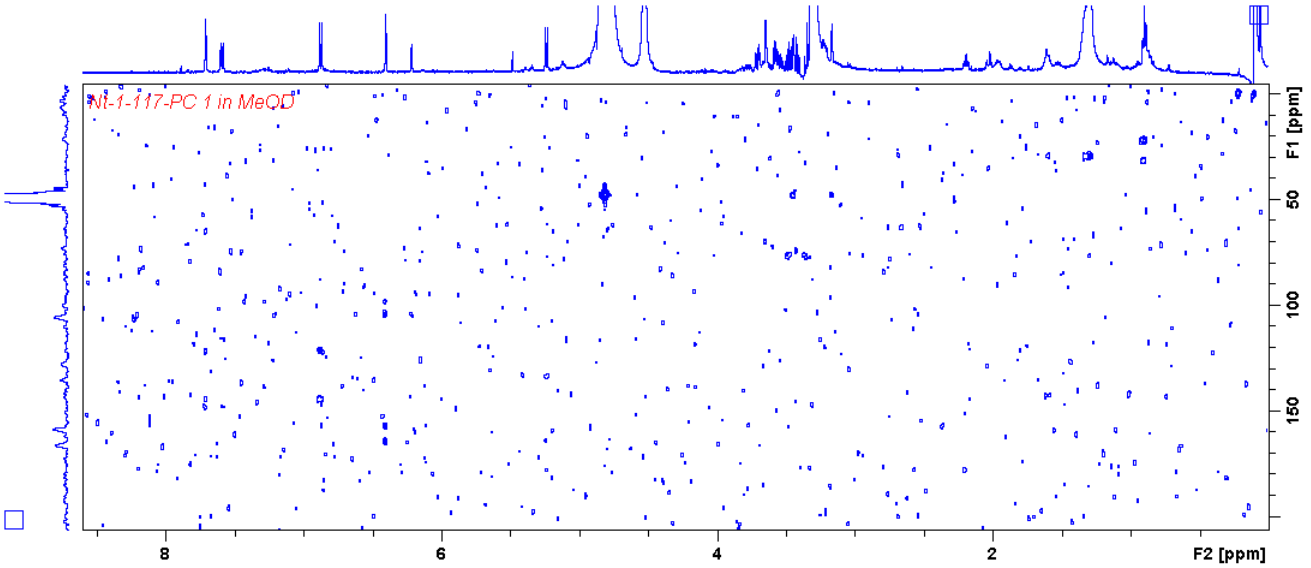

Plate 6.24: HMBC (500 MHz/125 MHz, CD_3OD) spectrum of quercetin 3-*O*-glucopyranoside (6.5).

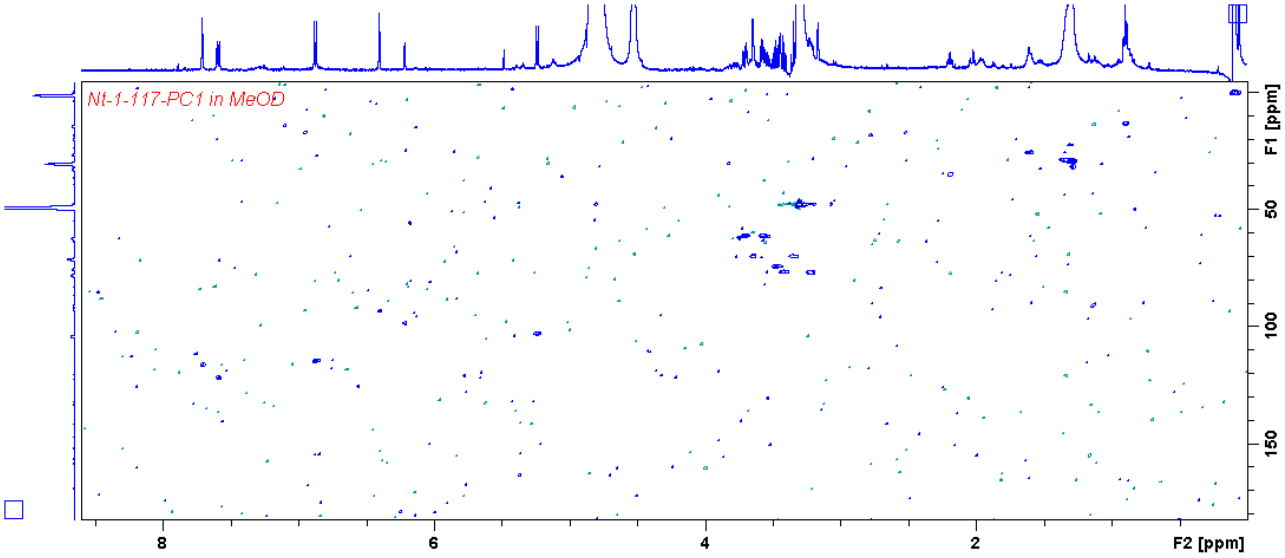

Plate 6.25: HSQC (500 MHz/125 MHz, CD_3OD) spectrum of quercetin 3-*O*-glucopyranoside (6.5).

APPENDIX E. HRESIMS AND NMR SPECTRA OF COMPOUNDS DESCRIBED IN CHAPTER 7

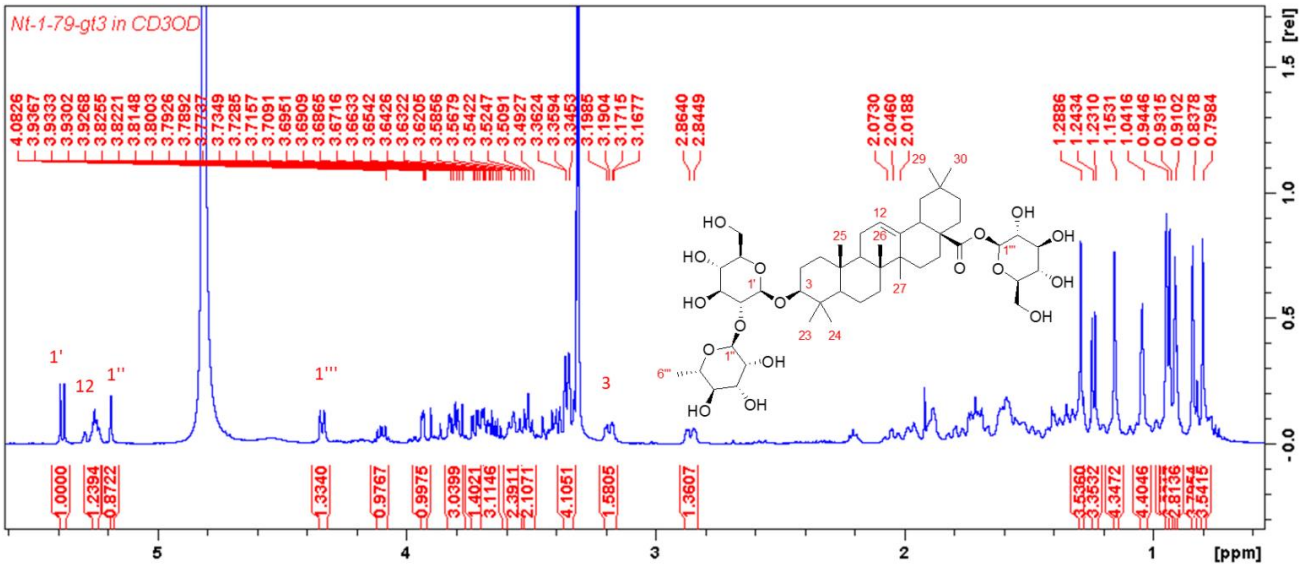

Plate 7.1: ^{1}H NMR (500 MHz, CD_3OD) spectrum of compound (7.1).

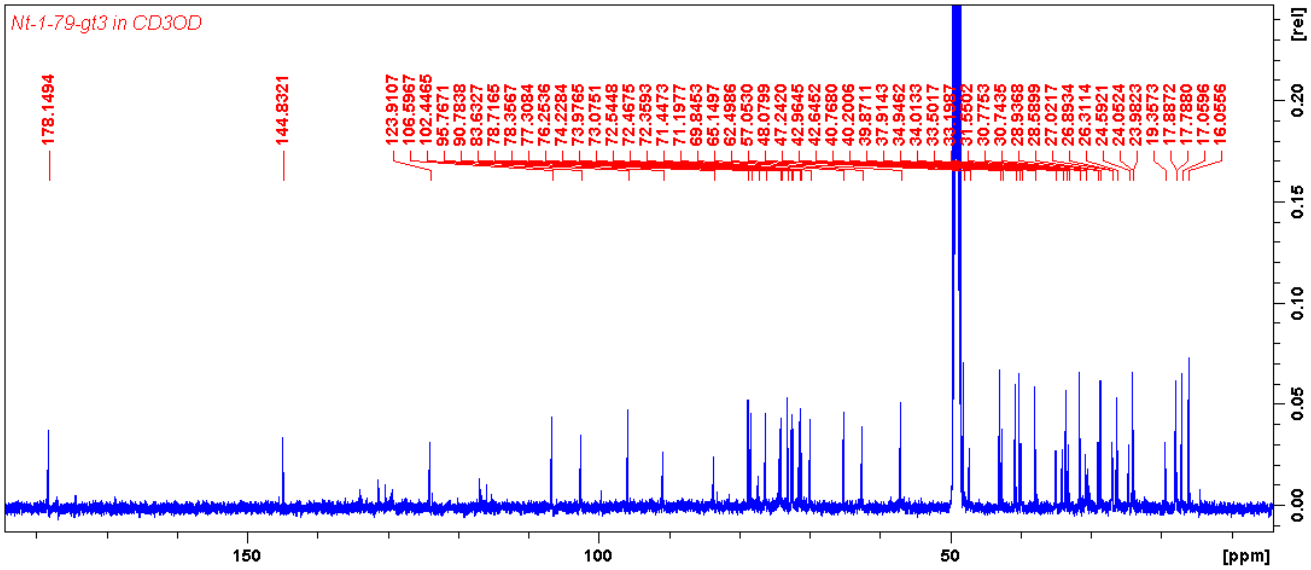

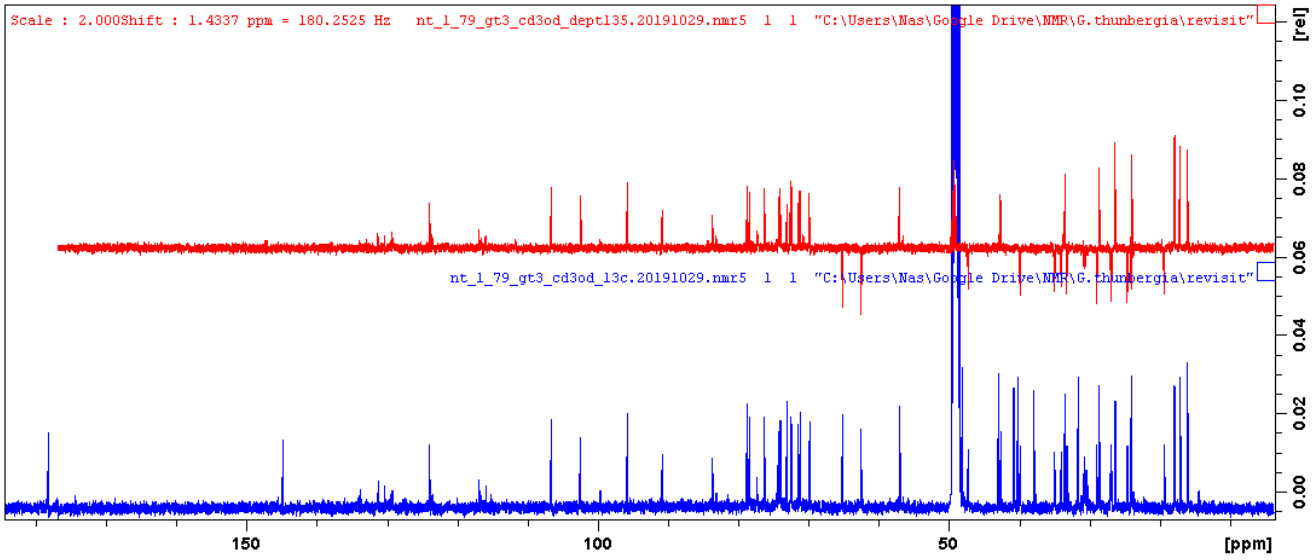

Plate 7.2: ^{13}C and DEPT (125 MHz, CD_3OD) spectra of compound (7.1).

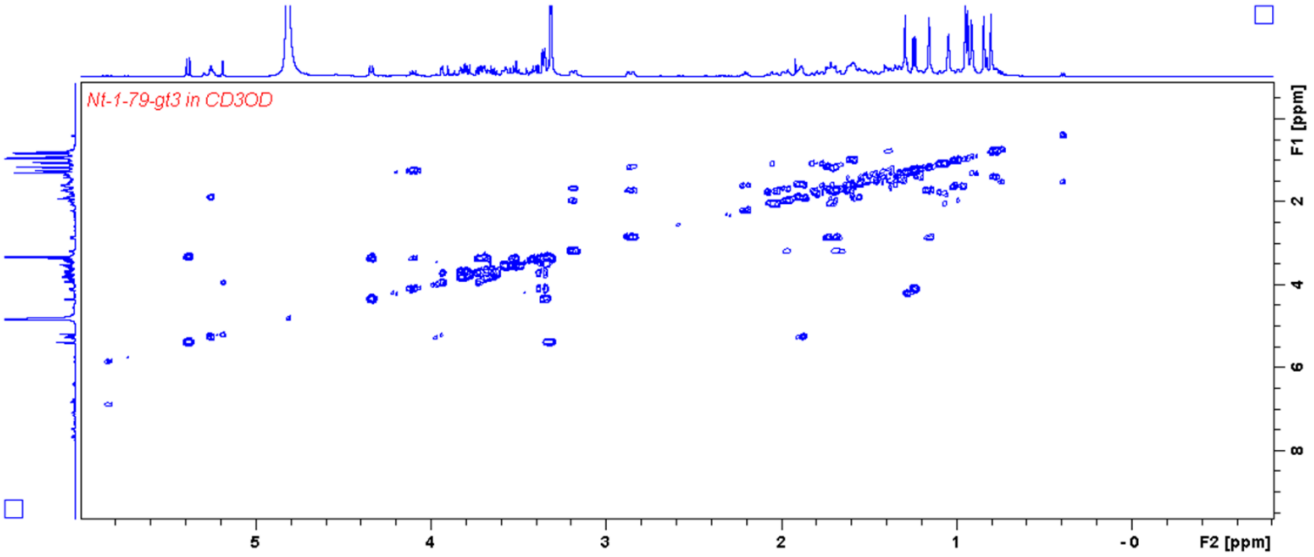

Plate 7.3: COSY (500 MHz, CD_3OD) spectrum of compound (7.1).

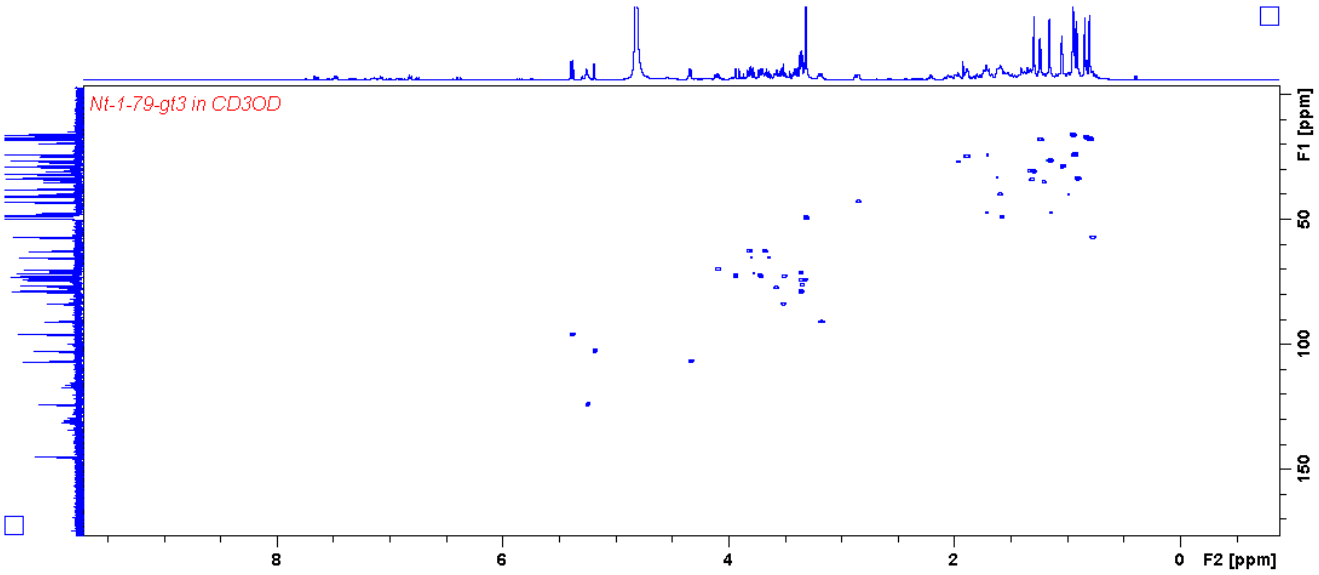

Plate 7.4: HSQC (500 MHz/125 MHz, CD_3OD) spectrum of compound (7.1).

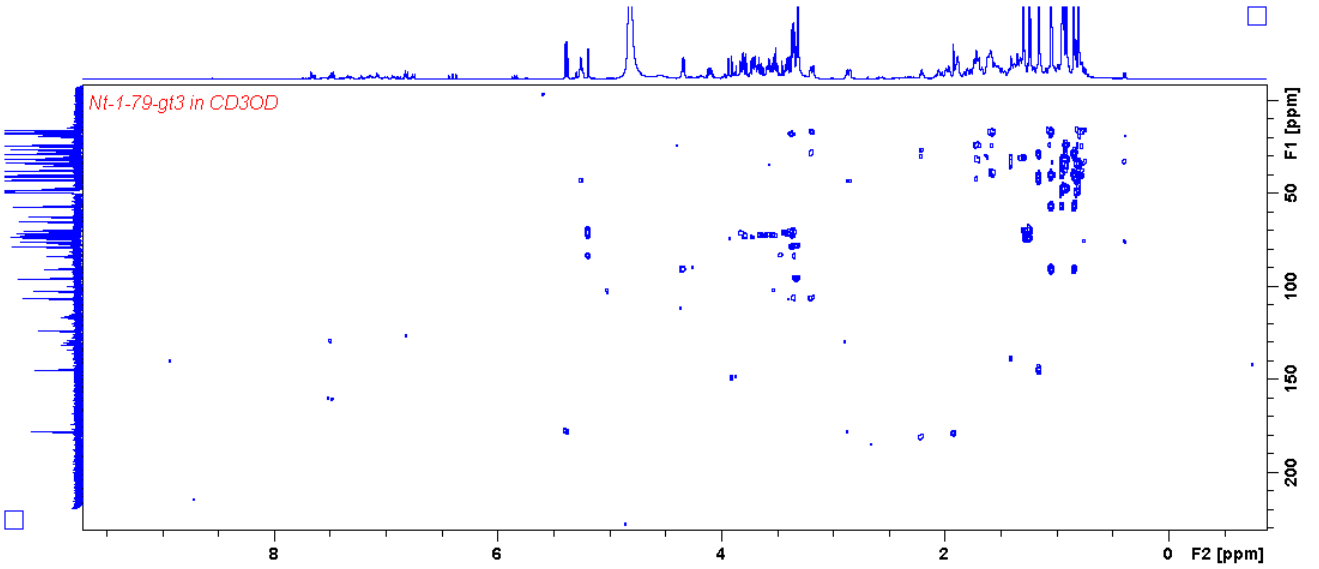

Plate 7.5: HMBC (500 MHz/125 MHz, CD_3OD) spectrum of compound (7.1).

Elemental Composition Report Page 1

Single Mass Analysis
Tolerance = 5.0 PPM / DBE: min = -1.5, max = 500.0
Element prediction: Off
Number of isotope peaks used for i-FIT = 2

Monoisotopic Mass, Even Electron Ions
199 formula(e) evaluated with 1 results within limits (up to 20 closest results for each mass)
Elements Used:
C: 20-25 1H: 10-20 2H: 0-4 O: 10-15 Na: 1-1
1,5a 48 (1.585) Cm (1:61)
TOF MS ES+

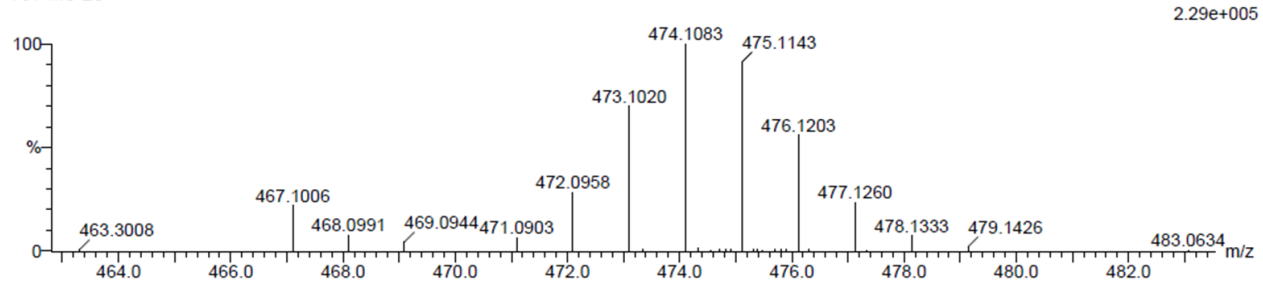

Minimum:				-1.5			
Maximum:		5.0	5.0	500.0			
Mass	Calc. Mass	mDa	PPM	DBE	i-FIT	i-FIT (Norm)	Formula
474.1083	474.1092	-0.9	-1.9	11.5	139.5	0.0	C21 1H17 2H3 O11 Na

Plate 7.6: HRESIMS of kaempferol 3-*O*-glucoside (7.2).

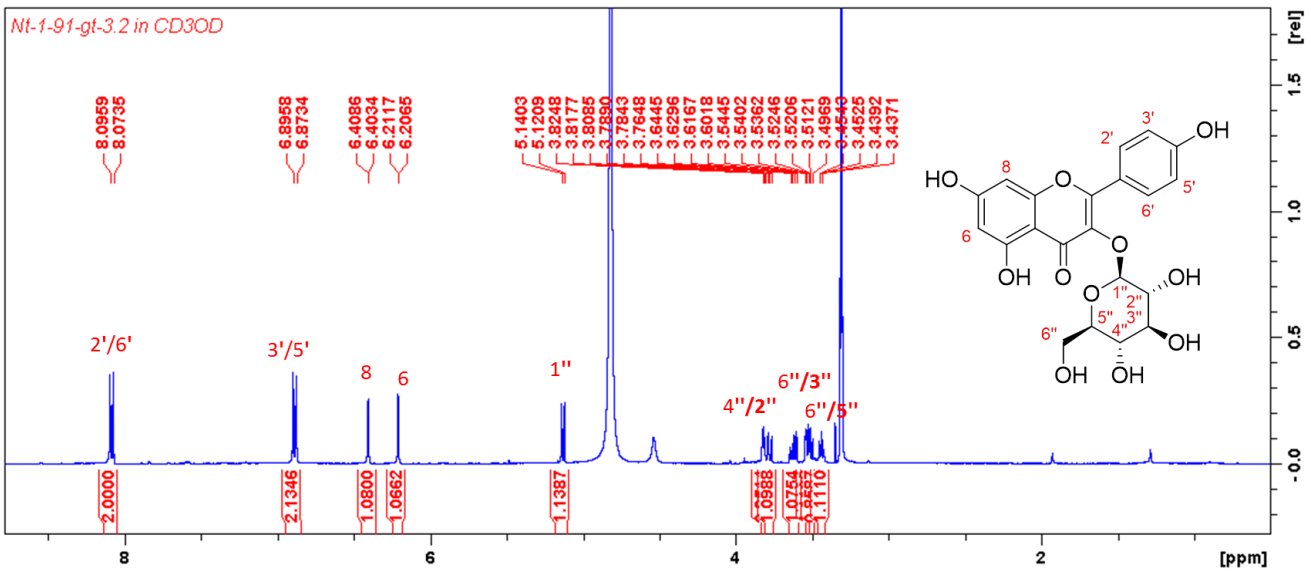

Plate 7.7: ^{1}H NMR (400 MHz, CD_3OD) spectrum of kaempferol 3-*O*-glucoside (7.2).

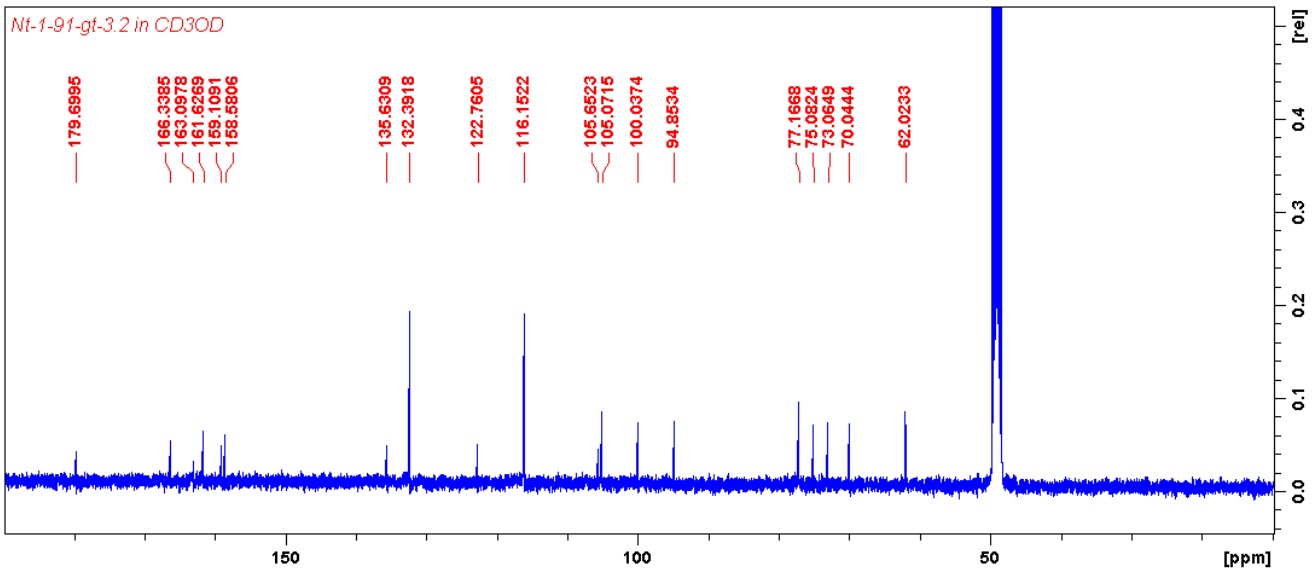

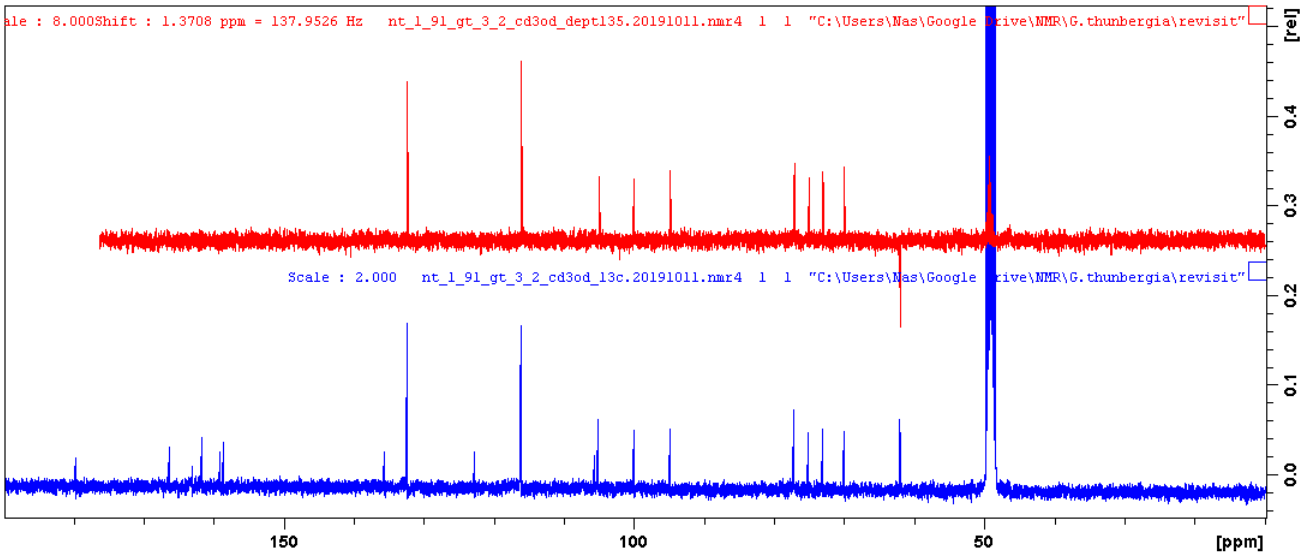

Plate 7.8: ^{13}C and DEPT (100 MHz, CD_3OD) spectra of kaempferol 3-*O*-glucoside (7.2).

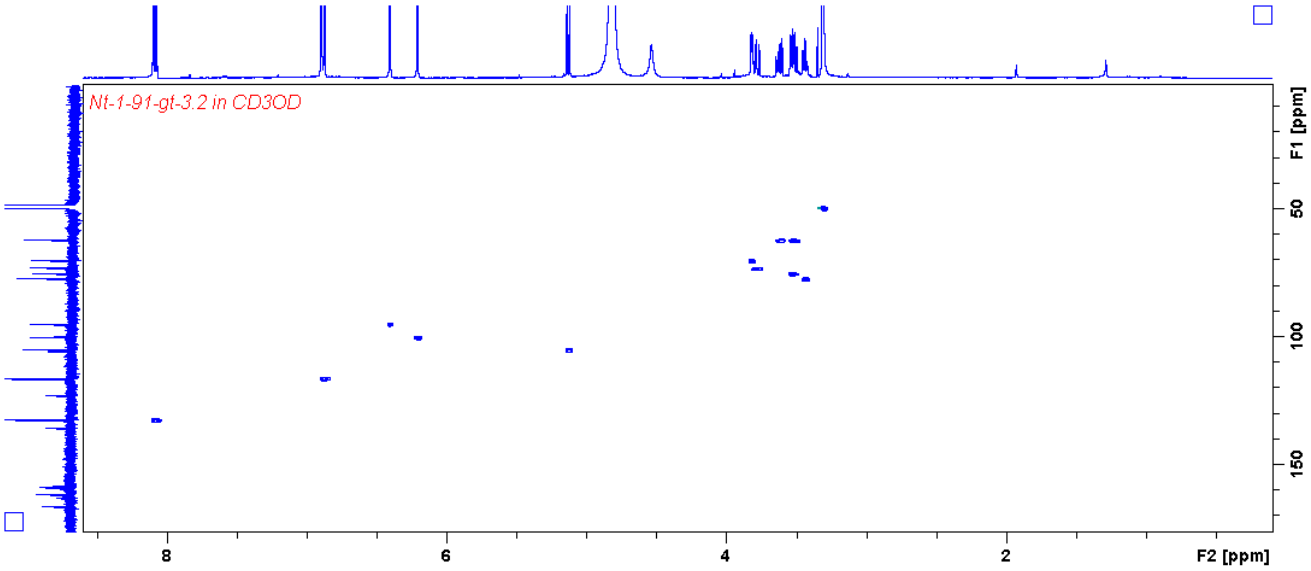

Plate 7.9: HSQC (400 MHz/100 MHz, CD_3OD) spectrum of kaempferol 3-*O*-glucoside (7.2).

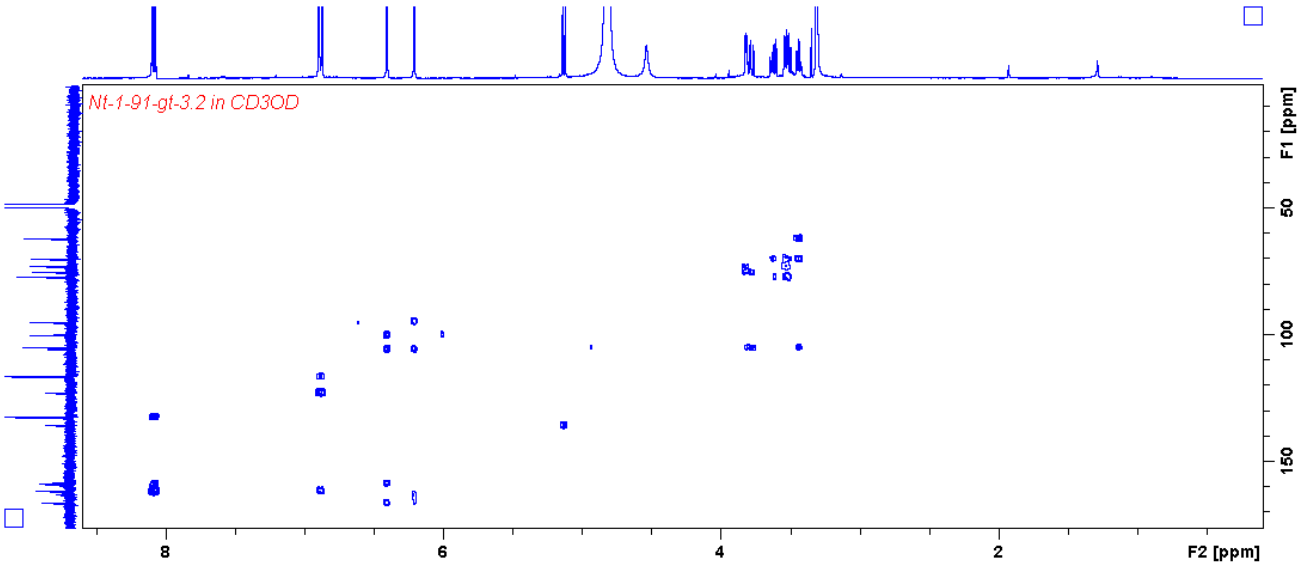

Plate 7.10: HMBC (400 MHz/100 MHz, CD_3OD) spectrum of kaempferol 3-*O*-glucoside (7.2).

Elemental Composition Report Page 1

Single Mass Analysis
Tolerance = 5.0 PPM / DBE: min = -1.5, max = 100.0
Element prediction: Off
Number of isotope peaks used for i-FIT = 3

Monoisotopic Mass, Even Electron Ions
1 formula(e) evaluated with 1 results within limits (all results (up to 1000) for each mass)
Elements Used:
C: 20-22 H: 18-20 O: 11-13
Nt-1-PC1 59 (1.957) Cm (1:61)
TOF MS ES-

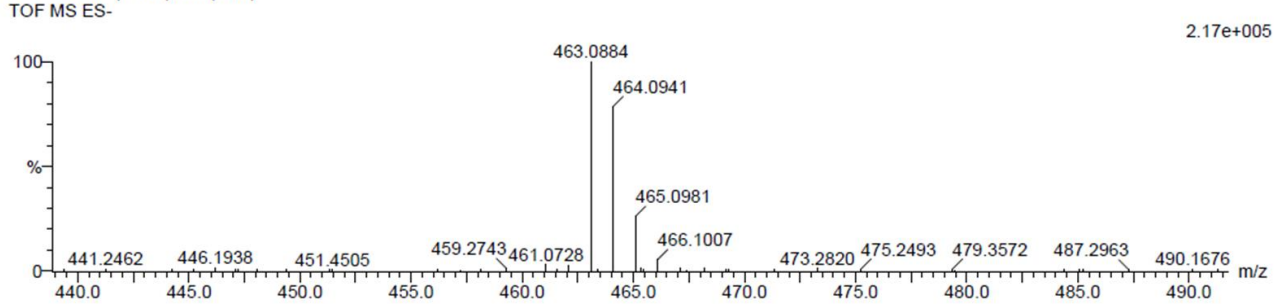

Minimum:				-1.5			
Maximum:		5.0	5.0	100.0			
Mass	Calc. Mass	mDa	PPM	DBE	i-FIT	i-FIT (Norm)	Formula
463.0884	463.0877	0.7	1.5	12.5	79.8	0.0	C21 H19 O12

Plate 7.11: HRESIMS of quercetin 3-*O*-glucoside (7.3).

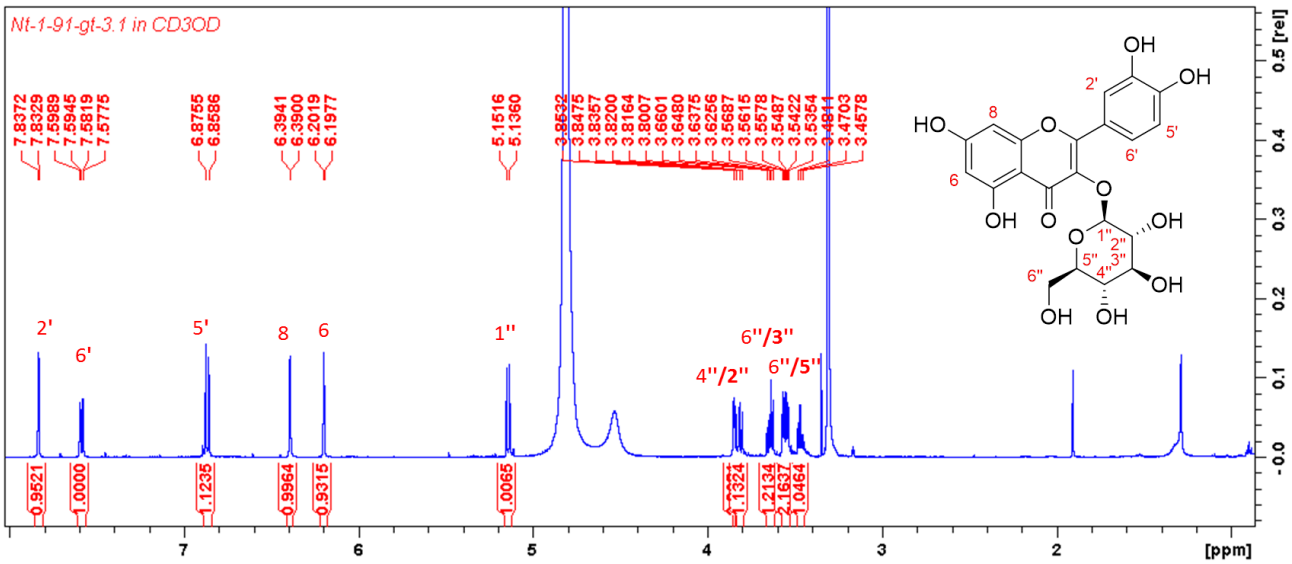

Plate 7.12: ^{1}H NMR (500 MHz, CD_3OD) spectrum of quercetin 3-*O*-glucoside (7.3).

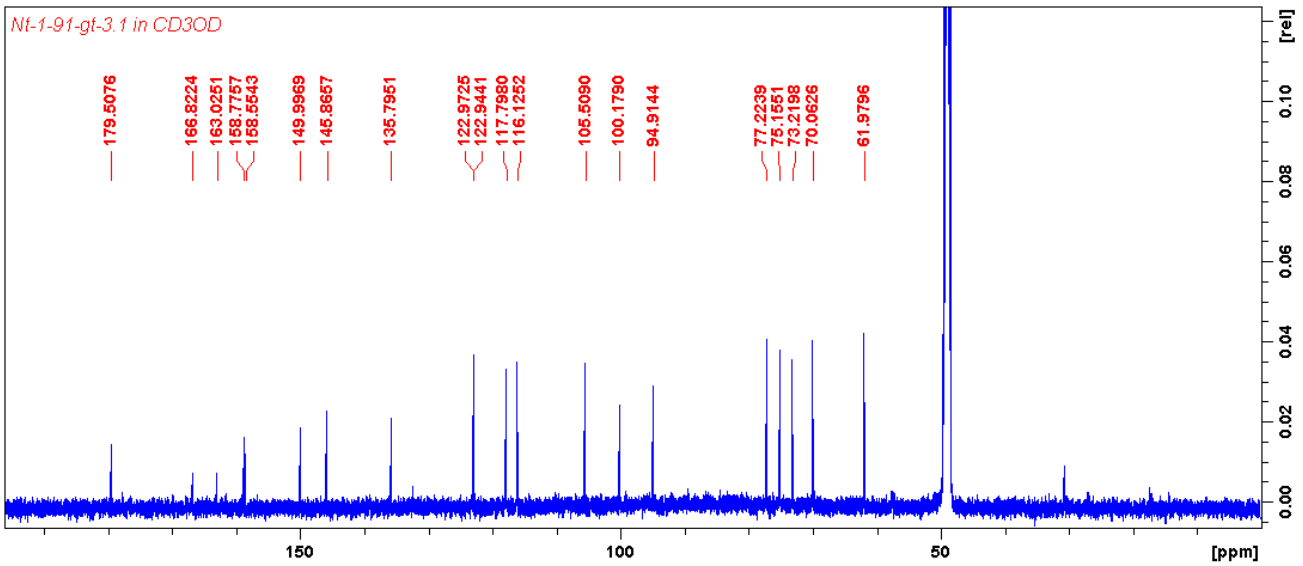

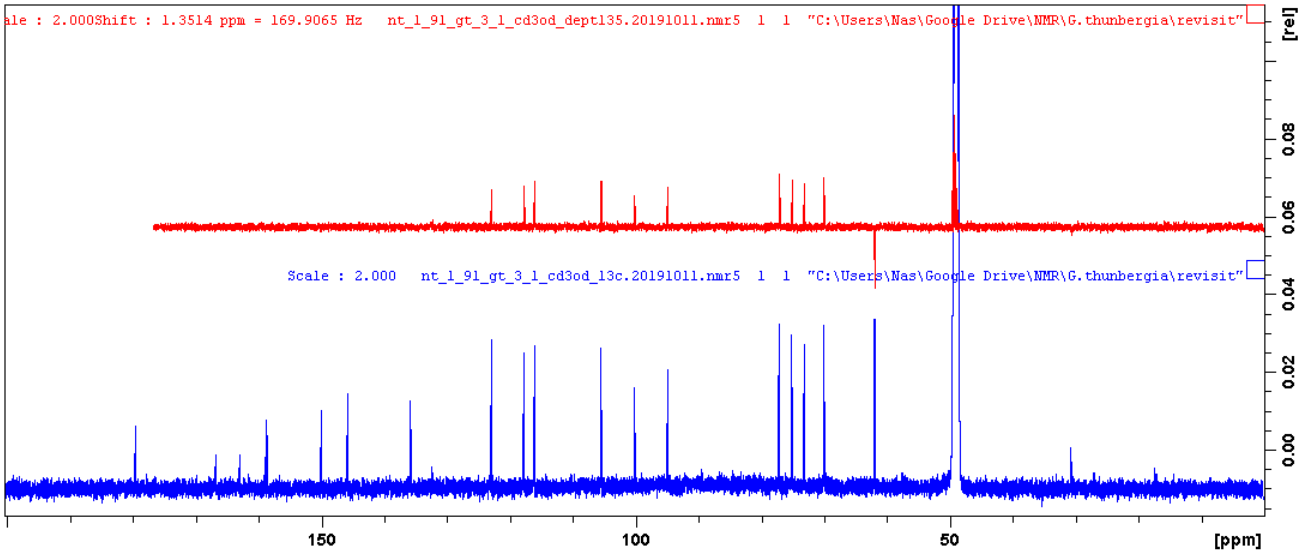

Plate 7.13: ^{13}C and DEPT (125 MHz, CD_3OD) spectra of quercetin 3-*O*-glucoside (7.3).

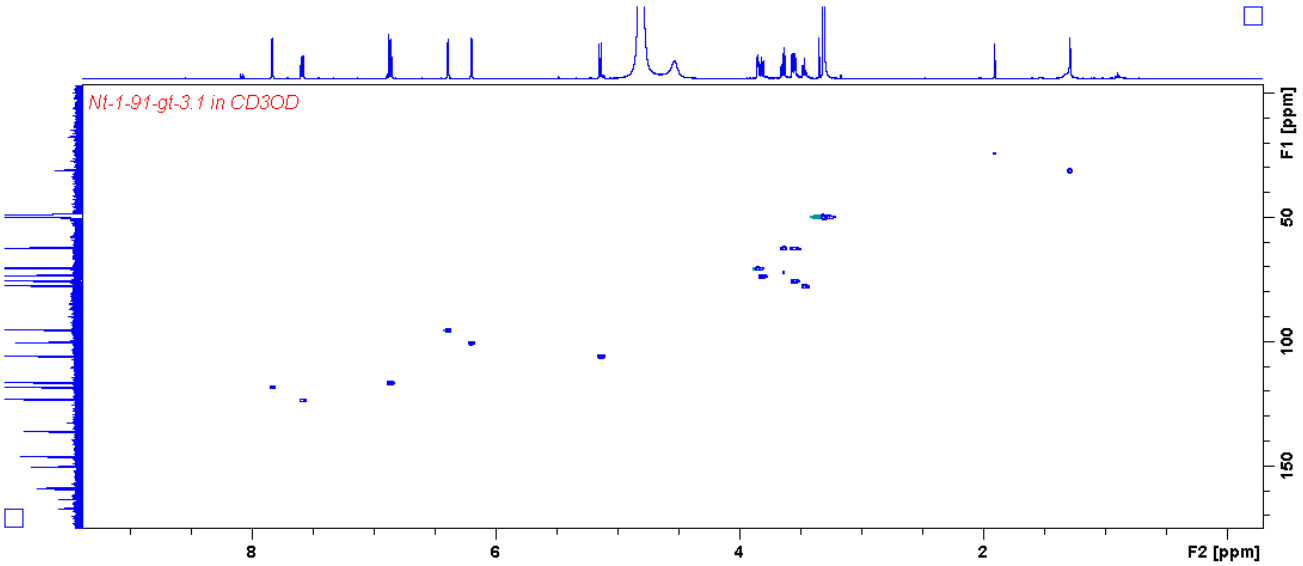

Plate 7.14: HSQC (500 MHz/125 MHz, CD_3OD) spectrum of quercetin 3-*O*-glucoside (7.3).

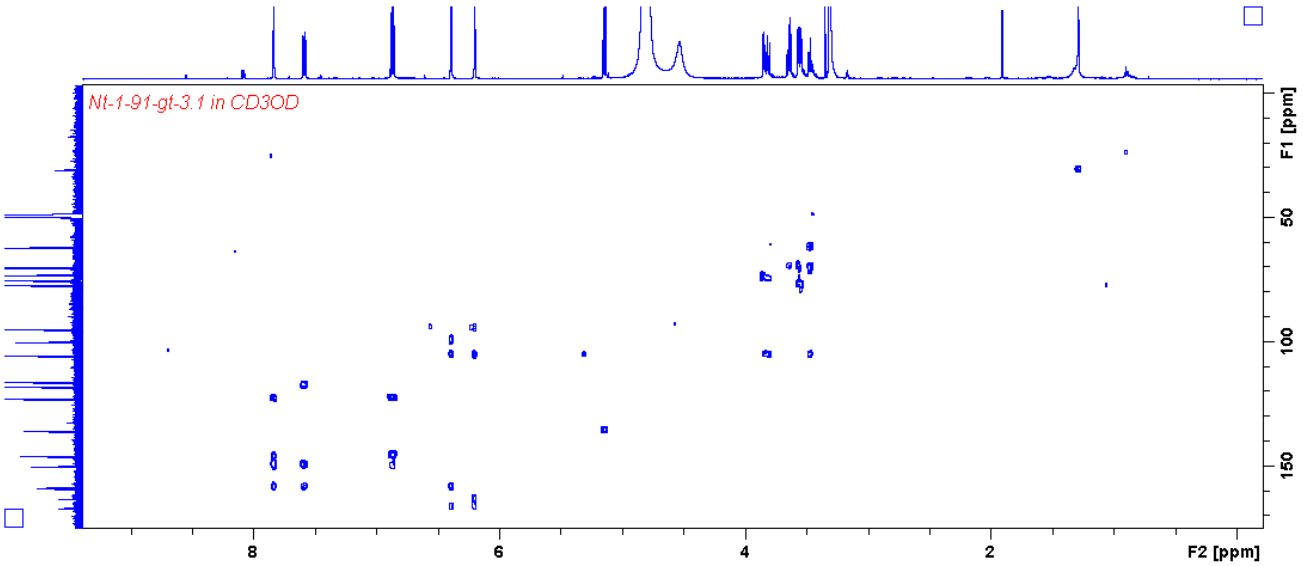

Plate 7.15: HMBC (500 MHz, CD_3OD) spectrum of quercetin 3-*O*-glucoside (7.3).

Elemental Composition Report **Page 1**

Single Mass Analysis
Tolerance = 5.0 PPM / DBE: min = -1.5, max = 50.0
Element prediction: Off
Number of isotope peaks used for i-FIT = 2

Monoisotopic Mass, Even Electron Ions
288 formula(e) evaluated with 1 results within limits (up to 20 closest results for each mass)
Elements Used:
C: 0-50 H: 0-50 N: 0-5 O: 0-10 Na: 0-1
1-4 2 (0.034) Cm (1:61)
TOF MS ES+

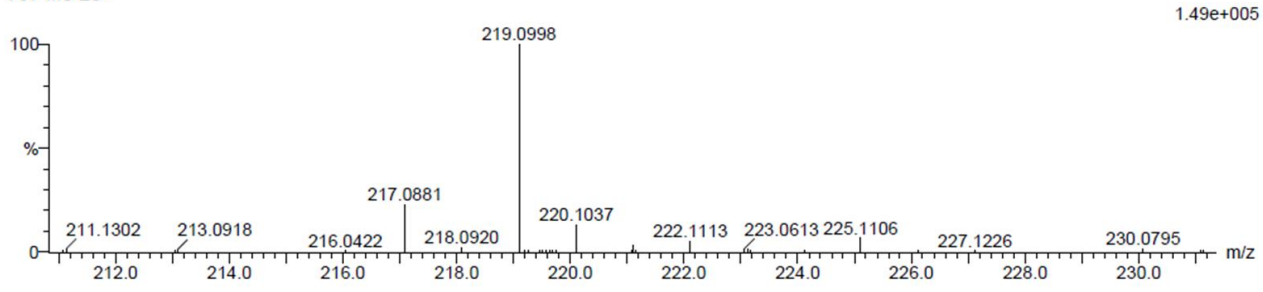

Minimum:				-1.5			
Maximum:		5.0	5.0	50.0			
Mass	Calc. Mass	mDa	PPM	DBE	i-FIT	i-FIT (Norm)	Formula
219.0998	219.0997	0.1	0.5	3.5	112.8	0.0	C11 H16 O3 Na

Plate 7.16: HRESIMS of Loliolide (7.4).

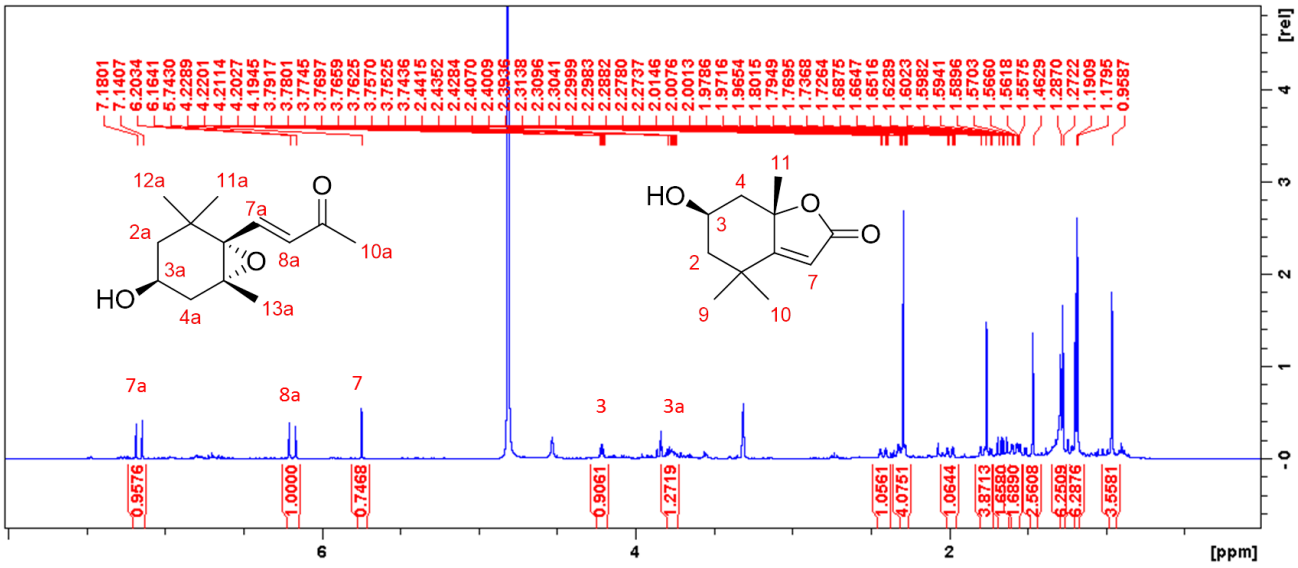

Plate 7.17: ^{1}H NMR (400 MHz, CD_3OD) spectrum of loliolide (7.4) and compound 7.5.

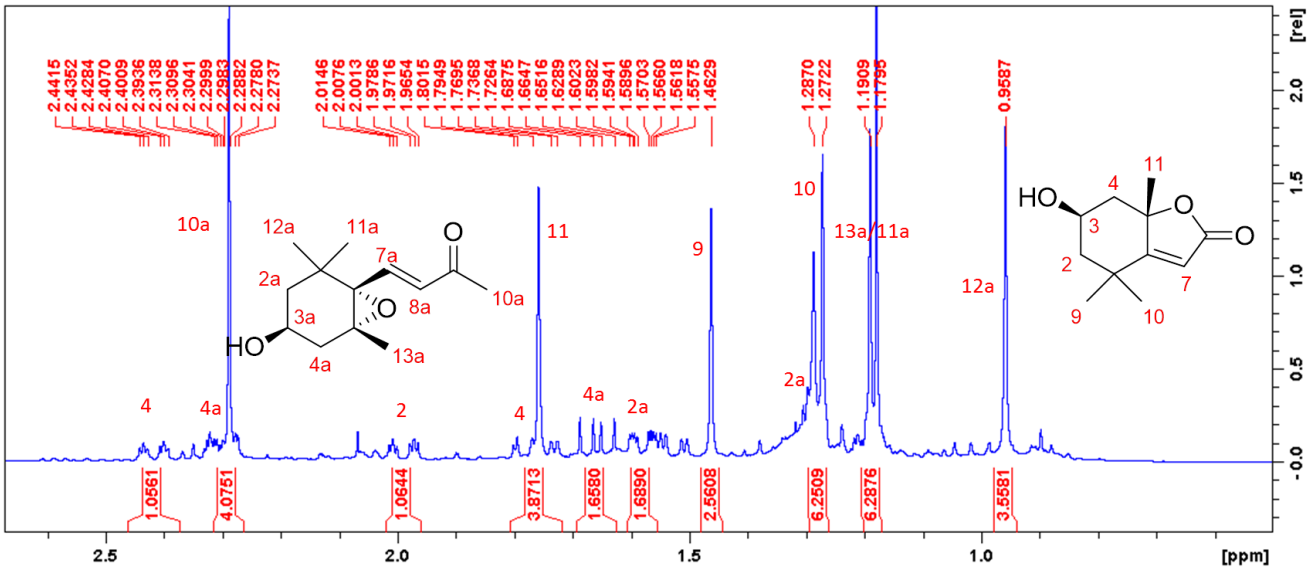

Expansion of ^{1}H NMR (400 MHz, CD_3OD) spectrum of Loliolide 7.4 and compound 7.5

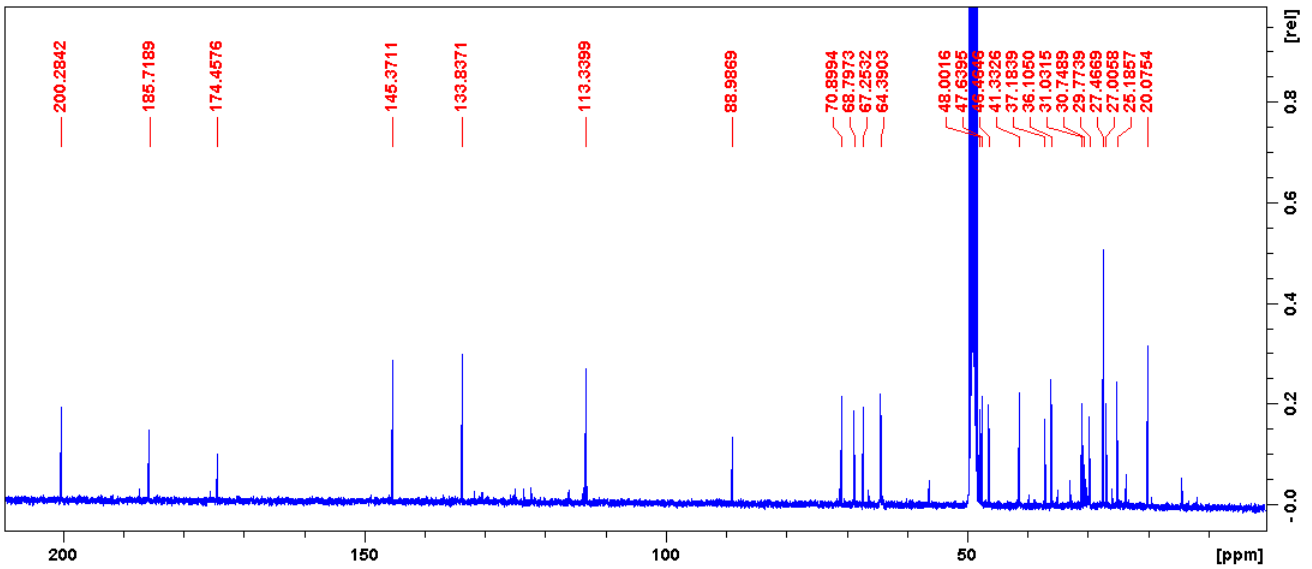

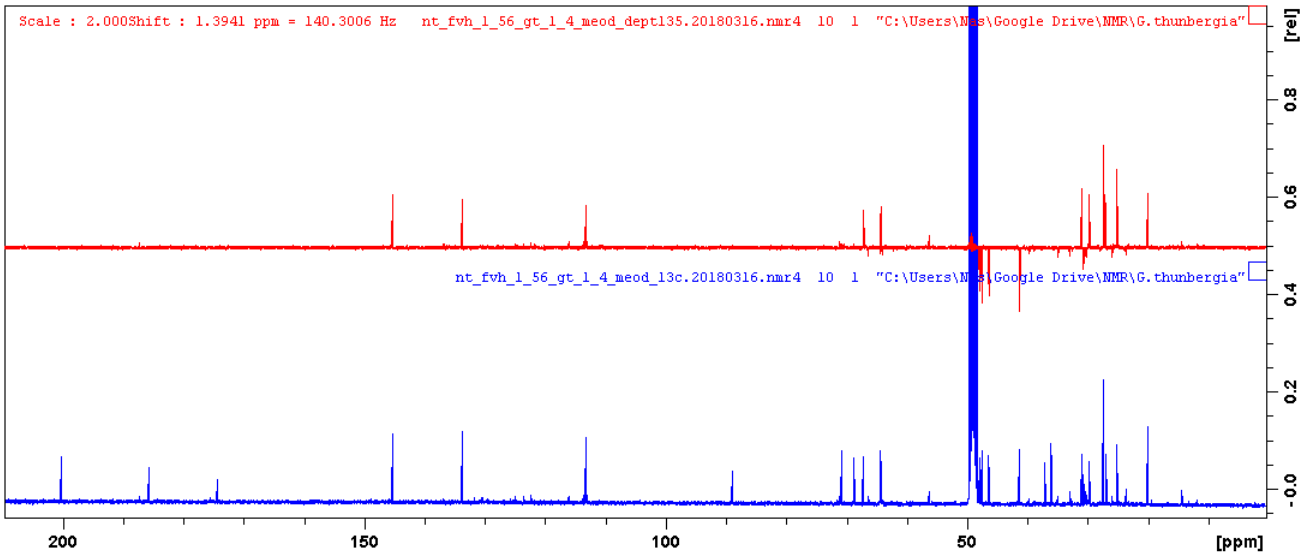

Plate 7.18: ^{13}C and DEPT (100 MHz, CD_3OD) spectra of loliolide (7.4) and compound 7.5

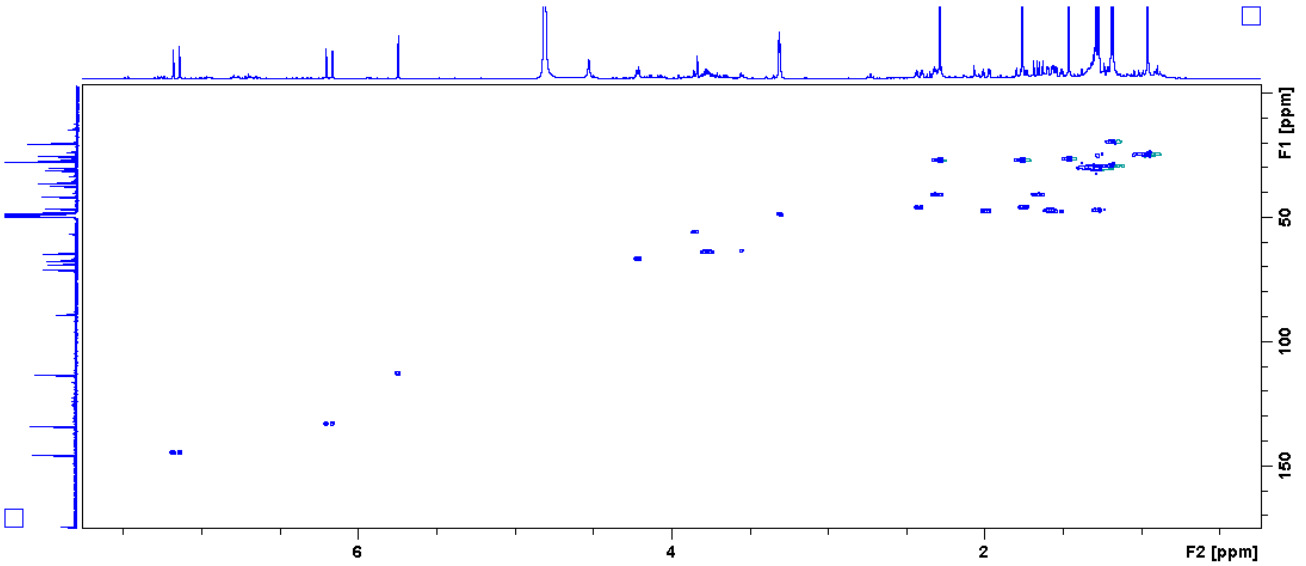

Plate 7.19: HSQC (400 MHz/100 MHz, CD_3OD) spectrum of loliolide (7.4) and compound 7.5.

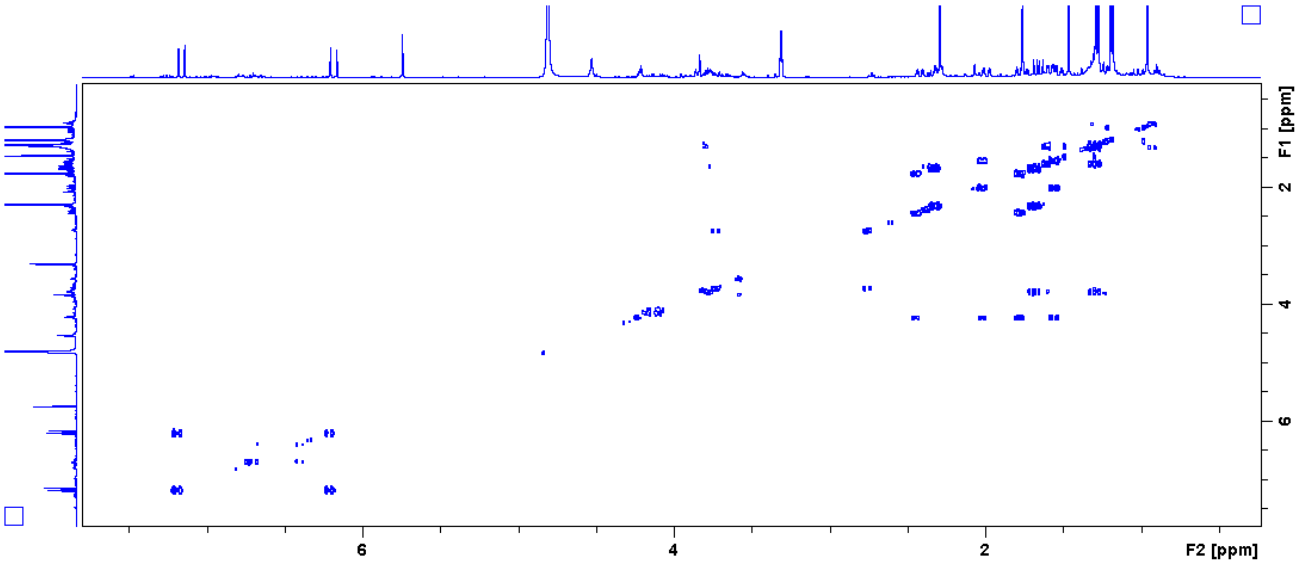

Plate 7.20: COSY (400 MHz, CD_3OD) spectrum of loliolide (7.4) and compound 7.5.

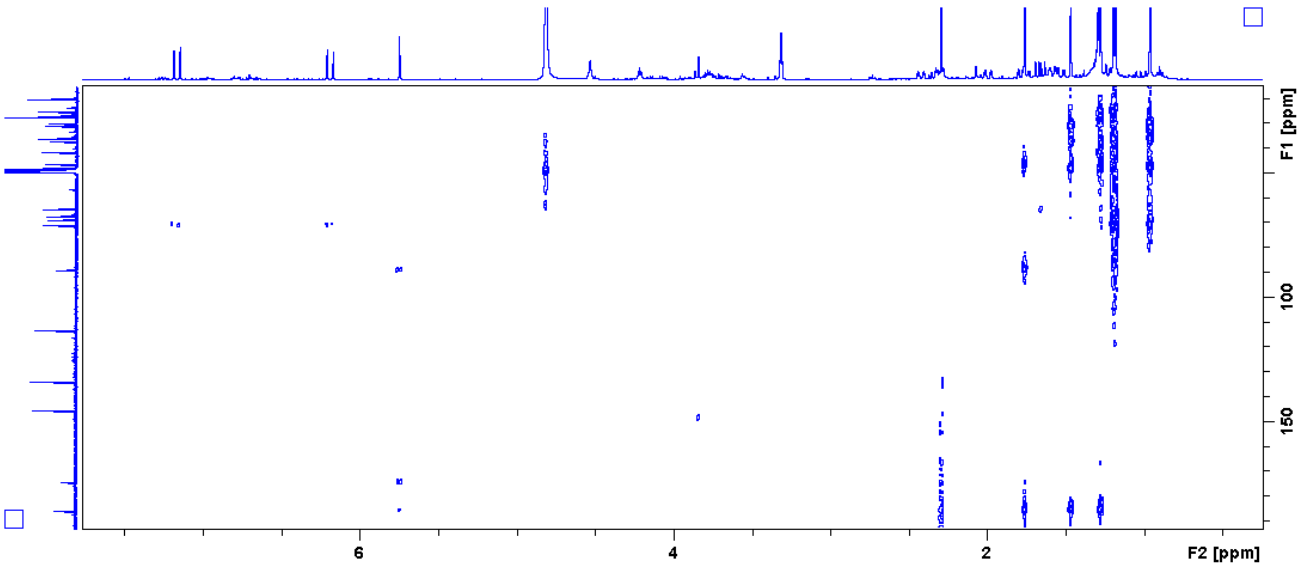

Plate 7.21: HMBC (400 MHz/100 MHz, CD_3OD) spectrum of loliolide (7.4) and compound 7.5.

Elemental Composition Report Page 1

Single Mass Analysis
Tolerance = 5.0 PPM / DBE: min = -1.5, max = 100.0
Element prediction: Off
Number of isotope peaks used for i-FIT = 3

Monoisotopic Mass, Even Electron Ions
3 formula(e) evaluated with 1 results within limits (all results (up to 1000) for each mass)
Elements Used:
C: 10-15 H: 5-10 O: 0-5
Nt-1-en1_2 34 (1.112) Cm (1:61)
TOF MS ES-

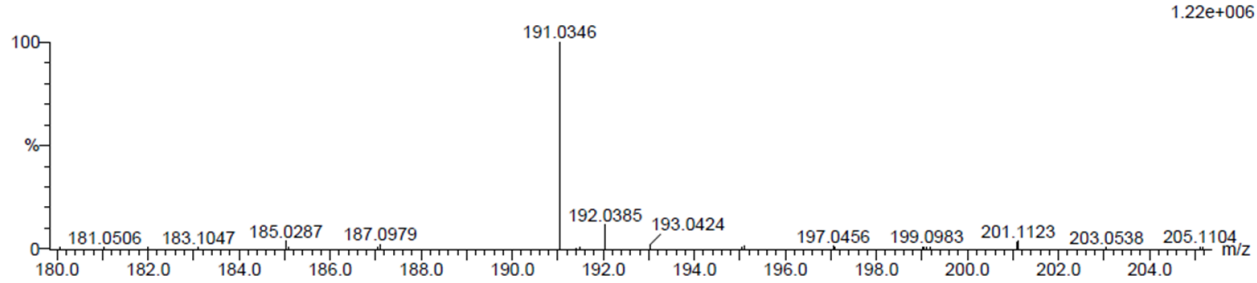

Minimum:				-1.5			
Maximum:		5.0	5.0	100.0			
Mass	Calc. Mass	mDa	PPM	DBE	i-FIT	i-FIT (Norm)	Formula
191.0346	191.0344	0.2	1.0	7.5	61.0	0.0	C10 H7 O4

Plate 7.22: HRESIMS of scopoletin (7.6).

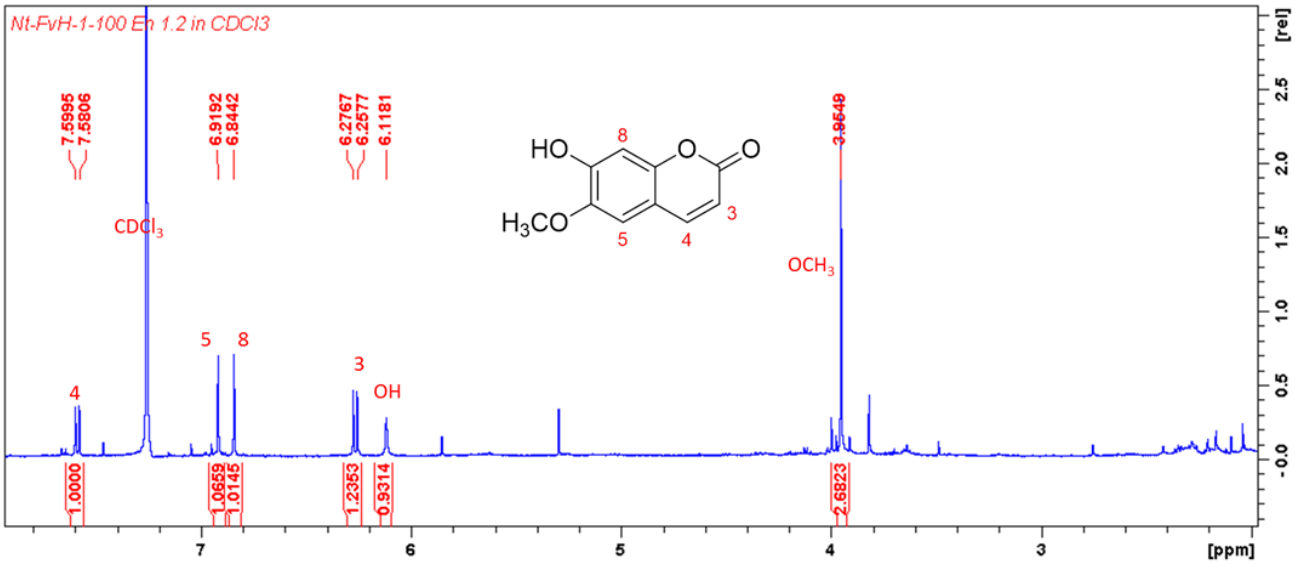

Plate 7.23: ^{1}H NMR (500 MHz, $CDCl_3$) spectrum of scopoletin (7.6).

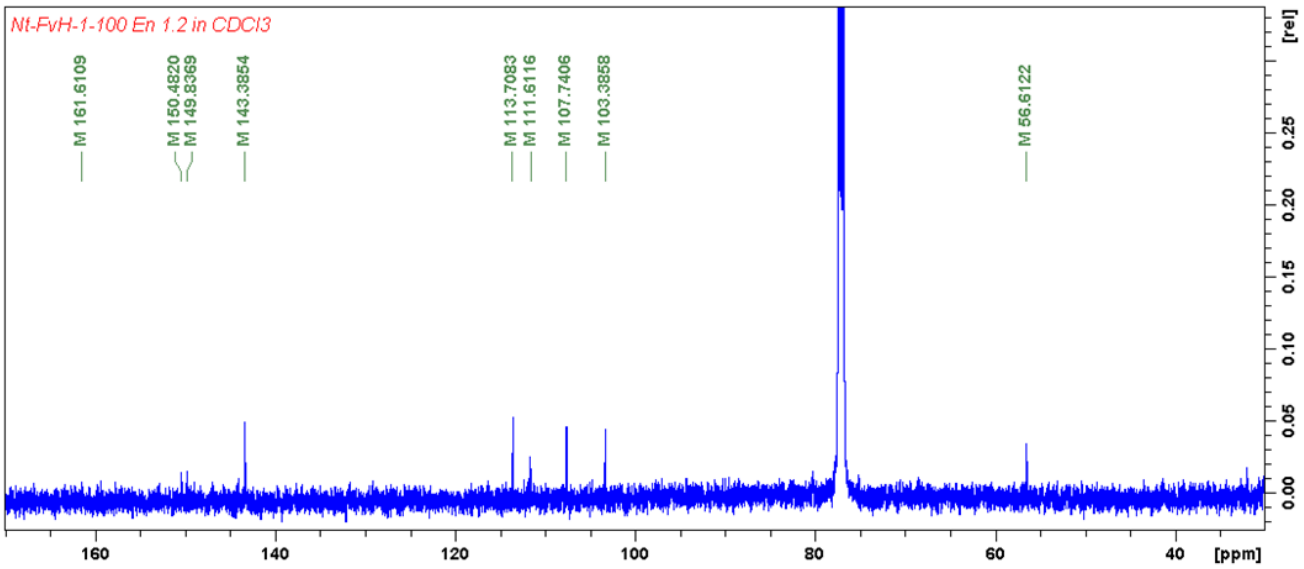

Plate 7.24: ^{13}C NMR (125 MHz, $CDCl_3$) spectrum of scopoletin (7.6).

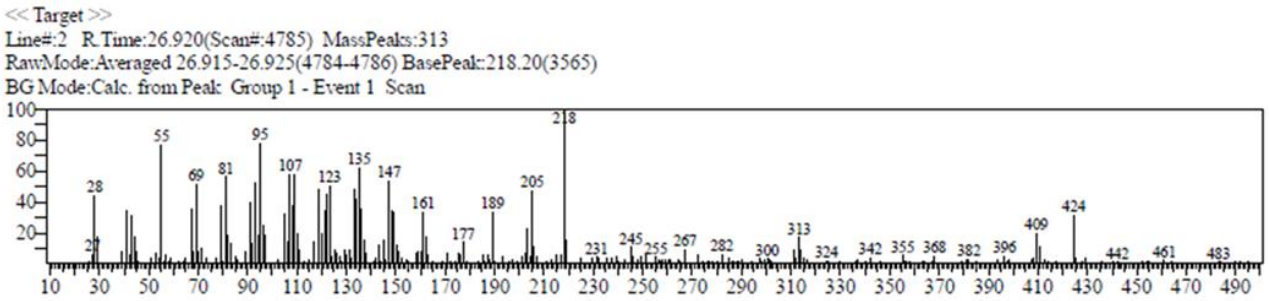

Plate 7.25: EIMS of lupeol (7.7).

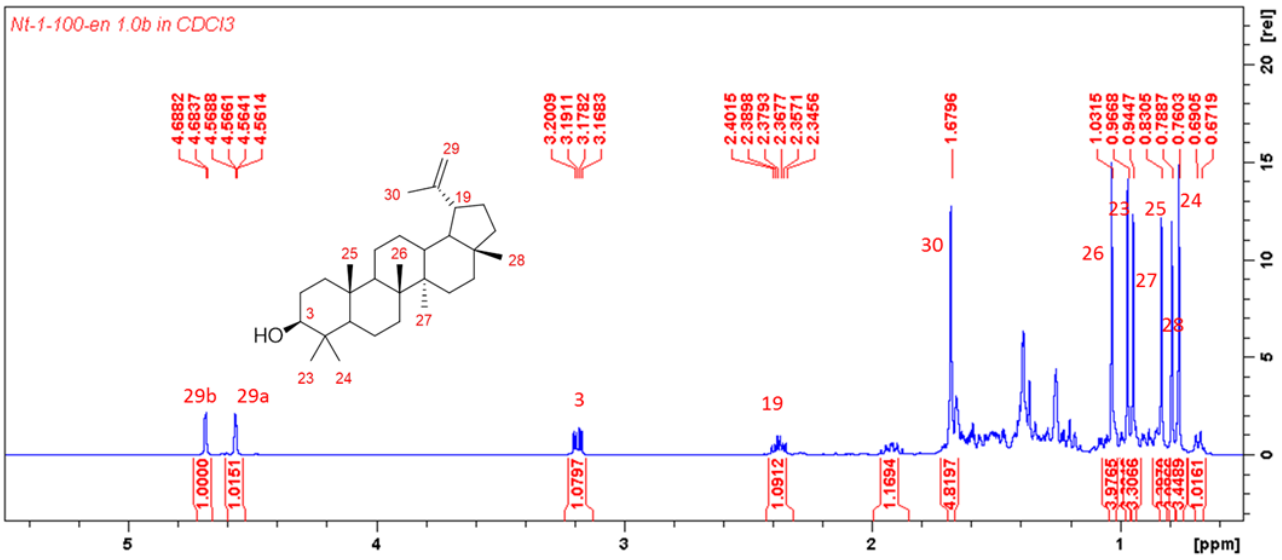

Plate 7.26: ^{1}H NMR (500 MHz, $CDCl_3$) spectrum of lupeol (7.7).

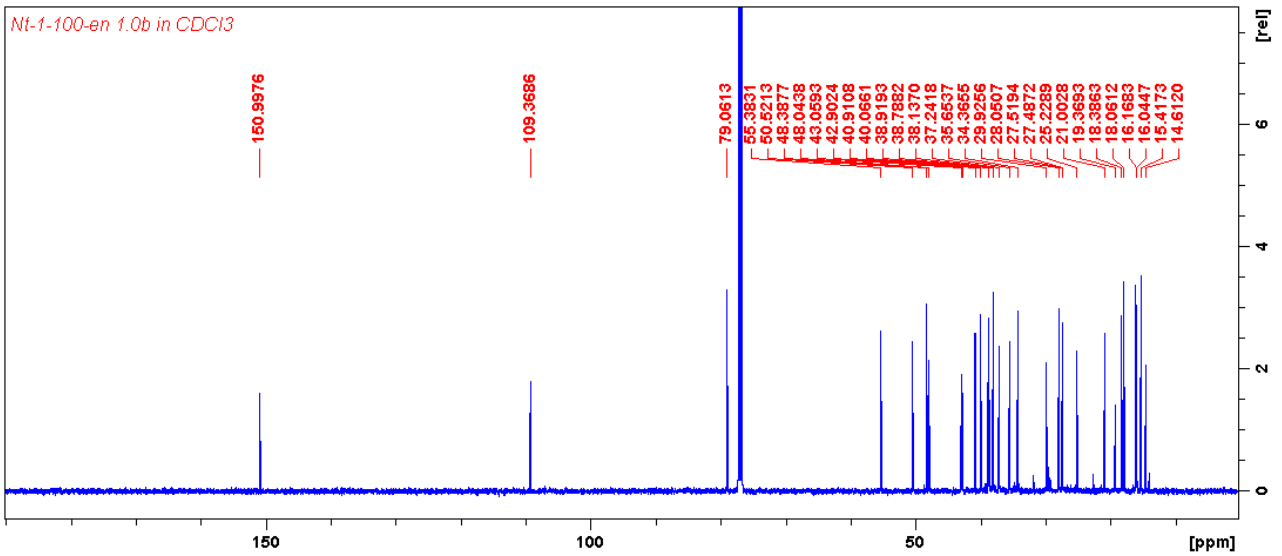

Plate 7.27: ^{13}C NMR (125 MHz, $CDCl_3$) spectrum of lupeol (7.7).

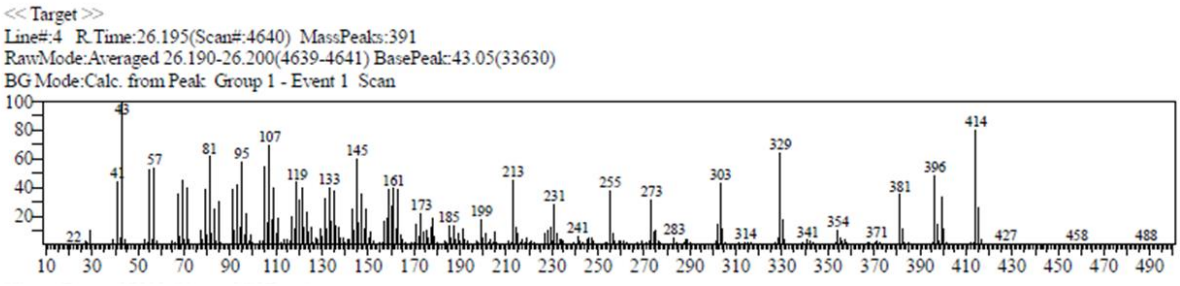

Plate 7.28: EIMS of β-sitosterol (7.8).

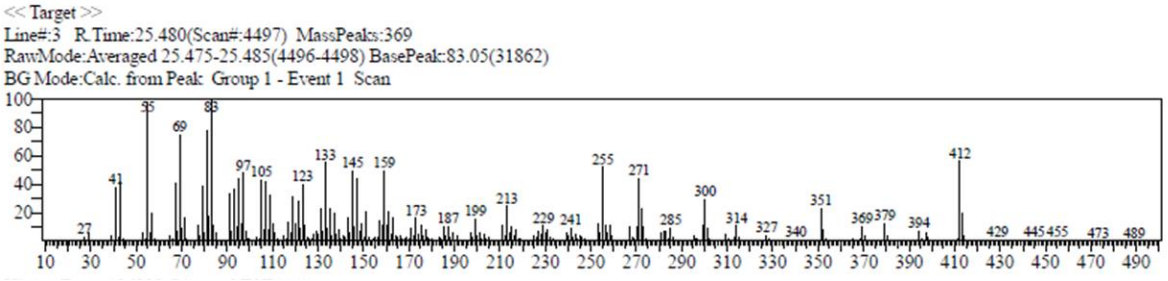

Plate 7.29: EIMS of stigmasterol (7.9).

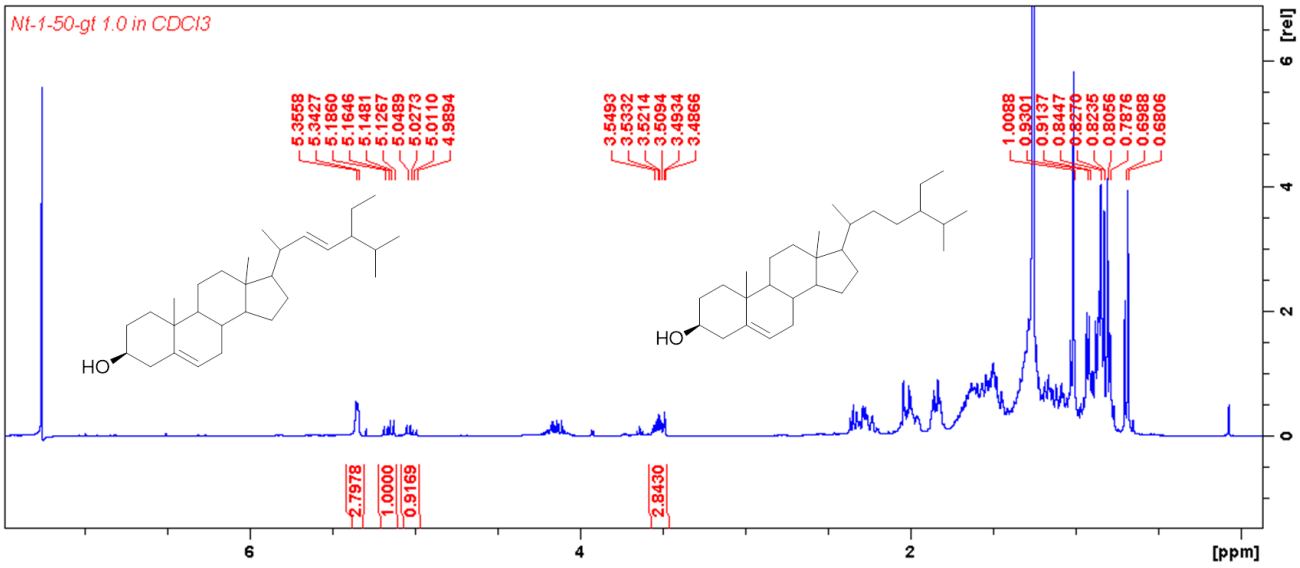

Plate 7.30: ^{1}H NMR (400 MHz, $CDCl_3$) spectrum of β-sitosterol (7.8) and stigmasterol (7.9).

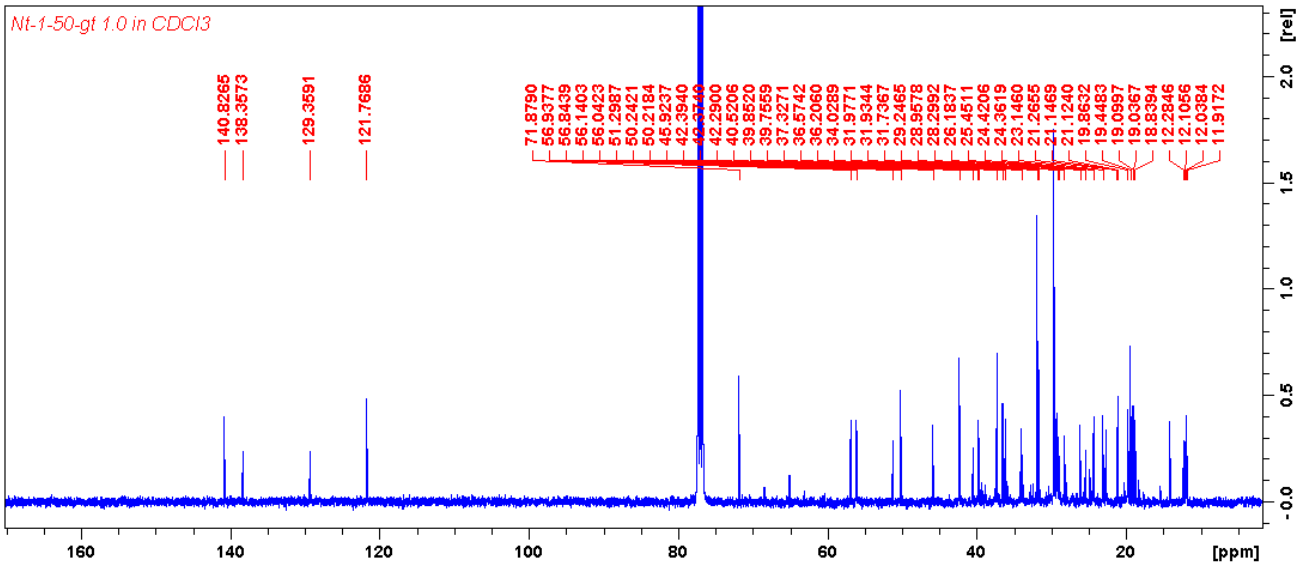

Plate 7.31: ^{13}C NMR (100 MHz, $CDCl_3$) spectrum of β-sitosterol (7.8) and stigmasterol (7.9).